ADVANCES IN PHYSIOLOGICAL SCIENCES

Proceedings of the 28th International Congress of Physiological Sciences Budapest 1980

Volumes

1 — Regulatory Functions of the CNS. Principles of Motion and Organization
2 — Regulatory Functions of the CNS. Subsystems
3 — Physiology of Non-excitable Cells
4 — Physiology of Excitable Membranes
5 — Molecular and Cellular Aspects of Muscle Function
6 — Genetics, Structure and Function of Blood Cells
7 — Cardiovascular Physiology. Microcirculation and Capillary Exchange
8 — Cardiovascular Physiology. Heart, Peripheral Circulation and Methodology
9 — Cardiovascular Physiology. Neural Control Mechanisms
10 — Respiration
11 — Kidney and Body Fluids
12 — Nutrition, Digestion, Metabolism
13 — Endocrinology, Neuroendocrinology, Neuropeptides — I
14 — Endocrinology, Neuroendocrinology, Neuropeptides — II
15 — Reproduction and Development
16 — Sensory Functions
17 — Brain and Behaviour
18 — Environmental Physiology
19 — Gravitational Physiology
20 — Advances in Animal and Comparative Physiology
21 — History of Physiology

Satellite symposia of the 28th International Congress of Physiological Sciences

22 — Neurotransmitters in Invertebrates
23 — Neurobiology of Invertebrates
24 — Mechanism of Muscle Adaptation to Functional Requirements
25 — Oxygen Transport to Tissue
26 — Homeostasis in Injury and Shock
27 — Factors Influencing Adrenergic Mechanisms in the Heart
28 — Saliva and Salivation
29 — Gastrointestinal Defence Mechanisms
30 — Neural Communications and Control
31 — Sensory Physiology of Aquatic Lower Vertebrates
32 — Contributions to Thermal Physiology
33 — Recent Advances of Avian Endocrinology
34 — Mathematical and Computational Methods in Physiology
35 — Hormones, Lipoproteins and Atherosclerosis
36 — Cellular Analogues of Conditioning and Neural Plasticity

(Each volume is available separately.)

ADVANCES IN
PHYSIOLOGICAL SCIENCES

Proceedings of the 28th International Congress of Physiological Sciences
Budapest 1980

Volume 8

Cardiovascular Physiology
Heart, Peripheral Circulation and Methodology

Editors

A. G. B. Kovách
E. Monos
G. Rubányi

Budapest, Hungary

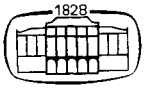

PERGAMON PRESS

AKADÉMIAI KIADÓ

Pergamon Press is the sole distributor for all countries, with the exception of the socialist countries.

HUNGARY	Akadémiai Kiadó, Budapest, Alkotmány u. 21. 1054 Hungary
U.K.	Pergamon Press Ltd., Headington Hill Hall, Oxford OX3 0BW, England
U.S.A.	Pergamon Press Inc., Maxwell House, Fairview Park, Elmsford, New York 10523, U.S.A.
CANADA	Pergamon of Canada, Suite 104, 150 Consumers Road, Willowdale, Ontario M2J 1P9, Canada
AUSTRALIA	Pergamon Press (Aust.) Pty. Ltd., P.O. Box 544, Potts Point, N.S.W. 2011, Australia
FRANCE	Pergamon Press SARL, 24 rue des Ecoles, 75240 Paris, Cedex 05, France
FEDERAL REPUBLIC OF GERMANY	Pergamon Press GmbH, 6242 Kronberg-Taunus, Hammerweg 6, Federal Republic of Germany

British Library Cataloguing in Publication Data

International Congress of Physiological Sciences
(28th. 1980: Budapest)
Advances in physiological sciences.
Vol. 8: Cardiovascular physiology, heart, peripheral circulation and methodology
1. Physiology-Congresses
I. Title II. Kovách, A. G. B.
III. Monos, E. IV. Rubányi G.
591.1 QP1 80-41875

Pergamon Press	ISBN 0 08 026407 7 (Series) ISBN 0 08 026820 X (Volume)
Akadémiai Kiadó	ISBN 963 05 2691 3 (Series) ISBN 963 05 2734 0 (Volume)

In order to make this volume available as economically and as rapidly as possible the authors' typescripts have been reproduced in their original forms. This method unfortunately has its typographical limitations but it is hoped that they in no way distract the reader.

Printed in Hungary

FOREWORD

This volume is one of the series published by Akadémiai Kiadó, the Publishing House of the Hungarian Academy of Sciences in coedition with Pergamon Press, containing the proceedings of the symposia of the 28th International Congress of Physiology held in Budapest between 13 and 19 July, 1980. In view of the diversity of the material and the "taxonomic" difficulties encountered whenever an attempt is made to put the various subdisciplines and major themes of modern physiology into the semblance of some systematic order, the organizers of the Congress had to settle for 14 sections and for 127 symposia, with a considerable number of free communications presented either orally or as posters.

The Congress could boast of an unusually bright galaxy of top names among the invited lecturers and participants and, naturally, the ideal would have been to include all the invited lectures and symposia papers into the volumes. We are most grateful for all the material received and truly regret that a fraction of the manuscripts were not submitted in time. We were forced to set rigid deadlines, and top priority was given to speedy publication even at the price of sacrifices and compromises. It will be for the readers to judge whether or not such an editorial policy is justifiable, for we strongly believe that the value of congress proceedings declines proportionally with the gap between the time of the meeting and the date of publication. For the same reason, instead of giving exact transcriptions of the discussions, we had to rely on the introductions of the Symposia Chairmen who knew the material beforehand and on their concluding remarks summing up the highlights of the discussions.

Evidently, such publications cannot and should not be compared with papers that have gone through the ordinary scrupulous editorial process of the international periodicals with their strict reviewing policy and high rejection rates or suggestions for major changes. However, it may be refreshing to read these more spontaneous presentations written without having to watch the "shibboleths" of the scientific establishment.

September 1, 1980

J. Szentágothai

President of the
Hungarian Academy of Sciences

Adv. Physiol. Sci. Vol. 8. Cardiovascular Physiology Heart, Peripheral Circulation and Methodology
A. G. B. Kovách, E. Monos, G. Rubányi (eds)

CENTRAL NERVOUS ORIGIN OF VASOMOTOR TONE

S. M. Hilton
Department of Physiology, University of Birmingham, England

The commonly accepted ideas about the origin of vasomotor tone are still influenced by nineteenth century concepts which led physiologists to imagine an assembly of centres in the brain, each controlling a single physiological variable. The origin of the notion of a vasomotor centre controlling arterial blood pressure is thus buried deep in history. This is largely why the idea persists, in spite of several attempts made over the past fifteen years to show it up as a naive notion which has hardly any experimental support.

The concept of a vasomotor centre - a source of confusion

Most of you probably know that the vasomotor centre controlling arterial blood pressure was placed in the medulla on the basis of the work over a 100 years ago of Dittmar (1870; 1873) and Owsjannikow (1871) : this comprised three separate studies of the effect on blood pressure of successive transections of the brainstem starting in the mid-brain and working through the medulla. The finding in these classical experiments was that blood pressure was only seriously affected when the section encroached upon the rostral medulla. More caudal sections reduced the blood pressure still further until a point was reached, about the caudal third of the medulla and some 3-4 mm rostral to the obex, at which the maximum fall was produced.

If findings such as these were made today, they would not be given the same significance; for we are so familiar with the syndrome of spinal shock. Indeed, all the attempts to analyse experimental information of this kind has led physiologists to be wary of assuming that it can be used simply to locate a specific centre whose influence has been removed. Nevertheless, in this particular case, and even more so following the discovery by Ranson and Billingsley (1916), on electrical stimulation, of pressor and depressor points in the floor of the 4th ventricle, the idea came about not only that the vasomotor centre exists but also that it is dorsally placed within this region of the brain stem. Much careful work followed, in which pressor and depressor regions were mapped in the medulla, (Ranson and Magoun, 1939) culminating in the maps made by Alexander (1946), which are those usually reproduced in textbooks, in which extensive pressor and depressor medullary areas are shown, the former being more dorsal and lateral, and the latter being a rather

smaller ventromedial zone.

We now know that the neuronal organisation within the so-called pressor area is exceedingly complex (Hilton, 1974; 1975); for it contains elements of the baroreceptor reflex pathway and others with inhibitory influences on individual vascular beds. Nevertheless, the idea that this is the vasomotor centre persists as the established view. A very recent investigation based upon it was that of Kumada et al. (1979) where, in the course of a study on the cerebral ischaemic reflex in rabbits, large lesions were made bilaterally in the dorsal medulla. Because of a marked fall in arterial blood pressure in 4 out of 15 of these rabbits, the suggestion was made by these authors that they may have located the site of the vasomotor centre. Reference back to the early work of Dittmar (1873), however, shows that this cannot be so; for in his experiments, which were also on rabbits, very careful extirpations of the dorsal medulla had been made with a knife specially constructed for the purpose, and the blood pressure found to be hardly affected by lesions which removed almost the dorsal two-thirds of this region of the brainstem. The area of the dorsal medulla common to all the lesions made by Kumada et al. (1979) was caudal to the site located by Dittmar (1873) as being of special significance for maintenance of blood pressure. He put it in the ventrolateral reticular formation near the facial nucleus — a conclusion to which I will return later. For now, however, it is sufficient to note that many investigators have made large lesions in the dorsal medulla and observed only small falls of blood pressure (e.g. Manning, 1965; Chai & Wang, 1968) which has led to the rather confusing conclusion that neurones with tonic vasomotor effects are diffusely distributed throughout the medulla. Although I have called this conclusion confusing, it appears to be supported when one looks at the results of experiments carried out as a search for specific vasomotor neurones within the medulla. A painstaking study of this kind was made by Hukuhara (1974) who looked for medullary neurones with a firing pattern which was correlated with the discharge in sympathetic efferent nerves, chiefly those to the kidney. His map of the location of these neurones show them to occupy almost all of the medullary reticular formation.

Something seems wrong with the conventional wisdom and this doubt is heightened by experimental evidence from a variety of sources. In a series of papers, published in the Chinese Journal of Physiology before the last war (Chen et al., 1936; 1937; Lim et al., 1938) stimulation experiments similar to those of Ranson and Billingsley (1916) were repeated, but in which measurements were made not only of arterial blood pressure, but also of heart-rate, pupil-size, the size of the spleen, tone of the bladder, small intestine and colon, and the level of the blood sugar. Piloerection, sweat gland activity, and effects on the bronchioles were also looked for. Such was the ubiquity of the changes found that there would appear to be no reason at all for isolating the arterial blood pressure from any of the other variables mentioned, or from any that could be measured or recorded, and hence for isolating a region that could be called specifically a pressor region. The clear implication of these findings is that if a section of the cord is made at the level that causes a profound fall in arterial blood pressure, every autonomic response organised at a lower level of the neuraxis would be expected to be profoundly depressed, and there is much clinical and experimental evidence that this is so. The problem of interpretation has arisen because of the original assumption that any physiological

variable which can be isolated experimentally, for independent measurement or registration, must have its appropriate controlling region in the brainstem, and that each of them can be regarded as a separate physiological and anatomical entity. As we now see, this assumption leads again and again to the unlikely conclusion that widespread, overlapping regions control each physiological variable.

Sympathetic rhythms

One way of attempting to deal with the dilemma has been to ignore the seemingly intransigent problems of topography and to speak instead of oscillating circuits. This is the approach of Gebber and his colleagues (Taylor and Gebber, 1975; Barman and Gebber, 1976) who have started out from the long-known observation (Adrian et al., 1932) that the discharges in sympathetic efferent nerves show several rhythmic variations. There is firstly a slow rhythm which is close to the respiratory rhythm but also apparently generated independently of it, as it often persists during hypocapnia of a degree sufficient to abolish the rhythmic discharge in the phrenic nerves and as it displays shifting phase relationships with the bursts of phrenic nerve discharge (Cohen and Gootman, 1970; Barman and Gebber, 1976). This rather capricious rhythm is superimposed upon a faster rhythm at 3-5 c/sec which is very close to the cardiac rhythm. However, as it persists after sino-aortic denervation, it in its turn is apparently independent of the baroreceptor input (Taylor and Gebber, 1975). These two rhythms have a supraspinal origin, whereas another at 8-12 c/sec (Green and Heffron, 1967; Cohen and Gootman, 1970) can be generated in the spinal cord (McCall and Gebber, 1975).

In Gebber's papers the hope is expressed that this approach will provide information on the intrinsic organisation of the brainstem circuits responsible for generating the background discharges of pre-ganglionic sympathetic neurones; but it is not easy to see how this may be realised. Even a close correlation between the discharge of a brainstem neurone and that in some sympathetic efferent nerve several synapses away is no proof that the former has actually generated the latter. Secondly, extensive investigations by Langhorst and his group of the activity in brainstem neurones, using cross-correlation techniques and power spectral analysis of their discharges in relation to potential inputs and outputs, has shown the shifting relations, both with time and the condition of the animal preparation, of the discharges recorded. This has led Langhorst (1980) to assert that there is nothing other than a "common brainstem system" of multiple potentiality. Indeed, in the light of all the arguments and data quoted already it seems unlikely that there can be any brainstem neurones which are dedicated to a single system —— sympathetic, parasympathetic or somatic —— or even to a single output.

Organisation of patterns of response

It seems to me that a straightforward way out of the dilemma which all these results appear to present is to regard the central nervous system as a mechanism for initiating and integrating patterns of response (Hilton, 1974; 1975). There is a number —— but only a small number —— of readily recognisable and biologically significant patterns of this kind, such as those comprising alimentary and sexual reactions, temperature regulation, and fear and rage reactions (usually described in physiology as the

defence reaction). All of these include important cardiovascular components, so if different but separate regions of the brainstem are responsible for the organisation of each pattern, there can be no separate brainstem region responsible for any single cardiovascular variable. Starting from this idea, everything falls into place and all the findings I have described so far can be explained. The only exception to my generalisation will be the medullary site of origin of the vagal neurones to the heart, for they must play a role similar to that of the sympathetic pre-ganglionic neurones in the intermediolateral cell column of the spinal cord. These are the origins of the final common paths for each output of the autonomic nervous system, and they must be the site of much of the integration that produces the final output to each effector unit (such as an individual vascular bed). But the response patterns are organised elsewhere and it is not only to the hypothalamus, but also to the more caudal brainstem, that we must look for the location of regions that serve this function. Of these various, complex responses, I believe the defence reaction to be that which is mostly concerned in the central nervous generation of vasomotor tone, so the rest of this paper will be concentrated upon it.

The role of the baroreceptor reflex

Before turning to it, however, I must say a few words about the baroreceptor reflex; for this is commonly thought to play the key role in blood pressure regulation. But this should now be carefully qualified for several reasons. In the first place, as pointed out by Scher and Young (1963), the reflex has too small an open-loop gain to function effectively as a control system. Indeed, we are familiar with the fact that blood pressure is far from constant; it fluctuates continually in normal daily-life above the resting, equilibrium level with every single activity, and large increases occur regularly with even a simple hand-grip or a casual act of micturition. The baroreceptors can cope reasonably well with steady-state changes, such as adjustments of the whole body from the lying to the upright position; but they are of little avail in coping with the rapid, phasic changes which are a feature of every interesting act we perform.

A second, and most telling finding that must carry a lot of weight is that of Cowley et al. (1973), who have made long-term observations of the arterial blood pressure of dogs, both normal animals and after sino-aortic denervation (which removes the baroreceptor input). The average pressure of the two groups of dogs is virtually the same, the latter group simply showing a larger variability. There has been much discussion as to whether an absolutely 100% complete baroreceptor denervation can be achieved, but this should not obscure the main point made by Guyton and his co-workers — and that is that the origin of the mean level of overall vasomotor tone does not lie with the baroreceptor reflex. Of course, Guyton (1976) argues strongly and eloquently that long-term homeostasis of arterial blood pressure is independent of the nervous system; but without denying the close relationship between body fluid colume and renal function, I think we cannot help but be impressed by the mass of evidence, both clinical and experimental, that the central nervous system plays an essential role in setting the general level of arterial blood pressure. In this connection there has been much interest in recent years in situations, both experimental and naturally occurring, in which

the baroreceptor reflex response is reset, so what we need to seek out are the central nervous mechanisms which tell the baroreceptors, so to speak, the range of arterial pressure around which they should work. As I have said before, I believe that the areas of the brain organising the defence reaction are those which play an essential role in this respect.

The alerting stage of the defence reaction

Most of you will probably know that, in experimental animals such as the cat, the cardiovascular pattern of response in this reaction consists of a mobilisation of venous reserves and an increase in chronotropic and inotropic actions on the heart, all leading to an increased cardiac output, with a vasodilatation in skeletal muscle and a strong and well-maintained vasoconstriction in the splanchnic area with some vaso-constriction also in the kidney and skin. In cats lightly anaesthetised with the steroid mixture, althesin (Timms, 1976), the pattern is elicited reflexly by stimulation of nociceptive afferents in a peripheral nerve, or most interestingly, of the peripheral chemoreceptors (Marshall, 1977; Hilton, 1979).

This pattern of response, which is easily understood as a preparation for the possibility of intense muscular exertion, occurs in the conscious animal in the early alerting stage of the response, which the animal will show to any sudden or novel stimulus in its environment (Abrahams et al., 1960; 1964). Exactly the same pattern of response is found in rabbits (Azevedo et al., 1980), dogs (Bolme et al., 1967) and monkeys (Schramm et al., 1971), and there is good evidence that it is readily provoked in human subjects, particularly in situations causing anxiety (Blair et al., 1959). In the early experiments of Brod et al., (1959) the pattern of response was found to be elicited by a simple test in mental arithmetic which the subject was asked to carry out rather rapidly. Kelly and Walter (1968) found the same pattern in patients suffering from a chronic anxiety state, when the muscle blood flow is almost double the normal value. Kelly and Walter (1968) also remarked that a return of muscle blood flow towards normal could be the earliest sign of recovery in these patients.

The efferent pathway for the cardiovascular response

We now know a very great deal about the anatomical location and organisation of the regions of the brain which initiate and integrate the whole pattern of cardiovascular response. This has been worked out chiefly in the cat, but the results of similar neurophysiological experiments suggest that the same parts of the limbic system, hypothalamus and brainstem are involved in all the animal species in which the central nervous organisation of the defence reaction has been studied so far, and the analogous regions in man are probably involved in a similar way. Mild electrical stimulation in the appropriate region of the hypothalamus of human subjects has been reported to produce feelings of restlessness, anxiety, depression, fright and horror, whilst stronger stimulation in the posterior hypothalamus has produced rage reactions (Heath and Mickle, 1960; Sem-Jacobsen and Torkildsen, 1960). Such stimulation also elicits rises in blood pressure. The detailed anatomy of these regions does not concern us today, except for a particular feature of the anatomical organisation of this response, and that is the location of the efferent

pathway from the hypothalamus and brainstem to the spinal cord. Our early work, and that of Lindgren and Uvnäs (1953) had shown this pathway to run in the ventral part of the medulla, while later work by Schramm and Bignall (1971) had indicated that, in the more caudal medulla, it may pass extremely close to its ventral surface. Bearing in mind that the pathway passes so close to the surface, a particularly interesting finding, made a few years ago, was that local applications of pentobarbitone sodium bilaterally onto the ventral surface of the medulla can cause a profound fall of arterial blood pressure (Feldberg and Guertzenstein, 1972). Guertzenstein and Silver (1974) later reported that bilateral applications of glycine to the same restricted region had the same vasodepressor effect, and so had small bilateral electrolytic lesions in the localised area to which glycine had been applied. This evidence leads naturally to the suggestion that nerve cells situated near the ventral surface of the caudal medulla play an essential part in tonically maintaining arterial blood pressure at its normal level.

We have recently shown that the bilateral application of glycine to the sensitive area blocks all the autonomic components of the defence reaction ordinarily seen on stimulation within the appropriate regions of the amygdala, hypothalamus or mid-brain (Guertzenstein et al., 1978). Over 5-10 minutes, as the block deepens the arterial blood pressure falls. The first component of the cardiovascular pattern of arousal response to be abolished is the splanchnic vasoconstriction. Electrical stimulation within the medullary area sensitive to glycine, with microelectrodes and using small stimulating currents, elicits the response characteristic of the defence reaction, which includes a strong vasoconstriction in the splanchnic area and kidney. The response is elicited by stimulation on the surface of the medulla, or only just below it. A map of the points from which the response is obtained shows it to occupy a narrow longitudinal strip which is a few millimeters from the mid-line and extremely superficial within the glycine-sensitive area, 1-2 mm caudal to the trapezoid body. After an extremely small lesion restricted to this superficial section of the strip on one side, glycine applied to the contralateral medullary area produces all the changes that without the lesion are seen only after bilateral application of the amino acid. The lesion necessary to produce this profound effect is extremely small. Moreover, anatomical evidence is now accumulating of connections between the superficial region of the ventral medulla in its caudal one-third, and the intermediolateral cell column of the spinal cord (Amendt et al., 1978; Loewy et al., 1979).

From these results, therefore, the resting level of blood pressure would seem to be largely determined by the ordinary level of activity generated in the brainstem defence areas and relayed in the pathway in the caudal medulla. It can be concluded that the general level of blood pressure in the normal awake animal is also determined, mainly, by that level of activity in these areas which is necessary for the state of arousal leading to the awake condition. It is particularly interesting that these results are fully in accord with those reported so long ago by Dittmar (1873), for they explain the result which he obtained without needing to postulate a vasomotor centre. There is probably a group of relay neurones very near the ventral surface of the medulla that form the final link in the efferent pathway to the various autonomic effectors, because glycine is not known to act elsewhere than at synapses : this will be a fascinating topic

for future study. If the conclusion can be confirmed, this is a most important group of neurones, constituting a functional nucleus in the ventral medulla essential for the normal level of sympathetic activity leading to vasomotor tone.

Comparison with the pattern of cardiovascular change during sleep

It is particularly interesting to recall that during desynchronised sleep in cats, the arterial blood pressure falls to a level similar to that we found in our experiments with glycine (Kumazawa et al., 1969). Mancia et al (1970) have shown that this fall results from vasodilatation in the splanchnic area and the kidney, whereas in the vascular beds of the limbs, which consist mostly of skeletal muscle, there is a concomitant vasoconstriction. This combination of changes is the exact opposite of that seen in the arousal state of the defence reaction, and is just what would be expected if desynchronised sleep entails a suppression of the activity of the defence areas. In the awake state, the defence areas can strongly inhibit the baroreceptor reflex response (Coote et al., 1979). In the sleeping state, therefore, the baroreceptor reflex might be expected to be strongly manifested and there is evidence in human subjects of exaggerated baroreceptor reflex responses during sleep (Smyth et al., 1969).

The genesis of hypertension

By contrast with the situation postulated during sleep, circumstances are conceivable in which the defence areas would become overactive, and these could be relevant to the genesis of hypertension. Brod and his coworkers have long espoused a hypothesis of this kind, ever since they showed that the resistance vessels of skeletal muscle do not participate to the same extent as those elsewhere in the general increase in vascular tone in hypertension (Brod et al., 1962). By emphasising the extensive splanchnic vasoconstriction elicited during arousal I have actually implied that the vascular resistance in the splanchnic area is the main effector mechanism through which the central nervous setting of vasomotor tone is achieved. It is therefore striking that the increase in blood pressure in the early stage of hypertension in spontaneously hypertensive rats has been shown to be due to an increase in vascular tone in the splanchnic area (Iriuchijima, 1973). With this in mind, I cannot help recalling that spontaneously hypertensive rats show exaggerated cardiovascular responses to alerting stimuli (Hallback, 1975). It will be of great interest to follow the further exploration of this idea in man. Moreover, in view of the activation of the arousal pattern by peripheral chemoreceptor stimulation, as shown in our laboratory (and mentioned already), the possible significance of this input as a "non-physiological" stimulus enhancing vasomotor tone will need to be explored.

Conclusion

In conclusion, therefore, the evidence from many different sources points to the important role of the arousal system in setting the general level of arterial blood pressure. The effect of blocking the pathway connecting the brainstem regions which organise the pattern of response characteristic of this system with the pre-ganglionic effector neurones is so profound as to suggest that the arousal system plays a key role in the generation of vasomotor tone in the awake state. Thus, this is not only a visceral

activating system which, when suddenly or strongly engaged, intensifies all the visceral components of the defence response as part of a fully-fledged and coordinated reaction. In addition, I now believe that it shows a moderate, though fluctuating, level of engagement at all times in the waking state, and that this is what mainly determines the general level of arterial blood pressure in daily life. Finally, as the results I have described can explain the findings of early workers such as Dittmar without the necessity of postulating the existence of a separate vasomotor centre, may I end by expressing the hope that, at last, the writers of text-books will recognise the inevitable and quietly forget it.

REFERENCES

Abrahams, V.C., Hilton, S.M. & Zbrozyna, A.W. (1960) Active muscle vasodilatation produced by stimulation of the brainstem : its significance in the defence reaction. J. Physiol., 154, 491-513.

Abrahams, V.C., Hilton, S.M. & Zbrozyna, A.W. (1964) The role of active muscle vasodilatation in the alerting stage of the defence reaction. J. Physiol., 171, 189-202.

Adrian, E.D., Bronk, D.W. & Phillips, G. (1932) Discharges in mammalian sympathetic nerves. J. Physiol. (Lond). 74, 115-133.

Alexander, R.S. (1946) Tonic and reflex functions of medullary sympathetic cardiovascular centres. J. Neurophysiol., 9, 205-217.

Amendt, K., Czachurski, J., Dembowsky, K. & Seller, H. (1978) Neurones within the "chemosensitive area" on the ventral surface of the brainstem which project to the intermediolateral column. Pflügers Arch. 375, 289-292.

Azevedo, A.D., Hilton, S.M. & Timms, R.J. (1980) The defence reaction elicited by midbrain and hypothalamic stimulation in the rabbit. J. Physiol., 301, 56-57P.

Barman, S.M. & Gebber, G.L. (1976) Basis for synchronization of sympathetic and phrenic nerve discharges. Am. J. Physiol., 231, 1601-1607.

Blair, D.A., Glover, W.E., Greenfield, A.D.M. & Roddie, I.C. (1959) Excitation of cholinergic vasodilator nerves to human skeletal muscles during emotional stress. J. Physiol. (Lond). 148, 633-647.

Bolme, P., Ngai, S.H., Uvnäs, B., & Wallenberg, L.R. (1967) Circulation and behavioural effects on electrical stimulation of the sympathetic vasodilator areas in the hypothalamus and the mesencephalon in unanaesthetized dogs. Acta Physiol. Scand. 70, 334-346.

Brod, J., Fencl, V., Hejl, Z. & Jirka, J. (1959) Circulatory changes underlying blood pressure elevation during acute emotional stress (mental arithmetic) in normotensive and hypertensive subjects. Clin. Sci., 18, 269-279.

Brod, J., Fencl, V., Hejl, Z. & Jirka, J. (1962) General and regional haemodynamic pattern underlying essential hypertension. Clin. Sci., 23, 339-349.

Chai, C.Y. & Wang, S.C. (1969) Integration of sympathetic cardiovascular mechanisms in medulla oblongata of the cat. Amer. J. Physiol., 215, 1310-1315.

Chen, M.P., Lim, R.K.S., Wang, S.C. & Yi, C.L. (1936) On question of myelencephalic sympathetic centre; effect of stimulation of pressor area on visceral function. Chin. J. Physiol., 10, 445-473.

Chen, M.P., Lim, R.K.S., Wang, S.C. & Yi, C.L. (1937) On question of myelencephalic sympathetic centre; experimental localization of centre. Chin. J. Physiol., 11, 367-384.

Cohen, M.I. & Gootman, P.M. (1970) Periodicities of efferent discharges of splanchnic nerve of the cat. Am. J. Physiol., 218, 1092-1101.

Cowley, Jr., A.W., Laird, J.F. & Guyton, A.C. (1973) Role of the baroreceptor reflex in daily control of arterial blood pressure and other variables in dogs. Circulat. Res., 32, 564-576.

Coote, J.H., Hilton, S.M. & Perez-Gonzalez, J.F. (1979) Inhibition of the baroreceptor reflex on stimulation in the brainstem defence centre. J. Physiol., 288, 549-560.

Dittmar, C. (1870) Ein neuer Beweis für die Reizbarbeit der centripetalen Fasern des Rückenmarks. Ber. verh. sächs. Ges. der Wiss. Math. Phys. Kl. 22, 18-48.

Dittmar, C. (1873) Über die Lage de sogenannten Gefässcentrums der Medulla Oblongata. Ber. verh. sächs. Ges. der Wiss. Math, Phys. Kl. 25, 449-469.

Feldberg, W. & Guertzenstein, P.G. (1972) A vasodepressor effect of pentobarbitone sodium. J. Physiol., 224, 83-103.

Green, J.H. & Heffron, P.F. (1967) Observations on the origin and genesis of a rapid sympathetic rhythm. Arch. Intern. Pharmacodyn., 169, 403-411.

Guertzenstein, P.G. & Silver, A. (1974) Fall in blood pressure produced from discrete regions of the ventral surface of the medulla by glycine and lesions. J. Physiol., 242, 489-503.

Guertzenstein, P.G., Hilton, S.M., Marshall, J.M. & Timms, R.J. (1978) Experiments on the origin of vasomotor tone. J. Physiol., 275, 78-79P.

Guyton, A.C. (1976) Personal views on mechanisms of hypertension. In : Hypertension. Ed. J. Genest, E., Koiw, O., Kuchel, O., McGraw-Hill, New York. 566.

Hallback, M. (1975) Interaction between central neurogenic mechanisms and changes in cardiovascular design in primary hypertension : Experimental studies in spontaneously hypertensive rats. Acta. Physiol. Scand., Suppl. 424.

Heath, R.G. & Mickle, W.A. (1960) In : Electrical studies on the unanaesthetized brain. (Eds. E.R. Ramey & D.S. O'Doherty(p. 214. Paul B. Hoeber, New York.

Hilton, S.M. (1974) The role of the hypothalamus in the organisation of patterns of cardiovascular response. Int. Symp. Calgary pp. 306-314 (Karger, Basel).

Hilton, S.M. (1975) Ways of viewing the central nervous control of the circulation - old and new. Brain Res. 87, 213-319.

Hilton, S.M. (1979) The defence reaction as a paradigm for cardiovascular control. In : Integrative functions of the autonomic nervous system. (Eds. C. McC. Brooks, K. Koizumi & A. Sato). Tokyo University Press. 443-449.

Hukuhara, T. (1975) Neuronal organisation of central vasomotor mechanisms in the brain stem of the cat. Brain Res. 87, 419-429.

Iruichijima, J. (1973) Sympathetic discharge rate in spontaneously hypertensive rats. Jap. Heart. J., 14, 350-356.

Kelly, D.H.W. & Walter, C.J.S. (1968) The relationship between clinical diagnosis and anxiety, assessed by forearm blood flow and other measurements. Brit. J. Psychiat., 114, 611-626.

Kumada, M., Dampney, R.A.L. & Reis, D.J. (1979) Profound hypotension and abolition of the vasomotor component of the cerebral ischaemic reflex response produced by restricted lesions of medulla oblongata in rabbit. Circulation Res., 44, 63-70.

Kumazawa, T., Baccelli, G., Guazzi, M., Mancia, G. & Zanchetti, A. (1969) Hemodynamic patterns during desynchronised sleep in intact cats and in cats with sinoaortic deafferentation. Circulation Res., 24, 923-937.

Langhorst, P., Schulz, G., Lambertz, M., Stroh-Werz, M., Krienke, B., Keyserlingk, D., Graf von (1980) Is there an influence of discharge patterns of neurones of the "unspecific brain stem system" on neuronal activity in the dorso-medial part of the NTS? In : Koepchen, H.P., Hilton, S.M. & Trzebski, A. (Eds). Central interaction between respiratory and cardiovascular control systems. Springer, Berlin, Heidelberg, New York.

Lim, R.K.S., Wang, S.C. & Yi, C.L. (1938) On question of myelencephalic sympathetic centre; depressor area a sympatho-inhibitory centre. Chin. J. Physiol., 13, 61-77.

Lindgren, P. & Uvnäs, B. (1953) Activation of sympathetic vasodilator and vasoconstrictor neurones by electrical stimulation in the medulla of the cat. Circulation Res., 1, 479-485.

Loewy, A.D. & McKellar, S. (1979) The neuroanatomical basis of central cardiovascular control. (From : American Physiological Society Symposium 'Central Integration of Cardiovascular Control' presented at the 63rd Annual Meeting of the Federation of American Societies for Experimental Biology, Dallas, Texas). pp 2495-2503.

McCall, R.B. & Gebber, G.L. (1975) Brain stem and spinal synchronization of sympathetic nervous discharge. Brain Res., 88, 139-143.

Mancia, G., Baccelli, G., Adams, D.B. & Zanchetti, A. (1971) Vasomotor regulation during sleep in the cat. Amer. J. Physiol., 220, 1085-1093.

Manning, J.W. (1965) Cardiovascular reflexes following lesions in medullary reticular formation. Amer. J. Physiol., 208, 283-288.

Marshall, J.M. (1977) The effect of uptake by adrenergic nerve terminals on the sensitivity of arterial vessels to topically applied noradrenaline. Br. J. Pharmac. 61, 429-432.

Owsjannikow, P. (1871) Die tonischen and reflektorischen Centren der Gefässnerven. Ber. verh. sächs. Ger. der Wiss. Math. Phys. Kl. 23, 135-147.

Ranson, S.W. & Billingsley, P.R. (1916) Vasomotor reactions from stimulation of the floor of the fourth ventricle. Amer. J. Physiol., 41, 85-91.

Ranson, S.W. & Magoun, H.W. (1939) Hypothalamus. Ergebn. Physiol., 41, 56.

Sem-Jacobsen, C.W. & Torkildsen, A. (1960) In : Electrical studies on the unanaesthetized brain. (Eds. E.R. Ramey & D.S. O'Doherty). p. 275. Paul Hoeber, New York.

Scher, A.M. & Young, A.C. (1963) Servoanalysis of carotid sinus reflex effects on peripheral resistance. Circulation Res., 12, 152-162.

Schramm, L.P., Honig, C.R. & Bignall, K.E. (1971) Active muscle vasodilatation in primates homologous with sympathetic vasodilatation in carnivores. Amer. J. Physiol., 22, 768-777.

Smyth, H.S., Sleight, P. & Pickering, G.W. (1969) Reflex regulation of arterial pressure during sleep in man. - A quantitative method of assessing baroreflex sensitivity. Circulation Res., 24, 109-121.

Taylor, D.G. & Gebber, G.L. (1975) Baroreceptor mechanisms controlling sympathetic nervous rhythms of central origin. Am. J. Physiol., 228, 1002-1013.

Timms, R.J. (1976) The use of the anaesthetic steroids alphaxalone - alphadalone in studies of the forebrain in the cat. J. Physiol., 256, 71-72P.

Adv. Physiol. Sci. Vol. 8. Cardiovascular Physiology. Heart, Peripheral Circulation and Methodology
A. G. B. Kovách, E. Monos, G. Rubányi (eds)

A COMPUTER AND EXPERIMENTAL ANALYSIS OF ARTERIAL PRESSURE REGULATION AND HYPERTENSION

Arthur C. Guyton, John E. Hall, David B. Young, Thomas E. Lohmeier, Thomas E. Jackson and Philip R. Kastner

Department of Physiology and Biophysics, University of Mississippi Medical Center, Jackson, Mississippi, USA

The goal of this paper is to examine some of the important arterial pressure control mechanisms and also to develop an overall concept of long-term arterial pressure regulation. In addition, we will discuss some of the basic mechanisms of hypertension.

Arterial pressure is not controlled by a single mechanism but instead by several, each of which plays its specific role. Figure 1 illustrates the degree of response of eight of the more important pressure control mechanisms following a sudden change in arterial pressure caused by some acute effect such as rapid hemorrhage. Each of the mechanisms immediately attempts to return the pressure back toward the normal level, and Figure 1

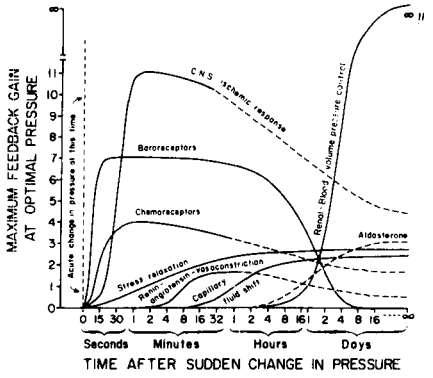

Figure 1. Degree of activation, expressed in terms of feedback gain, of different pressure control mechanisms following a sudden change in arterial pressure. (From Guyton: Arterial Pressure and Hypertension, p. 7. W. B. Saunders Co., Philadelphia, 1980.)

illustrates the responses expressed in terms of feedback gain. These mechanisms are the following:

First, three different nervous reflexes begin within seconds to cause reflex return of the pressure back toward normal. These include the

baroreceptor system, the chemoreceptor system (which is stimulated by poor delivery of oxygen and poor removal of carbon dioxide from the peripheral chemoreceptors), and the central nervous system ischemic response (which is stimulated when the pressure falls so low that the medulla becomes ischemic).

Second, another group of mechanisms begins to function within minutes. These include stress relaxation or reverse stress relaxation of the circulation, the renin-angiotensin-vasoconstrictor system, and the capillary fluid shift mechanism which causes fluid to shift either into or out of the capillaries to readjust pressure back toward normal.

Finally, the figure also illustrates two other control mechanisms that function very little at first but begin to function within hours and continue to function thereafter. One of these is the aldosterone mechanism and the other is the renal-blood volume pressure control mechanism. Note especially that this latter mechanism is shown to have a feedback gain of infinity at infinite time. We shall say more about this later.

It will not be possible to discuss all of these pressure control mechanisms in this short paper. Instead, we will consider several representative mechanisms of pressure control, especially the baroreceptor mechanism for acute pressure control and the renal-blood volume pressure control mechanism for long-term pressure control.

ROLE OF THE BARORECEPTOR MECHANISM FOR ACUTE CONTROL OF ARTERIAL PRESSURE

Though many investigators have suggested that the baroreceptor mechanism might be important for long-term control of arterial pressure, recent experiments have not substantiated this hypothesis. The reason for this is that the baroreceptors reset to new pressure levels whenever the pressure remains elevated or depressed for long periods of time. Nevertheless, the baroreceptors do respond very forcefully for the first few hours following a sudden change in pressure, and during that time they play a very important role in pressure control.

Figure 2 illustrates a study by Cowley and his colleagues [1] showing two two-hour periods of pressure recording, first, in a normal dog and, second, in a dog that had had its baroreceptors denervated several weeks previously. Note the difference in the degree of stability of the pressure. In the denervated dog, the pressure rose or fell when the dog stood up or sat down, when it became excited, when it defecated, when it ate food, or when any other abnormality of the surroundings stimulated the dog's psyche. However, note also that the averages of the arterial pressures of both the normal and the denervated dogs were approximately the same. Figure 3 illustrates this even more fully. This figure shows histograms of the mean arterial pressures recorded for 24-hour periods. Note again that the central points of the normal and of the denervated pressures correspond almost exactly. In studies on more than 60 dogs, Cowley has now shown that these two mean pressure levels are within 1 mm Hg of each other, whether the dog be denervated or normal.

Therefore, it seems clear that the baroreceptor system functions as an extremely important arterial pressure damping mechanism to prevent rapid changes in arterial pressure but not to prevent long-term changes. Indeed, it is exceedingly important that the baroreceptor system has the capability of resetting its control pressure level to high or low pressures because this allows the damping mechanism to function effectively at all

pressure levels, whether the person has normal pressure or various degrees of hypertension.

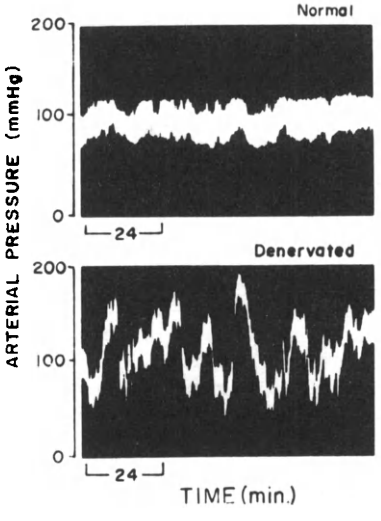

Figure 2. Extreme lability of the arterial blood pressure in a baroreceptor-denervated dog (bottom) contrasted with the arterial pressure in a normal dog (top). [Reprinted from Cowley et al., Circ. Res. 32:564, 1973, with permission from the American Heart Association, Inc.]

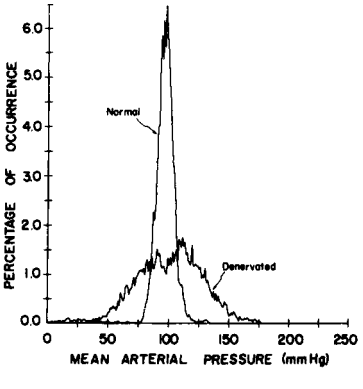

Figure 3. Histogram showing the percentage of each day that each pressure level was recorded in a normal dog and in a baroreceptor-denervated dog. These curves were constructed automatically by the computer from 24 hour pressure recordings in the two respective animals. Note that the 24 hour mean arterial pressure is almost the same in the denervated animal as in the normal animal. [Reprinted from Cowley et al., Circ. Res. 32:564, 1973, with permission from the American Heart Association, Inc.]

Figure 1 showed the renal-blood volume mechanism of pressure control to become progressively more powerful in its pressure controlling capability over long periods of time. Therefore, one would expect this mechanism to play an especially important role in long-term pressure abnormalities, such as hypertension.

The renal-blood volume mechanism of pressure control is based on the pressure diuresis and pressure natriuresis phenomena. That is, when the arterial pressure rises above normal, the kidney output of both water and salt increases tremendously. This causes the body fluid volumes to decrease and in turn reduces the pressure back to normal.

One of the important features of the renal-blood volume mechanism is that it does not cease to function until the pressure returns all the way to normal [2]. To state this another way, this mechanism has infinite capability for returning the pressure back to the normal level. For this reason, this mechanism has been said to have infinite gain.

Figure 4 illustrates an experimental demonstration of the renal pressure diuresis and pressure natriuresis mechanism for returning the pressure back to normal [3]. In this experiment a series of dogs were transfused in a period of 4 minutes with an amount of blood equal to 30 per cent of the original blood volume. The heads of the dogs had been removed to eliminate the nervous system. Note the instantaneous effects

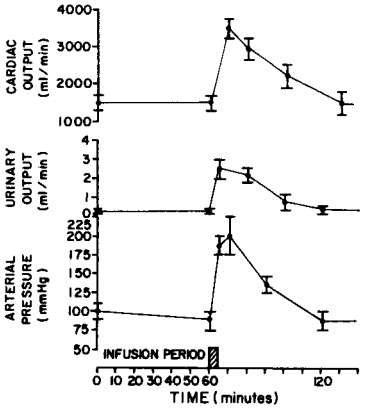

Figure 4. Function of the kidney-blood volume feedback mechanism to return the arterial pressure back to normal following transfusion of blood into dogs without nervous reflexes. [Modified from Dobbs et al., Am. J. Cardiol. 27:507, 1971.]

of the increased volume on both cardiac output and arterial pressure. In fact, the average increase in arterial pressure was greater than 100 per cent. Note also the tremendous increase in urinary output, an average increase of 12-fold. This increase continued as long as the arterial pressure remained above normal, but as the arterial pressure returned to normal, so also did the urinary output return to normal. In other words, as long as the arterial pressure was too high, pressure diuresis and pres-

sure natriuresis continued, until the pressure returned to normal.

The results of Figure 4 cannot be demonstrated with ease in a normal animal because the baroreceptor mechanism and other nervous feedback control mechanisms prevent the immediate effect of increased volume to increase the arterial pressure. This is illustrated in Figure 5 which presents results of the same experiment but in normal dogs, with the head intact. Almost identically the same increase in cardiac output occurred,

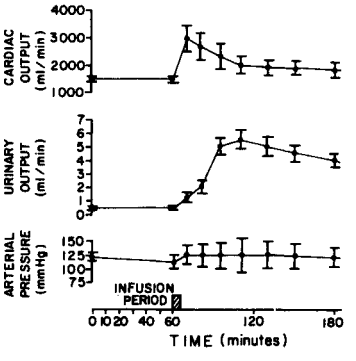

Figure 5. Same experiment as in Figure 4, except that the animals had normal nervous reflexes. Note that the nervous reflexes prevented significant rise in arterial pressure and obscured the kidney-blood volume-pressure feedback mechanism for control of arterial pressure [Modified from Dobbs et al., Am. J. Cardiol. 27:507, 1971.]

but the arterial pressure rose only 1/8th as much as it did in the dogs without nervous reflexes of Figure 4. Even so, the urinary output still increased 12-fold. But at the end of two hours the arterial pressure still had not returned all the way back to the normal level. In other words, when the nervous mechanisms are functioning normally, they prevent rapid changes in pressure, but they do not prevent the background effect of the blood volume pressure control mechanism. They merely delay these effects rather than preventing them.

Volume-Loading Hypertension

If the renal-blood volume mechanism for pressure control is the most important one for long-term control of pressure, then one would expect that abnormalities of this system could lead to hypertension. Figure 6 illustrates an experiment to demonstrate this [4]. In this series of dogs, the two poles of one kidney were removed at Point A in the diagram. Then two weeks later the entire opposite kidney was removed at Point B. For another period of two weeks, between the 38th day and the 54th day, control pressures were measured. This was followed by a two-week period of forcing the dogs to drink 0.9 per cent sodium chloride solution instead of water. Then another period of drinking pure water ensued, followed once more by drinking 0.9 per cent sodium chloride. Note the very rapid increase in arterial pressure that occurred during the periods of saline drinking. In general, the dogs drank 3 to 5 times

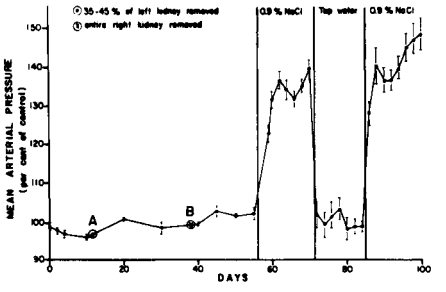

Figure 6. Volume-loading hypertension recorded in four dogs. The two poles of the left kidney were first removed, and later the entire right kidney was removed. After two weeks of recovery from all surgery, the dogs were made to drink 0.9 per cent sodium chloride instead of tap water for a period of two weeks, followed by tap water for another two weeks, and finally by saline solution again for three weeks. [Reproduced from Langston et al.: Circ.Res. 12:508, 1963, with permission of the American Heart Association, Inc.]

as much of the saline solution as they did of normal water, and they showed evident signs of fluid retention, including development of transient edema during the first few days of the saline drinking.

The experiment of Figure 6 proved to be such an excellent means for creating volume-loading hypertension that over a period of years we have now studied this hypertension in much greater detail [5,6]. Figure 7 illustrates a composite diagram showing the transient changes in extracellular fluid volume, blood volume, mean circulatory filling pressure, pressure gradient for venous return, cardiac output, total peripheral resistance, and arterial pressure during the period of saline loading. In these more precise experiments, the saline was infused at 5 to 7 times the normal rate of salt intake, instead of simply allowing the animal to drink the saline at will.

Note in Figure 7 that the values in all 5 of the top curves increased markedly during the first few days of saline-loading, but then they returned almost all the way back to the control level by the end of 16 days. All of the factors represented by these 5 curves are normally associated with increased body fluid volumes -- extracellular fluid volume, blood volume, mean circulatory filling pressure, pressure gradient for venous return, and cardiac output.

However, note also in Figure 7 that the total peripheral resistance decreased for the first few days of salt-loading and then secondarily increased to a very high level by the 16th day.

Finally, note that the arterial pressure began to rise on the first day but not nearly so rapidly as did the cardiac output. The reason for

this is that the decrease in total peripheral resistance actually opposed part of the early rise in arterial pressure. However, by the 4th day the total peripheral resistance was no longer decreased and then began to rise above normal. A careful study of the figure will show that the arterial pressure did not rise quite as rapidly as did the cardiac output but rose much more rapidly than the total peripheral resistance. In other words, the cardiac output changes "led" the arterial pressure changes, and the arterial pressure changes "led" the total peripheral resistance changes. These time relationships of the changes are very important because they illustrate that the primary cause of this type of hypertension was not a primary increase in total peripheral resistance.

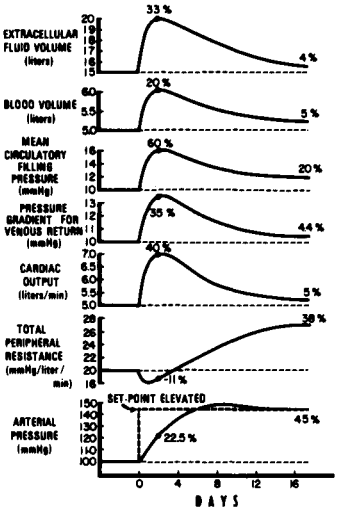

Figure 7. Progressive changes in the important variables that make up the kidney-blood volume feedback system following a sudden increase in the "set-point" of the system from 100 mm Hg to 145 mm Hg. Note especially the hyperdynamic state of the volume and cardiac output changes during the first few days but a decrease in total peripheral resistance. Then note the return of the volume and cardiac output factors almost to normal along with a very marked increase in total peripheral resistance in the chronic state. [Based on quantitative measurements made by Langston, Douglas, Coleman, and Manning.] (From Guyton: Arterial Pressure and Hypertension, p. 150. W.B. Saunders Co., Philadelphia, 1980.)

Role of Autoregulation in Volume-Loading Hypertension

There has been much discussion in recent years of the role of "autoregulation" in the development of hypertension. This can be explained: Beginning in the early 1960's a number of different research workers in the hypertension field attempted to answer the following question: When it is impossible to find an obvious vasoconstrictor substance in the circulating blood of hypertensive patients, and yet the total peripheral resistance is greatly increased, what is the cause of this increased resistance? Many research workers still have faith that eventually a vasoconstrictor substance will be found, but thus far, no increase in vasoconstrictor substances has been found in most patients with essential hypertension. In fact, two-thirds of such patients have either normal or low renins, indicating that renin almost certainly is not a significant factor in most patients with essential hypertension.

On the other hand, we noted in Figure 7 that volume-loading hypertension during the first few days of the hypertension is caused by greatly

increased cardiac output. Yet, within a week or two the cardiac output returns to normal and the total peripheral resistance becomes greatly elevated. Thus, in the final stage of this type of hypertension the total peripheral resistance is greatly elevated, the same as occurs in most patients with essential hypertension. Yet, because of the way that the experiment is performed, we know that the cause of hypertension is excess salt- and water-loading. Furthermore, cessation of the salt and water loading causes the pressure to return to normal in approximately two days. Therefore, after several weeks, volume-loading hypertension has essentially the same characteristics as essential hypertension, that is normal cardiac output but high resistance. Furthermore, the fluid volumes are also essentially normal, despite the fact that the hypertension itself is caused by excess fluid and salt-loading.

The only plausible explanation that has thus far been forthcoming to explain the shift of volume-loading hypertension from high cardiac output hypertension to high total peripheral resistance hypertension has been the autoregulation theory [5,6,7]. This theory holds that whenever the blood flow through the body's tissues is too great, an automatic response occurs in the blood vessels to cause constriction. This returns the blood flow back toward normal but at the same time also increases the resistance. Such a mechanism as this has been demonstrated many times in individual body tissues and also in the whole animal body. Yet, most of these studies have been performed as acute experiments lasting for only a few minutes to a few hours; and the degree of autoregulation that occurs during these short periods of time is not very great. On the other hand, there are many indications that the degree of autoregulation becomes progressively greater over a period of days, weeks, and months. The most outstanding evidence is the fact that the blood flow in the upper part of the body and also the blood flow in the lower part of the body of patients with coarctation of the aorta are as nearly normal as can be measured despite the fact that the arterial pressure in the upper body is very high and the pressure in the lower body is low [8]. This indicates that a long-term mechanism of blood flow autoregulation returns the blood flow of the tissues essentially to normal regardless of the pressure. Therefore, when the arterial pressure becomes too high and causes the tissue blood flow to increase, the autoregulation mechanism returns the tissue flow, and the cardiac output, back to normal.

Thus, the autoregulation theory suggests that in the volume-loading type of hypertension total peripheral resistance is determined by the arterial pressure rather than arterial pressure being determined by the total peripheral resistance.

However, it should be noted that autoregulation is not required for the renal-body fluid mechanism to cause hypertension. It is only required to convert the volume-loading type of hypertension from its initial high cardiac output character to a high total peripheral resistance character. In other words, the autoregulation mechanism is a blood flow regulator, not a blood pressure regulator.

ROLE OF VASOCONSTRICTOR SUBSTANCES IN ARTERIAL PRESSURE CONTROL -- VASOCONSTRICTOR HYPERTENSION

Since the time when Goldblatt [9] showed that renal artery constriction, whether applied to one kidney or to both kidneys, will cause hypertension, most investigators in the field of high blood pressure research have been possessed with the idea that the basic cause of hypertension is some circulating vasoconstrictor substance. This concept was

propelled forward by the early studies of Page and his co-workers [10] and Braun-Menendez and his co-workers [11], both of whom discovered and characterized angiotensin. Also, it is well-known that other vasoconstrictors when infused into an animal, can cause acute hypertension. Yet, a remaining difficulty with the idea that a vasoconstrictor agent in the cause of chronic essential hypertension is that it has not been possible to demonstrate excess vasoconstrictor substances in most patients with essential hypertension.

Nevertheless, in special circumstances long-term hypertension can occur. It especially occurs in patients who have tumors that secrete excess amounts of renin [12] or catecholamines [13]. Furthermore, in most of these patients, the hypertension is cured when the tumors are removed.

Figure 8 illustrates composite studies of vasoconstrictor hypertension based on work by Young [14] and Cowley [15], both of whom caused vasoconstrictor hypertension by infusing angiotensin II continuously into dogs for several days or several weeks at rates equal to 3 to 15 times

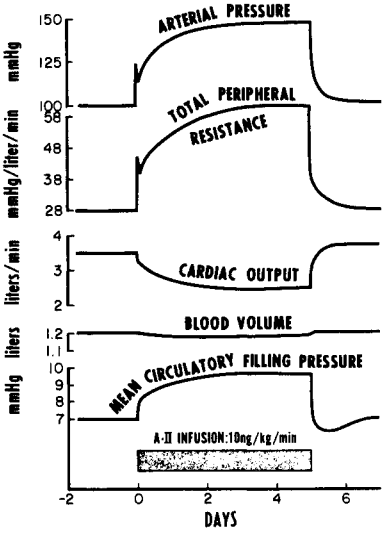

Figure 8. Vasoconstrictor hypertension caused in dogs by infusion of angiotensin II. This figure is a composite of results obtained by Young and Cowley working in our laboratory. (From Guyton: Arterial Pressure and Hypertension, p. 399. W. B. Saunders Co., Philadelphia, 1980.)

the normal rate of angiotensin II formation. The composite curve of Figure 8 is for angiotensin II rates of infusion approximately 6 times the normal rate of formation. Note the instantaneous rise in total peripheral resistance and moderate increase in arterial pressure. But note also that the cardiac output fell rather than rising. Furthermore, the total peripheral resistance and arterial pressure continued to increase during the next few days. On the other hand, the blood volume hardly changed even though the mean circulatory filling pressure did increase.

It is immediately clear that many of the hemodynamic changes in vasoconstrictor hypertension are quite different from the changes that occur in volume-loading hypertension. Most notably, the total peripheral resistance rises at the outset of this type of hypertension while the cardiac output falls. These are exactly opposite to the effects that occur in volume-loading hypertension.

One's initial impulse is to state that the cause of the chronic hypertension in vasoconstrictor hypertension is the increased total peripheral resistance caused by direct constriction of the peripheral blood vessels. However, later in this paper we shall see that, though the initial elevation of pressure is undoubtedly caused by the immediate increase in total peripheral resistance, the chronic phase of the hypertension most likely is caused by a renal vasoconstrictor effect.

Role of Autoregulation in Vasoconstrictor Hypertension

Since autoregulation is a blood flow regulator and not a pressure regulator, one would expect that peripheral vasoconstriction caused by a vasoconstrictor agent would be opposed by the autoregulation mechanism. This has been demonstrated many times in isolated tissues. For instance, eithe sympathetic stimulation of the gut or infusion of norepinephrine causes immediate vasoconstriction, but within minutes the blood flow to the gut "escapes." This is known as "autoregulatory escape" because the autoregulatory mechanism overcomes the effect of the vasoconstrictor stimulus.

Therefore, it is logical to assume that the autoregulation phenomenon plays a role in vasoconstrictor hypertension that is exactly opposite to its role in volume-loading hypertension. In volume-loading, the problem is excess cardiac output. Therefore, autoregulation reduces the cardiac output toward normal while increasing the total peripheral resistance. In vasoconstrictor hypertension, the problem is excess resistance and too little flow to the tissues. Therefore, autoregulation theoretically should increase the cardiac output while decreasing the total peripheral resistance. There is much reason to believe that this does indeed occur in vasoconstrictor hypertension, because vast amounts of vasoconstrictor agents are secreted by catecholamine or renin secreting tumors, and yet the tissues do not suffer irreparable ischemic damage. Infusion of similar amounts of vasoconstrictor substances acutely can reduce tissue blood flow to levels that would be incompatable with life if the autoregulation mechanism (or some other mechanism) did not protect the tissues.

Effect of Primary Changes in Total Peripheral Resistance on Arterial Pressure

Let us return for a moment to the following question: Is the high total peripheral resistance that occurs in essential hypertension the cause of the hypertension or the result of the hypertension? One way to study this question is to analyze all those conditions in the circulation which are known to cause primary changes in total peripheral resistance and see what happens to the arterial pressure in these same conditions.

Figure 9 illustrates a graph based on data from the literature showing the effect of different levels of total peripheral resistance on arterial pressure and cardiac output in nine different circulatory states [16]. The abnormal total peripheral resistances, both high and low, in this figure were all caused by primary changes in the peripheral vasculature itself. Note from the figure that it is cardiac output that changes and not arterial pressure!

Therefore, one must immediately question the idea that an increase in total peripheral resistance will necessarily cause hypertension. To take a simple example from Figure 9, in beriberi the peripheral blood

vessels dilate markedly. Unless the patient develops chronic congestive heart failure, the blood pressure does not decrease. Instead, the cardiac output becomes greatly elevated, which is well-known in patients with beriberi. Then when the patient is treated for the beriberi, the total peripheral resistance actually increases about 100 per cent. Yet, after an appropriate period of adjustment, the arterial pressure is still at the normal level. Instead, the cardiac output has been reduced from 100 per cent above normal back to normal.

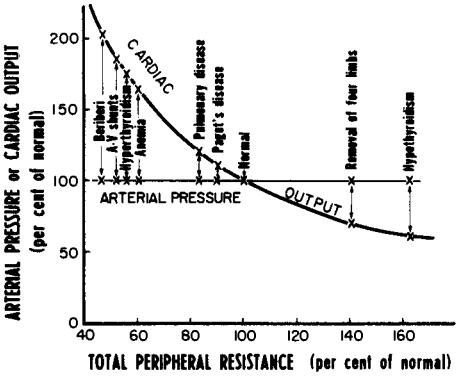

Figure 9. Effect of primary changes in total peripheral resistance on arterial pressure and on cardiac output. Eight different clinical conditions are represented, along with their effects on total peripheral resistance as well as on both arterial pressure and cardiac output. Note that there is no relationship between total peripheral resistance and arterial pressure, but an exact reciprocal relationship between total peripheral resistance and cardiac output. (From Guyton: Arterial Pressure and Hypertension, p. 362. W.B. Saunders Co., Philadelphia, 1980.)

Therefore, it seems clear that long-term primary changes in total peripheral resistance control cardiac output, not arterial pressure. One can easily understand this if he remembers that the renal-blood volume mechanism for pressure control has infinite gain for pressure control. That is, whatever the total peripheral resistance, whether low or high, if the arterial pressure is above normal then the kidney will excrete excess amounts of water and salt until the pressure returns to the normal level. On the other hand, if the pressure is below normal, whatever the total peripheral resistance, the kidneys will retain water and salt until the pressure again returns to normal.

MATHEMATICAL ANALYSIS OF ARTERIAL PRESSURE CONTROL

Along with our studies of experimental hypertension, we have also conducted simultaneous mathematical analysis of pressure control using the systems analysis approach. It will not be possible to present the

details of these analyses in the present paper because of limited space. However, they have been published in a number of different papers or books during the past 15 years [2, 16-19].

The basic essential of these analyses has been to develop mathematical equations for the different circulatory mechanisms and then to solve these as simultaneous equations using a digital computer. Some of the earlier mathematical models had as few as a dozen equations. However, the models that we have used lately have approximately 500 equations.

The importance of mathematical analyses is that one can discover new concepts that are not immediately apparent from usual logical thinking. One of the concepts that we discovered using the systems analysis approach was the so-called "infinite gain principle" of the renal-blood volume mechanism for pressure control. Using computer analysis it was possible to show that as long as the renal-blood volume mechanism is not disturbed in its function, the arterial pressure will always return exactly back to its original level regardless of what happens to the other pressure control mechanisms. For instance, the baroreceptor mechanism can return the arterial pressure only part of the way back to the normal level. Therefore, this pressure control system is said to be a proportional control system. And, whenever it competes with the renal-blood volume mechanism for pressure control, this renal mechanism completely overrides the baroreceptor mechanism in controlling the pressure. These principles are not easy to see without a deeper understanding of the systems analysis approach to blood pressure control. Therefore, the reader is referred to our previous reviews on this subject [2, 16-19].

Examples of Counter-Intuitive Concepts Derived From Computer Simulation

Figure 10 illustrates a computer simulation of arterial pressure control over a period of several weeks while various parameters of circulatory function were altered tremendously. Yet, in this simulation, the renal-blood volume mechanism for pressure control was not altered at all. The following sequence of hemodynamic changes was studied:

(1) An arteriovenous fistula was opened for two days and then closed.

(2) Two days later the total peripheral resistance (but not including the renal resistance) was increased 50 per cent for two days and then increased to 100 per cent for another two days. Then the total peripheral resistance was returned entirely to normal.

(3) After several days of recovery, the total vascular capacity of the circulatory system was decreased to one-half normal for two days and then returned back to normal.

(4) After another two days of recovery, the strength of the heart was increased 500 per cent.

Note that immediately after each one of these changes, either when it was begun or when it was stopped, the arterial pressure became abnormal. However, in two to three days the arterial pressure always returned exactly back to the normal level. On the other hand, the cardiac output and the blood volume were both adjusted to whatever levels were required to return the pressure to normal. Note also that immediately after each change in pressure there was either loss of fluid through the kidneys when the pressure rose or retention of fluid when the pressure fell. It was these changes in fluid output by the kidneys that caused the blood volumes and cardiac outputs to change, and it was through the changes in blood volume and cardiac output that the arterial pressure returned to normal.

Thus, mathematical analyses, as well as experimental studies, have demonstrated several non-causes of long-term blood pressure changes. These are (1) primary changes in total peripheral resistance, (2) primary changes in vascular capacitance, and (3) primary changes in heart strength.

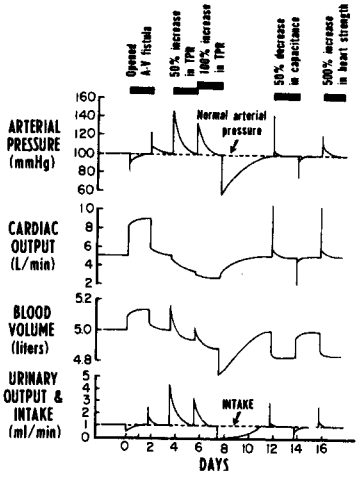

Figure 10. Computer simulation of changes in urinary output, blood volume, cardiac output, and arterial pressure under several different conditions as explained in the text. (From Guyton: Arterial Pressure and Hypertension, p. 315. W. B. Saunders Co., Philadelphia, 1980.)

Yet, it is common knowledge that changes in total peripheral resistance, vascular capacitance, and heart strength are often associated with changes in arterial pressure. How is this possible? The answer is quite simple. Many factors that change total peripheral resistance, vascular capacitance, or heart strength also alter the function of the renal-blood volume mechanism for pressure control at the same time. This does not necessarily mean a cause-effect relationship. For instance, let us return to the vasoconstrictor hypertension illustrated in Figure 8. In this case the initial rise in arterial pressure was almost certainly caused by initial vasoconstriction throughout the body, that is by increased total peripheral resistance. But, if the renal-blood volume mechanism for pressure control was still operating normally, why did the arterial pressure not return exactly to the normal level in the same way that this occurred in all the examples of Figure 10? The answer to this is that angiotensin also alters the renal-blood volume mechanism for pressure control. It increases the level of arterial pressure required to cause pressure diuresis and pressure natriuresis. A large number of studies have been completed in the past few years demonstrating this fact -- that angiotensin has both indirect and direct effects on the kidneys to cause salt and water retention [20-22]. Therefore, increased arterial pressure is required to cause even normal excretion of water and salt. And, in the vasoconstrictor hypertension in Figure 8, it is not the increase in total peripheral resistance that is responsible for the chronic phase of the hypertension. Instead the effect of the angiotensin on the kidneys to increase the functional pressure level of the kidneys is the necessary step for chronic maintenance of the elevated pressure.

SUMMARY

In this paper we have discussed some of the major arterial pressure control mechanisms. Especially, it has been pointed out that the hemodynamic changes in volume-loading hypertension and in vasoconstrictor hypertension are often exactly opposite to each other. But most importantly, the infinite gain principle of the renal-blood volume mechanism for pressure control has been discussed. This infinite gain characteristic makes this control system the final long-term determiner of the arterial pressure level, whether the hypertension be the volume-loading type or the vasoconstrictor type. Furthermore, any factor that causes chronic hypertension must of necessity increase the pressure controlling level of the renal-blood volume pressure control system.

REFERENCES

1. Cowley, A.W., Jr., J.F. Liard, and A.C. Guyton (1973). Role of the baroreceptor reflex in daily control of arterial blood pressure and other variables in dogs. Circ. Res. 32:564.

2. Guyton, A.C., T.G. Coleman, A.W. Cowley, Jr., R.D. Manning, Jr., R.A. Norman, Jr., and J.D. Ferguson (1974). A systems analysis approach to understanding long-range arterial blood pressure control and hypertension. Circ. Res. 35:159.

3. Dobbs, W.A., Jr., J.W. Prather, and A.C. Guyton (1971). Relative importance of nervous control of cardiac output and arterial pressure. Am. J. Cardiol. 27:507.

4. Langston, J.B., A.C. Guyton, B.H. Douglas, and P.E. Dorsett (1963). Effect of changes in salt intake on arterial pressure and renal function in nephrectomized dogs. Circ. Res. 12:508.

5. Coleman, T.G., and A.C. Guyton (1969). Hypertension caused by salt loading in the dog. III. Onset transients of cardiac output and other circulatory variables. Circ. Res. 25:152.

6. Manning, R.D., Jr., T.G. Coleman, A.C. Guyton, R.A. Norman, Jr., and R.E. McCaa (1979). Essential role of mean circulatory filling pressure in salt-induced hypertension. Am. J. Physiol. 236:R40.

7. Ledingham, J.M., and R.D. Cohen (1964). Changes in the extracellular fluid volume and cardiac output during the development of experimental renal hypertension. Can. Med. Assoc. J. 90:292.

8. Wakim, K.G., O. Slaughter, and O.T. Clagett (1948). Studies on the blood flow in the extremities in cases of coarctation of the aorta: determination before and after excision of the coarctate region. Proc. Mayo Clin. 23:347.

9. Goldblatt, H., J. Lynch, R.F. Hanzal, and W. Summerville (1934). Studies on experimental hypertension. I. The production of persistent elevation of systolic blood pressure by means of renal ischemia. J. Exp. Med. 59:347.

10. Page, I.H. (1939). On the nature of the pressor action of renin. J. Exp. Med. 70:521.

11. Braun-Menendez, E., J.C. Fasciolo, L.F. Leloir, and J.M. Muñoz (1939). La sustancia hipertensora de la sangre del riñón isquemiado. Rev. Soc. Argent. Biol. 15:420.

12. Brown, J.J., A.F. Lever, J.I.S. Robertson, R. Fraser, J.J. Morton, M. Tree, P.R.F. Bell, J.K. Davidson, and I.S. Ruthven (1973). Hypertension and secondary hyperaldosteronism associated with a renin-secreting renal juxtaglomerular-cell tumour. Lancet 2:1228.

13. Manger, W.M., and R.W. Gifford, Jr. (1977). Pheochromocytoma. Springer-Verlag, New York.

14. Young, D.B., R.H. Murray, R.G. Bengis, and A.C. Guyton (1977). Increased mean circulatory filling pressure (MCFP) in angiotensin hypertension. Fed. Proc. 36:531.

15. Cowley, A.W., Jr., and J.W. DeClue (1976). Quantification of baroreceptor influence on arterial pressure changes seen in primary angiotensin-induced hypertension in dogs. Circ. Res. 39:779.

16. Guyton, A.C. (1980). Arterial Pressure and Hypertension. W.B. Saunders Co., Philadelphia, p. 362.

17. Guyton, A.C. and T.G. Coleman (1967). Long-term regulation of the circulation: interrelationships with body fluid volumes. In Physical Bases of Circulatory Transport Regulation and Exchange. W. B. Saunders Co., Philadelphia, p. 179.

18. Guyton, A.C. and T.G. Coleman (1969). Quantitative analysis of the pathophysiology of hypertension. Circ. Res. 24(Suppl. 1): I-1.

19. Guyton, A.C., T.G. Coleman, and H.J. Granger (1972). Circulation: Overall regulation. Ann. Rev. Physiol. 34:13.

20. Fagard, R.H., A.W. Cowley, Jr., L.G. Navar, H.G. Langford, and A.C. Guyton (1976). Renal responses to slight elevations in renal arterial plasma angiotensin II concentration in dogs. Clin. Exp. Pharmacol. Physiol. 3:19.

21. Hall, J.E., A.C. Guyton, N.C. Trippodo, T.E. Lohmeier, R.E. McCaa, and A.W. Cowley, Jr. (1977). Intrarenal control of electrolyte excretion by angiotensin II. Am. J. Physiol. 232: F174.

22. Lohmeier, T.E., A.W. Cowley, Jr., N.C. Trippodo, J.E. Hall, and A.C. Guyton (1977). Effects of endogenous angiotensin II on renal sodium excretion and renal hemodynamics. Am. J. Physiol. 233:F388.

Adv. Physiol. Sci. Vol. 8. Cardiovascular Physiology. Heart, Peripheral Circulation and Methodology
A. G. B. Kovách, E. Monos, G. Rubányi (eds)

MECHANISMS OF CAPILLARY RECRUITMENT: RELATION TO FLOW, TISSUE PO_2 AND MOTOR UNIT CONTROL OF SKELETAL MUSCLE

Carl R. Honig and Thomas E. J. Gayeski

Department of Physiology and Department of Anesthesiology, University of Rochester, School of Medicine and Dentistry, Rochester, New York 14642, USA

INTRODUCTION

We seek answers to the following questions: 1) What are the functions of capillary recruitment? 2) What are the sites and mechanisms of capillary control? 3) Can flow and capillary density (C.D.) vary independently? 4) How is vasomotor control coupled to the motor unit organization of skeletal muscle? Our approach is to observe recruitment and derecruitment in a 3-dimensional, red, postural muscle, and relate the data to blood flow, $\dot{V}O_2$, and O_2 saturation of myoglobin.

METHODS

All experiments are performed on dog gracilis, which contains about 0.5 mM myoglobin (Mb). Muscles are vascularly isolated, taking care to preserve all vessels. Venous outflow either recirculates, or is diverted for measurement of flow and blood composition. Phasic twitch contraction is induced by stimulating the cut obturator nerve with supramaximal pulses too brief to excite autonomic fibers. Muscles are frozen in situ with a copper heat sink, cooled to -196°C in liquid nitrogen and applied at 0.1 Kg/cm^2 with an air-driven piston. A switch turns off the stimulator 10 ms before contact. Freezing rate is on the order of 10 μ/ms. Freezing "stops the clock", so we can make as many measurements as we like and consider all to have been made simultaneously, at the instant the muscle was frozen. In this way spatial and temporal heterogeneities can be dissociated. Though events at different times or work rates must be studied on different muscles, the intermuscle component of variability is small for both C.D. and Mb saturation relative to the changes of interest. Flow, blood gases, $\dot{V}O_2$, and rate of lactate production are co-variates.

Blocks 1 x 0.5 x 0.3 cm are cut under liquid nitrogen and examined in cross-section by reflection microscopy at 250X. Cell outlines and microvessels can be visualized without fixation or staining. The cold stage is regulated at -110°C

for spectroscopy. At that temperature, Mb and hemoglobin (Hb) spectra are stable for 3 hrs. Mb saturation is calculated from isosbestic points at 588, 568 and 547 nm, and non-isosbestic points at 560 and 578 nm. Spatial resolution of 5-10 μ permits unequivocal separation of Mb and Hb; measurement error is <5%. The system and its operation are as described in (5), except that the output of the photomultiplier is now fed directly into a computer, and the wavelength drive is under computer control.

The number of capillaries around each fiber is recorded as a co-variate for Mb saturation. Our principal analysis of C.D., however, is based on much larger samples (generally more than 1000 capillaries) collected on a separate aliquot of each muscle. The sample is treated as for spectroscopy except that the cold stage is operated at -70°C. An objective sampling protocol is essential. To this end, the observer positions a 90 x 200 μ grid at a muscle edge, at least 400 μ from the surface which had been in contact with the heat sink. Only capillaries which contain erythrocytes can be seen. These are considered perfused. All such capillaries in a 50 μ optical section are counted at the microscope. Error due to stationary cells and plasma gaps between cells is <5% under conditions of the experiments. After counting the grid is moved to the next of 15 contiguous fields. Six blocks (90 fields) are examined per muscle. Technical details are described in (13).

We require a quantitative measure of the heterogeneity of C.D. from field to field. If C.D. depends solely on random factors operating at each individual capillary, local C.D. should be Poisson distributed. Random factors include the size distribution of red cells, presence of granulocytes, red cell velocities, arteriolar hematocrit, pre and post capillary pressure gradients, vessel geometry, etc. (4). If a control process such as active vasomotion coordinates flow in several capillaries, there will be additional variance, over and above the Poisson, due to the existence of a deterministic process. To model both variance components we use the negative binomial distribution parameterized to include the Poisson as a null case. The variance of the negative binomial is:

$$\sigma = \mu (1 + \delta) \qquad (1)$$

δ=0 if the distribution is Poisson (random), and increases as the distribution becomes influenced by deterministic processes. The fit to the negative binomial is excellent in all muscles, as judged by the Pearson chi-square goodness of fit statistic.

RESULTS AND DISCUSSION

Conditions at rest

Mean capillary density in 15 resting muscles was 550/mm^2. The distribution of capillaries/field was never Poisson. The sample estimate of δ ($\hat{\delta}$) was always significantly greater than 0 ($p<.01-.001$); its mean value was 61. This was due to the existence of many more regions of sparse capillarity than predicted if local C.D. were random. Indeed, some fields were devoid of any perfused capillaries. The existence of poorly perfused or unperfused loci is the principal characteristic of vascular supply to normal, resting muscle. The large value of δ is interpreted as a measure of active vasomotion in vessels capable of controlling flow in several true capillaries simultaneously.

Despite "holes" in the capillary array, O_2 supply everywhere is sufficient to meet demand, for Mb is well saturated at all locations at rest (5). The distribution of PO_2 in 100 randomly selected cells in vasoconstricted (low flow) muscles is shown in Fig. 1.

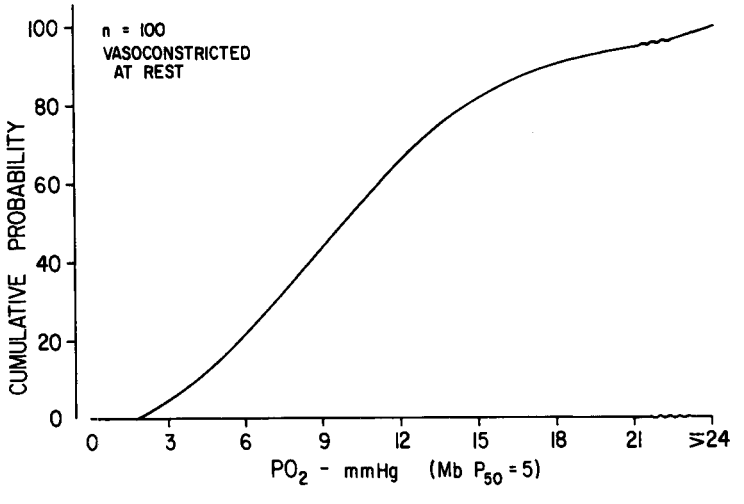

Fig. 1. PO_2 in resting muscles perfused at low flow.

Values are based on a Mb P_{50} of 5 torr at 37°C, in accord with measurements using improved systems for maintaining Mb fully reduced during tonometry (5,21). The P_{50} estimated by a spectroscopic method (21) in beating rat heart is not significantly different. The lowest PO_2 encountered was 2.5 torr, whereas the electron transport chain in resting muscle functions at maximum rate to <0.1 torr (1). Absence of anoxic loci at rest (Fig. 1) is confirmed by failure of $\dot{V}O_2$ to

increase during vasodilation (12). It would appear that total flow is sufficient, relative to $\dot{V}O_2$, to permit aerobic metabolism everywhere, despite restricted flow and C.D. in certain local regions. The high concentration and almost full saturation of Mb everywhere should "buffer" the transition from rest to work.

We emphasize that the above description does not apply to small animal species such as cat and rat, in which the Mb concentration is 10-100 times lower, resting $\dot{V}O_2$ is higher relative to flow, and C.D. is lower (12). Mb is highly desaturated in many cells in cat gracilis, and loci of fully desaturated Mb exist. As one might expect, the $\dot{V}O_2$ of such muscles is flow-limited. Mechanisms of vasomotor control may, therefore, be quite different from those of red fibers of large animals (dog, man).

Simulated phasic exercise

Twitch contraction at 4/min has almost no effect on flow, and increases $\dot{V}O_2$ only 30%. Nevertheless, C.D. almost doubles, and is about the same as at work rates which increase flow 2-10 fold and raise $\dot{V}O_2$ more than 50 fold; compare Fig. 2A & B.

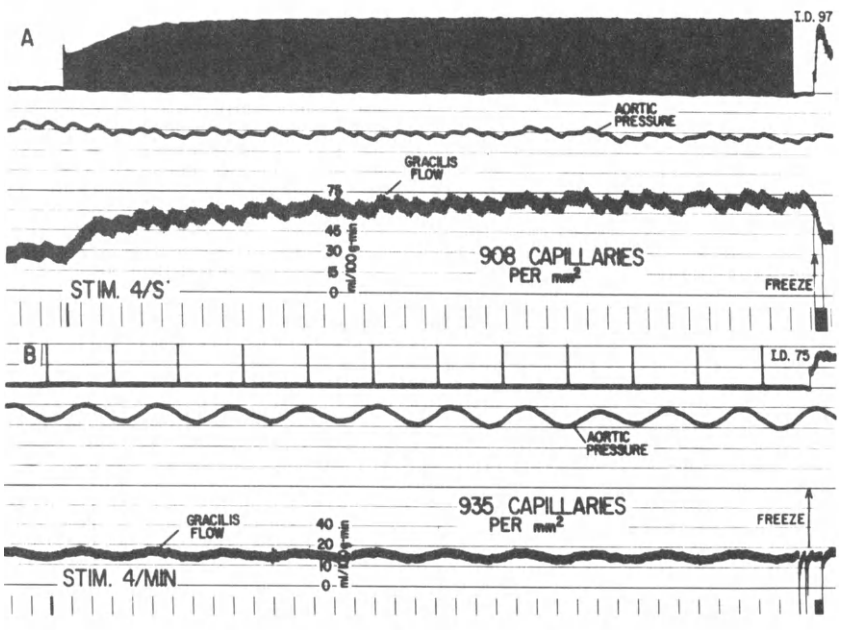

Fig. 2. Flow and C.D. during work at 4/s and 4/min.

A large component of capillary recruitment is therefore an ungraded, all-or-none process. Moreover, this ungraded component is not a "by-product" of flow regulation.

The time course of derecruitment provides further evidence to this point. Flow returns to the resting value 30 s after the last twitch at 6/s (90% of $\dot{V}O_2$ max). In contrast, C.D. exceeds 900/mm^2 for 5 min. Notice in Fig. 3 that $\hat{\delta}$ remains 0 for 5 min after contraction stops, indicating that capillary control vessels were relaxed even though vasomotor tone had fully recovered in vessels responsible for flow control. Complete recovery of C.D. and its frequency distribution requires about 30 min. Mechanisms responsible for such a protracted response are unknown.

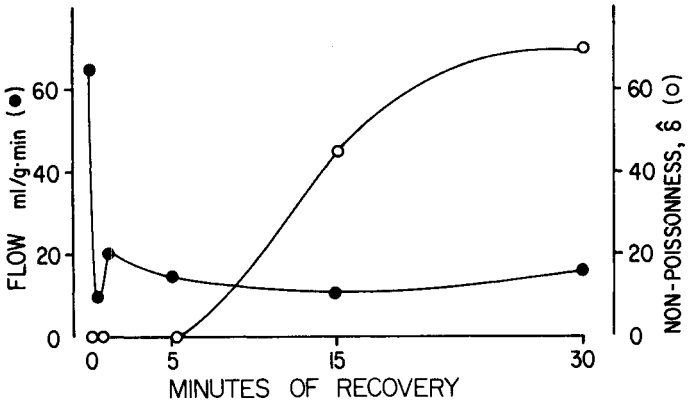

Fig. 3. Flow recovers 50 times faster than capillary distribution after work at 60% of $\dot{V}O_2$ max.

Our data confirm predictions of network models of microvascular beds (19). By use of such models one can compute the effect of changing the diameter of a particular class of vessels, while leaving all others unchanged. Such computations indicate that selective dilation of the smallest pre-capillary vessels (4th-6th order arterioles) influences flow in several capillaries but has almost no effect on overall bed resistance (19). We conclude that flow and C.D. can be controlled independently.

The time course of recruitment is shown in Figs. 4 & 5. Notice the long lower tail of the frequency distribution of local C.D. at rest is eliminated within 5 s. This renders the distribution random. $\hat{\delta}$ therefore goes to 0. It remains 0 throughout exercise and for several minutes thereafter, whether flow is held constant or free to vary (Fig. 5). These distributional changes were observed in each of 65 muscles. We interpret them to mean that all capillaries are

immediately rendered equally accessible to erythrocytes because active capillary control is switched off.

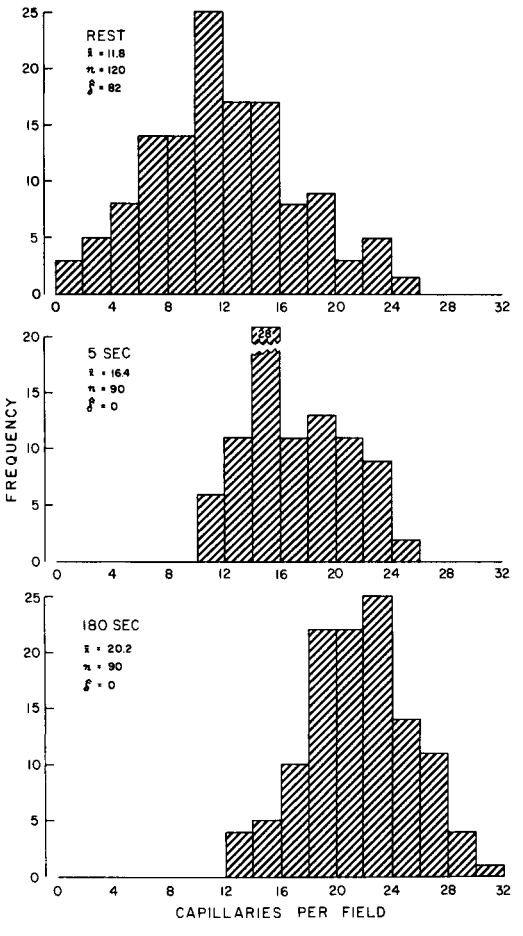

Fig. 4. Distributional changes in local C.D.

According to Gorczynski and Duling (6), the initial rate of arteriolar dilation is about 1 μ/s. This accounts for both the rapid rate of recruitment and its all-or-none character, for once a vessel exceeds 2.8 μ it cannot control passage of red cells (7). Calculations and Mb spectroscopy indicate that anoxia during exercise would be largely confined to those regions of exceptionally low C.D. represented by the lower tail of the resting distribution. We shall see that

maximum C.D. is not essential for aerobic metabolism, even at $VO_{2\ max}$. It is therefore likely that the almost instantaneous elimination of the longest diffusion paths is the principal function of recruitment in skeletal muscle. Indeed, if C.D. (and hence aggregate capillary cross-sectional area) increase out of proportion to blood flow, red cell transit times in some capillaries will be too long relative to VO_2, and respiration will become limited by $P_{cap}O_2$. As in most biologic systems, if a little is good, more is not necessarily better.

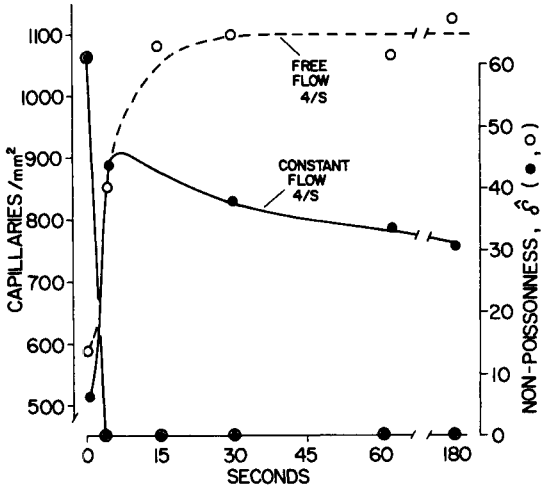

Fig. 5. Time course of recruitment during free and constant flow.

Excessive recruitment does not occur because the probability an erythrocyte will actually enter an accessible (open) capillary depends on hemodynamic factors closely related to flow. Notice in Fig. 5 that when flow is held constant at the resting value the increase in C.D. after 5 s fails to occur. Instead, C.D. falls in parallel with perfusion pressure. Experiments on autoperfused muscles indicate that both flow and perfusion pressure influence functional C.D.

The effect of work rate is shown in Fig. 6. Maximum functional C.D. is attained at 4/s, and is about 1100/mm^2. This is 700/mm^2 less than the anatomical maximum as determined by histologic methods (18). Just such a discrepancy should exist. Since red cell entry into capillaries is governed by stochastic factors, it is not possible to perfuse every one simultaneously, even if all are accessible. The expansion factor for C.D. in dog gracilis is about 2, in good agreement

with inferences drawn from indicator dilution measurements on this muscle (3). A larger expansion factor may exist in the unanesthetized state, for anesthetics suppress active vasomotion and thereby increase C.D. at rest.

Work at 4/s requires about 2/3 of maximum flow and VO_2. If C.D. at 4/s were the same as the resting value flow per capillary and red cell velocity would double. Capillary transit time (the ratio of capillary length to mean velocity), would be half normal and on the order of 80 ms. This is somewhat less than the estimated time for release of O_2 from capillaries under these conditions (14). Moreover, transit times have an important variance, so some values in the population would be substantially less than the mean (14). Failure of recruitment would therefore produce a physiologically significant O_2 shunt, and necessitate additional blood flow to meet O_2 requirements. The recruitment actually observed at 4/s is sufficient to prevent these inefficiencies.

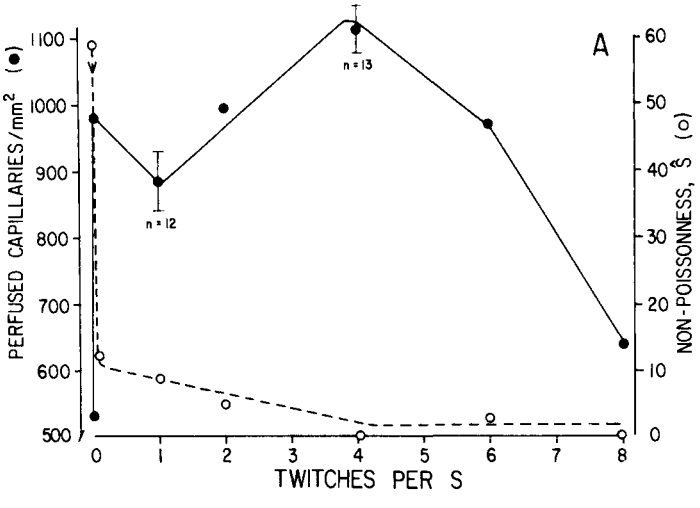

Fig. 6. Effect of work rate on local C.D.

VO_2 and flow are maximal at 8/s. The means for 7 muscles are 120 ml/100g·min and 15.2 ml/100g·min, respectively. Note that maximal C.D. is not required for maximal VO_2, as often assumed in the past. This is possible because there are no "holes" in the capillary array; the frequency distribution is typical of exercising muscle and $\hat{\delta}$ is 0 as shown in Fig. 6. Diffusion distances capable of producing anoxic loci are therefore absent according to calculations, and measurements of Mb saturation (Fig. 7). The process which restricts capillary perfusion at 8/s evidently affects all capillaries uniformly. The most likely explanation is tissue pressure, since contraction at 6 and 8/s produces partial fusion. The combination of maximal

flow and low mean C.D. results in mean transit times on the order of 50 ms. A physiological O_2 shunt should have been present, and was in fact observed. S_vO_2 at 8/s averaged 41% and was 53% in the muscle with the shortest mean transit time (45 ms). S_vO_2 was 16 torr higher than at 6/s, even though VO_2 was greater and Mb saturation lower (Fig. 7). Since cell PO_2 and lactate measurements indicate that work at 8/s is done aerobically, it is difficult to escape the conclusion that restricted C.D. produced a large O_2 shunt. Paradoxically, low mean C.D. at $VO_{2\ max}$ may be adaptive in that short transit times raise $P_{cap}O_2$ and provide for a higher capillary-to-tissue O_2 gradient. Maintenance of a high transcapillary O_2 gradient is essential at $VO_{2\ max}$ because cell PO_2 cannot be decreased significantly due to the shape of the Mb dissociation curve. In this view the transcapillary PO_2 gradient rather than capillary surface area or mean diffusion distance sets the limit on O_2 uptake. Though different intensities of work may require different mean capillary densities, a change from the frequency distribution at rest is always essential, and was observed in every exercised muscle regardless of the rate or duration of work.

Answers to the first 3 questions posed in the Introduction can now be summarized:

#1. The functions of capillary recruitment are:
*a) Eliminates longest diffusion paths immediately.
b) Promotes interaction of diffusion fields.
This compensates for low PO_2 in a particular capillary caused by long transit time and/or low capillary hematocrit.
c) Matches transit times to rates of O_2 release.
d) Decreases requirement for flow.

#2. C.D. at rest is controlled by active vasomotion of terminal arterioles. During exercise this vasomotion is switched off, and C.D. is controlled passively by stochastic hemodynamic factors acting at the capillary orifice.

#3. C.D. can be controlled independently of flow.

To answer our 4th question we must determine how vascular smooth muscle "knows" what the skeletal muscle is doing. Our data dispose of the possibility that an O_2-linked signal is involved. Fig. 7 shows the results of measurements at the center of randomly chosen cells after 3 min of work at 8/s. The arrows indicate median PO_2. The lowest saturation found is 5% (0.3 torr). In only 4% of loci is Mb less than 9% saturated (0.5 torr). Even if the older estimates of P50 (roughly half our value) are used the conclusion would be the same: There are no anoxic loci detectable with spatial resolution on the order of 2-3 mitochondria. This conclusion is consistent with the fact that the VO_2 of dog gracilis working at 80-90% of $VO_{2\ max}$ does not increase if more O_2 is delivered (15).

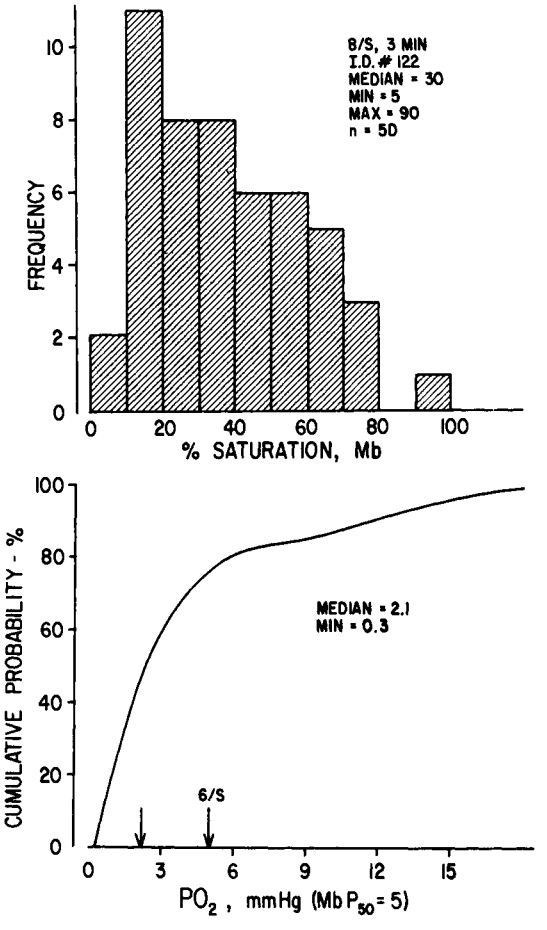

Fig. 7. Mb saturation and calculated PO_2 in a muscle working at VO_2 max.

K^+ and metabolites linked to ATP hydrolysis can also be excluded. Their concentrations would not be high enough after only 2-3 twitches, yet such metabolically trivial stimulii evoke 80% of maximum C.D. and drive $\dot{\delta}$ to 0. The same argument applies to exercise hyperemia; note in Fig. 8 that clear-cut dilation of vessels capable of flow control can be evoked by a single twitch if the initial resistance is high. This cannot be accounted for by any known metabolite. The short latency, rapid initial rate of dilation, stimulus-response relations, and recovery time course all strongly suggest a neural process. It is therefore significant that vasodilation after brief exercise can be blocked completely by local anaesthetics without affecting VO_2 or tension; see (9,10) and Fig. 8.

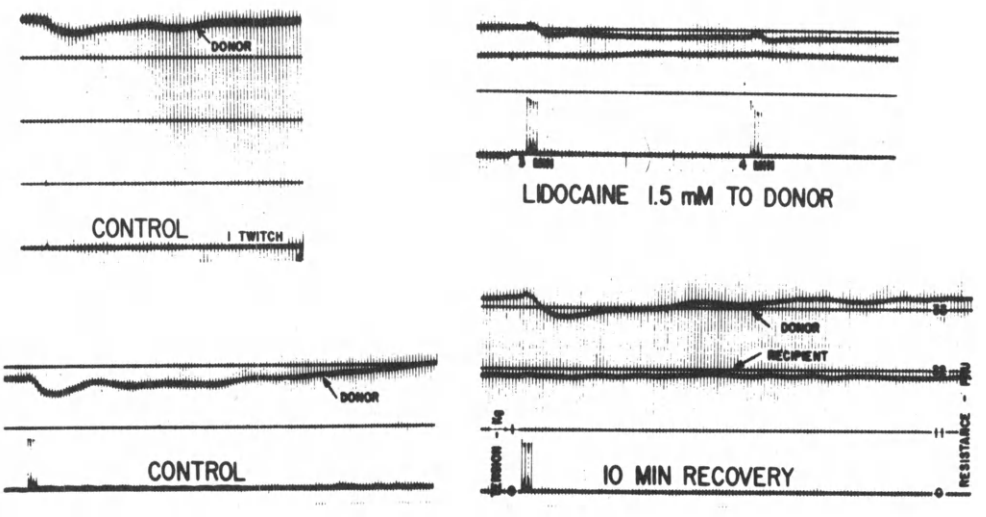

Fig. 8. Lidocaine reversibly blocks exercise dilation during perfusion at constant flow. Note effect of one twitch. The venous effluent from the exercised muscle (donor) perfused the resting gracilis of the opposite leg (recipient). Recipient resistance is a bioassay for metabolites. It did not change during contraction of donor in presence or absence of lidocaine.

If nerves are involved their cell bodies must lie within the muscle, because the main features of exercise vasodilation persist after chronic extrinsic denervation. Indeed, this observation has been the most persuasive argument in support of the metabolic (or myogenic) hypothesis (16). We recently reported, however, that neuronal cell bodies exist in the walls of arterioles of gracilis muscles from dog, cat and rat (20). About 10% exhibit typical catecholamine fluorescence, and the rest stain for specific acetylcholinesterase. Despite the above findings, the neural hypothesis for exercise dilation did not gain general acceptance when we proposed it a few years ago (10) because we could neither suggest a plausible stimulus to the intrinsic nerves nor identify the putative mediator. Exercise vasodilation is unaffected by blockers of acetylcholine, catecholamines, histamines or purines (2,9,10,11).

Quite recently, vasoactive intestinal peptide (VIP), has been identified by immunohistochemistry in sympathetic ganglia and peripheral sympathetic nerves (17). VIP is known to act as a neurotransmitter. Moreover, the sympathetic neurons which stain for VIP closely resemble the neurons observed in gracilis blood vessels, including strong staining for specific acetylcholinesterase (17). Existence of VIP (or other peptide

mediators) in acetylcholinesterase-positive neurons seems characteristic of tissues generally. Nerve fibers which stain for both VIP and acetylcholinesterase exist in sciatic nerve, and are found in close association with muscle blood vessels (17). VIP evokes changes in blood flow and C.D. in gracilis identical to those produced by heavy exercise; see Fig. 10. It is therefore possible that neurally released VIP initiates exercise vasodilation.

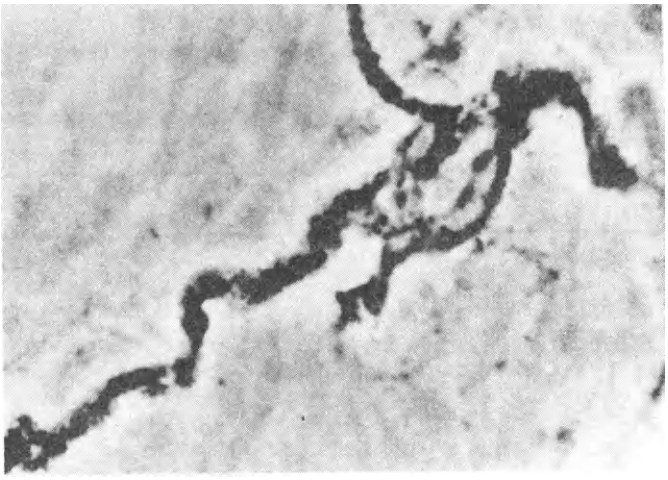

Fig. 9. Acetylcholinesterase-containing neuron in arteriole of dog gracilis, courtesy of Dr. Eric Schenk.

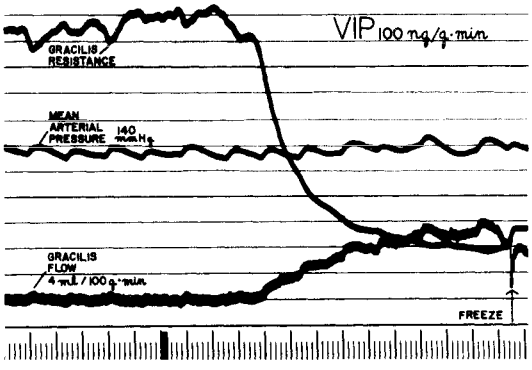

Fig. 10. Effect of intra-arterial infusion of VIP; mean C.D. was 1050/mm^2, and $\hat{\delta}$ was 0.

What stimulates the intrinsic nerves? Cutaneous sensory nerves are known to possess axon collaterals which make contact with vessels and sweat glands (8). They are thought to release a peptide mediator. A homologous peptidergic axon collateral, either from a spindle afferent or an alpha motor fiber could explain the short latency, tight coupling, and other features of exercise hyperemia and recruitment. This idea is especially attractive in that it allows us to relate vascular change to the motor unit function of muscle in vivo.

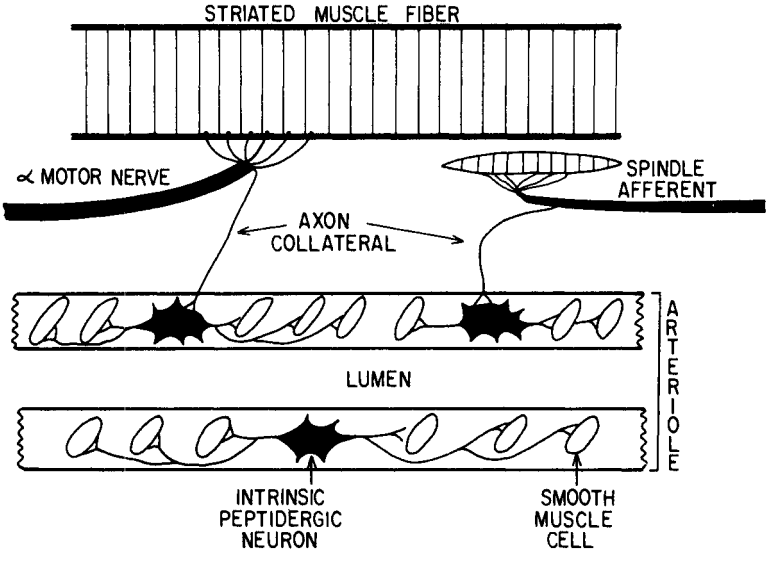

Fig. 11. A neural hypothesis for hyperemia and capillary recruitment in exercise. The transmitter released by the intrinsic nerves is thought to be a peptide such as VIP.

During a normal motor act only a few fibers uniformly distributed within the muscle are active, while the bulk of the muscle is at rest. The active units always function above the frequency for partial fusion (6-8/s in gracilis). Consequently, their VO_2 is always maximal, even if VO_2 of the whole muscle is low for ordinary work loads. From the standpoint of the active fibers local, all-or-none, instantaneous recruitment of surrounding capillaries would be highly advantageous. Indeed it may be essential for aerobic metabolism if the active unit happens to be in a portion of the muscle devoid of capillaries when work begins. Because of the nature of the vascular network, local recruitment could be accompanied by internal redistribution of flow to the active fibers, without

change in flow per gram of whole muscle. Local hyperemia would facilitate entry of red cells into capillaries and defend $P_{cap}O_2$. O_2 flux from well saturated Mb in adjacent resting fibers would supplement O_2 delivery. If the foregoing local changes were indeed produced by axon collaterals they could be initiated more quickly and confined more precisely to the working fibers than if control were dependent on diffusible substances. This would facilitate aerobic respiration and permit greater efficiency and economy in the use of cardiovascular reserves. As work increases, more motor units would be recruited, each with its complement of capillaries. Tension, flow and C.D. in the muscle as a whole would increase due to summation of local responses. Finally, during maximal effort, which is brief and infrequent, maximal dilation of large arterioles would produce the flows, capillary hematocrits, and short transit times required for maximal VO_2.

According to the above conceptions, aerobic metabolism during exercise depends on intrinsic neural mechanisms which match local O_2 delivery to the motor unit organization of skeletal muscle.

REFERENCES

1. Chance, B., Oshino, N. and Mayevsky, A. Basic principles of tissue oxygen determination from mitochondrial signals. Adv. Exper. Med. Biol. 37a: 277-292, 1973.

2. Daniel, A. and Honig, C.R. Does histamine influence vasodilation caused by prolonged arterial occlusion or heavy exercise? J. Pharmacol. Exper. Therap. In Press.

3. Durán, W.N. Effects of muscle contraction and of adenosine on capillary transport and microvascular flow in dog skeletal muscle. Circ. Res. 41: 642-647, 1977.

4. Fung, Y.-C. Stochastic flow in capillary blood vessels. Microvasc. Res. 5: 34-48, 1973.

5. Gayeski, T.E.J. and Honig, C.R. Myoglobin saturation and calculated PO_2 in single cells of resting gracilis muscles. Adv. Exper. Med. Biol. 94: 77-84, 1978.

6. Gorczynski, R.J. and Duling, B.R. Interrelations between contracting striated muscle and precapillary microvessels. Am. J. Physiol. 235: H494-504, 1978.

7. Henquell, L., LaCelle, P.L. and Honig, C.R. Capillary diameter in rat heart in situ: relation to erythrocyte deformability, O_2 transport and transmural O_2 gradients. Microvasc. Res. 12: 259-274, 1976.

8. Hökfelt, T., Johansson, O., Kellerth, J.-O., Ljungdahl, Å., Nillson, G., Nygårds, A. and Pernow, B. Immunohistochemical distribution of substance P. in: Substance P. Nobel Symposium 37. U.S. von Euler and B. Pernow, eds., Raven Press, New York, 1977.

9. Honig, C.R. Contributions of nerve and metabolites to exercise vasodilation: a unifying hypothesis. Am. J. Physiol. 236: H705-719, 1979.

10. Honig, C.R. and Frierson, J.L. Neurons intrinsic to arterioles initiate postcontraction vasodilation. Am. J. Physiol. 230: 493-507, 1976.

11. Honig, C.R. and Frierson, J.L. Role of adenosine in exercise vasodilation in dog gracilis muscle. Am. J. Physiol. 238: H703-715, 1980.

12. Honig, C.R., Frierson, J.L. and Nelson, C.N. O_2 transport and $\dot{V}O_2$ in resting muscle: significance for tissue-capillary exchange. Am. J. Physiol. 220: 357-363, 1971.

13. Honig, C.R., Odoroff, C.L. and Frierson, J.L. Capillary recruitment in exercise: rate, extent, uniformity and relation to blood flow. Am. J. Physiol. 238: H31-42, 1980.

14. Honig, C.R. and Odoroff, C.L. Calculated dispersion of capillary transit times; significance for O_2 exchange. Am. J. Physiol. In Press.

15. Horstman, D.H., Gleser, M. and Delehunt, J.C. The effect of adenosine infusion on oxygen consumption of contracting in situ gracilis muscle. Physiologist 17: 250, 1974.

16. Jones, R.D. and Berne, R.M. Intrinsic regulation of skeletal muscle blood flow. Circ. Res. 14: 126-138, 1964.

17. Lundberg, J.M., Hökfelt, T., Schultzberg, M., Uvnäs-Wallensten, K., Köhler, C. and Said, S.I. Occurrence of vasoactive intestinal peptide (VIP)-like immunoreactivity in certain cholinergic neurons of the cat: evidence from combined immunohistochemistry and acetylcholinesterase staining. Neuroscience 4: 1539-1559, 1979.

18. Martin, E.G., Wooley, E.C. and Miller M. Capillary counts in resting and active muscles. Am. J. Physiol. 100: 407-416, 1932.

19. Mayrovitz, H.N., Wiedeman, M.P. and Noordergraaf, A. Microvascular hemodynamic variations accompanying microvessel dimensional changes. Microvasc. Res. 10: 322-330, 1975.

20. Myers, H.A., Schenk, E.A. and Honig, C.R. Ganglion cells in arterioles of skeletal muscle: role in sympathetic vasodilation. Am. J. Physiol. 229: 126-138, 1975.

21. Tamura, M., Oshino, N., Chance, B. and Silver, I.A. Optical measurements of oxygen consumption of rat heart in vitro. Arch. Biochem. Biophys. 191: 8-22, 1978

ACKNOWLEDGEMENT

We appreciate the advice and assistance of our colleagues, Richard J. Connett, James L. Frierson, Charles L. Odoroff and Eric Schenk. Our research is supported by Grant HLB 03290 from the United States Public Health Service.

Adv. Physiol. Sci. Vol. 8. Cardiovascular Physiology. Heart, Peripheral Circulation and Methodology
A. G. B. Kovách, E. Monos, G. Rubányi (eds)

INTRODUCTION TO CATION REGULATION IN THE MYOCARDIUM

H. Reuter
Department of Pharmacology, University of Bern, 3010 Bern, Switzerland

A finely balanced ionic milieu in the cardiac cell is essential for the proper function of the heart. The major inorganic cations, K^+, Na^+, Ca^{2+} and Mg^{2+}, are not only unequally distributed between extracellular space and cell interior, but also within the cell. In recent years it has become apparent that cell organelles, like sarcoplasmic reticulum, mitochondria, or nuclei may contain an ionic composition quite different from that of the cytosol. While the distribution of Na^+ and K^+ ions across the cell membrane profoundly affects excitability of the membrane, small variations of the distribution of, for example, Ca^{2+} ions within the cell have considerable effects on the conformation of contractile proteins and, thereby, regulate contractility of the heart.

In recent years much progress has been made in designing methods that enable us to study membrane permeabilities, uphill transports and cellular concentrations of cations and anions in greater detail. Refinement of tracer flux techniques, of electrophysiological methods, notably voltage clamp methods, and the development of ion-selective electrodes and dyes have contributed to recent advances in our understanding of the function of the heart.

The present symposium deals with various aspects of cation regulation in the myocardium. Intracellular Na^+ and H^+ ion activities measured with ion-sensitive microelectrodes (see J.W. Deitmer and D. Ellis) may have profound effects on cardiac function such as cell-to-cell spread of excitation (see R. Weingart). A major route through which K^+ions pass through the plasma membrane is a set of ion channels that exhibit inward going rectification. Some properties of this class of ion channels will be discussed by E. Carmeliet. The cholinergic muscarinic receptors in the heart are linked to another set of K^+ channels, the functional state of which are regulated by acetylcholine (see W. Trautwein). Several functional apects of ion regulation in the myocardium will be dealt with in

5 short communications incorporated in the symposium. Obviously it is impossible to discuss all known mechanisms and functional consequences of cation regulation in cardiac cells. However, it is hoped that a few selected topics in this symposium may stimulate future research in this area.

Adv. Physiol. Sci. Vol. 8. Cardiovascular Physiology. Heart, Peripheral Circulation and Methodology
A. G. B. Kovách, E. Monos, G. Rubányi (eds)

REGULATION OF THE INTRACELLULAR SODIUM AND pH IN MAMMALIAN CARDIAC TISSUE STUDIED USING ION-SENSITIVE MICROELECTRODES

Joachim W. Deitmer* and David Ellis**

** Abteilung Biologie, Ruhr-Universität, D-4630 Bochum, FRG; ** Department of Physiology, University Medical School, Edinburgh EH8 9AG, UK*

INTRODUCTION

The performance of the mammalian heart during its excitation-contraction cycle is greatly influenced by the movements of ions across the cell membrane and between intracellular compartments (for review see Fozzard, 1977). The key ion for regulating the strength of the heart beat is Ca^{2+}. Other ions, such as Na^+, H^+ and K^+ have also been found to affect cardiac performance. The maintainance of extra- and intracellular ionic homeostasis in cardiac tissue is therefore important in providing the conditions for a normal cyclic heart contraction. The effect of ions other than Ca^{2+} on the heart beat might be due to direct interaction of the ion species with excitation-contraction coupling, or produced by changing the intracellular Ca^{2+} level. Alteration of the extracellular Na concentration e.g. has been shown to considerably affect the contractility of cardiac muscle (Lüttgau & Niedergerke, 1958; Orkand, 1968), presumably by changing the Ca fluxes across the cell membrane (Reuter & Seitz, 1968; Glitsch, Reuter & Scholz, 1970). Interactions between the regulation of different ion species have been demonstrated in a variety of tissues. It appears as if the regulation of intracellular and extracellular Ca^{2+}, Na^+, H^+ and K^+ does not occur independently from each other.

We have used Na^+- and pH-sensitive microelectrodes as described by Thomas (1978) to study the regulation of intracellular Na^+ and of intracellular pH in quiescent sheep heart Purkinje fibres. These types of electrodes allow continuous monitoring of the intracellular Na^+ and intracellular pH simultaneously.

MATERIAL AND METHODS

The experimental procedures have been extensively described elsewhere (Ellis & Thomas, 1976; Ellis, 1977; Deitmer & Ellis, 1978a,b; 1980). Purkinje fibres were dissected from fresh sheep hearts and pinned into a small superfusion chamber where the exchange rate of solutions was 6 to 10 bath volumes/min.

The ion-sensitive microelectrodes (Na^+ and pH) were pre-

pared as described by Thomas (1970; 1974). The tip of the ion-sensitive microelectrodes used in cardiac muscle cells was usually less than 1 μm. They were used to penetrate cells between 0.3 and 1.2 mm apart along the Purkinje fibre. The Na^+-sensitive microelectrodes used had a response of at least 54 mV (and up to 61 mV) for a tenfold change in the external Na concentration (at 35 °C), the response being more than 90% complete within 30 to 90 s. If the response of the Na^+-sensitive microelectrode calibrated in activity is to be converted to concentration, it has to be divided by the activity coefficient for Na^+, which is approximately 0.75 (in the bathing solution). The pH-sensitive microelectrodes responded with 55 to 60 mV (at 35 °C) to a unit change of the pH in the bathing solution, the response being more than 90% complete within 30 to 150 s. The response times of the ion-sensitive microelectrodes used in our experiments were much faster than the changes in the intracellular ion activities measured. The time courses of these intracellular ion changes measured were therefore not limited by the response time of the electrodes used.

The normal saline contained (in mM): Na 140, K 6, Ca 2, Mg 1, Cl 145, pyruvate 2, glucose 10, buffered with 10 mM HEPES to give a pH of 7.4 (±0.05), and was gassed with 100% O_2. The extracellular Na concentration was altered by exchange of NaCl by either TrisCl or LiCl. The pH was changed by the addition of NaOH (at the expense of NaCl) or HCl. For further details concerning the solutions and drugs used see Deitmer & Ellis (1978a,b; 1980). The temperature of the solutions was maintained at 35 °C.

RESULTS AND DISCUSSION

At the normal extracellular Na concentration of 140 mM, the intracellular Na activity of sheep heart Purkinje fibres is around 7 mM (see Table 1). Thus the Na^+ equilibrium potential is about 147 mV more positive than the membrane resting potential of approximately -75 mV in these cells. The intracellular pH of Purkinje fibres varies between 7.0 and 7.3, depending upon the buffer system used in the extracellular solution (see Table 1).

Table 1: Intracellular activities and electrochemical potentials of Na and H in quiescent sheep heart Purkinje fibres

		intracellular activity	equilibrium potential	electrochemical gradient
Na^+	(K_o=4mM)	7.2 mM	+71 mV	147 mV
	(K_o=6mM)	6.6 mM	+73 mV	146 mV
H^+	(HEPES)	7.2 - 7.3	-13 mV	62 mV
	(CO_2/HCO_3^-)	7.0 - 7.1	-22 mV	51 mV

In 5% CO_2/22 mM HCO_3^- (pH 7.4) the intracellular pH is between 0.1 and 0.3 pH units more acid than in HEPES-buffered solu-

tions. The electrochemical gradient thus varies between 50 and 65 mV, against which the intracellular pH has to be actively maintained. If the H^+ distribution across the cell membrane were in equilibrium, an intracellular pH of approximately 6.2 would be expected. The steady-states of the intracellular Na activity and the intracellular pH depend upon the concentration of Na and H in the extracellular solution (Fig. 1A,B). The relationship reveals that the intracellular levels of both ions appear to be a linear function of the extracellular levels over the range shown. It is interesting that this relationship remains linear for the Na^+ distribution, even if the Na/K pump is inhibited by 10^{-5} M strophanthidin.

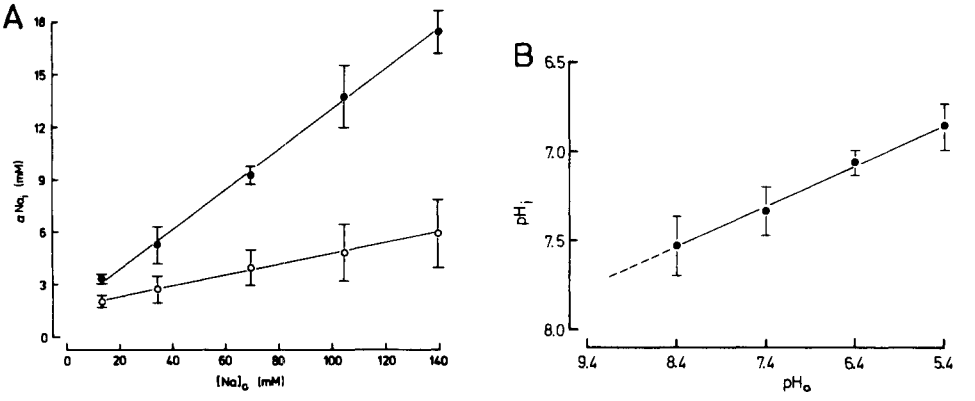

Fig. 1: The steady-state levels of the intracellular Na activity, aNa_i, (A), and the intracellular pH, pH_i,(B), of sheep heart Purkinje fibres. (A) The steady-state levels of intracellular Na^+ were measured at various extracellular Na concentrations in the absence (open circles), and in the presence (filled circles) of 10^{-5} M strophanthidin. Na was substituted by Tris. (B) The intracellular pH at extracellular pH between 5.4 and 8.4. All lines are regression fits to the points.

At all times the Na gradient across the membrane was such that Na^+ should tend to enter the cells. The large decreases in intracellular Na^+ as the extracellular Na concentration was lowered could not be due to passive Na movement. It is still not clear what mechanism produces the decrease in intracellular Na^+ in the absence of extracellular K^+ or in the presence of the cardio-active steroid strophanthidin (Ellis, 1977;Ellis & Deitmer, 1978). It seems likely that Ca^{2+} and/or H^+ gradient might be involved in this process.
The intracellular pH changed by 0.22 pH units for a unit change in the extracellular pH. This demonstrates that the H^+ distribution across the cell membrane is far from its equilibrium over the extracellular range between 5.4 and 8.4. The membrane potential changed by less than 10 mV over this pH range. Thus, the electrochemical gradient for H^+ ions across the cell mem-

brane changed considerably as the extracellular pH was varied. There was a linear relationship between the H^+ equilibrium potential, as calculated from the Nernst equation, and the extracellular pH, indicating a change of approximately 47 mV in the H^+ equilibrium potential, when the extracellular pH is altered by one unit. If a relatively constant membrane potential is assumed even at extracellular pH values higher than 8.4, the H^+ ion distribution across the cell membrane would be expected to be in equilibrium at an extracellular pH of about 8.7, where, by extrapolation, the intracellular pH should be approximately 7.6 (Deitmer & Ellis, 1980).

The addition of various concentrations of strophanthidin indicated that very low concentrations ($< 10^{-7}$ M) of strophanthidin can produce a decrease of the intracellular Na activity (Deitmer & Ellis, 1978a). Higher concentrations of this cardio-active steroid caused an increase of the intracellular Na level due to the inhibition of the Na/K pump. The half-maximal effect on the rate of rise of the intracellular Na activity was achieved at a concentration near to 10^{-6} M, and a maximal effect was apparent at a strophanthidin concentration near to 10^{-5} M. This strophanthidin dose caused the intracellular Na activity to rise with a mean maximum rate of 0.5 mM/min. This rise of intracellular Na^+ probably reflects the net passive Na influx into the cells. Taking a value for the cell surface area to volume ratio of 0.39 μm^{-1} (Mobley & Page, 1972), this increase of intracellular Na^+ indicates a net Na influx of 2.8 pmole/s cm^2. An apparent Na permeability coefficient can then be calculated to be about 6.7×10^{-9} cm/s. The effect of strophanthidin on the intracellular Na activity and intracellular pH is shown in Fig.2. The intracellular Na^+ began to rise within 3 min after the addition of strophanthidin due to the inhibition of the Na/K pump, and increased from about 6 mM up to 15 mM in the first 20 min. During this time there was only a small decrease of the intracellular pH from 7.27 to 7.22. In the following 25 min the intracellular Na activity increased at a much reduced rate up to 19 mM, while the intracellular pH now rapidly decreased to 7.05. The major increase of intracellular Na^+ had thus occurred while the intracellular pH remained almost unchanged, and the faster intracellular acidification coincided with intracellular Na^+ only increasing very slowly. The intracellular Na^+ appeared to approach a 'plateau' (Deitmer & Ellis, 1978a; Ellis & Deitmer, 1978), in spite of the fact that there was still a large Na^+ ion gradient into the cells. Addition of 5×10^{-4} M ouabain under these conditions produced only a very small rise in intracellular Na^+ (Deitmer & Ellis, 1978a). The results might indicate that the intracellular acidification is linked to the intracellular Na^+ approaching a 'plateau' level. Since a rise in intracellular Na^+ would also cause an increase of the intracellular Ca^{2+} (Glitsch, Reuter & Scholz, 1970), the intracellular acidification might also be due to an increased Ca level. In snail neurones Meech & Thomas (1977) have shown that intracellular injection of Ca^{2+} ions caused an immediate decrease of the intracellular pH.

Following the removal of strophanthidin, both the intracellular Na^+ and the intracellular pH recovered towards their initial levels. The membrane potential reversibly depolarized in the

presence of strophanthidin by about 7 mV. Upon removal of the Na/K pump inhibitor the membrane transiently hyperpolarized beyond the control level, presumably due to electrogenic Na^+ pumping.

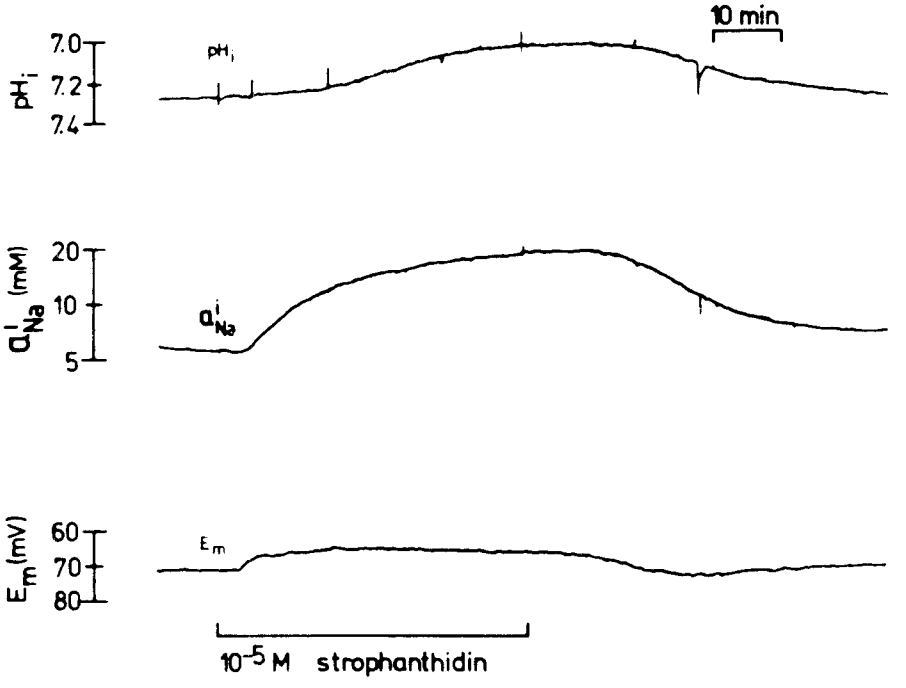

Fig. 2: The effect of 10^{-5} M strophanthidin (applied for about 45 min) on the intracellular pH (pH_i, upper trace), the intracellular Na activity (aNa_i, middle trace), and the membrane potential (E_m, lower trace) in the same Purkinje fibre. The E_m-recording microelectrode served as reference for both the pH- and the Na^+-sensitive microelectrode.

Effects of NH_4Cl and amiloride

Addition and removal of NH_4Cl cause changes in the intracellular pH which have been demonstrated in a variety of tissues (Thomas, 1974; Boron & de Weer, 1976; Aickin & Thomas, 1977). These changes are believed to be mainly due to movements of the uncharged NH_3 through the cell membrane. Fig. 3 shows an experiment, where the effects of NH_4Cl on the intracellular pH and the intracellular Na^+ of heart Purkinje fibres. There was a rapid intracellular alkalinization followed by a slower acidification when 20 mM NH_4Cl was added to the bathing solution. The intracellular Na activity decreased in the presence of NH_4Cl from 7 mM to 5.5 mM, and the membrane depolarized by

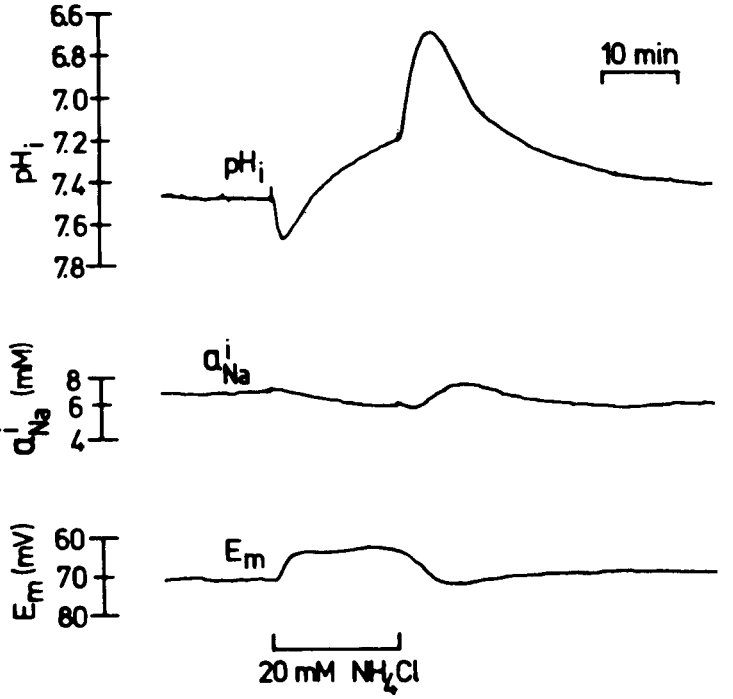

Fig. 3: The effects of the addition and removal of 20 mM NH_4Cl on the intracellular pH (upper trace), the intracellular Na activity (middle trace) and the membrane potential (lower trace).

10 mV. Upon removal of NH_4Cl the intracellular pH dropped by 0.5 pH units from 7.2 to 6.7, and than rapidly recovered towards the initial level. This pH recovery occurred against the H gradient, and must therefore be due to some active H^+ extrusion mechanism. The maximum rate of this intracellular pH recovery was 0.07 pH units/min, which is equivalent to a change in the amount of intracellular H^+ of 2.5 mequiv/l/min, assuming an intracellular buffering power of 35 mequiv H^+/pH unit/l (Ellis & Thomas, 1976). The intracellular Na activity transiently increased upon removal of NH_4Cl beyond the control level. This 'Na hump' occurred at the same time as the rate of the intracellular pH recovery was maximal. This suggests that the active regulation of the intracellular pH might be linked to an increased Na influx. The rise in the intracellular Na^+ could mean that internal H^+ ions are exchanged for external Na^+ ions. The net rise in intracellular Na^+ would be kept small by an increased activity of the Na/K pump, which might be indicated by the transient hyperpolarization of the cell membrane.
The diuretic amiloride, which is known to inhibit Na fluxes across epithelial membranes (Bentley, 1968), had some influence on both intracellular pH and Na^+ of heart Purkinje fibres.

In the presence of 10^{-3} M amiloride the intracellular pH decreased by up to 0.2 pH units, and the intracellular Na^+ also tended to decrease by a small amount. We have tested the effect of amiloride on the intracellular pH and Na^+ during the addition and the removal of NH_4Cl. Fig. 4 shows an experiment of this kind. There were two conspicuous changes upon the removal of NH_4Cl in the presence of amiloride: (1) the rate of recovery of the intracellular pH was much reduced (by up to 80 %), and (2) the transient rise of the intracellular Na^+ ('Na hump') was abolished. This supports the idea that part of the intracellular pH recovery was linked to an influx of Na^+ ions. When the extracellular Na concentration was reduced to 1/10, the intracellular pH recovery following the removal of NH_4Cl was also greatly inhibited. It must be mentioned, however, that the recovery from intracellular acidosis induced by lowering the extracellular pH was unaffected by changing the extracellular Na concentration. This discrepancy of the effects of extracellular Na^+ on the intracellular pH recovery is still unexplained, thus caution is needed in interpreting results obtained by the use of a single technique for inducing an acid load in cardiac tissue.

The evidence so far obtained for a Na/H exchange is not conclusive in all aspects, and other mechanisms may well be responsible for the effects observed. The reduction of the intracellular pH in the presence of high concentrations of cardio-active steroids might e.g. be due to an increase of the intracellular Ca^{2+}. These Na/K pump inhibitors are known to

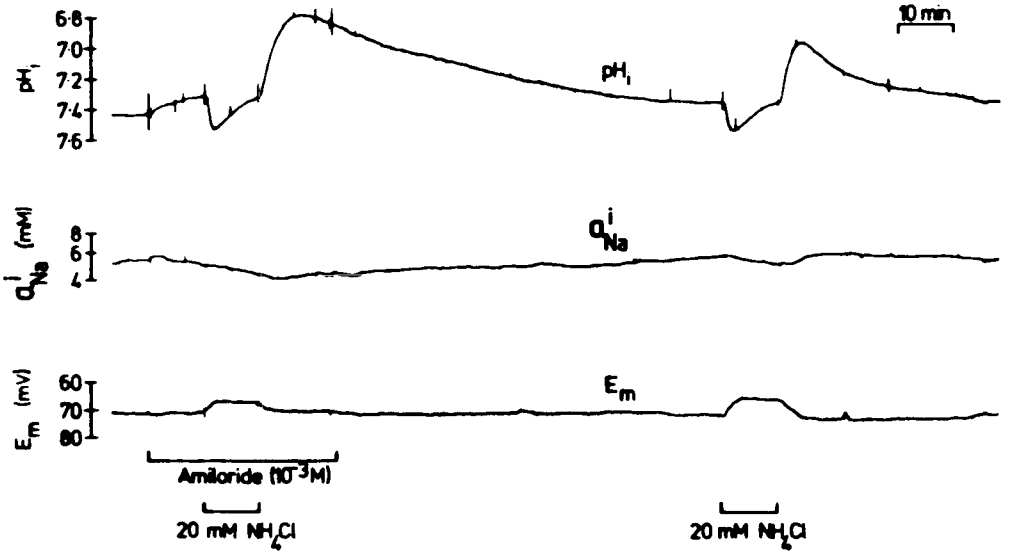

Fig. 4: The effects of 10^{-3} M amiloride on the intracellular pH and the intracellular Na activity, and on their changes produced by the addition and the removal of 20 mM NH_4Cl (indicated by bars).

produce contractures in cardiac muscle (Weingart, 1977), indicating that the intracellular Ca level is high. This high intracellular Ca^{2+} is probably directly caused by the rise in intracellular Na^+ via a Na/Ca exchange mechanism (Reuter & Seitz, 1968). Increasing the extracellular Ca concentration under these conditions could produce a marked decrease of the intracellular Na activity in sheep heart Purkinje fibres (see Fig. 5). The decrease of intracellular Na^+ became larger as the intracellular Na activity rose due to the inhibition of the Na/K pump. These experiments suggested that in the presence of cardio-active steroids, when the Na/K pump is inhibited, the intracellular Na activity is maintained at a relatively low level (< 30 mM) by a Na/Ca exchange across the cell membrane. When the extracellular Ca^{2+} was completely replaced by another divalent cation, e.g. Mg^{2+}, the intracellular Na^+ increased further to approach an electrochemical equilibrium (Deitmer & Ellis, 1978b). Thus, in the absence of extracellular Ca^{2+} the relatively low 'plateau' of intracellular Na^+ could not be maintained. Under conditions where the Na/K pump was inhibited, the level of intracellular Na^+ was directly dependent on the extracellular Ca concentration, i.e. the higher the extracellular Ca concentration the lower the level of the intracellular Na activity.

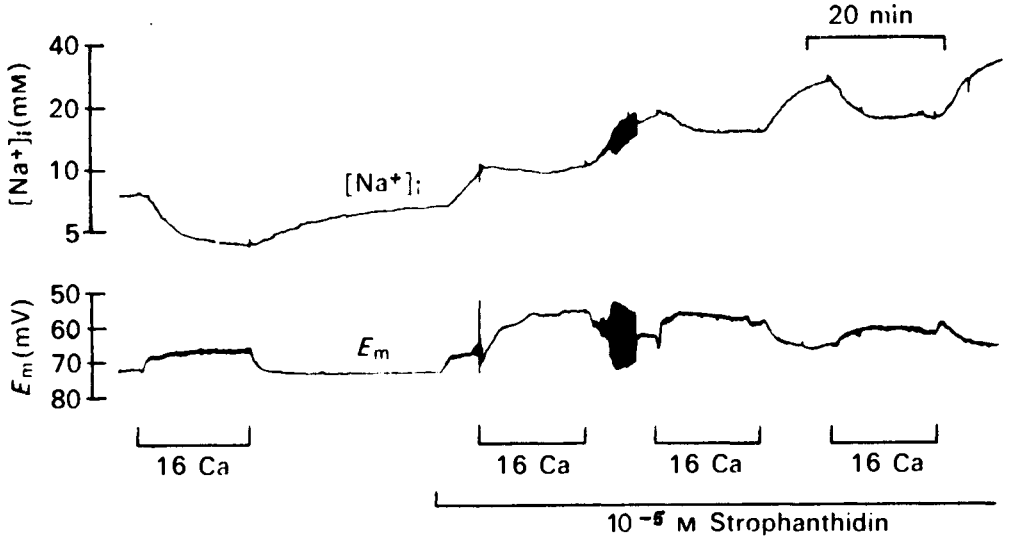

Fig. 5: Changes in the intracellular Na concentration, $[Na^+]_i$ (logarithmic scale), produced by successively raising the extracellular Ca concentration from 2 mM to 16 mM in the absence and presence of 10^{-5} M strophanthidin. Note that the decrease of intracellular Na^+ produced by raising the Ca concentration depended upon the level of intracellular Na^+.

CONCLUSIONS

The intracellular Na activity of cardiac tissue is- under normal physiological conditions- maintained primarily by the operation of the Na/K pump. Only when the Na/K pump is inhibited do other ion exchange processes become significantly involved in preventing a break-down of the Na gradient across the cell membrane. These processes may include Na/H and Na/Ca exchange. The regulation of the intracellular pH of cardiac muscle is still much less understood. It seems that the Na gradient across the cell membrane does affect the regulation of the intracellular pH under certain conditions. An exchange of Cl^- and HCO_3^- across the cell membrane also contributes to the maintainance of the normal intracellular pH (Vaughan-Jones, 1979). It appears likely that the intracellular pH in cardiac muscle is controlled by a multi-ionic exchange process across the cell membrane, as has been suggested for snail neurones (Thomas, 1977) and for mammalian skeletal muscle (Aickin & Thomas, 1977).

This work was supported by the Medical Research Council (U.K.) and the Deutsche Forschungsgemeinschaft (De 231/1,2).

REFERENCES

Aickin, C.C. & Thomas, R.C. (1977). An investigation of the ionic mechanism of intracellular pH regulation in mouse soleus muscle fibres. J. Physiol. 273, 295-316.

Bentley, P.J. (1968). Amiloride: a potent inhibitor of sodium transport across the toad bladder. J. Physiol. 195, 317-330.

Boron, W.F. & de Weer, P. (1976). Intracellular pH transients in squid giant axons caused by CO_2, NH_3 and metabolic inhibitors. J. gen. Physiol. 67, 91-112.

Deitmer, J.W. & Ellis, D. (1978a). The intracellular sodium activity of cardiac Purkinje fibres during inhibition and re-activation of the Na-K pump. J. Physiol. 284, 241-259.

Deitmer, J.W. & Ellis, D. (1978b). Changes in the intracellular sodium activity of sheep heart Purkinje fibres produced by calcium and other divalent cations. J. Physiol. 277, 437-453.

Deitmer, J.W. & Ellis, D. (1980). Interactions between the regulation of the intracellular pH and sodium activity of sheep cardiac Purkinje fibres. J. Physiol. 304, 471-488.

Ellis, D. (1977). The effects of external cations and ouabain on the sodium activity in sheep heart Purkinje fibres. J. Physiol. 273, 211-240.

Ellis, D. & Deitmer, J.W. (1978). The relationship between the intra- and extracellular sodium activity of sheep heart Purkinje fibres during inhibition of the Na-K pump. Pflügers Arch. 377, 209-215.

Ellis, D. & Thomas, R.C. (1976). Direct measurement of the

intracellular pH of mammalian cardiac muscle. J. Physiol. 262, 755-771.

Fozzard, H.A. (1977). Heart: excitation-contraction coupling. Ann. Rev. Physiol. 39, 201-220.

Glitsch, H.G., Reuter, H. & Scholz, H. (1970). The effect of the internal sodium concentration on calcium fluxes in isolated guinea-pig auricles. J. Physiol. 209, 25-43.

Lüttgau, H.C. & Niedergerke, R. (1958). The antagonism between Ca and Na ions on the frog's heart. J. Physiol. 143, 486-505.

Meech, R.W. & Thomas, R.C. (1977). The effect of calcium injection on the intracellular sodium and pH of snail neurones. J. Physiol. 265, 867-879.

Mobley, B.A. & Page, E. (1972). The surface area of sheep cardiac Purkinje fibres. J. Physiol. 220, 547-563.

Orkand, R.K. (1968). Facilitation of heart muscle contraction and its dependence on external calcium and sodium. J. Physiol. 196, 311-325.

Reuter, H. & Seitz, N. (1968). The dependence of calcium efflux from cardiac muscle on temperature and external ion composition. J. Physiol. 195, 451-470.

Thomas, R.C. (1970). New design for sodium-sensitive glass micro-electrode. J. Physiol. 210, 82-83 P.

Thomas, R.C. (1974). Intracellular pH of snail neurones measured with a new pH-sensitive glass micro-electrode. J. Physiol. 238, 159-180.

Thomas, R.C. (1977). The role of bicarbonate, chloride and sodium ions in the regulation of intracellular pH in snail neurones. J. Physiol. 273, 317-338.

Thomas, R.C. (1978). Ion-sensitive intracellular microelectrodes. Acad. Press, London.

Vaughan-Jones, R.D. (1979). Regulation of chloride in quiescent sheep heart Purkinje fibres studied using intracellular chloride and pH-sensitive micro-electrodes. J. Physiol. 295, 111-137.

Weingart, R. (1977). The actions of ouabain on intercellular coupling and conduction velocity in mammalian ventricular muscle. J. Physiol. 264, 341-365.

Adv. Physiol. Sci. Vol. 8. Cardiovascular Physiology. Heart, Peripheral Circulation and Methodology
A. G. B. Kovách, E. Monos, G. Rubányi (eds)

CELL-TO-CELL COUPLING IN CARDIAC TISSUE

Robert Weingart
Department of Physiology, University of Berne, Bühlplatz 5, 3012 Berne, Switzerland

1. INTRODUCTION

The classical cell theory, formulated back in the last century (Schleiden, 1838), defined an organism as an "aggregate of fully circumscribed and selfcontained unit beings, the cells". However, over the last twenty years or so, it was realized that the development of complex biological systems was only possible because individual cells communicate with each other via chemical and electrical messages. This principle seems now nearly a universal feature of organs, including heart. The only known exceptions are skeletal muscle cells and most nerve fibres, but only once they are fully differentiated.

In cardiac tissue, as in other excitable structures, impulse conduction occurs by means of local circuit currents. This concept presumes an intracellular path for the current flow from one cell to another via a low resistance barrier. Its resistance, among other parameters, determines the speed with which the electrical impulse propagates.

2. MORPHOLOGICAL ASPECT

As a consequence of Sjöstrand and Andersson's studies in 1954, it was realized that cardiac muscle represents not an anatomical syncytium, but is composed of isolated cells separated by specialized areas of contact, the intercalated disks. The development of improved preparation techniques in electronmicroscopy made it possible to investigate more closely the area of contact between cells. It was found that the disks include three types of junctional specializations, the fasciae adherentes, the maculae adherentes or desmosomes which provide mechanical connections, and the nexus, the pre-

sumed structure for current flow from one cell to the next (McNutt and Weinstein, 1973). In the area of the nexus, the two cell membranes are in intimate contact. In spite of the appearance of a narrow gap, the cells are not truly separated by an extracellular space. By using lanthanum as extracellular tracer or with freeze fracture techniques, it was shown that the nexus is composed of a regular arrangement of subunits, which span the narrow extracellular gap. A combined study by electronmicroscopy and low angle X-ray diffraction gave some insight into tne ultrastructural organization of the nexus. The subunits appear to be packed in a hexagonal array with a 10 nm center-to-center spacing, leaving a central hole, probably an aequous channel, with a diameter of the order of 1-2 nm. From this a picture emerged, indicating that six protein subunits compose a junctional channel, the connexon (Makowski et al., 1977). The connexons are embedded in the apposed membranes. Operational channels consist of connexons in register, linked to each other.

Nexal structures of this kind have not only been found in the working myocardium (ventricular and auricular muscle) but also in the specialized tissues of the heart, such as Purkinje fibres, AV-nodal and SA-nodal tissue (for references, see Pollack, 1976, and De Mello, 1977; Irisawa, 1978; Pévet-Masson, 1979). Furthermore, nexus have been described for hearts of various species, including vertebrates and invertebrates.

3. FUNCTIONAL PROPERTIES OF THE NEXUS

The functional significance of the nexus was first convincingly demonstrated by Barr, Dewey and Berger (1965). They found interruption of current flow from cell to cell under the experimental conditions of stretch and hypertonicity. EM pictures showed a separation of the nexal membranes caused by these interventions, thus providing evidence that the nexus must be responsible for normal intercellular current flow.

Cardiac tissue may be looked at as either a diffusional or as an electrical syncytium. As a matter of fact, both points of view have led to a number of studies in which attempts were made to determine the properties of the nexus as a chemical or a physical barrier. Diffusional investigations made it clear that the nexus might play an important role in the metabolic cooperation between cardiac cells, whereas the electrical studies clearly

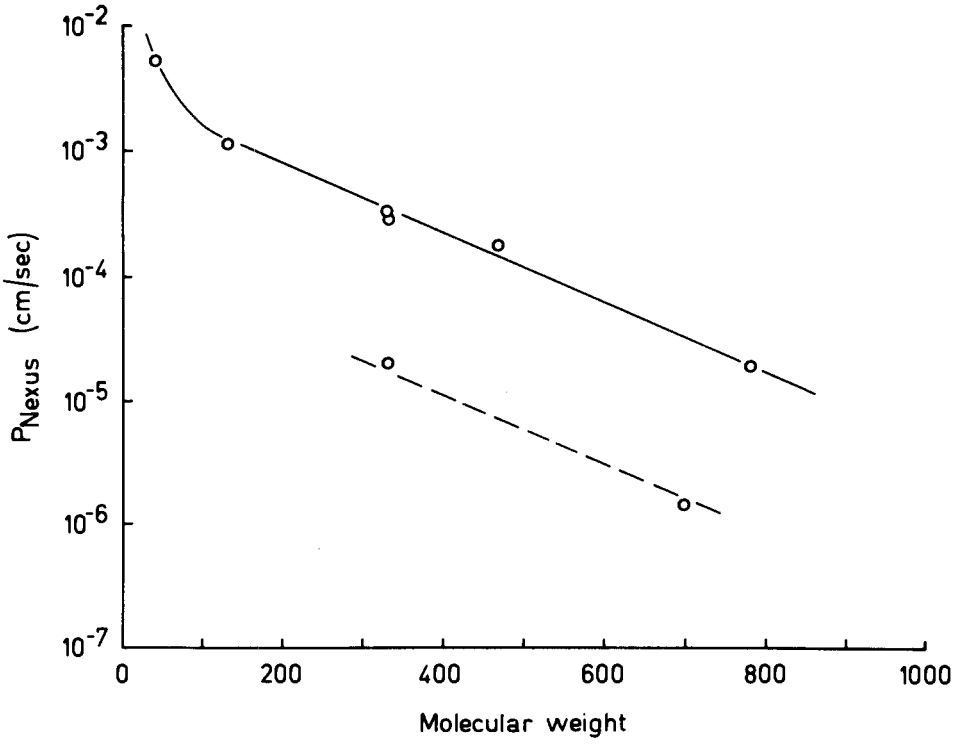

Fig. 1. Permeability of the nexal membrane to substances of various molecular weight: K^+, 39; TEA^+, 130; $cAMP^-$, 328; $fluoresceinate^-$, 332; $DBcAMP^-$, 469; procion $yellow^{3-}$, 697; digoxin, 781 (cf. Weingart, 1974; Pollack, 1976; Tsien and Weingart, 1976; Hess and Müller, in prep.). P_{nexus} has been re-calculated in some cases in order to use consistent values for h (interdisk distance) and q (ratio nexal membrane area to cross-section area of a cell). Ventricular muscle: h = 125 μ; q = 0.382; Purkinje fibre: h = 82 μ; q = 2.79. All values are normalized to 37° C.

demonstrated that impulse propagation is via electrotonic current spread from cell to cell.

Weidmann (1966) measured the ^{42}K diffusion within ventricular muscle bundles. He found that the tracer redistributed over many cell lengths, supporting the idea that K^+ ions are the major carrier for intercellular current flow. The diffusivity of a number of larger particles has been

characterized by other investigators. Fig. 1 compares the calculated permeability of the nexal membrane to the tested substances with their molecular weight. Purkinje fibres (- - -) seem to possess less permeable nexus than ventricular muscle (——). This surprising finding could either reflect a genuine difference in pore size or a difference in the connexon packing density of the two tissues. Fig. 1 also suggests that the cut-off limit for permeation must be beyond the largest tested particle in this tissue, i.e. 800 daltons (digoxin; Hess and Müller, in prep.). The dimensions of procion yellow (0.5 x 1 x 2.7 nm) establish 1 nm as a plausible lower limit for the effective diameter of a nexal channel.

The functional significance of the nexus is further documented by electrical measurements. A convenient way to study the current spread in an excitable tissue is by means of cable analysis. It is usually performed by passing current at one point, and measuring the resulting voltage deflections at various distances. Over the length of a space constant λ, the size of the membrane voltage deflection decreases by a factor of e, i.e. from 100 % to 37 %. In cardiac tissue, values of λ range from 0.4 mm in the AV-node (De Mello, 1977) to 2.0 mm in the Purkinje fibre (Weidmann, 1952). The length of an individual cell in these tissues has been estimated as 20 μ and 80 μ, respectively, suggesting that λ is one order of magnitude larger. Electrotonic current spread over many cell lengths implies that the cell-to-cell resistance must be low.

Structurally, cardiac tissue is highly anisotropic, and yet, most studies of λ were performed by forcing current to flow parallel to the main axis of the individual cells. Only few investigations dealt with current spread transversely to the long cell axis. In these studies, performed on mammalian working myocardium (Woodbury and Crill, 1961; Sakson, 1974; Clerc, 1976) and SA-node (Bukauskas et al., 1977), the ratio of the resistance in the transverse and the longitudinal direction was found to be 2 to 4. Differences in conduction velocity measured in the two directions can fully be accounted for by the disparity in intracellular resistances (Clerc, 1976).

How do the results of the chemical and the physical analysis compare with each other? Quantitative information about the nexal properties can be extracted from both experimental approaches. For a comparison, the data by Weidmann (1966; 1970) on calf ventricular muscle have been chosen. In both

DIFFUSIONAL ANALYSIS (^{42}K)	ELECTRICAL ANALYSIS
$P_{disk} = \frac{1}{h} \cdot \frac{D_s \cdot D_{app}}{D_s - D_{app}} = 2.0 \cdot 10^{-3}$ CM/SEC	$R_i = 470$ ΩCM $R_s = 180$ ΩCM $R_{disk} = 3.6$ ΩCM^2
$G_{disk} = a_K^i \cdot P_{disk} \cdot \frac{F^2}{RT} = 0.66$ S/CM^2	$G_{disk} = 0.28$ S/CM^2

ASSUMPTION: $D_s = 0.5\ D_{H_2O}$

$h = 125\ \mu$ (INTERDISK DISTANCE)

Fig. 2. Conduction of the intercalated disk, G_{disk}, of calf ventricular muscle. In one case, the calculation is based on the apparent axial diffusion coefficient for ^{42}K, D_{app} (Weidmann, 1966), and in the other case, it is based on the intracellular longitudinal resistance, R_i (Weidmann, 1970) and the sarcoplasmic resistivity, R_s (Chapman and Fry, 1978), corrected for 37° C ($Q_{10} = 1.37$).

cases, the experimentally determined quantity (apparent diffusion coefficient, D_{app}, and inside longitudinal resistance, R_i) was considered to reflect the contribution of two elements in series, the sarcoplasm (D_s and R_s, respectively) and the nexus. Fig. 2 summarizes the formalism used to calculate the conductance of the intercalated disk, G_{disk}. The values obtained for G_{disk} of 0.66 S/cm^2 and 0.28 S/cm^2 are reasonably close, suggesting that the two methods presumably investigate the same basic structure.

4. MODULATION OF THE NEXUS RESISTANCE

It has been known for some time that the "transfer" properties of the nexus show a degree of plasticity. Loewenstein (1975) suggested that, in insect salivary glands, the nexal conductance might be controlled in a

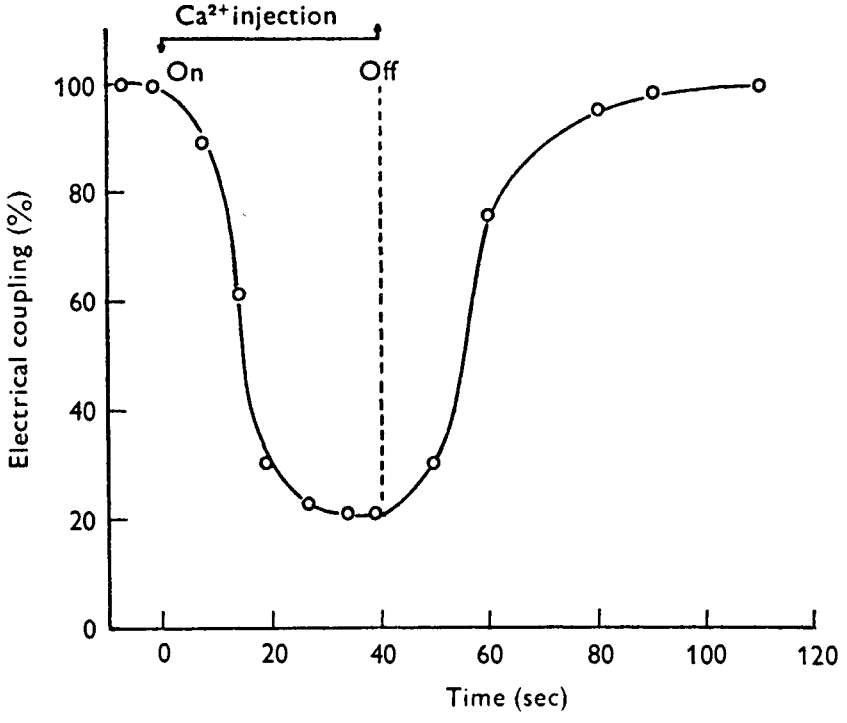

Fig. 3. Effect of Ca^{2+} on cell communication in a dog Purkinje fibre. Electrophoretic injection of Ca^{2+} into a single cell caused partial electrical uncoupling. The cell coupling was spontaneously re-established after interruption of the injection. From De Mello, J. Physiol. 250 (1975).

graded fashion by the $[Ca^{2+}]_i$. Recent observations seem to indicate that such a mechanism also operates in cardiac tissue.

De Mello (1975), when electrophoretically injecting Ca^{2+} into a single cell of a Purkinje fibre, observed a gradual decrease in electrical coupling (Fig. 3). The subsequent recovery from this uncoupling takes place presumably because the extra Ca^{2+} is either extruded from the cell or sequestered by intracellular stores (SR or mitochondria). A number of experimental interventions are known which produce partial or total uncoupling by way of a secondary increase in $[Ca^{2+}]_i$, such as Na^+ injection, exposure to cardiac glycosides, dinitrophenol, or hypoxia (for references, see De Mello, 1980;

Wojtczak, 1979). Injection studies also revealed that different cations, Sr^{+}, Mn^{2+}, or La^{3+}, can substitute for Ca^{2+} in the cell uncoupling process (De Mello, 1980). Very recently, Hermsmeyer (1980) reported that angiotensin II, a polypeptide, produces an increase of the electrical coupling in mammalian ventricular muscle. The mechanism of this so far unique observation is not clear.

How much Ca is required to induce decoupling? We know that the first signs of electrical uncoupling occur at an intracellular Ca^{2+} higher than that for tension activation (Weingart, 1977). This information comes from a comparison of the electrical uncoupling and the development of resting tension under the influence of ouabain. A different approach has been taken by Nishiye et al. (1980), who studied the Ca^{2+} binding of isolated cardiac nexus membranes by means of atomic absorption spectroscopy. The Ca^{2+} binding appears to take place in two discrete steps, displaying apparent dissociation constants of 1.3×10^{-7} M and 5.4×10^{-4} M respectively. It is tempting to speculate that one process controls the maintenance of the structural organization, while the other might be responsible for the reversible reactions involved in electrical uncoupling. Dahl and Isenberg (1980) attempted to correlate electrical decoupling in Purkinje fibres, induced by either dihydro-ouabain or dinitrophenol, with changes in the cellular Ca^{2+} level as monitored by a Ca^{2+}-sensitive microelectrode. Assuming a homogeneous distribution of Ca^{2+} inside the cells, 1.5 µM might represent the threshold Ca^{2+} concentration for the first measurable signs of decoupling.

Recently, it has been reported that intracellular H^{+} play a role in the control of the nexal conductance in early embryos of Xenopus frogs (Turin and Warner, 1980) and in pancreatic acinar cells from mice (Iwatsuki and Petersen, 1979). We have investigated whether protons exert a similar effect in sheep cardiac Purkinje fibres (Weingart and Reber, 1979). Two sets of experiments were carried out to monitor pH_i and to determine the cable parameters by performing conventional linear cable analysis. pH_i was manipulated either by addition of 15 mM NH_4Cl or by varying P_{CO_2} in the bathing medium. Intracellular alkalinization led to a moderate and reversible decrease in R_i (15 %), whereas acidification produced an increase (30 %). In a separate study we have investigated possible changes in pCa_i under the same pH interventions, using Ca-sensitive microelectrodes (Hess and Weingart, 1980). We

found that the cellular alkalinization was accompanied by an increase of $[Ca^{2+}]_i$, whereas acidification was associated with a decrease of $[Ca^{2+}]_i$. These observations suggest that protons might have a direct effect on the nexal membrane rather than an indirect one via secondary alteration of pCa_i. Thus it seems as if Ca^{2+} and H^+ could independently modify the properties of the nexal junction.

5. MODULATION OF THE NEXUS STRUCTURE

Ultrastructural changes of the nexus correlated with functional uncoupling have recently been observed by several investigators. Peracchia and Dulhunty (1976) studied the influence of dinitrophenol on the gap junction of the crayfish axon. They found an increase in R_j which was parallelled by a change in the structure of the junction. The structural change was characterized by a tighter and more regular packing of the intermembrane particles, a decrease in the overall width of the junction and the thickness of the gap. In experiments on Purkinje fibres, Dahl and Isenberg (1980) found a good temporal correlation between functional and similar structural alterations of the nexus induced by dinitrophenol or dihydro-ouabain. The critical $[Ca^{2+}]_i$ required for the particles to aggregate into regular hexagonal arrays seems to be somewhat larger than 5×10^{-7} M (Peracchia, 1977; Dahl and Isenberg, 1980). Peracchia and Peracchia (1978) tested the effect of protons on the gap junctions isolated from fibre cells of calf lens. At pH 6.5 or lower, they observed a transition from a disorderly to a crystalline particle packing. But quite different from the modifications induced by Ca^{2+}, each particle seemed to be composed of 4 instead of 6 subunits only. In conjunction with the physiological results (previous page), these data suggest that both Ca^{2+} and H^+ may independently cause cell uncoupling by acting directly on the junctional molecules.

What is the current view about the closing mechanism of a nexal channel? Unwin and Zampighi (1980) investigated the three-dimensional structure of isolated rat hepatocyte junctions by using Fourier methods for the analysis of the electronmicrographs. Depending on the preparation procedure, they found two different configurations of the connexons, presumably corresponding to the open and closed state of a junctional channel. According to their study, the 6 protein subunits forming a connexon are at different angular positions about the 6-fold axes on the two faces of the embedding

membrane, and thus must be inclined in their passage through the membrane. The transition from the open to the closed configuration of the hexagon seems to be produced by a radial inward motion of the subunits and a reduction of their inclination tangential to the 6-fold axis. It remains to be seen whether or not this model also applied to the structural changes of the nexus induced by Ca^{2+} and H^{+}.

Supported by the Swiss National Science Fouancation (3.565.0.79).

REFERENCES

Barr, L., Dewey, M.M. and Berger, W. (1965). Propagation of action potentials and the structure of the nexus in cardiac muscle. J. gen. Physiol. 48, 797-823.

Bukauskas, F.F., Veteikis, R.P., Gutman, A.M. and Mutskus, K.S. (1977). Intercellular coupling in the sinus node of the rabbit heart. Biofizika 22, 108-112.

Chapman, R.A. and Fry, C.H. (1978). An analysis of the cable properties of frog ventricular myocardium. J. Physiol. (Lnd.) 283, 263-282.

Clerc, L. (1976). Directional differences of impulse spread in trabecular muscle from mammalian heart. J. Physiol. (Lnd.) 255, 335-346.

Dahl, G. and Isenberg, G. (1980). Decoupling of heart muscle cells: Correlation with increased cytoplasmic calcium activity and with changes of nexus ultrastructure. J. Membr. Biol. 53, 63-75.

De Mello, W.C. (1975). Effect of intracellular injection of calcium and strontium on cell communication in heart. J. Physiol. (Lnd.) 250, 231-245.

De Mello, W.C. (1977). Passive electrical properties of the atrio-ventricular node. Pflüg. Arch. 371, 135-139.

De Mello, W.C. (1980). Intercellular communication and junctional permeability. In: Membrane Structure and Function, Vol. 3, Ed. E.E. Bittar, John Wiley & Sons, New York, pp. 127-170.

Hermsmeyer, K. (1980). Angiotensin II increases electrical coupling in mammalian ventricular myocardium. Circul. Res. (in press).

Hess, P. and Müller, P. Extra- and intracellular digoxin effects on contraction of cow and calf trabecular myocardium, using a digoxin-albumin macromolecule, its fab-antibody and a cut-end method for intracellular glycoside application (in preparation).

Hess, P. and Weingart, R. (1980). Intracellular free calcium modified by pH_i in sheep cardiac Purkinje fibres. J. Physiol. (Lnd.) (in press).

Irisawa, A. (1978). Fine structure of the small sinoatrial node specimen used for the voltage clamp experiment. In: The Sinus Node, Ed. F.I.M. Bonke, Martinus Nijhoff Medical Division, The Hague, pp. 311-319.

Iwatsuki, N. and Petersen, O.H. (1979) Pancreatic acinar cells: The effect of carbon dioxide, ammonium chloride and acetylcholine on intercellular communication. J. Physiol. (Lnd.) 291, 317-326.

Loewenstein, W.R. (1975). Permeable junctions. Cold Spring Harbor Symp. Quant. Biol. 40, 49-63.

Makowski, L., Caspar, D.L.D., Phillips, W.C. and Goodenough, D.A. (1977). Gap junction structures. II. Analysis of the X-ray diffraction data. J. Cell Biol. 74, 629-645.

McNutt, N.S. and Weinstein, R.S. (1973). Membrane ultrastructure at mammalian intercellular junctions. Progr. Biophys. Mol. Biol. 26, 45-101.
Nishiye, H., Mashima, H. and Ishida, A. (1980). Ca binding of isolated cardiac nexus membranes related to intercellular uncoupling. Jap. J. Physiol. 30, 131-136.
Peracchia, C. (1977). Changes in gap junctions with uncoupling are a calcium effect. J. Cell Biol. 75, 65a.
Peracchia, C. & Dulhunty, A.F. (1976). Low resistance junctions in crayfish. J. Cell Biol. 70, 419-439.
Peracchia, C. and Peracchia, L.L. (1978). Orthogonal and rhombic arrays in gap junctions exposed to low pH. J. Cell Biol. 79, 217a.
Pévet-Masson, M.A. (1979). The fine structure of cardiac pacemaker cells in the sinus node and in tissue culture. Ph.D. Thesis, University of Amsterdam, 1979.
Pollack, G.H. (1976). Intercellular coupling in the atrioventricular node and other tissues of the rabbit heart. J. Physiol. (Lnd.) 255, 275-298.
Sakson, M.E., Bukauskas, F.F., Kukushkin, N.I. and Nasanova, V.V. (1974). Study of electronic distribution on the surface of cardiac structures. Biofizika 19, 1045
Schleiden, M.J. (1838). Beiträge zur Phytogenesis. Arch. Anat. Physiol. Wiss. Med., 137-176.
Sjöstrand, F.S. and Andersson, E. (1954). Electron microscopy of the intercalated disks of cardiac muscle tissue. Experientia 10, 369-370.
Tsien, R.W. and Weingart, R. (1976). Inotropic effect of cyclic AMP in calf ventricular muscle studied by a cut end method. J. Physiol. (Lnd.) 260, 117-141.
Turin, L. and Warner, A.E. (1980). Intracellular pH in early Xenopus embryos: its effect on current flow between blastomeres. J. Physiol. (Lnd.) 300, 489-504.
Unwin, P.N.T. and Zampighi, G. (1980). Structure of the junction between communicating cells. Nature 283, 545-549.
Weidmann, S. (1952). The electrical constant of Purkinje fibres. J. Physiol. (Lnd.) 118, 348-360.
Weidmann, S. (1966). The diffusion of radiopotassium across intercalated disks of mammalian cardiac muscle. J. Phyisol. (Lnd.) 187, 323-342.
Weidmann, S. (1970). Electrical constants of trabecular muscle from mammalian heart. J. Physiol. (Lnd.) 210, 1041-1054.
Weingart, R. (1974). The permeability to tetraethylammonium ions of the surface membrane and the intercalated disks of sheep and calf myocardium. J. Physiol. (Lnd.) 240, 741-762.
Weingart, R. (1977). The actions of ouabain on intercellular coupling and conduction velocity in mammalian ventricular muscle. J. Physiol. (Lnd.) 264, 341-365.
Weingart, R. and Reber, W. (1979). Influence of internal pH on r_i of Purkinje fibres from mammalian heart. Experientia 35, 929.
Wojtczak, J. (1979). Contractures and increase in internal longitudinal resistance of cow ventricular muscle induced by hypoxia. Circul. Res. 44, 88-95.
Woodbury, J.W. and Crill, W.E. (1961). On the problem of impulse conduction in the atrium. In: Nervous Inhibition, Ed. E. Florey, Pergamon Press, Oxford, pp. 124-135.

Adv. Physiol. Sci. Vol. 8. Cardiovascular Physiology. Heart, Peripheral Circulation and Methodology
A. G. B. Kovách, E. Monos, G. Rubányi (eds)

INTRACELLULAR CHLORIDE ACTIVITY IN CAT VENTRICULAR MUSCLE

Kenneth W. Spitzer and John L. Walker
Department of Physiology, College of Medicine, University of Utah, Salt Lake City, Utah, USA

High levels of intracellular chloride activity, $a_i(Cl)$, have been reported for cardiac Purkinje fibers (Spitzer, et al, 1978; Vaughan-Jones, 1979a). However, except for brief reports (Baumgarten and Fozzard, 1978; Vaughan-Jones, 1979a) we are unaware of any other studies of intracellular chloride activity in mammalian ventricular muscle. Non-passive distribution of chloride could have important physiological implications. This report examines the state of intracellular chloride in resting mammalian ventricular muscle cells.

METHODS

Papillary muscles isolated from the ventricles of young cats were used for this study. The preparations were placed in a tissue bath where they were left unstimulated while being superfused with Tyrode's solution at a constant temperature, either 25°C or 37°C. pH was maintained at 7.4. Intracellular chloride activity was determined from multiple impalements (5 - 15) of cells near the endocardial surface using chloride liquid ion exchanger microelectrodes (Walker, 1971) and conventional microelectrodes for measurement of the resting membrane potential, E_M. In a given muscle, E_M and ΔE, the transmembrane potential difference measured with the chloride electrode (Walker, 1971), varied no more than 1 to 4 mv from cell to cell. Calibration of the chloride microelectrodes and the calculation of $a_i(Cl)$ have been previously described (Spitzer and Walker, 1980). The chloride equilibrium potential, E_{Cl}, and the predicted $a_i(Cl)$ were calculated from the Nernst equation. The reference electrode for E_M and chloride electrode measurements was either a 3 M KCl flowing liquid junction or a chloridized silver wire inside a glass tube filled with the same solution as that in the tissue bath.

Normal Tyrode's solution contained 146 mM chloride, 2.7 mM calcium, 0.5 mM magnesium, 5.5 mM glucose and either 2.7 mM, 4.4 mM or 5.4 mM potassium. Sodium concentrations were 155.0 mM, 153.3 mM and 152.3 mM respectfully. Bicarbonate buffered solutions contained 18.0 mM bicarbonate and were equilibrated with 5% CO_2-95% O_2. HEPES buffered solutions contained 12.0 mM HEPES and were gassed with 100% O_2. Low chloride solutions were prepared by replacing sodium chloride with sodium glucuronate and in some cases by also replacing potassium chloride with potassium bicarbonate. The chloride microelectrode has a high selectivity for chloride with respect to glucuronate but, glucuronate has the disadvantage of binding

calcium and thus reducing the calcium activity in the Tyrode's solution (Spitzer and Walker, 1980). Calcium activity in glucuronate containing solutions was measured with a calcium electrode and adjusted to the control value by addition of calcium chloride.

RESULTS

The relationship between $a_i(Cl)$ and the elapsed time after removal of the heart is illustrated in Figures 1 and 2 for muscles exposed to both 2.7 mM and 5.4 mM $[K]_o$. The average value of E_M is shown in parentheses for muscles for which more than one set of measurements are included. Both $a_i(Cl)$ and E_M remained fairly constant for up to ten hours. Furthermore, $a_i(Cl)$ was 2-4 times greater than predicted assuming chloride distribution was passive, i.e. $E_M = E_{Cl}$.

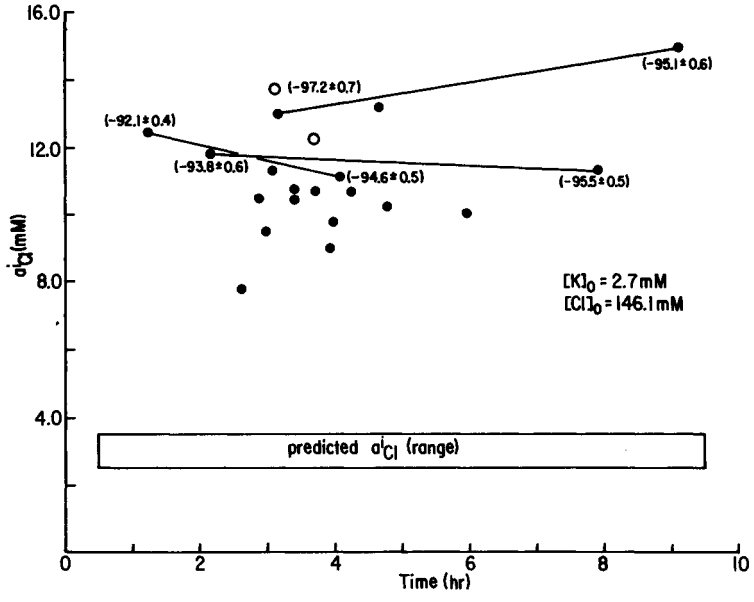

Fig. 1. Intracellular chloride activity in cat papillary muscle as a function of elapsed time between removal of the heart and the first chloride measurement. The measurements were carried out at 37°C in the presence of 2.7 mM $[K]_o$ and bicarbonate buffer. Points connected by lines are measurements in the same muscle. The open circles are trabecular muscles. The numbers in parentheses are means and standard errors.

Since the chloride microelectrode is not perfectly selective for chloride, interference from other anions must be considered. The only significant interfering anion in the Tyrode's solution is bicarbonate, i.e. the electrode is only approximately ten times more sensitive to chloride than to bicarbonate. This error was taken into account during the calibration of the microelectrode. However, the contribution of intracellular interferents to the measured (apparent) value of $a_i(Cl)$ is difficult to assess.

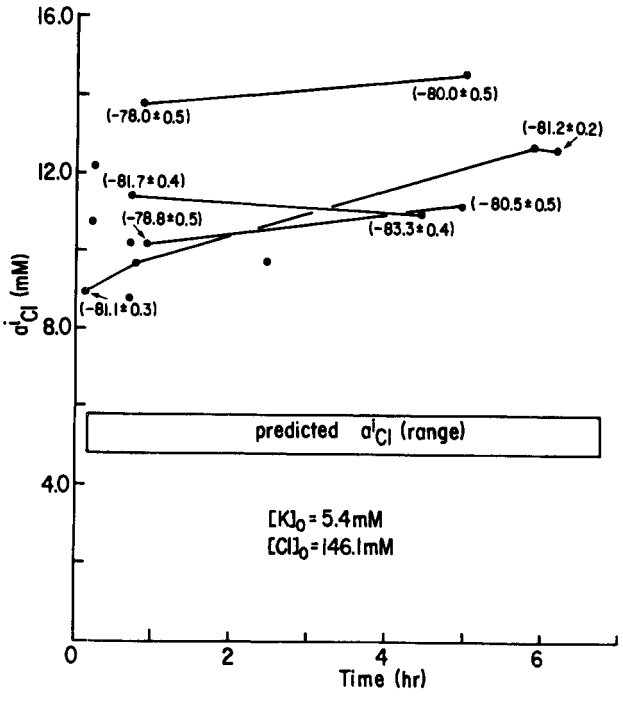

Fig. 2. Intracellular chloride activity in cat papillary muscle as a function of elapsed time between removal of the heart and the first chloride electrode measurement. The measurements were carried out at 37°C in the presence of 5.4 mM $[K]_o$ and bicarbonate buffer. Points connected by a line are measurements in the same muscle. The numbers in parentheses are means and standard errors. (From Spitzer and Walker, 1980).

Experimental estimates of interference were made by exposing muscles to low chloride solutions, the assumption being that the measured chloride activity under these conditions estimates the maximum intracellular interference. Figure 3 illustrates the effects of lowering $[Cl]_o$ from 146 mM ($a_o(Cl)$ = 108.3 mM) to 13.3 mM ($a_o(Cl)$ = 9.8 mM). The membrane potential remained constant while $a_i(Cl)$ decrease from 9.5 mM to 2.8 mM. Upon return to control $[Cl]_o$, $a_i(Cl)$ fully recovered. In several muscles continuous impalements of the same cell were maintained while changing from normal to low chloride solution. Under these conditions transient changes in E_M were observed which were the result of a liquid junction potential between the interstitial space of the muscle and the bulk solution (Spitzer and Walker, 1979).

The results of superfusing five other muscles with 13.3 mM $[Cl]_o$ are summarized in Figure 4. Data points from Figure 3 are included. Intracellular chloride activities ranged from 2.4 mM to 2.9 mM following at least two hours of exposure to low $[Cl]_o$. The same results were obtained from two muscles superfused with 5.4 mM $[K]_o$ and exposed to low $[Cl]_o$. In addition, reduction of $[Cl]_o$ to 6.4 mM ($a_o(Cl)$ = 4.7 mM) did not

significantly lower $a_i(Cl)$ below that found in 13.3 mM $[Cl]_o$ in either 2.7 mM or 5.4 mM $[K]_o$.

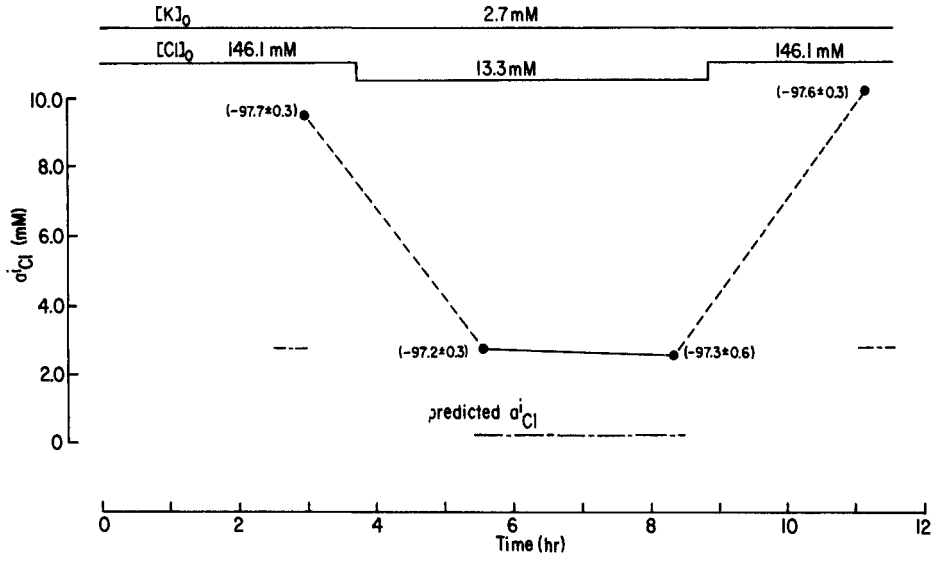

Fig. 3. Change in $a_i(Cl)$ as the result of changing $[Cl]_o$. The muscle was isolated at zero time and placed in the control solution, after which $[Cl]_o$ was reduced and then returned to normal. The measurements were carried out at 37°C in the presence of bicarbonate buffer. The numbers in parentheses are means and standard errors.

Glucuronate reduced the calcium activity in the low chloride solution of Figure 3 by 56%. However three other experiments in which calcium activity was held constant (closed circles, Figure 4) yielded essentially the same value of $a_i(Cl)$ in low $[Cl]_o$. Also shown in Figure 4 are two experiments demonstrating that there was no further reduction in $a_i(Cl)$ in the absence of external bicarbonate. This is in accord with the calculations indicating that interference from intracellular bicarbonate should be no greater than 1-2 mM.

Assuming that the apparent $a_i(Cl)$ measured during low chloride superfusion actually represents intracellular interferents, the upper limit of interference, in either 2.7 mM or 5.4 mM $[K]_o$, is 2-5 mM. Thus, $a_i(Cl)$ in the control chloride solution would be overestimated by the same amount assuming interference was the same in control and low chloride solutions. Even when this correction is made however, measured $a_i(Cl)$ exceeds predicted $a_i(Cl)$ at each level of $[K]_o$, as shown in Figure 5. This correction has not been applied to any of the data presented here. Also included in Figure 5 are $a_i(Cl)$ values from nine muscles equilibrated for several hours in HEPES buffered solutions.

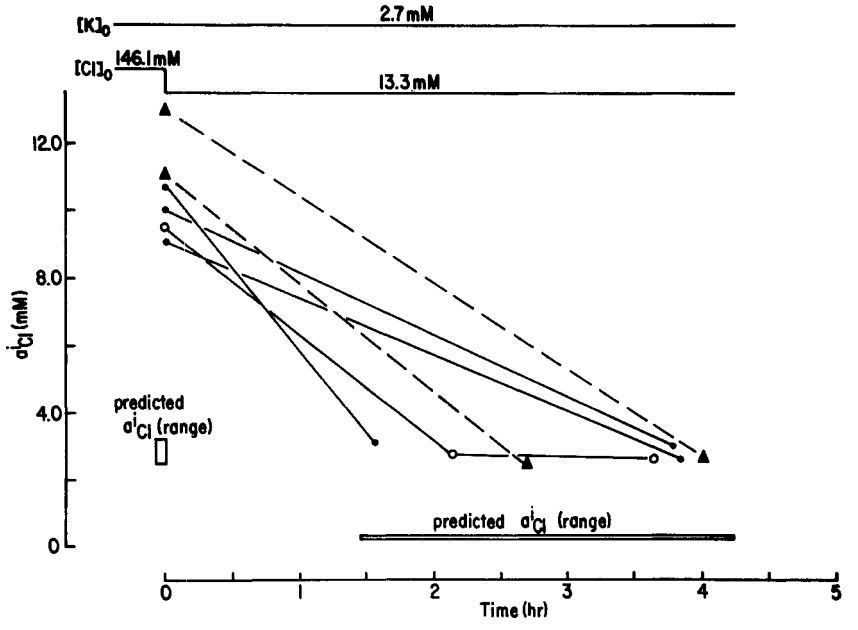

Fig. 4. Change in $a_i(Cl)$ as the result of reducing $[Cl]_o$. Data points for individual muscle are connected only for clarity of presentation and the lines are not intended to represent actual time courses. The triangles represent HEPES buffered solution, closed circles bicarbonate buffered solution with normal calcium activity and open circles low calcium activity in the low chloride solution. (From Spitzer and Walker, 1980).

A summary of the measurements of E_M, E_{Cl} and $a_i(Cl)$ is provided in Table 1. Each of the forty seven muscles was equilibrated in only one of the solutions. E_{Cl} ranges from 20-30 mv positive with respect to E_M. Ten muscles equilibrated for at least two hours in either 2.7 or 5.4 mM $[K]_o$ at 25°C, gave mean values of $a_i(Cl)$ that were not significantly different from those at 37°C. The values are means and standard errors. All solutions contained 146 mM $[Cl]_o$ and all were buffered with bicarbonate except the one in the second row which was buffered with HEPES.

DISCUSSION

These experiments demonstrate that intracellular chloride activity in quiescent cat papillary muscle is greater than expected assuming $E_{Cl} = E_M$, even after the upper limit of intracellular interference, 2-3 mM, is subtracted from the measured value. Thus chloride appears to enter these cells against its electrochemical gradient.

If chloride was passively distributed in the beating heart the mean membrane potential would be such that $a_i(Cl)$ and E_{Cl} would be about what

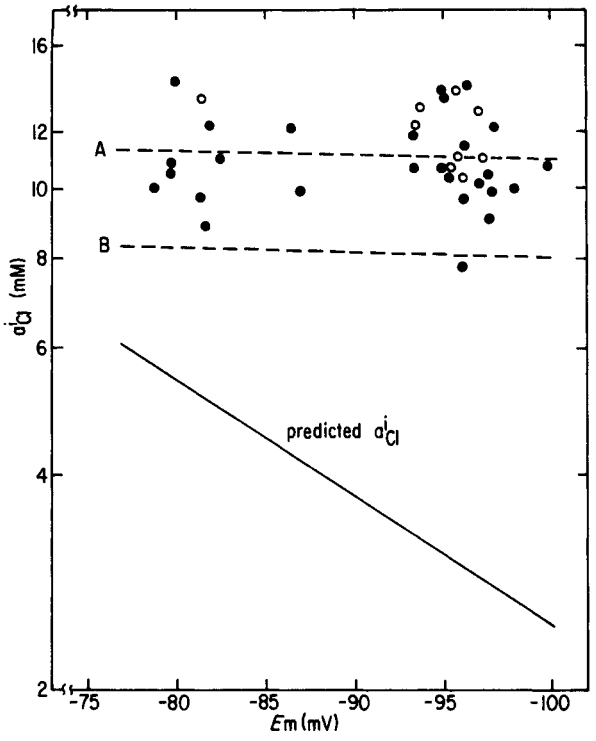

Fig. 5. Intracellular chloride activity as a function of membrain potential. For the left most group of points $[K]_o$ = 5.4 mM, for the two points in the center 4.4 mM and for the points to the right 2.7 mM. The open circles represent HEPES buffered solution and the closed circles bicarbonate buffered solution. Line A is the least squares linear regression and line B is the result of subtracting 3 mM from line A to correct for intracellular interference. The correlation coefficient for line A is -0.06 and the slope is not significantly different from zero. The line for predicted $a_i(Cl)$ assumes passive distribution. (From Spitzer and Walker, 1980.)

we are reporting for quiescent myocardium (Hutter and Noble, 1961). It seems reasonable to expect however, that $a_i(Cl)$ and E_{Cl} would decrease (i.e. E_{Cl} become more negative) with time after the muscle becomes quiescent. This should be especially evident in 2.7 mM $[K]_o$ which produces a resting potential of -96 mv. That value is 20-30 mv more negative than the average membrane potential during a cardiac cycle in a beating preparation. A rough calculation indicates that $a_i(Cl)$ should decline with a time constant of about thirteen minutes even if chloride conductance was as low as 0.008 mmho/cm^2. No such decline was observed in 2.7 mM $[K]_o$ despite up to nine hours of constant $a_o(Cl)$ and E_M (see Figure 1). The return of $a_i(Cl)$ to its original high level following low chloride superfusion is also incompatible with a passive distribution.

Table 1. Membrane potential, $a_i(Cl)$ and E_{Cl} in cat ventricular myocardial cells.

$[K]_o$ (mM)	E_M (mv)	E_{Cl} (mv)	$a_i(Cl)$ (mM)	No. of Muscles
		37°C		
2.7	-96.2 ± 0.2	-60.9 ± 0.9	11.2 ± 0.4	18
2.7	-95.8 ± 0.2	-59.0 ± 0.9	12.0 ± 0.4	8
4.4	-86.8 ± 0.3	-61.1 ± 2.6	11.1 ± 1.1	2
5.4	-80.6 ± 0.2	-60.9 ± 1.0	11.2 ± 0.4	9
		25°C		
2.7	-94.7 ± 0.3	-60.3 ± 0.9	10.4 ± 0.4	5
5.4	-79.2 ± 0.2	-55.4 ± 1.72	12.8 ± 0.8	5

Although we found similar values of steady state $a_i(Cl)$ at both 37°C and 25°C, chloride flux has been reported to be temperature sensitive in Purkinje fibers (Vaughan-Jones, 1979b). We did not examine this point but a temperature sensitivity of chloride flux would likely have produced changes in steady state $a_i(Cl)$ had we subjected the muscles to lower temperatures for longer periods of time. It is of interest to note however, that Lee and Fozzard (1975) reported that $a_i(K)$ was essentially the same at 35°C and 25°C in rabbit papillary muscle.

In summary, the results of the present study indicate that a significant component of chloride movement into cat ventricular muscle cells occurs against an electrochemical gradient. The mechanism of the process is unclear, although links with sodium and bicarbonate have been suggested (Russell, 1979; Vaughan-Jones, 1979b). The results presented here provide base line data for further studies of the problem of chloride distribution in heart muscle.

REFERENCES

Baumgarten, C.M. and Fozzard, H.A. (1978). Intracellular Cl activity of skeletal and heart muscle. Biophys. J. 21, 182a.

Hutter, O.F. and Noble, D. (1961). Anion conductance of cardiac muscle. J. Physiol. (London) 157, 335-350.

Lee, C.O. and Fozzard, H.A. (1975). Activities of potassium and sodium ions in rabbit heart muscle. J. Gen. Physiol. 65, 695-708.

Russell, J.M. (1979). Chloride and sodium influx: A coupled uptake mechanism in the squid giant axon. J. Gen. Physiol. 73, 801-818.

Spitzer, K.W., Walker, J.L. and Weir, W.G. (1978). Intracellular chloride activity in cardiac Purkinje fibers. Biophys. J. 21, 182a.

Spitzer, K.W. and Walker, J.L. (1979). Changes in liquid-junction potential following chloride replacement in cat papillary muscle. Pflügers Arch. 382, 281-284.

Spitzer, K.W. and Walker, J.L. (1980). Intracellular chloride activity in quiescent cat papillary muscle. Am. J. Physiol. 238, H487-H493.

Vaughan-Jones, R.D. (1979a). Non-passive chloride distribution in mammalian heart muscle: Micro-electrode measurement of the intracellular chloride activity. J. Physiol. (London) 295, 83-109.

Vaughan-Jones, R.D. (1979b). Regulation of chloride in quiescent sheep heart Purkinje fibres studied using intracellular chloride and pH-sensitive micro-electrodes. J. Physiol. (London) 295, 111-137.

Walker, J.L. (1971). Ion-specific liquid ion exchanger micro-electrodes. Anal. Chem. 43, 89A-93A.

Supported by NIH Grant HL-18053.

Adv. Physiol. Sci. Vol. 8. Cardiovascular Physiology. Heart, Peripheral Circulation and Methodology
A. G. B. Kovách, E. Monos, G. Rubányi (eds)

Ca-DEPENDENT ACTIVATION OF THE K CONDUCTANCE IN VENTRICULAR MUSCLE FIBERS

M. Hiraoka, Y. Okamoto and K. Ikeda
Institute for Cardiovascular Diseases, Tokyo Medical and Dental University, Tokyo 113, Japan

There have been considerable evidences in various tissues that the increased intracellular calcium can activate the membrane potassium conductance (Meech, 1978). In cardiac Purkinje fibers using Ca^{++}-injection technique, Isenberg (1975, 1977 a, b) observed changes compatible with the control of the K conductance by increased internal Ca^{++}. Similar conclusions were given by several others with different experimental approach (Kass and Tsien, 1976; Siegelbaum et al. 1977; Siegelbaum and Tsien, 1980). In mammalian cardiac muscles, evidences supporting this idea were rather few (Bassingthwaighte et al. 1976) and are less direct than the ones presented in Purkinje fibers or in other nervous tissues. Therefore, we investigated this problem in dog ventricular muscle fibers by changing external K^{+} and Ca^{++} concentrations.

METHODS

All the experiments were carried out with fine papillary or trabecular muscles excised from the right ventricle of the dog heart. The usual size of the preparations used for the potential measurement was 2-4 mm in length and 1-2 mm in diameter. The one used for the voltage clamp method was 0.8 mm or less in diameter. Preparations were placed in the tissue chamber and superfused with a normal Tyrode solution having following composition (mM/L); NaCl 137, KCl 2.7, $CaCl_2$ 1.8, $MgCl_2$ 1.0, NaH_2PO_4 0.42, $NaHCO_3$ 15.9, glucose 5.5. The K^{+}-free and the K^{+}-free, Ca^{++}-free solutions were prepared by omitting KCl and/or $CaCl_2$ from the Tyrode solution. Low Cl^{-} solution was made up by replacing NaCl with Na-isethionate. Osmolarity was kept constant by adding sucrose. Ouabain (g-strophanthin; Merck Co., Darmstadt) were added to the bathing media in appropriate amount. The volume of the tissue chamber was about 1.0 ml and the flow rate of superfusates was kept at 3.0-3.5 ml/min. The pH of the solution was adjusted to 7.2-7.3. All the solutions were bubbled with 95% O_2 + 5% CO_2. Temperature of the superfusates was maintained at 37 $\pm$ 0.5°C, except the experiments at low temperature.

Conventional microelectrode technique was used for recording the membrane potential. The membrane current was measured with a single sucrose gap voltage clamp technique. The tension was measured by using an isometric transducer (ME-4021, Medical Electronics Commercial Co., Tokyo).

RESULTS

Resting membrane potential (RMP) in different external K^+ and Ca^{++}

When ventricular muscle fibers were superfused with solutions containing different external K^+ and Ca^{++}, RMP of the preparation varid with the concentrations of both ions. In the Tyrode solution containing 2.7 mM-K^+ and 1.8 mM-Ca^{++}, RMP was -83.4 ± 1.92 mV (mean ± S.D., n = 8). Then, the preparations were superfused with the K^+-free, 1.8 mM-Ca^{++} solution for 30 min. They hyperpolarized and RMP reached to -90.1 ± 3.98 mV at the end of the K^+-free, 1.8 mM-Ca^{++} perfusion. The preparations were, next, soaked in the K^+-free, Ca^{++}-free solution for another 45 min. RMP of the preparation showed some depolarization reaching to -75.0 ± 2.44 mV at the end of this perfusion. After the K^+-free, Ca^{++}-free superfusion, Ca^{++} concentration of the superfusate was suddenly increased to 5.4-7.2 mM while keeping the K^+-free condition. The preparation hyperpolarized to about -90 mV within 10 min. of the start of the K^+-free, high-Ca^{++} superfusion. RMP at this stage was -96.9 ± 5.31 mV. Therefore, the preparation hyperpolarized by 22 mV upon changing the superfusate from the K^+-free, Ca^{++}-free solution to the K^+-free, high-Ca^{++} solution.

We examined whether or not Cl ions might be involved in developing the hyperpolarization in the K^+-free, high-Ca^{++} solution. Four preparations were similarly treated as in the previous experiments described above. RMP in the K^+-free, Ca^{++}-free solution containing 140 mM-Cl was -69.8 ± 16.51 mV (mean ± S.D.; n = 4) and it was -97.3 ± 8.84 mV in the K^+-free, 7.2 mM-Ca^{++} solution, which was most of Cl being replaced by less permeable anion, isethionate, and contained only 16 mM-Cl. Thus, the hyperpolarization was similarly observed as in the normal Cl solution.

The possibility that the hyperpolarization in the K^+-free high-Ca^{++} solution might be caused by the activation of an electrogenic Na-pump was examined, although the K^+-free condition was expected to reduce Na^+-K^+ pump activity (Glynn, 1956). At first, we studied the effect of low temperature on the high-Ca^{++} induced hyperpolarization. At 37°C, the preparation hyperpolarized by 18.2 ± 6.42 mV (mean ± S.D., n = 6) upon changing the superfusate from the K^+-free, Ca^{++}-free solution to the K^+-free, 7.2 mM-Ca^{++} solution. The same procedure was repeated with all six preparations at temperature of 25-27°C. The hyperpolarization was similarly observed as the one at 37°C and the amount of hyperpolarization at low temperature was 14.8 ± 9.38 mV. There was no statistical significance between the degree of hyperpolarization at 37°C and that at 25-27°C.

The effect of ouabain which is known to block Na^+-K^+ pump activity (Skou, 1965) was also studied. The fiber was treated with 10^{-5} M ouabain during the last 15 minutes of the superfusion by the K^+-free, Ca^{++}-free solution. Then, the superfusate was switched to the K^+-free, 7.2 mM-Ca^{++} solution. Six amongst nine preparations showed hyperpolarization of RMP within 10 min of the start of the K^+-free, high-Ca^{++} superfusion. The degree of hyperpolarization was 9.3 ± 3.56 mV (mean ± S.D., n = 6). Three other preparations showed no change or 2-3 mV of depolarization in RMP.

Tension development and RMP in the K^+-free, high-Ca^{++} solution

To see whether or not there are any change in the resting tension associated with the change of the superfusate from the K^+-free, Ca^{++}-free solution to the K^+-free, high-Ca^{++} solution, the isometric tension was measured simultaneously with the membrane potential recording. Figure 1 shows one of actual experimental records. When the superfusate was

switched from the K^+-free solution to the K -free, 7.2 mM-Ca^{++} solution, the resting tension rose quickly within minutes after the start of the latter solution. Then, RMP gradually showed hyperpolarization and it reached a plateau after 5-10 minutes of the start of the K^+-free, high-Ca^{++} superfusion. Six preparations gave similar results as the one in Figure 1. The rise in the resting tension always preceded the hyperpolarization of RMP in all the preparations.

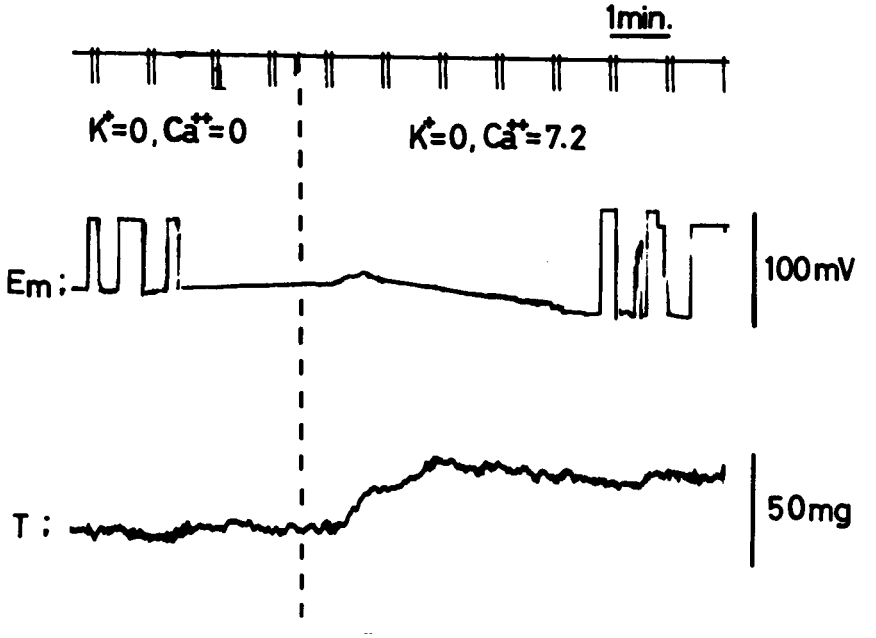

Fig. 1 Simultaneous recordings of RMP and resting tension uppon sudden increase in external Ca^{++} concentration with the K^+-free condition. The upper trace indicates the membrane potential (Em) and the lower is the resting tension (T). Dashed line indicates the time of the solution change from the K^+-free, Ca^{++}-free solution to the K^+-free, 7.2 mM-Ca^{++} solution. In the potential measurements (Em), the electrode was withdrawn repeatedly from the cell in both solutions to assure the zero level.

Membrane current change in the K^+-free, high-Ca^{++} solution

The membrane current was examined by a single sucrose gap voltage clamp technique. Figure 2 shows a steady-state current-voltage relation examined in the different K^+ and Ca^{++} concentrations. The steady-state current was taken from the current value at the end of 1 sec depolarizing or hyperpolarizing pulses. The steady-state current increased in the K^+-free, 7.2 mM-Ca^{++} solution than that in the K^+-free, Ca^{++}-free solution. Similar results as in Figure 2 were obtained in three preparations.

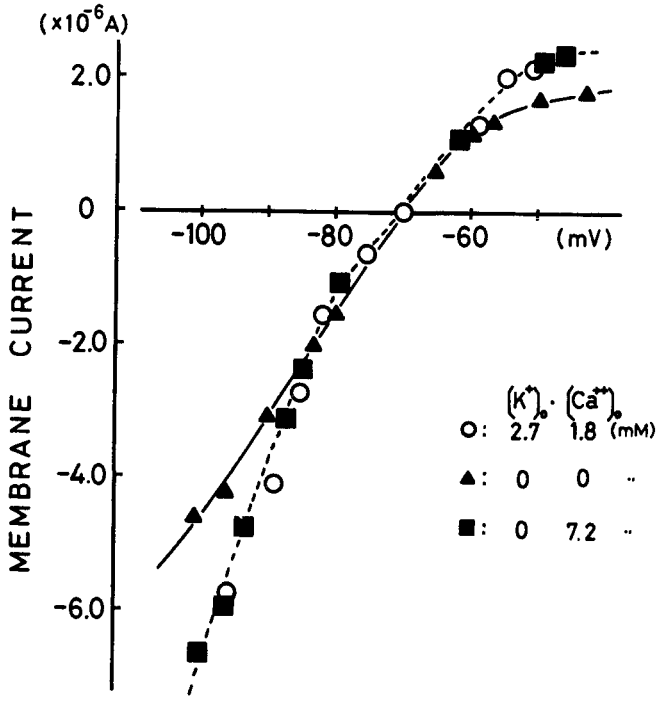

Fig. 2 Current-voltage relationship in different external K^+ and Ca^{++}. Current values were taken from the final values of 1 second - pulses. Note that the current in the K^+-free, 7.2 mM-Ca^{++} solution was larger than the one in the K^+-free, Ca^{++}-free solution.

DISCUSSION

When ventricular muscle fibers were immersed in the K^+-free solution, they hyperpolarized by about 7 mV in RMP, and this behavior contrasted to that of Purkinje fibers which showed marked depolarization in reduced external K^+ (Carmeliet, 1961). The muscle fiber depolarized by 15 mV when it was superfused with the K^+-free, Ca^{++}-free solution. In this state, an abrupt increase in the external Ca^{++} concentrations while keeping the K^+-free condition resulted in hyperpolarization of RMP by 20 mV.

The hyperpolarization in the K^+-free, high-Ca^{++} solution was not caused by Cl^- distribution, since it was also observed in the low Cl^- solution. The hyperpolarization seems not due to the activation of an electrogenic Na^+ pump, since it was seen in the K^+-free condition and with

ouabain-treated fibers, both of which are known to block the Na^+-K^+ pump activity (Glynn, 1956; Skou, 1965). The above assumption was further supported by the fact that lowering the temperature of the superfusate by 10°C did not affect the extent of hyperpolarization.

The hyperpolarization was always preceded by a rise in the resting tension, which indicated an increase in intracellular free Ca^{++}. It was also found that the steady-state current, which represented mostly in iK_1 in ventricular muscles (Trautwein, 1973), was actually increased in the K^+-free, high-Ca^{++} solution. These results might be interpreted that an increase in internal Ca^{++} activated the membrane K conductance in the ventricular muscle, although a direct proof of it was still lacking. In Purkinje fibers, DiFrancesco and McNaughton (1979) concluded that the effects of external Ca^{++} on outward current was an indirect one resulting from K^+ accumulation in the narrow external clefts rather than a direct one on the K channel. If this is the case, the fiber must depolarize, before hyperpolarization occurrs, due to accumulation of K^+ in the narrow spaces in the clefts, thus reducing an electrochemical gradients for K ions across the membrane. Although the record in Figure 1 showed some tendency of slight depolarization before hyperpolarization, we could not see this as a constant findings in other five preparations examined and most of them hyperpolarized without preceding depolarization in RMP. Further, there have been no direct evidences that high external Ca^{++} increased the accumulation of K^+ in heart muscles, so far. Therefore we suppose that K^+ accumulation, solely, can not explain the reason for the hyperpolarization in the K^+-free, high-Ca^{++} solution.

Bassinghwaighte et al. (1976) supposed Ca^{++} accumulation at the inner side of the membrane, judged by reduced E_{Ca}, caused an increase in K^+ current without producing muscle contracture. In contrast to their findings, we observed that a rise in the resting tension always preceded the hyperpolarization. The differences between the two observations must have been in the different experimental approach, since we suddenly increased Ca^{++} gradient across the membrane possibly admitting a large quantity of Ca^{++}-influx into the cells.

The present results showed that the hyperpolarization was easily produced in the K^+-free, high-Ca^{++} solution after the K^+-free, Ca^{++}-free perfusion. In heart muscles, the reduction of external K^+ was shown to reduce the K^+ conductance (Carmeliet, 1961). This may indicate that Ca^{++}-dependent K^+ conductance was more easily activated if the K^+ conductance was reduced than the normal level.

SUMMARY

When the ventricular muscle fiber from the dog heart was superfused with the K^+-free, high-Ca^{++} solution (Ca^{++} = 5.4-7.2 mM) after the K^+-free, Ca^{++}-free superfusion, the fiber hyperpolarized by 20 mV in the resting membrane potential. Hyperpolarization was also observed in the low Cl solution, at low temperature (25-27°C) and with ouabain-treated fibers. Hyperpolarization was always preceded by a rise in the resting tension. The steady-state current, mainly iK_1, was shown to increase in the K^+-free, high-Ca^{++} solution.

These results support the hypothesis that increased internal Ca^{++} activates the membrane K^+ conductance of the ventricular muscle fiber.

This work was supported in parts by the Grant-in-Aid for Scientific

Research from the Ministry of Education, Science and Culture of Japan.

REFERENCES

Bassinghthwaighte, J. B., Fry, C. H. and McGuigan, J. A. S. 1976. Relationship between internal calcium and outward current in mammalian ventricular muscle: a mechanism for the control of the action potential duration? J. Physiol. 262, 15-37.

Carmeliet, E. 1961. Chloride and potassium permeability in cardiac Purkinje fibres. Brussels : Editions Arscia S. A.

DiFrancesco, D. and McNaughton, P. A. 1979. The effects of calcium on outward membrane currents in the cardiac Purkinje fibre. J. Physiol. 289, 347-373.

Glynn, I. M. 1956. Sodium and potassium movements in human red cells. J. Physiol. 134, 278-310.

Isenberg, G. 1975. Is potassium conductance of cardiac Purkinje fibres controlled by (Ca^{2+})? Nature, 253, 273-274.

Isenberg, G. 1977a Cardiac Purkinje fibres. $(Ca^{2+})_i$ controls steady-state potassium conductance. Pflügers Arch. 371, 71-76.

Isenberg, G. 1977b. Cardiac Purkinje fibres. $(Ca^{2+})_i$ controls the potassium permeability via the conductance components gK_1 and gK_2. Pflügers Arch. 371, 77-85.

Kass, R. S. and Tsien, R. W. 1976. Control of action potential duration by calcium ions in cardiac Purkinje fibres. J. gen. Physiol. 67, 599-617.

Meech, R. W. 1978. Calcium dependent potassium activation in nervous tissues. Ann. Rev. Biophys. Bioeng. 7, 1-18.

Siegelbaum, S. A. and Tsien, R. W. 1980. Calcium-activated transient outward current in calf cardiac Purkinje fibres. J. Physiol. 299, 485-506.

Siegelbaum, S. A., Tsien, R. W. and Kass, R. S. 1977. Role of intracellular calcium in the transient outward current of calf Purkinje fibres. Nature, 269, 611-613.

Skou, J. C. 1965. Enzymatic basis for active transport of Na^+ and K^+ acvoss cell membrane. Physiol. Rev. 45, 596-617.

Trautwein, W. 1973. Membrane currents in cardiac muscle fibers. Physiol. Rev. 53, 793-835.

Adv. Physiol. Sci. Vol. 8. Cardiovascular Physiology. Heart, Peripheral Circulation and Methodology
A. G. B. Kovách, E. Monos, G. Rubányi (eds)

ELECTROCHEMICAL INHOMOGENEITY IN UNGULATE PURKINJE FIBERS: MODEL OF ELECTROGENIC TRANSPORT AND ELECTRODIFFUSION IN CLEFTS

J. M. Kootsey*, E. A. Johnson* and J. B. Chapman**

* *Department of Physiology, Duke University Medical Center, Durham, NC, USA*
** *Department of Physiology, Monash University, Clayton, Victoria, Australia*

INTRODUCTION

In any tissue that generates action potentials at a regular rate, such as cardiac muscle, a stationary state is reached at a given constant rate when active transport exactly balances passive transport. Since every cycle in stationary state must be exactly like any other, the passive flux of an ion integrated over one cycle is exactly equal to the active flux of the same ion integrated over the cycle. If the active transport is electrogenic, for example three sodium ions transported for every two potassium ions, then the integrated passive fluxes of those ions must be in the same ratio and the integrated pump current generated by that active flux is equal to the difference between the integrals of the two passive fluxes, i.e. one. Because the duration of the cardiac action potential is comparable to the length of the cardiac cycle, the instantaneous ratio of the fluxes must be of the same order of magnitude as the ratio of the integrated fluxes. Therefore, whatever the magnitudes of the passive ionic currents incurred in generating the action potential, the transport-generated current must be of the same order of magnitude.

Changing the electrical activity, for example increasing the rate of stimulation, must change the passive ionic fluxes; active transport must change accordingly to accommodate the changes in passive fluxes. Such an increase or decrease in pump activity must be reflected in an increase or decrease in pump current. Whenever active transport is electrogenic, then, an inescapable consequence of changing electrical activity is a time-dependent change in membrane current. Such a time-dependent current would be expressed as a change in action potential shape or as a time-varying current in a voltage-clamp experiment.

The generally-accepted mechanism by which the pump changes its activity in response to electrical activity is through a change in chemical composition (i.e. ionic concentrations) on one or both sides of the membrane. The time scale of the current due to changing pump activity depends on the geometry of the space in which the controlling change in ion concentration occurs. In particular, the time scale of the current varies inversely with the surface-to-volume ratio of the space. For a cylindrical cell of diameter 12 μm and a resting membrane potassium permeability that gives a slope resistance of 20 KΩ-cm^2, the time constant of

equilibration of internal concentration is about 100 sec. An extracellular cleft of width 30 nm, on the other hand, has a surface-to-volume ratio 400 times larger and thus produces currents on the time scale of 250 msec. Isolated preparations have yet another kind of space -- the unperfused vascular space -- which would have a time constant in between the other two. Thus, changing pump activity could be responsible for many (if not all) of the changes in action potential shape with rate and for voltage-clamp currents slower than a few milliseconds.

PUMP MODEL AND SMOOTH-SURFACED CELL

We previously developed a kinetic model of electrogenic active transport of sodium and potassium ions in which the influences of voltage and chemical composition are explicitly defined from thermodynamic laws and experimental facts. The steps in obtaining such an expression have been described in the literature (Chapman, 1973; Gibbs and Chapman, 1979; Chapman, Kootsey and Johnson, 1979) and are based on recent developments in chemical kinetic theory (Boudart, 1976; Chapman and McKinnon, 1978). To this description of electrogenic transport, we added a system of passive permeabilities and out of the resulting membrane, constructed a model of a smooth-surfaced cell. The passive permeabilities were made to be time-independent and of the minimum degree of complexity sufficient to generate an action potential of realistic shape and to produce a resting potential and resting membrane slope resistance corresponding to measured values. The ion concentrations outside the cell were treated as parameters and the internal concentrations were allowed to change in response to changes in the rate of stimulation and to changes in outside concentration. We assumed that only two types of ions -- Na^+ and K^+ -- contribute to the generation of the action potential and that the permeabilities of the membrane to these two ions, P_{Na} and P_K, were independent of time: P_K was assumed to be constant and P_{Na} an instantaneous function of potential only. The magnitudes of both permeabilities were not arbitrarily adjustable, but were fixed by known electrophysiological properties. For a given value of A, the free energy available from ATP, the magnitude of P_K was determined by the resting value of membrane slope resistance, the magnitude of resting P_{Na} was determined by the resting membrane potential, and the form of the voltage-dependent function for P_{Na} was determined by the shape of the action potential.

Analysis of the behavior of the model cell described above revealed time-varying currents on the time scale of tens of seconds for surface-to-volume ratios appropriate to cardiac cells. The long-term changes in configuration of the action potential that follow a change in stimulation rate (Gibbs, Johnson and Tille, 1963) were predicted by the model through a shift in the steady-state current-voltage relationship (predominantly that of the pump) caused by small changes in inside ion concentrations. The diastolic hyperpolarization observed following an increase in rate (Browning, et al, 1979) was also predicted, including the linear relationship between the maximum diastolic depolarization and the rate of stimulation. Varying the outside potassium concentration in the model produced changes in the rest potential and in the current-voltage relationship similar to published data (Carmeliet, 1961; McAllister and Noble, 1966). Deviations from ideal potassium electrode behavior occurred at both high and low concentrations because of effects on the pump. The model not only

predicted the observed shift of the current-voltage curve in the depolarizing direction with increasing $[K^+]_o$, but also the "cross-over effect", the crossing of the curve in normal $[K^+]_o$, without having to assume a dependency of g_K on K_o. The model also accounted for the observation of Weidmann (1956) that a sudden injection of high-potassium perfusate into the coronary circulation of a turtle caused an acceleration of repolarization, albeit to a more depolarized resting potential. Anoxia was introduced into the model by changing the concentrations of ATP and ADP and the model was able to account for the rapid initial diastolic depolarization observed in myocardial ischemia (Cohen and Kaufman, 1975). In addition to these electrophysiological effects, electrogenic active transport was also shown to greatly complicate the interpretation of isotopic flux measurements.

CELL MODEL WITH CLEFT

We have now developed a preliminary version of a cell model with a cleft representing restricted extracellular space and, from a small number of computations, this model has shown promise in accounting for action potential changes and voltage-clamp currents on the time scale of tens or hundreds of milliseconds as well as the slower currents characteristic of the smooth-surfaced cell model. The model is based on the following assumptions:

1) Ion movement in the cleft was represented in only one dimension -- the distance in from the surface -- because diffusion in the restricted spaces between cardiac cells is primarily in that direction. Although the direction is radial, we assumed this single dimension to be a linear one because much of cardiac muscle is composed of more-or-less-tightly-packed bundles of roughly cylindrical cells. In such a structure, restricted extracellular spaces produced by tight packing can be approximated by a lengthwise, narrow groove in a long cylinder (Fig. 1A). Other types of spaces might be better represented by a true radial dimension, e.g. the T-system in mammalian ventricular muscle and some atrial fibers. We chose to begin our studies with the linear type because we wanted, initially, to model the geometry of ungulate Purkinje fibers and frog atrial and ventricular trabeculae. Thus, we are in effect considering a thin slice (dotted line in Fig. 1A) of a long, cylindrical cell.

2) Ions in the cleft were assumed to move under the influence of diffusional and electrical forces, i.e. ion movement was described by an electrodiffusion equation. Solving for the ion concentrations in the cleft required simultaneous solution of electrodiffusion equations for all the ions -- cations and anions -- that carry significant charge; we solved simultaneous equations for sodium, potassium, and chloride. Incidentally, it is incorrect to represent electrodiffusion by trying a simultaneous numerical solution of an electrical cable equation and a one-dimensional diffusion equation; the two forces on the ions must be combined in one equation.

3) The diffusion coefficients for ions in the cleft were assumed to be equal to the values measured in bulk solutions at the same activity. The diffusion coefficients are probably lower in such a restricted space, but measurements are not available. If they were actually lower, the

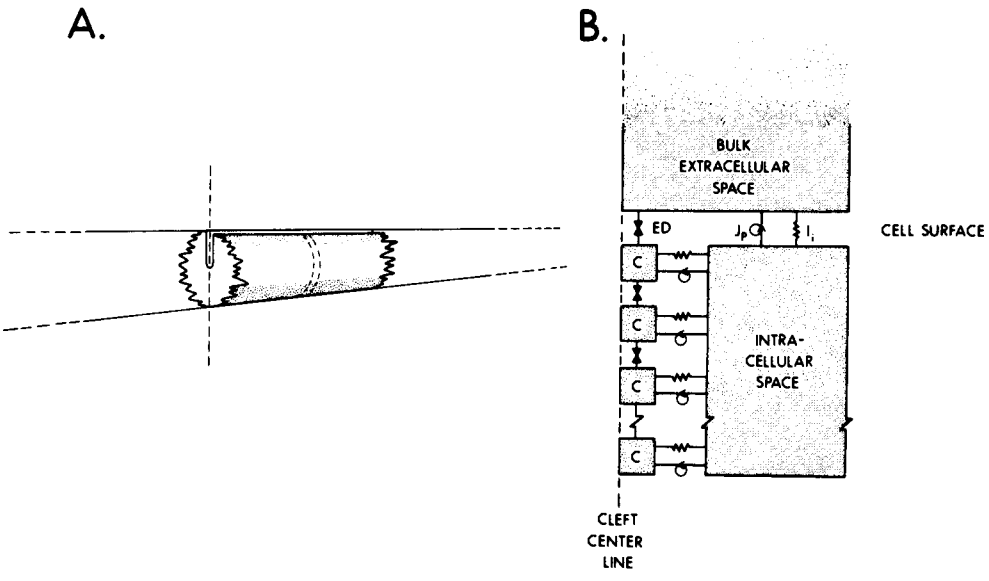

Figure 1. A: Idealized cylindrical cell with groove-like cleft forming an extracellular compartment. B: Block diagram of model. C = cleft segment; ED = coupling by electrodiffusion; J_p = pump current; I_i = passive current.

effects of our assumption would be to cause an underestimate of the magnitude of concentrations changes and an overestimate of the speed at which the ion concentrations change in the restricted space.

4) We assumed that the membrane facing the cleft was of the same type as on the surface of the cell and was also "uniform" along the length of the cleft (i.e. all the membrane was given the same dependence on inside and outside ion concentrations and transmembrane potential). The instantaneous current-voltage relationship of the membrane will, however, generally vary along the cleft because of variations in ionic concentrations along the cleft. We began with the same description of active and passive transport as was developed previously for the smooth-surfaced cell.

5) As with the simulations for the smooth-surfaced cell, we approximated depolarization by displacing the membrane potential along the cleft at the moment of stimulation to some positive potential by incrementing the ionic concentrations. This approximation is essential to keep the amount of computation within reason for simulations on the time scale of repolarization or longer. To compute depolarization, when the ionic currents through the membrane are large, it would be necessary to reduce the spatial increment in the numerical solution of the electrodiffusion equations (i.e. more segments are necessary to represent a cleft of given

length). The size of the time increment must also be reduced, both as a consequence of the smaller spatial increment and because of the fast kinetics of the sodium current responsible for the depolarization. As a result, computing depolarization as well as repolarization would slow the problem solution time by a factor of about 100. To be certain that our approximation is reasonable, we plan later to compute the first few milliseconds of an action potential with the fast sodium current equations of Ebihara and Johnson (1980) to verify that propagation down the cleft is such that the depolarization of membrane in the cleft is nearly synchronous with that of the surface.

6) We assumed that the mouth of the cleft communicates freely with a bulk extracellular space having fixed ionic concentrations. The bottom of the cleft was assumed to be sealed, i.e. no ion fluxes, representing either a closed end of the cleft or the center of a symmetric bundle.

The model of the cell with a cleft thus consists (see Fig. 1B) of a single compartment representing intracellular space, a distributed compartment representing the cleft, and a fixed bulk extracellular space in which the ion concentrations are parameters.

The equations representing the model of a cell with a cleft included: three second-order partial differential equations representing the electrodiffusion of sodium, potassium, and chloride in the cleft (these equations include derivatives in both concentration and potential); a set of transcendental equations representing active and passive transport of Na^+ and K^+ at each segment along the cleft and through the surface membrane; and a set of ordinary differential equations for the internal ion concentrations. The numerical methods for solving the partial differential equations were adapted from the Crank-Nicolson implicit method (Crank and Nicolson, 1947) for solving parabolic partial differential equations. A significant difference encountered in solving the electrodiffusion equations (as compared with previous solutions of the electrical cable equation) is that there is no mesh ratio rule to aid in the selection of the time step of integration. We thus found it necessary to find an appropriate time step by trial and error, making the time step as large as possible to improve computation speed, but small enough to preserve accuracy and to prevent spurious oscillations.

In previous cable simulations that we have done, the transmembrane potential has been the primary variable -- the variable of integration. In the cleft model, however, the ion concentrations became the integrated variables and the transmembrane potential was calculated on the basis of net charge on the membrane capacitance. With this change in variables, we were forced to increase the precision of the variables in the numerical solution because the potential now depends on small differences between large numbers (the ion concentrations). Since the individual concentrations may change substantially during the course of a simulation, the problem cannot be rectified by resorting to storing the difference between the instantaneous value of a concentration and some reference value rather than the instantaneous value itself.

Parameter values and initial conditions for the simulations were taken from measurements in the literature for sheep Purkinje fibers and are shown in Table I. Note that the ion concentrations which are parameters for the bulk extracellular space were used as initial conditions for concentrations in the cleft.

TABLE I:

PARAMETER VALUES AND INITIAL CONDITIONS

$[Na^+]_i$ = 9.6 mM		D_K =	2.04×10^{-8} cm^2/msec
$[Na^+]_o$ = 140 mM		D_{Na} =	1.39×10^{-8} cm^2/msec
$[K^+]_i$ = 130 mM		D_{Cl} =	2.11×10^{-8} cm^2/msec
$[K^+]_o$ = 4.0 mM		V_{rest} =	-90 mV
$[Cl^-]_i$ = 139.6 mM		Δx =	10 μm
$[Cl^-]_o$ = 144 mM		Δt =	0.1 msec
surf/vol (IC comp.)	= 10^6 m^{-1}		
cleft width	= 30 nm		
cleft length	= 100 μm		
cleft/total (membrane area)	= 0.8		

RESULTS

Figure 2A shows one well-known electrophysiological effect predicted by the cleft model. The first action potential shown is that produced by a single stimulus after a long pause. The second action potential generated 500 msec later has a substantially shorter duration. The time dependency of the membrane current-voltage relationship which is responsible for this shortening of the action potential clearly cannot be attributed to time-dependent changes in membrane permeability since we have made the passive permeabilities time-independent. The time dependency must arise from changes in active transport brought about by changes in chemical composition similar to the time scale expected for the cleft. Figure 3A shows the potassium concentration at the bottom of the cleft $[K^+]_l$ as a function of time after the moment of stimulation for a single action potential. Note that $[K^+]_l$ increases steadily throughout the action potential to a maximum value almost three times that in the bulk extracellular space. During the fast phase of repolarization, $[K^+]_l$ starts to fall and continues to decrease during diastole. By the end of 1000 msec, $[K^+]_l$ has almost returned to its initial value. The changes in cleft potassium concentration $[K^+]_c$ with distance are shown in Figure 3B for various times after stimulation. It can be seen that at depths greater than 40-50 μm, the chemical composition in the cleft is essentially independent of that in the bulk extracellular space, the deeper part of the cleft behaving essentially as a closed compartment during the action potential!

This change in $[K^+]_c$ and the corresponding change in cleft sodium concentration are large enough to significantly alter the membrane current-voltage relationship. A current-voltage relationship which generated an action potential of normal duration in the smooth-surfaced cell

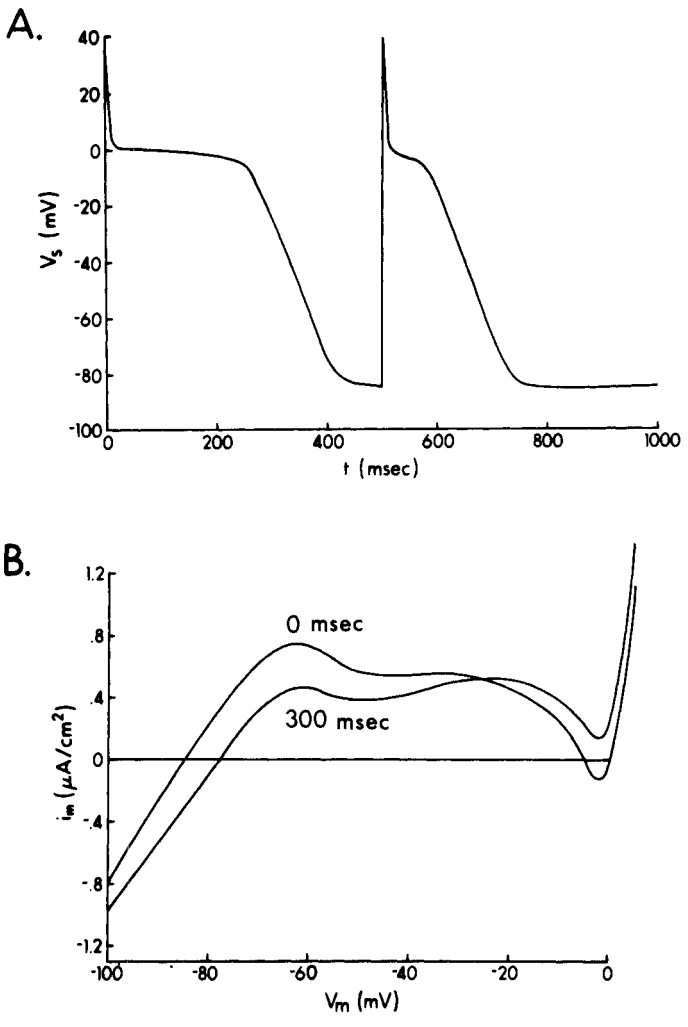

Figure 2. A. Response of model to two stimuli after long quiescent period. The surface transmembrane potential is shown as a function of time. B. Current-voltage relationship for membrane at the bottom of the cleft at two instants during the simulated experiment shown in part A.

model was so distorted that the duration was abnormally short. In order to generate an action potential of reasonable duration, the quiescent membrane current-voltage relationship had to be made to cross the voltage axis (see Fig. 2B, t=0 msec curve). During the course of the action potential, the change in chemical composition caused the current-voltage relationship to shift upwards in the plateau region, eliminating the region of inward current (see Fig. 2B, t=300 msec curve), initiating fast

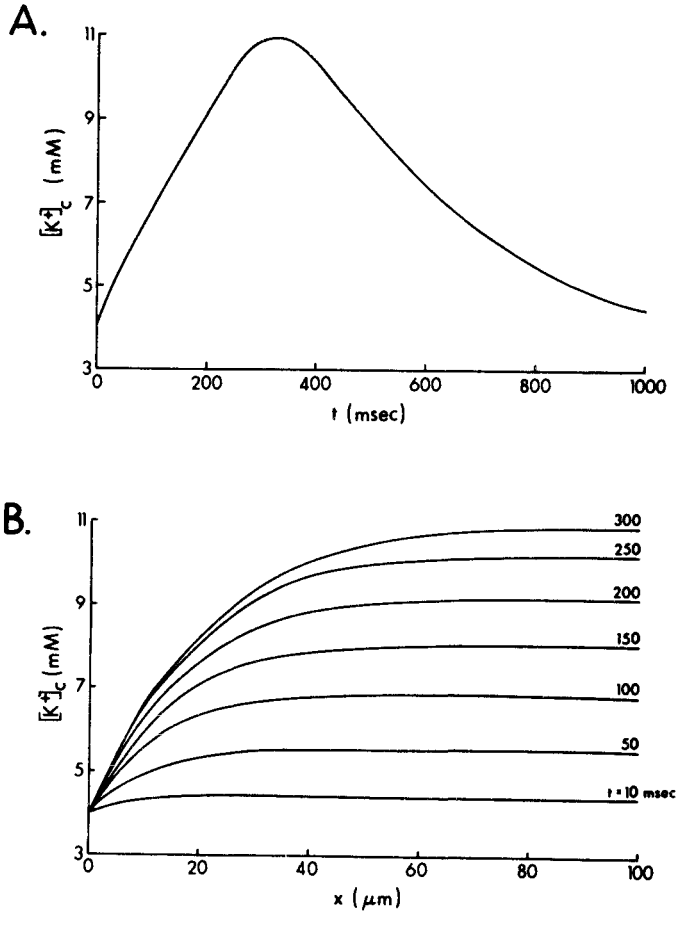

Figure 3. A: Potassium concentration at the bottom of a 100 μm deep cleft as a function of time after a single stimulus. (For comparison, the surface transmembrane potential for this simulated experiment is identical to the first 500 msec in Fig. 2A.) B: Potassium concentration along the cleft at several times during the same simulated experiment as part A. The distance x is measured from the mouth of the cleft.

repolarization. The necessity for the quiescent current-voltage relationship to cross the axis implies that if the capacity of the pump were decreased (for example by cooling), the cell might have a second stable state at a less negative potential because the chemical stimulation of the pump may be insufficient to raise the current-voltage relationship above the voltage axis.

The reason for the shortening of the second action potential is now clear. This action potential is initiated before the current-voltage relationship has returned to its quiescent form. In the plateau region, the current-voltage curve does not dip as far below the axis and thus requires less time to drift up to the axis. The duration of the plateau is a measure of the time taken for the curve to be lifted just beyond the voltage axis.

CONCLUSIONS

We have shown with a distributed cleft model that the ion concentrations in much of the volume of a realistic-sized cleft are independent of concentrations in bulk extracellular space on the time scale of an action potential. The changes in sodium and potassium ion concentrations in such a cleft are substantial and may be responsible for apparent membrane currents on the time scale of tens to hundreds of milliseconds, e.g. the shortening of an extra action potential. These results are only the beginning of our exploration of the contribution that clefts make to the electrophysiology of cardiac muscle. We are curious to see how much of the electrophysiology on this time scale can be accounted for by this model, including voltage-clamp currents. We believe that the major obstacles to be overcome before the generation of the cardiac action potential is understood have moved from concern with voltage inhomogeneity to concern with chemical inhomogeneity and its resultant effects on active as well as passive transport.

(This work was supported by NIH grant HL 12157 and by the Australian National Heart Foundation.)

REFERENCES

Boudart, M. (1976). Consistency between kinetics and thermodynamics. J. Phys. Chem. 80:2869-2870.

Browning, D.J., J.S. Tiedemann, A.L. Stagg, D.G. Benditt, M.M. Scheinmann, and H.C. Strauss. (1979). Aspects of rate-related hyperpolarization in feline Purkinje fibers. Circ. Res. 44:612-624.

Carmeliet, E. (1961). Chloride and Potassium Permeability in Cardiac Purkinje Fibres. Press Acad. Europ. Bruxelles.

Chapman, J.B. (1973). On the reversibility of the sodium pump in dialyzed squid giant axons. A method for determining the free energy of ATP breakdown? J. Gen. Physiol. 62:643-646.

Chapman, J.B., J.M. Kootsey, and E.A. Johnson. (1979). A kinetic model for determining the consequences of electrogenic active transport in cardiac muscle. J. Theor. Biol. 80:405-424.

Chapman, J.B., and I.R. McKinnon. (1978). Consistency between thermodynamics and kinetic models of ion transport processes. Proc. Aust. Soc. Biophys. 21:3-7.

Cohen, D., and L.A. Kaufman. (1975). Magnetic determination of the relationship between the S-T segment shift and the injury current produced by coronary artery occlusion. Circ. Res. 36:414-424.

Crank, J., and P. Nicolson. (1947). A practical method for numerical evaluation of solutions of partial differential equations of the heat-conduction type. Proc. Cambridge Phil. Soc. 43:50-67.

Ebihara, L., and E.A. Johnson. (1980). The fast sodium current of cardiac muscle. A quantitative description. Biophys. J., in press.

Gibbs, C.L., and J.B. Chapman. (1979). Cardiac energetics. pp. 775-804 in Handbook of Physiology - The Cardiovascular System I, ed. by Berne and Sperelakis, Am. Physiol. Soc.

Gibbs, C.L., E.A. Johnson, and J. Tille. (1963). A quantitative description of the relationship between the area of rabbit ventricular action potentials and the pattern of stimulation. Biophys. J. 3:433-458.

McAllister, R.E., and D. Noble. (1966). The time and voltage dependence of the slow outward current in cardiac Purkinje fibers. J. Physiol. (Lond.) 186:632-662.

Weidmann, S. (1956). Resting and action potentials of cardiac muscle. Ann. N.Y. Acad. Sci. 65:663-678.

Adv. Physiol. Sci. Vol. 8. Cardiovascular Physiology. Heart, Peripheral Circulation and Methodology
A. G. B. Kovách, E. Monos, G. Rubányi (eds)

TWO MEMBRANE POTENTIAL DEPENDENT PROCESSES CONCERNED IN THE GENERATION OF THE AMPHIBIAN HEART BEAT

R. A. Chapman and J. Tunstall
Department of Physiology, University of Leicester, England

When sodium ions are withdrawn from the fluid bathing a frog atrial trabecula, a contracture develops. The strength of this contracture, which occurs in the absence of significant membrane depolarization, is dependent upon the concentration of calcium and sodium ions in the bathing medium and upon the intracellular sodium concentration. (8, 29,). In sodium free fluid this contracture spontaneously relaxes at which time another contraction can be evoked by the application of caffeine, hypertonic fluids or by the rapid cooling of the preparation. This contracture is relatively insensitive to $[Ca]_o$, being unaltered by perfusion in a calcium free fluid containing E.G.T.A., but can be inhibited by local anaesthetics. (9, 11, 13,). Because of its immediate dependence upon the concentration of calcium and sodium ions, the sodium withdrawal contracture is thought to originate in the activity of a Na/Ca exchange in the cell membrane. On the other hand, the subsequent contracture would seem to originate from an intracellular store of Ca^{2+} probably the sarcoplasmic reticulum.

When a preparation of mammalian or amphibian cardiac muscle is depolarized, either by the elevation of the potassium concentration, by voltage clamp pulses or by prolonged action potentials, the contractile response which develops can often be resolved into two components. First, an initial phasic response, associated with the development of a slow inward current and possibly with the release of Ca^{2+} from the sarcoplasmic reticulum and second, a delayed tonic tension which depends upon $[Ca]_o$ and $[Na]_o$. (2, 17, 21, 22, 26, 28, 34, 37).

The similarities between the two types of response in sodium depleted non-depolarized preparations and the two phases of the response to depolarization suggest that there are two processes which can raise $[Ca]_i$ sufficiently to generate tension.

In new experiments, using a rapid perfusion technique applied to frog atrial trabeculae 20-100μ in diameter, we have further characterized these two processes and obtained quantitative data of their dependence upon membrane potential. This technique allows us to clear the extracellular space very quickly, as estimated by the effects of changing $[K]_o$ when the resulting membrane potential change is 90% complete in less than 3 seconds. (12, 15,).

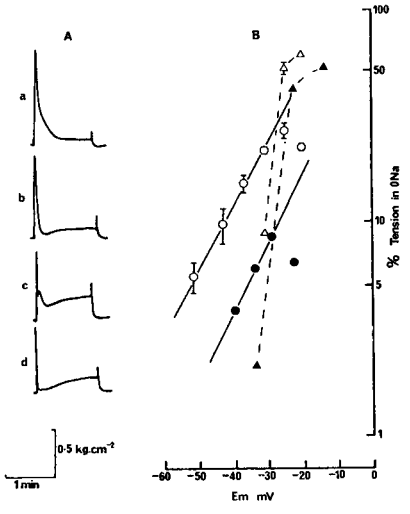

Fig.1.

A) K. contractures evoked in 100mM Na, illustrating the contribution of a phasic and a tonic component.

B) Log. contracture tension of the phasic Δ and tonic O components plotted against membrane potential.
Open symbols 0.5mM Ca.
Closed symbols 0.25mM Ca.

When $[K]_o$ is raised to depolarize the membrane in the presence of sodium ions, the resulting contracture can be seen to have two phases (Fig.1A). These are the initial phasic tension, which has a threshold at a membrane potential of -31mV (± 1.3mV S.D.) and a strength which varies steeply with membrane voltage, an e-fold change in tension occurring for each 6.2mV (± 0.6mV S.D.) change in membrane potential. (Fig.1B). The phasic tension gives way to a delayed but sustained tonic tension (Fig.1A). This tonic phase shows no discrete threshold (in fact the preparation may relax if [K] in normal Ringer is reduced) and a much shallower dependence upon membrane potential showing an e-fold change in tension for each 15.8mV (± 0.8mV S.D.) of depolarization. (Fig.1B).

Our experimental technique allows us to exchange virtually all the extracellular spaces within 30 seconds. If for this time the $[Na]_o$ or $[Ca]_o$ is changed the exponential relationships between both the phasic and tonic components of a subsequent potassium contracture are unaltered, however the amptitude of the tonic, but not the phasic component is much affected. This change means that the relationship between tonic tension and membrane potential is shifted along the voltage axis (Fig.1B). The magnitude of these shifts associated with various changes in the outside ionic concentrations are shown in Table 1.

When these observations are repeated in the presence of 1mM tetracaine the phasic component of the potassium contracture is inhibited (Fig.2). The remaining tonic component shows virtually unaltered dependence upon membrane potential and upon $[Na]_o$ and $[Ca]_o$ as indicated in Table 1.

TABLE 1

Experimental Conditions	Depolarization for e-fold increase in tension		Shift in tension - depolarization curve caused by changes in extracellular ion concentrations of:					
			x 2 in $[Ca]_o$ mV		x 5 in $[Ca]_o$ mV		x ½ in $[Na]_o$ mV	
	Phasic response	Tonic response	Phasic response	Tonic response	Phasic response	Tonic response	Phasic response	Tonic response
Normal Ringer	6.2 ± 0.6 (n = 19)	15.8 ± 0.8 (n = 26)	-3.8 ± 1.3 (n = 6)	-15.8 ± 0.6 (n = 6)	-10.2± 2.4 (n = 4)	-34.0 ± 2 (n = 4)	-12.1± 3.7 (n = 4)	-35.0 ± 1.8 (n = 4)
Normal Ringer + 1mM Tetracaine		18.9 ± 1.0 (n = 22)		-16.2 ± 1.7 (n = 7)		-44.5 ± 1.7 (n = 2)		-45.5 ± 1.0 (n = 3)
Na-free Ringer	8.0 ± 0.4 (n = 10)				1.2 ± 1.9 (n = 5)			
Predictions of $3Na^+ - 1Ca^{++}$ exchange (eq 2 & 5)	>14.0		-17.3		-40.5		-50.5	

Table 1.
The collected experimental data for the phasic and tonic components of the K-contracture induced in frog atrial trabeculae, in normal Ringer, Na-free Ringer and in the presence of tetracaine are compared to the predictions of a model for the Na-Ca exchange.

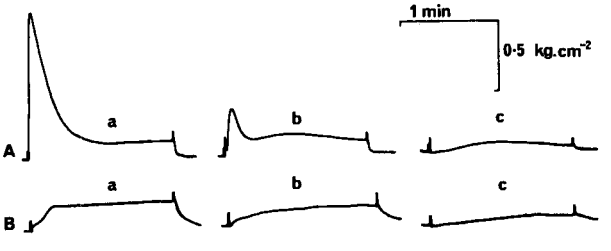

Fig.2.
The effects of tetracaine upon the phasic component of K contractures in a) 100mM K b) 50mM and c) 35mM K.

A: In 100mM Na Ringer
B: In 100mM Na Ringer and 1mM Tetracaine

If all the sodium ions bathing the preparation are removed and the resulting zero sodium contracture is allowed to spontaneously relax to resting levels, depolarization of the preparation (by raising $[K]_o$) leads to a further development of tension. This contracture in Na-free fluid is unaffected by $[Ca]_o$ but shows, like the phasic response, a steep dependence upon membrane potential, Table 1. This response is inhibited by tetracaine where 1mM tetracaine shifts the tension depolarization relationship by 42mV (± 3mV S.D.) towards less negative membrane potentials. Fig.3.

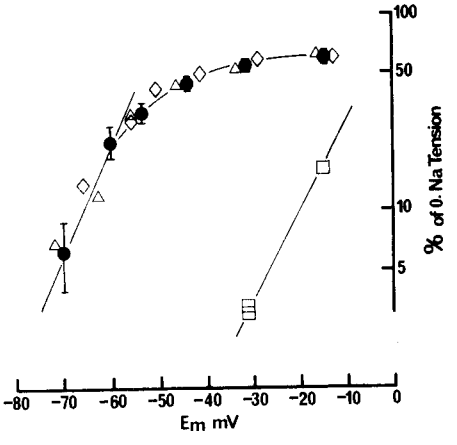

Fig.3
The strength of the K contracture evoked in sodium free fluid following the spontaneous relaxation of the low sodium contracture, plotted against membrane potential and its dependence upon $[Ca]_o$ and Tetracaine.

● - 1mM Ca △- 5mM Ca ◇- 0.2mM Ca
□ - Ringer and 1mM Tetracaine.

These results show that in the amphibian heart tension induced, in the presence of sodium ions, by depolarization is associated with two processes, one, a rapid and tetracaine sensitive process which has a steep dependence upon membrane potential, and is unaffected by $[Ca]_o$ and $[Na]_o$, and a delayed slower process insensitive to tetracaine, with a shallow dependence upon membrane potential and highly sensitive to $[Ca]_o$ and $[Na]_o$. Further the phasic component of the potassium contracture shows much in common with those contractures evoked in sodium free fluid by caffeine, rapid cooling or hypertonic solutions which are considered to result from a release of Ca^{2+} from the sarcoplasmic reticulum. In addition the tonic component shows features in common with the sodium withdrawal contractures, which are suggestive of a common origin in a Na/Ca exchange at the Sarcolemma. By logical inference then we should expect the Na/Ca exchange to be membrane potential dependent.

A dependence of the Na/Ca exchange upon membrane potential was considered for cardiac tissue by (5, 23, 30, 33, 38). Such a dependence has also been extensively investigated in squid axon (3). In both tissues the experiments involved measurements of calcium and sodium fluxes. A clear dependence of a coupled sodium-calcium movement upon membrane potential has been shown for squid axon however in cardiac tissue the results are more equivocal.

A clear effect of membrane potential (or $[K]_o$) on the sodium withdrawal contracture can be obtained on isolated frog atrial trabeculae, Fig.4. In these experiments the relationship between the contracture tension and various $[Na]_o$ was determined at the beginning and end of an experiment in Ringers solution containing 3mM potassium (membrane potential = -83mV). The relationship was then determined in low sodium solutions 30 seconds after raising the $[K]_o$ to either 15mM (membrane potential = -55mV) or to 30mM (membrane potential = -43mV). The figure shows that a substantial shift occurs in the relationship between tension and $[Na]_o$ when the preparation is depolarized.

This interrelationship between membrane potential $[Na]_o$ and tension is similar to that of the tonic phase of the potassium contracture where in both cases the effects upon tension of halving the $[Na]_o$ or depolarizing the membrane by 40mV (i.e. 10 x inc in $[K]_o$) are approximately the same. Furthermore changes in $[Ca]_o$ also effect the tension low sodium relationship in ways quantitatively similar to the effect of $[Ca]_o$ on the tonic phase of the potassium contracture. This is strong evidence in favour of an electrogenic Na/Ca exchange which is responsible for a) the low sodium contracture and b) the tonic phase of the potassium contracture.

We have compared the results of the low sodium contracture experiments to values of tension predicted by a number of theoretical schemes for the Na/Ca exchange which would depend on membrane potential or $[K]_o$. We first assumed that tension is controlled at the unit level of the contractile proteins by either a simultaneous or a sequential binding of two calcium ions according to equation 1 or 2 (1, 10, 35) where:-

$$\text{Relative Tension} = \frac{[Ca]_i^2 K_T^2}{1 + [Ca]_i^2 K_T^2} \quad \text{------} \quad 1.$$

$$\text{Relative Tension} = \left[\frac{[Ca]_i K_T}{1 + [Ca]_i K_T}\right]^2 \quad \text{------} \quad 2.$$

where K_T is the apparent binding constant of the controlling proteins for Ca^{2+}.

We then computed the expected $[Ca]_i$ for a Na/Ca exchange by way of a charged carrier, equation 3 (30); by way of a mechanism which exchanges not only calcium and sodium ions but maintains electroneutrality by also exchanging potassium as proposed by equation 4 (4); and by way of a mechanism which exchanges more than two sodium ions for each calcium ion, equation 5 (4).

$$[Ca]_i = \frac{[Ca]_o [Na]_i^2}{[Na]_o^2} \exp \frac{EmFz}{RT} \quad \text{-----} \quad 3.$$

where z is the charge on the carrier, Em the membrane potential and $Fz/RT = 1/25mv^{-1}$

$$[Ca]_i = \frac{[Ca]_o [Na]_i^n}{[Na]_o^n} \frac{[K]_o^{n-2}}{[K]_i^{n-2}} \quad \text{----} \quad 4.$$

$$[Ca]_i = \frac{[Ca]_o [Na]_i^n \exp \frac{EmF}{RT}}{[Na]_o^n} \quad \text{----} \quad 5.$$

where n = the number of sodium ions exchanging for each calcium ion.

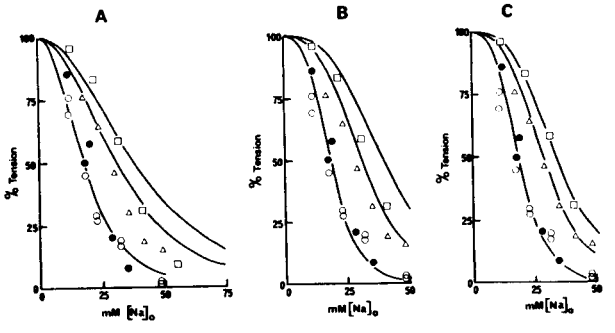

Fig.4.
The relationship between tension and $[Na]_o$ for two trabeculae. One exposed to 3mM K ○ and to 15mM K △ ; the other to 3mM K ● and to 30mM K □

The experimental data are compared to the predictions of three versions of a Na/Ca exchange:

in A) where each Ca^{++} exchanges for $2Na^{++}$

in B) when a Ca^{++} and a K^+ exchange for $3Na^+$

in C) when $3Ca^{++}$ exchange for each sodium ion.

Relative tension is calculated

as $$\frac{\text{Tension}}{\text{Max Tension}} = \left[\frac{[Ca]_i K_T}{1 + [Ca]_i K_T}\right]^2$$

In solving these equations for $[Ca]_i$ we assumed a value for $[Na]_i$ = 7mM, a figure obtained for sodium flux studies on frog heart (24, 31) and with sodium sensitive microelectrodes in mammalian cardiac cells, (16, 25)

The other experimental parameters $[Ca]_o$, $[Na]_o$ and membrane potential ($[K]_o$) are known. In order to convert the relationship between $[Ca]_i$ and $[Na]_o$ predicted by these models into values of tensions using equations 1 and 2, it is necessary to derive a value for K_T which best fits the computed data to the experimental results. This fit was made for experimental data obtained for the preparation in 1mM Ca and 3mM $[K]_o$ (Em = -83mV). Using this value of K_T we tested the ability of the various models to predict the experimental results for tension on 15mM K (Em = -55mV) and in 30mM K (Em = -43mV).

Of the numerous schemes the predictions of those that came closest to the experimental behaviour of the preparation are illustrated in Fig.4. They are: Fig.4A the solution to equations 2 and 3 with z = 1, Fig.4B equations 2 and 4 when n = 3, and Fig.4C equations 2 and 5 when n = 3. It is clear that a sequential binding of calcium and the exchange of three sodium ions for each calcium ion best fits the experimental observations. Further these relationships provide a value for K_T of $2.6 \times 10^{-6} M^{-1}$ close to that found for skinned cardiac muscle cells or isolated cardiac myofibrils (20, 35). This model will also provide the best fit to experimental data when $[Ca]_o$ is altered or that recorded following manoeuvres likely to raise $[Na]_i$.

The membrane potential dependence of the tension predicted by the three sodium for one calcium exchange (eq.2 and 5) and the shifts in this relationship expected when either $[Ca]_o$ or $[Na]_o$ is altered are also listed in Table.1. and agree with experimental data for the tonic tension of the potassium contracture.

The similarities between the phasic tension of potassium contractures, the potassium contracture in zero sodium and caffeine contractures in zero sodium, which suggest that they result from the release of Ca^{2+} from the sarcoplasmic reticulum, have already been noted. In particular that these contractures are blocked by tetracaine.

The action of tetracaine in inhibiting specifically the phasic component the K-contracture could be due to its ability to block the slow inward current (18). Indeed other inhibitors of the slow inward current, Mn^{2+} and D 600 also block the phasic component of the contraction observed in voltage clamp experiments on frog heart (17, 26, 37). A close functional link between slow inward current and phasic tension has been established in a variety of cardiac tissues by voltage clamp techniques, and yet there is evidence that the Ca^{2+} carried into the cell by this current is insufficient to activate significant contraction. (see (10) for references and discussion). Furthermore the strength of the initial tension is altered by manoeuvres likely to increase the Ca^{2+} in intracellular stores (2, 21, 30). Local anaesthetics, unlike D 600 and Mn^{2+} block the contractures evoked by caffeine in both frog and mammalian heart (12, 13), indicating an additional reaction of these agents, presumably related to their ability to inhibit the release of Ca^{2+} from the S.R. (19). This notion is supported by voltage clamp experiments on frog muscle which show that tetracaine inhibits tonic tension in a non-competitive way but is a competitive inhibitor of slow inward current. (Chapman & Leoty, unpublished).

It is important to consider how these two processes, a Na/Ca exchange and the release of Ca from the sarcoplasmic reticulum, both of which can

generate tension, interact in the intact normally beating heart. During diastole the membrane potential is well below the threshold for the phasic tension, i.e. for the release of Ca from the sarcoplasmic reticulum. In this condition the sarcoplasmic reticulum and other stores of intracellular calcium ions are likely to be filled to an extent dependent upon the heart rate and temperature, in so far as it effects the metabolism of the Ca sequestering systems. These stores must play a part in controlling $[Ca]_i$ as both the zero sodium and potassium contractures spontaneously relax. This spontaneous relaxation has a large Q_{10} and is slowed by metabolic inhibitors. When spontaneous relaxation is absent in metabolically poisoned preparations caffeine fails to evoke a contracture suggesting that the sarcoplasmic reticulum plays an important role in removing calcium from the sarcoplasm to bring about spontaneous relaxation. (6, 7). In addition at this membrane potential the Na/Ca exchange will maintain an $[Ca]_i$ at a level where little activation of the contractile proteins will occur. It would in fact be close to its equilibrium potential calculated as $3E_{Na} - 2E_{Ca}$ and would tend to cause the efflux of Ca to compensate either its spontaneous release from the sarcoplasmic reticulum or its passive influx known to occur in resting hearts.

On depolarization by the cardiac action potential both processes would be activated. The phasic component would contribute an amount to $[Ca]_i$ and to tension, which would depend upon the status of the intracellular stores, i.e. upon heart rate etc. That this is probable comes from the observation that the strength of a regularly beating heart is reduced by tetracaine, D 600 or by Mn^{++}, and would account for the staircase phenomenon. The Na/Ca exchange will now also cause the influx of Ca^{++} but as it acts more slowly, to produce the delayed tonic tension, the strength of the heart beat will depend upon the duration of the action potential, and upon the $[Ca]_o$ and $[Na]_o$ (14, 27). It is interesting to note that in normal frog Ringer and at a membrane potential equivalent to the peak of the action potential of frog heart equations 2 and 5 predict a tension some 20% of the maximum tension recorded in zero sodium. This is a typical value for the amplitude of the amphibian heart beat at a high heart rate. In the depolarized heart, if the $[Ca]_i$, due to its release from intracellular stores, exceeds the value set by the Na/Ca exchange the exchange will reverse and be in competition with the contractile proteins for the available $[Ca]_i$. In this competition it will be hampered by increasing $[Ca]_o$ or by reducing $[Na]_o$, factors known to increase the heart beat. On the other hand it will be favoured by the reduction of $[Ca]_o$ or the elevation of $[Na]_o$, when $[Ca]_i$ will fall and tension subside. In addition such an arrangement would explain the inability of caffeine to cause a contracture in frog muscle bathed by sodium ions when a large contracture can be evoked in low sodium solutions.

This scheme may also operate in mammalian heart. In this tissue large caffeine contractures can be evoked in normal sodium concentrations. These contractures are blocked by tetracaine (12) which also blocks contractures evoked by depolarization in zero sodium (36). A close link between the phasic tension on depolarization and slow inward current is well established for mammalian heart under voltage clamp (see 32, for review) so one process known to raise intracellular calcium seems common to the two vertebrate classes.

Sodium withdrawal contractures which would indicate the activity of a Na/Ca exchange in these hearts are rarely reported. They have been shown

in guinea pig atria by Jundt et al (23) but rarely reach maximum twitch tension. Recent experiments on isolated guinea pig trabeculae (R.A. Chapman, A. Corey and J.A.S. McGuigan - reported at this Congress) show that rapid large Na withdrawal contractures can be evoked which show a similar dependence upon $[Na]_o$ $[Ca]_o$ and membrane potential as those reported for frog. In some preparations these contractures are not maximal i.e. the addition of caffeine induces a further development of tension implicating the activity of the sarcoplasmic reticulum which is reducing the Na-withdrawal contracture.

It seems that the two types of heart show no qualitative differences but rather quantitative differences in the relative contributions of the sarcoplasmic reticulum, which is much more abundant in mammalian heart, and the Na/Ca exchange to the control of $[Ca]_i$ and the generation of tension.

It could be that mammals are merely warm frogs with more sarcoplasmic reticulum or vice versa.

The authors would like to thank Miss A. Gardner and Mrs. D. Williams for their help in the preparation of the manuscript.

References:-

[1] Ashley, C.C. & Moisescu, D.G. (1972) Nature New Biology 237 208
[2] Beeler, G.W. & Reuter, H. (1970) J. Physiol. 207 211-229
[3] Blaustein, M.P. (1974) Rev.Physiol.Biochem.Pharmac. 70 33
[4] Blaustein, M.P. & Hodgkin, A.L. (1969) J. Physiol. 200 497
[5] Busselen, P. & Van Kerkhove, E. (1978) J. Physiol. 282 263
[6] Chapman, R.A. (1973a) J. Physiol. 231 209
[7] Chapman, R.A. (1973b) J. Physiol. 231 233
[8] Chapman, R.A. (1974) J. Physiol. 237 295
[9] Chapman, R.A. (1978) Q.Je.exp.Physiol. 63 291
[10] Chapman, R.A. (1979) Prog.Biophys.molec.Biol. 35 1
[11] Chapman, R.A. & Ellis, D. (1974) J. Physiol. 232 101P
[12] Chapman, R.A. & Leoty, C. (1976) J. Physiol. 258 1P
[13] Chapman, R.A. & Miller, D.J. (1974) J. Physiol. 242 589
[14] Chapman, R.A. & Niedergerke, R. (1970) J. Physiol. 211 423
[15] Chapman, R.A. & Tunstall, J. (1971) J. Physiol. 215 139
[16] Deitmer, J.W. & Ellis, D. (1978) J. Physiol. 277 437
[17] Einwachter, H.M., Haas, H.G. & Kern, R. (1972) J. Physiol. 227 141
[18] Eisner, D.A., Lederer, W.J. & Noble, D. (1979) J. Physiol. 293 76P
[19] Endo, M. (1977) Physiol. Rev. 57 1
[20] Fabiato, A. & Fabiato, F. (1978) Ann.N.Y.Acad.Sci. 307 491
[21] Gibbons, W.R. & Fozzard, H.A. (1971) J. gen. Physiol. 58 483
[22] Goto, M., Kimoto, Y. & Kato, Y. (1971) Jap.J.Physiol. 22 637
[23] Jundt, H., Porzig,H., Reuter, H. & Stucki, J.W. (1975) J. Physiol. 246 229

[24] Keenan, M.J. & Niedergerke, R. (1967) J. Physiol. 188 235
[25] Lee, C.O. & Fozzard, H.A. (1975) J.gen.Physiol. 65 695
[26] Leoty, C. & Raymond, . (1972) Pflugers Arch. 334 114
[27] Morad, M. & Orkand, R.K. (1971) J. Physiol. 219 167
[28] Morad, M. & Trautwein, W. (1968) Pflugers Arch. 299 66
[29] Miller, D.J. & Moisescu, D.G. (1976) J. Physiol. 259 283
[30] Niedergerke, R. (1963) J. Physiol. 167 515
[31] Novotny, Z. & Bianchi, C.P. (1973) Pflugers Arch. 339 113
[32] Reuter, H. (1973) Prog.Biophys.Molec.Biol. 26 1
[33] Reuter, H. & Seitz, N. (1968) J. Physiol. 195 451
[34] Scholz, H. (1969) Pflugers Arch. 308 315
[35] Solaro, R.J. (1975) J.Supramol.Struct. 3 368
[36] Thorens, S. (1971) Pflugers Arch. 324 56
[37] Vassort, G. & Rougier, O. (1972) Pflugers Arch. 331 191
[38] Wollert, U. (1966) Pflugers Arch. 289 191

Adv. Physiol. Sci. Vol. 8. Cardiovascular Physiology. Heart, Peripheral Circulation and Methodology
A. G. B. Kovách, E. Monos, G. Rubányi (eds)

CONCLUDING REMARKS ON CATION REGULATION IN THE MYOCARDIUM

H. Reuter
Department of Pharmacology, University of Bern, 3010 Bern, Switzerland

During the time available for this Symposium only a few aspects of cation regulation in myocardial cells could be dealt with. The work by DEITMER and ELLIS clearly shows that the intracellular sodium ion activity /aNa_i/ is not only regulated by the activity of the sodium pump. If the pump is inhibited by storphanthidin aNa_i increases, but reaches a new steady state after some time. This steady state is due to an exchange of external Ca^{2+} against internal Na^+ /Na-Ca exchange/. The possibility exists that also hydrogen ions exchange for Na^+ across the plasma membrane.

The functional importance of keeping the intracellular ionic milieu constant is indicated by WEINGART's presentation, who showed that an increase in free Ca^{2+} within the cell beyond approximately 5×10^{-6} M reduces the permeability of intercalated discs /nexus/ between two neighbouring cells. Such a reduction in cell-to-cell coupling can also be brought about by injection of Na^+ into the cells which causes a subsequent increase in Ca^{2+} /via Na-Ca exchange/. Moreover, not only Ca^{2+} but also H^+ seem to reduce nexus permeability.

One of the most prominent outward currents in heart sarcolemma is the inwardly rectifying K current /i_{K1}/. CARMELIET has combined ^{42}K efflux and voltage clamp measurements in cardiac Purkinje fibres. Unidirectional K efflux decreases when the membrane is depolarized. This component of inward rectification of K permeability is voltage- and time-dependent and

can be inhibited by Cs ions in a voltage-dependent manner. The component of outward rectification of K current is not much affected by Cs^+.

Another type of K^+ permeability is induced by acetylcholine /ACh/ in sinus node of the rabbit heart. In this tissue ACh causes an opening of K channels by its reaction with muscarinic receptors. A detailed analysis of this muscarinic response by TRAUTWEIN shows considerable similarity of the muscarinic ACh response in sinus node with nicotinic ACh effects on the neuromuscular endplate. But there are also important differences:

/1/ The density of ion channels induced by ACh in the sinus node is approximately 10^4 times smaller than at the endplate;

/2/ ACh-induced ion channels in the sinus node are very selective for K^+ while endplate channels are not;

/3/ The single channel conductance of the sinus node is approximately 5-10 times smaller than that of the endplate;

/4/ There may be a delay in the onset of the muscarinic response.

All these results contribute significantly to our /still very incomplete/ understanding of the importance of monovalent and divalent cations for cardiac cell function. It becomes increasingly clear that at least some of the adaptability of the heart is attributable to the control of ion permeation across the membrane and ion concentration changes within the cell.

Adv. Physiol. Sci. Vol. B. Cardiovascular Physiology. Heart, Peripheral Circulation and Methodology
A. G. B. Kovách, E. Monos, G. Rubányi (eds)

FREE FATTY ACIDS AND MYOCARDIAL METABOLISM

O. D. Mjøs
Institute of Medical Biology, University of Tromsø, Tromsø, Norway

Free fatty acids (FFA), lactate and glucose are the main substrates for myocardial metabolism. Their relative contribution is mainly determined by their plasma concentrations. After overnight fasting FFA cover about 50-60% of the total substrate utilization. During prolonged fasting or stimulation with catecholamines the FFA-fraction may increase up to 100%. A positive correlation has been demonstrated between arterial concentration of FFA and myocardial uptake of FFA. Transport of FFA into the myocardial cells has therefore been regarded as following the general rules of transcapillary exchange of metabolites - without being subjected to active transport. Usually the uptake and rate of oxidation of fatty acids are neatly balanced, and consequently the intracellular lipid pool through which the FFA pass remains constant, with only minor fluctuations. However, during fasting and catecholamine-stimulation, the amount of FFA taken up by the myocardium exceeds the oxidative needs, resulting in storage of the additional amount of FFA as triglycerides within the heart. In addition, under conditions of high uptake of FFA the amount of intracellularly unbound FFA may also increase and influence myocardial function and oxygen consumption (Challoner and Steinberg 1966). Traditionally, two mechanical factors - myocardial contractility and tension - are assumed to be the main determinants of myocardial oxygen consumption ($M\dot{V}O_2$) (Sonnenblick et al 1968). The present results indicate that $M\dot{V}O_2$ may also be determined by the substrate supply to the heart. Consequently, in the intact dog heart, high plasma concentrations of FFA - in contrast to glucose and lactate-effected a marked rise in $M\dot{V}O_2$ without influencing the mechanical activity of the heart (Mjøs 1971a, Mjøs 1971b). $M\dot{V}O_2$ is therefore not only determined by the mechanical performance, but also influenced by high plasma concentrations of FFA.

REFERENCES

Challoner, D.R. and Steinberg, D. (1966). Effects of free fatty acid on the oxygen consumption of perfused rat heart. Amer. J. Physiol. 210, 280-286.

Mjøs, O.D. (1971a). Effect of free fatty acids on myocardial function and oxygen consumption in intact dogs. J. clin. Invest. 50, 1386-1389.

Sonnenblick, E.H., Ross, J. jr. and Braunwald, E. (1968). Oxygen consumption of the heart. Newer concepts of its multifactorial determination. Amer. J. Cardiol. 22, 328-336.

Mjøs, O.D. (1971b). Effect of inhibition of lipolysis on myocardial oxygen consumption in the presence of isoproterenol. J. clin. Invest. 50, 1869-1873.

Adv. Physiol. Sci. Vol. 8. Cardiovascular Physiology. Heart, Peripheral Circulation and Methodology
A. G. B. Kovách, E. Monos, G. Rubányi (eds)

FACTORS REGULATING NORMAL AND ISCHAEMIC MYOCARDIAL SUBSTRATE METABOLISM

Rudolph Arend Riemersma

Lipid Research Laboratory, Department of Clinical Chemistry, Royal Infirmary, Lauriston Place, Edinburgh, EH3 9YW, Scotland

INTRODUCTION

The metabolism of the heart has been studied extensively. The main substrates have been identified: free fatty acids (FFA) and glucose, accounting for 80-95% of the myocardial oxygen consumption (24,25,21). Lactate and ketone bodies play a quantitatively less important role. The regulatory mechanism are largely understood (22). Much less in known about controlling factors during acute myocardial ischaemia, but recently progress has been made (15,34) and will be highlighted here.

THEORY AND FORMULATION OF METABOLIC CONTROL

The general approach to define where and how metabolic control is exerted in a pathway has been reviewed (22). Briefly, 1) Identification of non-equilibrium reactions - a reflection of insufficient enzyme activity to bring a reaction to completion, 2) Study of the properties of identified regulatory enzymes in vitro, culminating in the postulation of a theory of metabolic control, 3) The hypothesis can then be tested by perturbing the flux in the pathway and study whether the changes in concentrations of pathway intermediates are in accordance to the theory.

Often control is most efficiently exerted by a reaction at the beginning of a pathway (e.g. glucose transport under certain conditions) or immediately after a branching point in the pathway. When metabolic processes are controlled by non-equilibrium reactions, it is thermodynamic prerequisite that energy must be lost in the form of heat. Control by non-equilibrium reactions lacks the flexibility of increasing the flux extensively, since the cellular environment (ATP, and cofactor concentrations) must be kept within relatively small boundaries, lest severe secondary effects would result: changes in ionic strength, cessation of other pathways, etc. Increased flexibility can be achieved by substrate cycling. In this process a forward regulatory enzymatic step in the pathway is opposed by another, separate non-equilibrium reaction:

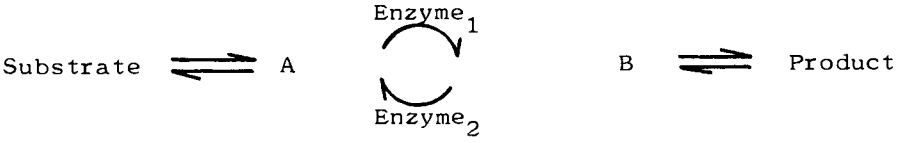

At the expense of increasing energy loss, the effect of the limiting pathway intermediate concentration (A) on the overall flux in the pathway can be amplified (22). Although this mechanism may be very useful for the cell to cope with sudden large increases in energy (ATP) demand, it may potentially be an energy sink during energy limiting conditions such as ischaemia (31).

METABOLISM OF THE WELL OXYGENATED HEART

Fatty Acid Metabolism

FFA utilised by the heart originate mainly from adipose tissue triglycerides (TG). After hydrolysis they diffuse into the blood, where they are bound to plasma albumin. FFA are extracted by the myocardium according to their FFA/albumin molar ratio (25,21) and to their chemical nature (5). There is evidence that they are protein bound within the cell (23), and it has been suggested that myoglobin may also be important (9).

Fatty acids are converted in an active intermediate acyl-CoA, an energy requiring reaction catalysed by acyl-CoA synthetase, before they can be oxidised. The major fate of FFA taken up by the heart is oxidation (28), and the remainder stored in the form of TG. (Incorporation into structural lipids has been omitted). The fate of circulating TG which are hydrolysed by endothelial lipoprotein lipase (33) is assumed to be similar as that of plasma FFA. The metabolism of FFA has been reviewed previously (21).

Control of Myocardial FFA Metabolism at Peripheral Level.

The main control on myocardial FFA metabolism is exerted by the regulation of fatty acid mobilisation from adipose tissue is controlled by a substrate cycle: triglyceride lipolysis and reesterification of FFA into triglyceride. Reesterification is stimulated by insulin, which increases glucose uptake thereby the availability of α-glycerophosphate for the adipocyte. Hence after insulin secretion reesterification is stimulated and FFA mobilisation is reduced (22). Although the concentrations of α-glycerophosphate are generally assumed to limit reesterification (despite the fact that Km is unknown), the addition of FFA enhances reesterification without affecting α-glycerophosphate levels.

The activity of adipose tissue triglyceride lipase is 10-100 lower than that of diglyceride and monoglyceride lipase. It may exist in enzymatically interconvertible forms. The

inactive form is phosphorylated by a cAMP sensitive protein kinase catalysed reaction under hydrolysis of ATP. Catecholamines by stimulating adenylcyclase enhance lipolysis, as do agents (caffeine, theophylline) which inhibit cAMP-phosphodiesterase. The theory of control whereby stimulation of adenylcyclase leads to a cascade effect resulting in lipolysis has been well tested (22) mainly in isolated fat pads, and is generally accepted as representative for the in vivo situation. However, the inactivation of the active form by lipase phosphatase appears not to have been examined in great detail. The variable result with nerve stimulation has been explained (7) by noradrenaline induced vasoconstruction opposing the diffusion of hydrolysed fatty acids into the general circulation. Lipolysis is also stimulated by starvation, possibly due to combined effects of growth and glucagon and the lowered insulin level (22).

Control at Myocardial Level

A close correlation has been reported between myocardial FFA uptake and oxidation (28), with control of this pathway by substrate supply. The concentration of intracellular FFA have been reported (24), but have been questioned (24,31). Hydrolysis during the extraction of as little as 0.1% of stored triglycerides could double the apparent cytoplasmic FFA level. Despite these technical difficulties it appears that fatty acid oxidation is not determined by the intracellular FFA levels, since at high FFA/albumin molar ratios the activity of the citric acid cycle (accumulation of acetyl-CoA) or the respiratory chain (NADH accumulation) may be the limiting factors (28).

Pyruvate and ketone bodies but not glucose can reduce fatty acid oxidation (24) and pyruvate in high concentrations stimulate the incorporation of (^{14}C)-palmitate into tissue lipids (28). L-carnitine can also effect the oxidation of fatty acids and after depletion of its myocardial stores, depressed oxidation and accumulation of myocardial triglycerides is observed (8). The activation of short chain fatty acids occurs within the mitochondria and, therefore, is not inhibited by carnitine deficient states. However, it is not clear whether carnitine is a limiting factor under normal conditions. The development of sensitive radioactive enzymatic essays will stimulate further work in this area.

Studies stimulating FFA metabolism have been hampered by technical problems. Direct infusion to modify plasma FFA levels can only be achieved using expensive and complicated equipment (10). The identification of regulatory enzymes of the fatty acid oxidation pathway is also hampered by the poor solubility of the intermediates. The activity of enzymes in vitro is largely dependent on the nature of the substrate:

whether in micellular form, or bound by protein, etc. Hence, their Km values may have little or no meaning. Intermediates of the pathway are compartmentalised, rendering concentrations at the site of the 'regulatory' enzyme doubtful.

However, it has been suggested that AMP inhibits palmityl-CoA synthetase (22), but increased ventricular performance, which is associated with increased levels of AMP (22), has been associated with enhanced FFA uptake (28).

Control of Endogenous Triglyceride Metabolism

It is generally assumed that myocardial lipolysis is under similar control as has been discussed for adipose tissue. It is sensitive to catecholamines (3), mediated by alteration in cAMP levels, and presumably increased activity of protein kinase. Raised plasma FFA concentrations have a sparing effect on the utilisation of myocardial TG stores (22) and also inhibit myocardial lipolysis stimulated by glucagon (41). The mechanism of this end-product inhibition is not clear. It could be a reflection of the low amount of free binding sites on the binding protein. An effect on cAMP seems unlikely since FFA do not affect adenyl-cyclase (14). Myocardial triglyceride synthesis is assumed to be dependent on the provision α-glycerophosphate and acyl-CoA. Whenever the capacity of the cell to oxidize fatty acids is exceeded or inhibited using drugs (hypoglycin,4-pentenoate) enhanced triglyceride synthesis results. Thus it appears that cytoplasmic acyl-CoA is a main controlling factor. Provision of α-glycerophosphate from glycolysis does not affect the oxidation and incorporation of fatty acids into lipids (22).

Myocardial Glucose Metabolism

The cytoplasmic process, by which glucose is degraded after activation to glucose-6-phosphate via fructose-1,6-diphosphate to pyruvate is commonly referred to as glycolysis. Pyruvate is oxidized intramitochondrially. However, glycolysis is not dependent on the completion of oxidative part of the metabolic pathway, since the necessary NAD^+ can be provided by the conversion of pyruvate to lactate. The heart can store glucose as glycogen as a fuel reserve. The synthesis and breakdown of glycogen constitute two separately controlled pathways.

Control of Glucose Metabolism

Glucose extraction by the heart is related to arterial glucose concentrations, and those of other substrates, the availability of insulin and the intracellular pH (24,21). Investigations of the concentrations of glycolytic intermediates (mass action ratios) and of the properties

of the glycolytic enzymes suggest that control may be exerted at four points: glucose transport and at the level of hexokinase, phosphofructokinase and pyruvate kinase (22). Insulin can stimulate the transport of glucose as well as of non-utilisable sugars, and oxidation of fatty acids has an inhibitory effect (22). However, our knowledge of the transport system is limited in comparison to other key enzymes: hexokinase and phosphofructokinase. Hexokinase is inhibited in a non-competitive manner by its product glucose-6-phosphate. This fact alone allows it to regulate the glycolytic flux in a concerted manner with phosphofructokinase since stimulating its actiivity will lower the glucose-6-phosphate level. Phosphofructokinase is a regulatory enzyme under most conditions. Its activity is inhibited by high ATP concentrations (22) and this effect of ATP can be overcome by AMP. ATP levels are well controlled within the cell. Adenylate kinase is thought to amplify small ATP changes by the conversion:

$$2\ ADP \rightleftharpoons ATP + AMP$$

A reduction of 6% in ATP levels should raise theoretically AMP concentrations by 800% (22). Inorganic phosphate also relieves the ATP inhibition of phosphofructokinase and stimulates further the action of AMP. The operation and control of glycolysis at two levels may seem unnecessary but it allows the heart to synthesize glycogen at rest under the influence of insulin, stimulating glucose transport and glycogen synthetase (glucosyltransferase).

Control of Glycogen Metabolism

Glucosyltransferase is considered to be the regulatory enzyme for glycogen synthesis. It occurs in two forms I and D. The D form which is dependent for its activity on glucose-6-phosphate (D = dependent), is strongly inhibited by ATP, ADP and inorganic phosphate that under most physiological conditions it will be inactive. The activation of glycosyltransferase involved another enzyme glycosyltransferase-D phosphatase, which converts the D to the I form. This phosphatase is inhibited by glycogen. In this manner glycogen exerts a negative feedback control on its synthesis by converting glucosyltransferase into the 'inactive' D form. This process is catalysed by protein kinase under influence of cAMP (22).

Neely and coworkers have contributed most to our understanding of control of ischaemic metabolism. In their elegant work using the isolated perfused working rat heart, factors responsible for the initial accelleration of glycolytic flux is approximately 2 min after induction of ischaemia and its subsequent inhibition was examined (reviewed in reference 34). Sequential analysis of glycolytic intermediates showed that the concentrations of all hexosephosphates, glucose-6-phosphate, fructose-6-phosphate, fructose 1,6-di phosphate were elevated at peak glycolytic flux (2 min). However, the

largest changes were found in the concentrations of dihydroacetone phosphate and glyceraldehyde-phosphate. It is noteworthy that pyruvate and lactate levels were only slightly raised. These findings are compatible with restricted glycolysis at the level of glyceraldehyde-3-phosphate dehydrogenase. Insulin in the presence of high glucose levels was able to stimulate glucose transport and as a result glucose utilisation was stimulated. However, even in the presence of insulin glycolytic flux remained restricted at the level of glyceraldehyde-phosphate dehydrogenase. This enzyme is sensitive to the cytoplasmic NADH/NAD ratio (22) and indirect evidence (lactate/pyruvate ratios) suggested that a significant increase may have occurred as early as 2 min after induction of ischaemia (35). Glyceraldehyde phosphate dehydrogenase is pH sensitive (22). In view of the difficulties in measuring intracellular pH it is not clear whether the intracellular acidity might have contributed as early as this.

Later during ischaemia when the total glucose utilisation is becoming inhibited control of glycolytic flux is essentially the same. Measurements of glycolytic intermediates support the view that control remains exerted at the level of glyceraldehyde-3-phosphate dehydrogenase (34). Relief of the control at the glyceraldehyde phosphate dehydrogenase level can be demonstrated using external buffering solutions. These effects are strongly dependent on the residual blood flow (34).

Glycogenolysis is controlled by the activity of phosphorylase. This enzyme occurs in two forms, phosphorylase a and b. These two enzymes differ in their sensitivity to the inhibitors ATP and glucose-6-phosphate. Phosphorylase b is only active when AMP and Pi levels are high enough to overcome the inhibitory effects of ATP and glucose-6-phosphate. The interconversion to phosphorylase a is regulated by phosphorylase b kinase, which in its turn exists in an active and inactive form. The interconversion of these enzymes is catalysed by a cyclic AMP dependent protein kinase.

METABOLIC EVENTS DURING ACUTE MYOCARDIAL ISCHAEMIA

The heart requires a constant supply of oxygen to maintain its functional activity. Whenever the oxygen demand can not be met by increased supply acute ischaemia ensues. It is apparent that different degrees of residual regional myocardial blood flow may occur. (This in contrast to experimentally induced anoxia: where increased coronary flow enhances wash-out of waste products H^+ and lactate.)

The onset of myocardial ischaemia is characterised by a locally reduced myocardial O_2 tension (36), despite increased O_2 extraction (27). There is a shift of intracellular redox pairs towards a more reduced state (increased NADH/NAD ratios, etc.). Contractility in the ischaemic area is depressed within seconds after occlusion and the

myocardium virtually ceases to contract at a time when ATP levels are not yet, but CP levels are decreased (29). These reductions of CP and ATP are accompanied by accumulations of ADP, AMP and inorganic phosphate, as well as their degradation products (4). cAMP is soon raised but the exact reason for this is not clear.

Electrolyte gradients are no longer held and the ischaemic cell loses K^+, while it gains Na^+ and Ca^{++} (6). The intracellular pH falls rapidly and is probably responsible for the rise in pCO_2 (17). All these changes during acute ischaemia (up to 10-20 min) are reversible upon reflow.

Glucose Metabolism During Ischaemia

It is becoming evident that the metabolic pattern of glucose is strongly dependent on the residual flow (34). There is an acceleration of glucose transport during ischaemia, and the extraction of glucose is enhanced (27), but the mechanism for this appears not to have been studied. Glycolytic flux is stimulated mainly due to enhanced glycogenolysis, which in its turn is stimulated by the action of cAMP on protein kinase - phosphorylase b kinase cascade. In addition, the increased levels of AMP and inorganic phosphate will enhance the activity of phosphorylase b.

Competition of Substrates During Ischaemia

It was generally assumed that the well known competition between substrates to be utilised by the well perfused, normoxic heart (22) was also valid during ischaemia. However, recent findings do not support this view. Thus FFA do no longer impede the extraction of glucose (15,31). The effect of lactate on glucose utilisation appears to be more complex. The main effect is on basal rather than on ischaemia induced glucose utilisation (34). The competition of pyruvate with glucose utilisation has also been examined (18). Pyruvate increased glucose utilisation, presumably by relieving control of glycolytic flux at glyceraldehyde phosphate dehydrogenase to either pyruvate kinase or pyruvate dehydrogenase (18). However, pyruvate was studied in the presence of a buffer. Pyruvate may have affected the intracellular acidosis due to the following reaction:

$$\text{Pyruvate} + \text{NADH} + H^+ \rightleftharpoons \text{Lactate} + NAD^+$$

The influence of acute ischaemia and residual blood flow on glycogenolysis and glycogen synthesis has not extensively been investigated, despite the fact that glycogen levels have a protective effect against the development of serious complications during acute ischaemia (31). It is assumed that glycogenolysis is stimulated by the action of cAMP on protein kinase (26), and increased levels of phosphorylase a have been demonstrated (12). On the other hand, it is possible that the rise in AMP and inorganic phosphate is sufficient to maximally stimulate phosphorylase b.

The reason for the sudden cessation of glycogenolysis, at a time when glycogen stores have not been depleted (34) is not clear. The effect of lactate, FFA and pyruvate on glycogenolysis has not been examined in great detail. Pyruvate (in the presence of a buffer) stimulated in addition to its effect on glycolysis glycogenolysis during ischaemia (34). Although this is very encouraging more work is required.

Control of Fatty Acid Metabolism in Ischaemic Myocardium

Control of fatty acid metabolism during acute ischaemia has hardly been investigated. Extraction of fatty acids (14C-palmitate) may (38) or may not be decreased (32). However, when measured chemically, extraction is reduced (27). The most likely explanation is the release of FFA from enhanced intramyocardial lipolysis into the effluent blood. Intracellular concentrations of free fatty acids might be raised (19). However, in view of the major technical difficulties of such measurements (see above) they can only be considered with reservations. That oxidation of fatty acids is inhibited is well established (32,27,15), and in a flow dependent fashion (15).

As a result intermediates of this pathway acyl-CoA, acyl-carnitine, hydroxyacyl-CoA all accumulate (15,40,13). The accumulation of these intermediates (particularly acyl-CoA and acyl-carnitine) seem to preclude an early inhibtion of acyl-carnitine acyl-transferase. However, this enzyme may be reduced in chronic ischaemia (39). The available data suggest that the increase in NADH/NAD ratio is largely responsible for the reduced β-oxidation, rather than reduced oxidation of acetyl-CoA (15). This may also explain why glucose can compete 'better' with fatty acids for oxidation (27). The incorporation of fatty acids into triglycerides is increased (38,15), presumably due to the increased levels of α-glycerophosphate and acyl-CoA. On the other hand lipolysis is stimulated (27,12,42). Despite this, tissue levels of triglyceride rise, particularly in the 'border' zone surrounding the severely ischaemic myocardium (2). The implication of these findings is that a energy wasting cycle is operative (31). Quantitative analysis of the amount of energy wasted is not available.

Mitochondrial Function During Ischaemia

Several groups have investigated the function of mitochondria, isolated from ischaemic myocardium (16,20,39). Such mitochondria are fragile and yields are only half of these obtained from non-ischaemic myocardium (16). Using manometric and polargraphic techniques it appears that their function phosphorylation-oxidation (P/O) ratios and respiratory control are decreased. However, inclusion of fat free albumin and EDTA in the homogenisation medium can nullify the effect of ischaemia (20). The effect of reoxygenation *in vitro* appears not to have been examined, but reperfusion *in*

vivo is known to cause extensive mitochondrial damage (11). This area deserves much more attention. Maximising the efficiency of the residual oxygen utilisation should be one of the main priorities. However, such studies may have to await the development of new in vivo techniques.

New Developments

The recent introduction of several techniques, allowing the study of the biochemistry of the ischaemic heart in vivo is most promising. Nuclear magnetic resonance of ^{31}P labelled intermediates of glucose and of adenine nucleotides have provided valuable information on intracellular pH and on control of glycogenolysis (1). Regional myocardial metabolism in healthy men has been attempted with ^{11}C labelled substrates (37). The method has not yet been validated for the ischaemic myocardium. The use of reflectance fluorescence and dual wavelength absorbtion already provides valuable information on redox states and control of the function of ischaemic myocardial mitochondria.

These techniques may help to solve many of the outstanding questions on the regulation of metabolism during acute ischaemia and will stimulate the application of the principle of metabolic intervention (discussed during this symposium by Mjøs et al) for the treatment of ischaemia.

REFERENCES

1. Bailey, I.A., Personal Communication, 1980.

2. Bryant, R.E., Thomas, W.A., O'Neal, R.M., Cir Research 6, 699-709, 1958.

3. Crass III, M.F., Shipp, J.C., Pieper, G.M., Am J Physiol 228, 618-627, 1975.

4. De Jong, J.W., Verdouw, P.D., Remme, W.J.,J Molec Cell Cardiol 9, 297-312, 1977.

5. Evans, J.R., Canad J Biochem 42, 955-969, 1964.

6. Flear, C.T.G., Riemersma, R.A., Nandra, A., Nandra, G., Rec Adv Studies Card Struct Metab 7, 297-305, 1976.

7. Fredholm, B., Rosell, S., J Pharmac Exp Ther 159, 1-7, 1968.

8. Fritz, I.B., Adv Lipid Res 1, 285-334, 1963.

9. Gloster, J., J Molec Cell Cardiol 9 (Suppl), 15, 1977.

10. Greenough III, W.B., Crespin, S.R., Steinberg, D., J Clin Invest 48, 1923-1933, 1969.

11. Hearse, D.J., Humphrey, S.M., Rec Adv Studies Card Struct Metab 7, 327-334, 1976.

12. Hough, F.S., Gevers, W., S Afr Med J, 49, 538-543, 1975.

13. Hull, F.E., Radloff, J.F., Rec Adv Studies Card Struct Metab 7, 13-21, 1976.

14. Hülsmann, W.C., J Mol Cell Endocrinol 12, 1-8, 1978.

15. Idell-Wenger, J.A., Neely, J.R. in Pathophysiology and therapeutics of myocardial ischaemia, Lefer, A.M. (Ed), Spectrum Publications Inc, p 227-238, 1977.

16. Jennings, R.B., Ganote, C.E.,Circ Research 38 (Suppl) I, 80-91, 1976.

17. Khuri, S.F., Flaherty, T.J., O'Riordan, J.B.,Circ Research 37, 455-463, 1975.

18. Liedtke, A.J., Nellis, S.H.,Circ Research 43, 189-199, 1978.

19. Lochner, A., Kotze, J.C., Benade, A.J., Gevers, W., J Molec Cell Cardiol 10, 857-875, 1978.

20. Lochner, A., Opie, L.H., Owen, P., Kotze, J.C.N., J Molec Cell Cardiol 7, 203-217, 1975.

21. Neely, J.R., Morgan, H.E., Ann Rev Physiol 36, 413-459, 1974.

22. Newsholme, E.A., Start, C., Regulation in Metabolism, JohnWiley and Sons, London, 1973.

23. Ockner, R.K., Manning, J.A., Poppenhausen, R.B., Ho, W.K.L Science 177, 56-58, 1972.

24. Opie, L.H., Am Heart J 76, 685-695, 1968.

25. Opie, L.H., Am Heart J 77, 100-122, 1969.

26. Opie, L.H., J Molec Cell Cardiol 1, 107-115, 1970.

27. Opie, L.H., Owen, P., Riemersma, R.A., Eur J Clin Invest 3, 419-435, 1973.

28. Oram, J.F., Bennetch, S.L., Neely, J.R., J Biol Chem 248, 5299-5309, 1973.

29. Puri, P.S., Rec Adv Studies Card Struct Metab 7, 161-169, 1976.

31. Riemersma, R.A., Metabolic aspects of acute myocardial ischaemia, University of Edinburgh, Ph.D. thesis, 1979.

32. Riemersma, R.A., Holland, A., Owen, P., Lewis, B., Opie, L.H., Cardiology, 56, 364-369, 1972.

33. Robinson, D.S., Adv Lipid Res, 1, 133-182, 1973.

34. Rovetto, M.J., Neely, J.R., in Pathophysiology and therapeutics of myocardial ischaemia, Lefer, A.M. (Ed), Spectrum Publications Inc, p 169-191, 1977.

35. Rovetto, M.J., Whitmer, J.T., Neely, J.R., Circ Research 32, 699-711, 1973.

36. Sayen, J.J., Sheldon, W.F., Peirce,G., Kuo, P.T., Cir Research 6, 779-798, 1958.

37. Schelbert, H.R., Personal communication, 1980.

38. Scheuer, J., Brachfeld, N., Metabolism 15, 945-954, 1966.

39. Schwartz, A., Wood, J.M., Allen, J.C., Bornet, E.P., Entman, M.L., Goldstein, M.A., Sordahl, L.A., Suzuki, M., Am J Cardiol 32, 46-61, 1973.

40. Sug, A.L., Thomsen, J.H., Folts, J.D., Bittar, N., Klein, M.I., Koke, J.R., Hutch, P.J., Arch Biochem Biophys 187, 25-33, 1978.

41. Stam, H., Geelhoed-Mieras, T., Hülsmann, W.C., Lipids 15, 242-250, 1980.

42. Vik-Mo, H., Riemersma, R.A., Mjøs, O.D., Oliver, M.F., Scand J Clin Lab Invest 39, 559-568, 1979.

Adv. Physiol. Sci. Vol. 8. Cardiovascular Physiology. Heart, Peripheral Circulation and Methodology
A. G. B. Kovách, E. Monos, G. Rubányi (eds)

IMPORTANCE OF ISCHEMIA-INDUCED MYOCARDIAL LIPOLYSIS IN DOGS

H. Vik-Mo, O. D. Mjøs, R. A. Riemersma and M. F. Oliver
Institute of Medical Biology, University of Tromsø, Norway and Department of Cardiology, The Royal Infirmary, Edinburgh, UK

The severity of an acute myocardial ischemic injury is determined by factors which alter the oxygen requirement of the heart relative to oxygen supply (Braunwald and Maroko 1974). Plasma fatty acid (FFA) concentration has been shown to be an important determinant of myocardial oxygen consumption (Mjøs 1971a). Consequently raised availability of FFA from arterial blood increase the extent of an acute myocardial ischemia (Miller et al. 1976). Reduction of arterial FFA concentration by several antilipolytic agents have been reported to reduce the myocardial ischemic injury in experimental studies (Kjekshus and Mjøs 1973, Mjøs et al. 1976) and in patients with myocardial infarction (Kjekshus and Grøttum 1978). In vitro experiments in the isolated rat heart have suggested that infusion of catecholamines or induction of myocardial ischemia might enhance hormone-sensitive lipase activity with consequent hydrolysis of endogenous triglycerides (Crass et al. 1975). Thus, local release of FFA within the ischemic myocardium might further aggravate the extent of myocardial ischemia.

The purpose of the present investigation was, firstly to study if induction of myocardial ischemia per se might stimulate myocardial lipolytic activity with breakdown of endogenous triglycerides in the in vivo situation. If so, part of the beneficial effect of antilipolytic agents on the severity of myocardial ischemia might be due to inhibition of myocardial lipolysis with reduced local FFA release to the ischemic myocardium, in addition to reduced extraction of FFA from plasma, as earlier shown in the non-ischemic myocardium (Mjøs 1971b). The second purpose of the investigation was to study possible mechanisms of action of the antilipolytic agents nicotinic acid and sodium salicylate which both have been shown to reduce an acute myocardial ischemic injury (Vik-Mo 1977).

METHODS

Experiments were performed in overnight fasted mongrel dogs anesthetized with sodium pentobarbital and ventilated on a volume controlled respirator. The heart was exposed through an incision in left fifth intercostal space. Myocardial ischemia was induced by occlusion of a branch from left anterior descending artery by a metal clip. A local coronary vein draining the ischemic myocardium and coronary sinus draining predominantly non-ischemic tissue were cannulated by plastic catheters (Vik-Mo et al. 1979). Blood samples were drawn simultaneously from aorta, coronary sinus and the

local coronary vein, and myocardial metabolism was assessed by arterio-venous differences of FFA, glucose, glycerol, lactate and oxygen saturation Metabolism in ischemic myocardium was calculated as arterio-local coronary vein (a-lv) differences and in non-ischemic myocardium as arterio-coronary sinus (a-cs) differences. Glycerol is not used in any significant amount in the myocardium (Most et al. 1969), and glycerol released from the myocardium was therefore used as a measure of lipolytic activity in the myocardium. Left ventricular systolic pressure (LVSP, left ventricular dP/dt (LV dP/dt) and heart rate (HR) were measured continuously. Wilcoxon nonparametric test for paired data (twotailed) was used to calculate probabilities.

EXPERIMENTAL DESIGN

Measurements of hemodynamic and metabolic variables and epicardial electrocardiographic mapping were performed before and 10 min after coronary artery occlusion. The following sequence of registrations were performed in each animal:

1. Basal conditions
2. During isoprenaline infusion (0.10 - 0.20 μg/min·kg b.w.)
3. During nicotinic acid (0.3 mg/min·kg b.w.) or sodium salicylate infusion (60 mg/kg b.w. followed by 0.15 mg/min·kg b.w.).
4. During nicotinic acid or sodium salicylate + isoprenaline infusion.

Four intermittant occlusions were performed in each animal, and a recovery period of 45 min was allowed after each occlusion period. Each dog served as its own control. Myocardial blood flow measurements were done in separate experiments before and after administration of nicotinic acid or sodium salicylate.

RESULTS

In the basal state, induction of myocardial ischemia produced release of glycerol from the ischemic area, as reflected in negative a-lv differences of glycerol, while a-cs differences measured simultaneously were not different from zero (Fig. 1). The glycerol release calculated as a-lv differences before induction of myocardial ischemia minus a-lv differences during myocardial ischemia was -30.9 $\pm$ 12.9 μmol/l, while during nicotinic acid administration the glycerol release was reduced in 4 of 5 experiments to -6.5 $\pm$ 10.2 μmol/l. During isoprenaline infusion no glycerol release across the ischemic myocardium was observed (Fig. 2). Infusion of isoprenaline markedly increased arterial FFA concentration and a concomitant elevation of FFA extraction across ischemic myocardium from 78 $\pm$ 14 to 380 $\pm$ 62 μmol/l ($p < 0.01$, $n = 14$) was observed. Arterial FFA concentration and FFA extraction in the ischemic myocardium correlated positively ($r = 0.52$, $p < 0.01$, $n = 28$) (Fig. 3). Pretreatment with nicotinic acid (Fig. 4) or sodium salicylate (Fig. 5) markedly depressed FFA extraction across the ischemic myocardium both in basal state and during isoprenaline infusion.

Induction of myocardial ischemia markedly increased the extraction of glucose and oxygen and the release of lactate across ischemic myocardium both in basal state and during isoprenaline infusion. Nicotinic acid reduced the oxygen extraction during isoprenaline infusion from

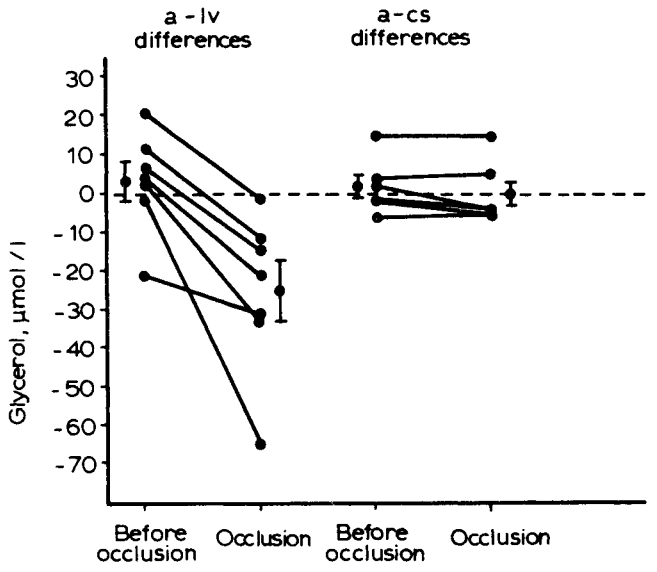

Fig. 1. The effect of coronary artery occlusion on arterio-venous differences across ischemic (a-lv) and non ischemic (a-cs) myocardium.

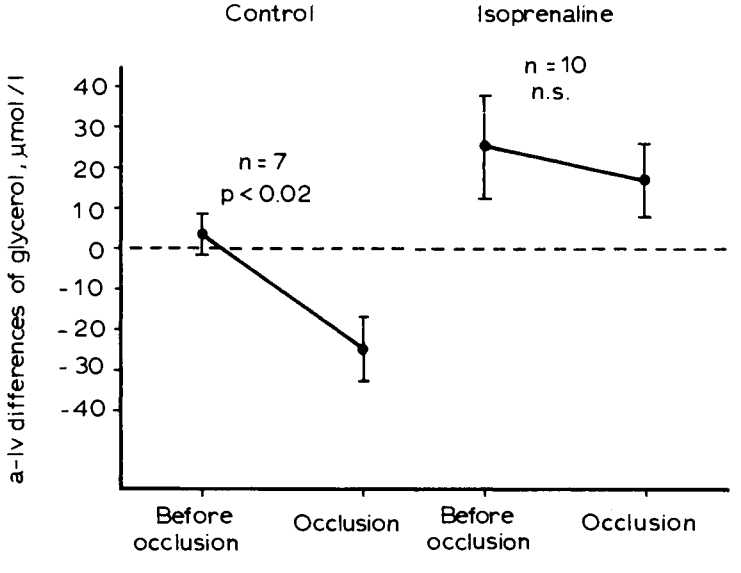

Fig. 2. The effect of coronary artery occlusion on arterio-venous differences across ischemic (a-lv) myocardium before and during isoprenaline infusion. n = number of experiments.

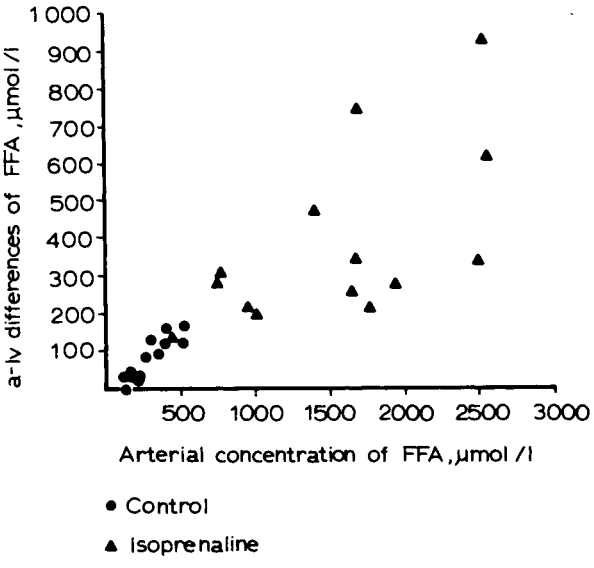

Fig. 3. Arterio-venous differences of free fatty acids (FFA) across ischemic myocardium (a-lv) as a function of arterial FFA concentration.

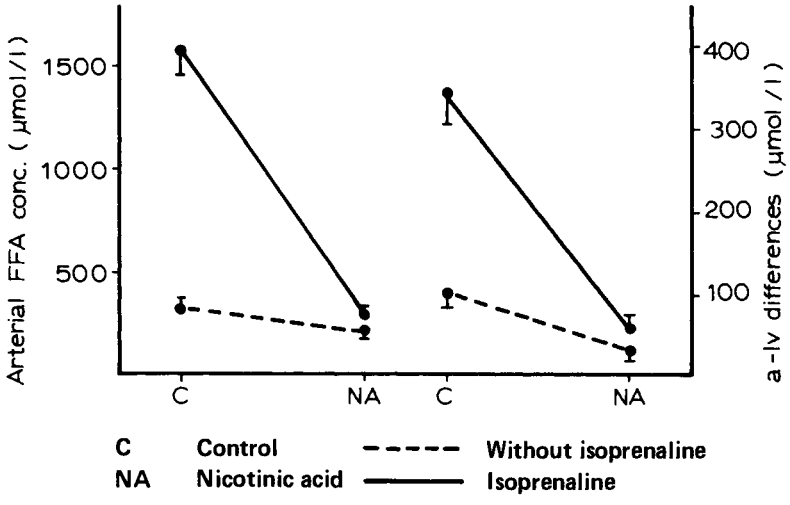

Fig. 4. Effects of nicotinic acid on arterial concentrations and arterio-venous differences of free fatty acids (FFA) across ischemic myocardium (a-lv) before (------) and during isoprenaline infusion (————). n = number of experiments.

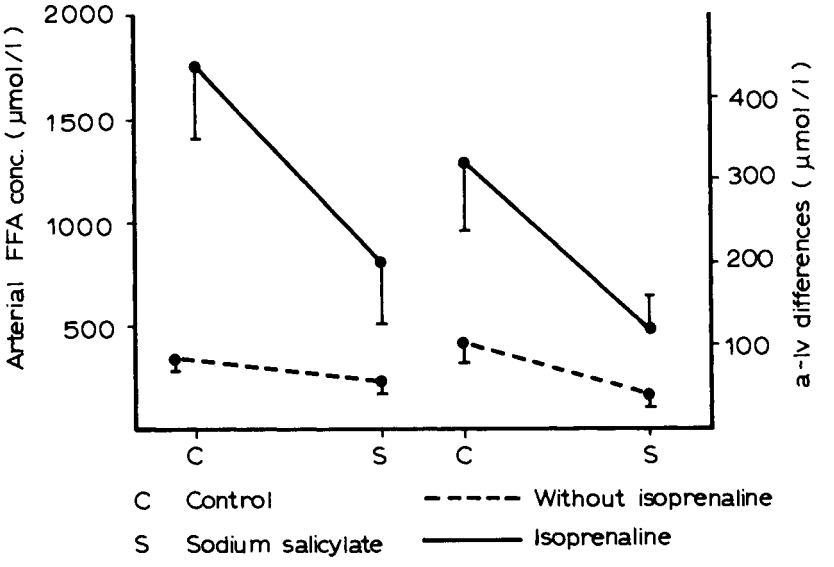

Fig. 5 Effect of sodium salicylate on arterial concentrations and arterio-venous differences of free fatty acids (FFA) across ischemic myocardium (a-lv) before and during isoprenaline infusion.

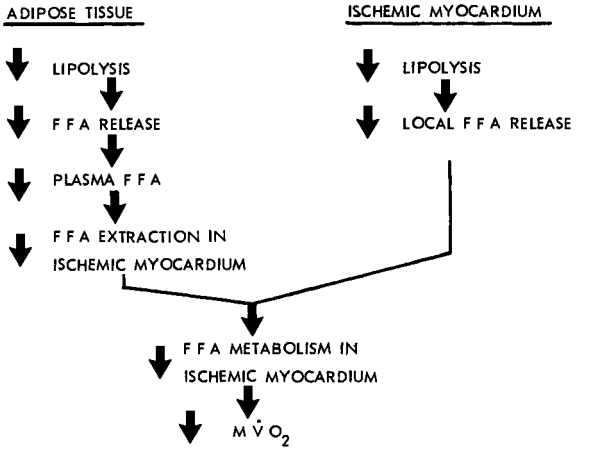

Fig. 6. Possible mechanisms for the action of antilipolytic agents on an acute ischemic myocardium. $M\dot{V}O_2$ = myocardial oxygen consumption. FFA = free fatty acids.

58.8 ± 3.4 to 53.4 ± 2.7% ($p < 0.02$, $n = 1$), whereas no significant changes in exchange of glucose or lactate occured either in basal state or during isoprenaline infusion.

LVSP, LV dP/dt and HR were not changed by nicotinic acid or sodium salicylate.

DISCUSSION

Induction of myocardial ischemia induced glycerol release from ischemic area, whereas no glycerol uptake/release was observed in/from nonischemic area. Since glycerokinase activity (Robinson and Newholm 1967), glycerol oxidation (Most et al. 1969) and lipoprotein lipase activity (Kessler and Senderoff 1962) are presumed to be low in ischemic myocardium, it is reasonable to assume that glycerol released from ischemic myocardium is a measure of endogenous lipolysis. Our finding of enhanced lipolysis in the intact dog myocardium during ischemia is in accordance with *in vitro* studies by Hough and Gevers (1975) reporting increased activity of hormon-sensitive lipase in ischemically perfused rat hearts. They found that the lipolytic activity was markedly reduced after reserpinization, indicating that local release of noradrenaline within ischemic myocardium might be the stimulus for enhanced lipolysis.

During isoprenaline infusion, however, we could not demonstrate any ischemia-induced enhancement of myocardial lipolysis. Possibly the high arterial FFA concentration during isoprenaline infusion might have effected an inhibition of myocardial lipolysis. Accordingly, Crass et al. (1975) found in the isolated rat heart that the stimulatory effect of adrenaline on mobilization of triglycerides was abolished when FFA was included in the perfusate.

Although the oxidation of FFA is impaired in ischemic myocardium (Scheuer and Brachfeld 1966), we observed a substantial extraction of FFA in the ischemic area during high plasma concentrations, indicating increased esterification of FFA. Reduction of plasma FFA by the antilipolytic agents nicotinic acid or sodium salicylate markedly reduced the extraction in ischemic myocardium, as earlier shown in the non-ischemic myocardium (Mjøs 1971b).

Antilipolytic agents have been shown to reduce the extent of an acute myocardial ischemic injury in experimental studies (Kjekshus and Mjøs 1973, Mjøs et al. 1976, Vik-Mo 1977) and in patients with acute myocardial infarction (Kjekshus and Grøttum 1978). Possible mechanisms of action of antilipolytic agents on acute myocardial ischemia are shown in Fig. 6. Firstly, reduced lipolysis in adipose tissue might decrease the FFA availability from plasma with consequently reduced extraction of FFA in the ischemic myocardium. Secondly, antilipolytic agents might also inhibit lipolysis within the ischemic myocardium.

REFERENCES

Braunwald, E. and Maroko, P.R. (1974). The reduction of infarct size - an idea whose time (for testing) has come. Circulation 50, 206-209.

Crass, M.F. III, Shipp, J.C. and Pieper, G.M. (1975). Effects of catecholamines on myocardial endogenous substrates and contractility. Amer. J. Physiol. 228, 618-627.

Hough, F.S. and Gevers, W. (1975). Catecholamine release as mediator of intracellular enzyme activation in ischaemic perfused rat hearts S. Afr. Med. J., 49, 538-543.

Kessler, J.I. and Senderoff, E. (1962). Effect of experimental infarction, manual massage, and electrical defibrillation on myocardial lipoprotein lipase activity of dogs. J. clin. Invest. 41, 1531-1536.

Kjekshus, J.K. and Grøttum, P. (1978). Effect of lipolysis on infarct size in man. In A. Hjalmarson and L. Wilhelmsen (eds.). Acute and Longterm Medical Management of Myocardial Ischaemia, L. Lindal & Søner AB, Mølndal, Sweden, Pp. 373-381.

Kjekshus, J.K. and Mjøs, O.D. (1973). Effect of inhibition of lipolysis on infarct size after experimental coronary artery occlusion. J. clin. Invest. 52, 1770-1778.

Miller, N.E., Mjøs, O.D. and Oliver, M.F. (1976). Reduction of myocardial free fatty acid extraction and epicardial ST segment elevation by albumin infusion during coronary occlusion in dogs. Clin. Sci. Molec. Med. 51, 209-213.

Mjøs, O.D. (1971a). Effect of free fatty acids on myocardial function and oxygen consumption in intact dogs. J. clin. Invest. 50, 1386-1389.

Mjøs, O.D. (1971b). Effect of inhibition of lipolysis on myocardial oxygen consumption in the presence of isoproterenol. J. clin. Invest. 50, 1869-1873.

Mjøs, O.D., Miller, N.E., Riemersma, E.A. and Oliver, M.F. (1976). Effects of p-chlorophenoxyisobutyrate on myocardial free fatty acid extraction, ventricular blood flow, and epicardial ST-segment elevation during coronary occlusion in dogs. Circulation 53, 494-500.

Most, A.S., Brachfeld, N., Gorling, R. and Wahren, J. (1969). Free fatty acid metabolism of the human heart at rest. J. clin. Invest. 48, 1177-1188.

Robinson, J. and Newsholm, E.A. (1967). Glycerol kinase activities in rat heart and adipose tissue. Biochem. J. 104, 2c.

Scheuer, J. and Brachfeld, N. (1966). Myocardial uptake and fractional distribution of palmitate-1-C^{14} by the ischemic dog heart. Metabolism 15 945-954.

Vik-Mo, H., Riemersma, R.A., Mjøs, O.D. and Oliver, M.F. (1979). Effect of myocardial ischaemia and antilipolytic agents on lipolysis and fatty acid metabolism in the in situ dog heart. Scand. J. clin. Lab. Invest. 39, 559-568.

Vik-Mo, H. (1977). Distribution of coronary blood flow during acute coronary artery occlusion in dogs: Effect of nicotinic acid and sodium salicylate. Scand. J. clin. Lab. Invest. 37, 697-703.

Adv. Physiol. Sci. Vol. 8. Cardiovascular Physiology. Heart, Peripheral Circulation and Methodology
A. G. B. Kovách, E. Monos, G. Rubányi (eds)

CALCIUM AND THE CO-ORDINATION OF METABOLISM AND MECHANICAL PERFORMANCE IN RABBIT PAPILLARY MUSCLE

T. Russell Snow
Department of Physiology, Duke University, Durham, NC, USA

The traditional view of myocardial homeostasis portrays the processes responsible for substrate catabolism and oxidative phosphorylation as responding passively to the energetic needs of the contractile proteins. This in part is based on studies of skeletal muscle (17). However, as a result of numerous experiments, a quite different model is beginning to emerge. In this model, the performance of any of the three processes- substrate catabolism, oxidative phosphorylation and contractility - is in part determined by the state of the other two. This tight coupling of the three processes has led to the proposal that an "M" should be added to E-C coupling ie E.C.M. coupling (7). One immediate question posed by this model is what messengers are responsible for co-ordinating the function of these three systems.

In addition to its well established role in determining contractility (26,29), recent studies clearly suggest that Ca^{++} may play an important role as a messenger. The work by Fabiato & Fabiato (11,12) has shown that sarcolemmal (SL) Ca^{++} may be the trigger for release of contractile Ca^{++} from the sarcoplasmic reticulum (SR). These studies along with those showing the importance of ATP in determining the Ca^{++} mediated slow inward current (15,24) suggest one mechanism by which the three systems are co-ordinated. Another site at which these processes may be synchronized is the SR membrane. Studies by Entman and his colleagues have shown that the SR membrane contains a Ca^{++} sensitive glycogenolytic complex capable of high rates of glycogen catabolism (8,9,10). In addition to the SL and SR, the work by Carafoli et al (2,3) and by Lehninger (19) suggest that the mitochondria may also be a site at which the performance of the systems responsible for substrate catabolism, oxidative phosphorylation and force generation are coordinated.

While these studies have demonstrated the capability for coordination in isolated vesicles, few studies have attacked the problem in the intact tissue. However, Hartley & McNeil (14) have shown that changes in inotropic state alter the phosphorylase b:a ratio. These studies have been extended by Thompson et al (27) and show a similar shift during the course of a single contraction. Possibly more germane are the studies by Snow et al (22) which show that changes in extracellular $[Ca^{++}]$ induce both a change in contractile performance and in the redox state of the respiratory chain.

The experiments described below were designed to further explore this relation and specifically to investigate two questions: 1. does Ca^{++} affect the dynamic relation between the rate of substrate catabolism and of mechanical power expenditure and 2. which pools/sources of Ca^{++} are most involved in insuring synchrony between the three systems. The results show that SL Ca^{++} is involved in coordinating these systems but not via Na^{+}-Ca^{++} exchange; that endogenous catacholamines do not contribute appreciably and that the SR Ca^{++} probably plays a major role.

METHODS

Right ventricular papillary muscles were excised from stunned female (2-3 Kg) New Zealand rabbits. These were isometrically mounted in a Ringer bath containing 10 mU/cc insulin and one of four substrates (10 mM): d-glucose (Glc), pyruvate (Pyr), butyric acid (BA) or β-OH- butyrate (BOB). The different substrates were used to accentuate the separate catabolic pathways. This permitted determination of the importance Ca^{++} plays in coordinating each with mechanical function. Metabolic function was evaluated (5) by measuring (16) the maximum extent of the intra mitochondrial (25) pyridine nucleotide (PN) oxidation (P_{mx}) which accompanies contractile activity. The slope of the least squares fitted line of P_{mx} vs $\tau \cdot \nu$ was used as a measure of the coupling between metabolism and mechanical function: P_{mx} = maximum PN oxidation, τ = maximum developed tension and ν = frequency of stimulation. In a separate set of experiments, the product $\tau \cdot \nu$ has been shown to be well correlated ($p = .94$ Fisher $z = 1.74$) with the rate of oxygen consumption. A decrease in the slope, coupling coefficient (M), indicates a decrease in the extent of PN oxidation per unit change in mechanical power ($\Delta \tau \cdot \nu$). This is interpreted as signifing a more sensitive coupling between metabolism and mechanical performance.

RESULTS

The first series of experiments were designed to determine the effects of changes in extracellular [Ca^{++}] on the coupling coefficient. Each muscle was exposed to four levels of Ca^{++} (1,2,4 and 6 mM) presented in random order. The top panel in Fig. 1 shows a typical force-frequency (τ vs ν) response for one muscle at each Ca^{++} level. The lower panel of Fig. 1 shows the plot of P_{mx} vs $\tau \cdot \nu$ for the same muscle. The cumulative data are presented in Table I where the results are given as percent relative to control ([Ca_o^{++}] = 1 mM). As expected, increases in [Ca^{++}] elicited greater contractile performance.

Figure 1

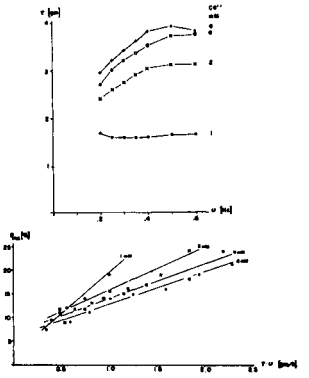

Figure 2

The response of the coupling coefficient, M, to $\Delta[Ca_o^{++}]$ are also presented in Fig. 2. Because of the flat force-frequency response with $[Ca_o^{++}]$ = 1 mM, subsequent experiments used 2 mM as the control. From Fig. 2 it is evident that M is significantly affected by $\Delta[Ca_o^{++}]$ with Glc, Pyr or BA as the substrate. With BOB, there was no appreciable effect.

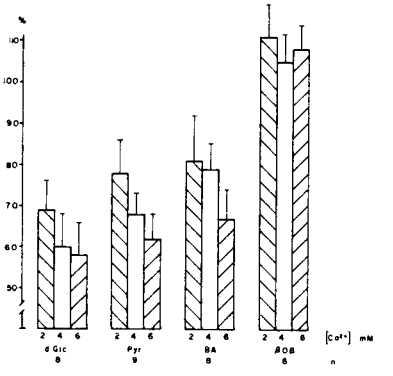

TABLE I

n		$[Ca^{++}]$	τ	$\dot{\tau}_{mx}$	TPT	M
8	Glu	2	132 ± 6	134 ± 10	109 ± 11	69 ± 7
		4	163 ± 6	172 ± 14	104 ± 11	60 ± 8
		6	182 ± 7	188 ± 16	97 ± 10	58 ± 8
9	Pyr	2	149 ± 7	172 ± 19	103 ± 3	78 ± 8
		4	188 ± 16	233 ± 20	96 ± 4	68 ± 5
		6	194 ± 19	248 ± 24	92 ± 2	62 ± 6
8	BA	2	121 ± 9	123 ± 9	102 ± 7	81 ± 11
		4	149 ± 20	155 ± 19	91 ± 4	79 ± 6
		6	157 ± 17	163 ± 14	82 ± 5	67 ± 7
8	βOB	2	134 ± 7	146 ± 8	94 ± 3	1.11 ± 8
		4	149 ± 6	180 ± 11	86 ± 5	1.05 ± 7
		6	154 ± 8	194 ± 12	82 ± 6	1.08 ± 6

Values given are mean ± SEM in percent (%) relative to control ≡ 1 mM Ca^{++}

Figure 3

To determine whether endogenous catacholamines contribute to the effects observed with $\Delta[Ca_o^{++}]$ (20), the next set of experiments examined the effect of propranolol on the coupling coefficient response to $\Delta[Ca_o^{++}]$. The results are given in Table II and Fig. 3. Comparing Fig. 3 to Fig. 2 shows that with Glc or BA, propranolol did not appreciable alter the response to $\Delta[Ca_o^{++}]$. However, with Pyr, there was an attenuation. Thus it would appear that at least part of the change in M induced by $\Delta[Ca_o^{++}]$ with Pyr is due to cAMP.

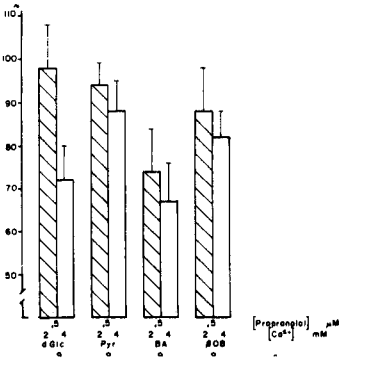

Table II

n			τ	$\dot{\tau}_{mx}$	TPT	M
9	d Glc	Prop	97 ± 4	97 ± 4	95 ± 3	98 ± 10
		Ca=4	104 ± 5	117 ± 6	83 ± 5	72 ± 8
9	Pyr	Prop	110 ± 4	105 ± 3	101 ± 5	94 ± 5
		Ca^{++}=4	118 ± 4	119 ± 8	94 ± 5	88 ± 7
9	BA	Prop	97 ± 5	97 ± 5	95 ± 3	74 ± 10
		Ca^{++}=4	97 ± 9	102 ± 10	88 ± 4	67 ± 9
9	βOB	Prop	94 ± 12	89 ± 7	100 ± 2	88 ± 10
		Ca^{++}	91 ± 13	88 ± 14	104 ± 3	82 ± 6

Since $\Delta[Ca_o^{++}]$ will affect both the slow inward current and Na^+-Ca^{++} exchange, the next set of experiments examined the effect of ouabain on M. This agent was selected because of its effect on Na^+-Ca^{++} exchange (18). As expected, ouabain produced a concentration dependent positive inotropic response - Fig. 4. The cumulative results are given in Table III with the effect upon M shown in Fig. 5. As is evident, ouabain had virtually no effect. In a second set of experiments, the effect of ouabain on the response of M to $\Delta[Ca_o^{++}]$ was examined. As Table IV shows, ouabain had a slight effect with BA as the substrate.

Figure 4

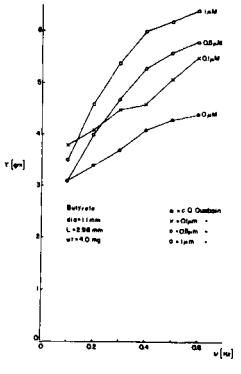

Figure 5

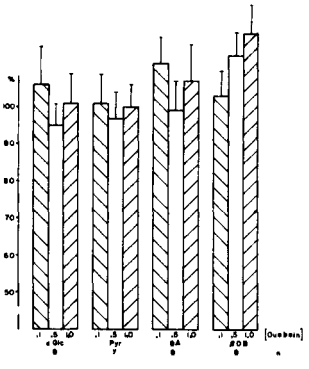

Table III

n		[Ouab]	τ	$\dot{t}_{mx}$	TPT	M
8	d Gcl	.1	115 ± 5	107 ± 8	93 ± 3	106 ± 9
		.5	114 ± 6	105 ± 9	86 ± 2	95 ± 11
		1.0	123 ± 9	117 ± 7	83 ± 1	101 ± 8
7	Pyr	.1	101 ± 8	104 ± 10	97 ± 3	101 ± 8
		.5	108 ± 12	106 ± 8	90 ± 7	97 ± 7
		1.0	110 ± 11	114 ± 8	87 ± 5	100 ± 6
8	BA	.1	102 ± 7	107 ± 8	94 ± 5	112 ± 7
		.5	104 ± 7	112 ± 9	91 ± 5	99 ± 8
		1.0	97 ± 10	108 ± 11	87 ± 3	107 ± 10
9	OB	.1	97 ± 4	100 ± 8	90 ± 11	103 ± 6
		.5	95 ± 7	103 ± 10	87 ± 11	114 ± 6
		1.0	86 ± 10	93 ± 7	81 ± 16	121 ± 8

Values given are mean ± SEM in percent

Control = 2 mM Ca^{++}, 0 μM Ouabain

Table IV

n		$[Ca^{++}]/[Ouab]$	τ	$\dot{t}_{mx}$	TPT	M
6	d Glc	2/.5	107 ± 8	104 ± 8	91 ± 6	99 ± 7
		4/.5	115 ± 7	117 ± 8	80 ± 4	78 ± 6
7	Pyr	2/.5	120 ± 9	117 ± 5	89 ± 6	97 ± 6
		4/.5	129 ± 14	128 ± 7	79 ± 9	65 ± 10
7	BA	2/.5	114 ± 8	118 ± 9	95 ± 4	94 ± 6
		4/.5	121 ± 7	135 ± 11	85 ± 11	60 ± 7
6	OHB	2/.5	98 ± 4	104 ± 7	87 ± 3	102 ± 5
		4/.5	112 ± 9	128 ± 8	85 ± 4	99 ± 6

Values given are mean ± SEM in percent

Control = 2 mM Ca^{++}; 0 μM Ouabain

Figure 6

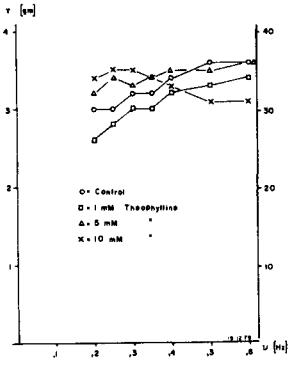

The final set of experiments examined the importance of SR Ca^{++} in determining the coupling coefficient. To do this, theophylline was used to modify the Ca^{++} sequestering ability of the SR (1,28). A typical force-frequency response is shown in Fig. 6. As expected, the maximum inotropic response occurs at the slower stimulation frequencies (1). The metabolic response to theophylline was unexpected - Fig. 7. The upper trace is a measure of the PN fluorescence intensity with a downward deflection indicating an oxidation ie decrease in fluorescence intensity. With Glc and 10 mM theophylline, the initial response to the onset of contractile activity is the expected oxidation (4). However, this is immediately followed by a stable and more reduced state of the PN after approximately 1 min. With cessation of contractile activity, there is a transient reduction of the PN then a slow oxidative return to the rest level. The cumulative data are presented in Table V and Fig. 8. With Glc and BA, 10 mM theophylline essentially nullifies the normal oxidative response to increases in contractile activity.

Figure 7

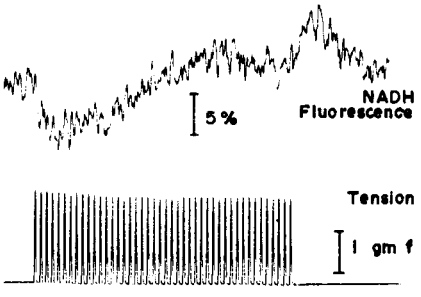

Figure 8

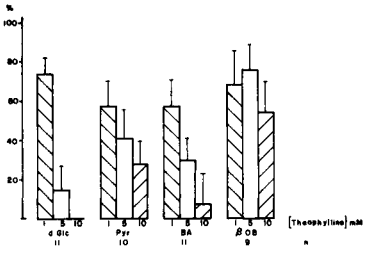

Table V

n						
11	d Glc	1	94 ± 7	100 ± 7	93 ± 1	74 ± 12
		5	98 ± 11	110 ± 11	95 ± 6	15 ± 15
		10	91 ± 8	104 ± 9	95 ± 7	-
10	Pyr	1	101 ± 13	103 ± 11	94 ± 11	58 ± 12
		5	110 ± 11	102 ± 12	105 ± 5	41 ± 15
		10	102 ± 12	106 ± 14	102 ± 5	28 ± 11
11	BA	1	91 ± 7	94 ± 5	92 ± 11	58 ± 13
		5	101 ± 12	97 ± 5	102 ± 15	24 ± 11
		10	100 ± 12	97 ± 9	113 ± 13	7 ± 18
9	OB	1	99 ± 3	104 ± 5	93 ± 8	68 ± 18
		5	112 ± 9	128 ± 12	104 ± 11	76 ± 13
		10	101 ± 6	111 ± 3	101 ± 7	55 ± 15

Values given are mean ± SEM in percent

Control = 2 mM Ca^{++}; 0 mM Theophylline

SUMMARY:

The data from these studies demonstrate that Ca^{++} does play an important role in determining the relation between metabolism and mechanical function. In particular, increases in $[Ca_o^{++}]$ improve the coupling between these systems as evidenced by the extent of the decrease in PN oxidation per unit increase in mechanical power. This is particularly true for Glc, Pyr and BA. From Table II, endogenous catacholamines do not contribute to this effect.

The effects of ouabain, Table III, suggest that the Ca^{++} associated with Na^{+}-Ca^{++} exchange does not contribute to the messenger pool with any of the substrates. However, as Table IV shows, ouabain does affect the response of M to $\Delta[Ca_o^{++}]$ with Pyr and BA. Previous studies (6,27) have shown that different substrates alter mechanical performance of the mammalian myocardium. These data along with the results just presented suggest an explanation for this differential effect. Specifically, the difference in performance with different substrates may be due to their altering the relative contributions of the separate pools in providing Ca^{++} for E.C.M. coupling.

The extraordinary response of the coupling coefficient to theophylline in the presence of Glc indicates that the glycogenolytic complex demonstrated in SR vesicles by Entman et al (8,9,10) may well play a significant role in coordinating metabolism and contractile function in-vivo. Thus the SR may provide the Ca^{++} necessary for both troponin activation (13,23) and for stimulation of substrate catabolism (9,10). In addition to this provocative hypothesis/model, the response to theophylline also suggests that

the relation between the redox state of the respiratory chain and the rate of ADP rephosphorylation is not as simple as sometimes assumed. The data presented here and elsewhere (22) show that external factors besides oxygen can dramatically affect this relation.

ACKNOWLEDGEMENTS

Support for this work was provided by USPHS SCOR HL 17670.

REFERENCES

1. Blinks, J.R., Olson, C.B., Jewell, B.R. and Braveny, P. Influence of caffeine and other methylxanthines on mechanical properties of isolated mammalian heart muscle (Kitten). Circ. Res. 30, 367-392, 1972.
2. Carafoli, E., Dabrowska, R., Crovetti, F., Tiozzo, Drabikowski, W. An in vitro study of the interaction of heart mitochondria with troponin bound Ca^{++}. Biochem. Biophys Res Com. 62, 908-912, 1975.
3. Carafoli, E. Mitochondrial Ca^{++} transport and the regulation of heart contraction and metabolism. J. Mol. Cell Card. 7, 83-87, 1975.
4. Chance, B., Williams, G.R. The respiratory chain and oxidative phosphorylation. Adv. Enzymol. 17, 65-134, 1956.
5. Chance, B. Pyridine nucleotide as an indicator of the oxygen requirements for energy linked functions of mitochondria. Circ. Res. Suppl I. 38, 31-38, 1976.
6. Chapman, J.B., Gibbs, C.L. and Gibson, W.R. Heat and fluorescence changes in cardiac muscle. Effects of substrates and calcium. J. Mol. Cell Card. 8, 545-558, 1976.
7. Dhalla, N.S., Ziegelhoffer, A. and Harrow, J.A.C. Regulatory role of membrane systems in heart function. Can. J. Physiol. Pharm. 55, 1211-1234, 1977.
8. Entman, M.L., Kaniike, K., Goldstein, M.A., Nelson, T.E., Bornet, E.P. Futch, T.W. and Schwartz, A. Association of glycogenolysis with cardiac sarcoplasmic reticulum. J. Biol. Chem. 251, 3140-3146, 1976.
9. Entman, M.L., Bornet, E.P., Garber, A.J., Schwartz, A., Levey, G.S. Lehotay, D.C., and Bricker, L.A. The cardiac sarcoplasmic reticulum-glycogenolytic complex. A possible effector site for cyclic AMP. Biochem. Biophys Acta 499, 228-237, 1977.
10. Entman, M.L., Keslensky, S.S., Chu, A., and Van Winkle, W.B. The sarcoplasmic reticulum-glycogenolytic complex in mammalian fast twitch skeletal muscle: Proposed in-vitro counter part of the contraction activated glycogenolytic pool. J. Biol. Chem., in press.
11. Fabiato, A. and Fabiato, F. Calcium induced release of calcium from the sarcoplasmic reticulum of skinned cells from adult human, dog, cat, rabbit, rat and frog hearts and from fetal and new-born rat ventricles. Ann. NY Acad. Sci. 307, 499-521, 1978.
12. Fabiato, A., and Fabiato, F. Calcium and cardiac excitation-contraction coupling. Ann. Rev. Physiol. 41, 473-484, 1979.
13. Fuchs, F., Reddy, Y., and Briggs, F.N. The interaction of cations with the calcium binding site of troponin. Biochem. Biophys. Acta. 221, 407-409, 1970.
14. Hartley, E.J. and McNeill, J.H. The effect of calcium on cardiac phosphorylase activation contractile force and cyclic AMP in euthyroid and hyperthyroid rat hearts. Can. J. Physiol. Pharm. 54, 590-595, 1976.

15. Hui, C.W., Drummond, M. and Drummond, G.I. Calcium accumulation and cyclic AMP stimulated phosphorylation in plasma membrane enriched preparations of myocardium. Arch. Biochem. Biophys. 173, 415-427, 1976.
16. Jöbsis, F.F., Legallais, V., and O'Connor, M. A regulated differential fluorometer for the assay of oxidative metabolism in intact tissue. IEEE Trans. BME 13, 93-99, 1966.
17. Jöbsis, F.F. and Duffield, J.C. Oxidative and glycolytic recovery metabolism in muscle. J. Gen. Physiol. 50, 1009-1047, 1967.
18. Langer, G.A. Relationship between myocardial contractility and the effects of digitalis on ionic exchange. Fed. Proc. 36, 2231-2234, 1977.
19. Lehninger, A.L., Vercesi, A., and Bababunmi, E.A. Regulation of Ca^{++} release from mitochondria by the oxidation-reduction state of pyridine nucleotides. Proc. Natl. Acad. Sci. 75, 1690-1694, 1978.
20. Rasmussen, H., Jensen, P., Lake, W., Friedmann, N. and Goodman, D.B.P. Cyclic nucleotides and cellular calcium metabolism. Adv. Cyclic Nucleoti. Res. 5, 375-394, 1975.
21. Snow, T.R. Study of the mechanical and metabolic performance of rabbit papillary muscle during normoxia and hypoxia. Am. J. Physiol. 235, H144-H149, 1978.
22. Snow, T.R., Rubanyi, G., Dora, T., Dora, E. and Kovach, A.G.B. Effect of perfusate Ca^{++} on the relation between metabolism and mechanical performance in the rat heart. Can. J. Physiol. Pharm. in press.
23. Solaro, R.J., Wise, R.M., Shiner, J.S., and Briggs, F.N. Calcium requirements for cardiac myofibrillar activation. Circ. Res. 34, 525-530, 1974.
24. Sperelakis, N., and Schneider, J.A. A metabolic control mechanism for calcium ion influx that may protect the ventricular myocardial cell. Am. J. Card. 37, 1079-1085, 1976.
25. Steenbergen, C., Deleeuw, G. and J.R. Williamson. Analysis of control of glycolysis in ischemic hearts having heterogenous zones of anoxia. J. Mol. Cell Card. 10, 617-639, 1978.
26. Szent-Györgyi, A.G. Calcium regulation of muscle contraction. Biophys. J. 15, 707-723, 1975.
27. Thompson, C.I., Rubio, R. and Berne, R.M. Changes in adenosine and glycogen phosphorylase activity during the cardiac cycle. Am. J. Physiol. 238, H389-H398, 1980.
28. Thorpe, W.R. Some effects of caffeine and quinidine on sarcoplasmic reticulum of skeletal and cardiac muscle. Can. J. Physiol. Pharm. 51, 499-503, 1973.
29. Trithart, H., Volkmann, R., Weiss, R., and Eibach, H. The interrelationship of calcium mediated action potentials and tension development in cat ventricular myocardium. J. Mol. Cell Card. 8, 249-261, 1976.

Adv. Physiol. Sci. Vol. 8. Cardiovascular Physiology. Heart, Peripheral Circulation and Methodology
A. G. B. Kovách, E. Monos, G. Rubányi (eds)

EFFECT OF CALCIUM AND NICKEL IONS ON OXIDATIVE AND GLYCOLYTIC METABOLISM IN THE PERFUSED RAT HEART

Gábor Rubányi
Experimental Research Department, Semmelweis Medical University, Budapest, Hungary

In addition to its key role in excitation-contraction /E-C/ coupling process /12/, Ca has been shown to activate phosphorylase-b-kinase /7,13/ in the myocardium, without any change in tissue cyclic AMP content /6/, to increase the rate of glucose uptake and oxidation and to accelerate breakdown of glycogen and trygliceride /6/. Earlier studies have shown /21/ that with glucose perfusion the elevation of perfusate calcium concentration /Ca_p/ resulted in a biphasic tissue NADH fluorescence response: consisting of an initial NADH oxidation followed by NAD reduction. Intracellular NADH/NAD ratio is not only an indicator of glycolytic and respiratory rates, but at the same time is of great importance in the regulation of the aforementioned metabolic processes /9/.

The present study was therefore designed to analyse changes in tissue NADH fluorescence at various extracellular Ca levels in parallel with contractile activity, oxygen consumption and myocardial lactate production in the presence of glucose or pyruvate as exogenous substrates. In order to further clarify action mechanism of Ca, contractile and metabolic effects of nickel ion /Ni/, a well known antagonist of Ca in the E-C coupling process of the myocardium /10/ were also studied.

MATERIALS AND METHODS

Hearts were rapidly excised from Wistar rats, cooled and the aortic stump cannulated to allow retrograde coronary perfusion by modified Krebs-Henseleit bicarbonate /KHB/ solution containing 10 mU/ml insulin and 10 mM glucose or 10 mM pyruvate, via constant flow peristaltic pump, bubble-trap, thermostate /37°C/ and filter.
Left ventricular pressure development /LVPD/, dp/dt_{max}, and perfusion pressure /PP/ were monitored. Left ventricular mechanical performance was characterized by the product of heart rate and dp/dt_{max}.

Myocardial oxygen consumption /MVO_2/ was calculated from AV-pO_2 difference and coronary flow.
Using a time-sharing fluorometer redox changes of the heart were monitored by alterations in the fluorescence intensity from tissue NADH /3/. In order to eliminate fluorescence artifacts, reflectance /R/ and corrected fluorescence /CR/ were monitored as well /4/. Only CR values will be given in the figures.
Myocardial lactate production was characterized by changes of perfusate lactate concentration in lieu of total lactate production /i.e. lactate in tissue plus perfusate/ since 1. this allowed serial measurements from a single heart in various conditions and 2. changes in lactate release qualitatively reflect changes in total lactate production /5, 16/. Values given are mean ± S.E.M. unless otherwise noted.

RESULTS

Effects of Ca^{2+}

The product of heart rate and dp/dt_{max} was linearly related to the rate of oxygen consumption with either glucose or pyruvate as the exogenous substrate /Figure 1/. These findings indicate that the effect of Ca on mechanical performance and rate of respiration is independent of the substrate present, under the present experimental conditions.

Tissue NADH fluorescence intensity would be expected to decrease linearly with increased rate of oxygen consumption /9/. However, NADH fluorescence changes following Ca_p elevation followed a different pattern in the presence of glucose /Figure 2/. At Ca_p levels of 0.32 and 0.65 mM,

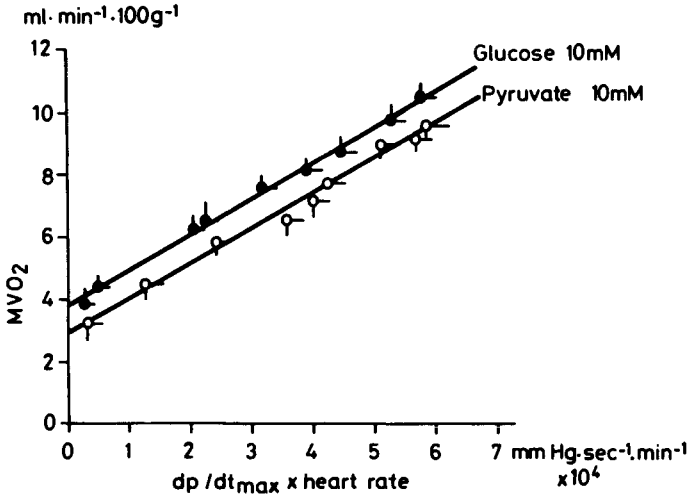

Figure 1. Effects of cardiac work and substrate on oxygen consumption during stepwise elevation of perfusate Ca from 0.32 to 7.8 mM.

tissue NADH fluorescence intensity was by 10 to 12 % higher than in the control state /i.e. fluorescence intensity was taken as 100 % in the presence of 1.3 mM Ca and 10 mM glucose in the perfusate/, indicating a more reduced state of the respiratory chain due to a decrease of mechanical activity. Elevation of Ca_p from 0.65 to 1.3 caused a considerable NADH oxidation, analogous to the State 4 to 3 transition observed in isolated mitochondria /1/. Further elevation of Ca_p evoked an unexpected Ca-dependent increase of NADH fluorescence intensity.

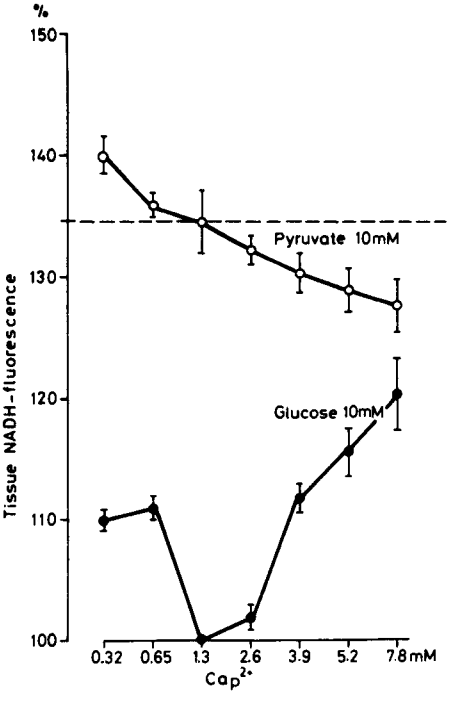

Figure 2. Tissue NADH fluorescence changes with elevation of perfusate Ca-concentration in the presence of either glucose or pyruvate as the sole exogenous substrate in isolated rat hearts.

Switching the exogenous substrate from glucose to pyruvate caused a significant increase in fluorescence intensity /34.8±4.7 %/. Elevation of Ca_p in the presence of pyruvate induced tissue NADH fluorescence changes fundamentally different from those observed in the presence of glucose. Pyruvate totally abolished the development of NAD reduction at higher Ca levels, and instead a Ca-dependent NADH oxidation could be observed. At 7.8 mM Ca_p the intensity of NADH fluorescence was almost similar with glucose and pyruvate perfusion /Figure 2/.

Ca_p elevation caused a significant increase of myocardial lactate release in the presence of glucose /Figure 3/. Pyruvate induced a continuous slow decline in lactate production. Elevation of Ca_p from 1.3 to 5.2 mM caused also an increase in lactate output, but significantly less pronounced than that observed in the presence of glucose.

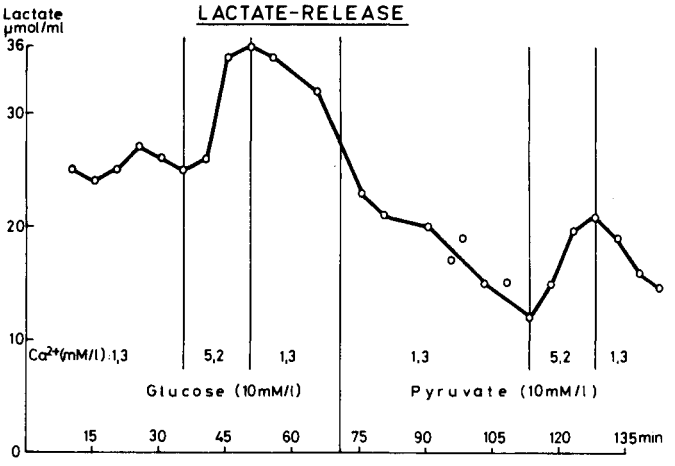

Figure 3. Effects of four-fold elevation of perfusate Ca concentration and substrate on myocardial lactate production. Circles represent the mean of 6 experiments.

Effects of Ni^{2+}. Ni-Ca antagonism

Addition of 1 mM Ni to the perfusate /first vertical bar in Figure 4/ abolished contractile activity and increased coronary resistance /TCR/. Immediately after cessation of heart beat NADH fluorescence intensity rose, which was followed by a decrease of it /NADH oxidation/ of much greater extent. Inhibition of contractile activity was accompanied by a significant decrease of oxygen consumption.
Threefold elevation of Ca_p from 1.3 to 3.9 mM /second vertical bar in Figure 4/ restored contractile activity and caused further increase of TCR. Excess Ca restored NADH fluorescence intensity and the rate of MVO_2 in the presence of glucose as the exogenous substrate.
In the presence of pyruvate /Figure 5/ $NiCl_2$ caused also a decrease of NADH fluorescence intensity, the magnitude of which, however, was significantly less pronounced than that observed in the presence of glucose /10.4±1.8 % and 25.4 ±

3.5 % respectively; p 0.01/. Excess Ca had no effect on the Ni-induced more oxidized state in the presence of pyruvate which is in sharp contrast to those observed with glucose /see Figure 4/.

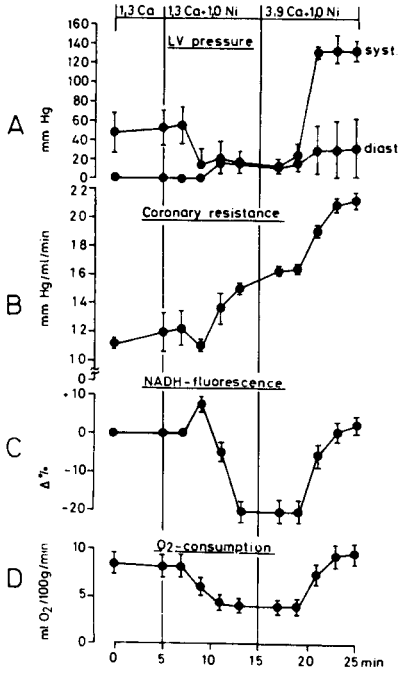

Figure 4. Effect of Ni and Ca on contractility, coronary resistance /TCR/, NADH-fluorescence and oxygen consumption in the isolated rat heart.

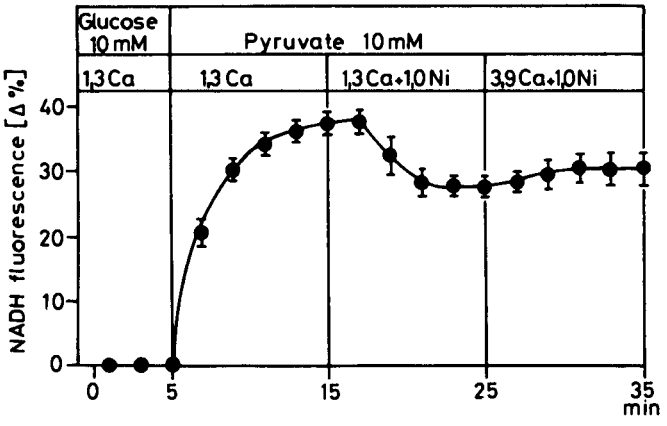

Figure 5. Effect of Ni and Ca on tissue NADH fluorescence in the presence of pyruvate as the sole exogenous substrate.

DISCUSSION

Cardiac Metabolism and Ca^{2+}

The increase of NADH fluorescence intensity /i.e. tissue NADH accumulation/ in aerobic hearts, when the rate of oxygen consumption was continuously accelerated by elevation of Ca_p, could have been due to either increased rate of cytosolic /glycolytic/ NADH production or to increased substrate /reducing equivalent/ availability for mitochondrial respiratory chain. Tissue hypoxia, a well known cause of increased tissue NADH /15, 18/ can be excluded, since 1. contractile activity increased continuously with elevation of Ca_p; 2. oxygen supply and tissue oxygen tension were proved to be adequate, and 3. high Ca induced NADH oxidation in the presence of pyruvate

Cytosolic NADH accumulation

The rise in cytosolic NADH production in aerobic hearts may occur because an acceleration of phosphofructokinase /PFK/ /which was reported to develop during raising cardiac performance /9// results in higher tissue levels of glyceraldehyde-3-phosphate /G-3-P/, which in turn activates G-3-P-dehydrogenase /GAPD//Figure 6/. Increased flux through this step apparently produces NADH faster than can be oxidized by any of the two major reactions operating in cardiac muscle /i.e. malate-aspartate shuttle /19/ and lactate production from pyruvate//see Figure 6/.

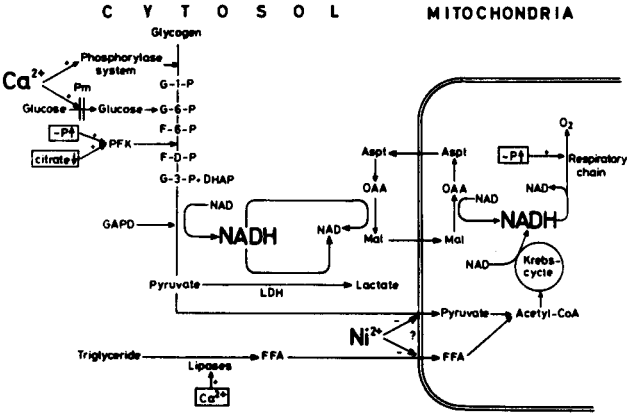

Figure 6. Pathways for cytosolic and mitochondrial NADH production and oxidation, and possible sites of action of Ca and Ni ions in the intermediary metabolism of cardiac tissue.

The suggestion that cytosolic NADH does increase is supported by the analysis of lactate production. In accordance with Opie /15/ and Rovetto et al /17/ isolated rat hearts always produced lactate in the present experiments as well. Significant elevation of tissue lactate production after Ca_p elevation in the aerobic hearts assumes that either pyruvate and/or cytosolic NADH production increases as a result of Ca-stimulation of cardiac metabolism. Neely et al /14/ found that when glycolysis is accelerated with insulin treatment a larger percent of pyruvate is converted to lactate - due to an increased production of cytosolic NADH. The reduction of both basal and Ca-stimulated lactate production in the presence of pyruvate /Figure 3/ - when cellular pyruvate level is in excess - can only be explained by the previously demonstrated decrease of cytosolic NADH production /9/ due to an inhibition of glycolysis. These data strongly suggest that excess Ca enhances glycolytic rate in the presence of glucose as the exogenous substrate.

Mitochondrial NADH accumulation

Mitochondrial production of NADH may be explained by the following two possibilities: 1. accelerated transport of reducing equivalents into mitochondria via malate-aspartate shuttle, and 2. increased substrate /pyruvate,FFA/ availability for NADH production via the citric-acid-cycle /Figure 6/.
The rate of malate transport is proportional to its concentrations /11/. Accelerated transport requires a high level of cytosolic NADH, which is probably present during Ca-induced activation of glycolysis /see above/. Increased mitochondrial NADH production by excess pyruvate, on the other hand, is substantiated by previous /22/ and present demonstration of increased tissue NADH fluorescence intensity after switching from glucose to pyruvate perfusion /Figure 4/, when cytosolic NADH production was reported to be inhibited /9/. The finding that in the presence of pyruvate /when both cytosolic NADH- and pyruvate-production accelerating actions of Ca are abolished/ high Ca_p causes only NADH oxidation, strongly emphasizes the probability of the aforementioned mechanisms.

The possibility that increased triglyceride breakdown through Ca-activation of myocardial lipases /8/ may contribute to mitochondrial NADH accumulation can not be ruled out /Figure 6/. Previous demonstration of a decrease in triglyceride content and elevated levels of free fatty acid /FFA/ in the myocardium as well as increased release of glycerol in the perfusate upon elevation of Ca_p in the presence of glucose as the sole exogenous substrate /6/ substantiates this possibility.

The difference in metabolic response to increase in Ca_p between glucose and pyruvate would suggest that the metabolic site/s/ affected by Ca must occur prior to pyruvate oxidation. The two reasonable sites are the transport of glucose into the cell /20/ and phosphorylase-b-kinase /7, 13/, but increased production of FFA should also be considered /Figure 6/.

In aerobic hearts most of the ATP is synthetized from oxidation of NADH produced in the mitochondria /9/. Experimental data clearly indicate that the increase of Ca_p enhances the delivery of reducing equivalents to respiratory chain /affecting both cytosolic and mitochondrial NADH compartments/ above that necessary to compensate for the increase in the rate of NADH reoxidation. This action of Ca could serve to guarantee adequate rates of ADP rephosphorylation in response to increasing mechanical demands.

Cardiac Metabolism and Ni^{2+}

The biphasic NADH fluorescence response following Ni addition to the perfusate of isolated rat hearts suggests that at least two different mechanisms are responsible for Ni-induced changes in cardiac metabolism. The initial NAD reduction is the consequence of reduced ATP-splitting due to cessation of heart beat, analogous to the State 3 to 4 transition observed in isolated mitochondria /1/. Significant decrease of MVO_2 substantiates this assumption.
The second phase of NADH response starts several minutes after the cessation of contractile activity by Ni, when no further changes in MVO_2 were observed /Figure 4/.
The first explanation for NADH oxidation is that the myocardium was hypoxic prior to Ni administration. Among other evidences, the fact that with pyruvate as the substrate excess Ca restores contractility and MVO_2 without any change in NADH fluorescence, argues against this theory.
The possibilities that Ni uncouples oxidative phosphorylation or that there is an active mitochondrial uptake of Ni, may be excluded since MVO_2 did not increase during the second phase of NADH response. Hence, the only reasonable explanation for the more oxidized fluorescence state is that Ni inhibits the flow of reducing equivalents to the mitochondria /analogous to State 2 observed in isolated mitochondria //1, 22/.
The fact that inhibition of glycolysis by pyruvate did not abolish Ni-action on NADH fluorescence indicates that the site of Ni-action should be between pyruvate dehydrogenase and the first member of the respiratory chain /NADH/ /Figure 6/.
The experimental finding that excess Ca restored Ni-induced decrease of tissue NADH/NAD ratio in the presence of glucose only, substantiates the assumption that the increase of Ca_p enhances the flow of reducing equivalents to the respiratory chain primarily by activating glycogenolysis/glycolysis /see above/.

REFERENCES

1. Chance,B.,Williams,G.R. - Adv.Enzymol. 17:65. 1956
2. Chance,B. - J.Biol.Chem. 240:2729. 1965.
3. Chance,B., Salkovitz,A., Kovách,A.G.B.-Am.J.Physiol. 223:207. 1972
4. Chapman,J.B. - J.gen.Physiol. 59:135. 1972
5. Chiong,M.A. - Can.J.Physiol.Pharmacol. 51:482. 1973
6. Dhalla,N.S., Yates,J.C., Proveda,V.- Can.J.Physiol.Pharmacol. 55:925. 1977
7. Friesen,A.J.D.,Oliver,N.,Allen,G. - Am.J.Physiol. 217:445. 1969
8. Jesmok,G.J.,Mogelnicki,S.R.,Lech,J.J., Calvert,D.N. - J.Mol.Cell.Cardiol. 8:283. 1976
9. Kobayashi,K.,Neely,J.R. - Circ.Res. 44:166. 1979
10. Kohlhardt,M.,Minich,Z.,Haap,K. - J.Mol.Cell.Cardiol. 11:1227. 1979
11. La Nou,K.F., Williamson,J.R.- Metabolism 20:119. 1971
12. Langer,G.A. In: The mammalian myocardium. Ed. G.A.Langer, A.J.Brady. J.Wiley and Son, New York, 1974. p.193.
13. Namm,D.H.,Mayer,S.E.,Maltbie,M. - Mol.Pharmacol. 4:522. 1968
14. Neely,J.R.,Denton,R.M.,England,P.J.,Randle,P.J. - Biochem J. 128:147. 1972
15. Opie,L.H. - Am.Heart J. 76:685. 1968
16. Opie,L.H., Mansford,K.R.L. -Eur.J.Clin.Invet.1:295. 1971
17. Rovetto,M.J.,Whitmer,J.T.,Neely,J.R. -Circ.Res. 32:669. 1973
18. Rovetto,M.J.,Lamberton,W.F.,Neely,J.R.-Circ.Res. 37: 742. 1975
19. Safer,B. - Circ.Res. 37:527. 1975
20. Schwartz,A., Lindemayer,G.E.,Allen,J.C. - Curr.Top.Membr. Transp. 3:118. 1972
21. Snow,T.R.,Rubányi,G.,Dora,T.,Dóra,E.,Kovách,A.G.B. - Can.J.Physiol.Pharmacol. 1980 - in press
22. Williamson,J.R. - J.Biol.Chem. 240:2309. 1965

Adv. Physiol. Sci. Vol. 8. Cardiovascular Physiology. Heart, Peripheral Circulation and Methodology
A. G. B. Kovách, E. Monos, G. Rubányi (eds)

REGULATION OF ADENINE NUCLEOTIDE TRANSLOCATION BY LONG CHAIN FATTY ACYL CoA ESTERS*

Earl Shrago and Gebretateos Woldegiorgis
Departments of Medicine and Nutritional Sciences, University of Wisconsin, Madison, Wisconsin 53706, USA

The adenine nucleotide translocase which carries out a one-to-one exchange of ADP for ATP across the inner mitochondrial membrane confers the specificity of oxidative phosphorylation on the adenine nucleotides, and, by coordinating their concentrations in the mitochondria and cytosol, determines the phosphate potential of the cell (Klingenberg, 1970). Moreover, recent evidence provides added support for the hypothesis that the adenine nucleotide translocase is the rate limiting step in overall energy linked respiration (LaNoue and Schoolwerth, 1979). There seems good reason to believe, therefore, that such an important biochemical reaction would be carefully regulated. As in the analogous case of the morphine receptor and the endorphins, the many studies on the binding to and inhibition of the adenine nucleotide translocase by atractylate, carboxyatractylate and bongkrekic acid (Klingenberg, 1970), indicate the likelihood of an endogenous effector for the ADP/ATP carrier. We and others have postulated that long chain fatty acyl CoA esters are the natural effectors and physiological modulators of the adenine nucleotide translocase (for review see Meijer and VanDam, 1975; Vignais, 1976).

Heart muscle which preferentially utilizes fatty acids for energy purposes (Neely and Morgan, 1974) provides an excellent model system to study the potential effects of fatty acyl CoA esters on adenine nucleotide transport and myocardial energy metabolism. The experimental evidence suggests that during periods of ischemia or hypoxia concentrations of fatty acyl CoA esters build up in the mitochondrial matrix and/or cytosol of the cell in sufficient quantities to inhibit the ADP/ATP carrier and thereby impair the synthesis and distribution of high energy phosphate compounds (Shrago *et al.* 1976).

MATERIALS AND METHODS

Heavy beef heart mitochondria were prepared according to Green *et al.* (1957) and submitochondrial particles by the method of Hanson and Smith (1964). The procedure for purification of the ADP/ATP carrier by hydroxyapatite chromatography (Klingenberg *et al.* 1978) was followed to prepare the homogeneous palmitoyl CoA-protein complex (Woldegiorgis and Shrago,1980). Assay of adenine nucleotide translocase activity was carried out according to standard methods used in this laboratory (Lerner *et al.* 1972). Long

*This work was supported by U.S.P.H. Grant GM-14033

chain acyl CoA esters were determined by the method of Williamson and Corkey (1969). Atractylate, carboxyatractylate and acyl CoA esters were purchased from commercial sources. The bongkrekic acid was kindly provided by Professor Berends, Delft University of Technology, The Netherlands.

RESULTS

Inhibitions of the adenine nucleotide translocase by atractylate, bongkrekic acid and oleoyl CoA was compared in intact beef heart mitochondria (Figure 1). Atractylate and oleoyl CoA, at concentrations below 5 μM, produced a marked inhibition of adenine nucleotide translocation whereas bongkrekic acid only exerted an inhibition at comparatively higher concentrations. In addition, it was necessary to preincubate the mitochondria with bongkrekic acid for at least seven minutes and the pH lowered to 6.5 to permit a significant fraction of the bongkrekic acid to be protonated and thus penetrate the inner mitochondrial membrane where it binds to and inhibits the carrier on the matrix (m) side.

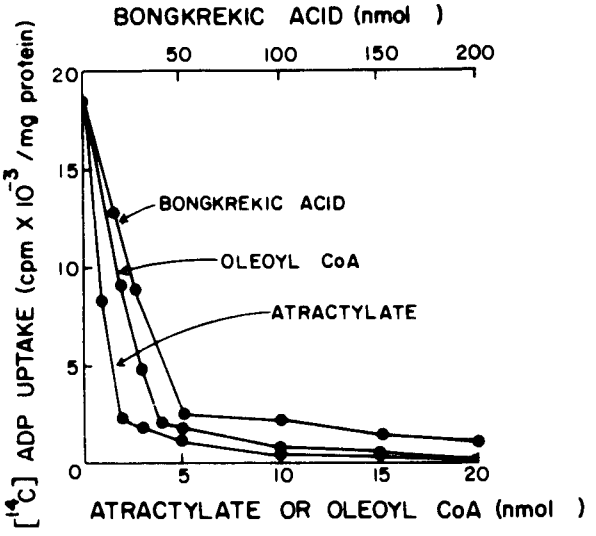

(Fig. 1) Effect of increasing concentration of oleoyl CoA, atractylate and bongkrekic acid on [^{14}C]ADP uptake by beef heart mitochondria.

The similar inhibition pattern of adenine nucleotide translocation in isolated beef heart mitochondria by atractylate and palmitoyl CoA is shown in panel A of Figure 2. Neither of the ligands can penetrate the inner mitochondrial membrane and the binding which occurs on the cytosolic (c) side of the membrane initiates marked inhibition of the translocase which is competitive in type (Shrago et al. 1974). After preincubation of the mitochondria with [^{14}C]ADP atractylate is able to remove the nucleotide bound specifically to the carrier site and, as shown in panel B, palmitoyl CoA acts in an identical manner to atractylate under the same experimental conditions. The results clearly demonstrate that on the c side of the inner membrane long chain acyl CoA esters have a specific atractylate-like effect on the adenine nucleotide translocator.

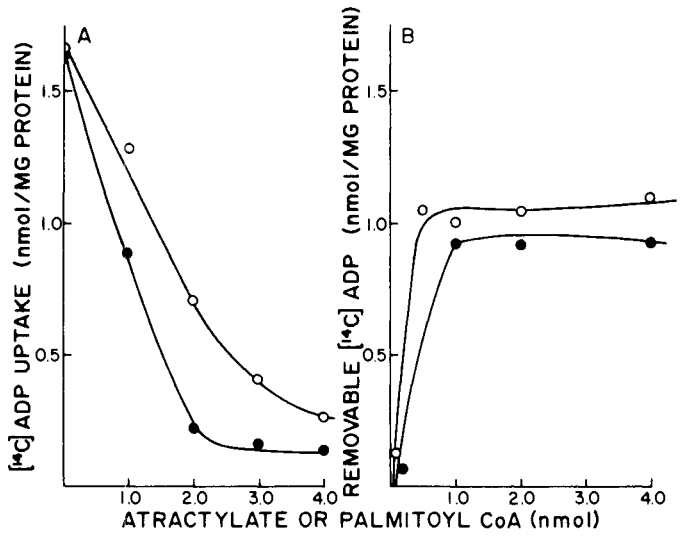

(Fig. 2) Effect of atractylate and palmitoyl CoA on ADP uptake and removal from bovine heart mitochondria. Panel A: The uptake of ADP was determined using intact mitochondria and carrier free [^{14}C]ADP. Panel B: Removal of bound ADP was measured with mitochondria partially depleted of endogenous nucleotides and then preincubated for 2 min. with [^{14}C]ADP following which atractylate or palmitoyl CoA was added to the incubation mixture.

Submitochondrial particles prepared by sonication contain inner membranes with inverted sidedness. Schertzer and Racker (1974) made the observation that with "inside out" particles atractylate, which would be able to interact directly with the m side of the inner membrane, was unable to inhibit the adenine nucleotide translocase. Experiments demonstrating inhibition of the adenine nucleotide translocase by long chain acyl CoA esters as compared with the effects of atractylate and bongkrekic acid in the inverted submitochondrial particles are shown in Figure 3. The atractylate sensitivity of the adenine nucleotide translocase of approximately 20% suggests two populations of mitochondria with 80% of the submitochondrial particles being inverted. As expected, bongkrekic acid which could now interact directly with the m side of the inner membrane became a very potent inhibitor of the adenine nucleotide translocase. The most significant observation was that one showing the inhibition by oleoyl CoA to be as severe in the inverted submitochondrial particles as in the intact mitochondria. Thus, in contrast to their effect with intact mitochondria, long chain fatty acyl CoA esters exert a bongkrekic acid-like effect on the m side of the inner membrane with submitochondrial particles.

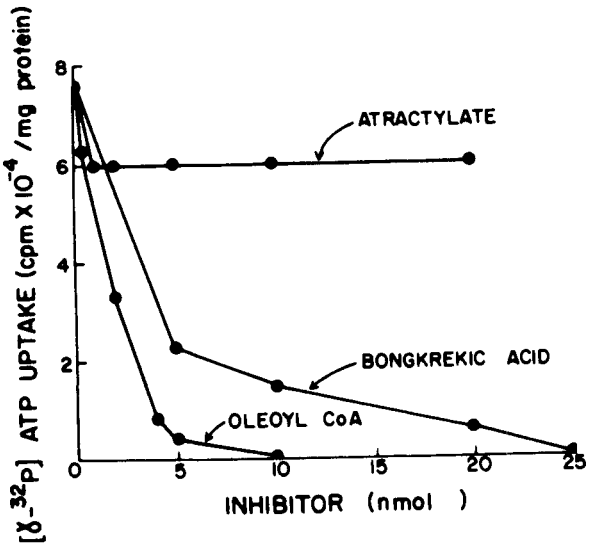

(Fig. 3) Effect of increasing concentrations of oleoyl CoA, atractylate and bongkrekic acid on [γ^{32}P]ATP by beef heart inverted submitochondrial particles.

Results of a related experiment are shown in Table 1.

TABLE 1

Effect of Inhibitory Ligands of the Adenine Nucleotide Translocase on the Uptake and Removal of [^{14}C]ADP from Submitochondrial Particles.

In experiment 1, submitochondrial particles were preincubated with or without the ligands, [^{14}C]ADP was added and the incubation continued. The reaction mixture was then filtered on a 0.45 mμ Millipore filter, the residue on the filter washed twice with the incubation medium, dried and the radioactivity of the filter counted. In experiment 2 the submitochondrial particles were preincubated with [^{14}C]ADP and then incubated with ADP or bongkrekic acid or palmitoyl CoA. Subsequent treatment of the reaction mixture was as described in experiment 1.

ADDITIONS	BOUND [^{14}C]ADP nmol	% OF CONTROL
Expt. 1		
None	1.74	100
Atractylate	1.76	100
Bongkrekic Acid	0.12	7
Palmitoyl CoA	0.33	19
Expt. 2		
None	1.70	100
ADP	0.40	23
Bongkrekic Acid	1.64	96
Palmitoyl CoA	1.65	97

In the case represented by experiment 1 atractylate is unable to inhibit the binding and subsequent transport of ADP into the submitochondrial

particle. By contrast palmitoyl CoA which acts in a similar manner to atractylate when incubated with intact mitochondria inhibits more like bongkrekic acid when added to inverted submitochondrial particles. The critical observations are shown with particles preincubated with [^{14}C]ADP in experiment 2. When [^{14}C]ADP is preincubated with submitochondrial particles, bongkrekic acid does not remove the bound nucleotide though the bound [^{14}C]ADP is able to exchange freely with added cold ADP. More important, palmitoyl CoA which was shown to remove [^{14}C]ADP from the c side is unable to remove a nucleotide from the m side of the membrane. Thus, the experiments clearly demonstrate: 1) In contrast to either atractylate or bongkrekic acid, which bind and inhibit asymmetrically, acyl CoA esters are able to bind to and inhibit the adenine nucleotide translocase effectively from either side of the inner mitochondrial membrane. 2) The acyl CoA esters which bind to the translocator on either side of the inner mitochondrial membrane initiate effects typical of atractylate on the c side and bongkrekic acid on the m side of the inner membrane.

Klingenberg and co-workers (1978,1979) purified the carboxyatractylate and bongkrekic acid binding proteins which had the properties of the ADP/ATP carrier. The purification scheme makes use of the selective elution of the homogeneous protein from a hydroxyapatite column. The purification is followed by loading the mitochondria with the radioactive ligands carboxyatractylate or bongkrekic acid which bind tightly to the carrier. An identical purification scheme was carried out except that the mitochondria were loaded with [^{14}C] palmitoyl CoA (Woldegiorgis and Shrago, 1980). Following extraction of the mitochondria with Brij 58 and solubilization with Triton X-100 the radioactivity resided primarily with the protein in the void volume of the hydroxyapatite column and ligand bound protein appeared as a homogeneous band of 30,000 daltons by gel electrophoresis (Figure 4).

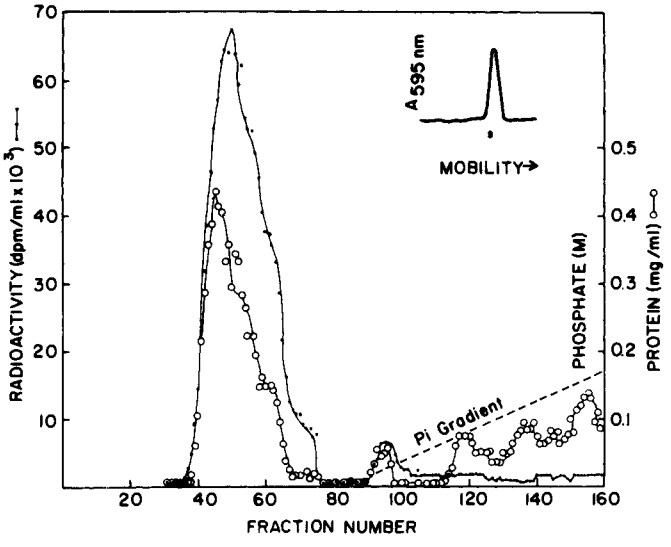

(Fig. 4) Purification of the [^{14}C] palmitoyl CoA protein complex by hydroxyapatite chromatography.

It was found that prior loading of the mitochondria with carboxyatractylate or bongkrekic acid is necessary not only to follow the purification of the carrier but also to insure its stability, particularly at temperatures higher than 4°C. In Figure 5 the electrophoretic peak of the purified unliganded protein is compared with that of the palmitoyl CoA protein complex when both were purified at 22°C. The important finding is that palmitoyl CoA, like carboxyatractylate, prevented the disaggregation of the purified protein. This experiment demonstrates that the acyl CoA ligand binds to a specific receptor site on the carrier and provides additional support for its biological function in adenine nucleotide transport.

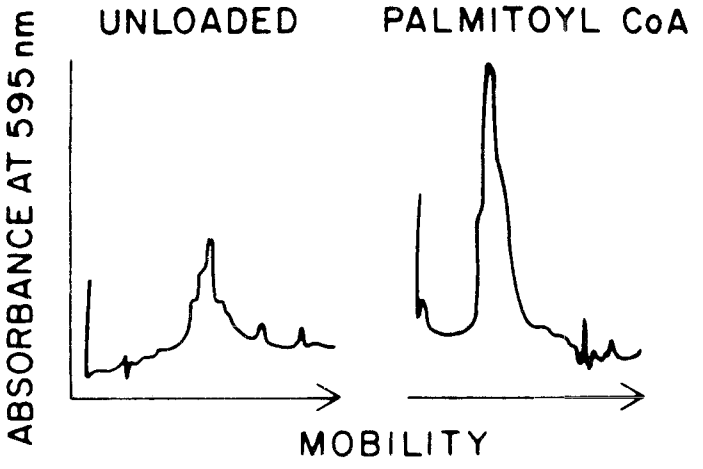

(Fig. 5) Sodium dodecyl sulfate gel electrophoresis patterns of the unliganded and palmitoyl CoA loaded protein following hydroxyapatite chromatography.

An attempt to show an in vivo effect of long chain fatty acyl CoA esters on adenine nucleotide translocation was carried out under experimental conditions of myocardial ischemia (Shug et al. 1974). At timed intervals following the development of myocardial ischemia in dogs subjected to coronary ligation, hearts were removed and tissue appropriately handled for preparation of mitochondria and long chain fatty acyl CoA esters. A time curve comparing mitochondrial adenine nucleotide translocase activity and tissue long chain acyl CoA esters following myocardial ischemia is shown in Figure 6. Within 15 minutes following ligation of the anterior coronary artery there was a sharp increase of long chain acyl CoA esters in the infarct area associated with a decline in the adenine nucleotide transport. These reciprocal changes continued for up to 60 minutes when the experiment was terminated.

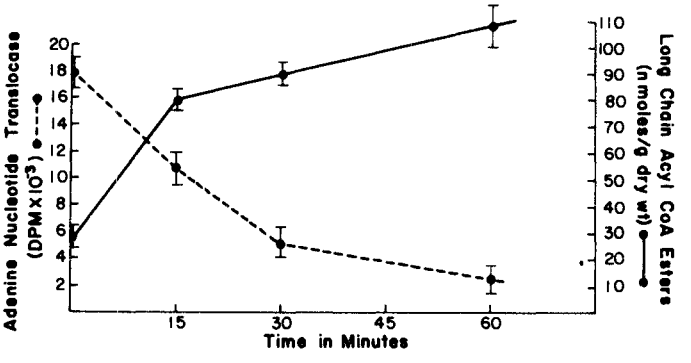

(Fig. 6) Comparison of adenine nucleotide translocase activity and long chain acyl CoA ester concentration in dog heart following onset of myocardial ischemia. Results are expressed as the average and standard deviation from five animals.

DISCUSSION

The adenine nucleotide translocase is recognized to be one of the most important enzymes in cell bioenergetics. The characterization of this transport protein particularly in the laboratories of Klingenberg (1970) and Vignais (1976) was based primarily on the effects of specific inhibitors, atractylate and bongkrekic acid. A model for the mechanism of adenine nucleotide translocation had to take into consideration the asymmetry of the binding of the inhibitors; atractylate acting on the c side and bongkrekic acid on the m side of the inner mitochondrial membrane. Long chain acyl CoA esters can be physiologically translocated across the inner mitochondrial membrane by the acylcarnitine transferase enzymes and the carnitine-acylcarnitine translocase system (Pande 1975; Ramsey and Tubbs 1975). As natural effectors of the ADP/ATP carrier they are able to bind and inhibit the translocator from both sides of the inner membrane. The specificity of long chain acyl CoA esters for receptors on the carrier indicate that the asymmetry with respect to binding of the ligands atractylate and bongkrekic acid must be intrinsic to the carrier since the long chain acyl CoA esters act like atractylate on the c side and bongkrekic acid on the m side of the membrane (Woldegiorgis and Shrago, 1979). This difference in the interaction of the acyl CoA esters with the carrier on the c and m sides indicates that there must either be two distinct receptors or the translocator must exist in at least two different conformational states.

A critical question is whether or not the long chain fatty acyl CoA esters modulate adenine nucleotide transport under in vivo conditions. Results have shown that during ischemia or hypoxia there is an accumulation of long chain acyl CoA esters in the myocardium which, in turn, is

associated with a decrease in activity of the adenine nucleotide translocase (Shug et al. 1974; Shrago et al. 1976). Figure 7 illustrates the interaction of fatty acid oxidation and adenine nucleotide translocation in the heart cell.

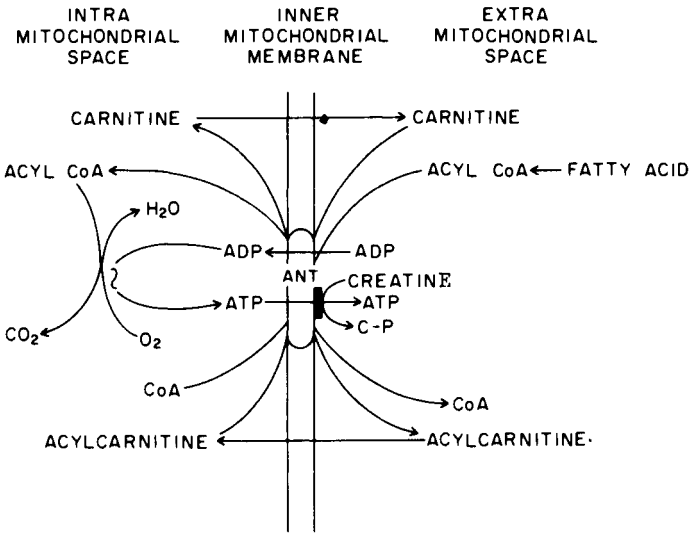

(Fig. 7) Interrelationship of fatty acid oxidation and adenine nucleotide translocation of the inner membrane of heart mitochondria.

Under normal conditions the flow of fatty acids into the mitochondria for β oxidation is promoted by the conversion of the fatty acyl CoA to the acylcarnitine ester which penetrates the inner mitochondrial membrane via the carnitine-acylcarnitine translocase. Under conditions of ischemia there is a marked build-up of long chain acyl CoA and long chain acylcarnitine esters (Neely and Morgan, 1974). Whereas the acylcarnitine esters are ineffective, long chain acyl CoA esters bind to and are strong inhibitors of the adenine nucleotide translocase. Of importance is the observation that the majority of long chain acyl CoA esters in heart tissue are located in the mitochondrial matrix (Idell-Wenger and Neely, 1978). It seems likely, therefore, that inhibition of the adenine nucleotide translocase would occur from the m side of the inner membrane. The creatine phosphokinase isozyme in heart tissue is located on the c side of the inner membrane which permits it to trap the ATP transported across the membrane on the adenine nucleotide translocator (Jacobus and Lehninger, 1973). The results stemming from inhibition of adenine nucleotide transport by long chain fatty acyl CoA esters would be a diminution in the formation of creatine phosphate as well as ATP. This, in turn, would cause a disruption of the phosphate potential in the cytosol and mitochondria with ensuing complications in electrical conductivity and muscle contraction.

SUMMARY

Evidence has been provided to show that long chain fatty acyl CoA esters are the natural effectors of the adenine nucleotide translocator. The receptors on the ADP/ATP carrier for the acyl CoA esters are asymmetric or in different conformational states in that when the acyl CoA is bound to the cytosolic side of the inner membrane it inhibits like atractylate, whereas when it is bound to the matrix side of the inner membrane, the acyl CoA inhibits like bongkrekic acid. A homogeneous acyl CoA-protein complex with characteristics identical to the ADP/ATP carrier has been isolated from heart mitochondria. Results from physiological studies in dogs whose anterior descending coronary arteries have been ligated show that there is a decrease in adenine nucleotide translocase activity concomitant with an increase in the concentration of fatty acyl CoA esters in the ischemic heart muscle. These studies provide independent evidence for the hypothesis that the adenine nucleotide translocase is rate limiting for oxidative phosphorylation and indicate that such an important biochemical reaction must be carefully regulated.

REFERENCES

1. Aquila, H., Eiermann, W., Babel, W. and Klingenberg, M. (1978) Isolation of the ADP/ATP translocator from beef heart mitochondria as the bongkrekate protein complex. Eur. J. Biochem. 85: 549-560.

2. Green, D. E., Lester, R. L. and Ziegler, D. M. (1957) Studies on the mechanism of oxidative phosphorylation. 1. Preparation and properties of a phosphorylating electron transfer particle from beef heart mitochondria. Biochim. Biophys. Acta 23: 516-524.

3. Hansen, M. and Smith, A. L. (1964) Studies in the mechanism of oxidative phosphorylation. VII. Preparation of a submitochondrial particle which is capable of fully coupled oxidative phosphorylation. Biochim. Biophys. Acta 81: 214-222.

4. Idell-Wenger, J. A. and Neely, J. R. (1978) Coenzyme A and carnitine distribution in normal and ischemic hearts. J. Biol. Chem. 253: 4310-4318.

5. Jacobus, W. E. and Lehninger, A. L. (1973) Creatine kinase of rat heart mitochondria. J. Biol. Chem. 248: 4803-4810.

6. Klingenberg, M. (1970) Metabolite transport in mitochondria: An example for intracellular membrane function, In Essays in Biochemistry, Campbell, P. N. and Dickens, F., Eds. Vol. 6, Academic Press, New York, pp. 119-159.

7. Klingenberg, M., Riccio, P. and Aquila, H. (1978) The isolation of the ADP/ATP carrier as the carboxyatractylate protein complex from mitochondria. Biochim. Biophys. Acta 503: 193-210.

8. LaNoue, K. F. and Schoolwerth, A. C. (1979) Metabolite transport in mitochondria. Annu. Rev. Biochem. 48: 871-922.

9. Lerner, E., Shug, A. L., Elson, C. and Shrago, E. (1972) Reversible inhibition of adenine nucleotide translocation by long chain fatty acyl Coenzyme A esters in the liver of mitochondria of diabetic and hibernating animals. J. Biol. Chem. 247: 1513-1519.

10. Meijer, A. J. and VanDam, K. (1974) The metabolic significance of anion transport and mitochondria. Biochim. Biophys. Acta 346: 213-244.

11. Neely, J. R. and Morgan, H. (1974) Relationship between carbohydrate and lipid metabolism and the energy balance of heart muscle. Annu. Rev. Physiol. 36: 413-459.

12. Pande, S. V. (1975) A mitochondrial carnitine acylcarnitine translocase system. Proc. Natl. Acad. Sci. USA 72: 883-887.

13. Pande, S. V. and Blanchaer, M. C. (1971) Reversible inhibition of mitochondrial adenosine diphosphate phosphorylation by long chain Coenzyme A esters. J. Biol. Chem. 246: 402-411.

14. Ramsey, R. R. and Tubbs, P. D. (1975) A mechanism for fatty acid uptake by heart mitochondria: an acylcarnitine-carnitine exchange. FEBS Lett. 54: 21-25.

15. Schertzer, H. G. and Racker, E. (1974) Adenine nucleotide transport in submitochondrial particles and reconstituted vesicles derived from bovine heart mitochondria. J. Biol. Chem. 249: 1320-1321.

16. Shrago, E., Shug, A., Elson, C., Spennetta, T. and Crosby, C. (1974) Regulation of metabolite transport in rat and guinea pig liver mitochondria by long chain fatty acyl Coenzyme A esters. J. Biol. Chem. 249: 5269-5274.

17. Shrago, E., Shug, A. L., Sul, H., Bittar, N. and Folts, J. D. (1976) Control of energy production in myocardial ischemia. Circ. Res. Suppl. 1,38: 75-79.

18. Shug, A. L., Shrago, E., Bittar, N., Folts, J. D. and Koke, J. R. (1975) Acyl CoA inhibition of adenine nucleotide translocation in ischemic myocardium. Am. J. Physiol. 228: 689-692.

19. Vignais, P. V. (1976) Molecular and physiological aspects of adenine nucleotide transport in mitochondria. Biochim. Biophys. Acta. 456: 1-38.

20. Williamson, R. and Corkey, B. E. (1969) Assays of intermediates of the citric acid cycle and related compound by fluorometric enzyme methods, In Methods in Enzymology, Lowenstein, J. M., Ed., Vol. 13 Academic Press, New York pp. 437-440.

21. Woldegiorgis, G. and Shrago, E. (1979) The recognition of two specific binding sites of the adenine nucleotide translocase by palmitoyl CoA in bovine heart mitochondria and submitochondrial particles. Biochem. Biophys. Res. Commun. 89: 837-844.

22. Woldegiorgis, G. and Shrago, E. (1980) Isolation of a palmitoyl CoA protein complex with properties of the ADP/ATP carrier from bovine heart mitochondria. Biochem. Biophys. Res. Commun. 92: 1160-1165.

Adv. Physiol. Sci. Vol. 8. Cardiovascular Physiology. Heart, Peripheral Circulation and Methodology
A. G. B. Kovách, E. Monos, G. Rubányi (eds)

THE CREATINE PHOSPHOKINASE SYSTEM — A FURTHER TARGET OF CALCIUM IONS IN HEART MUSCLE CELLS?

R. Vetter and V. A. Saks
Institute of Physiology, Humboldt University of Berlin, GDR, and Cardiology Research Center of the USSR Academy of Medical Sciences, Moscow, USSR

INTRODUCTION

The important role of the cardiac creatine-phosphorylcreatine-creatine phosphokinase system in the process of intracellular energy transport from mitochondria to myofibrils and other sites of energy utilization has been stressed repeatedly (Seraydarian and Abbott 1976; Saks et al. 1978) .
A heterogeneous distribution of different creatine phosphokinase (CPK) isoenzymes in the intracellular space and functional coupling of these to key reactions of myocardial energy metabolism at the mitochonrial site and the myofibrillar and membrane sites are well established (Saks et al. 1975, 1976 a,b; Baba et al. 1976; Sharov et al. 1977; Levitzky et al. 1977; Saks et al. 1978).
Divalent metal ions (Me^{2+}) like Mg^{2+}, Ca^{2+} and Mn^{2+} are essential in the Lohmann reaction (ATP + Cr $\underset{}{\overset{CPK}{\rightleftharpoons}}$ PCr + ADP) since the adenine nucleotides ATP and ADP react only as metal complexes (Morrison and Uhr 1966; Watts 1973). As clearly demonstrated previously Mg^{2+} and Ca^{2+} are almost equally active in CPK reactions catalyzed by different myocardial isoenzymes (Saks et al. 1979). Additionally, a regulatory action of Mg^{2+} in the mitochondrial CPK reaction was found (Saks et al. 1975).
Since the Mg^{2+} concentration remains practically unchanged under normal cellular conditions this observed Mg^{2+} effect can hardly be realized in CPK reactions of cardiac cells. On the other hand, the concentration of Ca^{2+} changes in a wide range in the contraction-relaxation cycle (Langer 1974) and remarkably under special pathological conditions (Fleckstein 1971/75; Dhalla 1976).
According to the importance of cardiac CPK isoenzymes for the energy supply of contraction the possible influence of Ca^{2+} upon the CPK reaction was studied.

MATERIALS AND METHODS

White rats from 200 to 300g were used in the experiments. The hearts were removed after opening the thoracic cages of anestetized animals.
MM-CPK isoenzym was obtained after chromatographic separation of the cytosolic fraction of rat heart muscle as described earlier (Saks et al. 1977).

The MM-CPK containing fraction was used in the experiments without further purification.
The overall rate of CPK reaction was determined in the presence of both the substrates and the reaction media containing 0.25M sucrose, 20mM Tris-HCl, pH 7.4 and 0.3mM dithiothreitol. ATP, creatine (Cr) and phosphoryl-creatine (PCr) were present in variable concentrations indicated in the figures. The concentration of Mg^{2+} ranged from zero to 2.5mM and of Ca^{2+} from zero to 1.8mM. To 3ml of the reaction media at 30° C, 0.1 - 0.2 ml of the MM-CPK containing fraction was added to start the reaction. Aliquotes of 1.0 ml were taken from the reaction mixture at 30 s and at 60 s after initiation of the reaction. The samples were mixed with 0.2 ml 6% perchlorci acid on Millipore filters (0.45um) and immediatly filtered under suction. The filtrate was neutralized by addition of 5N K_2CO_3 in the presence of methyl orange. After centrifugation of this mixture ADP concentration was measured by spectrophotometric method using lactate dehydrogenase and pyruvate kinase as described earlier (Saks et al. 1975). The imitial velocity of the reaction was determined as the rate of ADP concentration change (per min per ml of reaction mixture) and calculated for two points in time to assure the linearity. The determined velocities were relativated to the maximal velocity of the forward CPK reaction V_1 to get comparable values.
The Mg^{2+} and Ca^{2+} concentrations were determined by titration with EDTA solution in the presence of Eriochrom black.
The methods of the kinetic analysis of CPK reaction in the presence of Mg^{2+} and Ca^{2+} and all substrates and products are given in previous papers (Saks et al. 1975, 1979).

RESULTS

The experiments were performed in the presence of all substrates and products of the CPK reaction thus that both forward and reverse CPK reaction could occur. This reaction system will be designated in this paper complete CPK system. Figure 1 shows the behaviour of this system in the presence of different Ca^{2+} and Mg^{2+} concentrations. Curve 1 demonstrates the overall reaction rate in the direction of ADP and PCr formation if no Ca ions are present in the reaction media. An increase in Mg^{2+} concentration from zero leads to an increase of the rate of ADP and PCr synthesis due to an privileged binding of Mg^{2+} to ATP (Saks et al. 1975). Further increase in Mg^{2+} concentration reverses the reaction as a result of an appearance of the Mg ADP and beginning with a Mg^{2+} concentration value of 0.85mM, there is only a formation of ATP and creatine in the system. In the presence of Ca^{2+} the reaction is reversed from ADP and PCr formation to ATP and creatine formation

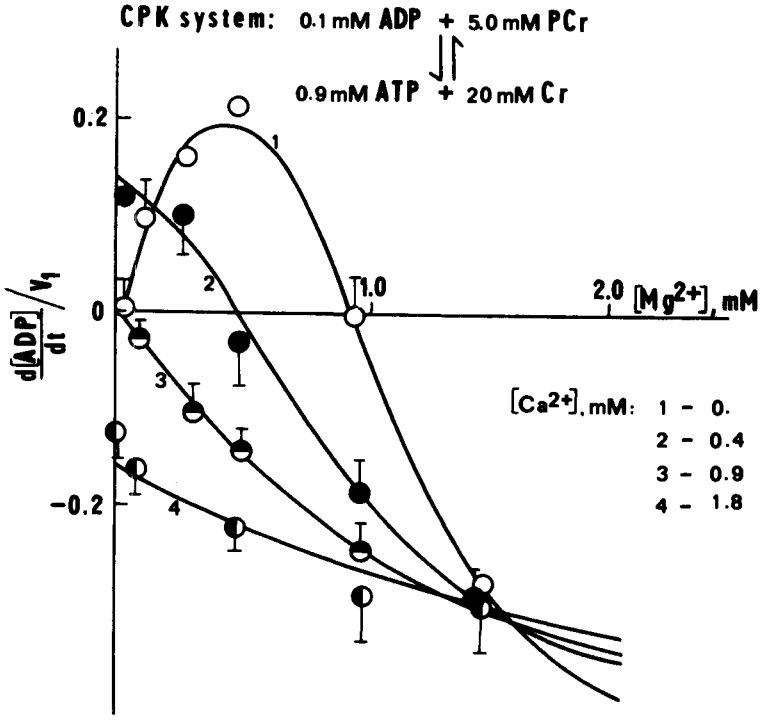

FIG. 1 Dependence of the overall CPK reaction rate on the total Mg^{2+} concentration at different Ca^{2+} concentrations. The initial concentrations of the substrates and the metal ion concentrations are given in the figure. Separate dots - experimental determined rates of ADP formation (average $\pm$ S.D. n=5). Solid lines - theoretical dependences. V_1 - the maximal ratio of forward MM-CPK reaction equal to 57 mmol x min^{-} x ml^{-}.

at lower Mg^{2+} concentration values (curve 2, fig. 1). If the Ca^{2+} concentration is sifficiently high only ATP creatine production is observed (curve 3, 4, fig. 1). In figure 1 the measured experimental values of the overall CPK reaction rate are represented by separate dots and the solid lines represent the results of theoretical calculated dependences based on the kinetic model of the CPK reaction and the characteristics of metal adenine nucleotide complex formation. This theoretical analysis is described in detail elsewhere (Saks et al. 1975, 1976 a).

It is of special interest to study the complete CPK system at a Mg^{2+} concentration which keeps the CPK reaction in equilibrium in the absence of Ca^{2+}. This is the case where curve 1 in figure 1 crosses the abscisse axis.

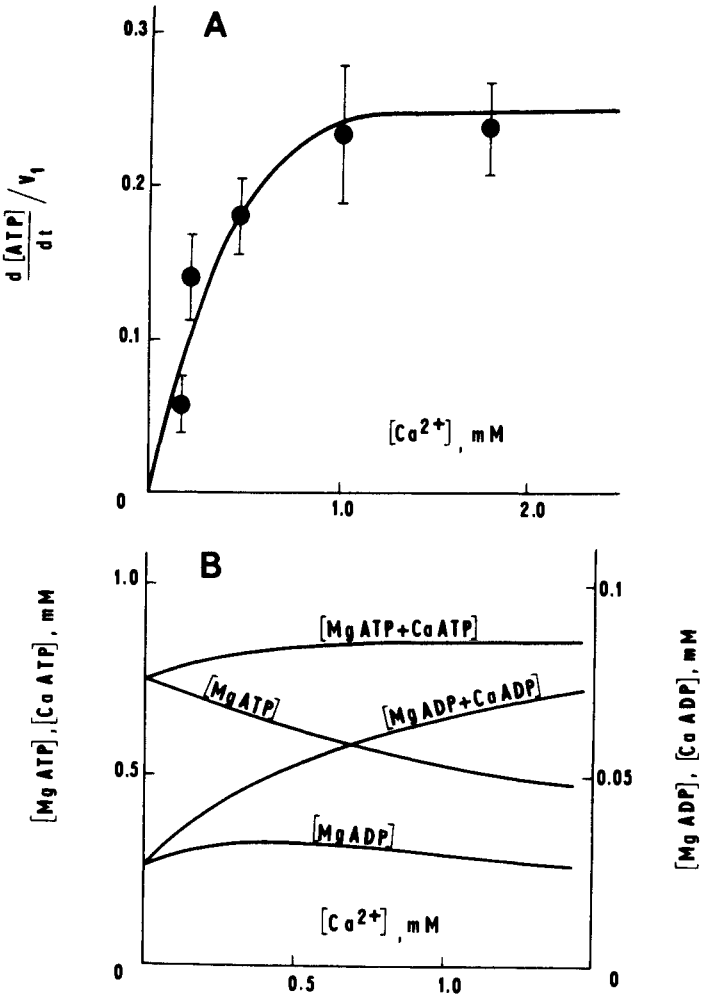

FIG. 2 A Increase in the ATP formation rate in the CPK reaction as a result of elevation in Ca^{2+} concentration. Total Mg^{2+} concentration was fixed at the point of equilibrium equal to 0.85mM. Substrate concentrations as shown in figure 1. Separate dots - experimental values.
Solid lines - theoretical dependences.

B Changes in concentration of the complexes $MgADP^-$, $MgADP^-$ + $CaADP^-$, $MgATP^{2-}$, $MgATP^{2-}$ + $CaATP^{2-}$ under conditions described in figure 2A. These concentrations were calculated by aid of a mathematical model using the stability constants for complex formation. The actual metal complex concentrations were introduced in the rate equation of CPK to get the theoretical dependences shown in figure 2A.

At this point the values of the forward and reverse reaction rate are equal and the system is very sensitive to changes in $Me\,ADP^{-}$ concentration. As is demonstrated in figure 2A an increase in Ca^{2+} concentration under these conditions shifts the system very rapidly from the equilibrium in the direction of ATP and creatine formation. Thus, Ca^{2+} induces a PCr breakdown in the complete CPK system. As can be seen in figure 2B an increase of Ca^{2+} concentration in the system does not change the concentration of the complexes ($MgATP^{2-}$ + $CaATP^{2-}$) significantly. The deerease of $MgATP^{2-}$ concentration due to a competition between

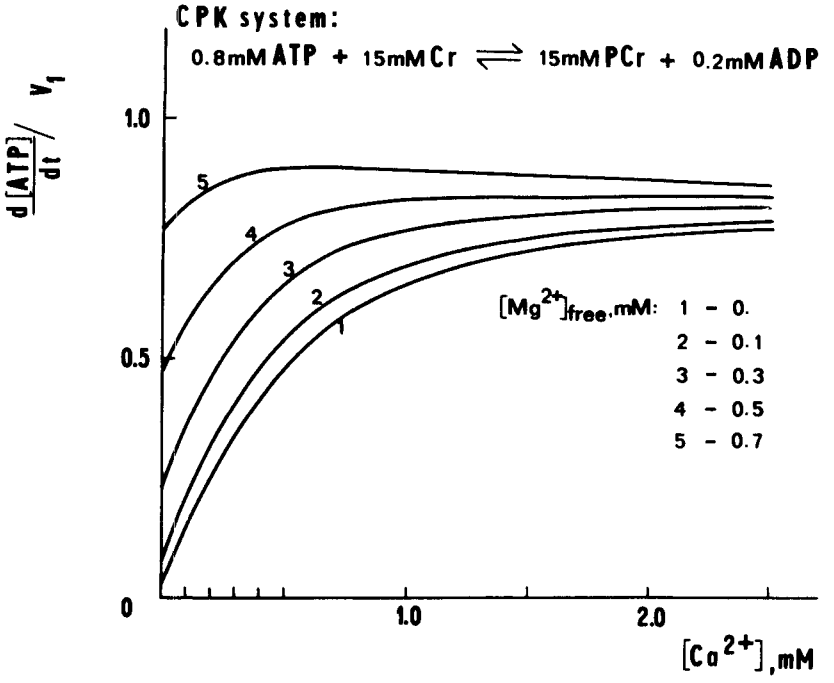

FIG. 3 Dependence of the ATP formation rate on the total Ca^{2+} concentration in the complete CPK-MM system at different fixed free Mg^{2+} concentrations in a range from zero to 0.7mM. The mathematical calculation was the same as in figure 2. Substrate concentrations are outlined in the figure. V_1 - as in figure 1.

Mg^{2+} and Ca^{2+} in the process of complex formation is compensated by an increase of the $CaATP^{2-}$ concentration. On the other hand, an increase in Ca^{2+} concentration produces a significant increase in the concentration of the ADP complexes with Mg^{2+} and Ca^{2+} ($Mg\,ADP^{-} + CaADP^{-}$). This increase in $MeADP^{-}$ concentration is responsible for the observed shift of the equilibrium in the direction of ATP and creatine formation. Using the kinetic model mentioned above, the observed Ca^{2+} effects can be quantitatively described by the rate equation of the CPK reaction if the exact metal adenine nucleotide complex concentrations are accounted for (see Saks et al. 1979). By aid of this model the dependences shown in figure 3 were obtained for conditions proved in this figure. The behaviour of the complete CPK system at several fixed free Mg^{2+} concentrations is similar to those shown in figure 2A. It is remarkable that a distinct raising in the ATP and creatine formation rate (that is an increase in PCr breakdown rate) can be observed in a Ca^{2+} concentration range from zero to $5 \cdot 10^{-4}$ M for each fixed free Mg^{2+} concentration.

DISCUSSION

The results demonstrate a modifying influence of Ca^{2+} on the complete (ATP, ADP, Cr and PCr containing) CPK system against the background of Mg^{2+} concentration. Both the regulatory action of Ca^{2+} and Mg^{2+} have been analyzed in other publications in detail (Saks et al. 1976, 1979). As to this analysis it has been concluded that changes in the ratio of the active substrates $MeADP^{-}$/ $MeATP^{2-}$ are due to differences in the values of the stability constants of the complexes $MgADP^{-}$, $MgADP^{2-}$, $CaADP^{-}$ and $CaATP^{2-}$. A good fitting between the experimentally determined and the theoretically calculated dependences obtained by introduction of the actual $MeATP^{2-}$ and $MeADP^{-}$ concentrations into the overall rate equation of the CPK reaction can be seen in figures 1 and 2. In the absence of Ca^{2+} the CPK system is characterized by the state of equilibrium at a Mg^{2+} concentration of nearly 1mM (crosspoint of curve 1 with the abscisse axis in figure 1). At this Mg^{2+} concentration nearly all ATP in the system is present as $MgATP^{2-}$. In this case Ca^{2+} added to the system competes with Mg^{2+} in the reaction of complex formation due to very similar stability constants of $MgATP^{2-}$ and $CaATP^{2-}$, equal to $5{,}9 \times 10^{4}$ and $2.1 \times 10^{4} M^{-}$ respectively (Sillen and Martell 1964; Saks et al. 1975, 1979). The decrease of $MgATP^{2-}$ concentration in figure 2B is the result of this competition. The released Mg^{2+} and the added Ca^{2+} simultaneously cause an increase in $MgADP^{-}$ and $CaADP^{-}$ concentrations, but the formation of these complexes is less effective than the $MeATP^{2-}$ complex formation due to weaker stability constants of $MgADP^{-}$ and $CaADP^{-}$ equal to 3.37×10^{3} and $2.2 \times 10^{3}\ M^{-}$ respectively (Saks et al. 1975, 1979). The affinity of these complexes to the enzyme is very high (Watts 1973, Saks et al. 1975, 1976 a, b, Levitzky 1977) resulting in a rapid shift from a equilibrium state in the direction of ATP an creatine synthesis.

Due to the nature of this regulatory Ca^{2+} mechanism in the CPK reaction and due to very close kinetic properties of all cardiac CPK isoenzymes (Saks et al. 1975, 1976 a, b, Levitzky et al. 1977) the obtained Ca^{2+} effect should be the same in all reactions catalyzed by several CPK isoenzymes. This conclusion

has been confirmed in the case of cardiac mitochondrial CPK (Saks et al. 1976b). This study does not allow one to decide wether or not the found Ca^{2+} effect can be realized under cellular conditions, if the Ca^{2+} concentration changes in a range between 10^{-7} and 10^{-4} M. In all likelihood the realization of the regulatory Ca action in vitro is unlike in cardiac cells under normal physiological conditions. But serous attention should be paid to stress situations when the intracellular Ca^{2+} content can be increased extremely (Fleckstein 1971, Dhalla 1976). It has been demonstrated by Fleckenstein (1971) that isoproterenol can increase the myocardial Ca^{2+} content 36-fold. Under these conditions a rapid breakdown of PCr and also ATP causes a drastic decrease in myocardial high energy phosphate level leading to cell death (Fleckenstein 1971/75).

Considering the regulatory Ca^{2+} effect on the CPK reaction, the role of Ca^{2+} in the reactions of cardiac energy metabolism under conditions of Ca overload described by Fleckenstein (1971/75) should be extended in the following way: A higher intracellular Ca^{2+} concentration causes an additional activation of the myofibrillar and other ATPases causing a higher rate of ATP splitting (Fleckenstein 1974/75).

Simultaneously the cellular CPK reactions are shifted in the direction of an increased PCr breakdown for ATP synthesis.

In cardiac cells ATP probably is saturated with Mg^{2+} where as ADP is not complexed with Mg^{2+} completely (Sols and Marco 1970; Polimeni and Page 1973). This is accomplished in the experiment in figure 1 at a total Mg^{2+} concentration of about 1mM, where the free Mg^{2+} concentration is very low. As a consequence the enhancement in Ca^{2+} concentration is responsible for an accelaration in PCr breakdown. In addition, the inhibition of mitochondrial ATP producing reactions (Vinogradov et al. 1972; Eboli et al. 1974) lowers the resynthesis of PCr at the mitochonrial site. The factors mentioned above should be the reason for the loss of cellular PCr and ATP, respectively which can induce irreversible cell demage. This can be prevented if the Ca^{2+} entrance into the cell is inhibited for instance by verapamil (Fleckenstein 1971/75).

Thus the Ca^{2+} effect on CPK reactions should be taken into account if energy metabolism in heart muscle cells is studied under conditions of calcium overload.

REFERENCES

Baba, H., Kim, S., and Farrell, E.C. (1976) J. Mol. Cell. Cardiol., 8, 599 - 617

Dhalla, N.S. (1976) J. Mol. Cell. Cardiol. 8, 661 - 667

Eboli, M.L., Cittadini, A., and Tarranova, T. (1974) Experentia 30, 1125 - 1127

Fleckenstein, A. (1971) In : Calcium and the heart. Edited by P. Harris and L. Opie. Academic Press., New York, pp. 135 - 188

Fleckenstein, A., Lanke, J. Döring, H.J., Leder, O. (1975) In : Rec. Adv. Stud. Card. Struct. Metabl. Edited by A. Fleckenstein and G. Rona. v.6, University Park Press , Baltimore, pp. 21 - 32

Langer, G.A. (1974) In : The mammalian myocardium. Edited by G.A. Langer and A. Brady. John Wiley & Sons Inc., New York, pp. 193 - 216

Levitzky, D.C., Levchenko, T.S., Saks, V.A., Sharov, V.G., and Smirnov, V.N., (1977) Biokhimia, 42, 1766 - 1773

Morrison, J.F., and Uhr, M.L. (1966) Biochim. Biophys. Acta 122, 57 - 74

Polimeni, P.I., and Page, E. (1973) Circul. Res. 33, 367 - 374

Saks, V.A., Chernousova, G.B., Gukovsky, D.E., Smirnov, V.N., and Chazov, E.I. (1975) Eur. J. Biochem. 57, 273 - 290

Saks, V.A., Chenousova, G.B., Vetter, R., Smirnov, V.N., and Chazov, E.I. (1976 a) FEBS Lett. 62, 293 - 296

Saks, V.A., Lipina, N.V., Chernousova, G.B., Sharov, V.G., Smirnov, V.N., Chazov, E.I., and Grosse, R. (1976 b) Biokhimia 41 2099 - 2109

Saks, V.A., Seppet, E.K., and Lyulina, N.V. (1977) Biokhimia 42, 579 - 588

Saks, V.A., Rosenshtraukh, L.V., Smirnov, V.N., and Chazov, E.I. (1978) Can. J. Physiol. Pharmacol. 56, 691 - 706

Saks, V.A., Kats, V.M., Vetter, R., Lyulina, V.N., and Shell, W.E. (1979) Biokhimia 44, 1600 - 1613

Seraydarian, M.W., and Abbott, B.C. (1976) J. Mol. Cell. Cardiol. 8, 741 - 746

Sharov, V.G., Saks, V.A., Smirnov, V.N., and Chazov, E.I., (1977) Biochim. Biophys. Acta 468, 495 - 501

Sillen, L.G., Martell, A.E. (1964) Chem. Soc. Spec. Publ. 17, 117 - 130

Sols, A., and Marco, R. (1970) Curr. Top. Cell. Regul. 2 , 227 - 273

Vinogradov, A.D., Scarpa, A., and Chance, B. (1972) Arch. Biochem. Biophys. 152, 646 - 654

Watts, D.C. (1973) In : The Enzymes. vol. 8. Edited by P. Boyer. Academic Press. Inc., New York, pp. 383 - 455

Adv. Physiol. Sci. Vol. 8. Cardiovascular Physiology. Heart, Peripheral Circulation and Methodology
A. G. B. Kovách, E. Monos, G. Rubányi (eds)

REGULATION OF LIPOLYSIS AND TRIGLYCERIDE-LIPASE IN THE DIABETIC RAT HEART

P. Rösen, C. Ubrig, T. Budde and H. Reinauer

Department of Biochemistry, Diabetes-Forschungsinstitut, Auf'm Hennekamp 65, 4000 Düsseldorf, FRG

INTRODUCTION

An increased supply of fatty acids and triglycerides from the adipose tissue of diabetics was assumed to be responsible for the preferential oxidation of fatty acids by heart muscle and their almost exclusive utilization as energy source for heart action according to the glucose-fatty acid cycle as suggested by Randle and coworkers in 1963 (1). A disturbancy in the glyceride metabolism was, therefore, considered as the primary defect in the diabetic metabolic disorder. Thus, the impaired glucose utilization of the diabetic heart tissue would reflect the prevalent degradation of fatty acids and/or ketone bodies as substrates. Substitution of fatty acids by glucose should then favour the oxidation of glucose. However, isolated perfused hearts of diabetic rats did not show the corresponding changes. Rather, the supply of exogenous fatty acids was replaced by the delivery of fatty acids derived from hydrolysis of stored, endogenous triglycerides. A 15-fold increase in the glycerol release reflects this accelerated lipolysis in the diabetic heart (fig. 1). Assuming a complete oxidation, these fatty acids can account for about 80% of the oxygen uptake by the diabetic heart, whereas in controls over 90% of the oxygen consumption can be related to the oxidation of glucose (3). An increased activity of a triglyceride lipase activity could be responsible for the persistence of the impaired glucose utilization of the diabetic heart. The regulation of the lipase activity was, therefore, studied in the isolated perfused heart and heart homogenate preparations.

METHODS

Hearts were prepared and perfused according to Langendorff (2) in a non-recirculating perfusion system using a modified Krebs-Henseleit bicarbonate buffer saturated with 5% CO_2 in oxygen and containing 11.1 mM glucose as previously published (3,4). Oxygen uptake was measured by the polarographic method described by Clark (5), glycerol outflow by a standard enzymatic method (6). Lipase activity was measured using ^{14}C-triolein as substrate following the procedure of Debeer (7). Fatty acids

were extracted (8) with a recovery of about 80%. For comparison lipase activity was determined in some experiments by monitoring glycerol production, measured after deproteinization (0.6 M $HClO_4$) and neutralization. To exclude interferences with the myocardial lipoproteinlipase activity, hearts were preperfused with heparin (1250 U) which has been shown to remove the surface bound lipoproteinlipase activity from heart tissue (9).

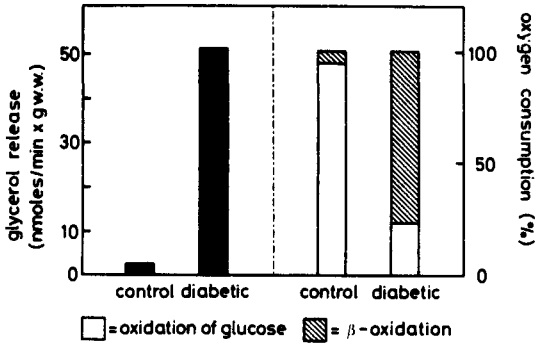

Fig. 1: Lipolysis of endogenous, myocardial triglycerides by isolated perfused hearts of control and streptozotocin-diabetic rats. Isolated hearts were perfused with a Krebs-Henseleit buffer containing 11.1 mM glucose saturated with 5% CO_2 in oxygen. The data are given as the mean of 6 determinattions in the steady state between the 35th and 45th min. of perfusion. Oxygen consumption was determined and related to the oxidation of glucose measured by the formation of radioactive CO_2 from glucose. Oxygen related to β-oxidation of fatty acids was calculated from the glycerol release assuming an amount of 26.5 µmoles oxygen consumed/µmole fatty acid.

RESULTS AND DISCUSSION

In heart homogenates lipase activity increased in a linear fashion with time for about 90 min. and with a protein concentration up to 2 mg/assay, when the substrate concentration was higher than 1.5 mM. The activity measured in the pH-range between 4 and 9 revealed 2 maxima: around pH 4.5 and at about 7.5. Above pH 8.0 a sharp decrease in activity is observed demonstrating the effectiveness of the heparin wash step in removing lipoproteinlipase activity (fig. 2). In agreement with this conclusion only a minimal lipase activity was observed in the presence of calcium and serum.
From differential centrifugation studies the lipase activity at acidic pH can be totally attributed to a membrane bound enzyme activity originating from a mitochondrial-lysosomal fraction. In contrast, the distribution pattern of the neutral lipase activity is not so unequivocal. About 30% of the total activity was found in the cytosolic compartment as a soluble

enzyme, whereas the remaining activity was distributed equally between the microsomal and the mitochondrial fraction. Studies are in progress to reveal the cellular distribution of the neutral lipase activity. The differences, however, to the distribution of the enzyme from the adipose tissue are obvious (10).

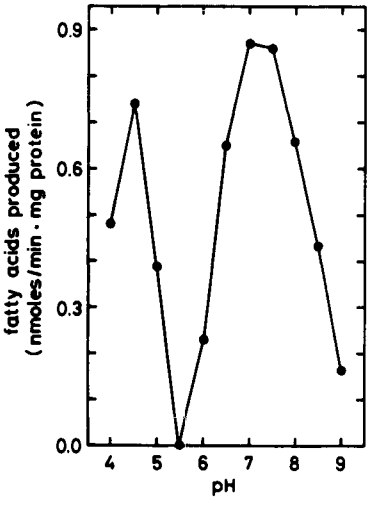

Fig. 2:
pH-dependency of the myocardial lipase activity.
The lipase activity was measured in homogenates of rat hearts using ^{14}C-triolein as substrate (1.8 mM, 37°C, 60 min.).
pH 4-6: acetate buffer, 0.1 M,
pH 6-8: phosphate buffer, 0.1 M,
pH 8-9: glycin buffer, 0.1 M.
The data represent the mean of two different experiments done in triplicates.

If the lipase activity was not measured by the production of fatty acids, but by the glycerol formation, a significant release and formation of glycerol was observed only at pH 7.4 at an amount expected from the fatty acid production. At pH 4.5 no glycerol release could be measured (fig. 3) demonstrating the absence of a monoglyceride lipase activity in the membrane bound lipase fraction, whereas neutral lipolytic activity represents a complex enzyme system containing mono-, di- and triglyceride lipase activities. That means the membrane bound lipase activity with the acidic pH optimum (presumably a lysosomal enzyme cannot be involved in the observed glycerol formation as suggested by others (9).

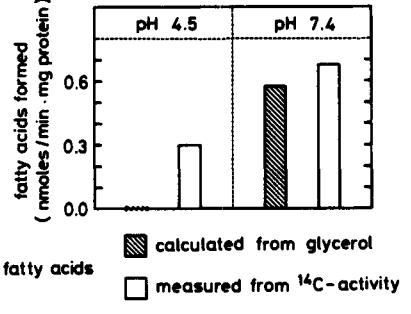

Fig. 3:
Comparison of lipase activity measured in heart homogenates by the production of glycerol and by the formation of fatty acids (1.8 mM triolein, 37°C, 60 min.).

Because the neutral lipase activity determined from the glycerol formation (which may be derived from exogenous and endogenous, presumably enzyme-bound triglycerides) equals the value

measured by the formation of fatty acids from radioactive triolein as substrate, a significant hydrolysis of endogenous triglycerides may be excluded under the experimental conditions of the enzyme assay. This may be of importance because in adipose tissue differences in lipase activity were discribed, depending on the exogenous or endogenous substrates used for the measurement of lipase activity (11, 12).

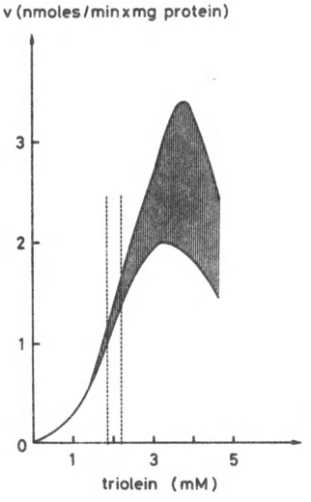

Fig. 4:
Dependency of myocardial lipase activity on the substrate concentration.
Lipase activity was measured in heart homogenates using ^{14}C-triolein as substrate at 37°C and pH 7.4. The linear initial velocity is given as a function of the triolein concentration. The range obtained for the activities of 4 different preparations is indicated.

The substrate dependency measured at pH 7.4 in a concentration range up to 7 mM shows a saturation curve reaching a maximum at about 3-4 mM and reflects a K_m of approximately 2 mM for exogenous triolein as substrate. From these observations it might be concluded that the low triglyceride content found in hearts of control rats would allow a minimal lipolysis and glycerol production in agreement with data obtained from isolated perfused hearts (13-15). The increase in the triglyceride content as observed in ketotic, diabetic rat hearts (13, 16) would shift the enzymatic activity to a range of substrate saturation, and the reaction would approach maximal velocity. This would explain well the high glycerol release observed in perfusion experiments with diabetic rat hearts.

However, the lipase activity measured in hearts of acutely diabetic animals (100 mg streptozotocin/kg b.w., 3 days before the experiment) and in chronically diabetic rats (30 mg streptozotocin/kg b.w., 28 days before the experiments) was reduced at the 3 different pH-values studied (13, 14).
Insulin therapy restored these reduced activities at least partially. The following 3 observations might help to understand these unexpected results: (1) In the isolated perfused diabetic heart the glycerol release is inhibited by 5-hydroxybutyrate (data not shown). (2) Preperfusion of the diabetic heart with

a Krebs-Henseleit buffer containing glucose as substrate (37°C, 30 min.) leads to an increase in the lipase activity in heart homogenates corresponding to the high glycerol release observed in these hearts under perfusion conditions (3, 13). (3) As shown in fig. 6 the lipase activity can be inhibited by

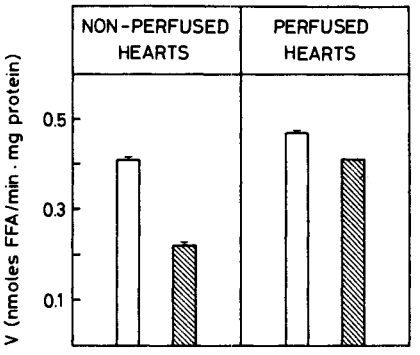

Fig. 5:
Lipase activity in perfused and non-perfused hearts of control and streptozotocin-diabetic rats. Lipase activity was measured in heart homogenates at a triolein concentration of 1.8 mM at pH 7.4 (37°C, 60 min.)
If indicated, hearts were perfused with a Krebs-Henseleit buffer containing 11 mM glucose for 30 min. (37°C).

increasing concentrations of palmitoyl-carnitine. Thus, it is tempting to propose that the triglyceride lipase is inhibited in the ketotic, diabetic heart, presumably by intermediates of the lipid metabolism, explaining the rapid triglyceride synthesis and accumulation of triglycerides described (16). Perfusion with a buffer containing glucose, free from fatty acids and ketone bodies, would allow a reactivation of the lipase activity and results in the utilization of endogenous triglycerides by the diabetic heart (fig. 5).

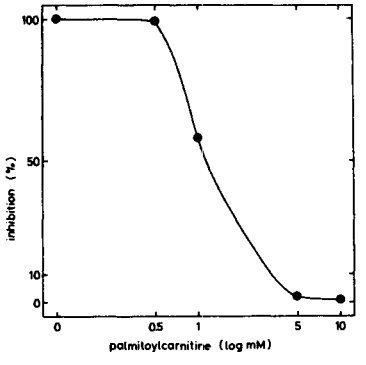

Fig. 6:
Inhibition of triglyceride-lipase activity measured in heart homogenates by palmitoyl-carnitine (37°C, 60 min., 1.8 mM triolein).

On the other hand, a reduction in the triglyceride stores by prolonged perfusion would decrease the lipase activity proportionately to the substrate saturation curve shown in agreement with perfusion studies. As a consequence of the reduced

availability of fatty acids from endogenous triglycerides the disturbed carbohydrate metabolism becomes improved as shown in the fig. 7.
In conclusion, our data suggest that the triglyceride-lipase activity is inhibited in the ketotic, diabetic rat heart by intermediates of the fatty acid metabolism as shown for palmitoyl-carnitine explaining the accumulation of triglycerides in vivo.

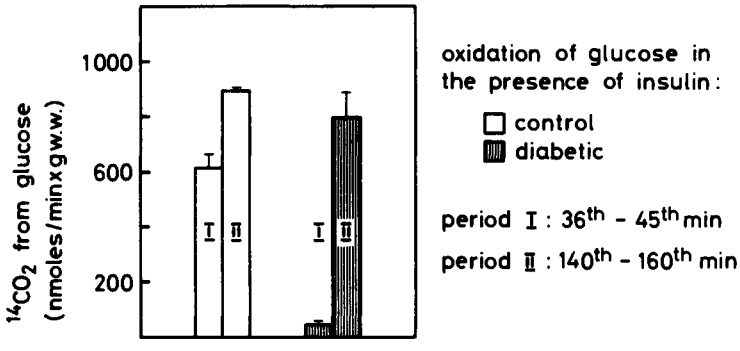

Fig. 7: Normalization of the rate of glucose oxidation after depletion of myocardial triglycerides by prolonged perfusion time. Rate of glucose oxidation were measured in isolated hearts of control and diabetic rats perfused with Krebs-Henseleit buffer containing 11.1 mM glucose and insulin (5 U/l). The data given (mean ± SEM) represent the rate of oxidation in period I: 35th-45th min., and in period II: 140-160 min. after depletion of myocardial triglyceride stores in diabetic hearts.

Changes of the substrate and perfusion of the isolated heart with a buffer containing glucose, but no fatty acids and ketone bodies, would lead to an activation of the lipase activity resulting in an utilization of the endogenous triglyceride stores as shown by the increased glycerol outflow from these hearts. In agreement with the glucose-fatty acid cycle discussed by Randle and coworkers (1) this supply of endogenous fatty acid would be, then, responsible for the depressed glucose oxidation demonstrated in the isolated perfused heart of the streptozotocin-diabetic rat. Only unsufficient delivery of fatty acids after an inhibition of triglyceride lipase activity or depletion of the triglyceride stores would improve the disturbed glucose oxidation which could be shown in our experiments. Thus, the regulation of the triglyceride lipase activity is directly involved in the persistence of the insulin resistence observed in the perfused diabetic heart.

REFERENCES

1. Randle, P.J., Garland, P.B., Hales, C.N., Newsholme, E.A.: The glucose-fatty acid cycle: its role in insulin sensitivity and the metabolic disturbancies of diabetes mellitus. Lancet, I, 785-789 (1963)
2. Langendorff, O.: Untersuchungen am überlebenden Säugetierherzen. Arch. Ges. Physiol. 61, 291-332 (1895)
3. Rösen, P., Reinauer, H.: Interrelationship between carbohydrate and lipid metabolism. Hoppe-Seyler's Z. Physiol. Chem. 361, 785-786 (1980)
4. Reinauer, H., Müller-Ruchholz, E.R.: Regulation of pyruvate dehydrogenase activity in isolated perfused heart of guinea-pig. Biochim. Biophys. Acta 444, 33-42 (1976)
5. Clark, C., Wolf, R., Granger, O., Taylor, Z.: Continuous recording of blood oxygen tension by polarography. J. appl. Physiol. 6, 189-193 (1953)
6. Eggstein, M., Kühlmann, E.: Triglyceride und Glycerin in: Methoden der enzymatischen Analyse (ed. H.U. Bergmeyer), Verlag Chemie, Weinheim, Vol. II, 1871-1874 (1974)
7. Debeer, L.J., Thomas, J., Mannaerts, G., De Schepper, P.J.: Effect of sulfonylureas on triglyceride metabolism. J. Clin. Invest. 59, 185-192 (1977)
8. Severson, D.L.: Characterization of lipase activity in rat heart. J. Mol. Cell. Cardiol. 11, 569-583 (1979)
9. Hülsmann, W.C., Stam, H.: Intracellular origin of hormone-sensitive lipolysis in the rat heart. Biochem. Biophys.Res. Commun. 82, 53-59 (1978)
10. Steinberg, D.: Interconvertible enzymes in adipose tissue regulated by c-AMP dependent proteinkinase. Adv. Cycl. Nucleotide Res. 7, 157-198 (1976)
11. Wise, L.A., Jungas, R.L.: Evidence for a dual mechanism of lipolysis activation by epinephrine in rat adipose tissue. J. Biol. Chem. 253, 2624-2627 (1978)
12. Smith, R.A., Jarett, L.: Surface structure changes of rat adipocytes during lipolysis stimulated by various lipolytic agents. J. Cell. Biol. 84, 57-65 (1980)
13. Budde, T., Rösen, P., Reinauer, H.: Rate of lipolysis and triglyceride lipase activity in hearts diabetic rats. Submitted (1980)
14. Denton, R.M., Randle, P.J.: Concentrations of glycerides and phospholipids in rat heart and gastrocnemius muscle. Biochem. J. 104, 416-422 (1967)
15. Denton, R.M., Randle, P.J.: Measurement of flow of carbon atoms from glucose and glycogen to glyceride glycerol and glycerol in rat heart and epididymal adipose tissue. Biochem. J. 104, 423-434 (1967)
16. Murthy, V.K., Shipp, J.C.: Accumulation of myocardial triglycerides in ketotic diabetes. Diabetes 26, 222-229 (1979)

* This work was supported by the Ministerium für Jugend, Familie und Gesundheit, Bonn, and the Ministerium für Wissenschaft und Forschung des Landes Nordrhein-Westfalen, Düsseldorf.

Adv. Physiol. Sci. Vol. 8. Cardiovascular Physiology Heart, Peripheral Circulation and Methodology
A. G. B. Kovách, E. Monos, G. Rubányi (eds)

LACTATE–FATTY ACID COMPETITION IN THE HEART DURING SHOCK

John J. Spitzer
Louisiana State University Medical Center, New Orleans, USA

The myocardium is a most versatile tissue capable of oxidizing a variety of substrates. Although under physiologic conditions in the post-absorptive state, free fatty acid (FFA) serve as the major metabolites other metabolites may replace FFA as energy yielding substrates under certain conditions. Thus we have demonstrated that elevated arterial ketone body concentration may depress myocardial FFA oxidation and increase the utilization of these substrates by the heart (1).

The findings discussed in this report were obtained in studies designed to answer two questions: 1) since impairment of myocardial function has been demonstrated 3-4 hrs following endotoxin administration (2,3) and since endotoxin is known to cause marked elevation of arterial lactate concentration, is there an early metabolic alteration in the myocardium evident following the administration of E.coli endotoxin, and 2) if so, can arterial lactate elevation alone (without the administration of endotoxin) simulate these changes of myocardial metabolism.

Anesthetized dogs were prepared with indwelling arterial and coronary sinus catheters to enable the monitoring of hemodynamic parameters, coronary sinus blood flow and myocardial uptake of FFA and lactate. A continuous infusion of tracer doses of albumin-bound palmitic acid-1-^{14}C was used to determine the oxidation of this substrate by the myocardium. The animal preparation and analytical techniques have been described previously (4,5,6,7).

Figure 1 indicates changes in myocardial metabolism 1 hr following E.coli endotoxin administration. It may be observed that myocardial FFA oxidation decreased markedly while only trivial changes were noted in the concentration of arterial FFA. Myocardial lactate uptake increased significantly and this change was accompanied by a marked increase in arterial lactate concentration. Thus while during the control period a larger fraction of metabolic CO_2 was

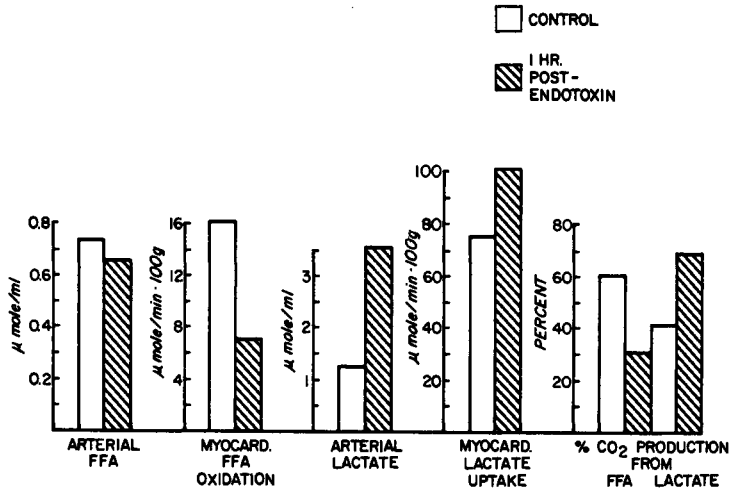

Fig. 1 Changes in myocardial metabolism following E.coli endotoxin administration.

derived from FFA oxidation than from lactate utilization, following endotoxin administration this situation was reversed: more most of the metabolic CO_2 was derived from lactate than from the oxidation of FFA. Thus alterations in myocardial metabolism were evident following endotoxin administration and they occurred at a time which preceeded the appearance of functional derangements of myocardial performance.

In order to determine whether the above changes were due to an increased availability of blood lactate or other changes that accompanied the administration of endotoxin, arterial lactate concentrations were elevated by infusing sodium lactate to anesthetized dogs. The results of these studies are summarized in Figure 2 . It can be seen that myocardial FFA oxidation decreased markedly with relatively small changes in arterial FFA concentration. Lactate uptake by the myocardium increased as did the arterial lactate concentration. As in the previous experiments, a much larger fraction of the metabolic CO_2 was derived from lactate following lactate infusion than under control conditions. The opposite was true for myocardial CO_2 production derived from FFA oxidation. Thus lactate appears to be the preferred myocardial substrate over FFA and the alterations in myocardial substrate utilization that were found following endotoxin administration could be imulated by elevating the arterial lactate concentrations without producing the other effects of endotoxin.

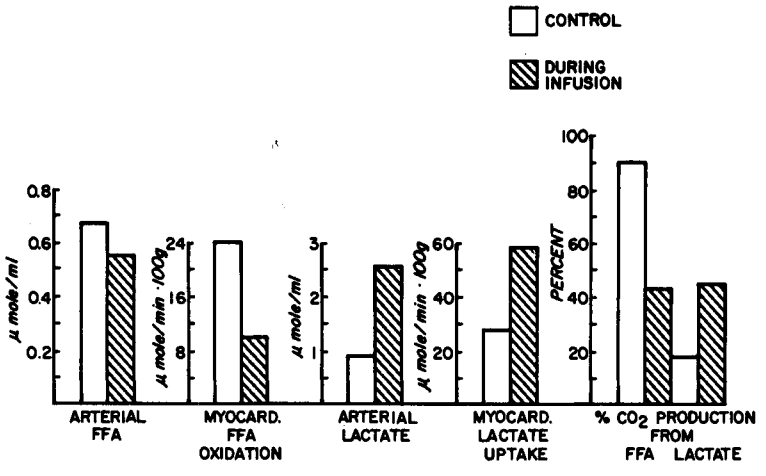

Fig. 2 Changes in myocardial metabolism following Na-lactate infusion

These data reaffirm the notion that lactate a water soluble metabolite which undergoes considerable daily variations under physiologic conditions, is a preferred substrate to FFA for myocardial metabolism under in vivo conditions. The statement also implies that lactate should not be merely considered as a metabolic waste product but also as an actively utilizable metabolite. Furthermore, the preference of myocardium to utilize lactate over FFA may have a potentially important survival value as well, under at least two different circumstances: a) Following severe trauma or in shock when adipose tissue FFA release may be impaired (8) and the availability of FFA for myocardial utilization is diminished while at the same time arterial lactate concentration is markedly elevated. b) In conditions that are accompanies by actual or impending myocardial hypoxia, it has been repeatedly demonstrated (9,10,11) that high myocardial concentration of FFA may be deleterious to cardiac function. Under such circumstances an alternate fuel source may be of considerable benefit. Lactate is a reasonable candidate for this role, as arterial lactate concentration is frequently elevated under these conditions. The potential role of lactate as an alternate fuel source for the myocardium under pathologic conditions will require further study.

Acknowledgement

The author's research efforts are being supported by grant HL 23157 from the NIH.

References

1. Little, J.R., M. Goto and J.J. Spitzer. Effect of ketones on metabolism of FFA by dog myocardium and skeletal muscle in vivo. Am. J. Physiol. 219:1458-1463, 1970.

2. Hinshaw, L.B., L.T. Archer, M.R. Black, L.J. Greenfield and C.A. Guenter. Prevention and reversal of myocardial failure in endotoxin shock. Surg. Gynecol. Obstet. 136:1-11, 1972.

3. Hinshaw, L.B., L.J. Greenfield, S.E. Owen, L.T. Archer and C.A. Guenter. Precipitation of cardiac failure in endotoxin shock. Surg. Gynecol. Obstet. 135:39-48, 1972.

4. Scott, J.G., J.T. Weng and J.J. Spitzer. Myocardial metabolism during endotoxin shock. In: Neurohumoral and Metabolic Aspects of Injury. Eds: A.G.B. Kovach, B. Stoner and J.J. Spitzer. Plenum Press:New York. pp. 375-386, 1973.

5. Spitzer, J.J. Myocardial metabolism during acute shock induced by hemorrhage, endotoxin or physostigmine infusion. In: Recent Advances in Studies on Cardiac Structure and Metabolism. University Park Press:Baltimore, pp. 161-167, vol. 3, 1973.

6. Spitzer, J.J., A.A. Bechtel, L.T. Archer, M.R. Black and L.B. Hinshaw. Myocardial substrate utilization in dogs following endotoxin administration. Am. J. Physiol. 227 :132-136, 1974.

7. Spitzer, J.J. Effect of lactate infusion on canine myocardial free fatty acid metabolism in vivo. Am. J. Physiol. 226:213-217, 1974.

8. Romanosky, A.J., G.J. Bagby, E.L. Bockman and J.J. Spitzer. Free fatty acid utilization by skeletal muscle following endotoxin administration. Am. J. Physiol. (In press).

9. Hoak, J.C., W.E. Connor and E.D. Warren. Toxic effects of glucagon-induced acute lipid mobilization in geese. J. Clin. Invest. 47:2701-2715, 1968.

10. Kurien, V.A., P.A. Yates and M.F. Oliver. Free fatty acids, heparin and arrhythmias during experimental myocardial infarction. Lancet 2:185-187, 1969.

11. Henderson, A.H., A.S. Most, W.W. Parmley, R. Gorlin and E.H. Sonnenblick. Depression of myocardial contractility in rats by free fatty acids during hypoxia. Circ. Res. 26:439-449, 1970

Adv. Physiol. Sci. Vol. 8. Cardiovascular Physiology. Heart, Peripheral Circulation and Methodology
A. G. B. Kovách, E. Monos, G. Rubányi (eds)

CONCLUDING REMARKS ON FACTORS REGULATING MYOCARDIAL SUBSTRATE METABOLISM

O. D. Mjøs
Department of Physiology, Institute of Medical Biology, University of Tromsø, Tromsø, Norway

Dr. NOBLE and Dr. SPITZER pointed out that lactate is a preferred substrate for the myocardium if it is present in high blood concentrations, e.g. during exercise and in shock. Dr. DANIEL expressed that lactate after all was an intermediate substrate,and it my be that the heart is removing this intermediate from the blood rather than preferring lactate for energy production. Dr.MACKENZIE expressed that acetate is also used by the heart, e.g. during exercise. Acetate is also a coronary vasodilator. More attention should be directed to the role of acetate in myocardial metabolism.

Dr. MJØS stressed that ischaemia-induced myocardial lipolysis might contribute to accumulation of free fatty acids within the myocardium in the very early phase of acute myocardial infarction. This might contribute to the extension of infarct size. A good antilipolytic agent must also inhibit the myocardial lipase activity. Dr. ROSEN pointed out that lipolysis is enhanced in the isolated diabetic rat heart. Lipolysis could be further enhanced by catecholamines, but was inhibited by addition of fatty acids in the perfusate.

Dr. SZEKERES and Dr. BORBOLA expressed that excess free fatty acids might have an arrhythmogenic effect in the ischaemic myocardium.

Dr. BENADE expressed that ischaemia might induce increased phospholipase activity with production of lysophospholipids which might inhibit oxidative phosphorylation.Dr. RIEMERSMA pointed out that he had investigated this question and found

no release of lysophospholipids from the ischaemic dog heart.

Dr. SNOW and Dr. RIEMERSMA stressed that one should be careful in describing whether studies were performed during ischaemia or hypoxia. Marked metabolic differences can be demonstrated between the two situations.

Dr. SNOW and Dr. RUBÁNYI pointed out that calcium is a key factor in regulation of myocardial metabolism in addition to its role in the excitation/contraction coupling. Non-invasive methods will give much more insight into the regulation of myocardial substrate metabolism.

Dr. SCOW asked whether there is data on increased triglyceride synthesis in the ischaemic myocardium. Dr. RIEMERSMA answered that there is clear evidence for this. Dr. SCOW said that he had evidence from adipose tissue that accumulation of free fatty acids can be observed as lamellar structures in the electron microscope with very high magnification. He suggested that this might also be demonstrated in the ischaemic myocardium.

Adv. Physiol. Sci. Vol. 8. Cardiovascular Physiology. Heart, Peripheral Circulation and Methodology
A. G. B. Kovách, E. Monos, G. Rubányi (eds)

INTRODUCTION: CONTRIBUTION OF WALL COMPONENTS TO ARTERIAL MECHANICAL PROPERTIES

Robert H. Cox
Bockus Institute and Department of Physiology, University of Pa., Philadelphia, Pa., USA

The mechanical properties of arteries are important determinants of their role in the function of the cardiovascular system. In addition, the arterial wall is the target organ of peripheral vascular disease. As a result it plays a major role in the pathogenesis and altered cardiovascular function that occurs in a number of common states such as atherosclerosis and hypertension. The arterial wall is a complex structure composed of a number of important components. As a result, the properties of the arterial wall are dependent upon the relative content and properties of the individual components. This symposium will consider the contribution of a number of these components to arterial wall properties.

Work in recent years has produced considerable gains in our understanding of the manner in which various components contribute to arterial wall properties and function. However, a number of important gaps remain in our understanding of this topic. Three such gaps will be considered in this presentation in the following areas: a) the contribution of connective tissue to passive arterial wall properties, b) the relationship between the ability of smooth muscle to generate increases in wall stress and decreases in wall diameter, and c) the representation of the mechanics of arterial smooth muscle by models of muscle function.

Passive Properties. The passive properties of arteries are primarily determined by the connective tissue elements, collagen and elastin. The connective tissue proteins primarily serve a structural function and serve to provide a framework for the active structures: vascular smooth muscle and endothelial cells of the blood vessel wall. Elastin, which is a composite of amorphous and microfibrillar components, is a compliant low elastic modulus matrix that primarily acts to ensure uniform distribution of wall forces and prevent potentially damaging stress concentrations within the blood vessel wall. Collagen is also a complex structure composed of a number of different and separable substructures, i.e. α chains (1). The collagen matrix is characterized by extensive inter- and intra molecular crosslinking. This characteristic imparts to the collagen matrix a relatively high stiffness characterized by high elastic modulus. Connective tissue proteins primarily function to maintain the structural integrity of the arterial wall.

Studies relating passive mechanical properties of blood vessels with connective tissue composition have presented the following model (2,3).

At low values of wall stress or strain, wall load is primarily borne by the elastin matrix. As the blood vessel is stretched collagen fibers are progressively recruited to support wall load. At high degrees of stretch, wall load is primarily borne by collagen fibers. This suggests that the low stress passive stiffness of blood vessels is closely related to elastin content while the high stress stiffness of blood vessels is determined primarily by the collagen content. Furthermore, the mid-range stress/strain relation of blood vessels should be determined by the characteristics of the recruitment of collagen fibers.

As a result of the large differences in the mechanical properties of these two components, variation or differences in the relative composition of collagen and elastin can produce large differences in the mechanical properties of different blood vessels. Recent studies have documented the contribution of collagen and elastin to mechanical properties of arteries. These studies have shown that in general the stiffness of a blood vessel is determined by total connective tissue content as well as by the ratio of collagen to elastin (4). Figure 1 shows a summary of the relationship between mechanical properties at a number of different arterial sites and the collagen/elastin content of those vessels. The low stress elastic modulus (E_5) showed a linear correlation to the elastin content expressed on the basis of a percentage of wet tissue weight. The high stress elastic modulus (E_{240}) also showed a reasonably good correlation with the collagen

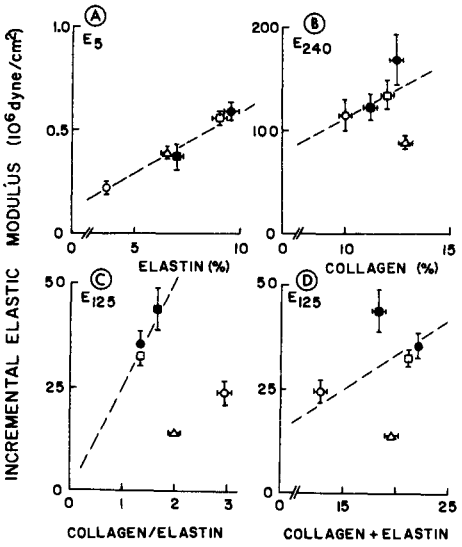

Figure 1. Correlation of incremental elastic modulus with connective tissue content. Values of elastic modulus are as follows: E_5 = modulus at 5 mmHg, E_{125} = modulus at 125 mmHg, and E_{240} = modulus at 240 mmHg. Connective tissue values are given as % of dry tissue weight. Arterial sites are identified as follows: carotid (Δ), iliac (●), mesenteric (□), coronary (○) and renal (■) arteries.

content. The one exception to this correlation were data from the carotid artery. The results in the lower two panels of Figure 1 show the relation between values of the elastic modulus in the mid-stress range to collagen/elastin ratio as well as to total connective tissue content (collagen plus elastin). The lack of correlation here can be explained on the basis of differences in the manner in which collagen fibers are recruited to support wall load (5).

While much of the mechanical properties of blood vessels can be explained on the basis of this previously described model, there are some results which cannot be explained. The data shown in Figure 2 summarize passive tangential stress/strain relations for carotid and tail arteries from normotensive (WKY) and spontaneously hypertensive (SHR) rats. These mechanical data show that arteries from the hypertensive animals are stiffer relative to their control counterparts. This conclusion is in consonance with generally accepted views. However, an analysis of connective tissue content does not support the previously described relationship between mechanics and connective tissue. These connective tissue data are summarized in Table 1. As indicated there, arteries from hypertensive animals possess a lower total connective tissue content as well as a lower collagen to elastin ratio. Based upon connective tissue data one would predict that the arteries from the hypertensive animals should be more compliant than arteries from the control counterpart. This prediction is certainly not in agreement with the mechanical data presented in Figure 2. Accordingly, this suggests that additional factors influence the relationship between passive mechanics and connective tissue content.

One could hypothesize a number of different factors contributing to

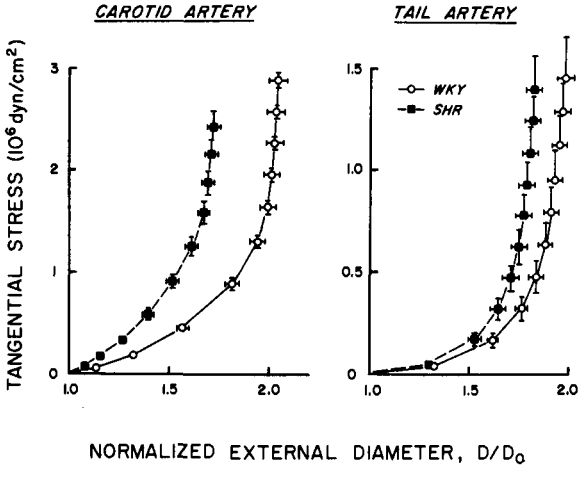

Figure 2. Variation of tangential wall stress with normalized external diameter under passive conditions of arteries from normotensive (WKY) and spontaneously hypertensive rats (SHR). Symbols are means and bars are $\pm$ SE. D_0 is the diameter value at zero stress.

TABLE 1. Connective Tissue Content of Carotid and Tail Arteries

Vessel	C	E	C+E	C/E
Carotid Artery				
WKY	40.7±2.5	31.0±1.1	71.6±3.2	1.36±.10
SHR	31.1±1.6*	34.5±2.4	65.0±1.5*	0.94±.10*
Tail Artery				
WKY	49.8±3.6	13.8±1.3	63.7±4.4	3.85±.43
SHR	35.5±2.7*	15.9±1.3	51.4±2.5*	2.38±.35*

*Statistically significant difference ($P<.05$)
C=collagen, E=elastin (given as % of dry solids)

this apparent discrepancy. These factors range from differences in the primary structure of the collagen and elastin matrices in normotensive and hypertensive animals to differences in the manner in which collagen fibers are recruited to support wall forces in the two animal groups. Collagen fibers are composed of polypeptide chains wound together (1). In addition, recent studies have documented the existence of a number of different types of collagen (1). The possibility of differences in either amino acid composition of the individual collagen chains or differences in the relative content of different collagen types could theoretically contribute to differences observed in passive mechanical properties. In addition, because the collagen and elastin matrices are in a state of rapid turnover in hypertension, the possibility of the existence of differences in cross-linking of connective tissue matrices between the two groups could also contribute to differences in mechanical properties (1). At the present time, however, these suggestions remain as hypotheses to be tested.

Active Mechanics. Numerous studies have documented that arterial smooth muscle possesses many characteristics in common with striated muscle. Active force-muscle length relationships show a similar variation as in striated muscle (6). An optimum length exists at which active force development is a maximum. Force development is smaller for muscle lengths both higher and lower than the optimum value. The maximum force generating capacity of arterial smooth muscle, however, appears to be much larger on the basis of cellular content or actomyosin content than striated muscle (7). Arterial smooth muscle also possesses hyperbolic force velocity relationships that are also qualitatively similar to that of striated muscle. The principal difference being that maximum velocities of shortening of arterial smooth muscle are substantially smaller than that of striated muscle reflecting the much smaller rate of ATP hydrolysis by myosin ATPase during contraction.

From the point of view of classical muscle mechanics the force-length relationship is a very important characteristic of muscle relative to its function. This is particularly true in the case of striated muscle. However, in the case of vascular smooth muscle this is not necessarily true. When analyzed from the point of view of the role of the arterial wall in the regulation of the circulation, isometric force development is not a very good predictor of vascular wall function. Vascular smooth muscle in

the arterial circulation primarily acts to influence the caliber of blood vessels under the influence of neural and humoral mechanisms. As a result, the ability of smooth muscle to produce constriction of the lumen is an important characteristic relative to the function of smooth muscle in the arterial wall. As a result, a better measure of smooth muscle function is its ability to produce shortening in response to activation. The shortening characteristics of arterial smooth muscle show a number of interesting characteristics (6). An optimum initial state exists (either load or pressure) at which activation of vascular smooth muscle will produce a maximum response in terms of vessel wall constriction. At high pressures, the constriction capacity of blood vessels decreases significantly in a manner that depends upon the site studied.

A number of recent studies have documented that significant differences exist in the ability of smooth muscle to produce constriction responses as contrasted to its ability to generate isometric force (8,9). An example of such a comparison is shown in Figure 3. This figure summarizes data on active force development and constriction responses of arterial smooth muscle from canine carotid and iliac arteries. The data shown in this figure document relatively small differences in the constriction capacity of these two blood vessels. No significant difference exists in the maximum constriction response for the two sites with the exception that the maximum response occurs at a higher value of transmural pressure in the case of the iliac artery. For pressures between 60 and 100 mmHg

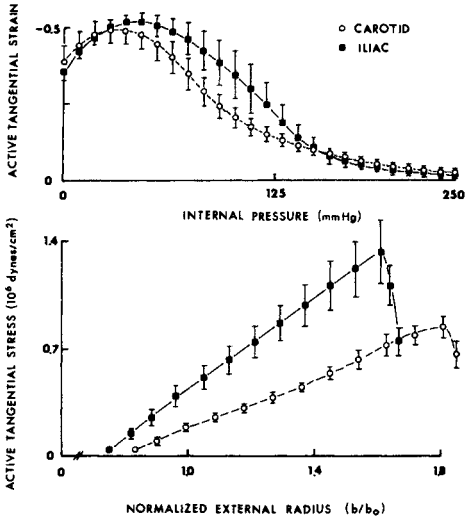

Figure 3. Active mechanics of canine carotid and iliac arteries. The upper panel shows the pressure variation of the diameter decrease with activation divided by the initial passive diameter (active tangential stress). The lower panel shows the increase in tangential wall stress produced by activation at different values of external radius normalized by dividing by the value at zero passive stress.

constriction responses are slightly better maintained in the iliac compared to the carotid artery. The iliac artery, however, has the capacity to generate a much larger maximum isometric force compared to the carotid artery. This conclusion holds also when active force development is normalized on the basis of wall cross sectional area or wall cellular content. We find a situation, therefore, in which the smooth muscle of one vessel has the capacity to generate a much larger active force compared to another and yet cannot produce a larger maximum constriction of the vessel lumen.

This observation raises a very interesting question. What is the relationship between force development and constriction or shortening capacity of arterial smooth muscle? One of the characteristics that arterial smooth muscle has in common with other muscles relates to this question: series elasticity. Series elasticity means that a muscle behaves mechanically as if the compliant structure were coupled in series with the contractile system. Sudden changes in load associated with sudden changes in length produce extension or retraction of the series elastic elements followed by changes associated with movement of the contractile system. Series elasticity also has the characteristic that it distorts the external manifestation of the properties of the contractile system. Stated in another way, the mechanical properties of the contractile system only manifest their behavior in the function of intact muscle on the basis of the properties of series elastic elements. Series elastic elements have the capacity to distort active force development and active shortening characteristics of the contractile system such that those actually measured from total muscle responses are less than those that could be produced by the contractile system under truly isometric or isotonic conditions. In addition, an analysis of the mechanical properties of classical models of muscle show that the mechanical characteristics of passive elastic elements functionally connected in parallel with the contractile system also contributes to a determination of a relationship between shortening characteristics and force development of the total muscle and that of the contractile system. The principal reason for this is that changes in muscle length and load do not directly reflect changes in contractile element length and load but reflect changes also in length and load of the passive elements functionally connected both in series (series elasticity) and in parallel (parallel elasticity) with the contractile elements. Analysis of simple mechanical models of muscle document that muscles with a specific capacity for force development will produce a larger constriction response if they possess stiffer series elastic elements compared to ones with more compliant series elastic elements. Vessels with stiffer parallel elastic elements, on the other hand, will produce smaller constriction responses. In addition, another important factor that can contribute to this relationship is the relative wall thickness of the blood vessel. Arteries with greater wall thicknesses/radius ratios will generate larger constriction responses for a given amount of maximum active force development.

These findings have several important implications. First of all, they indicate that measurements of isometric force-length relationships may not be adequate measures of the active mechanical characteristics of arterial smooth muscle from the point of view of the role of the arterial wall in circulatory control. Secondly, they suggest that differences in the active mechanical properties of intact muscle can occur as a result of changes in the passive elastic characteristics of blood vessels independent

of changes in the properties of the contractile elements per se. This is not to indicate that changes in the contractile system are not important in determining the active mechanical properties of intact muscle. Simply, that changes in the active properties of intact muscle reflect differences or changes in either the active or passive components of the blood vessel wall. This conclusion is of particular importance related to pathological states of the peripheral circulation because changes in the passive properties of arteries occur in such states (eg., hypertension and atherosclerosis) which may contribute to changes in the mechanics of arterial smooth muscle independent or in addition to changes in the contractile system per se.

Muscle Models. The results of studies described in the previous section indicate the importance of mechanical models in the evaluation of active mechanics of arterial smooth muscle. Development of an adequate mechanical model of muscle is important for at least two reasons. Firstly, as a means of determining the relationship between properties of the contractile system and properties of the intact muscle. A model would allow an ability to determine contractile element properties based upon measurements obtained from intact muscle. A determination of the mechanical properties of the contractile system per se are important for correlation with biochemical characteristics of muscle and represent a fundamental requirement for understanding the physiology of arterial smooth muscle. A second use of a mechanical model of muscle is for the determination of the contribution of active and passive components of the arterial wall to changes in intact muscle responses. Such information would be important in evaluating the relative contributions of active and passive elements to alterations associated with peripheral vascular diseases, for example.

Recent studies have indicated that the classical three parameter mechanical models developed to describe the characteristics of striated muscle are inadequate for describing the properties of arterial smooth

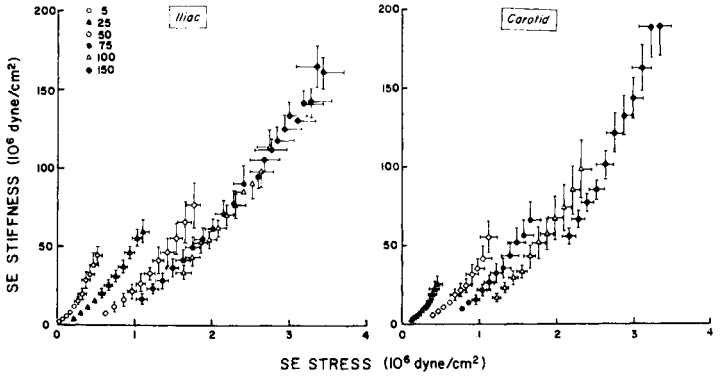

Figure 4. Variation of the stiffness of series elastic elements with stress at different muscle lengths for canine carotid and iliac arteries. Initial lengths are values obtained at specific values of pressure shown in the figure under passive conditions.

muscle (10). Figure 4 summarizes values of series elastic (SE) properties of canine carotid and iliac arteries as a function of muscle length. The classical models predict that these curves should be independent of initial muscle length and dependent on muscle stress only. These data document the inadequacy of these classical muscle models.

It is possible to develop a model that produces a similar apparent muscle length dependency of series elasticity by the addition of one passive element to the classical three element models as shown in Figure 5. Indeed, it is always possible to phenomenologically represent responses such as those shown in Figure 4 by the addition of elements to a model. However, such representations are of little value if they have no morphological basis. The model labelled Model 1 in Figure 5, does in fact have some resemblence to morphological features of arterial smooth muscle.

Figure 6 shows an electron micrograph of a portion of the media of the canine carotid artery. A region is shown in the center where the ends of two smooth muscle cells come together. The two cells do not show direct contact but appear to be coupled by a combination of amorphous and fibrillar material. This is the position one would expect to find structures contributing to series elasticity (SE in Model 1). One also sees in the spaces between smooth muscle cells quantities of collagen (fibrils) and elastin (dark amorphous material) which in some areas come in close proximity and perhaps in continuity with the basement membrane of the cells. This material could contribute to the element labelled PE_2 in Model 1. Other connective tissue elements present in the adventitia could contribute to the element labelled PE_1 in Model 1 as they would circumscribe the lumen without directly coupling with medial smooth muscle cells.

This discussion suggests an extracellular morphological basis for the three passive elements in Model 1. This should not be interpreted to

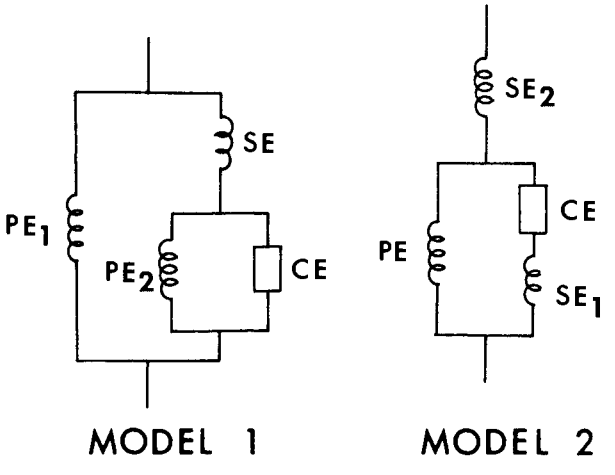

Figure 5. Mechanical models of muscle. CE = contractile elements, PE = parallel elastic element, SE = series elastic element.

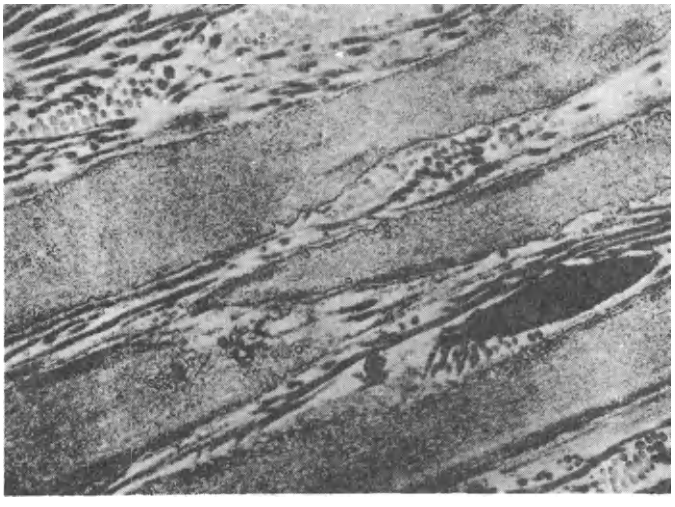

Figure 6. Electron micrograph of area of the media of the canine carotid artery. Vessel was pressure-fixed with gluteraldehyde X21,600.

indicate that intracellular structures do not also contribute to the properties of these passive elements. Indeed some information does exist in the literature which suggests that a portion of series elasticity is associated with intracellular structures (11). The above discussion is designed to show that Model 1 could have a real morphological basis.

REFERENCES

1. Prockop, D. J. et al. The biosynthesis of collagen and its disorders. I. New Eng. J. Med. 301:13-23, 1979.

2. Roach, M. R. and Burton, A. C. The reason for the shape of the distensibility curves of arteries. Can. J. Biochem. Physiol. 35:681-690, 1957.

3. Wolinsky, H. and Glagov, S. Structural basis for the static mechanical properties of the aortic media. Circ. Res. 14:400-413, 1964.

4. Cox, R. H. Regional, species, and age related variations in the mechanical properties of arteries. Biorheology 16:85-94, 1979.

5. Cox, R. H. Passive mechanics and connective tissue composition of canine arteries. Am. J. Physiol. 234:H533-H541, 1978.

6. Cox, R. H. Contribution of smooth muscle to arterial wall mechanics. Basic Res. Cardiol. 74:1-9, 1979.

7. Murphy, R. A. Filament organization and contractile function in vertebrate smooth muscle. Ann. Rev. Physiol. 41:737-748, 1979.

8. Cox, R. H. Comparison of carotid artery mechanics in the rat, rabbit and dog. Am. J. Physiol. 234:H280-H288, 1978.

9. Cox, R. H. Regional variation of series elasticity in canine arterial smooth muscle. Am. J. Physiol. 234:H542-H551, 1978.

10. Cox, R. H. Influence of muscle length on series elasticity in arterial smooth muscle. Am. J. Physiol. 234:C146-C154, 1978.

11. Mulvany, M. J. and Warshaw, D. M. The active tension-length curve of vascular smooth muscle related to its cellular components. J. Gen. Physiol. 74:85-104, 1979.

The research performed in the author's laboratory was supported in part by research grants HL-17840, HL-23348 and HL-23779 from D.H.E.W.

Adv. Physiol. Sci. Vol. 8. Cardiovascular Physiology. Heart, Peripheral Circulation and Methodology
A. G. B. Kovách, E. Monos, G. Rubányi (eds)

MECHANICAL PROPERTIES OF VASCULAR SMOOTH MUSCLE RELATED TO ITS CELLULAR COMPONENTS

M. J. Mulvany and D. M. Warshaw
Biophysics Institute, Aarhus University, 8000 Aarhus C., Denmark, and Department of Physiology, University of Massachusetts Medical Center, Worcester, MA 01605, USA

INTRODUCTION

Under relaxed conditions the resistance of the vascular system is determined by the connective tissue components of the blood vessel walls. Under physiological conditions however the vasculature is normally activated, that is the smooth muscle cells in the blood vessel walls are producing tension and playing an important role in the determination of vessel caliber. The purpose of this paper is twofold. First, to show the relationship between the mechanical properties of smooth muscle cells and those of whole blood vessels. Second, to show how these properties might be related to those of the contractile apparatus. This is illustrated mainly with results from our own work using a resistance vessel preparation [1, 2, 3, 4].

In some veins the smooth muscle cells are arranged longitudinally [5], but in most veins and in all arteries the cells are arranged either circumferentially or in a slight helix [6]. The cells are small having lengths of about 70 μm and maximum diameters of about 4 μm [1], and their method of interconnection appears complex. Unlike skeletal muscle fibres the intracellular structure of smooth muscle seems to lack a regular organization, although the presence of actin and myosin filaments [7] suggests that the basic contractile mechanism of smooth and skeletal muscle is similar [8, 9], i.e. that smooth muscle also operates on a sliding filament basis, force being generated by the interaction of myosin crossbridges with actin.

The small size of vascular smooth muscle cells has so far prevented mechanical experiments being performed on isolated cells (although such experiments have been performed by Fay on visceral smooth muscle cells which are larger (see [9])). Therefore our knowledge of the mechan-

ical properties of vascular smooth muscle cells has to be inferred from the mechanical properties of whole vascular preparations. Some indication of the relationship of these properties to those of smooth muscle cells can be obtained from histological studies [6]. However the complex interconnection of the cells makes interpretation of such studies difficult.

Our approach has been to use a very small whole muscle preparation, namely a 150-μm artery, which is transparent enough to permit visualization of the smooth muscle cells within it. Using this preparation we have been able to make a direct correlation between the behaviour of the cells and the behaviour of the preparation under various mechanical perturbations.

METHODS

The method of mounting segments of 150-μm arteries on a myograph has been described earlier [1, 2]. They were taken from the mesenteric bed of rats, threaded onto fine wires and mounted as a ring preparation which permitted direct measurement of their isometric wall tension while their internal circumference was controlled. Vessels were either held relaxed in a normal saline solution or activated by exposing them to a cocktail of 10 μM noradrenaline and 125 mM potassium. The myograph was mounted on a microscope so that the vessels' morphological and mechanical characteristics could be determined simultaneously.

As the cells in this preparation are arranged circumferentially the 'length' of the preparation corresponds to the internal circumference. The term length is therefore where appropriate used here as a synonym for internal circumference.

FORCE GENERATION AND CONTRACTION VELOCITY

In our rat mesenteric preparation, as in other vascular smooth muscle preparations, the active force produced per unit cell crosssection is about 360 mN/mm^2 and therefore similar to that found in whole skeletal muscle (Table 1). As smooth muscle contains only about one fifth the amount of myosin found in skeletal muscle [10], the force production per myosin molecule is much greater in smooth muscle. By contrast the velocity of shortening of vascular smooth muscle (Table 1) is about 100 times slower than skeletal muscle at the same temperature. One possible explanation for this difference is that the method by which the cells are interconnected gives them a mechanical advantage. This would be the case if cells which were arranged in

series were connected in parallel [11]. This possibility can be tested by measuring the change in cell length which accompanies a change in internal circumference. If the method of cell interconnection gives the cells a mechanical advantage greater than unity, then the percentage change in cell length will exceed the percentage change in internal circumference.

We have investigated this possibility in our mesenteric artery preparation [2]. This was done by making direct measurements of the change in separation of intracellular markers when the internal circumference of the relaxed preparation was changed. We found (Fig.1) that the percentage change in cell length was the same as the percentage change in internal circumference. We concluded that the method of interconnection of the smooth muscle cells did not confer any mechanical advantage. Similar results have been obtained by Murphy and his colleagues (see [8]) from a hog carotid artery preparation using a histological method. It may therefore be deduced that the comparatively high force production of vascular smooth muscle and its low velocity of shortening are properties of the smooth muscle cells, and not of the method of cell interconnection.

TABLE 1

Mechanical characteristics of smooth and skeletal muscle preparations

	(a)	(b)	(c)	(d)	(e)
Active force per unit cell cross-section (mN/mm^2)	360	370	236	200	350
Maximum velocity of shortening (L_o/s)	0.13	0.12	0.53	18.7	2.0
Active dynamic stiffness (P_o/L_o)	49	58	28	84	200

(a) Rat 150-μm mesenteric artery [1,3])
(b) Hog carotid artery [8,10]) 37^oC
(c) Rat portal vein [5,12])
(d) Rat fast skeletal muscle [13])
(e) Frog skeletal muscle fibres [11,14,15] 0^oC

L_o is preparation length at which maximum active force P_o is developed.

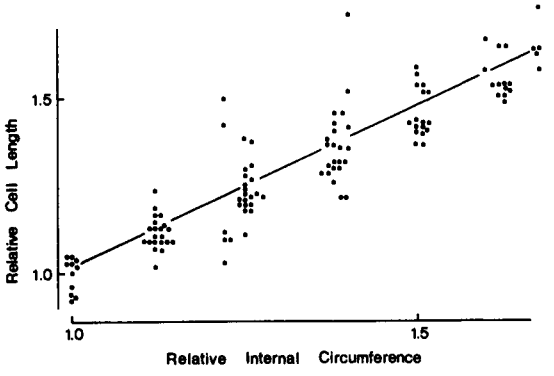

Fig. 1

Relation between relative spacing of intracellular structures (relative cell length) and relative internal circumference of rat 150-μm mesenteric arteries. Reproduced from reference [2].

ACTIVE TENSION-LENGTH RELATION

In skeletal muscle the active tension-length relation is closely correlated with the sarcomere structure, particularly at lengths above L_o, the length at which maximum active tension is developed. At such lengths the active tension is proportional to the amount of overlap between the contractile filaments. Since, as indicated above, smooth muscle may also operate on the basis of a sliding filament system, it has been of interest to investigate the active tension-length relation of smooth muscle.

At lengths below L_o the active tension-length characteristic is similar to that of skeletal muscle, although vascular smooth muscle is able to contract to shorter lengths (down to about 0.4 L_o). The characteristic has not been much studied at lengths longer than L_o, partly because the high resting tension makes it difficult to distinguish the active tension and partly because the characteristic is not normally reversible. However, for our mesenteric artery preparation we have been able to obtain conditions under which this characteristic is in part reversible. Under these conditions we showed [2] that the active tension-length relation above L_o also resembles that of skeletal muscle (Fig. 2).

We now consider whether the active tension-length characteristic of the whole preparation also represents that of the smooth muscle cells. As we have shown above, under relaxed conditions the internal circumference is proportional to cell length. However when activated isometrically, even

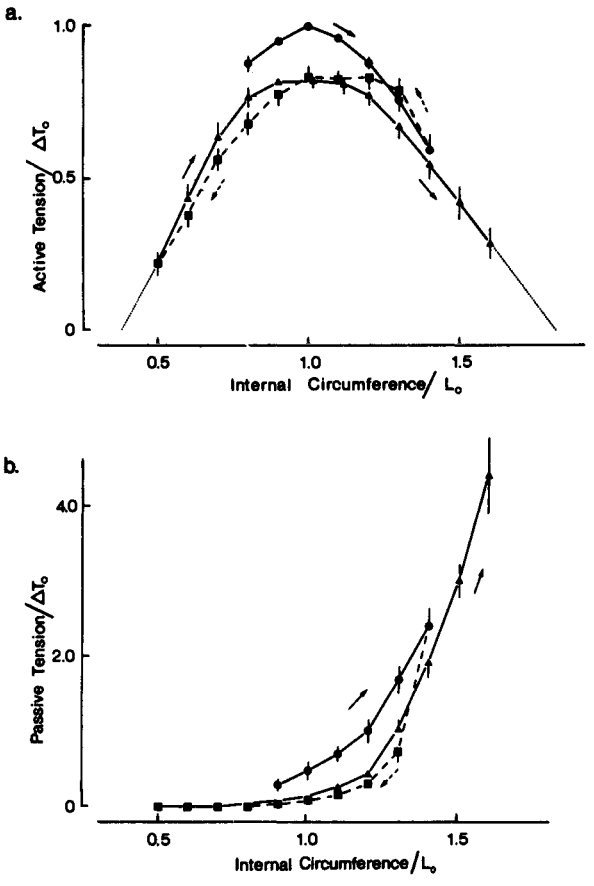

Fig. 2

(a) active and (b) passive tension as function of length (internal circumference) in 8 rat 150 μm arteries. Bars show SE. Points obtained in order indicated by arrows. Note difference in ordinate scales of (a) and (b). Reproduced from reference [2].

though the internal circumference remains constant, the smooth muscle cells may be expected to shorten at the expense of the compliance of the extracellular components. The series elastic component (SEC) of activated smooth muscle is considerable, that is a release of 5-10% is required to reduce the tension to zero [1, 5, 16]. Therefore if a substantial portion of the SEC is extracellular, the active tension-length relation will be distorted to the left with respect to that of the cells [6].

We have investigated this possibility by observing the behaviour of cells within our mesenteric artery preparation during and after a rapid (5 ms) release. This was done using a microscope flash technique which permitted the location of intracellular structures at precisely defined times with a resolution of 0.5 ms [4]. The results indicated (Fig. 3) that there was little movement during recovery of the tension produced by a rapid release, the average movement cor-

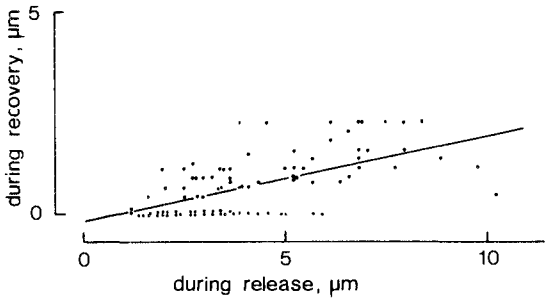

Fig. 3

Relation between movement of intracellular structures during rapid decrease in length (internal circumference) of activated rat 150-μm mesenteric artery (abscissa) and the movement of these structures during the recovery of tension (ordinate). Measurements made using Nomarski microphotography and flash illumination. From data previously published in reference [4].

responding to about 21% of the movement during the release. The results therefore indicated that only about one fifth of the SEC of this smooth muscle preparation is due to extracellular structures, the majority of the SEC being due to intracellular structures. Thus the active tension-length relation does not seem, in this smooth muscle preparation, to be greatly distorted by the presence of extracellular compliance.

We may therefore conclude that the active tension-length characteristic of this preparation is a reasonable indication of the average active tension-length characteristics of the smooth muscle cells. The results are therefore consistent with, but do not of course prove, the hypothesis that vascular smooth muscle operates on a sliding filament basis.

LOCATION OF THE SERIES ELASTIC COMPONENT

In skeletal muscle, and more particularly in skeletal muscle fibres, much of the SEC has been attributed to the contractile apparatus [15]. A number of investigators have therefore measured the SEC of vascular [5, 16, 17] and visceral [5, 18, 19] smooth muscle, with a view to determining whether this too can be attributed to the compliance of the contractile apparatus. It seems from the results presented

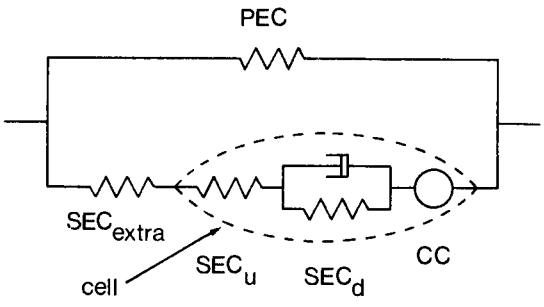

Fig. 4

Model of vascular smooth muscle preparation which accounts for mechanical characteristics of rat 150-μm mesenteric arteries. The passive tension is accounted for by a parallel elastic component (PEC). The force generating structures are represented by a contractile component (CC) obeying Hill's equation [17]. In series with the CC is a series elastic component (SEC) which is partly extracellular (SEC_{extra}) and partly intracellular. The intracellular SEC is represented by the series combination of an undamped-SEC (SEC_u) and a damped-SEC (SEC_d). As indicated in the text, in rat 150-μm mesenteric arteries SEC_{extra} is small compared with SEC_u.

above that in our rat mesenteric artery preparation most of the SEC is intracellular. We have investigated the properties of the SEC by determining the mechanical responses to rapid (5 ms) changes in length or load. We [3] have shown that the responses can be explained in terms of the SEC consisting of the series combination of an undamped-SEC and a damped-SEC (Fig. 4). We investigated whether these components could be associated with the contractile apparatus as follows.

First, we have investigated the length dependence of the stiffness of the undamped-SEC [2]. This was done by determining how the 'dynamic stiffness' of the preparation varied with length. The dynamic stiffness is the ratio of the immediate change in tension accompanying a rapid (5 ms) change in length to the change in length. As shown in Fig. 5, below L_o the active dynamic stiffness (increase in dynamic stiffness upon activation) falls less rapidly than the active tension. However above L_o the active dynamic stiffness and active tension are proportional. These findings are similar to those obtained in skeletal muscle fibres [15], and there the correlation between active tension and active dynamic stiffness is attributed to both being proportional to the overlap between the actin and myosin filaments. Our results

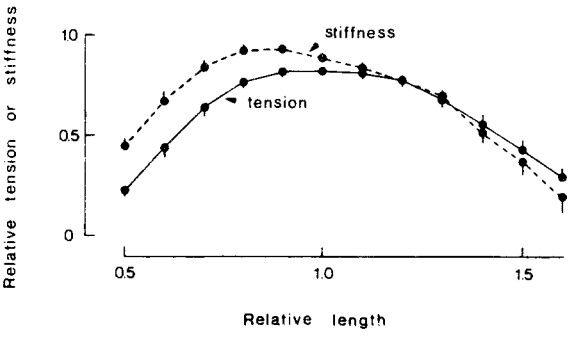

Fig. 5

Active tension (full lines) and active dynamic stiffness (stippled lines) as a function of length (internal circumference) in rat 150-μm mesenteric arteries. Data obtained during the second ascending sequence from the vessels shown in Fig. 2. Length is expressed in terms of L_o, the length at which maximum active tension was developed during the first ascending sequence. Active tension and active dynamic stiffness are expressed as fractions of these parameters at L_o during the first ascending sequence. Bars show SE.

are therefore consistent with the hypothesis that part of the undamped-SEC is within the contractile apparatus. However the absolute value of the stiffness of the undamped-SEC is much less than that found in skeletal muscle fibres (Table 1), so that the majority of the undamped-SEC is probably located in structures connecting the contractile apparatus to the cell membrane [3].

Second, we have investigated the temperature dependence of the undamped- and damped-SEC [3]. Although the undamped-SEC was essentially independent of temperature, the coefficient of damping in the damped-SEC had a Q_{10} of about 1.8. This temperature dependence is higher than would be expected for passive components and suggests that the damped-SEC may in part be attributed to the transitory behaviour of the contractile apparatus.

We therefore conclude that while the majority of the undamped-SEC of our preparation lies in the structures connecting the contractile apparatus to the cell membrane, part of the undamped-SEC may be directly associated with the contractile apparatus.

CONCLUSIONS

In rat mesenteric vessels the smooth muscle cells appear to be coupled in series and the compliance of the extracellular connections appears to be a small fraction of the total compliance of the activated preparation. The mechanical properties of the whole preparation therefore appear to be a reasonable indication of the average properties of the smooth muscle cells within it. On this basis the force production of vascular smooth muscle cells correspondends to about 360 mN/mm^2, while their maximum velocity of contraction at 37°C is about 0.13 L_o/s. Their average active tension-length relation appears to be similar to that of skeletal muscle fibres. Finally their series elastic component can be accounted for in terms of undamped and damped components, these possibly representing in part the transitory behaviour of the contractile apparatus when subjected to rapid mechanical perturbations.

Whether these conclusions are generally applicable to blood vessels, in particular to other resistance vessels, remains to be seen. If however this is the case, then our results imply that smooth muscle cells, rather than extracellular connective tissue, play the dominant role in the control of peripheral resistance under physiological conditions.

ACKNOWLEDGEMENTS

This work was supported by a NATO-fellowship Exchange Program and by the Danish Medical Research Council. We thank Michael Stoltze for excellent technical assistance.

REFERENCES

1. Mulvany, M.J. and Halpern, W. (1976). Mechanical properties of vascular smooth muscle cells in situ. Nature, 260, 617-619.
2. Mulvany, M.J. (1979). The undamped and damped series elastic components of a vascular smooth muscle. Biophys. J., 26, 401-413.
3. Mulvany, M.J. and Warshaw, D.M. (1979). Dynamic stiffness of activated vascular smooth muscle cells. Biophys. J., 25, A116.
4. Mulvany, M.J. and Warshaw, D.M. (1979). The active tension-length curve of vascular smooth muscle related to its cellular components. J. gen. Physiol., 74, 85-104.
5. Johansson, B., Hellstrand, P. and Uvelius, B. (1978). Responses of smooth muscle to quick load change at high time resolution. Blood Vessels, 15, 65-82.

6. Dobrin, P.B. (1978). Mechanical properties of arteries. Physiol. Rev., 58, 397-460.

7. Ashton, F.T., Somlyo, A.V. and Somlyo, A.P. (1975). The contractile apparatus of vascular smooth muscle: Intermediate high voltage stereo electron microscopy. J. Mol. Biol., 98, 17-29.

8. Murphy, R.A. (1979). Filament organization and contractile function in vertebrate smooth muscle. Ann. Rev. Physiol., 41, 737-748.

9. Fay, F.S., Rees, D.D. and Warshaw, D.M. Contractile mechanism of smooth muscle. In Membrane structure and function. Ed E. Bittar. Wiley (In Press).

10. Murphy, R.A., Herlihy, J.T. and Megerman, J. (1974). Force-generating capacity and contractile protein content of arterial smooth muscle. J. of General Physiol., 64, 691-705.

11. Huxley, A.F. (1957). Muscle structure and theories of contraction. Prog.Biophys., 1, 255-318.

12. Mulvany, M.J., Ljung, B., Stoltze, M. and Kjellstedt, A. Contractile and morphological properties of the portal vein in spontaneously hypertensive and Wistar-Kyoto rats. Blood Vessels (In Press).

13. Close, R.I. (1972). Dynamic properties of mammalian skeletal muscle. Physiol. Rev., 52, 129-197.

14. Hill, A.V. (1938). The heat of shortening and the dynamic constants of muscle. Proc. Roy. Soc. B, 126, 136-195.

15. Huxley, A.F. (1974). Review lecture, muscle contraction. J. Physiol., 243, 1-44.

16. Cox, R.H. (1977). Determination of the series elasticity in arterial smooth muscle. Am. J. Physiol., 233, H248-H255.

17. Dobrin, P.B. (1974). Vascular muscle series elastic element stiffness during isometric contraction. Circ. Res., 34, 242-250.

18. Meiss, R.A. (1978). Dynamic stiffness of rabbit masotubarium smooth muscle: effect of isometric length. Am. J. Physiol., 234, 614-626.

19. Peterson, J.W. (1978). Relation of stiffness, energy metabolism, and isometric tension in a vascular smooth muscle. In Mechanisms of Vasodilation. Ed. Vanhoutte, P.M. and Leusen, I. pp 79-88. Karger, Basel.

Adv. Physiol. Sci. Vol. 8. Cardiovascular Physiology. Heart, Peripheral Circulation and Methodology
A. G. B. Kovách, E. Monos, G. Rubányi (eds)

THE EFFECT OF ALTERATIONS IN SCLEROPROTEIN CONTENT ON THE STATIC ELASTIC PROPERTIES OF THE ARTERIAL WALL

S. E. Greenwald and C. L. Berry
Department of Morbid Anatomy, The London Hospital, London, E1 1BB, UK

The elastic properties of the arterial wall are governed by the elastic properties of its components, by their relative amounts and by the manner that stress is distributed between them.

Attempts have been made by a number of workers to correlate the static and dynamic elastic constants of conduit arteries with their chemical composition and morphology. Roach and Burton (1959) and Apter et al. (1966) have found that the elastic constants of the aorta measured at a low level of strain are associated with its elastin content. In the earlier study an increase in elastance was associated with an age related increase in collagen content. However, the quantitative approach used in the latter work failed to reveal a correlation between the parallel elastic constant (analogous to the static circumferential modulus) and collagen content.

The frequently observed increase in stiffness of conduit arteries with increasing distance from the heart has been associated qualitatively with an increase in the ratio of collagen to elastin (Fischer and Llaurado 1966, McDonald 1974). This suggestion is consistent with an association between an increase in the collagen elastin ratio in arteries from aged and hypertensive subjects and a corresponding increase in elastic modulus values, and has been verified in a number of animal studies by Cox. (For example, Cox et al. 1974; Cox 1977).

In this paper we shall review our attempts to explain in quantitative terms, the relationship between the static elastic properties of the rat aorta and its chemical composition. This is based on a simple model of the aorta in which collagen and elastin fibres bear stress in parallel. The results are compared to those from a study by Cox (1978) in which the relationship between pressure and the fraction of collagen fibres bearing stress is considered.

Finally we describe some recent elasticity measurements on rats treated with βeta-amino propionitrile, which inhibits the formation of scleroprotein cross links and was therefore expected to modify the elastic properties of the large arteries.

METHODS AND RESULTS

The methods used in this study have been described in detail previously (Berry and Greenwald 1976). The variation of radius with pressure in the rat aorta was measured in-situ by a radiographic method. Exposures were obtained at pressure increments of 0.26 kPa (20mm Hg) in the range 0 to 40 kPa (300mm Hg). Circumferential incremental elastic modulus was calculated from an expression for the variation of internal radius with pressure.

$$Einc = 1.5\Delta P R_I R_O^2 / \Delta R_I (R_O^2 - R_I^2)$$

where R_O and R_I are the average outside and inside radii over a pressure increment ΔP and ΔR_I is the corresponding increase in internal radius.

Following the distensibility experiments the vessel segments were dried to constant pressure and hydrolysed in water to render the collagen soluble. The aqueous fraction was further hydrolysed in 6M and HCℓ and collagen estimated by measurement of hydroxyproline in an autoanalyser. After boiling the solid residue in NaOH, non-alkali soluble elastin was estimated gravimetrically.

Animals were made hypertensive at the age of 4 weeks by uni-nephrectomy, DOCA implantation and salt loading. Systolic blood pressure in the caudal artery of lightly anaesthetised animals was measured using an occluding tail-cuff and a Doppler flow-velocimeter. Experiments were carried out on normotensive animals ranging in age from 4 weeks to 2 years, on hypertensives, from 6 to 20 weeks and on a number of ex-hypertensive animals aged 12 weeks to 1 year in which the steroid and salt treatment was stopped at the age of 10 weeks.

The detailed results of the elasticity experiments and chemical determinations have been reported elsewhere. Those that are relevant to the discussion are summarised below.

Figure 1 shows the variation with age, of Einc measured at an arbitrarily low value of distension ($R/R_O = 1.05$) (lower curve). In normotensive animals the modulus falls with age. Values for the hypertensive and previously hypertensive animals are close to but higher than normal. Similar changes are observed in the abdominal aorta (not shown) although for each group the modulus is lower by approximately 10%.

When measured at the maximum distension achieved in each group (corresponding to a pressure of 40 kPa) (Figure 1, upper curve) Einc in normotensive animals increases with increasing age. Values for the two groups of treated animals are scattered about the normal points, as are those for the abdominal aorta. This scatter is associated with the large errors caused by measuring small diameter changes close to the resolution limit of the X-ray film and measurement procedure (ca 3×10^{-3} cm).

In the thoracic aorta the elastin content expressed as a percentage of the wet weight of the vessel decreases with age (Figure 2, upper panel). Vessels from hypertensive animals contain more elastin than normal

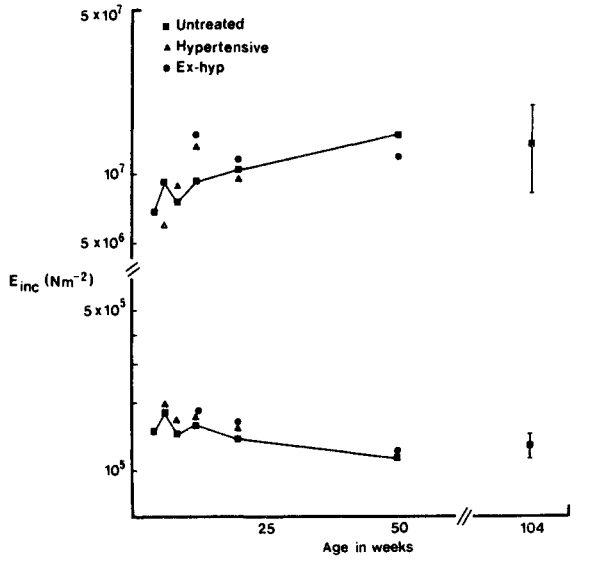

Figure 1: Variation with age of incremental elastic modulus measured at a distension (R/R_O) of 1.05 (lower curve) and the mean maximum distension observed for each group of animals (upper curve).
(In all diagrams vertical lines represent standard errors)

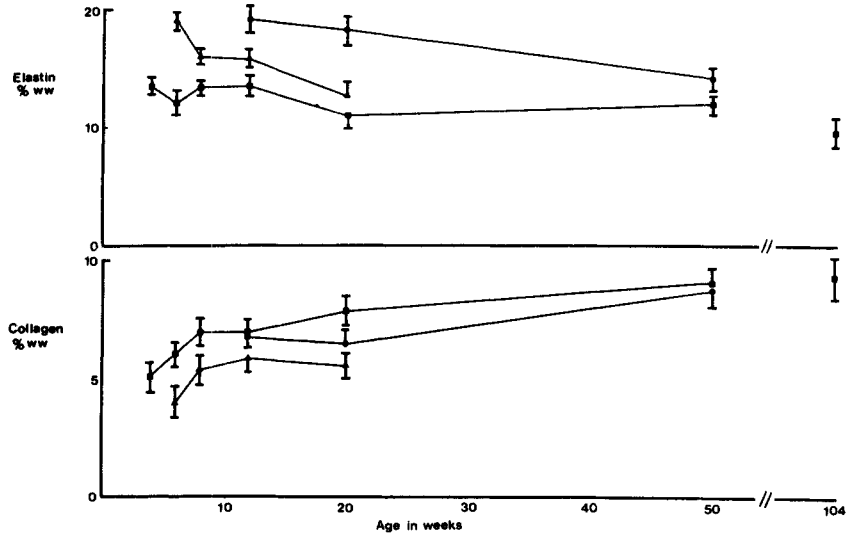

Figure 2: Effect of age on elastin (upper panel) and collagen (lower panel) content of the thoracic aorta, expressed as a fraction of its wet weight. Symbols as Figure 1.

although this difference diminishes with age. The elastin content of the aortae of ex-hypertensive animals is still higher than normal up to the age of 1 year. A similar pattern of changes is seen in the abdominal aorta, although the elastin content within each group of animals is lower by approximately 4%.

In common with most tissues the collagen content of the aorta increases with age (Figure 2, lower panel). Hypertension is associated with a lower than normal collagen content and reversal of hypertension does not result in a return to normal values. The changes seen in the abdominal aorta again resemble those seen in the thoracic, although in all groups of animals the collagen content is higher by approximately 4%.

DISCUSSION

In a composite material in which all the components bear stress in parallel the observed elastic modulus (E_{OBS}) will be related to those of the components by the expression:

$$E_{OBS} = \frac{E_1A_1 + E_2A_2 + \ldots\ldots E_nA_n}{A_1 + A_2 \ldots\ldots A_n} \qquad (2)$$

Where E_n is the modulus of the Nth component and A_n is the cross section area it occupies.

The evidence that the major components of the arterial wall bear stress in parallel is largely circumstantial. It is based on the form of the stress strain (or pressure radius) curve and selective digestion experiments such as those of Roach and Burton (1957). Morphological data is also consistent with this assumption.

In a vessel in a dead animal that has been flushed with saline and subjected to several stretch cycles up to 40 kPa no stress/strain hysteresis is observed and it is, therefore, reasonable to assume that the smooth muscle is inactive. Under these conditions its elastic modulus and those of all components other than collagen and elastin are assumed to be negligibly small. Provided that the moduli of the two scleroproteins are constant equation (2) may be written as:

$$E_{OBS} = \frac{E_EA_E + E_cA_c}{A_{TOTAL}} \qquad (3)$$

where the subscripts E and c refer to elastin and collagen. If it is assumed that the specific gravities of both collagen and elastin are close to 1 then (3) may be written:

$$E_{OBS} \qquad E_EW_E \; 1 \; fE_cW_c \qquad (4)$$

where W_E and W_c are the weights of elastin and collagen relative to the wet weight of the vessel and f is the fraction of collagen fibres that bear stress at any given value of strain (Cox 1978).

At low strains we assume that, due to folding or kinking, f approaches zero. If the model is correct a plot of E_{OBS} against W_E for each group of animals (Figure 3) should give a straight line of gradient E_E and zero intercept. The value of the gradient (bivariate regression coefficient) is 4.93 $\pm$ 1.5(SD) x $10^5 Nm^{-2}$, and of the intercept 0.6 $\pm$ 0.18(SD) x $10^5 Nm^{-2}$. This value for the modulus of elastin differs from that given in our previous report (5.8 x $10^5 Nm^{-2}$) due to the inclusion of data from more hypertensive animals. However both estimates agree well with values quoted in the literature (see for example McDonald 1974).

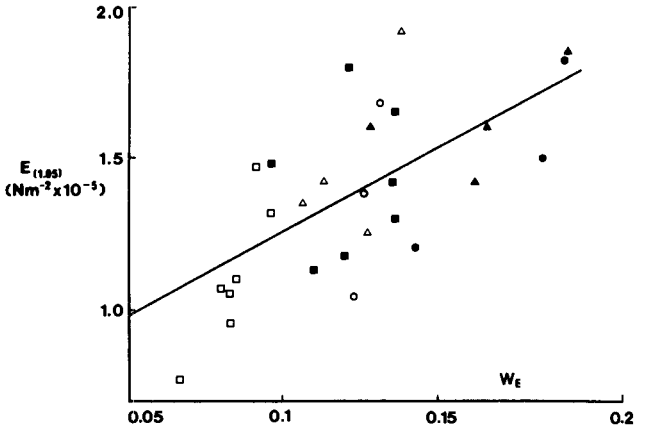

Figure 3: Relationship between elastic modulus measured at distension of 1.05 and elastin as a fraction of vessel wet weight. Symbols as Figure 1 Closed - thoracic aorta, open - abdominal. Correlation coefficient = 0.71

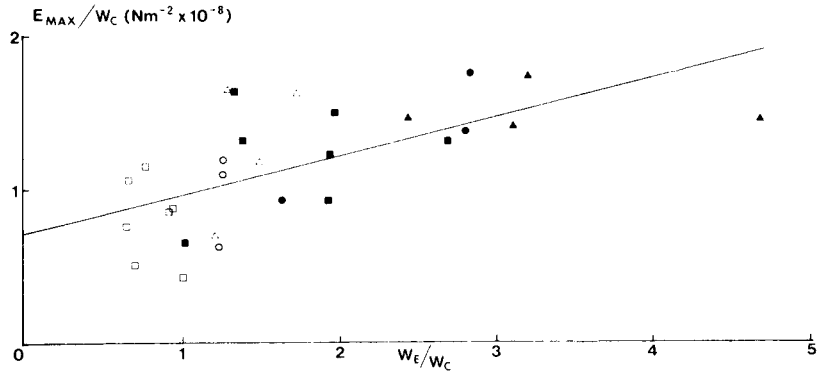

Figure 4: Relationship between elastic modulus measured at high degree of distension/collagen fraction and ratio of elastin to collagen. Symbols as Figure 3. Correlation coefficient = 0.66.

At high strains f in equation (4) approaches unity, hence a plot of E_{OBS}/W_C against W_E/W_C (Figure 4) should give a straight line of gradient E_E and intercept E_C. The values for the moduli of collagen and elastin

are 6.5 ± 1.3(SD) x $10^7 Nm^{-2}$ and 2.6 ± 0.7(SD) x $10^7 Nm^{-2}$. The value for collagen is within the accepted range whereas that for elastin is not. However since the modulus of elastin is probably about 2 orders of magnitude smaller than that of collagen, small errors in the ratio of W_E/W_C and E_{OBS}/W_C, while causing relatively small errors in E_C, will cause relatively large errors in E_E. We conclude, therefore, that the simple model propsed provides a useful description of the static mechanical properties of the rat aorta.

Following the procedure outlined by Cox (1978) we may calculate the manner in which the fraction of collagen fibres bearing stress varies with pressure or strain. The values of E_E obtained from equation (4) with f = 0 and that of E_C, with f = 1 may be used in equation (4) to calculate f for each value of E_{OBS}. Thus:

$$f = \frac{E_{OBS} - E_E W_E}{E_C W_C}$$

Figure 5 shows the result of this procedure for the thoracic aorta in normotensive animals. The shape of the curve differs from that obtained by Cox (1978) from normal dogs of unknown age which was convex with respect to the x axis. At 15 kPa (110mm Hg) the fraction of collagen fibres bearing stress is in the range 6.0 to 12.9% (mean 8.7% ± 0.55(SEM). For the abdominal aorta (not shown) the mean for all ages is lower (5.9% ± 1.2 SEM) but not significantly so ($t = 1.88$, $P > 0.1$). This is in accord with the results of Cox who found that at a given pressure the values of f from a number of different sites were closely comparable although the carotid artery was exceptional in this respect. At 15 kPa (110mm Hg) the fraction of collagen fibres bearing stress was approximately 10% for the mesenteric, coronary, iliac and renal arteries; and approximately 6.5% for the carotid.

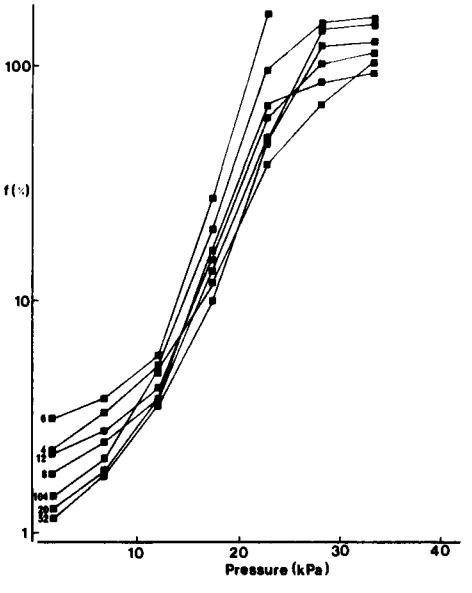

Figure 5: Variation of fraction of collagen fibres bearing stress with pressure. Thoracic aorta normal animals. Numbers at the origin of each curve refer to age in weeks of each group of animals.

When measured at a particular pressure (15 kPa) there is a small reduction in f between 4 and 52 weeks followed by a slight increase (Figure 6, lower curve). Values for the two treated groups remain close to normal.

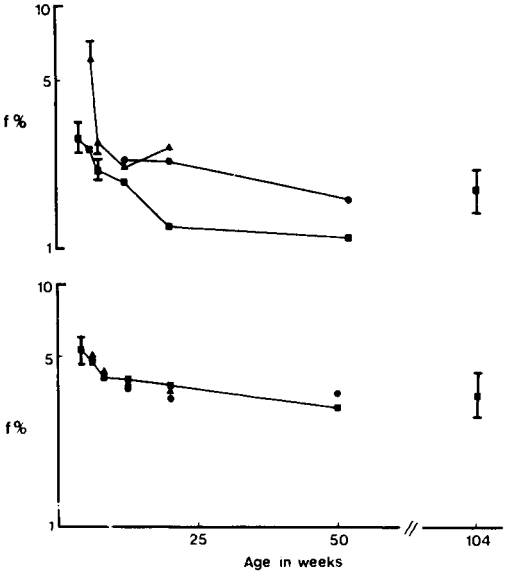

Figure 6: Effect of age on fraction of collagen fibres bearing stress - measured at a pressure of 15 kPa (lower curve) and a distension of 1.5 (upper curve)

The variation of E_{OBS} (and hence f) with pressure is governed not only by the chemical composition of the vessel wall but also by its thickness relative to the internal radius. An increase in age is associated with a decrease in the relative wall thickness of the aorta; and hypertension, with an increase.

In order to compare values of f from these different groups of animals in a manner which is independant of relative wall thickness, it is necessary to express the fraction (f) at a given degree of distension (R/R_O).

Figure 6 (upper panel) shows the effect of age and hypertension on f evaluated at a distension of 1.5. There is a steady decline with age in the fraction of collagen fibres bearing stress. At a given age the fraction is higher in the hypertensive animals. In previously hypertensive animals the fraction does not return to normal. Values for the abdominal aorta (not shown) again follow a similar pattern but are, in general, lower by a factor of 2.

We may conclude from these data that, at a given degree of distension, an increase in collagen content is associated with a decrease in the proportion of the total that is bearing stress. A possible explanation is that the mean unstretched length of collagen fibres relative to the unstretched radius of the vessel increases with age. This suggestion is in contradiction to the results of Roach and Burton (1959) and is inconsistent with evidence of an increase in the number of collagen cross links with age (e.g. Davison 1978).

A second and simpler explanation may be proposed if it is assumed that for all vessels a given degree of distension is associated with a fixed absolute amount of collagen bearing stress. The production of more collagen with, for example, increasing age would simply dilute the fixed stress bearing component and thus reduce the numerical value of f.

THE EFFECT OF BETA-AMINO PROPIONITRILE ON THE STATIC ELASTIC PROPERTIES OF THE AORTA

Iwatsuki et al. (1977) have observed that treatment of rats by β-amino propionitrile (BAPN) results in a reduction in vascular collagen deposition. The blood pressure in animals made hypertensive by nephrectomy, DOCA implantation and salt loading was reduced when they were given BAPN.

BAPN inhibits the activity of lysyl oxidase (Iwatsuki et al. 1977) and thereby reduces the degree of scleroprotein cross linking and deposition. It has no other known pharmacological action. Since its administration has been associated with changes in the elastic properties of other tissues (Harkness et al. 1962), we have subjected rats to a similar treatment in order to measure possible changes in aortic distensibility.

Fifty-five four week old rats of the AS strain, which exhibit spontaneous mild hypertension were divided into 5 groups and given the following treatment:

1) The left renal artery was partially occluded with a silver clip
2) Arterial occlusion plus daily administration of BAPN (100mg/kg i.p.)
3) BAPN injection
4) Saline injection
5) Untreated

Systolic blood pressure in the caudal artery was measured at weekly intervals. At the age of 12 weeks the animals were killed and distensibility measurements were carried out. The systolic pressures of all groups increased from an overall average of 10.5 $\pm$ 0.25(SEM) 79mmHg to the following values in kPa, (figures in brackets, mmHg)
Group (1) 22.6 $\pm$ 0.67 (170), Group (2) 17.5 $\pm$ 0.8 (132),
Group (3) 17.3 $\pm$ 0.53 (130), Group (4) 18.6 $\pm$ 0.4 (140) and
Group (5) 16.0 $\pm$ 0.53 (120). These results show that rats treated with a single renal artery clip develop marked hypertension but concomitant treatment with BAPN inhibits this change.

Figure 7 shows the variation of pressure strain elastic modulus (Ep) with pressure in the thoracic aorta. Points for the saline injected group, which are close to control values over the entire pressure range, are omitted for clarity. At pressures below 14.6 kPa (110mm Hg) in none of the treated groups do the Ep values differ significantly from that of the controls. At pressures between 17.2 and 26.6 kPa the values for all the treated groups are significantly lower than that of the controls.

That these changes in functional stiffness are caused by alterations in vessel structure may be seen in Figure 8, which shows the variation of

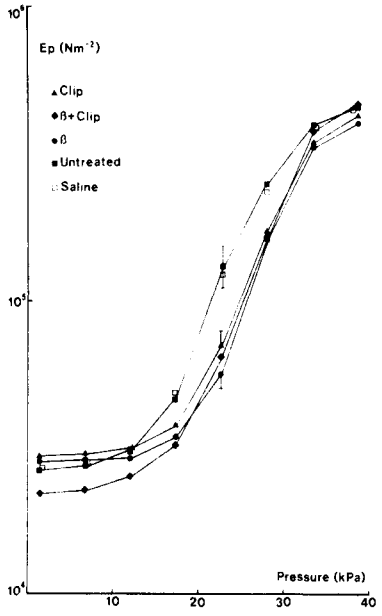

Figure 7: Variation of pressure strain elastic modulus with pressure.

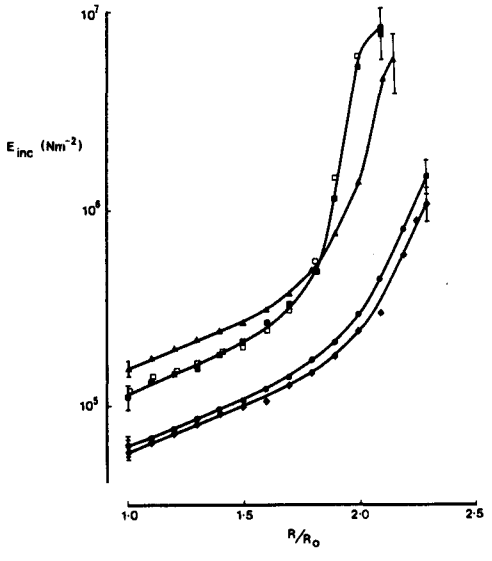

Figure 8: Variation of incremental elastic modulus with distension (R/R_O). Symbols as Figure 7.

incremental elastic modulus with distension. When compared at any given degree of distension both groups teated with BAPN are more distensible than the control and hypertensive animals. The difference increases from a factor of 2 at low strains to 20 at high strains. The decrease in elastic modulus associated with BAPN treatment at high and low strains is consistent with biochemical evidence for an inhibition of cross link formation in both collagen and elastin (Page and Benditt 1967; Iwatsuki et al. 1977).

What is the relationship between BAPN treatment and the inhibition of experimentally induced hypertension?

If the increased distensibility observed in the aorta is manifest in vessels containing baro-receptors, their rate of firing at any given pressure would, at least in the short term, be increased, although this effect would also apply to the clipped hypertensive animals.

As a step towards investigating this process we propose to carry out simultaneous measurement of baro-receptor activity and vessel elasticity under dynamic conditions, in animals treated with BAPN.

REFERENCES

Apter J.T., Rabinowitz M. and Cummings M.T. (1966) Correlation of visco-elastic properties of large arteries with microscopic structure. Circulation Res. 19, 104-121

Berry C.L. and Greenwald S.E. (1976) Effects of hypertension on the static mechanical properties and chemical composition of the rat aorta. Cardiovascular Res. 10, 437-451

Cox R.H. (1977) Carotid artery mechanics and composition in renal and DOCA hypertension in the rat. Cardiovascular Med. 2, 761-766

Cox R.H. (1978) Passive mechanics and connective tissue composition of canine arteries. Am. J. Physiology 234, H533-H541

Cox R.H., Jones A.W. and Fischer G.M. (1974) Carotid artery mechanics, connective tissue and electrolyte changes in puppies. Am. J. Physiology 227, 563-568

Davison, P.F. (1978) Bovine tendons, aging and collagen cross linking. J. Biological Chemistry 253, 5635-5641

Fischer G.M. and Llaurado J.G. (1966) Collagen and elastin content in canine arteries selected from functionally different vascular beds. Circulation Res. 19, 394-399

Fry P., Harkness M.L.R., Harkness R.D. and Nightingale M. (1962) Mechanical properties of tissues of lathyritic animals. J. Physiology 164, 77-89

Iwatsuki K., Cardinale G.J., Spector S. and Udenfriend S. (1977) Reduction of blood pressure and vascular collagen in hypertensive rats by beta-aminopropionitrile. Proceedings of National Academy of Science U.S.A. 74, 360-362

McDonald D.A. (1974) The elastic properties of the arterial wall. In: "Blood flow in arteries" 2nd edn. Edward Arnold Ltd., London Chap.10

Page R.C. and Benditt E.P. (1967) Diseases of connective and vascular tissues. IV The molecular basis for lathyrism. Lab. Invest 26, 22-25

Roach M.R. and Burton A.C. (1959) The effect of age on the elasticity of human iliac arteries. Canadian J. Biochem. Physiology 37, 557-570

Roach M.R. and Burton A.C. (1957) The reason for the shape of the distensibility curves of arteries. Canadian J. Biochem. Physiology 35, 681-690

Adv. Physiol. Sci. Vol. 8. Cardiovascular Physiology. Heart, Peripheral Circulation and Methodology
A. G. B. Kovách, E. Monos, G. Rubányi (eds)

BIOMECHANICAL PROPERTIES OF CONDUIT ARTERIES IN VIVO: MYOGENIC AND NERVOUS CONTROL

M. Gerová and J. Gero
Institute of Normal and Pathological Physiology, Centre of Physiological Sciences, Slovak Academy of Sciences, Bratislava, Czechoslovakia

Smooth muscle is the only element of the vascular wall which by active waving of its tonus influences the dimensions of the vessel, as well as the inner architecture of the wall and so determines the biomechanical properties of vessels. As a contractile element it is subjected to the hierarchy of control machinery of the body: myogenic, humoral and nervous: the first /myogenic/ and the last /nervous/ being most poorly understood.

Myogenic control

The impetus for triggering of a myogenic response, provides various shapes of deformation of the smooth muscle cell which is transferred to the contractile intracellular apparatus. Some data available deal with the by pressure induced deformation of smooth muscle and/or myogenic response of conduit arteries. The Baylis's original idea on contractile response of conduit common carotid artery to an increase in intravascular pressure has never been confirmed; on the contrary, data have been provided on the increasing diameter to the increase of intravascular pressure in conduit arteries /Zatzman et al 1954, Gero and Gerová 1962/. Fortunately, this fact did not preclude to open a wide field of search on Baylis's phenomenon in resistant vessels where it was demonstrated as fully operating.

Recently a renaissance of interest in conduit artery smooth muscle control related to blood flow has revived. Indeed, there is a considerable contraversy about the trigger mechanism itself, however, a dilation of conduit arteries in extremities to increase in blood flow has been taken generally as granted. /Schretzenmayr 1933, Fleisch 1956, Hilton 1959, Ingebrigsten et al 1970, Lie et al 1970, Smieško et al 1979/.

We studied this phenomenon in conduit coronary arteries as coronary vascular bed is an area well known where sudden raise in blood flow occurs. The ramus interventricularis ventralis /RIV/ of the heart of a dog killed by electric current /220 V, the heart nutritive vascular bed was blocked with mercury/, was joined to femoral artery and vein of an other

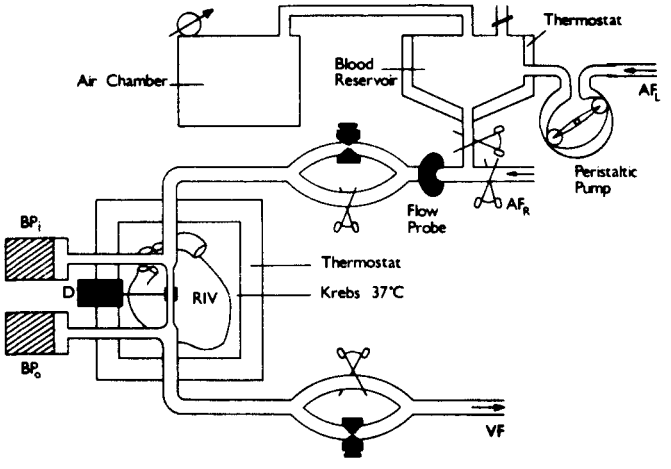

Fig.1 Diagram of experimental preparation

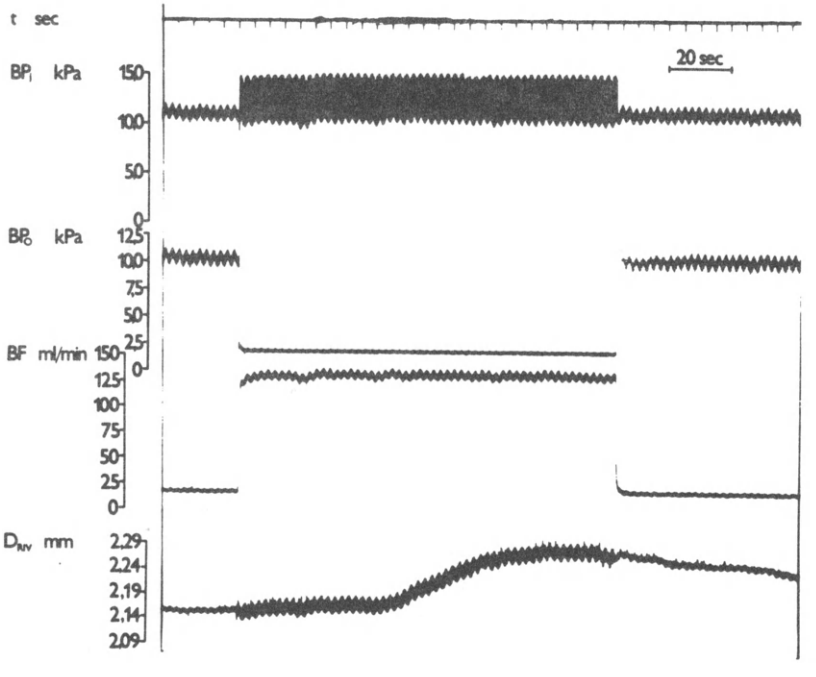

Fig. 2 Effect of increased BF on coronary artery diameter

anesthetized dog. RIV inflow pressure /BPi/, outflow pressure /BPo/, diameter /D_{RIV}/, and flow /BF/, were synchronously monitored /Fig. 1/. Operating the inflow rezistance and outflow rezistance, the blood flow raised 5 to 10 times of the resting value, in such a way, however, that at the segment where diameter was registered, no change in mean blood pressure occured. In that case diameter registered indicated the smooth muscle tonus /Fig.2/. An increase in blood flow from 11.3 ± 0.78 ml/min to 81.4 ± 6.2 ml/min induces a f t e r a p e r i o d of 24.4 ± 1.0 sec an increase in diameter which represents 3.4 ± 0.5 %.

To exclude the effect of pressure pulse amplitude changes /occuring simultaneously with blood flow increase/ in triggering the coronarodilation, in a series of experiments non-pulsating blood flow was used. The results confirmed that even increase in non-pulsating blood flow from 12.1 ± 2.2 ml/min to 90.33 ± 11.3 ml/min lasting more than 20 sec induced a dilation of ramus interventricularis ventralis /37.64 ± 5.4 um, i.e. 1.8 %/. /Fig. 3/

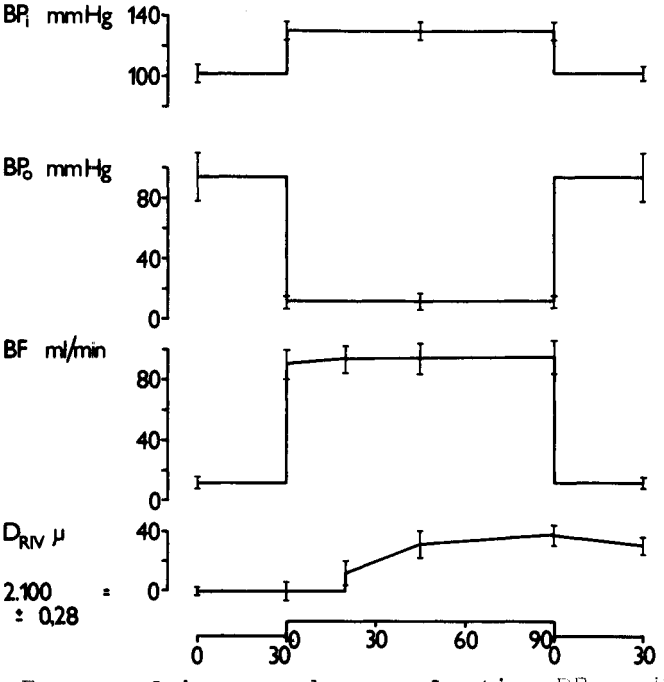

Fig. 3. Effect of increased non-pulsating BF on RIV diameter

The proper trigger pattern of deformation of smooth muscles in coronary wall during the high blood flow is unknown. One can suppose that by increasing shearing stress during the increased blood flow /Fry 1968/ the endothelial cells transfer the stress through the fenestrae in lamina elastica interna /Soret et al. 1976/ to smooth muscle cells in

the media and so the dilation is triggered.

An other type of conduit coronary artery dilation was observed at sudden increase in pressure pulse amplitude of certain magnitude. This dilation, in opposite to the high blood flow dilation, occurs i m m e d i a t e l y after the increase in pulse pressure amplitude, and remains - independently from blood flow /Fig. 4/. In a group of experiments increase in blood pressure amplitude from 16.0 ± 4.9 mmHg to 67.0 ± 9.8 mmHg induced - without any latency - increase in RIV diameter which after 90 seconds reaches 87.1 ± 19.2 μm, representing 3.9%.

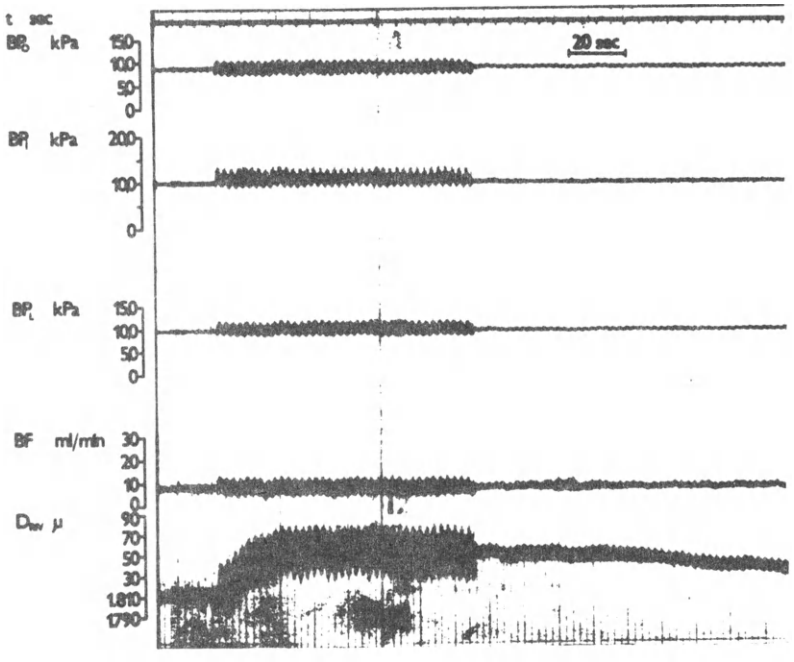

Fig. 4 Effect of increased pulse amplitude on coronary artery diameter

Moreover, the dilation triggered by high pulse pressure amplitude is independent even on mean blood pressure. It is to see when the high pulse pressure amplitude is accompanied by the decrease, increase, or no change in mean blood pressure /Fig. 5 / .

Both RIV dilation phenomena described may have an important role in cases of dilation of heart nutritive vascular bed due to increased heart work, e.g. induced by increased sympathetic activity. They may counterbalance the simultaneously occuring sympathetic constriction of RIV, /Gerová et al 1979 a, Gerová et al 1979 b /.

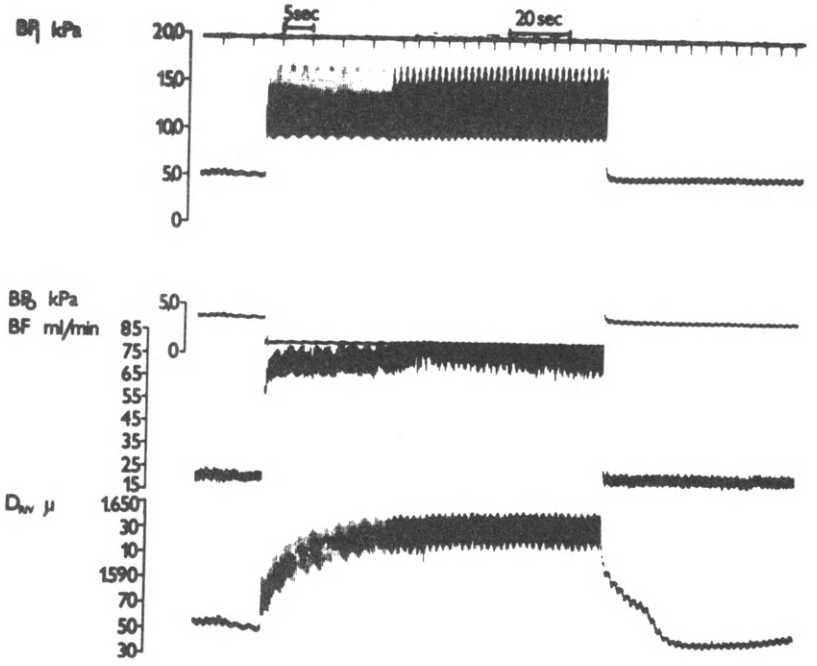

Fig. 5 Effect of increased pulse amplitude and mean BP on coronary artery diameter

Nervous /sympathetic/ control

Data concerning the nervous, namely sympathetic control are similarily very poor. The morphological studies using histochemical technique, as well as electronmicroscopy and autoradiography of H^3 noradrenaline, have convincingly proved during last two decades that adrenergic nerve terminals are located in adventitia of conduit arteries, in particular /Pease and Paule 1960, Falck 1962, Doležel et al 1975, 1978/. Having in mind the nowadays paradigm concerning the function of neurovascular synapse /release of transmitter, its diffusion, binding to smooth muscle receptors, $uptake_1$, $uptake_2$/ it could hardly be supposed that the smooth muscle in the whole media is uniformly activated; rather a gradient of activation /adventitia to intima/ and/or contraction, is to be expected /Gerová et al 1967, Bevan et al 1970, Török et al 1971/; the slope of the gradient being dependent on the density of nerve terminals and/or amounts of smooth muscle layers in the media. However, the control mechanisms are by far more complicated as the studies on diameter decrease of individual segments of

vascular tree at stimulation of respective sympathetic outflow have revealed.

From the experiments it can be derived:

/1/ Tonus of smooth muscle in individual conduit arteries and collecting veins is subjected to nervous control /despite the media is nerve free/; interruption of respective sympathetic pathways increases the diameter of the vessel /Gero et al 1968, Gerová et al 1969/.

/2/ A great variability in range of the sympathetic control /expressed as diameter reduction induced by supramaximal stimulation/ of individual segments of vascular tree is documented at the table 1.

Table 1

The extent of sympathetic control of individual portions of vascular tree.

Vessel	Diameter mm	Stimulation	Max. D decrease u	Max. D decrease %
abd. aorta I	11.1 ± 0.7	LG_1	329.5 ± 41.1	2.9 ± 0.3
abd. aorta II	9.6 ± 0.7	LG_1	496.9 ± 60.1	5.1 ± 0.5
abd. aorta III	8.8 ± 0.7	LG_1	755.8 ± 77.8	8.6 ± 0.8
carotid a.	4.7 ± 0.1	cran.cerv.g.	141.9 ± 9.9	3.0 ± 0.2
		stell.g.	126.9 ± 23.0	2.7 ± 0.4
r.interventricularis ventr.	1.7 ± 0.1	stell.g.	71.2 ± 8.9	4.0 ± 0.5
		Th_{2-3-4}	21.3 ± 7.1	1.2 ± 0.4
brachial a.	2.0 ± 1.6	stell.g.	286.0 ± 26.0	13.4 ± 1.3
femoral a.	2.1 ± 1.8	LG_{3-4}	283.3 ± 25.1	13.4 ± 1.2
saphenous a.	1.9 ± 0.1	LG_{2-3}	390.1 ± 35.6	19.7 ± 1.8
dors.ped.a.	1.8	LG_{3-4}	262.0	14.1
*resistant vessels		LG_{3-4-5}		51.3
femoral v.	4.8 ± 0.5	LG_{3-4}	609.7 ± 65.1	12.7 ± 1.3
postcava	7.4 ± 0.4	LG_{1-2-3}	551.3 ± 30.5	7.4 ± 0.9

*Resistant vessels were included for comparison into the table 1 too; their diameter decrease was calculated according to Poiseuille equation.

The two poles of the sympathetic control of conduit arteries /the resting diameter about the same/, represent: saphenous a. with 19.7% diameter decrease and coronary a. with 4.0% diameter decrease.

There is no relation between density of nerve terminals in the vessel wall and extent of diameter decrease of the respective vascular segment at supramaximal sympathetic stimulation /Gerová et al 1973, Gero et al 1978/. A further series of impacts have to be searched for, which participate in effective dimension change of a vessel.

The response of individual segments to sympathetic stimulation is frequency dependent; plotting the frequency of stimulation and the diameter decrease yields a hyperboloid relation. The frequency-response curves of collecting veins are shifted to the left in comparison with concomittant conduit arteries.

/3/ The direct consequence of the remote location of nerve terminals from smooth muscle cells is the extremely slow constraction of individual conduit segments; maximum diameter decrease being reached at 90-120 seconds /coronary a./ or at 180 seconds /femoral artery and femoral vein/. These values are 3-6 times higher than those of resistant vessels /20-30 sec/. /Gerová et al 1969, 1979, Gero et al 1971, 1978/.

/4/ Sympathetic stimulation induces a significant decrease in both static and dynamic elastic moduli in femoral artery. As far as dynamic elastic modulus concerns, its decrease is brought about not only by the decrease of diastolic diameter, but simultaneously by a rise in diameter pulse amplitude /Gero et al 1971/.

Length deformation of vessels

The above data yield information on radial dimensions of vessels as influenced by myogenic and nervous control. No data are available describing the control of length dimensions of vessels in vivo. It is to understand, that waving the tonus of smooth muscle in the vessel wall had to be reflected in length dimensions of the vessel. The complicated length deformation of the vessel may be deduced from the in vitro experiments too: spiral and longitudinal strip from the same vessel /femoral artery/, in the same bath, respond to the same dosis of noradrenalin with shortening /spiral strip/ and/or lengthening /longitudinal strip/ /Gerová et al 1970/.

Even having in mind the unique studies by Patel and coworkers on length dimensions of the aorta and pulmonary artery /1964/ one can state that the most basic data have still been missing in this field.

Using an inductive transformer we monitored length movement of the, in situ, normally tethered, abdominal aorta in the dog during a heart beat in three points: below renal branching /I/, in the middle /II/ and just above iliac bifurcation /III/, and in one point below iliac bifurcation: on a. sacralis media /IV/. With increasing the pressure /anacrotic part of the pulse/ a caudadwards displacement in point

/I/ and /II/ was registered, a change in direction in point III and a clear-cut cranialwards displacement in point /IV/- - below iliac bifurcation was registered /Fig. 6/.

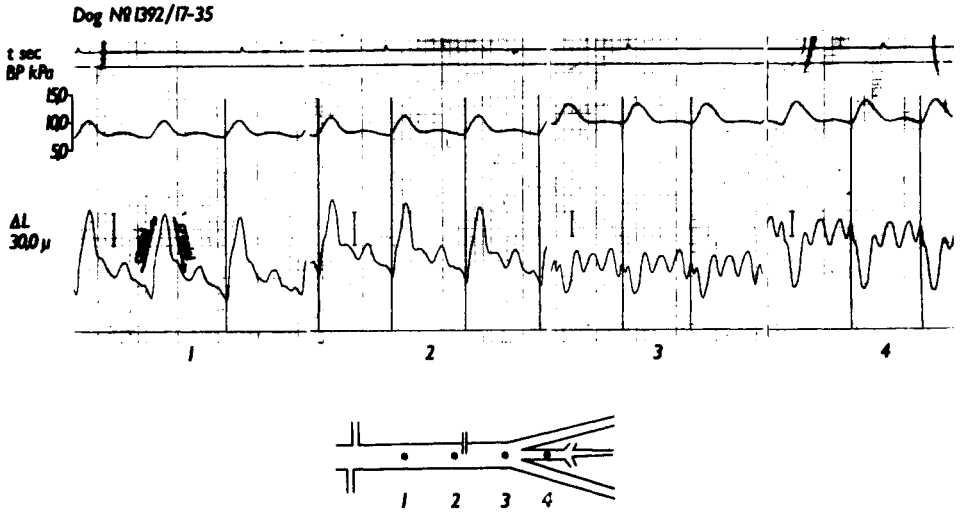

Fig. 6 Length displacement of individual points along the abdominal aorta and a. sacralis media.

At a pressure amplitude 30-40 mmHg the amplitude of the length pulse displacement in either direction represents 40 - 100 u with a gradient declining towards the iliac bifurcation.

The effect of smooth muscle tonus on length dimensions of vessels, however, remains still the goal for the future.

References

Bevan JA, Török J : Movement of norepinephrine through the media of rabbit aorta. Circ. Res. 27:325-331, 1970

Doležel S, Gerová M, Gero J, Feit J : Diffusion through the vessel wall of transmitter released by sympathetic stimulation. Blood Vessels 12:108-121, 1975

Doležel S, Gerová M, Gero J, Sládek T, Vašku J : Adrenergic innervation of the coronary arteries and the myocardium. Acta Anat. 100:306-316, 1978

Falck B : Observations on the possibilities of the cellular localization of monoamines by a fluorescence method. Acta Physiol. Scand. Suppl. 56:197, 1962

Fleisch A : Les réflexes nutritifs ascendants producteurs de dilatation arterielle. Arch. int. Physiol. 41:141-167, 1935
Fry DL : Acute vascular endothelial changes associated with increased blood velocity gradients. Circ. Res. 22:165-197, 1968
Gero J, Gerová M : Dynamics of carotid sinus elasticity during pressor reaction. Circ. Res. 11:1010-1020, 1962
Gero J, Gerová M : Sympathetic regulation of collecting vein. Experientia 24:811-812, 1968
Gero J, Gerová M : In vivo studies of sympathetic control of vessels of different function. in Physiol. Pharmacol. Vasc Neuroeffector Systems, Karger, Basel, 1971, pp. 86-94
Gero J, Gerová M, Doležel S, Török J : Vaskulárny nevroefektorový systém. Bratisl. lek. Listy 70:375-388, 1978
Gerová M, Gero J, Doležel S : Mechanisms of sympathetic regulation of arterial smooth muscle. Experientia 23:639-640, 1967
Gerová M, Gero J : Range of the sympathetic control of the dog femoral artery. Circ. Res. 24:349-359, 1969
Gerová M, Blašková J, Doležel S : Response of dog's femoral artery strips to vasoactive substances. Physiol. Bohemoslov. 19:217-221, 1970
Gerová M, Gero J, Doležel S, Blažková-Huzuláková I : Sympathetic control of canine abdominal aorta. Circ. Res. 33:149-159. 1973
Gerová M, Smieško V, Gero J, Barta E : A myogenic dilating mechanism operating in conduit coronary artery. Physiol. bohemoslov. 28:438, 1979 a
Gerová M, Barta E, Gero J : Sympathetic control of major coronary artery diameter in the dog. Circ. Res. 44:459-467, 1979 b
Hilton SM : A peripheral arterial conducting mechanism underlying dilatation of the femoral artery and concerned in functional vasodilatation in skeletal muscle. J. Physiol. 149:93-111, 1959
Ingebrigsten R, Leraand S : Dilatation of a medium-sized artery immediately after local changes of blood pressure and flow as measured by ultrasonic technique. Acta. Physiol. Scand. 79:552-562, 1970
Lie M, Sejersted OM, Kiil F : Local regulation of vascular cross section during changes in femoral arterial blood flow in dogs. Circ. Res. 27:727-737, 1970
Patel DJ, Greenfield JC, Fry DL : In vivo pressure - length--radius relationship of certain blood vessels in man and dog. in E.O.Attinger /ed/: Pulsatile blood flow, Mc Graw-Hill Inc., New York 1964, pp. 293-302
Pease DC, Paule WJ : Electron microscopy of elastic arteries: thoracic aorta of the rat. J. Ultrastruct. Res. 3:369-482, 1960
Schrentzenmayr A : Über kreislafregulatorische Vorgänge an den großen Arterien bei der Muskelarbeit. Pflüg. Arch. ges. Physiol. 232:743-748, 1933

Smieško V, Chajutin VM, Gerová M, Gero J, Rogoza AN : Čuvstviteľnosť maloj arterii myšečnogo tipa k skorosti krovotoka: reakciji samoprisposoblenija prosveta arterii. Fiziol. Ž. 65:291-298, 1979

Soret MG, Peterson T, Block EM : Ultrastructural study of cytoplasmatic bridges through the membrana elastica interna in the aorta of the chinese hamster. Artery 2:451-466, 1976

Török J, Bevan JA : Entry of ^{3}H-norepinephrine into the arterial wall. J.Pharmacol. exp. Ther. 177:613-620, 1971

Zatzman M, Stacy RW, Randall J, Eberstein A : Time course of stress - relaxation in isolated arterial segments. Am. J. Physiol. 177:299-305, 1954

Adv. Physiol. Sci. Vol. 8. Cardiovascular Physiology. Heart, Peripheral Circulation and Methodology
A. G. B. Kovách, E. Monos, G. Rubányi (eds)

CONTINUUM MECHANICAL METHODS AND MODELS IN ARTERIAL BIOMECHANICS

Antal G. Hudetz
Experimental Research Department, Semmelweis University Medical School, Budapest, Hungary

INTRODUCTION

In order to better understand cardiovascular processes, to clarify pathogenesis of frequent vascular diseases, and to design adequate vessel prostheses, accurate mathematical characterisation of mechanical behavior of blood vessels under a wide varieties of hemodynamical circumstances is necessary. Hopefully, the consequent application of continuum mechanics will help to develop mathematical models which can predict the mechanical behavior of vascular tissues under complex in vivo loading conditions (Monos and Szücs, 1978), where exact measurements of the rheological properties is not possible. Since rheological characteristics of blood vessels are too complex to describe by a single mathematical model, we have developed different continuum models for anisotropic, incremental elastic, nonlinear viscoelastic, and time dependent active responses of arterial walls

ANISOTROPIC ELASTIC PROPERTIES

Anisotropic properties of cylindrically orthotropic arteries were characterized by the three incremental Young's moduli and the six incremental Poisson ratios:

$$E_k = \Delta t_k / e_k \ , \qquad \sigma_{\ell k} = -e_\ell / e_k \qquad (k,\ell = r,\theta,z) \ , \quad (1)$$

where Δt_k and e_k are the normal components of the incremental stress and strain tensors in the (r,θ,z) cylindrical coordinate system, and $\Delta t_\ell = 0$ for $k \neq \ell$. The incremental moduli can be measured at both static and dynamic conditions but in the static case they can be determined more accurately from an adequate form of the strain energy function of the vessel wall.

In order to evaluate the incremental moduli of arteries we performed calculations with different polynomial and exponential forms of the strain energy function using the method of Vaishnav and co workers (1972). The best results were obtained with the following strain energy function:

$$W = W_1 \exp[A+B\varepsilon_\theta^2+C\varepsilon_\theta\varepsilon_z+D\varepsilon_z^2] \ , \quad (2)$$

where ε_θ and ε_z are Lagrangian strain components, A,B,C,D are constants of

elasticity, and W_1 is a scale factor. This essentially four parameter model gave better fit than the 7 constant polynomial, and it gave much smoother characteristic curves than the 12 or higher constant polynomials which usually resulted very "wavy" curves.

Fig. 1 shows computational results for a representative artery. The strong dependence of Young's moduli and Poisson ratios on the initial tangential and axial strains reflects a highly nonlinear anisotropic wall structure. It is noteworthy that the initial axial extension of the vessel segment had relatively small influence on the circumferential incremental modulus and the corresponding Poisson ratio. The calculated curves resemble closely those reported by Cox (1975) with the exeption that the initial value of $\sigma_{\theta z}$ was always less than 0.5.

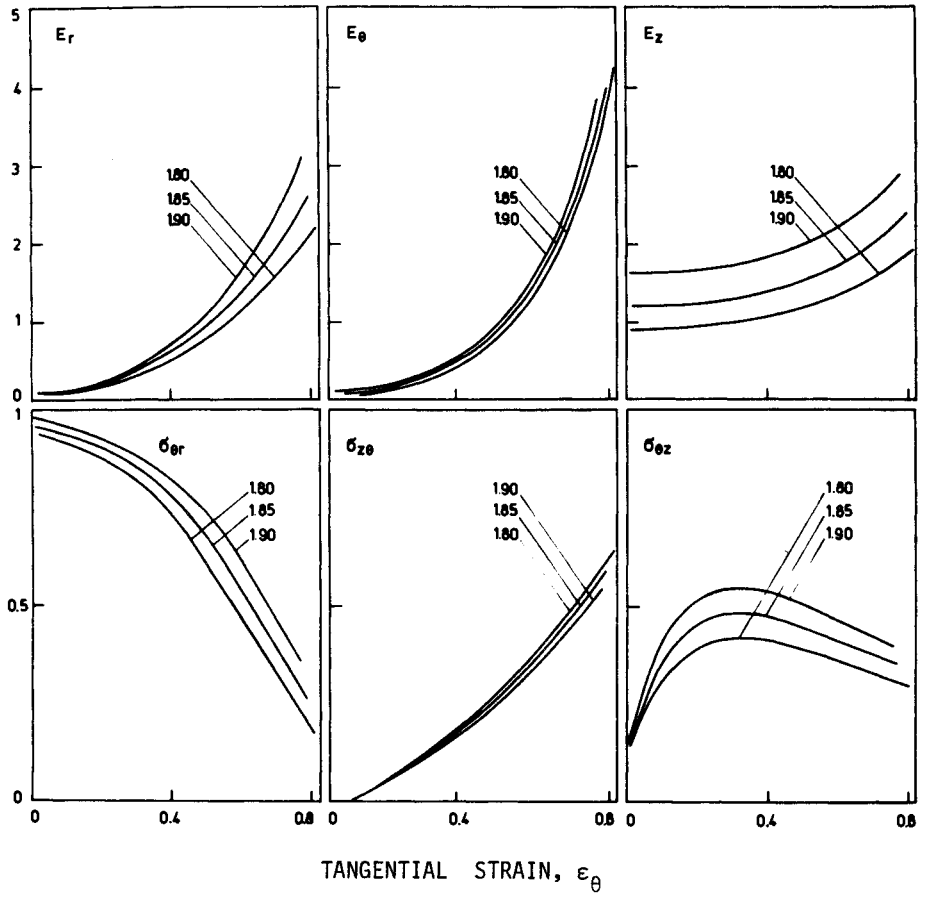

Fig. 1. Dependence of incremental Young's moduli and incremental Poisson ratios on the initial tangential strain at three different initial axial extension ratios of a canine common carotid artery.

STRUCTURAL MODEL OF ANISOTROPY

In order to investigate the possible architectural basis of nonlinear anisotropic properties of arteries, continuum mechanics of fiber reinforced materials was used to develop a two-dimensional structural model of the arterial wall. The model consisted of two helical families of infinitesimally thin, inextensible fibers embedded into a homogeneous, isotropic and linearly elastic matrix. The incremental constitutive equations of such a composite read

$$\begin{aligned} \Delta t_r &= -p+Be_r \ , \\ \Delta t_\theta &= -p+Be_\theta+2T\sin^2\phi \ , \\ \Delta t_z &= -p+Be_z+2T\cos^2\phi \ , \end{aligned} \qquad (3)$$

where in addition to the quantities already known, B is an elastic modulus of the matrix, p and T are reaction stresses appearing due to incompressibility and fiber inextensibility, and ϕ is the average angle between the fibers' direction and the vessel's axis.

Nonlinearity was introduced into the model by allowing the number and angle of fibers to change with deformation of the tissue. The fibers were assumed to be loose in the undeformed state and becoming aligned at increasing strain according to a distribution function. Based on these assumptions the following nonlinear constitutive equation was established (for costant vessel length):

$$t_\theta - t_r = 2B\int_{R_o}^{R} \frac{dr}{r[1-x(r)]} \ , \qquad (4)$$

where R is the vessel's midwall radius and x(r) is the distribution function of the aligned

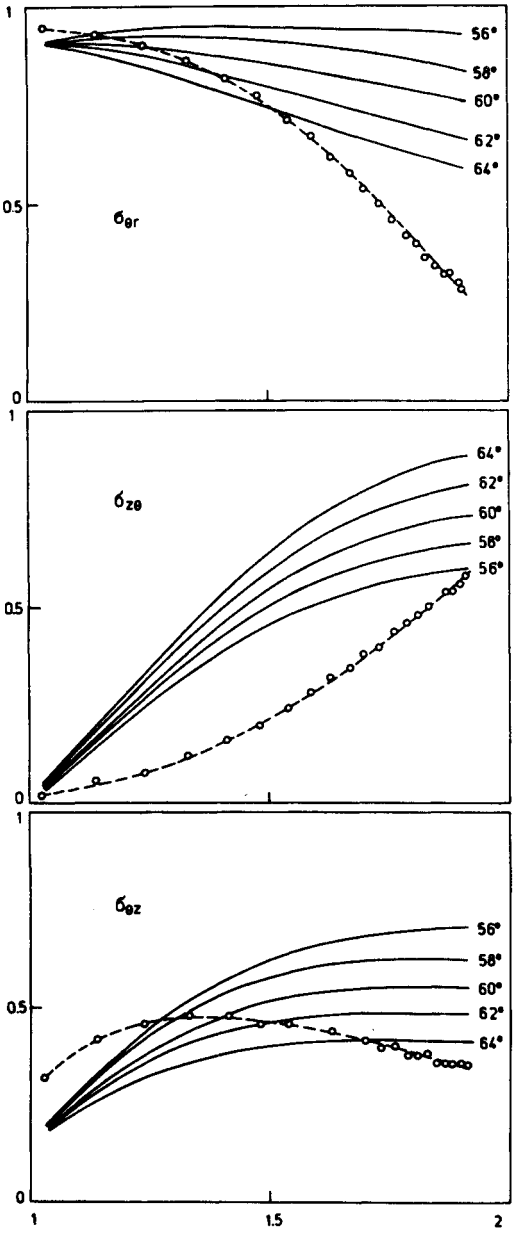

Fig. 2. Comparison of incremental Poisson ratios calculated from the structural model (continuous lines) and from the exponential strain energy function (broken line) at λ_z = 1.85.

fibers. The integral is the so called reduced tangential strain constructed to measure the deformation of the unconstrained part of the matrix. The angle of the loose fibers was calculated as

$$\phi = \arctan\left(\frac{\lambda_\theta}{\lambda_z}\tan\Phi\right) , \tag{5}$$

where λ_θ and λ_z are tangential and axial extension ratios, respectively, and Φ is the initial fiber angle in the unstrained state.

The structural model has been used to calculate the incremental Poisson ratios of the arterial wall. For this purpose, the distribution function x(r) was determined from experimentally measured stress-strain curves using Eq. (4). The Poisson ratios were calculated as ratios of the resultants of incremental strains in the free (1) and the constrained (2) part of the matrix:

$$\sigma_{k\ell} = -\frac{(1-x)e_k^{(1)}+xe_k^{(2)}}{(1-x)e_\ell^{(1)}+xe_\ell^{(2)}} . \tag{6}$$

The strain components in Eq. (6) were calculated from the kinematical constraint conditions of fiber inextensibility and from Eq. (3).

In Fig. 2 incremental Poisson ratios calculated from the model at different Φ, initial fiber angles can be compared with those taken from Fig.1 (λ_z = 1.85) for the same artery. The results suggest that a helical network of collagen fibers embedded in isotropic, linearly elastic media may explain the nonlinear anisotropy of arteries. The model predicts an average collagen fiber angle of 1.05±0.07 rad (60±4°) in the unstrained state of the carotid artery.

ISOTROPIC AND ORTHOTROPIC INCREMENTAL MODULI

From practical aspects of characterisation and measurements, it is often more convenient to use a single incremental modulus instead of three moduli. In 1961 Bergel introduced a useful formula for determination of the isotropic incremental Young's modulus of cylindrical arterial segments. It has been shown recently (Hudetz, 1979) that in order to apply this formula for incremental deformations correctly it must include an additional term responsible for the initial stress. For an incompressible, thin walled vessel the corrected expression of the isotropic incremental modulus reads

$$E = 0.75\,\frac{R^2\Delta P}{h\,\Delta R} + 0.75\,\frac{RP}{h} , \tag{7}$$

where R is the midwall radius and h is the wall thickness at the intraluminal pressure P. In the derivation of Eq. (7) stresses measuring force per unit area before incremental deformation were used. If stresses measuring force per unit area after incremental deformation are used, then the initial stress term will be different, and we obtain

$$E' = 0.75\,\frac{R^2\Delta P}{h\,\Delta R} + 1.5\,\frac{RP}{h} . \tag{8}$$

Since large arteries are not isotropic we introduced another icremental modulus for cylindrically orthotropic, incompressible vessels pressurized at constant length with the definition:

$$H = \frac{\Delta T_\theta}{e_\theta} + \frac{\Delta T_r}{e_r} \qquad \text{or} \qquad H' = \frac{\Delta t_\theta}{e_\theta} + \frac{\Delta t_r}{e_r} , \tag{9}$$

where the incremental stresses ΔT_θ, ΔT_r and Δt_θ, Δt_r measure force per unit area before and after incremental deformation respectively. Substituting common formulas of the average wall stresses into Eq. (9) we obtain

$$H = \frac{R^2 \Delta P}{h \Delta R} + \frac{RP}{h} \qquad \text{and} \qquad H' = \frac{R^2 \Delta P}{h \Delta R} + 2 \frac{RP}{h} . \tag{10}$$

Thus, the "orthotropic" modulus H (or H') can be determined from similar expressions and measurements to the isotropic modulus E (or E'), but it characterises tangential-radial elastic stiffness of cylindrically orthotropic, incompressible vessels at constant length.

H and H' are related to the tangential incremental Young's modulus through two incremental Poisson ratios:

$$H = \frac{E_\theta}{1 - \sigma_{\theta z}\sigma_{z\theta}} \qquad \text{and} \qquad H' = \frac{E'_\theta}{1 - \sigma'_{\theta z}\sigma'_{z\theta}} . \tag{11}$$

We note, that Eqs. (7)-(11) are valid for the complex modulus formulation, too.

NONLINEAR VISCOELASTIC PROPERTIES

When vascular smooth muscle is activated,mechanical properties of arteries become obviously time dependent. For describing large deformation time dependent behavior of vessels with contracting smooth muscle a simple nonlinear viscoelastic constitutive equation was developed. Our starting point was that (1) the area of the quasi static hysteresis loop of arteries is fairly insensitive to strain rate (Fung, 1972; Cox, 1976), and (2) arteries show markedly different responses to loading and unloading. These observations suggest that arteries do not belong to the class of "rate type" materials; thus, the commonly used differential viscoelastic constitutive equations are inappropriate for their material characterization. Instead, arteries can be preferrably considered as materials with fading memory, the mechanical responses of which are determined by the past strain/stress history.

The general nonlinear functional equations of this class of materials are too complicated for practical purposes. A quasi linear single integral and a nonlinear multiple integral representation of the general equations have been given by Fung (1972) and Patel and Vaishnav (1977) respectively, for vessels with passive smooth muscle. When smooth muscle is activated, however, strain and time dependence of the relaxation function contained by the single integral equation are not separable; thus the quasi linear costitutive equation is not applicable in this case. Also, for the required large range of deformation the necessarily high degree integral polynomial equations give unstable relaxation functions (Hudetz et al., 1978).

To avoid these difficulties we have developed the following viscoelastic constitutive equation (in one dimensional creep formulation):

$$\varepsilon(t) = \int_{-\infty}^{t} \partial_s C^{+}[S(\tau), t-\tau]\, h[\dot{S}(\tau)] + \int_{-\infty}^{t} \partial_s C^{-}[S(\tau), t-\tau]\, h[-\dot{S}(\tau)] \,, \qquad (12)$$

where ε and S are appropriate Lagrangian strain and stress components,

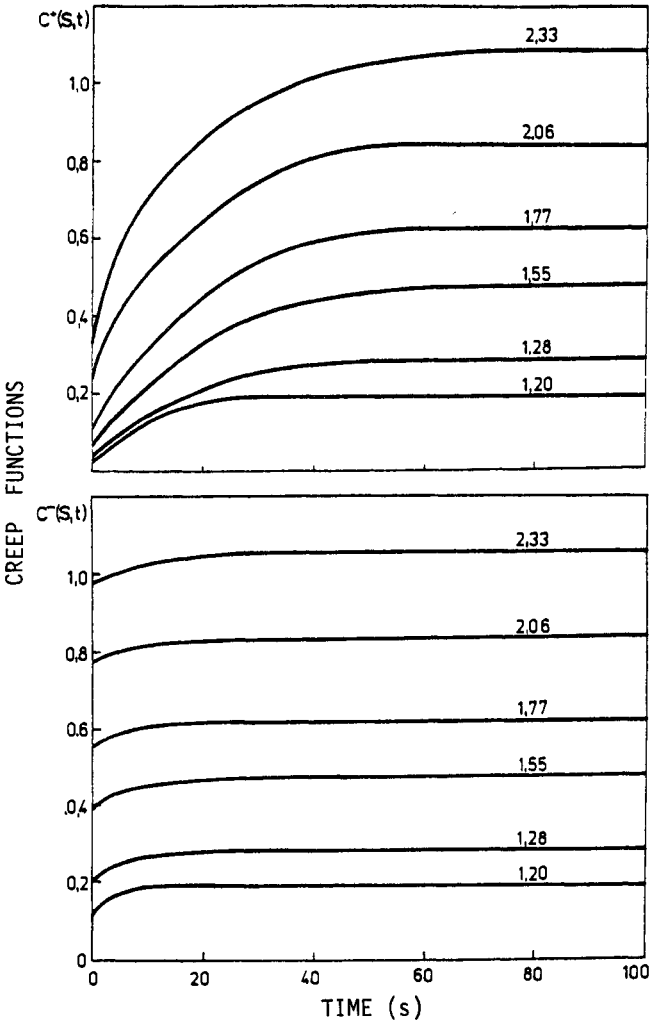

Fig. 3. Creep functions C^{+} and C^{-} of a NE-activated canine iliac artery as determined from six creep and recovery step tests of different amplitudes. (Values of stress steps above the curves are in KPa.)

C^+ and C^- are creep functions, and h is the unit step function. Equation (12) has the advantageous properties that (1) it is nonlinear in both stress and time, (2) the creep functions have definite physical meaning, and (3) responses to loading and unloading are treated separately through the two creep functions.

For determining creep functions of arteries a series of creep and recovery step tests were performed on NE-activated canine iliac artery segments at constant vessel length. The obtained creep functions reflect marked nonlinearities in both stress and time, and notable differences between loading and unloading behavior (Fig. 3).

Substituting the tabulated values of experimentally determined creep functions into Eq. (12), constant stress rate hysteresis curves were simulated on digital computer. Fig. 4 shows that the nonlinear viscoelastic model could predict some characteristics of arterial hysteresis, e.g., large loop area, small rate sensitivity, and sign changing dependence of stress-strain curves on the stress rate.

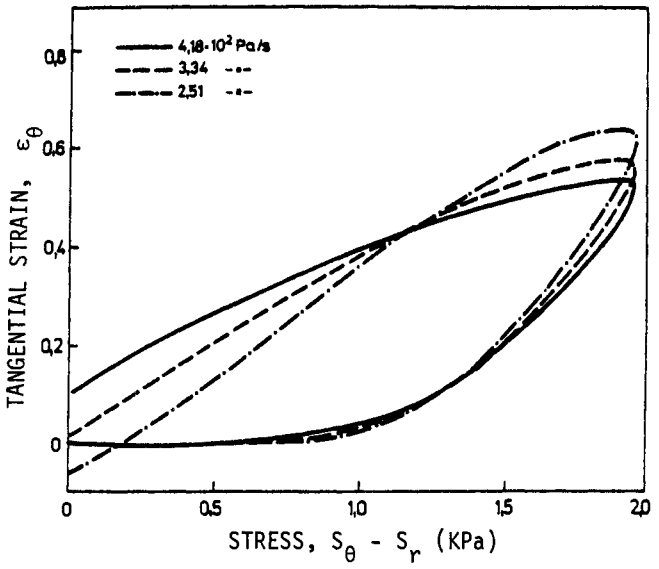

Fig. 4. Computer simulation of quasi static hysteresis loops at different constant stress rates using the viscoelastic constitutive equation (12).

MYOGENIC RESPONSE

The hypothesis of fading memory excludes time dependent active responses, such as icrease in stress at constant strain or decrease in strain at constant stress. To simulate stretch induced myogenic responses of vascular smooth muscle (VSM),spring and dashpot elements of the classical linear viscoelastic models were completed with a new stress generating

element (SGE) defined by the constitutive equation

$$\dot{\sigma} = \alpha e \ , \tag{13}$$

where $\dot{\sigma}$ is the rate of stress production, e is the strain, and α is a parameter depending on nonmechanical effects: rate of chemical energy production, ionic milieu, etc. Since the stress in the SGE must remain finite, Eq. (13) is valid as a short time approximation.

Small deformation myogenic reactions of VSM were simulated by a one dimensional four element model in which the SGE was associated with the undamped contractile component of the muscle. The parallel coupled SGE and viscous dashpot were completed with a series and a parallel elastic

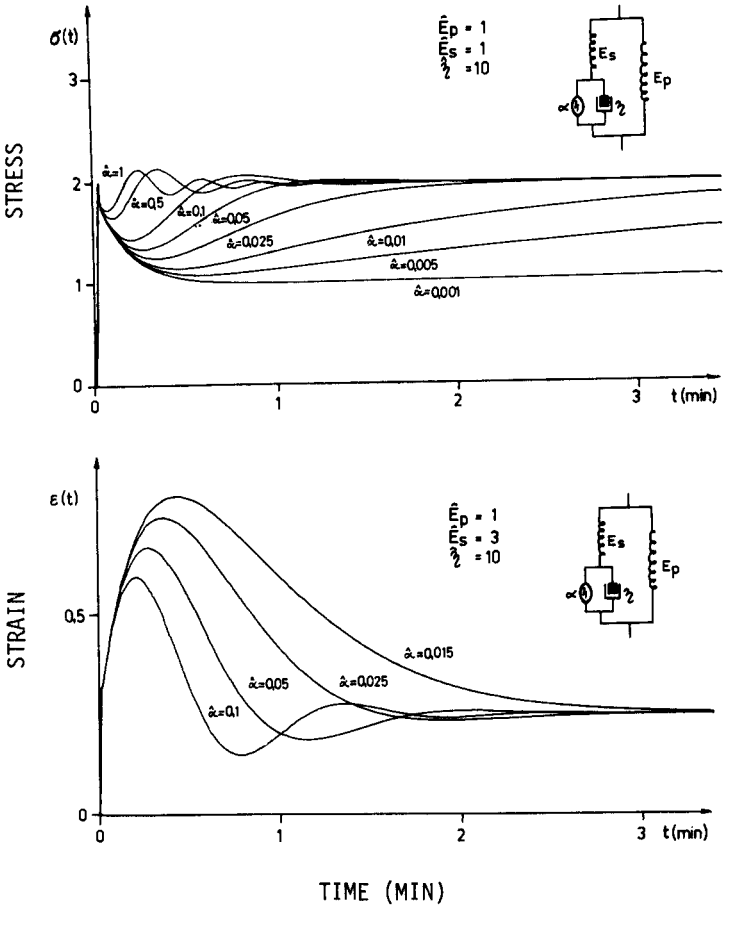

Fig. 5. Stretch induced isometric (upper panel) and isotonic (lower panel) responses simulated by the four element viscoelastic active model of VSM. (σ, e, $\hat{E}_p$, $\hat{E}_s$ and $\hat{\eta}$ are undimensional.)

element (Fig. 5). The differential equation of this model was

$$\eta\ddot{\sigma} + E_s\dot{\sigma} + \alpha\sigma = \eta(E_s + E_p)\ddot{\varepsilon} + E_sE_p\dot{\varepsilon} + \alpha(E_s + E_p)\varepsilon \ , \qquad (14)$$

where η is the viscosity of the dashpot, and E_s and E_p are the Young's moduli of the series and parallel coupled elastic elements, respectively.

Stress response to step change in strain, and strain response to step change in stress were simulated at different SGE rate constants on analog computer. Fig. 5 shows that α has an influence on the time course of the stress regeneration phase. Damped oscillations appear if $\alpha > \alpha_o$ where

$$\begin{aligned} \alpha_o &= E_s^2/4\eta \qquad \text{(at constant strain)}, \\ \alpha_o &= E_s^2E_p^2/4\eta(E_s + E_p)^2 \qquad \text{(at constant stress)}. \end{aligned} \qquad (15)$$

Amplification of spontaneous (intrinsic) oscillations of VSM could also be modelled by parametric resonance of the model. For achieving this α was modulated sinusoidally, simulating intrinsic pacemaker activity of the smooth muscle cells (Fig. 6).

The model predicted rate insensitive hysteresis around the frequency $\omega_o = \sqrt{\alpha/\eta}$, positive correlation between the loop area and strain rate at $\omega > \omega_o$, and negative correlation for $\omega < \omega_o$. The latter finding corresponds well to the experimentally observed slight reduction of arterial hysteresis with increasing strain rate at low frequency (.001-.01 Hz) which obviously can not be explained by classical dissipative viscoelastic models.

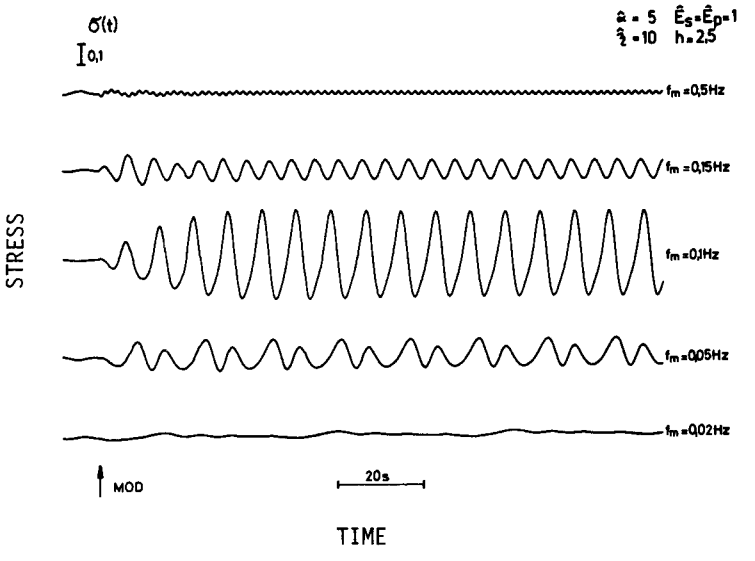

Fig. 6. Parametric resonance of the viscoelastic model with a natural frequency of 0.11 Hz. f_m, h: frequency and amplitude of modulation of α.

SUMMARY

Incremental and nonlinear continuum mechanics have been used to model anisotropic incremental elastic, nonlinear viscoelastic, and viscoelastic active behavior of vascular tissues. Incremental Young's moduli and Poisson ratios of the carotid artery determined experimentally using a four parameter exponential strain energy function reflected highly nonlinear anisotropic structure. Poisson ratios calculated from the fiber reinforced architectural model showed similar trends to those obtained from the strain energy function. The model predicted 1.05±0.07 rad for the angle of collagen fibers in the wall of the carotid artery. For characterizing tangential-radial elasticity of cylindrically orthotropic arteries, a new incremental modulus was defined at constant vessel length. Characteristics of quasi static arterial hysteresis were predicted by a nonlinear viscoelastic constitutive equation developed to model large deformation,time dependent behavior of vessels with contracting smooth muscle. Stretch induced (myogenic) contractions, spontaneous oscillation,and further properties of arterial hysteresis were simulated by a four element linear viscoelastic model containing a special stress generating element.

ACKNOLEDGEMENTS

I wish to express my thanks and appretiation to Prof. Dr. A. G. B. Kovách and to Dr. E. Monos for their continuous support and valuable discussions. This work was supported by Ministry of Health, Hungary (1-07-0301-00-1/K) and by the grant NINDS-10393, USA.

REFERENCES

Bergel, D. H. (1961) The static elastic properties of the arterial wall. J. Physiol. 156, 445-457

Cox, R. H. (1975) Anisotropic properties of the canine carotid artery in vitro. J. Biomechanics 8, 293-300

Cox, R. H. (1976) Mechanics of canine iliac artery smooth muscle in vitro. Am. J. Physiol. 230, 462-470

Fung, Y. C. (1972) Stress-strain history relations of soft tissues in simple elongation. In: Biomechanics: Its Foundations and Objectives, Y. C. Fung, N. Perrone, M. Anliker (eds.) Englewood Cliffs, New Jersey

Hudetz, A. G. (1979) Incremental elastic modulus for orthotropic incompressible arteries. J. Biomechanics 12, 651-655

Hudetz, A. G., Monos, E. and Kovách, A. G. B. (1978) Nonlinear viscoelastic properties of arteries. In: Proc. 3rd Int. Congr. Biorheol., Y. C. Fung, J. G. Pinto (eds.) La Jolla, p. 158

Monos, E. and Szücs, B. (1978) Effect of changes in mean arterial pressure on the structure of short-term blood pressure waves. Automedica 2, 149-160

Patel, D. J. and Vaishnav, R. N. (1977) Mechanical properties of arteries. In: Cardiovascular Flow Dynamics and Measurements, N. H. C. Hwang, N. A. Normann (eds.) Univ. Park Press, Baltimore, pp. 439-472

Vaishnav, R. N., Young, J. T., Janicki, J. S. and Patel, D. J. (1972) Nonlinear anisotropic elastic properties of the canine aorta. Biophys. J. 12, 1008-1027

Adv. Physiol. Sci. Vol. 8. Cardiovascular Physiology. Heart, Peripheral Circulation and Methodology
A. G. B. Kovách, E. Monos, G. Rubányi (eds)

ROLE OF ARTERIAL MECHANICS IN CIRCULATORY FUNCTIONS

E. Monos
Experimental Research Department, Semmelweis University Medical School, Budapest, Hungary

Spectral properties of circulatory waves. Complexity is characteristic for blood pressure and flow fluctuations. The power-density of short-term arterial pressure waves varies over a 60 dB range, its frequency components overlapping four to five decades from about 0.005 Hz upward. In addition to amplitude and frequency, these pressure fluctuations can also be characterized by the magnitude of their stochastic components /Monos and Szücs 1978/.

Utilizing electronic signal filtering techniques, Fourier-series, as well as statistical functions, like auto-, cross-correllograms, and power-density spectra, it was found that alterations of mean arterial pressure elicited profound changes in wave structure. For instance, amplitude of first Fourier-harmonic and magnitude of stochastic components of pulsatile "first-order" pressure waves exhibited in several cases a parabolic dependence on mean pressure in the 160-90 mmHg range with minimum value around 100-110 mmHg /Fig. 1. and 2./. Traube-Hering-Mayer "third-order" waves predominant-

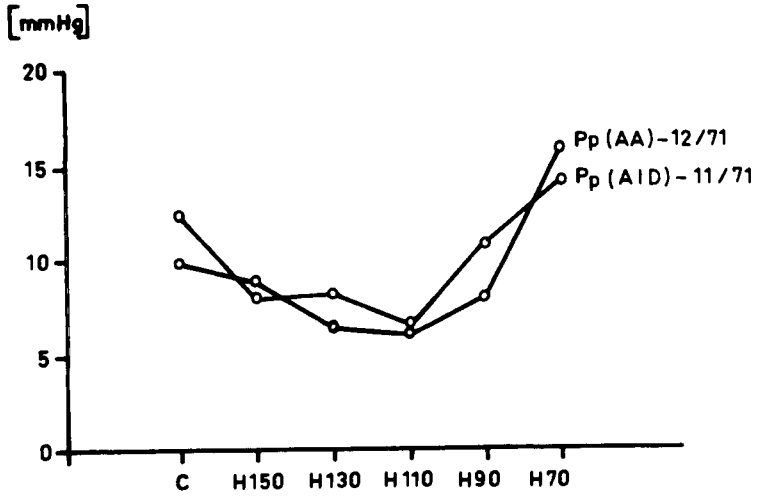

Figure 1. Amplitude of 1st Fourier-harmonic of aortic /AA/ and iliac /AID/ pulse pressure waves at various mean pressure levels set by bleeding. Mean pressure is given in mmHg by H. C: control pressure /160 mmHg/.

ly consisted of stochastic components. Their dominant frequency decreased gradually when mean arterial pressure was lowered in the range of baroreceptor control. A close dynamic correlation was found between the instantaneous third-order changes in absolute value as well as derivative maximum of pulsatile pressure and the third-order pressure fluctuations itself at each mean pressure level studied /Szücs and Monos 1977/.

The above outlined features of circulatory waves are results of characteristic changes in cardiac activity as well as in mechanical properties of the arteries. To understand the nature and control of these pressure changes, geometrical and elastic behavior of the arteries were studied under various loading conditions.

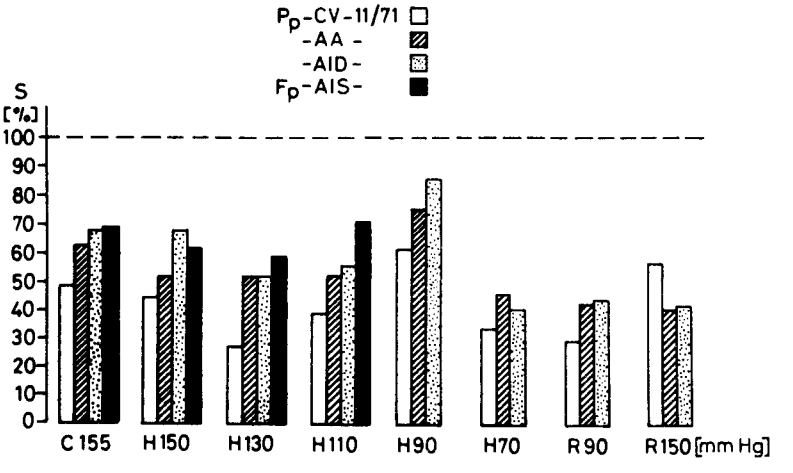

Figure 2. Changes in stochastic components /S/ of pulse pressures P_p in caval vein /CV/, ascending aorta /AA/ and iliac artery /AID/ as well as of blood flow velocity F_p in contralateral iliac artery /AIS/ as a function of mean arterial pressure.

Mechanical behavior of the arterial wall and its short-term control. Passive and active mechanical properties of isolated arterial segments /carotid, iliac, uterine, splenic/ were examined by applying a quasi-static large deformation test. Outer diameter and axial extending force of the segments were recorded at constant in vivo length as function of intraluminal pressure in 0-250 mmHg range. Recordings were made both with relaxed and norepinephrine activated smooth muscle. The following mechanical quantities were computed: three-dimensional normal wall stresses, strain-energy density, tangential elastic modulus, distensibility, characteristic impedance, and deformation measures /Fig. 3./. Details of the methods are published elsewhere /Cox 1974, Monos and Kovách 1979/.

Active geometrical response of the vessels, expressed as isobaric change in strain during activation with a physiological amount of norepinephrine, revealed that intraluminal pressure had a substantial, but varying influence on contractions depending on the type of vessel /Fig. 4./.

D E F I N I T I O N S

AVERAGE WALL STRESSES

$$S_\Theta = \frac{PR_i}{R_e - R_i}$$

$$S_R = -\frac{PR_i}{R_e - R_i}$$

$$S_Z = \frac{F}{(R_e^2 - R_i^2)\pi} + \frac{PR_i^2}{R_e^2 - R_i^2}$$

STRAIN ENERGY DENSITY

$$W = \frac{1}{V_w}\int_{V_o}^{V} P\,dV' = \frac{2\pi L}{V_w}\int_{R_{io}}^{R_i} PR_i'\,dR_i'$$

INCREMENTAL ELASTIC MODULUS

$$E = \frac{\Delta P}{\Delta R_e}\,\frac{2R_i^2 R_e}{R_e^2 - R_i^2}$$

INCREMENTAL DISTENSIBILITY

$$D = \frac{\Delta V}{V \Delta P} = \frac{1}{E}\,\frac{4R_e^2}{R_e^2 - R_i^2}$$

CHARACTERISTIC IMPEDANCE

$$Z_0 = \frac{\rho}{R_i^2 \pi}\sqrt{\frac{E(R_e^2 - R_i^2)}{4\rho R_e^2}}$$

INTERNAL RADIUS

$$R_i = \sqrt{R_e^2 - \frac{V_w}{\pi L}}$$

Figure 3. Definitions used for describing biomechanical properties of the vessels. S_Θ, S_R, S_Z tangential, radial, and axial stresses respectively;
P intraluminal pressure;
R_i internal radius;
Re external radius;
R_{io} initial internal radius;
F axial extending force;
V_w volume of the vessel wall;
V_i: volume of the vessel lumen;
V_O: initial value of luminal volume;
ρ blood density /≈1/;
L length of the vessel cylinder.

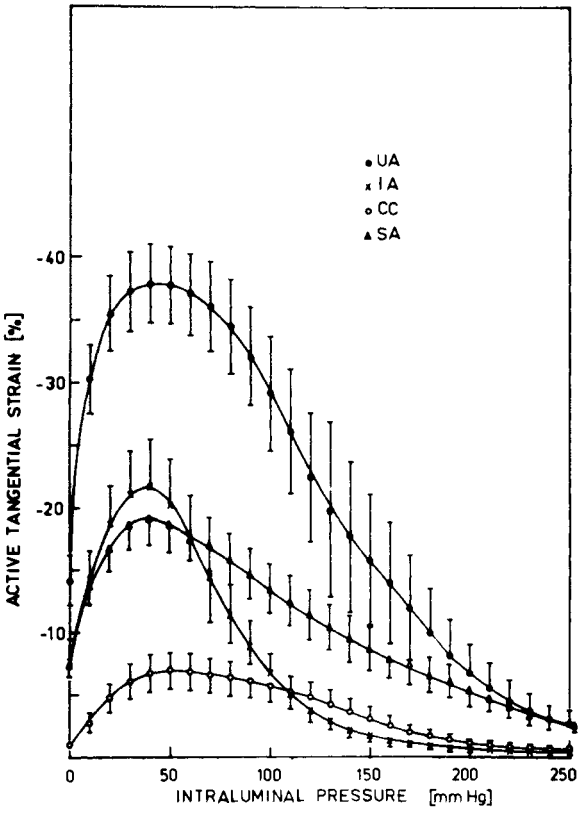

Figure 4. Isobaric geometrical response of noradrenaline-activated /0.5 μg/ml/ uterine UA, iliac IA, common carotid CC and splenic SA arteries.

This variability of responses indicates that regional differences in neural and humoral reactions of arteries are to be explained not only by receptor heterogeneity of the smooth muscle cells, but also by different biomechanical properties of various vessels. Maximum active strain, however appeared always at pressures below the normal 90-110 mmHg range. Conversely, the active elastic response, that is change in elastic modulus under norepinephrine, reached its peak value at normal or higher pressure levels /Fig. 5./.

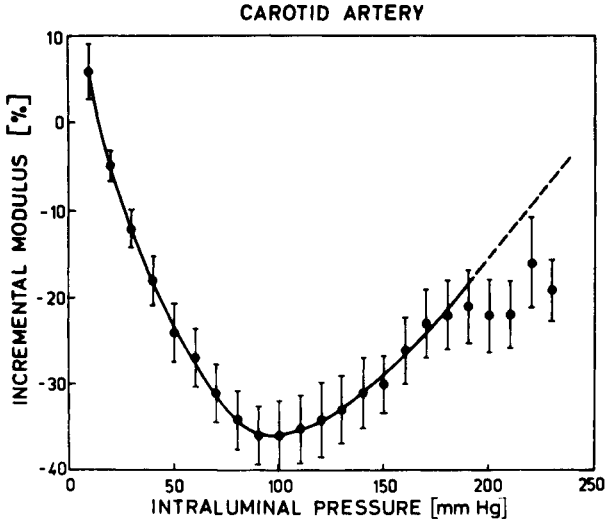

Figure 5. Change in arterial elastic modulus as a function of pressure after smooth muscle activation with 0.5 µg/ml norepinephrine. The decrease of the modulus amounted to 40 % in the physiological pressure range. Hog carotid arteries.

As a result of these responses, elastic parameters like characteristic impedance of both large /Cox 1978, Hudetz et al. 1980/ and middle size /Fig. 6./ arteries /Monos and Kovách 1980/ studied hitherto depend on intraluminal pressure parabolically when smooth muscle is activated. Minimum value of the impedance is in the normal physiological pressure range. The above observations suggest that, apart from caliber, also elastic properties of the arteries might represent controlled variables of short-term regulatory mechanisms.

Further studies revealed that the adrenergic pressure-dependent response characteristics of arteries are substantially influenced by hormonal and metabolic factors. E.g. physiological amount of vasopressin /150 µU/ml/, which alone is insufficient to induce smooth muscle contraction on isolated arteries, potentiates the contractile response to norepinephrine significantly /Fig. 7./. Similar effect of physiological dosis of vasopressin on major arteries has been proved in vivo as well /Monos et al. 1978a, b/. During the recovery period following one hour severe local ischemia /Monos and Kovách 1979/ a substantially enhanced reactivity to norepinephrine was observed on carotid arteries /Fig. 8./. Thus, consideration of the biomechanical, humoral and metabolic conditions alike is essential in estimating physiological significance of arterial contractile responses to various control effects.

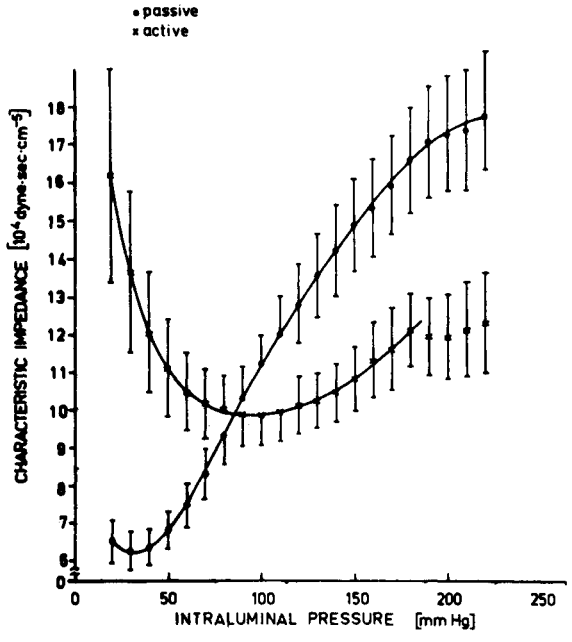

Figure 6. Theoretical characteristic impedance of canine splenic arteries with relaxed "passive", and with activated smooth muscle, respectively.

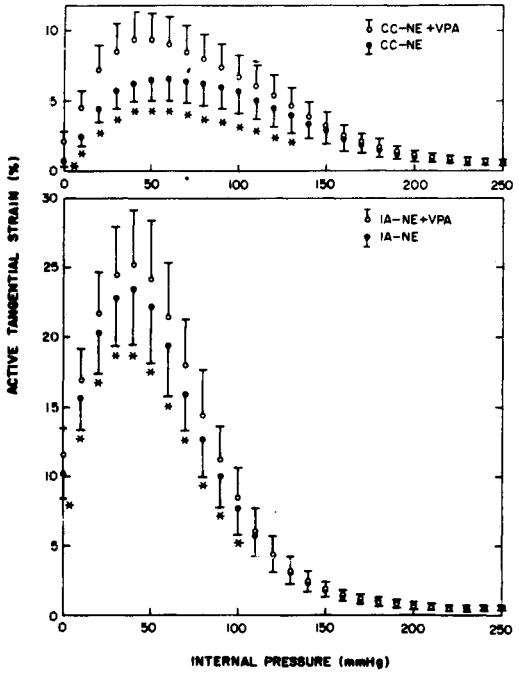

Figure 7. Outer diameter reduction of canine common carotid /CC/ and iliac /IA/ arteries as a function of pressure 3-4 minutes following 0.5 μg/ml norepinephrine /NE/ and NE plus 150 μg/ml arginine-vasopressin /VPA/ administration. Statistically significant /$p < 0.05$/ potentiating effect is indicated with asterisks.

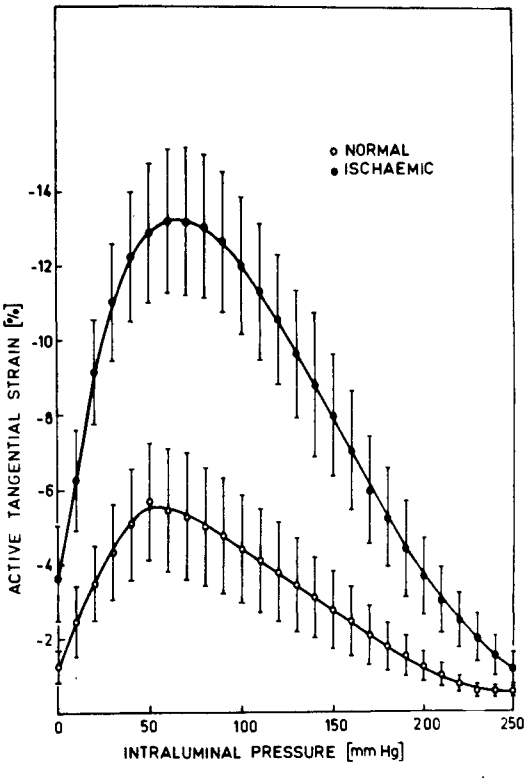

Figure 8. Changes in outer diameter of normal and post-ischemic canine carotid arteries with pressure following activation of smooth muscle by 0.5 /ug/ml norepinephrine.

A hypothetical optimizing mechanism for short-term circulatory control. Based upon observations outlined above the theory is advanced that a forced oscillation type optimizing mechanism contributes to the regulation of arterial pressure /Szücs and Monos 1977/ involving the control of arterial elasticity as well. Fig. 9. shows a block diagram of such optimizing system. For this type of control two interacting processes are essential: a searching one, and a considerably slower basic process. Pulsatile changes in arterial pressure can be regarded as searching process, and Traube-Hering-Mayer waves as basic one. If noise effects disturbe the system the pulsatile searching process will induce a control signal, magnitude of which depends on the position of operating point on the extremal characteristic; then the control signal, modifying the basic process, forces the operating point back to the minimum of the characteristic. This type of arterial pressure control mechanism might minimize the pulsatile work of the heart in various physiological conditions through minimizing the impedance in large arteries, and could shield the microcirculation against mechanical injury by reducing the pressure pulses onto optimal value in middle size arteries.

The functioning of a control system like this is subjected to several essential conditions, some of which are proven to be fulfilled in the cardiovascular system. E.g. parabolic extremal characteristics can be identified for such substantial system parameters as arterial impedance, and others characterizing the elastic properties of arteries. Further, there exist several processes in the circulation with considerably distinct frequencies; the close correlation between first- and third-order circulatory wave components indicates the interaction of these processes. An analogue and a digital computer model of this optimizing control mechanism with coefficients taken from physiological measurements has been constructed and tested successfully /Szücs and Monos, unpublished/. It should be emphasized however, that further investigations are required to identify exactly the structure of this control, and to decide how band-pass filter, discriminator and integrator functions are managed in the body, if this control mechanism exists at all.

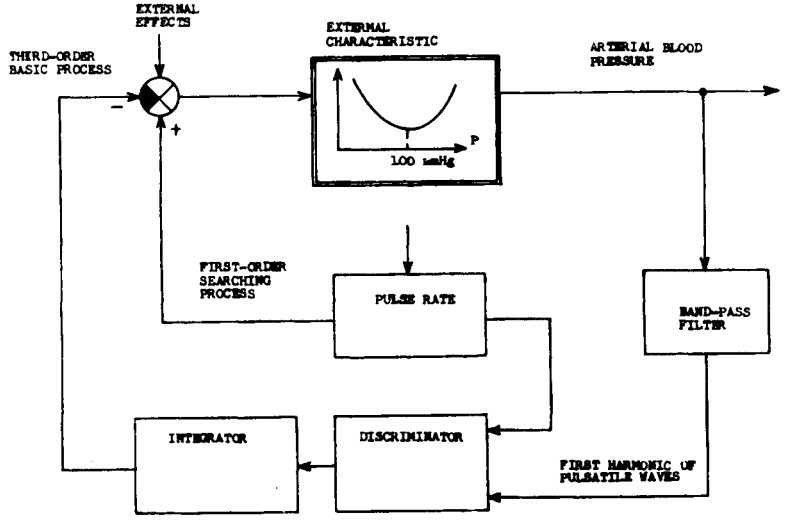

Figure 9. Block-diagram of a hypothetical forced oscillation control mechanism optimizing blood pressure. ⊗: error detector, P: blood pressure.

Some aspects of long-term control of the arterial wall mechanics. Biomechanical studies on fibrosclerotic and normal isolated human arteries /anterior cerebral, internal carotid/ suggest the existence of a tissue mechanism, which under certain conditions is capable to restore some rheological properties of the vessel wall. The following observations form the basis of this hypothesis. Fibrosclerotic arteries with relaxed smooth muscle were found to have much smaller elastic stiffness then the passive normal ones at

identical intraluminal pressures, but incremental distensibility of fibrotic arteries was not smaller than that of the normal vessels. /Fig. 10, 11./, because the decrease in elastic modulus was the result of the increase in wall thickness/radius ratio /Hudetz et al. 1977, Márk et al. 1977/. Similar observations were made on canine femoral vein /Monos and Csengődy 1980/ some months after grafting it into the femoral artery /Fig. 12, 13./.

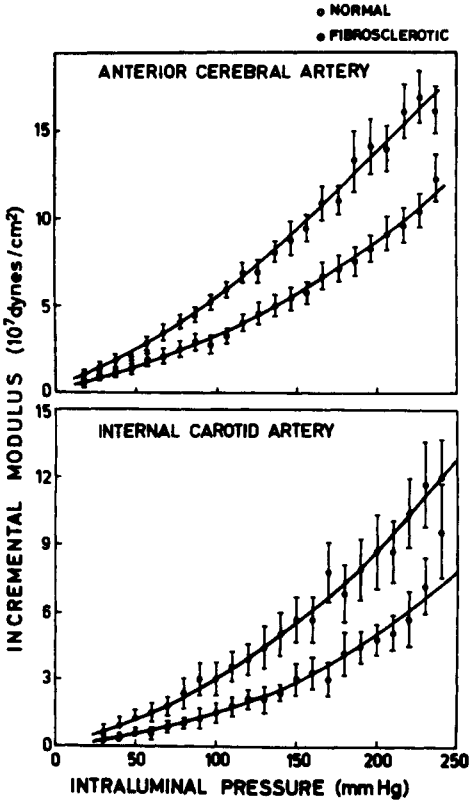

Figure 10. Dependence of elastic modulus on intraluminal pressure in the case of normal, as well as fibrosclerotic human anterior cerebral and internal carotid arteries.

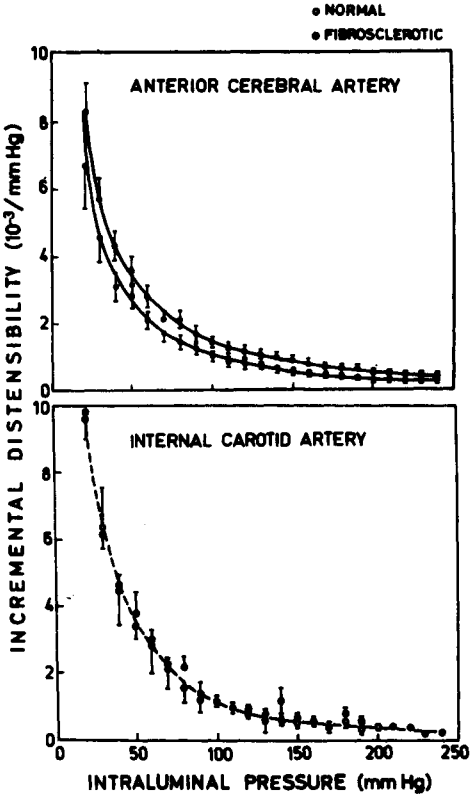

Figure 11. Changes in distensibility of normal, and fibrosclerotic human cerebral arteries with pressure.

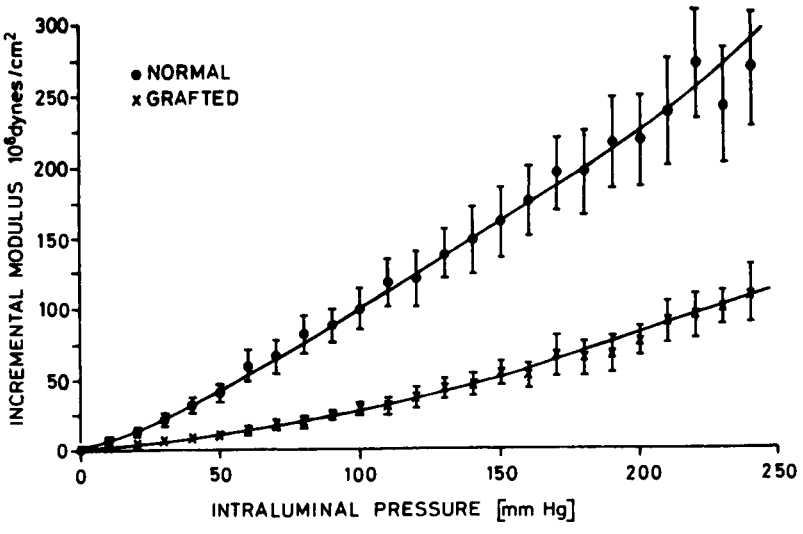

Figure 12. Elastic modulus of normal and "arterialized" veins plotted against pressure.

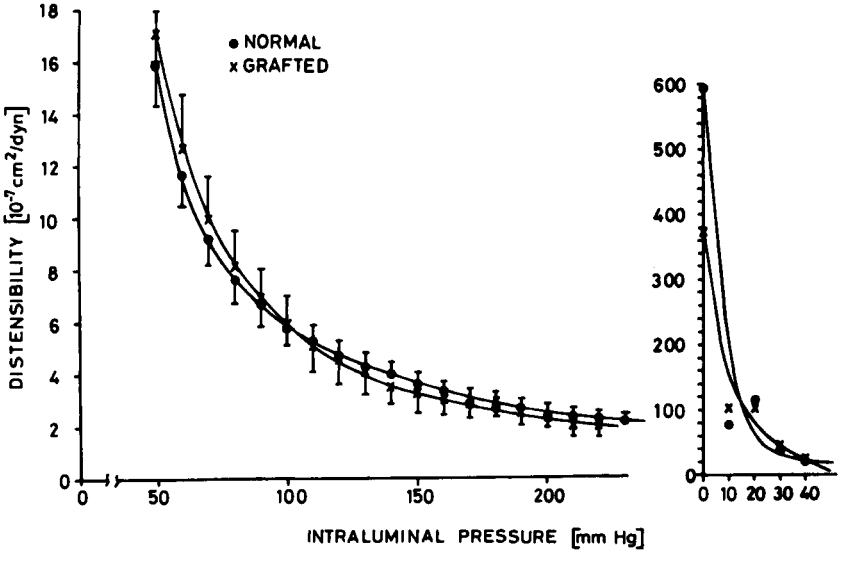

Figure 13. Incremental distensibility of normal and "arterialized" veins at different pressure levels.

In both cases, besides reduction in elastic modulus, a substantial decrease in tangential wall stress was found. It can be assumed that wall thickening of the vessels was induced initially by the abnormally elevated tangential stress elicited by hypertension and/or by weakened smooth muscle tone. The consequent change in wall thickness tended to maintain vascular distensibility and some other rheologically important properties close to the normal level.

It is concluded from the foregoing observations that apart from the caliber, the elastic properties of the arteries, e.g. distensibility and impedance, might also represent controlled variables of short-term and long-term regulatory mechanisms. Thus, it would be more apropriate to use the term "impedance vessel" instead of "Windkessel artery". It is hypothesized that the coordinated regulation of arterial mean pressure and the wave damping function of arteries might follow the rules of a forced oscillation type optimizing system.

Acknowledgement. This work was supported in part by Ministry of Health, Hungary, and by research grant NIN CDS-10939-6, USA. The fruitful discussions with Béla Szücs and Dr. Antal Hudetz are highly appreciated.

References

Cox, R.H.: Three-dimensional mechanics of arterial segments in vitro: methods. J. Appl. Physiol. 36:381-384, 1974.

Cox, R.H.: Arterial smooth muscle mechanics. In: "The Arterial System". eds. Bauer, R.D., Busse, R. pp. 63-79, Springer-Verlag, Berlin 1978.

Hudetz, A.G., Márk, G., Kovách, A.G.B., Monos, E.: The effect of smooth muscle activation on the mechanical properties of porcine carotid arteries. Acta physiol. Acad. Sci. hung., 1980. In Press.

Hudetz, A.G., Márk, G., Monos, E., Szutrély, J., Kovách, A.G.B.:Biomechanical properties of human cerebral arteries. In: Proc. Internat. U. Physiol. Sci., Vol. XIII., pp. 337, 1977.

Márk, G., Hudetz, A.G., Kerényi, T., Monos, E., Kovách, A.G.B.: Is the sclerotic vessel wall more rigid really than the normal one ? Prog. biochem. Pharmacol. 14:292-297, 1977.

Monos, E., Cox, R.H., Peterson, L.H.: Relationship between biomechanical factors and vascular reactions during activation by physiological doses of norepinephrine and vasopressin. Acta physiol. Acad. Sci. hung. 52:11-23, 1978a.

Monos, E., Cox, R.H., Peterson, L.H.: Direct effect of physiological doses of arginin-vasopressin on the arterial wall in vivo. Am. J. Physiol. 234:, H167-172, 1978b.

Monos, E., Csengődy, J.: Does hemodynamic adaptation take place in the vein grafted into an artery ? Pflügers Arch. 384:177-182, 1980.

Monos, E., Kovách, A.G.B.: Effect of acute ischemia on active and passive large deformation mechanics of canine carotid arteries. Acta physiol. Acad. Sci. hung. 54:23-31, 1979.

Monos, E., Kovách, A.G.B.: Biomechanical properties of splenic artery. Acta physiol. Acad. Sci. hung. 55:355-364, 1980.

Monos, E., Szücs, B.: Effect of changes in mean arterial pressure on the structure of short-term blood pressure waves. Automedica, 2:149-160, 1978.

Szücs, B., Monos, E.: Modelling of circulatory control system. In: Modern Trends in Cybernetics and Systems, eds. Rose, J., Bilciu, C., pp. 953-962, Vol. 3. Springer-Verlag, Berlin 1977.

Adv. Physiol. Sci. Vol. 8. Cardiovascular Physiology. Heart, Peripheral Circulation and Methodology
A. G. B. Kovách, E. Monos, G. Rubányi (eds)

ARTERIAL ELASTICITY AND TOTAL AND RELATIVE PROPORTION OF WALL CONSTITUENTS ARE INFLUENCED BY SYMPATHETIC NERVE TRAFFIC*

Rosemary D. Bevan and Hiromichi Tsuru**
Department of Pharmacology, UCLA School of Medicine, Center for the Health Sciences, Los Angeles, California 90024, USA

INTRODUCTION

It is recognized that the motor innervation of voluntary muscle is essential for maturation of skeletal muscle fibers, and in addition to initiating contraction, regulates many intracellular processes and membrane properties (Gutmann, 1977). Sympathetic nerves are the major regulators of neurogenic tone in vascular smooth muscle (VSM). Whether the sympathetic nervous system plays a role in influencing vascular wall maturation and cell characteristics has not been as well studied apart from the well recognized influence on cell sensitivity to agonists (Fleming, 1978). It has been shown that sympathetic nerves influence maintenance of mature smooth muscle characteristics in culture (Chamley and Campbell, 1976).

We have previously observed that sympathetic denervation impairs DNA synthesis in VSM of the ear artery of the growing male New Zealand rabbit (Bevan, 1975) and have now examined the effect of long-term denervation on the structure and function of this ear artery at 3 different ages, growing (3-4 weeks), young adult (10 weeks), and mature (over 4 months). Some of the studies have been previously reported (Bevan, 1979a, b; 1980).

METHOD

Only sympathetic nerves have been identified as efferent to this artery. Neurogenic contraction was prevented by superior cervical ganglionectomy or section of the preganglionic nerve fibers 'decentralization' (Bevan, 1979a). In the former method the axon terminals in the artery wall rapidly degenerate, but in the latter the postsynaptic adrenergic terminals remain in a normal distribution at the adventitio-medial junction.

Arteries from each age group were studied *in vitro* 8 weeks following surgery and compared with the control contralateral ear artery. Identical lengths from corresponding areas of vessel were dissected and sectioned *in situ* using blades of fixed standard distance. Denervation was confirmed by the absence of specific catecholamine fluorescence (Lindvall and

*Supported by USPHS Grant HL 20581

**Present address: Department of Pharmacology
Nagoya University School of Medicine
Tsuruma, Showa-ku
Nagoya 466, Japan

Bjorklund, 1974) on whole mounts of the most proximal and distal segments of vessel used, and decentralization confirmed by absence of choline acetyltransferase activity in the superior cervical ganglia (Fonnum, 1975). From each artery a ring segment was processed for light microscopy and measurement of medial cross sectional area and VSM cell counts from transverse sections. Two 3 mm ring segments were used for in vitro studies and set up in organ baths in a standard manner (Bevan, 1979a) to measure: (a) contractile responses to norepinephrine; (b) stress-strain relationships.

Stress-Strain Relationships

A 3 mm ring segment was stretched in steps of 50 microns every 5 - 10 minutes by turning a fine screw adjustment attached to a force displacement transducer. The distance between the outer edges of the wires suspending the segment was determined at each equilibrium level through the tissue bath wall, using a microscope with 10 x micrometer eyepiece. This was regarded as half internal circumference. Wall stress was expressed as passive stress (dynes/cross-sectional area cm^2), for each experimental length. Tangential moduli of elasticity (Bevan et al., 1964) were calculated at the half internal circumference at which wall stress was equivalent to that calculated to result from a blood pressure of 80 mm Hg in the control artery (Birmingham, 1970).

Statistical Analysis

Paired observations in the control and denervated ear arteries in each age group were compared using the paired t-test. Differences between the different age groups were analyzed by means of the unpaired t-test (Dixon and Massey, 1957). A statistical inference of significance was made when $P < 0.05$.

RESULTS

The mean body weights of rabbits from each age group, whether the ear artery was denervated or decentralized were similar at surgery and eight weeks later. The growing, young adult, and mature groups increased in weight about 6, 1.4 and 1.05 times respectively. Approximately 8 - 10 rabbits were in each of the 6 groups. For a more detailed account of methods, results and statistical analysis see Bevan (1979a, b; 1980).

Tissue weights: When the data from individual rabbits were paired for comparison, weights of 3 mm ring segments were significantly less at all ages in all groups of animals whether denervated or decentralized (Table 1).

Table 1. Mean Percentage Reduction in Tissue Weight

	Growing	Young Adult	Mature
Denervated	89.1 ± 3.04	87.5 ± 3.0	84.1 ± 2.51
Significance	$p < 0.005$	$p < 0.005$	$p < 0.005$
Decentralized	85.3 ± 3.2	93.8 ± 2.56	95.26 ± 1.91
Significance	$p < 0.001$	$p < 0.025$	$p < 0.025$

Dimensions: The cross-sectional area of the muscle layer in both denervated and decentralized ear arteries was significantly less than controls in growing and young adult rabbits only, being most marked at the

younger age (Table 2). This age relationship was also apparent in cell counts of VSM cells in transverse sections. In the denervated ears of growing, young adult and mature groups, cell counts expressed as a percentage of control values were 82.7, 93 and 105 percent respectively.

Table 2. Percentage Reduction in Cross-Sectional Area of Artery Media 8 Weeks after Denervation or Decentralization

	Growing	Young Adult	Mature
Denervated	72.8 ± 5.48	86.63 ± 4.1	95.1 ± 5.38
Significance	$p < 0.005$	$p < 0.005$	not significant
Decentralized	69 ± 3.39	81.6 ± 3.85	94.3 ± 5.18
Significance	$p < 0.0005$	$p < 0.002$	not significant

Maximum developed force: Chronic loss of neurogenic stimulation by either denervation or decentralization resulted in a decreased maximum force development to norepinephrine ranging from 70 - 80 percent of control values. These differences became less when corrected for cross-sectional area except in the youngest group.

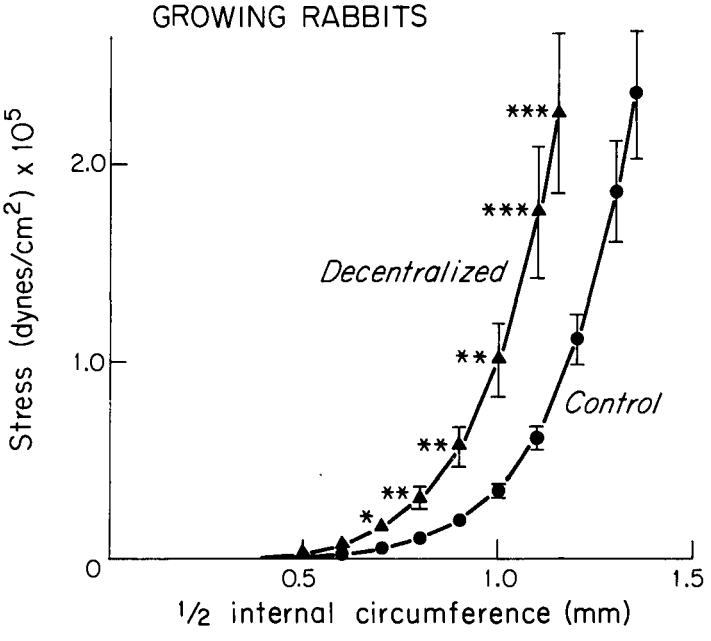

Fig. 1. Passive stress-strain curves of paired innervated and decentralized ear artery segments from growing rabbit group. Vertical bars refer to standard error of mean. Asterisks refer to significant p values of comparisons between denervated and innervated groups using paired t-test.

Stress-strain relationships: When neurogenic stimulation of the ear arteries had been absent for 8 weeks in the growing and young adult groups the stress-strain curves of ring segments of ear artery *in vitro* were significantly shifted to the left of controls (Fig. 1) indicating that the artery was stiffer. This was true also in the denervated mature group but not the decentralized.

The tangential modulus of elasticity was calculated from the curve in each denervated group at the circumference corresponding to a blood pressure of 80 mm Hg *in vivo* (Table 3). There was a tendency for the difference in the elastic modulus to be greatest in the youngest group.

Table 3. Denervated Rabbit Ear Artery
Tangential Modulus of Elasticity [Et] X 10^4 dynes/cm^2

Growing Rabbits		Young Adult Rabbits		Mature Rabbits	
Control	Denervated	Control	Denervated	Control	Denervated
5.28±0.28	10.96±0.99	5.35±0.14	8.94±0.24	5.32±0.23	7.99±1.22
$P < 0.001$		$P < 0.001$		$P < 0.05$	

In the growing group of rabbits the percentage reduction from control values of the structural and functional parameters tested in denervated ear arteries are summarized in Fig. 2.

DISCUSSION

Decentralization or denervation of the smooth muscle of the rabbit ear artery resulted in similar age-related structural and functional differences from control vessels. These changes suggest that nerve impulses influence the development and maintenance of the artery wall characteristics and the presence of the nerve terminals in the absence of nerve impulses does not modify the changes in cell parameters described. The effect of loss of neurogenic tone may be likened to the 'disuse' atrophy of voluntary muscle, although much less pronounced, possibly because the artery wall is subject to continuous rhythmic stretch. Leung et al. (1978) have shown that cyclical stretching and relaxation of aortic VSM cells in the culture on elastic membranes induces increased rates of synthesis of protein and extracellular material and a change in cell morphology compared to control unstretched cells. Postdenervation atrophy of voluntary muscle may also be overcomed by passive stretch (Tobary, 1972). In addition the arterial VSM is influenced by circulating vasoactive substances which may counteract the denervation effect.

Medial cross-sectional area and VSM cell number in the denervated ear artery was most reduced in comparison to control values in the artery deprived of sympathetic control from 4 weeks of age whereas after the rabbit was mature these parameters did not differ significantly from the control values. The young adult group values were in between. Postnatal proliferation of VSM in the normal ear artery is age related, being most pronounced in the first few weeks and then declining, so that in the normal mature animal in larger and medium sized arteries the population is relatively stable. Consequently if the sympathetic nervous system regulates the cell cycle it would be most apparent during growth. Our results showing a smaller number of VSM cells in the denervated growing ear artery are in agreement with this concept and a prior observation that less cells were seen in the DNA synthesis phase (Bevan, 1975). It is possible that denervated arteries retract less than controls so that

the difference in medial cross-sectional area and cell number is an artifact. However, the segments of identical in situ lengths weighed significantly less than controls at all ages (Bevan, 1980). Maximum contractile force was also significantly diminished following loss of nerve impulses at all age periods and although this could be accounted for by fewer cells during growth, in the mature animal it may represent a change in the contractile mechanism.

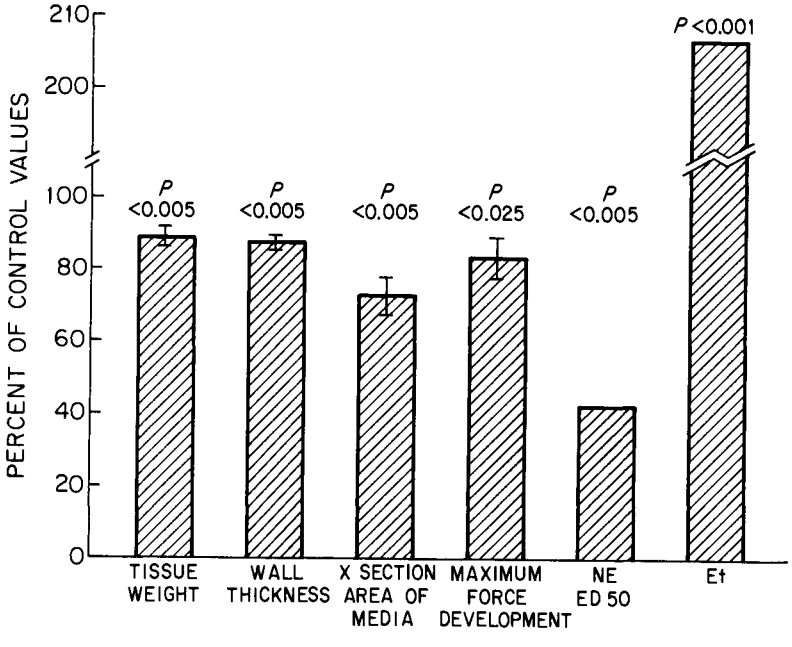

Fig. 2. Parameters of isolated ring segments of ear arteries from rabbits denervated at 4 weeks of age and examined 8 weeks later, expressed as a percentage of their innervated controls. NE ED_{50} refers to concentration of norepinephrine required to produce 50% of maximum contraction in the presence of propranolol (3×10^{-7}M), desmethylimipramine (3×10^{-7}M) and hydrocortisone (8.7×10^{-6}M). Et refers to tangential modulus of elasticity at internal circumference equivalent to 80 mm Hg. Vertical bars refer to standard error of mean (n = 8). p refers to comparisons between denervated and innervated vessels using paired t-test.

Stress-strain curves indicate that in the chronic absence of nerve impulses the vessel wall is stiffer, that is, less distensible. The difference in the tangential modulus of elasticity being greatest in the growing animals and just significant in the mature denervated but not the mature decentralized group. The exact age of the 2 different groups of mature animals is not known. Collagen synthesis has been shown to decrease with increasing age (Newman and Langer, 1975) and become increasingly stable due

to cross-linkage. Changes in passive mechanical properties of arteries are thought to be largely due to the collagen and elastin content (Roach and Burton, 1957), which may be increased in the denervated vessels. It is possible that the cellular processing of collagen is shifted towards the formation of a more stable cross-linked collagen as occurs in aging after denervation. An alternative explanation is that in the absence of neurogenic tone the vessel is dilated and therefore would be exposed to an increased wall tension which might induce an increase in extracellular components.

These results indicate that lack of nerve activity results in complex changes in VSM metabolism affecting growth regulation, synthesis of extracellular material and contractile properties of the smooth muscle. Nonspecific hypersensitivity of the cells to agonists are described elsewhere (Bevan, 1980). They are consistent with a change in cell membrane properties and are in agreement with those reported by Fleming (1979). The structural changes are age dependent.

REFERENCES

1. BEVAN, J.A., R.C. JOHNSON and M.A. VERITY (1964): Changes in elasticity of pulmonary reflexogenic area with sympathetic activity. Am. J. Physiol. 206:36-42.

2. BEVAN, R.D. (1975): Effect of sympathetic denervation on smooth muscle cell proliferation in the growing rabbit ear artery. Circ. Res. 37:14-19.

3a. BEVAN, R.D. and H. TSURU (1979): The trophic effect of the sympathetic neuron on the artery wall in growing rabbits. IN: Catecholamines: Basic and Clinical Frontiers, Vol. 1, pp. 465-467, edited by E. Usdin, I.J. Kopin and J. Barchas, Pergamon Press, New York.

3b. BEVAN, R.D. and H. TSURU (1979): Long-term denervation of vascular smooth muscle causes not only functional but structural change.

4. BEVAN, R.D. and H. TSURU (1980): Functional and structural changes in the rabbit ear artery following sympathetic denervation. Circ. Res. in press.

5. BIRMINGHAM, A.T. (1970): Sympathetic denervation of the smooth muscle of the vas deferens. J. Physiol. (Lond.) 206:645-661.

6. CHAMLEY, J.H. and G.R. CAMPBELL (1976): Tissue culture: interaction between sympathetic nerves and vascular smooth muscle. Proc. 2nd Intl. Symp. Vascular Neuroeffector Mechanisms, pp. 10-18, Karger, Basel.

7. DIXON, W.J. and F.J. MASSEY, JR. (1969): Introduction to Statistical Analysis, 3rd Edition, McGraw-Hill, New York.

8. FLEMING, W.W. (1978): The trophic influence of autonomic nerves on electrical properties of the cell membrane in smooth muscle. Life Sci. 22:1223-1228.

9. FONNUM, F. (1975): The rapid radiochemical method for the determination of choline acetyltransferase. J. Neurochem. 24:407-409.

10. GUTMANN, E. (1977): Trophic effects in nerve muscle cell relations. IN: Synapses, pp. 291-318, edited by G.A. Cottrell and N.R, Usherwood, Blackie, Glasgow.

11. LEUNG, D.Y.M., S. GLAGOV, J.M. CLARK and M.B. MATHEWS (1977): Mechanical influences on the biosynthesis of extracellular macromolecules by aortic cells. Exp. Cell Res. 285:285-298.

12. LINDVALL, O. and A. BJÖRKLUND (1974): The glyoxylic acid fluorescence histochemical method. A detailed account of the methodology for the visualization of central catecholamine neurons. Histochemistry 39: 97-127.

13. NEWMAN, R.A. and R.O. LANGER (1975): Age related changes in the synthesis of connective tissues in the rabbit. Conn. Tiss. Res. 3:231-236.

14. ROACH, M.R. and A.C. BURTON (1957): The reason for the shape of the distensibility curves of arteries. Can. J. Biochem. Physiol. 35:681-690.

15. TABARY, J.C., C. TABARY, C. TARDIEU, G. TARDIEU and G. GOLDSPINK (1972): Physiological and structural changes in the cat's soleus muscle due to immobilization of different lengths by plaster casts. J. Physiol. (Lond.) 224:231-244.

Adv. Physiol. Sci. Vol. 8. Cardiovascular Physiology. Heart, Peripheral Circulation and Methodology
A. G. B. Kovách, E. Monos, G. Rubányi (eds)

RELATIVE VOLUMES OF STRUCTURAL COMPONENTS IN VENTRAL INTERVENTRICULAR BRANCH (VIB) OF THE LEFT CORONARY ARTERY IN DOGS — FUNCTIONAL INTERPRETATION

V. Levický and M. Gerová

Institute of Normal and Pathological Physiology, Centre of Physiological Sciences SAS, Bratislava, Czechoslovakia

Major coronary arteries are the site, where spasms of smooth muscular elements have been clinically described(Feigl 1967, Rose et al. 1974, Cheng et al. 1972). Despite a relatively deep functional knowledge of the coronary vascular bed, the conditions of this phenomenon have not as yet been satisfactorily explained. A study of spasm provoking factors has shown that sympathetic stimulation produces only minor changes of VIB diameter. As has been demonstrated by Gerová et al. (1979), bilateral sympathetic stimulation of fibers originating in the stellate ganglion decreased the diameter by 4% only. This observation has toned down the assumptions according to which, the sympathetic nerve system innervating the coronary vascular bed, is the main factor of coronary artery closing in cases, when histo-pathological changes in the VIB wall could not be proved. Microscopical examinations have revealed the VIB structure to be different from other arteries (Boucek et al. 1963). Data of previous morphological descriptions and functional observations inadequate to explain the above phenomenon.

The present study deals with the relationship between the geometry of this blood vessel and its function, as well as with some structural components of the VIB wall from the aspect of their quantitative representation.

MATERIAL AND METHODS

Five mongrel dogs of both sexes (10.0-15.0 kg) were used. Immediately after each animal had been sacrificed by electroshock the heart was removed and a glass cannula connected (by a rubber tubing) to a buffer or a fixation medium reservoir was inserted into the ostium of the left coronary artery. The vascular bed was then perfused for 2 minutes with a phosphate buffer followed by 20 minutes perfusion fixation with Karnovsky solution (paraformaldehyde and glutaraldehyde solution in the phosphate buffer) at intravital blood pressure (120 mm Hg). The temperature of both solutions was 37 ^{o}C C.

After dissecting out the investigated blocks from parts of the VIB were postfixed with the same fixative and with 1% osmium tetroxide in the phosphate buffer solution. After fixation had been completed, the tissue blocks were washed in distilled water, dehydrated with acetone and embedded in Durcupan ACM for sectioning. The ultrathin (for electronmicroscopical examination) and semithin (for lightmicroscopical examination) sections were cut with a Tesla BS 490A ultramicrotome. The ultrathin sections were stained with uranylacetate and lead citrate and examined in a Tesla BS 500 electron microscope; the semithin sections were mounted on glass slides and stained with Weigert's resorcin fuchsin (staining for elastic tissue) and with Weigert's hematoxilin (staining for muscle cells nuclei).

The following sites of the VIB were dissected out:

I. the origin of the artery (just under the origin of the circumflex artery),
II. the middle part of the artery (25 mm from the preceding site),
III. the terminal part of the VIB (in the apex cordis region, at a distance of 30 mm from the site under II.),
IV. the branch of the VIB arising just under the site II.

The point -counting method (Haug 1962, Weibel et al.1966) was used to determine the volumes of both the elastic tissue and smooth muscle cells. The histological section of the arterial wall was observed by means of a test grid (an eyepiece micrometer) inserted in the eyepiece of the microscope. The total magnification was 1250.

First, the relative volumes of the elastic tissue and nuclei of smooth muscle cells in the arterial wall were determined. The volume of total smooth muscle was calculated from the volume of nuclei of smooth muscle cells. This procedure was adopted because the method used requires a precise delimitation of the evaluated structures, and this cannot be achieved through the simultaneous staining of elastic tissue and smooth muscle cells. Since the volume of smooth muscle cell is a 14.5 multiple of that of its nucleus, as was established in a previous study (Levický 1976, Levický Doležal 1980), the actual volume of smooth muscle cells was calculated by multiplying the nuclear volume by this coefficient.

Using an eyepiece micrometer, we determined also the internal and external vascular diameters and the ralion between thickness/external diameter.

RESULTS

Geometry of VIB

A low power light microscopical magnification reveals the VIB along its course as a thin walled blood vessel (Figs. 1, 2 and 3).

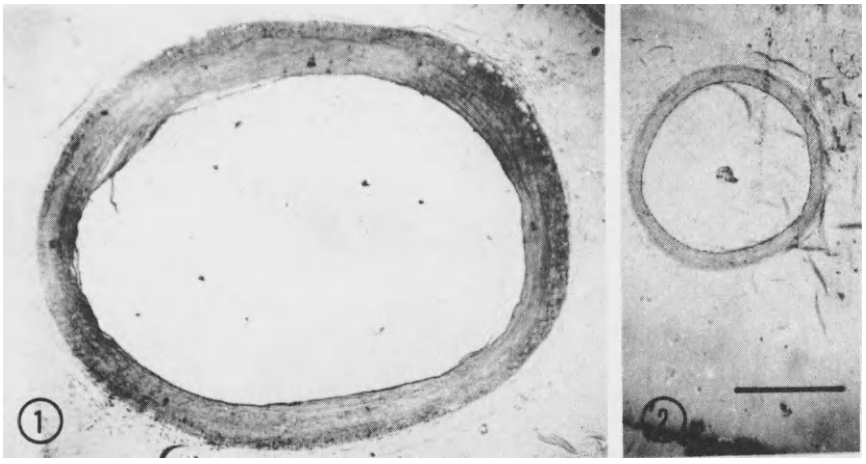

Figs. 1 and 2. Low power micrographs of ventral interventricular branch (VIB) of left coronary artery at two places of examination showing decrease of arterial caliber from proximal (VIB I., Fig. 1) to distal (VIB II., Fig. 2) parts of artery. In situ fixation, cross section. Bar indicates 0.5 mm.

At its origin the mean external diameter (Dext) measures 2.13 mm and the internal diameter (Dint) 1.72 mm (Fig. 4) The vascular wall thickness (Wth) calculated from these values is 0.22 mm. The values of all these parameters gradually decrease towards the perifery of the VIB, the lowest being at the site of VIB IV. - Dext = 0.71 mm, Dint = 0.63 mm and Wth = 0.04 mm. The values of the ratio vascular wall thickness external diameter shows the initial value 1/12.08 to decrease proportionally as the artery calibre decrease; finally it attains the value of 1/18.38 in VIB IV., thus giving an evidence that the vascular wall becomes relatively thinner towards the perifery.

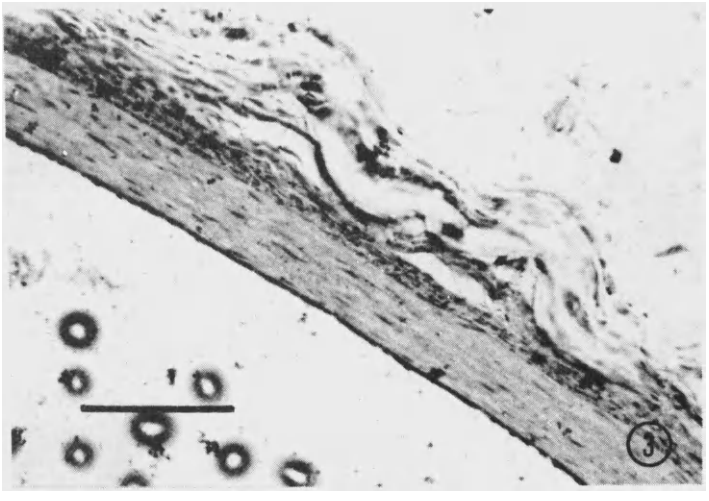

Fig. 3 Micrograph of VIB II. Note the thinness of arterial wall. In situ fixation, cross section. Bar indicates 0.1 mm.

Structure of VIB

The ventral interventricular branch, originating as a continuation of the left coronary artery, has all the three layers clearly differentiated at its beginning: tunica adventitia, tunica media and tunica intima. The artery is mostly located directly below the epicardium. In some cases, tunica adventitia loses its contours, becomes indistinct on the abluminal side, at sites adhering to the epicardium it becomes thinner, and its collagen fibrils intermingling with the subepicardial layer. The adventitia of the VIB is all along its course formed by tightly organized fibers of collagen fibrils and delicate fibers of elastic tissue (Fig. 5). Nerve endings, probably adrenergic, can also be found between these structures. Vasa vasorum are irregularly dispersed in the adventitia of the proximal part of the VIB.

The media at the beginning of the VIB is made up of 16 - 18 layers of smooth muscle cells. As the diameter of the VIB decreases, the number of smooth muscle cells also decreases: VIB III. and VIB IV. have only 4 - 6 layers of cells. The elastic tissue in the media of the VIB is sparse, but collagen fibers are abundant.

The intima consists of the endothelium, the subendothelial layer of collagen fibrils and a well formed internal elastic lamina.

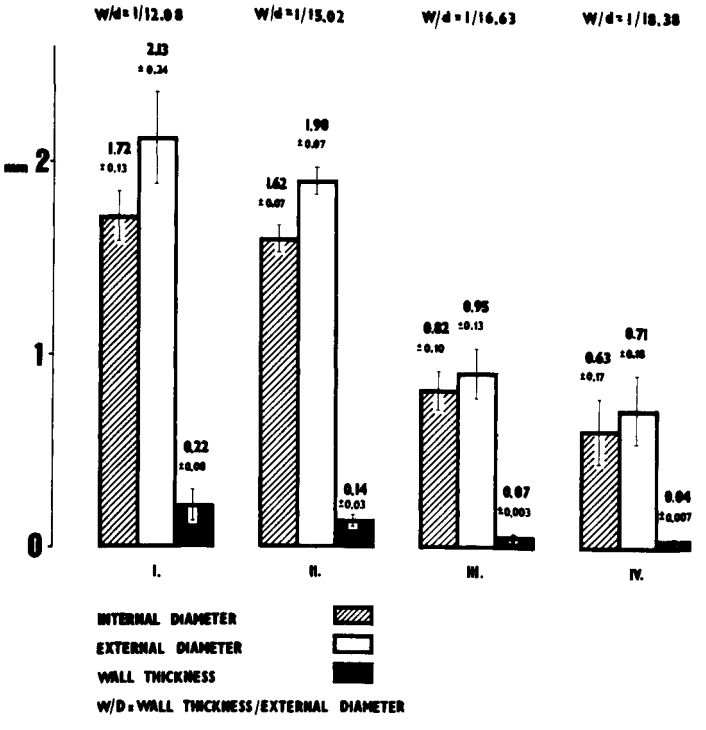

Fig. 4 Geometry of ventral interventricular branch (VIB) wall. I.-IV. are sites of examination.

The relative volumes

Elastic tissue

The quantitative proportions of two important components of the vascular wall - elastic tissue and smooth muscle - are showned in Fig. 6. The relative volume of elastic tissue at the beginning of the VIB represents 5.97 %. At other sites of the vascular bed this volume was found to change insignificantly only. VIB II. contains 5.45 %, VIB III. 5.02 % and VIB IV. 4.70 % of elastic tissue.

Smooth muscle

The volume of smooth muscle cell nuclei from which the total smooth muscle volume was calculated, represents at the origin of the VIB 3.23 % of the relative volume. After multiplication by the coefficient 14.5 this corresponds to 47.1 volume percent (for mode of calculation, see Material and Methods). The corresponding values at the other sites of

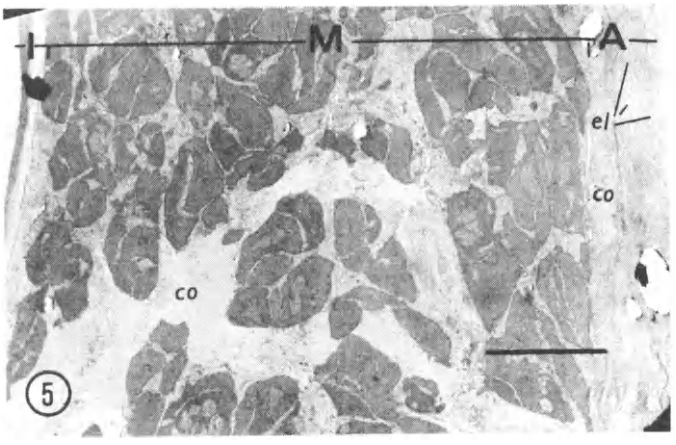

Fig. 5 Electron micrograph of VIB II. wall showing cross sectioned intima (I), media (M) and adventitia (A). Collagen fibrils (co) and elastic fibers (el) can be seen in adventitia and media. Internal elastic membrane (iem) is well formed. In situ fixation. Bar indicates 20 μm.

exstirpation are: VIB II. - 3.44 % and 49.9 %, VIB III. - 4.57 % and 66.4 %, VIB IV. - 5.81 and 84.2 %. A significant increase ($P < 0.05$) may be seen between VIB I. and VIB III., and between VIB I. and VIB IV.

DISCUSSION

This study is designed to describe the VIB from three aspects: its geometry, structure and relative amounts of its structural components.

Geometry of the vesel is characterised by the conspicious thinness of its wall, which is evident not only from the results of measurements (Fig. 3), but also from direct visual observation. With a decrease of intravascular pressure, the vessel wall becomes very slender and gives the impression of a vein. At a zero intravascular pressure, the vessel closes completely. The wall thinness of the VIB clearly stands out when the latter it is compared with other arteries of matched diameter (Tab. 1), e.g. the common carotid artery and dorsal pedal artery. The ratio of vascular wall thickness to external diameter differenciates this artery from blood vessels of a similar calibre, e.g. common carotid artery and dorsal pedal artery. A comparison with dorsal pedal artery in particular (Fig. 7) very clearly illustrates the VIB wall thinness. This thinness is caused principally by a reduction of the number of

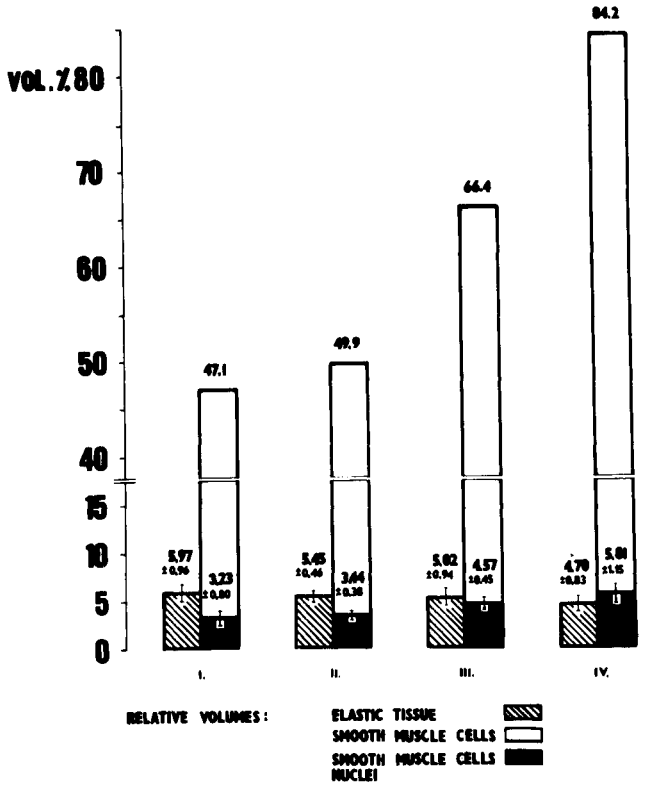

Fig. 6 Relative volumes of ventral interventricular branch (VIB) wall components. I.-IV.are sites of examination.

smooth muscle cell layers in the media of the VIB in comparison with the dorsal pedal artery (16 - 18 layers of smooth muscle cells in the VIB at its origin and 28 - 30 layers in the dorsal pedal artery). A characteristic trait of this thinness is that this ratio (Wth/Dext) does not rise with a decline of the diameter, as is the case with other arteries. On the contrary, this ratio decreased from 1/12.08 in VIB I. to 1/18.38 in VIB IV.

In judging of the structure of vascular walls it should be underlined that there is question here of the first-order branch of the aorta branching off it at the very origin. Hence, it is rather surprising that this artery has the appearance neither of one of an elastic type with an abundance of elastic lamellae in the media, nor of a large artery of the muscular type in which the elastic tissue is concentrated in the adventitia in the form of thick fibers. The only distinct elastic structure in the VIB wall is the internal elastic membrane

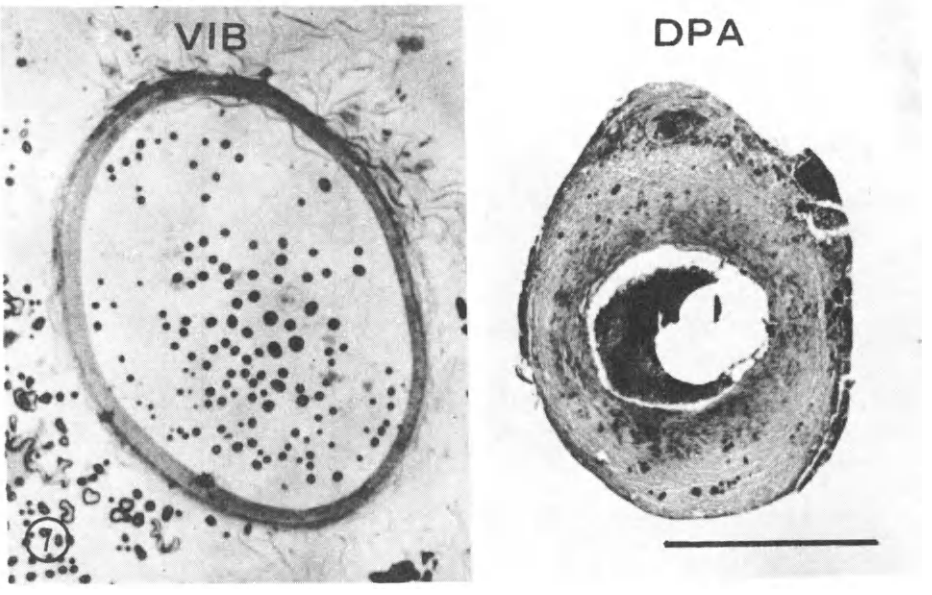

Fig. 7 Micrograph of VIB I. and dorsal pedal artery (DPA). The arteries have the same external diameter, but the wall of DPA is approximately two times thicker. Cross sections. Bar indicates 1 mm.

while an external elastic membrane is lacking. This feature is found in no other artery of a similar diameter. The smooth muscle fibers reveal generally a helical arrangement. Bundles of smooth muscle cells may be observed at the adventitia-media interface, which then pass on into the inner parts of the media and then assume a spiral course. This feature was described by Boucek et al. (1963).

The results of the present study on the relative volumes of the VIB components make it clear that the VIB wall throughout its entire length is made up of approximately an equal volume of elastic tissue (its values vary nonsignificantly around 5 volume percent). This share of elastic tissue is rather surprising, especially if we consider that the VIB is the first aortal branch in which the content of the elastic tissue is very high (22 volume percent). In no other artery branching off the aorta or whose diameter is close to that of the VIB do we find such low values (Tab. 2). Even typical arteries of the muscle type, such as the dorsal pedal artery, contain far higher values.

Tab. 1 Geometry of VIB II. and some other arteries.

ARTERY	N	D_e ± SEM	D_i ± SEM	W_{th} ± SEM	W_{th}:D_e
Ascend. aorta	6	12.92 ±1.10	10.95 ±1.57	0.990 ±0.032	1:14.0
Comm.carot. art.	5	2.25 ±0.31	1.86 ±0.33	0.19 ±0.13	1:11.8
VIB II.	4	1.90 ±0.066	1.62 ±0.067	0.14 ±0.03	1:15.0
Dors. pedal art.	2	1.36	0.88	0.24	1:5.7

Tab. 2 Relative volumes of elastic tissue and smooth muscle in VIB II. and in some other arteries.

ARTERY	N	ELAST. TISSUE vol. % ±SEM	SMOOTH MUSCLE NUCLEI vol. % ±SEM	SMOOTH MUSCLE CELLS vol. %
Ascend. aorta	6	21.82 ±1.96	3.45 ±0.52	50.07
Comm.carot. art.	5	15.49 ±0.48	3.63 ±0.38	52.72
VIB II.	4	5.45 ±0.46	3.44 ±0.38	49.90
Dors. pedal art.	10	7.92 ±2.51	3.76 ±0.72	54.52

As regards the spasms of coronary arteries, a plausible explanation seems to be that the principal role is here played by a deficiency of elastic skeleton of the vascular wall that would be capable of keeping the vascular lumen open in situations of a sudden decrease of wall tension, e.g. in consequence of an abrupt drop in the intraluminal pressure. In such a situation even the smooth muscle of the vascular wall may become contracted.

REFERENCES

Boucek R. J., Takashita R., Fojaco R.: Relation between microanatomy and functional properties of the coronary arteries. Anatom. Rec. 1963; 147: 199-207.

Cheng T. O., Bashour T., Singh B. K., Kelser G. A.: Myocardial infarction in the absence of coronary arteriosclerosis - result of coronary spasm ? Amer. J. Cardiol. 1972; 30: 680-689.

Feigl E. O.: Sympathetic control of coronary circulation. Circ. Res. 1967; 20: 262-271.

Haug H.: Bedeutung und Grenzen der quantitativen Messmethoden in der Histologie. In: Medizinische Grundlagenforschung 4: 299-344, edited by K. Fr. Bauer. Georg Thieme Verlag, Stuttgart, 1962.

Gerová M., Barta E., Gero J.: Sympathetic Control of Major Coronary Artery Diameter in the Dog. Circ. Res. 1979; 44: 459-467.

Levický V.: The volumes of elastic tissue and smooth muscle cells in the arterial wall. Proceedings of the Fourth International Congress for Stereology. Natl. Bureau of Stand. Spec. Publ. No. 431: 337-340. Gaithersburg 1976, Md., U.S.A.

Levický V., Doležal S.: Volume of elastic tissue and smooth muscle in elastic and muscular type arteries in the Dog. Physiol. bohemoslov. 1980 /in press/.

Rose F. J., Johnson A. D., Carleton R. A.: Spasm of the left anterior descending coronary artery. Chest 1974; 66: 719-721.

Weibel E. R., Kistler G. S., Scherle W. F.: Practical stereologic methods for morphometric cytology. J. Cell Biol. 1966; 30: 23-38.

Adv. Physiol. Sci. Vol. 8. Cardiovascular Physiology. Heart, Peripheral Circulation and Methodology
A. G. B. Kovách, E. Monos, G. Rubányi (eds)

ELASTIC PROPERTIES OF CORONARY ARTERIES IN CONSCIOUS DOGS

M. Pagani, A. Pasipoularides and S. F. Vatner

Departments of Medicine, Harvard Medical School and Peter Bent Brigham Hospital, Boston, MA and the New England Regional Primate Research Center, Southboro, MA 01772, USA and Istituto di Ricerche Cardiovascolari, G. Sisini, and CNR, Università di Milano, Italy

Knowledge of the elastic properties of coronary arterial walls is necessary for better understanding of the control of the coronary circulation. Moreover, changes in smooth muscle tone must also be considered (Gow, 1980). This is important both because coronary arterial walls contain a relatively large amount of smooth muscle, and also because the smooth muscle is thought to play a major role in alpha-adrenergic control of the coronary bed (Feigl, 1967; Holtz, et. al., 1977; Kelley and Feigl, 1978; Mudge, et. al., 1976; Schwartz and Stone, 1977; Vatner, et. al., 1970; Vatner, et. al., 1974; Vatner and McRitchie, 1975).

While caliber changes of large coronary arteries have been estimated indirectly from measurements of pressure and flow (Feigl, 1967; Holtz, et. al., 1977; Kelley and Feigl, 1978; Mudge, et. al., 1976; Schwartz and Stone, 1977; Vatner, et. al., 1970; Vatner, et. al., 1974; Vatner and McRitchie, 1975), there are only few studies in which direct measurements of coronary caliber and elastic properties were obtained either in isolated vessels (Cox, 1978; Gow and Hadfield, 1979) or in the intact heart (Douglas and Greenfield, 1970; Gerova, et. al., 1979; Gow and Hadfield, 1979, Patel and Janicki, 1970; Vatner, et. al., 1980). Significant reductions in coronary arterial caliber from control were observed at constant or elevated pressure levels with sympathetic stimulation (Gerova, et. al., 1979; Vatner, et. al., 1980).

The goal of this report is to describe pressure-diameter, stiffness-stress and stiffness-radius relationships of the circumflex coronary artery in the conscious dog, in the absence of the complicating influences of anesthesia and recent surgery (Vatner and Braunwald, 1975), both in the control state and after smooth muscle activation with alpha-adrenergic stimulation. This was accomplished by direct and continuous measurements of aortic root pressure and of circumflex coronary artery diameter using a modified ultrasound technique, in chronically instrumented animals.

METHODS

Successful experiments were performed on eight mongrel dogs that had been previously instrumented using pentobarbital, Na (30 mg/kg i.v.) for anesthesia. Through a thoracotomy in the fifth left intercostal space a pair of miniature ultrasonic transducers was implanted on opposing surfaces of the left circumflex coronary artery 3-6 cm from its origin. When feasible (five dogs) an electromagnetic flow probe, and a hydraulic occluder, were placed on the circumflex coronary artery 1-3 cm distal to the ultrasound

crystals. A miniature pressure gauge (Konigsberg Instruments, Inc., Pasadena, CA) was implanted in the left ventricle through the apical dimple. A hydraulic occluder was placed around the proximal aorta.

Proximal coronary arterial pressure was obtained from measurements of aortic root pressure made with a Millar pressure transducer advanced to the left ventricle through a femoral artery and then withdrawn so as to lie in the aortic root near the coronary ostia. Left ventricular pressure was measured with the implanted Konigsberg transducer. Left circumflex coronary arterial external diameter was measured with an improved ultrasound dimension technique which was further modified to allow measurements of these small dimensions (Feigl, 1967; Patrick, et. al., 1974; Vatner, et. al., 1980).

All experimental data were recorded on a 14 channel analog tape recorder and played back on a strip chart recorder. Pressure-diameter plots were obtained with a storage oscilloscope (Tektronix 912), after appropriate correction of the time delay between the pressure and diameter waveforms was made using an analog delay circuit connected in series with the oscilloscope. Coronary wall thickness was calculated for any external diameter from the weight of a segment of known in situ length, assuming a wall density of 1.06 g/cm^3 (Dobrin and Rovick, 1969).

Experiments were performed 7-10 days after operation, when the animals had recovered fully from surgery. All measurements were taken in the conscious state, during quiet respiration. Measurements were taken continuously at control, during inflation of the implanted aortic balloon to raise arterial pressure, and during i.v. methoxamine infusion (50 µg/kg/min for 7-10 min) to maximally activate arterial smooth muscle.

An effective diastolic incremental elastic modulus (E_{inc}) for the coronary arterial wall was derived from measurements of external diameter and pressure. A stress (σ) equal to the difference between circumferential and radial stresses at midwall was calculated according to the formula: $\sigma = 2\ P_t(R_iR_o/R)^2/(R_o^2 - R_i^2)$, where P_t is the distending pressure, R_i and R_o are the inner and outer radii, respectively, and $R = (R_i + R_o)/2$ is the midwall radius. E_{inc} was quantified according to the formula: $E_{inc} = 0.75R\ d\sigma/dR$. After curve-fitting parameters were obtained for an exponential form $\sigma = Ae^{\beta R}$, the local slope ($d\sigma/dR$) at any σ level was determined as $d\sigma/dR = \beta\sigma$ (Pagani, et. al., 1979; Pagani, et. al., 1978; Vatner, et. al., 1980). Baseline characteristics and changes in the elastic behavior of the coronary artery wall associated with activation of its smooth muscle were assessed using data derived from the diastolic phase of the pressure-diameter loop, thus minimizing viscous influences.

Values reported are mean ± SEM, and significance of changes from control was assessed with the paired t-test (Armitage, 1974).

Table 1: Measured Hemodynamic and Calculated Elastic Properties of the Circumflex Coronary Artery of the Conscious Dog.

Mean aortic root pressure	Heart Rate	Mean left circumflex coronary artery			
		Diameter	Thickness	Stress	Effective Elastic modulus
mmHg	beats/min	mm	mm	dyne/cm^2 x 10^5	dyne/cm^2 x 10^6
91±1	84±5	3.23±0.08	0.52±0.4	3.22±0.32	1.72±0.32

RESULTS

The resting control hemodynamic data for the eight conscious dogs are presented in Table 1. Figure 1 shows representative waveforms for aortic

root pressure, circumflex coronary diameter and flow, and left ventricular pressure at control. Notice the similarity between the pressure and diameter waveforms, although the latter exhibits downward deflections at the end of diastole, coincident in time with atrial and isvolumic ventricular contraction. This period at the end of diastole as well as systole were excluded when evaluating the data for stress-radius, stiffness-stress and stiffness-radius analyses.

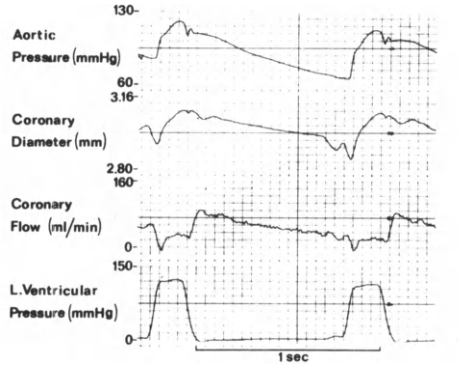

Figure 1: Representative phasic waveforms of aortic root pressure, left circumflex coronary artery diameter, blood flow, and left ventricular pressure in a conscious dog at rapid paper speed. (Reprinted with permission from the Journal of Clinical Investigation 65: 5-14, 1980).

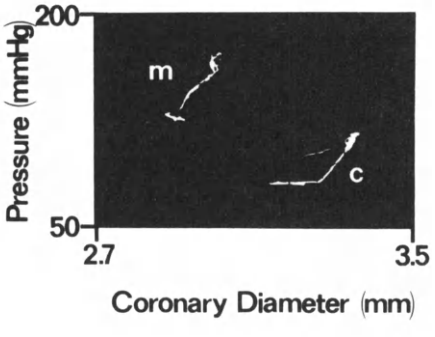

Figure 2: Pressure-diameter loops obtained in a conscious, chronically instrumented dog, after electronic correction for an ∿ 8 ms time-delay caused by the distance between the transducers. Note the dramatic shift, upward and to the left of the control (c) loop, that is induced by methoxamine (m), as well as concomitant near-elimination of the hysteresis loop area.

Figure 2 depicts the dynamic relationship between aortic root pressure and circumflex coronary artery diameter, after appropriate electronic correction of the time delay induced by the distance between the pressure and diameter transducers. Note the marked hysteresis, with pressure leading diameter that is present at control.

An important effect of methoxamine activation of smooth muscle is depicted in Figure 2. This shows a dramatic leftward shift of the pressure-diameter relationship, as well as the near-disappearance of the pronounced dysteresis loop, which is present at control.

An example of the effects of methoxamine is shown in Figure 3. Initially methoxamine i.v. increased both pressure and coronary diameter. However, at the end of the infusion (∿ 10 min) mean coronary diameter was reduced significantly below control, while mean arterial pressure had risen 65 ± 5% above control ($p<0.01$). When arterial pressure was raised mechanically by inflating the implanted aortic occluder for 10 minutes in absence of pharmacologic adrenergic stimulation, coronary arterial diameter increased and remained elevated throughout the intervention.

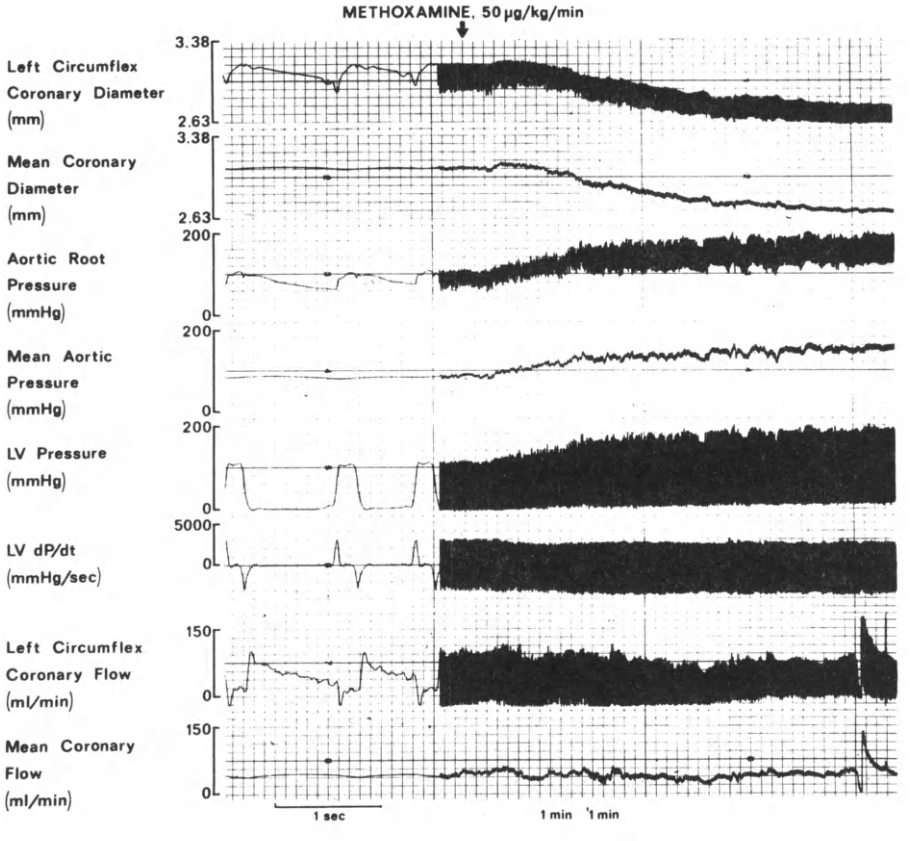

Figure 3: The effects of a 10 min. infusion of methoxamine, 50 µg/kg per min, in a conscious dog are shown on simultaneous measurements of phasic and mean left circumflex coronary artery diameter, aortic root pressure, left ventricular pressure, left ventricular dP/dt, and phasic and mean left circumflex coronary blood flow. (Reproduced with permission from the Journal of Clinical Investigation 65: 5-14, 1980.)

Figure 4 shows the effects of smooth muscle activation of the σ-midwall radius relationship. These relationships were all well described by the exponential curve fit $\sigma = Ae^{\beta R}$ ($r>0.94$). Alpha adrenergic stimulation by methoxamine induced a dramatic leftward shift of the σ-radius curve. At any common radius the level of stress was increased markedly above control.

Figure 5 shows E_{inc} plotted as a function of stress both at resting levels of smooth muscle tone and during the late response to methoxamine. Over the common stress range between 2.0 and 4.0 x 10^5 dyn/cm^2, E_{inc} was reduced significantly from baseline levels by smooth muscle activation.

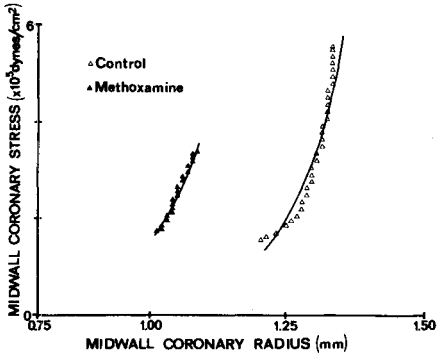

Figure 4: Midwall stress-radius relationships for the left circumflex coronary artery of conscious, chronically instrumented dogs are depicted with (▲) and without (△) methoxamine infusion. The stress employed here represents the difference between the circumferential and radial wall stresses at midwall. (Reproduced with permission from the Journal of Clinical Investigation 65:5-14, 1980).

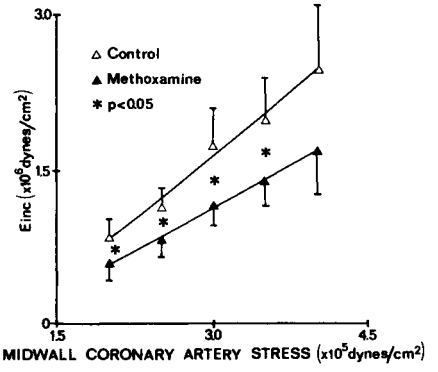

Figure 5: Mean (±SEM) values of E_{inc} plotted vs. midwall stress for the left circumflex coronary artery of conscious instrumented dogs. The significant ($p<0.05$) changes induced by methoxamine (▲) from control (△) are indicated by asterisks. Stress here denotes the difference between the circumferential and radial wall stresses at midwall. (Reproduced with permission from the Journal of Clinical Investigation 65:5-14, 1980).

DISCUSSION

The unique feature of this study of coronary arterial wall mechanics is that it was conducted in conscious animals, without the complicating influences of general anesthesia and recent surgery in acute animal studies. Moreover, vascular dimensions were measured instantaneously and continuously

using an ultrasonic dimension gauge. The ultrasonic dimension gauge used in this study was modified to provide measurements of small dimensions, such as those of the circumflex coronary artery of the dog, and to obtain calibrations in steps of 0.5 μ sec, i.e. 0.75 mm.

From pressure and diameter measurements the effective diastolic elastic properties of the circumflex coronary artery were assessed. The isotropic E_{inc} concept provides a practical means of quantifying vascular wall stiffness around any operating large deformation level along the highly nonlinear load-response curve (Fig. 4). In many physiologic studies, vascular compliance is quantified in terms of an incremental modulus of volume distensibility, defined $C_V \simeq (\Delta V/\Delta P_t) \times (1/V)$. Although E_{inc} pertains to the stiffness of the vascular segment as a hollow distensible structure, the two indices can be related quite readily according to the following formula: $C_V = (0.75/E_{inc}) \times (2R_i/R_o - R_i)$ (Vatner, et. al., 1980).

In this investigation, under baseline conditions of smooth muscle tone, the effective diastolic incremental modulus of the left circumflex coronary artery wall was $1.7 \pm 0.4 \times 10^6$ dyn/cm^2 at a stress of $\sim 3 \times 10^5$ dyn/cm^2 (Fig. 5). Allowing for an inner diameter to wall thickness ratio of $\sim$ 8-10, this E_{inc} estimate is slightly lower than that implied by the modulus of volume distensibility reported by Patel and Janicki (1970), which in turn is lower than the C_V values reported by Douglas and Greenfield (1970). Our representative E_{inc} is an order of magnitude lower than the E_{inc} reported by Cox (1978). The differences in these stiffness estimates may in part be attributed to differences in experimental design. For instance, the greatest disparities were found between our results and those of Cox (1978). Whereas our studies were conducted in intact, conscious animals, the data of Cox (1978) were obtained from isolated, in vitro vascular segments.

The elastic behavior of the left circumflex coronary artery of the conscious dog was altered by smooth muscle activation. Methoxamine induced a marked leftward shift in the pressure-diameter and stress radius relationships (Figs. 2 and 4). Thus, augmented alpha-adrenergic activation reduced vascular caliber for any given stress and pressure level. Moreover, smooth muscle activation raised the E_{inc} of the coronary arterial wall from control when the comparison was carried out at similar radii, but it reduced E_{inc} when the comparison was made at similar stress (Fig. 5) or pressure levels. Thus, for any given arterial pressure level, the effective incremental modulus of the wall of the left circumflex coronary artery can be reduced considerably by the enhanced smooth muscle activation elicited by methoxamine. The viscoelastic properties of the circumflex coronary artery were also likely to be modified by alpha-adrenergic mechanisms. In fact, the hysteresis in the pressure-diameter loop present at control was almost abolished during methoxamine infusion.

• In conclusion, we have examined the elastic properties of the circumflex coronary artery of the conscious dog at control and during alpha-adrenergic activation of smooth muscle. Alpha-adrenergic mechanisms were found to be powerful enough to reduce circumflex coronary radii and elastic wall moduli for any given pressure and stress levels. The working level of coronary arterial elasticity weems to be controlled by an alpha-adrenergic mechanism, capable of maintaining it constant in the face of a markedly increased pressure load.

REFERENCES

Armitage, P., 1974, Statistical Methods in Medical Research, Blackwell Scientific Press, London, p. 504.

Bergel, D.H., 1972, Cardiovascular Fluid Dynamics, Academic Press, New York.

Cox, R.H., 1978, Passive mechanics and connective tissue composition of canine arteries, Am. J. Physiol., 234: 4533-4541.

Dobrin, P.B. and Rovick, A.A., 1969, Influence of vascular smooth muscle on contractile mechanics and elastic of arteries, Am. J. Physiol., 217: 1644-1651.

Douglas, J.E. and Greenfield, J.C., 1970, Epicardial coronary artery compliance in the dog, Circ. Res., 27: 921-929.

Feigl, E.O., 1967, Sympathetic control of coronary circulation, Circ. Res., 20: 262-271.

Gerova, M., Barta, E. and Gero, J., 1979, Sympathetic control of major coronary artery diameter in the dog, Circ. Res., 44: 459-467.

Gow, B.S., 1980, Circulatory correlates vascular impedance, resistance and capacity, in: Handbook of Physiology, The Cardiovascular System, D.F. Bohr, A.P. Somlyo and H.V. Sparks, Jr., eds., American Physiology Society, Bethesda, MD.

Gow, B.S. and Hadfield, C.D., 1979, The elasticity of canine and human coronary arteries with reference to postmortem changes, Circ. Res., 45: 588-594.

Holtz, J., Mayer, E. and Bassenge, E., 1977, Demonstration of alpha-adrenergic coronary control in different layers of canine myocardium by regional myocardial sympathectomy, Pfluegels Arch. Em. Physiol., 372: 187-194.

Kelley, K.O. and Feigl, E.O., 1978, Segmental alpha-receptor-mediated vasoconstriction in the canine circulation, Circ. Res. 45: 908-917.

Mudge, G.H., Grossman, W., Mills, R.M., Lesch, M. and Braunwald, E., 1976, Reflex increase in coronary vascular resistance in patients with ischemic heart disease, N. Engl. J. Med., 295: 1333-1337.

Pagani, M., Schwartz, P.J., Bishop, V.S. and Malliani, A., 1975, Reflex sympathetic changes in aortic diastolic pressure-diameter relationship. Am. J. Physiol., 229: 286-290

Pagani, M., Vatner, S.F., Baig, H., Franklin, D.L., Patrick, T., Manders, W.T., Quinn, P. and Sherman, A., 1978, Measurement of multiple simultaneous small dimensions and study of arterial pressure-dimensions and study of arterial pressure, Am. J. Physiol.,4: H610-H617.

Pagani, M., Mirsky, I., Baig, H., Manders, W.T., Kerkhof, P. and Vatner, S.F., 1979, Effects of age on aortic pressure-diameter and elastic stiffness-stress relationships in unanesthetized sheep, Circ. Res., 44: 420-429.

Patel, D.J. and Janicki, J.S., 1970, Static elastic properties of the left coronary circumflex artery and the common carotid artery in dogs, Circ. Res., 27: 149-158.

Patrick, T.A., Vatner, S.F., Kemper, W.S. and Franklin, D., 1974, Telemetry of left ventricular diameter and pressure measurements from unrestrained animals, J. Appl. Physiol., 37: 276-281.

Schwartz, P.J. and Stone, H.L., 1977, Tonic influence of the sympathetic nervous system on myocardial reactive hyperemia and on coronary blood flow distribution in dogs, Circ. Res., 41: 51-58.

Vatner, S.F. and Braunwald, E., 1975, Cardiovascular control mechanisms in the conscious state, N. Engl. J. Med., 293: 970-976.

Vatner, S.F. and McRitchie, R.J., 1975, Interaction of the chemoreflex and the pulmonary inflation reflex in the regulation of coronary circulation in conscious dogs. Circ. Res., 37: 664-673.

Vatner, S.F., Franklin, D., Van Citters, R.L., and Braunwald, E., 1970, Effects of carotid sinus nerve stimulation on the coronary circulation of the conscious dog. Circ. Res., 27: 11-21.

Vatner, S.F., Higgins, C.B. and Braunwald, E., 1974, Effects of norepinephrine on coronary circulation and left ventricular dynamics in the conscious dog. Circ. Res., 34: 812-823.

Vatner, S.F., Pagani, M., Manders, W.T., and Pasipoularides, A.D., 1980, Alpha-adrenergic vasoconstriction and nitroglycerin vasodilation of large coronary arteries in the conscious dog, J. Clin. Invest., 65: 5-14.

Adv. Physiol. Sci. Vol. 8. Cardiovascular Physiology. Heart, Peripheral Circulation and Methodology
A. G. B. Kovách, E. Monos, G. Rubányi (eds)

A NEW MODEL FOR THE STATIC ELASTIC PROPERTIES OF THE AGING HUMAN AORTA

G. J. Langewouters, K. H. Wesseling and W. J. A. Goedhard
Department of Physiology, Free University, Amsterdam, The Netherlands

INTRODUCTION

Much information with regard to the elastic properties of the aorta can be obtained from the literature, except that publications on the elastic properties of the human aorta are scarce and inconsistent and generally not available for ages above 40 or 50 years. To study the effects of aging on arterial elasticity it is common usage to compare values of a modulus of elasticity of the arterial wall at a specific value of transmural pressure, i.e. 13.3 kPa (100 mmHg).
In this paper we present an alternative way to describe the passive static elastic properties of the human aorta and the effects of age on these properties. The measured pressure-volume relationships of 45 human thoracic aortas aged 30 to 88 years are described by a new non-linear three-parameter model. Since aortic distensibility is small, especially for the old aortas, and consequently difficult to measure accurately, we briefly describe some critical points of our measurement set-up.

MATERIAL AND METHODS

Aortic segments were obtained from autopsies at the pathalogic anatomy departments of two Amsterdam hospitals. A 10 cm long segment of the thoracic aorta just above the diaphragm was marked by two small incisions, excised and put into cold ($4^{o}C$) glucose-free Tyrode solution. This aortic segment is almost straight, of almost constant diameter and without many side branches.
The segments were trimmed of loose connective tissue and side branches were tightly ligated. Then the segments were mounted horizontally in the measurement apparatus while stretched to their in situ length. The segments were perfused with oxygenated (95% O2, 5% CO2) glucose-containing Tyrode at $37\pm1^{o}C$. The outside of the segments was kept moist with the same liquid.
Pressure inside the segment was measured with a Statham P23Db pressure transducer. Pressure was applied and stabilized to within 26Pa (.2 mmHg) by a column Tyrode of variable height.

Two diametrically opposed linear displacement transducers (SE Labs, type 351.02), precisely located at the pressure measurement site, gauged changes in the external diameter due to pressure changes (Fig. 1).

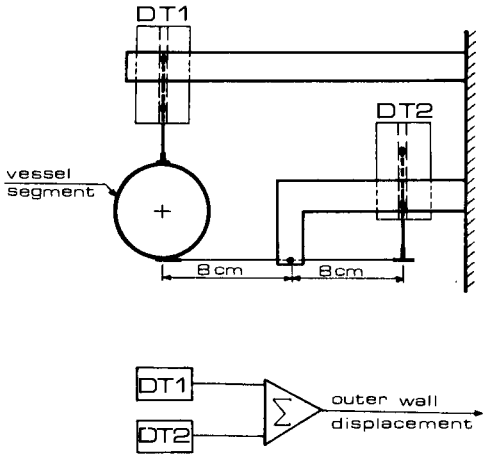

Fig.1 Transducer arrangement to measure arterial diameter changes in vitro. DT = displacement transducer. DT2 gauges the lower wall displacement via a balance.

The total linear displacement range of both transducers together was 10 mm. Sensitivity was such that changes of 1μm (10^{-6}m) in diameter could be measured with confidence. Such a high sensitivity is important since the diameter of the older vessels changes about 8 μm/kPa (1μm/mmHg) at higher pressures. A balanced arrangement to measure diameter was necessary; some vessels which were not perfectly straight showed a tendency to increase in curvature with increasing pressure, thus invalidating one-side measurements.
After being mounted in the measurement apparatus the segments were allowed to incubate for at least one hour. Pressure was set at 13.3 kPa (100 mmHg) during this time. Subsequently the segments were subjected to a series of 3 to 5 inflation-deflation cycles between 2.66 and 23.94 kPa (20-180 mmHg) at a rate of 133 Pa/s (1 mmHg/s). A thus conditioned vessel was assumed to have negligible smooth muscle tone.
Next passive pressure-diameter data were measured. Starting at 2.66 kPa (20 mmHg) pressure was changed stepwise in 2.66 kPa (20 mmHg) increments to 23.94 kPa (180 mmHg). The stepwise pressure changes facilitated the observation of the visco-elastic creep phenomenon (Langewouters et al, 1978). About 60 seconds after the onset of a pressure step the diameter reached a new steady state level, representing the static response of the aorta. At the end of the experiment an X-ray picture of the vessel and its connectors - with a known diameter - was made at a distending pressure of 13.3 kPa (100 mmHg) to obtain one absolute value of the vessels external diameter. The segments'

wall volume was determined by weighing it in air and while submerged in Tyrode.

Calculations

The internal cross-sectional area, A, of a vessel segment of length l, wall volume Vw and external diameter d at a given pressure level was computed from these data assuming that the vessel deformed isovolumetrically:

$$A = \frac{\pi}{4} d^2 - \frac{Vw}{l} \qquad (1)$$

Hemodynamically important quantities, such as the compliance per cm length, the characteristic impedance and the pulse wave velocity were computed as follows:

compliance $$C = \frac{dA}{dp} \qquad (2)$$

characteristic impedance $$Z_c = \sqrt{\frac{\varrho}{A} \frac{dp}{dA}} \qquad (3)$$

pulse wave velocity $$v = \sqrt{\frac{A}{\varrho} \frac{dp}{dA}} \qquad (4)$$

in which ϱ is the density of the fluid within the vessel. The circumferential incremental Young's modulus, E, was computed using the formula:

$$E = \frac{3A\ (Al + Vw)}{Vw} \frac{dp}{dA} \qquad (5)$$

Data reduction

The relationship between pressure and cross-sectional area of a vessel segment, further called the static response curve, was described by a non-linear equation:

$$A(p) = Am \left\{ \frac{1}{2} + \frac{1}{\pi} \tan^{-1} \left(\frac{p-p_o}{p_1} \right) \right\} \qquad (6)$$

This model is characterized by three parameters. For the determination of the parameters Am, p_o and p_1 appearing in Eq. (6) non-linear regression analysis was applied with the Marquardt method for obtaining the least squares fit (Marquardt, 1963).

RESULTS

The measured static response curves for all 45 thoracic aortas are shown in Fig. 2. It is emphasized that these curves are highly non-linear. Although there is a considerable inter-individual variability in the cross-sectional area of the aorta all curves have a more or less S-shaped appearance.
One typical example of these curves is shown in Fig. 3. The non-linear model according to Eq. (6) fitted to the measured data (+) is represented by the solid line.

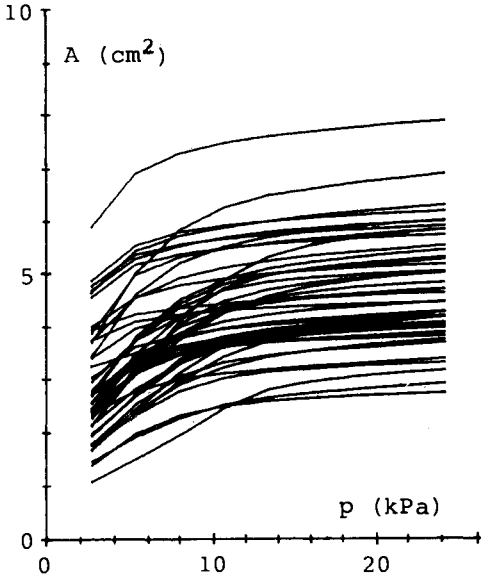

Fig.2 Static response curves of 45 human thoracic aortas aged 30 to 88 years. Note the highly non-linear shape of the curves. The younger vessels have a characteristic S-shaped curve.

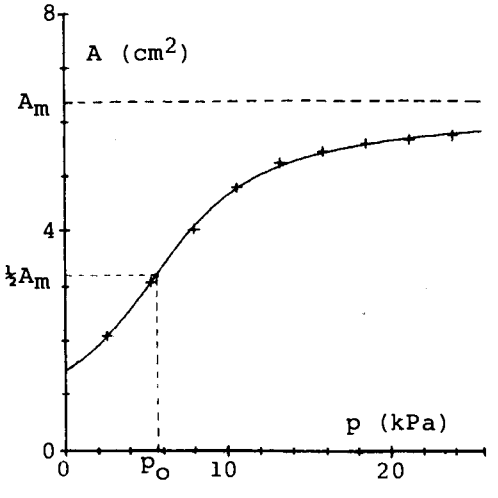

Fig.3 Static response curve of a 39 years old male aorta. Measurement data are indicated by a +. The solid curve represents the best fit curve (Eq. (6)). At the inflection point in the curve (p_o) the cross-sectional area of the aorta equals Am/2.

The physical meaning of the three parameters which characterize this curve is as follows:

- Am is the asymptotic cross-sectional area of the vessel at high pressure.
- p_o is the pressure level at which the inflection-point in the S-shaped curve is situated. At this pressure level the cross-sectional area of the vessel equals Am/2.
- p_1 is a measure of the steepness of the curve at the inflection point; this steepness being great as p_1 is small.

The least squares estimates of these parameters together with their estimated standard error are listed in Table 1.

Table 1: Best fit parameter values for the curve of Fig.3.

Parameter	Value	St.error	Unit
Am	6.37	0.04	cm^2
p_o	5.49 (41.3)	0.09 (0.68)	kPa (mmHg)
p_1	4.90 (36.8)	0.16 (1.25)	kPa (mmHg)

Coefficient of determination: $r^2 = .9996$

The standard error of the parameters is rather small, being about 3% in the worst case. Note the high value of the coefficient of determination, r^2, which is close to 1, indicating the close agreement between the measured data and the fitted curve.
Computed hemodynamical quantities C, Zc and v and the circumferential incremental Young's modulus E for this particular vessel are plottted as a function of pressure in Fig. 4. Compliance C and Young's modulus are plotted on a logarithmic vertical scale. The solid curves were drawn by inserting Eq. (6) into Eqs. (2)-(5). For all these quantities there is a close agreement between the solid curve and the discrete (+) values calculated from the measured data. Compliance C reaches a maximum at $p = p_o$, i.e. 5.5 kPa, and decreases strongly as pressure is raised beyond this level. In contrast, characteristic impedance Zc reaches a minimum at about 6.5 kPa. This minimum is situated somewhat beyond the pressure level corresponding to the inflection point in the static response curve. Pulse wave velocity is minimal at a pressure level somewhat below p_o. Note that the Young's modulus E is fairly constant in the pressure region below p_o ($E = 6.10^4\ Nm^{-2}$) but strongly increases as pressure is increased beyond p_o.

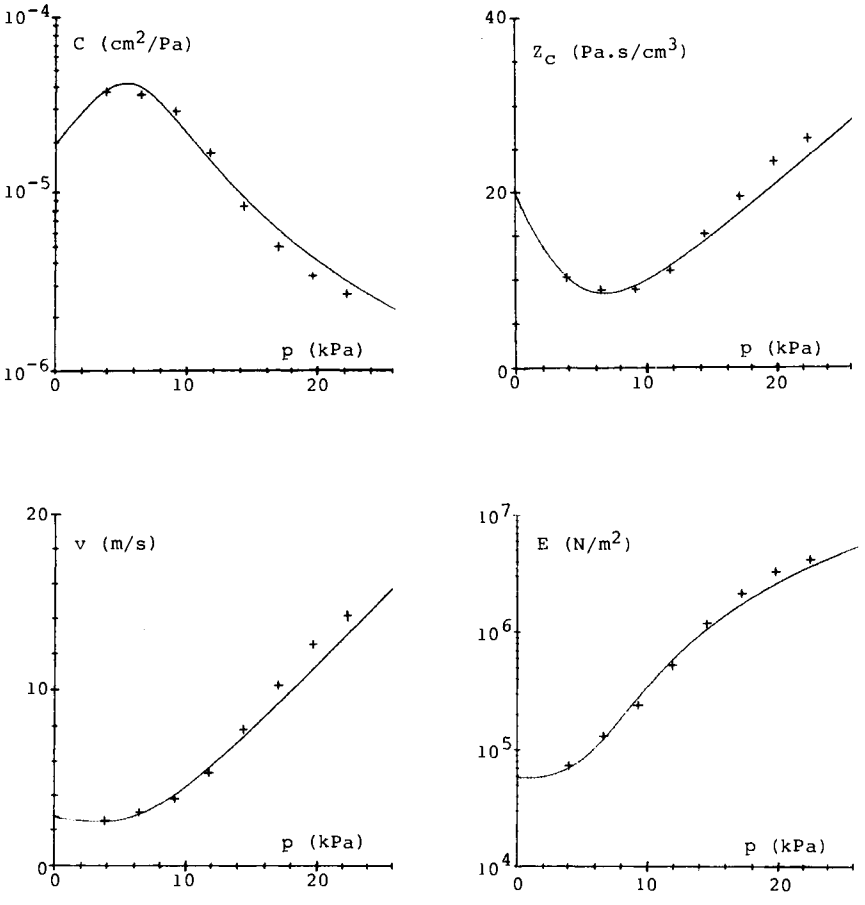

Fig.4 Compliance C, characteristic impedance Zc, pulse wave velocity v and the circumferential incremental Young's modulus E of the aorta from Fig.3 as a function of transmural pressure.
Values calculated from the measured data are indicated by a +.
Solid curves were calculated from the best fit curve shown in Fig.3. Equations (2)-(5) were used.
Note that the C-curve has a maximum, while the Zc- and v-curve have a minimum.

Aortic aging

The effect of aging on arterial elasticity was studied by relating the modelparameters to the chronological age of the aortas. Plots of Am, p_o and p_1 versus age are shown in Fig.5.

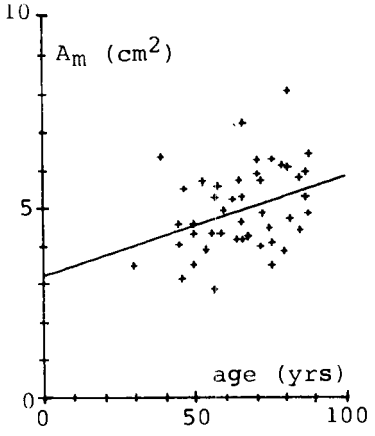

The maximum value of the cross-sectional area of the aorta slightly increases with age.

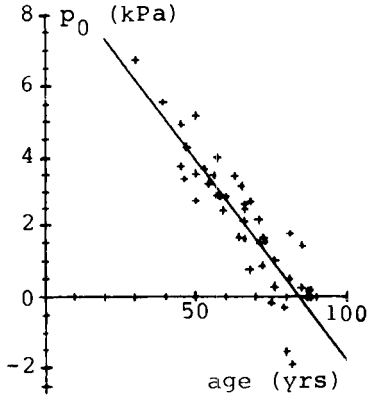

The inflection point in the static response curve shifts to lower pressure levels with increasing age. Note that the inflection point is situated in the negative pressure region for ages beyond 80 years.

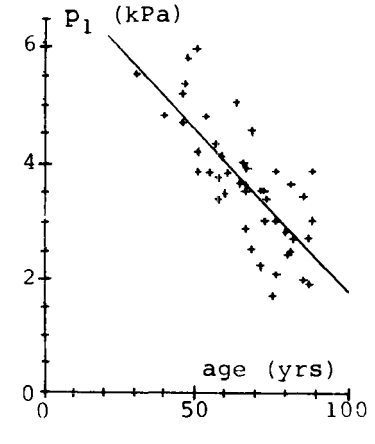

The steepness of the static response curve near the inflection point is inversely proportional to p_1 and increases with age.

Fig.5 Changes with age in the modelparameters Am, p_o and p_1. Linear regression lines are also shown.

Linear regression lines are also drawn. A summary of the linear regression analysis performed on the modelparameters is given in Table 2.

Table 2: Linear regressions of the modelparameters on age.
$y = a + bx$

Par.	a	b	SEE	r	F	p	unit
Am	3.25	0.026	1.05	.34	6	<0.05	cm^2
p_o	9.66(72.6)	-0.116(-0.87)	0.82(6.2)	-.90	180	<0.01	kPa(mmHg)
p_1	7.55(56.8)	-0.059(-0.78)	0.69(5.2)	-.78	66	<0.01	kPa(mmHg)

The asymptotic maximum surface area Am of the aorta increases by around 50% between 30 and 90 years. The pressure at the inflection point, p_o, is highly correlated with age ($r = -.90$). The decrease of p_o with age points out that the static response curve of the human aorta shifts to lower pressure levels with age. Finally the decrease of p_1 with age points to an increase of the steepness of the static response curve in the region around the inflection point.
The changes in the static response curve with age are elucidated in Fig. 6, in which this curve is shown for the age of 30, 60 and 90 years respectively.

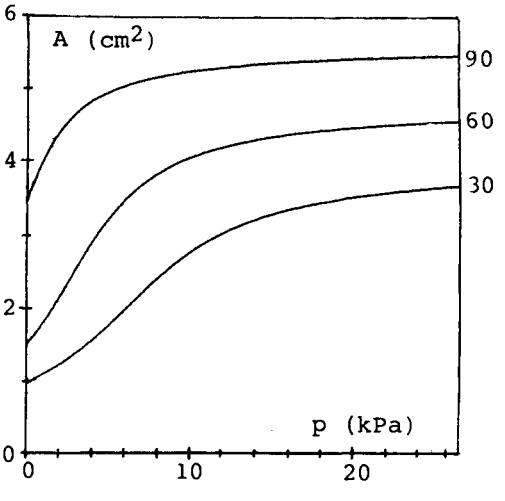

Fig.6 Changes with age in the shape of the static response curve of the human thoracic aorta. The curves were obtained by inserting parameter values corresponding to the age of 30, 60 and 90 years, calculated from the linear regressions on age (Table 2), into Eq. (6).

DISCUSSION

The results presented in this paper document the changes in passive mechanical properties of human thoracic aortas as a function of pressure and age. Younger and older vessels differed remarkably in their behaviour at low pressures, with the younger vessels having an S-shaped static response curve as shown in Fig. 2. Changes in the passive static elastic properties with pressure are well described by the non-linear three-parameter model proposed in this study.

To be able to use parameter techniques on individual measurements, accurate measurements are necessary. Therefore the reproducibility of the measurement apparatus and the influence of the time lapsed between the autopsy and the measurements were tested. Measurements were done twice or more on 10 vessels. The time lapsed between the autopsy and the first measurement varied from 3 to 99 hours. Most repeated measurements were done immediately after the first. Some segments were stored in cold (4°C) glucose-free Tyrode for 24 to 48 hours before repeating the measurements. Subsequent estimation of the modelparameters Am, p_o and p_1 from the repeated measurements yielded values which agreed with those of the first measurement to within the standard error of the parameters, which was always less than 3%. These results indicate not only a high degree of precision of the measurements but also suggest that a time lapse of up to 100 hours between the autopsy and the measurement has no influence on the static elastic properties if the vessels are stored in cold glucose-free Tyrode at 4°C.

As far as aging is concerned characteristic changes in the passive static elastic properties of the aging thoracic aorta were observed (Fig.5). The old aortas are dilated as compared with the young aortas. In addition the static response curve is shifted to the left for the old aortas. These results are in qualitative agreement with those reported by Bader (1967). The absence of a quantitative agreement is probably due to the fact that Bader measured whole thoracic aortas which were free to lengthen. In addition measurements were done at 20°C. Our results also showed a decrease of p_1 with age. The distensibility of the aorta (C/A) at the pressure p_o is inversely proportional to p_1. Since the cross-sectional area at the inflection point equals Am/2 and only slightly increases with age these observations indicate that the distensibility of the aorta at a constant diameter increases with age. In other words the arterial wall gets weaker with age. In this context it is interesting to note that Learoyd and Taylor (1966) found a significant decrease with age of the Young's modulus of the thoracic aorta at an external radius of 1.0 cm. In contrast Young's modulus at 13.3 kPa (100 mmHg) appeared to increase with age.

The results shown in Fig. 4 indicate that the hemodynamic quantities as well as the modulus of elasticity of the arterial wall can be satisfactorily calculated from the three-parameter model. In combination with the age-dependency of the model-parameters it is possible to calculate these quantities at any

given pressure level and age in the studied pressure- and age range. For instance Fig. 7 shows that the pulse wave velocity in the human thoracic aorta at 13.3 kPa (100 mmHg) increases more than two-fold between 30 and 90 years of age.

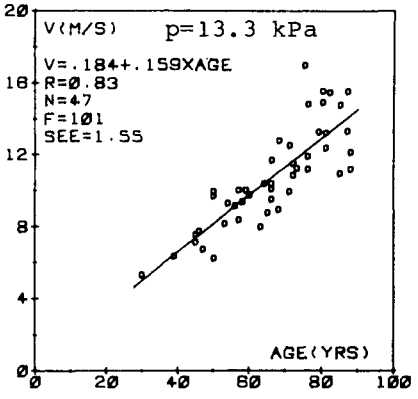

Fig.7 Pulse wave velocity in the human thoracic aorta at a transmural pressure of 13.3 kPa (100 mmHg) as a function of age. The solid line is the linear regression. Note that v increases from about 5 m/s at 30 years to around 14 m/s at 90 years.

In conclusion, the three-parameter model may serve as a tool to incorporate the pressure-dependent static elastic properties of the aging human aorta in arterial (computer) models.

SUMMARY

Human thoracic aortas were used to study age-related changes in the elastic properties of the aorta. Intact cylindrical segments (N = 45, age range 30-90 years) were studied in vitro at their in situ length. Pressure-volume relations were measured under passive conditions at 37°C. The S-shaped pressure-volume curves were described by a new non-linear three-parameter model. Model parameters were estimated from individual measurements by means of parameter estimation techniques. The greater part of the interindividual variability in the estimated parameters could be ascribed to aortic aging: pressure-volume curves were shifted to lower pressure levels with age. These results provide a means to compute passive hemodynamic quantities - such as arterial compliance, characteristic impedance and pulse wave velocity - at a given pressure level and age.

ACKNOWLEDGEMENT

The help of members of the pathologic anatomy departments of the Onze Lieve Vrouwe Gasthuis (OLVG) (Dr. E.L. Frensdorf) and the Free University Hospital (Prof.dr. R. Donner) is gratefully acknowledged.
This work was supported in part by the organization for Pure Scientific Research ZWO-FUNGO under Grant No. 13-26-16.

REFERENCES

Bader, H.: Dependence of wall stress in the human thoracic aorta on age and pressure. Circ.Res. 1967, 20: 354-361.

Langewouters, G.J., K.H. Wesseling and W.J.A. Goedhard: Dynamic behaviour of human aortas in vitro. Progr.Report 1978, 6: 133-143. Inst.Med.Phys. TNO, The Netherlands.

Learoyd, B.M. and M.G. Taylor: Alterations with age in the visco-elastic properties of human arterial walls. Circ.Res. 1966, 18: 278-292.

Marquardt, D.W.: An algorithm for least squares estimation of non-linear parameters. J.Soc.Industr. & Appl.Math. 1963, 11: 431-441.

Adv. Physiol. Sci. Vol. 8. Cardiovascular Physiology. Heart, Peripheral Circulation and Methodology
A. G. B. Kovách, E. Monos, G. Rubányi (eds)

A NONLINEAR TWO-LAYER CYLINDRICAL MODEL DESCRIBING THE ELASTIC PROPERTIES OF CAROTID ARTERIES

W. W. von Maltzahn, D. Besdo and W. Wiemer

Department of Biomedical Engineering, The University of Texas, Arlington, USA, Department of Mechanics, University of Hannover, FRG, Department of Physiology, University of Essen, FRG

INTRODUCTION

The following considerations were stimulated by investigations on the excitation mechanism of carotid baroreceptors (Wiemer et al., 1974; v. Maltzahn et al., 1980): As other muscular conduit arteries, the carotid sinus consists of three different layers: intima, media, and adventitia. Only the latter two contribute significantly to the mechanical properties of arteries. Also in the sinus area, structure and components of the media are quite different from those of the adventitia (Rees, 1968; Rees and Jepson, 1970); many baroreceptive nerve endings are embedded along the border between these layers (Knoche et al., 1974). When modelling the mechanical behavior of arterial walls, anatomical facts as well as experimental results and theoretical assumptions must be considered. Some of these shall be shortly reviewed.

Frank (1920) published the first thorough analysis of the mechanical properties of arteries. He found that arteries not only expanded considerably, but that the stress-strain relationship is different and highly nonlinear for each direction of measurement. These anisotropic and nonlinear properties are well established for arterial strips (Vonderlage, 1968; Laszt, 1968; Hardung, 1970; Sharma, 1974; Tanaka and Fung, 1974) as well as for arterial segments (Bergel, 1961; Tickner and Sacks, 1967; Attinger, 1968; Dobrin and Doyle, 1970; Patel and Janicki, 1970; Cox,1975b). In vivo arteries are tethered which usually increases the moduli of elasticity at any given point of operation (Kenner, 1964; Patel and Fry, 1969). Arteries are normally exposed to pulsatile blood pressure. In the course of a complete pressure cycle the stress-strain curves for expansion and relaxation do not superimpose indicating that energy is being dissipated. This introduces time and frequency dependence to the moduli of elasticity (Gow and Taylor, 1968; Hardung, 1970; Westerhof and Noordergraaf, 1970;Cox, 1972; Patel et al., 1973). The nonlinear large-deformation theory of elasticity was introduced to the analysis of arteries by Tickner and Sacks (1967). They used strain invariants as the independent variables in their energy density function which, therefore, describes an isotropic material. Hartung (1972, 1975), showed that this applies only to small arteries. Larger arteries have distinct anisotropic properties and thus need anisotropic energy density functions for their description (Vaishnav et al., 1972 ; Patel and Vaishnav, 1972; Cox, 1975b).

Respective experiments were carried out by Patel and Vaishnav (1972) and Cox (1975a,b). They recorded axial force and external diameter as a function of internal pressure while the arterial segment was held at a known

fixed length. The wall volume was determined at the conclusion of the experiment using Archimedes' principle. From these five parameters, completed by the resting length and the resting diameter, the coefficients of the energy density function were computed in the least square sense. Seven coefficients of a polynomial with two independent variables were necessary to describe elastic properties of arteries within 5 % accuracy.

However, none of the models proposed so far can assess the effects of arterial pressure and longitudinal tethering on structures within the vessel wall - for instance, baroreceptor nerve endings along the zone between media and adventitia. Therefore, a new cylindrical model comprising, at least, two layers has been devised for the stress-strain distributions across the arterial wall under the supposition that the essential force bearing layers in carotid arteries and the carotid sinus are media and adventitia. Other assumptions for this model, in accordance with Patel and Vaishnav (1972), are: symmetrical structure, anisotropy, nonlinearity and incompressibility. Hysteresis and viscoelasticity were not yet considered in this paper.

THEORY AND METHODS

The arterial wall deforms when external forces act on its surface. If the wall is assumed to be elastic, the work necessary to produce the deformation is stored inside the wall as potential energy. In arterial mechanics this energy is commonly referred to the unit volume of the undeformed wall and called the strain energy density W. Since W depends on the deformation of the wall, there exists a functional relationship between these two. Arteries are incompressible and orthotropic and, therefore, only two independent strain variables can be derived from the displacement field. This also implies that from the energy density function only stress differences can be computed and not the stresses themselves.

Anisotropic and isotropic constitutive equations

Patel and Vaishnav (1972) derived the constitutive equation for a thick-walled, cylindrical, orthotropic artery.

$$\sigma_t - \sigma_r = \frac{\partial W}{\partial \gamma_t} \lambda_t^2 \qquad \text{and} \qquad \sigma_z - \sigma_r = \frac{\partial W}{\partial \gamma_z} \lambda_z^2 \tag{1}$$

The theory for the description of the elastic properties of carotid arteries is based on reversible thermodynamic processes. These can be applied to continuum mechanics in general (c. f. textbooks by Green and Zerna,1968; Becker and Bürger, 1971) or to arterial mechanics as shown by Vaishnav et al. (1972), Hartung (1976) and v. Maltzahn (1979). The stretch ratios λ_t and λ_z are defined by

$$\lambda_t = \frac{r}{r_o} \qquad \text{and} \qquad \lambda_z = \frac{z}{z_o} \tag{2}$$

where r_o and z_o are undeformed lengths and r and z deformed lengths. σ_r, σ_t, σ_z are the actual stresses in the radial, tangential, and axial direction. The Green-St. Venant strains are defined by

$$\gamma_t = \tfrac{1}{2}(\lambda_t^2 - 1) \quad \text{and} \quad \gamma_z = \tfrac{1}{2}(\lambda_z^2 - 1) \tag{3}$$

Hartung (1975) published the constitutive equation for a thick-walled, cylindrical, isotropic artery

$$\sigma_t - \sigma_r = 2\left(\lambda_t^2 - \frac{1}{\lambda_t^2 \lambda_z^2} \right) \left(\frac{\partial W}{\partial I_1} + \lambda_z^2 \frac{\partial W}{\partial I_2} \right)$$
$$\sigma_z - \sigma_r = 2\left(\lambda_z^2 - \frac{1}{\lambda_t^2 \lambda_z^2} \right) \left(\frac{\partial W}{\partial I_1} + \lambda_t^2 \frac{\partial W}{\partial I_2} \right) \qquad (4)$$

I_1 and I_2 are two invariants which can be computed from the stretch ratios:

$$I_1 = \lambda_t^2 + \lambda_z^2 + 1/\lambda_t^2 \lambda_z^2 \quad \text{and} \quad I_2 = 1/\lambda_t^2 + 1/\lambda_z^2 + \lambda_t^2 \lambda_z^2 \qquad (5)$$

Sometimes it may be advantageous to use strain invariants different from those above. One set which yielded excellent results in this study is:

$$J_1 = I_1 - 3 \quad \text{and} \quad J_2 = I_2 - 2I_1 + 3 \qquad (6)$$

Equations (4) can be easily written in terms of these invariants.

The two-layer, cylindrical model

As was pointed out in the introduction a two-layer thick walled cylindrical model appears to be a reasonable representation of the arterial wall. The model and its boundary condition are given in figure 1. The boundary conditions state that the radial stresses have to be continuous at r_1, r_2, r_3, and the radial displacements at r_2. There must not be a discontinuity in these functions.

The parameters measured in typical experiments on arterial segments (Cox, 1975a; Patel and Vaishnav, 1972) are the axial force F_z, the internal pressure P_i, and axial length l, the outer diameter D and the total wall volume V. The inner radius r_1 can be calculated from the latter three parameters. The aim is now to determine the two energy density functions for the two layers so that the measured data can be computed from the two-layer model. First, the pressure drop across the arterial wall can be determined by integrating the equation of equilibrium for cylindrical coordinates:

$$p_i - p_o = \int_{r_1}^{r_2} \left(\overset{M}{\sigma_t} - \overset{M}{\sigma_r} \right) \frac{dr}{r} + \int_{r_2}^{r_3} \left(\overset{A}{\sigma_t} - \overset{A}{\sigma_r} \right) \frac{dr}{r} \qquad (7)$$

For the stress differences in (7) either equation (3) or (4) has to be inserted. The axial force F_z measured on a plate mounted to the artery is equal to the difference between force F_{zw} developed by the axial stress σ_z inside the wall and the difference between the forces developed by the internal and external pressures:

$$F_z = F_{zw} - \pi \left(r_1^2 p_i - r_3^2 p_o \right) \qquad (8)$$

The force in the wall F_{zw} is equal to the integral of the axial stress σ_z over the cross-sectional area of the wall. σ_z can be split up as shown below:

$$F_{zw} = 2\pi \int_{r_1}^{r_2} {}^{M}\sigma_z \, r\,dr + 2\pi \int_{r_2}^{r_3} {}^{A}\sigma_z \, r\,dr \qquad (9)$$

$$= 2\pi \int_{r_1}^{r_2} \left[{}^{M}\sigma_r - \left({}^{M}\sigma_z - {}^{M}\sigma_r \right) \right] r\,dr + 2\pi \int_{r_2}^{r_3} \left[{}^{A}\sigma_r - \left({}^{A}\sigma_z - {}^{A}\sigma_r \right) \right] r\,dr$$

The first term under the integral can be transformed by partial integration, the equilibrium equation, and the boundary conditions:

$$2\pi \int_{r_1}^{r_2} {}^{M}\sigma_r \, r\,dr + 2\pi \int_{r_2}^{r_3} {}^{A}\sigma_r \, r\,dr = \pi \left(r_1^2 p_i - r_3^2 p_o \right) - \pi \int_{r_1}^{r_2} \left({}^{M}\sigma_t - {}^{M}\sigma_r \right) dr - \pi \int_{r_2}^{r_3} \left({}^{A}\sigma_t - {}^{A}\sigma_r \right) dr \qquad (10)$$

Combining (9) and (10) gives:

$$F_{zw} = \pi \left(r_1^2 p_i - r_3^2 p_o \right) +$$

$$\pi \int_{r_1}^{r_2} \left[2\left({}^{M}\sigma_z - {}^{M}\sigma_r \right) - \left({}^{M}\sigma_t - {}^{M}\sigma_r \right) \right] r\,dr + \pi \int_{r_2}^{r_3} \left[2\left({}^{A}\sigma_z - {}^{A}\sigma_r \right) - \left({}^{A}\sigma_t - {}^{A}\sigma_r \right) \right] r\,dr \qquad (11)$$

The stress differences $(\sigma_t - \sigma_r)$ and $(\sigma_z - \sigma_r)$ in (11) are again taken from (3) and (4). For all practical purposes the external pressure p_o can be set equal to zero. Then the axial force F_z and the internal pressure p_i can be computed from a given set of values for λ_z, r_1, r_2 and r_3, if W is known. The problem is now: which form should W have, and how are these parameters to be obtained?

The energy density functions

The overall properties of large arteries are clearly anisotropic (Dobrin, 1978). This does not exclude, however, that parts of the wall may be isotropic. The elastic membranes, for instance, may very well have isotropic or transverse isotropic properties. Since there is no data available of either the media or the adventitia alone, the layers of the model were successively made transverse isotropic, isotropic, anisotropic, and any combination of these. In addition, various polynomials and exponential functions were tried for W. Using polynomials leads to semilinear systems and well behaved numerical algorithms. Exponential functions are superior to polynomials in modelling the large increase in the tangential stress-strain relationship, but they lead to transcendental equations and complicated numerical approximation procedures. Through trial and error finally the following functions for the two layers were obtained yielding very good agreements between measured and computed curves, and at the same time keeping computational efforts at a minimum:

$${}^{A}W = b_1 \gamma_t^4 + b_2 \gamma_t \gamma_z + b_3 \gamma_z^2 \qquad (12)$$

$${}^{M}W = b_4 J_1^2 + b_5 J_2^2 \qquad (13)$$

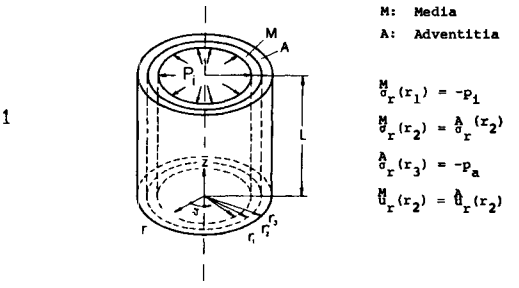

Fig. 1 Two-layer model of the carotid artery with boundary conditions for radial stresses and radial displacements.

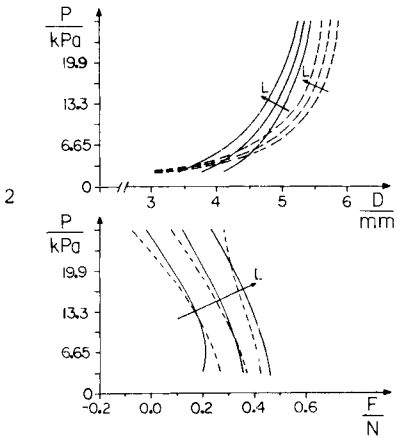

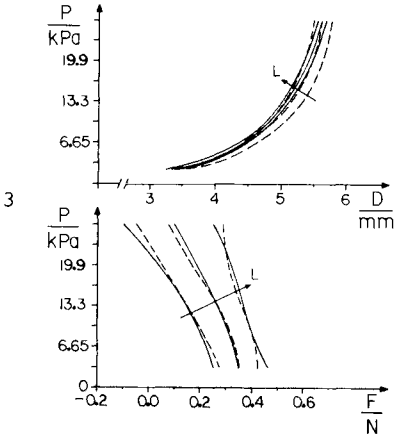

Fig. 2 One-layer model using equation (14).
The upper diagram shows the pressure-diameter relationship, the lower diagram the pressure-axial force relationship. The solid curves are computed, the dashed curves are taken from Cox (1975b). L indicates three different increasing axial lengths.

Fig. 3 Two-layer model using equations (15) and (16)
The upper diagram shows the pressure-diameter relationship, the lower diagram the pressure axial force relationship. The solid curves are computed, the dashed are taken from Cox (1975b). L indicates three different increasing axial lengths.

The superscipts A and M stand for adventitia and media, γ_t and γ_z are tangential and axial strains, and J_1 and J_2 are strain invariants defined by equation (6).

The iterative procedure for the computation of $b_1 \ldots b_5$ consists of two parts. First b_1, b_2, b_3 of the adventitia are calculated by a linear set of equations employing the common least square method. Then these parameters are held constant and b_4, b_5 of the media are determined by using a Newtonean gradient method. These two numerical procedures are repeated and the two sets of parameters are successively changed until the sum of the

differences between measured and computed datapoints reaches a minimum.

Stresses, strains, moduli of elasticity and Poisson's ratio

The procedure for obtaining the moduli of elasticity and the Poisson's ratios from the linearized form of equations (1) and (4) has been described in detail elsewhere (Vaishnav et al., 1973). Those derivations were used here, providing the basis for the results presented in this paper.

RESULTS

The two-layer model was tested with the experimental data of Cox (1975) obtained from canine carotid arteries. So far, no experiments seem to have been carried out on either the media or the adventitia alone.

First the seven parameters of the anisotropic strain energy density function used by Vaishnav et al. (1972) were computed from Cox's data with a conventional least square fit for the one-layer model:

$$W = \left(-33192\gamma_t^2 + 18503\gamma_t\gamma_z + 5005\gamma_z^2 + 40835\gamma_t^3 + 21844\gamma_t^2\gamma_z - 5980\gamma_t\gamma_z^2 + 6055\gamma_z^3 \right) \text{Pa} \tag{14}$$

It was then tried to retrieve the measured data from this function.The calculated and the measured sets of data for three different axial lengths are graphically displayed in figure 2.

Next the three parameters of the anisotropic and the two parameters of the isotropic strain energy function were computed by the method suggested in this paper for the two-layer model. These functions are:

$$\frac{A}{W} = \left(93118\gamma_t^4 + 20819\gamma_t\gamma_z + 15374\gamma_z^2 \right) \text{Pa} \tag{15}$$

$$\frac{M}{W} = 3507 \left(J_1^2 + J_2^2 \right) \text{Pa} \tag{16}$$

The best fit was obtained when the two parameters b_4 and b_5 were equal to each other, and when one layer(media) was isotropic, the other (adventitia) anisotropic. The calculated and measured sets of data are displayed in figure 3. They match within 2 % accurary.

The stress and strain distributions for three different internal pressures p_1 are shown in figure 4. To understand the highly nonlinear behavior of biological soft tissues some authors prefer to look at the moduli of elasticity and the Poisson's ratios rather at the stress strain distributions. Therefore, figure 5 and 6 present these parameters as a function of the stretch ratios λ_t and λ_z. The stretch ratios are chosen to lie within the normal physiological range.

DISCUSSION

Multi-layer models for the arterial wall have been suggested before (Müller, 1959), but to our knowledge they have never been used in conjunction with nonlinear energy density functions. On one hand, this may be due to the lack of experimental data on the mechanical properties of individual layers. Such data may become available in the future. On the other hand, there may not have been sufficient incentive to find out what is actually happening inside the arterial wall, although the answer to this question could be quite important to the understanding of baroreceptor functions,

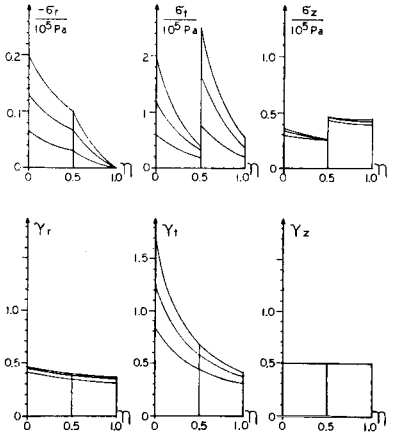

Fig. 4 Stresses and strains computed from the two-layer model. The upper diagrams show the radial, tangential, and axial stresses, the lower diagrams the corresponding strains as a function of the normalized radius $\eta = (r_1-r_2)/(r_1-r_3)$. The inner layer (media) is isotropic, the outer (adventitia) anisotropic. The three curves represent internal pressures of p_j = 6.65 kPa, 13.3 kPa, 19.9 kPa.

5

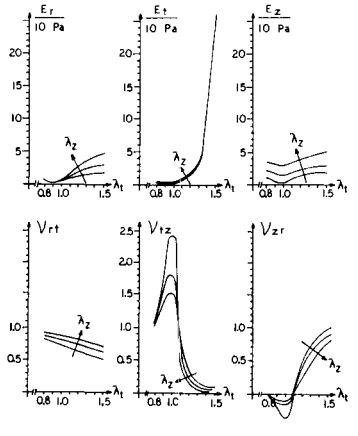

6

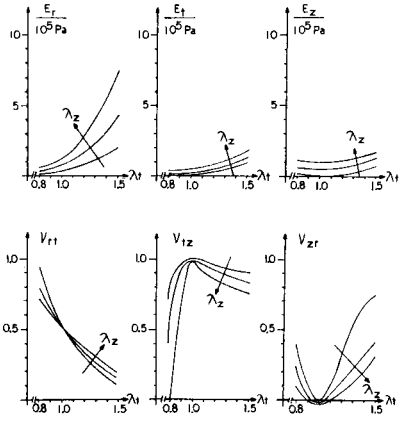

Fig. 5 Anisotropic layer: Moduli of elasticity and Poisson's ratios in the radial, tangential, and axial directions as functions of the tangential (abscissa) and axial (arrow) stretch ratios. The three axial stretch ratios are λ_z = 1.3, 1.5, 1.7.

Fig. 6 Isotropic layer: Moduli of elasticity and Poisson's ratios in the radial, tangential, and axial directions as functions of the tangential (abscissa) and axial (arrow) stretch ratios. The three axial stretch ratios are λ_z = 1.3, 1.5, 1.7.

hypertension, arteriosclerosis, atherosclerosis, and autoregulation (Cox, 1979).

Our model appears to provide an improved insight into the nonlinear stress-strain relationships of the multi-composite arterial wall. The graphs for both the one and two-layer models (figures 2 and 3) show the considerable advantages of the two-layer model. This improvement is accomplished despite the fact that only four parameters are needed in the two-layer model as compared to 7 or more parameters in the one layer model. These four parameters have direct mechanical implications: For the anisotropic layer, b_1 and b_3 determine the stress-strain relationships in the tangential and axial directions, while b_2 gives the interdependence of tangential stresses or strains on axial stresses or strains. For the isotropic layer there exists only one material constant. The more familiar incremental moduli of elasticity and the Poisson's ratios are far more complicated functions altogether.

The questions which layer is isotropic and which anisotropic, or whether both are anisotropic, cannot be answered satisfactorily as long as data is available for the whole wall only. The fact that the best agreement between the measured and computed data can be achieved by making the media isotropic and the adventitia anisotropic does not necessarily mean that this is so in reality. The data of Cox (1975b) used in this study was derived from carotid arteries with inactivated muscle cells, the main mechanical structures in the media thus being elastic membranes. These membranes may well have predominantly isotropic properties. It can also be visualized that the adventitia has primarily anisotropic properties because its main mechanical structures are collageneous fibers. In this respect, the results seem to correlate quite well with the specific composition of the arterial wall.

The coefficients $b_1 \ldots b_4$ give a best fit in the least square sense to measured forces, pressures and lengths and not to stresses or stress-differences. The latter are commonly derived from linearized equations which introduce intrinsic errors in the order of 5% or more (Vaishnav et al., 1973). These errors are avoided in the two-layer model without increasing the computational effort significantly.

On a statistical basis Hartung (1976) estimated the energies stored in elastic and collageneous components of thick walled arteries. The curves for these energies can be modelled and described by equations (15) and (16) of the two-layer model. The results (which are not shown in this paper) are in remarkable agreement.

In summary: the two-layer model appears to be superior to one-layer models in several ways; (a) it describes the elastic properties in the physiologic pressure range more accurately, (b) it employs simple polynomials with only one coefficient for the media and three coefficients for the adventitia and (c) it delivers more realistic stress-strain distributions inside the arterial wall.

The investigations were supported by a grant (SFB 114) form the Deutsche Forschungsgemeinschaft

REFERENCES

Attinger, F. M. L. (1968) Two-dimensional in-vitro studies of femoral arterial walls of the dog. Circulation Res., 22, 829-840.

Bagshaw, R. J., Fischer, G. M. (1971) Morphology of the carotid sinus in the dog. J. Appl. Physiol., 31, 198-202.

Becker, E., Bürger, W. (1971) Kontinuumstechnik. Teubner, Stuttgart.

Bergel, D. H. (1961) The static elastic properties of the arterial wall. J. Physiol. 156, 445-457.

Carew, T. E., Vaishnav, R. N., Patel, D. J. (1968) Compressibility of the arterial wall. Circulation Res. 23, 61-68.

Cox, R. H. (1972) A model for the dynamic mechanical properties of arteries. J. Biomechanics, 5, 135-152.

Cox, R. H. (1975a) Pressure dependence of the mechanical properties of arteries in vivo. Am. J. Physiol., 229, 1371-1375.

Cox, R. H. (1975b) Anisotropic properties of the canine carotid artery in vitro. J. Biomechanics, 8, 293-300.

Cox, R. H. (1979) Comparison of arterial wall mechanics in normotensive and spontaneously hypertensive rats. Am. J. Physiol., 237 (2), H159-H167.

Dobrin, P. B., Doyle, J. M. (1970) Vascular smooth muscle and the anisotropy of dog carotid artery. Circulation Res., 27, 105-119.

Dobrin, P. B. (1978) Mechanical properties of arteries. Physiol. Rev., 58, 397-460.

Frank, O. (1920) Die Elastizität der Blutgefäße. Z. Biol., 71, 255-272.

Fung, Y. C. (1976) Biomechanics. In: Theoretical and Applied Mechanics. (Ed. Koiter, W. T.), North Holland, Amsterdam.

Gow, B. S., Taylor, M. G. (1968) Measurement of viscoelastic properties of arteries in the living dog. Circulation Res., 23, 111-122.

Green, A. E., Zerna, W. (1968) Theoretical Elasticity, 2nd. Edition. Oxford University Press, Oxford.

Hardung, V. (1970) Dynamische Elastizität und innere Reibung muskulärer Blutgefäße bei verschiedener durch Dehnung und tonische Kontraktion hervorgerufener Wandspannung. Arch. Kreislaufforsch. 61, 83-100.

Hartung, C. (1972) Zur Biomechanik kleiner Blutgefäße. Biomedizinische Technik, 17, 212-217.

Hartung, C. (1975) Zur Biomechanik weicher Gewebe, Fortschrittberichte der VDI-Zeitschriften, 17.

Kenner, T. (1964) Über die Bedeutung der Längsvorspannung und deren Einfluß auf die Dehnbarkeit von Arterien. Zeitschrift f. Kreislaufforsch. 53, 865-870.

Knoche, H., Addicks, K., Schmitt, G. (1974) A contribution regarding our knowledge of pressoreceptor fields and the sinus nerve based on electron microscopic findings. In: Symposium Mechanoreception (Ed.: Schwarztkopff, J.) Abh.Rhein.-Westf.Akad.Wiss., 53, 57-76.

Laszt, L. (1968) Untersuchungen über die elastischen Eigenschaften der Blutgefäße im Ruhe- und im Kontraktionszustand. Angiologica, 5, 14-27.

Maltzahn, W.-W. v. (1979) "Über die elastischen Eigenschaften der Arterienwand im Sinus Caroticus", Dissertation Thesis, Universität Hannover, FRG.

Maltzahn, W.-W. v., Besdo, D., Wiemer, W. (1980) The elastic properties of the carotid sinus wall as described by a non-linear two-layer model of arteries (in print).

Müller, A. (1959) Die mehrschichtige Rohrwand als Modell für die Aorta.Helv. physiol. pharmacol. Acta 17, 131-145.

Patel, D. J., Fry, D. L. (1969) The elastic symmetry of arterial segments in dogs. Circulation Res., 24, 1-8.

Patel, D. J., Janicki, J. S. (1970) Static elastic properties of the left coronary circumflex artery and the common carotid artery in dogs. Circulation Res., 27, 149-159.

Patel, D. J., Janicki, J. S., Vaishnav, R. N., Young, J. T. (1973) Dynamic anisotropic properties of the aorta in living dogs. Circulation Res., 32, 93-107.

Patel, D. J., Vaishnav, R. N. (1972) The rheology of large blood vessels. In: Cardiovascular Fluid Dynamics (Ed.: Bergel, D. H.), Vol. 2, Academic Press, London, 1-64.

Rees, P. M. (1968) Electron microscopical observations on the architecture of the carotid arterial walls, with special reference to the sinus portion. J. Anat., 103, 35-47.

Rees, P. M., Jepson, P. (1970) Measurement of arterial geometry and wall composition in the carotid sinus baroreceptor area. Circulation Res., 26, 461-468.

Sharma, M. G. (1974) Viscoelastic behavior of conduit arteries. Biorheology, 11, 279-291.

Tanaka, T. T., Fung, Y. C. (1974) Elastic and inelastic properties of the canine aorta and their variation along the aortic tree. J. Biomechanics, 7, 357-370.

Tickner, E. G., Sacks, A. H. (1967) A theory for the static elastic behavior of blood vessels. Biorheology, 4, 151-168.

Vaishnav, R. N., Young, J. T., Janicki, J. S., Patel, D. J. (1972) Non-linear anisotropic elastic properties of the canine aorta. Biophysical J., 12, 1008-1027.

Vaishnav, R. N., Young, J. T., Patel, D. J. (1973) Distribution of stresses and of strain-energy density through the wall thickness in a canine segment. Circulation Res., 32, 577-583.

Vonderlage, M. (1968) Untersuchungen über die mechanischen Eigenschaften von Streifenpräparaten verschiedener Schnittrichtung aus der Aorta abdominalis des Kaninchens. Pflügers Arch., 301, 320-328.

Westerhof, N., Noordergraaf, A. (1970) Arterial viscoelasticity: a generalized model, J. Biomechanics, 3, 357-379.

Wetterer, E., Kenner, T. (1968) Grundlagen der Dynamik des Arterienimpulses. Springer-Verlag, Berlin, Heidelberg, New York.

Wiemer,W.,Kaack,D.,Kezdi,P.,Brügge,C.,Zmijewski,M.(1974) Response characteristics of carotid baroreceptors to steady pressure.In: Symposium Mechanoreception (Ed.: Schwartzkopff,J.) Abh.Rhein.-Westf.Akad.Wiss.,53, 77-98.

Adv. Physiol. Sci. Vol. 8. Cardiovascular Physiology. Heart, Peripheral Circulation and Methodology
A. G. B. Kovách, E. Monos, G. Rubányi (eds)

CONCLUDING REMARKS ON BIOMECHANICAL PROPERTIES OF ARTERIES

R. H. Cox
Bockus Institute and Department of Physiology, University of Pennsylvania, Philadelphia, Pennsylvania, USA

The presentations in this symposium have reemphasized the complexity and variablity of the mechanical properties of the arteries in health and disease. Regarding the smooth muscle cells of the arterial wall, MULVANY and WARSHAW demonstrated that the mechanics of arterial smooth muscle generally represent the properties of the cells they contain. However, individual cells within a given tissue may exhibit different properties at any given moment and condition. In addition, MONOS showed that substantial differences exist in the ability of smooth muscle to control vessel diameter under in vitro conditions at a specific degree of activation. GEROVA and GERO showed that a similar situation exists in vivo in terms of the effects of efferent nerve activity on arterial wall diameter at /constant/ physiological values of pressure.

The importance of passive structural elements was also stressed in several of the presentations. GREENWALD and BERRY described the effects of genetic and experimental forms of hypertension and aging on arterial wall scleroprotein content and mechanical properties. Both aging and hypertension were associated with substantial and predictable changes in the arterial wall. Elastin content declines and collagen increases with aging as does stiffness. Hypertension is associated with a decline in collagen content, an increase in elastin content, and a decreased stiffness. When rats with clipped renal arteries were given beta-

amino-propionitrile which inhibits the formation of collagen cross links they did not develop hypertension. This finding emphasizes the importance of the control of vascular wall content and circulatory function, a theme that was emphasized by MONOS. He discussed the relation between the mechanical properties of arteries, their composition, and a minimum that exists in a time series analysis of pressure waves *in vivo* in terms of a forced oscillation type of optimizing system.

BEVAN and TSURU reported that the composition and properties of arteries are strongly influenced by efferent sympathetic nerve traffic. Loss of sympathetic nerve traffic causes a stiffening of the arterial wall, and a decrease in wall thickness, smooth muscle content and active force development. This study stresses the importance of the trophic effect of sympathetic innervation on arterial wall structure and function.

In view of this complexity, the importance of the development of analytical models to represent the properties of the arterial wall was emphasized in two presentations. HUDETZ described models to represent the anisotropic behavior of arteries, their viscoelastic nature, and their myogenic response to quick stretch. Von MALTZAHN et al. presented a nonlinear two layer model for the arterial wall to represent indepently the media and adventitia.

Detailed studies of the properties of cronary arteries were presented by three authors. GEROVA and GERO described active responses of *in situ* coronary arteries to increases in coronary blood flow and pulse pressure, suggesting a myogenic basis. LEVICKY and GEROVA reported on the structural composition of coronary arteries demonstrating substantial differences from that of other similarly sized arteries. They consider these structural differences the basis for coronary artery spasm. PAGANI et al. presented data on the mechanical properties of coronary arteries in the conscious dog. They found values of elastic moduli

to be much lower than previously reported perhaps related to the presence of smooth muscle tone. They further found that alpha adrenergic stimulation produced a significant effect on these arteries.

LANGEWOUTERS et al. described experiments performed to determine the effects of transmural pressure and age on the mechanics of human arteries. They combined the experimental measurements with a model representation to obtain parameters describing the nonlinear quasi-static elasticity and time-dependent viscoelastic behavior. The variations of both functions were mainly due to age.

Adv. Physiol. Sci. Vol. 8. Cardiovascular Physiology. Heart, Peripheral Circulation and Methodology
A. G. B. Kovách, E. Monos, G. Rubányi (eds)

CIRCULATORY CONSEQUENCES OF FETAL NEPHRECTOMY

J. C. Mott
Nuffield Institute for Medical Research, University of Oxford, United Kingdom

INTRODUCTION

This paper summarises some features of the circulation of fetal lambs following bilateral nephrectomy at about 0.8 gestation (full-term ∿ 147 days).

Fetal plasma renin activity and angiotensin II concentration fall to very low levels in nephrectomized fetal lambs (Broughton Pipkin, Lumbers & Mott 1974). It seemed possible that following nephrectomy fetal arterial pressure would fail to be maintained in the normal range on account of a deficiency of circulating angiotensin II.

METHODS

Fetal vascular and amniotic pressures were measured by Devices transducers from catheters inserted at operation with the ewe under halothane anaesthesia. The arterial pressure signal corrected for amniotic pressure was sampled every few seconds and recorded continuously on a Cambridge Slow Recorder. A Devices heart rate meter was triggered by the arterial pulse and heart rate similarly displayed. Amniotic pressure was also recorded and in some lambs central venous pressure. 0.5 - 1 ml fetal blood was withdrawn daily for measurement of blood gas pressures and pH on Radiometer or Corning meters. A microhaematocrit centrifuge was used in the measurement of packed cell volume. Unless otherwise stated measurements refer to the forenoon.

RESULTS

Blood pressure and heart rate

Contrary to expectation fetal arterial pressure of most nephrectomized lambs rose within a few days and approached double that of comparable normal lambs (Table 1).

Similar hypertension follows ureteral occlusion which does not however abolish plasma renin activity (Dutton, Mott & Valdes Cruz 1978). The heart rate of nephrectomized lambs consistently exceeded ($P < 0.001$) that of normal lambs and this difference was apparent before arterial pressure rose. In 11 nephrectomized lambs the average heart rate over the first seven days was 186 beats/min $\pm$ 17 (S.D.) compared with 162 beats/min $\pm$ 17 (S.D.) in 8 normal lambs.

Table 1 Arterial Pressure

Arterial pressure of fetal lambs following bilateral nephrectomy at 111-125 days gestation age. Mean pressure in 8 control lambs was 44.6 $\pm$ 4.5 (S.D.) mm Hg.

Day	No. of lambs	Arterial pressure mm Hg mean	range	% of lambs with pressure more than 2 S.D. above mean control value.
1	11	46.3	35-54	9
2	11	46.5	36-60	18
3	11	51.4	38-68	27
4	11	58.4	44-82	54
5	11	61.6	44-78	81
6	11	64.0	43-80	73
7	9	70.0	38-94	78

Packed cell volume, pH and blood gas tensions.

Packed cell volume was consistently lower in nephrectomized than in otherwise comparable intact lambs; both groups showed the fall normally seen following operation (Table 2).

Table 2 Packed cell volume

Packed cell volume % (mean ± S.D.) in fetal lambs following bilateral nephrectomy at 111-125 days gestation age. Number of lambs in parentheses.

Lambs	Days following nephrectomy and/or catheterization		
	1	4	7
Nephrectomized	34.6 ± 5.5 (11)	26.6 ± 5.4 (11)	26.7 ± 6.3 (10)
Control	37.8 ± 6.9 (8)	30.7 ± 3.5 (6)	30.8 ± 7.6 (7)

Femoral arterial pH was within normal limits in nephrectomized lambs, pCO_2 slightly above and pO_2 somewhat below the values in comparable normal lambs. Table 3 summarizes the measurements taken on established preparations 7-15 days after catheterization.

Table 3 pH and blood gas tensions

pH and blood gas tensions (mm Hg) in 7 intact and 11 nephrectomized lambs before termination of observations 7-15 days after catheterization. Mean values ± S.D. No. of observations in brackets where different from no. of lambs.

	Lambs		
	Intact		Nephrectomized
Bodyweight (kg)	2.8 ± 0.6	P<0.01	3.9 ± 0.7
Gestation age (days)	131 ± 4		130 ± 5
Days post-catheterization	10 ± 3		9 ± 2
Arterial pressure (mm Hg)	47 ± 5		77 ± 14
Packed cell volume (%)	33 ± 9		26 ± 6
Femoral arterial pH	7.35 ± 0.04		7.34 ± 0.05 (9)
pO_2	20.0 ± 7.4		15.4 ± 4.8 (9)
pCO_2	43.1 ± 5.2		49.1 ± 5.9 (9)

Anatomical observations

The nephrectomized lambs were on average heavier ($P < 0.01$) than the controls (Table 3). Some lambs became conspicuously oedematous with a girth (at umbilical level)/crown-rump length ratio of up to 1. Lesser degrees of oedema such as some listed for illustration in Table 4 might pass unnoticed unless a normal lamb is available for comparison.

Table 4 Ratio of girth/crown-rump length in fetal lambs

This index in 4 catheterized normal fetal lambs 2-8 days after operation was 0.616 - 0.792.

Days		Lambs	
post-nephrectomy	gestation age	nephrectomized	unoperated sib
2	124	.734	.673
4	128	.872	.735
7	128	.95	.729
8	128	.833	.739
8	131	.805	.698 .657

The occurence of an apparently large heart in one nephrectomized fetal lamb suggested systematic measurement of cardiac ventricular muscle. As a percentage of body weight this averaged 0.57 $\pm$ 0.08 (S.D,) in 13 control lambs. In 9 lambs 7 days or more after nephrectomy, ventricular muscle was 0.81% $\pm$ 0.17 (S.D,) of bodyweight. Six of these lambs had a proportion of ventricular muscle more than two standard deviations above the mean control value. The corresponding arterial pressures averaged 78 mm Hg with 8/9 values exceeding the control level of 44.6 mm Hg $\pm$ 4.5 (S.D) (Table 1). When the girth/crown-rump length ratios of individual lambs (4 intact, 5 nephrectomized) were compared with their relative heart weights these were found to be correlated ($r = 0.757$, $P < 0.02$).

DISCUSSION

Circulation

The development of hypertension in approximately 80% of lambs bilaterally nephrectomized at about 0.8 term follows a consistent pattern. Within twenty four hours of operation, heart rate is about 10% above and packed cell volume (Table 2) about 9% below that of control lambs.

Between the third and fourth day (Table 1) arterial pressure has risen significantly in half the lambs. Cardiac enlargement has not been found before the seventh day. However, the casual measurements available from nephrectomized lambs before the seventh day arise from cases of accidental death or spontaneous delivery and should perhaps be viewed with caution. Seven days or more following nephrectomy hypertension was only found in lambs with enlarged hearts. The correlation of arterial pressure and relative ventricular weight in these established preparations was close to significance at the 5% level. Thus following bilateral nephrectomy there is a sequence of mild tachycardia and haemodilution preceding a dramatic and sustained rise of arterial pressure. The longer term maintenance of arterial pressure is strongly associated with the increase of the ventricular muscle. Arterial pH is in the normal range in nephrectomized lambs but the data of Table 3 suggests minimal asphyxia in some lambs. The slightly raised PCO_2 levels might be a contributory factor to the tachycardia but the arterial pressures reached by many nephrectomized lambs far exceed those induced by experimental hypoxaemia. (Boddy et al. 1974)

Phentolamine

Three lambs 121 - 130 days gestation received intravenous infusions of phentolamine (5.7 - 13.7 mg for 1 - 1.25 hr) 7 - 10 days post-nephrectomy. One of these lambs was not hypertensive and as in intact lambs there was little fall of arterial pressure (Jones & Ritchie 1978) but the heart rate in all three rose to 250 beats/min or more during the infusion. Arterial PO_2 fell and PCO_2 rose in all three lambs but pH fell in only two. These asphyxial changes were reversible and are summarized for one lamb in Table 5.

Table 5 Phentolamine

Effect of intravenous infusion of phentolamine ∿ 2.2 mg/kg on a nephrectomized fetal lamb 121 days gestation age.

	Before	During	After
Time	10.00	10.45	15.13
Arterial Pressure mm Hg	65	44	68
Heart rate beats/min	170	240	185
PO_2 mm Hg	22	15	27
PCO_2 mm Hg	45	50	34
pH	7.37	7.31	7.39

Perhaps these responses are due to a decrease of systemic peripheral resistance by inhibition of raised sympathetic outflow. This in turn might have reduced the placental fraction of cardiac output.

It is likely that the threshold for arterial baroreceptor stimulation in fetal lambs is above the normal range of arterial pressure in this age group (Dawes, Johnston and Walker in press). However, the pressures seen in hypertensive lambs might be sufficient to make some sustained baroreflex activity likely. It is thus possible that the tachycardia seen in nephrectomized lambs would be considerably greater in the absence of baroreceptor activity. The large further increases of heart rate seen during phentolamine infusion could be due to direct action as in intact lambs (Jones & Ritchie 1978) but the fall of pressure should also attenuate the baroreflexes.

The modest haemodilution and tachycardia seen in nephrectomized lambs are consistent with increased systemic arteriolar sympathetic outflow inferred from the response to phentolamine. It may be that most nephrectomized lambs only avoid significant asphyxia by becoming hypertensive. The relative contributions of increased peripheral resistance and/or increased cardiac output require definition. Unless haemopoiesis is reduced by nephrectomy, the low packed cell volumes may reflect an increased plasma volume. However it seems unlikely that such increase could exceed $\sim$ 6% (cf Table 2).

Two nephrectomized lambs survived nine days without arterial pressure rising above the normal range. One died suddenly in utero. When the other lamb was killed at the end of an acute experiment its heart muscle was found to be in the same range as in normal lambs. Neither of these lambs when alive was distinguishable from other nephrectomized lambs in respect of heart rate, packed cell volume, blood gas tensions or plasma sodium and potassium.

Oedema

Nephrectomized lambs were 40% heavier than intact lambs (Table 3). Some of this difference may be attributable to a preponderance (5/11) of single pregnancies whereas 6/7 in the control group were twin. On the other hand 3 of the nephrectomized lambs were one of triplets. Some of the greater weight of nephrectomized lambs probably represents oedema which the data of Table 4 suggest may account for between 13 and 30%. There is no evidence that bilateral nephrectomy restricts fetal growth.

Ventricular muscle was on average 40% heavier in lambs nephrectomized 7 or more days previously than in controls. It is unlikely that the cardiac muscle was disproportionately oedematous. Clearly fetal reserves must be adequate to support a high rate of growth at least in the cardiac muscle of nephrectomized lambs.

In normal lambs, pressure in the inferior cava was less than 4 mm Hg and often lower. Pressures of up to at least 8 mm Hg were recorded in some nephrectomized lambs though these were not always uniformaly maintained for extended periods. Such pressures may be indicative of cardiac failure. Furthermore the association ($P < 0.02$) between the girth/crown-rump length ratio and relative cardiac weight may also indicate cardiac failure. Nevertheless some anephric lambs are so well adjusted to their circumstances as to survive parturition unassisted and breathe on delivery. On the other hand, one lamb (Table 4) which died four days after nephrectomy was clearly oedematous with a girth/crown-rump length ratio of 0.872 but the percentage of cardiac muscle was only 0.416 of body weight. Arterial pressure was about 45 mm Hg until 5 hours before death when heart rate increased and intermittent rises of pressure occurred. High girth/crown-rump ratio and cardiomegaly have also been found following ureteral occlusion in fetal lambs.

A further possibility is that removal of the maturing fetal kidney removes a supply of a circulating vasodilator. However, in two nephrectomized lambs, the plasma levels of prostaglandins $F_{2\alpha}$, F metabolite and especially of E_2 were somewhat above normal. This makes it unlikely that the systemic hypertension can be attributed to lack of circulating PGE_2.

The occurrence of hypertension in lambs with only the ureters tied and in which plasma renin activity persists rules out angiotensin II as a vasoconstrictor causal agent. Another candidate, vasopressin, was found in plasma from two nephrectomized lambs to be in the normal range.

The responses to nephrectomy and ureteral occlusion may involve the fetal adrenal since plasma cortisol levels are raised (Dutton, Jones, Mott & Roebuck unpublished) and fetal plasma aldosterone is often high (Dutton & Mott 1980). Plasma sodium and potassium are also high in anuric lambs (Dutton & Mott 1979). The responses to fetal nephrectomy therefore probably involve both nervous and humoral elements of which both afferent and efferent pathways require further investigation.

Experiment suggests that fetal hypertension may initiate changes in pulmonary vascular muscle similar to those found in persistent pulmonary hypertension of the newborn (Ruiz et al 1972). It is possible that irrespective of preparation for independent life the fetal kidney performs an important function towards the end of gestation in the maintenance of arterial pressure at its normally low and presumably safe level.

SUMMARY

1. Lambs bilaterally nephrectomized at about 0.8 term have higher heart rates and lower packed cell volumes than normal lambs.

2. Arterial pressure rose to a mean value about 175% control in lambs which survived seven days after nephrectomy. In individual lambs significantly raised pressures were not reached in the absence of cardiac enlargement (ventricular weight/bodyweight %) which averaged 142% of control. Cardiac enlargement has not been seen before the seventh day following nephrectomy.

3. Girth/crown rump length ratio was increased in nephrectomized lambs. This ratio was correlated ($P < 0.02$) with relative cardiac ventricular weight and probably indicates the degree of oedema. A lamb which died in utero 4 days post-nephrectomy was already oedematous, although not hypertensive.

4. Venous pressures in the inferior cava of nephrectomized lambs were above normal. This and the oedema are consistent with incipient cardiac failure. In many lambs this appears to be contained by cardiac enlargement.

5. The raised heart rate, low packed cell volume and the response to phentolamine suggest that sympathetic outflow is increased following nephrectomy in mature fetal lambs.

REFERENCES

Boddy, K., Dawes, G.S., Fischer, R., Pinter, S., and Robinson, J.S. (1974) Foetal respiratory movements, electrocortical and cardiovascular responses to hypoxaemia and hypercapnia in sheep. J. Physiol. 243, 599-618.

Broughton Pipkin, F., Lumbers, E.R. and Mott, J.C. (1974). Factors influencing plasma renin and angiotensin II in the conscious pregnant ewe and its foetus. J. Physiol. 243, 619-636.

Dawes, G.S., Johnston, B.M. and Walker, D.W. Relationship of arterial pressure and heart rate in fetal, newborn and adult sheep. J. Physiol. in press.

Dutton, A. and Mott, J.C. (1979). Hypernatraemia in sheep pregnancy. J. Physiol. 290, 33-34P

Dutton, A., Mott, J.C. and Valdes Cruz, L.M. (1978). Development of hypertension in unanaesthetized fetal lambs after bilateral nephrectomy or ureteral occlusion. J. Physiol. 284, 155-156P.

Dutton, A., and Mott, J.C. (1980) Plasma aldosterone measurements in intact and nephrectomized fetal lambs. J. Physiol. In press.

Jones, C.T. and Ritchie, J.W.K. (1978) The cardiovascular effects of circulating catecholamines in fetal sheep. J. Physiol. 285, 381-393.

Ruiz, U., Piaseck, G.J., Balogh, K., Polansky, B.J. and Jackson, B.T. (1972). An experimental model for fetal pulmonary hypertension. Am.J.Surg. 123, 468-471.

This work was supported by the Wellcome Trust. In addition to my co-authors cited in the references I thank Dr. M. Mitchell for prostaglandin analyses, Dr. D. Rurak for vasopressin analyses and I. Fore and G. Haines for their help. I am grateful to A. Stevens and C. Hanson for surgical assistance and H. Elvidge for care of the animals.

Adv. Physiol. Sci. Vol. 8. Cardiovascular Physiology. Heart, Peripheral Circulation and Methodology
A. G. B. Kovách, E. Monos, G. Rubányi (eds)

THE DISTRIBUTION OF CARDIAC OUTPUT IN PREGNANT SHEEP

R. J. Barnes, R. S. Comline, A. Dobson and M. Silver
Physiological Laboratory, Downing Street, Cambridge CB2 3EG, England

SUMMARY

Cardiac output has been estimated in pregnant and non-pregnant ewes by the thermal dilution and radioactive microsphere techniques. In some ewes microspheres were injected into the foetus to assess placental blood flow. Cardiac output in the ewe rose from 4131 ± 135 ml/min (121.5 ± 3.9 ml/kg/min) in non-pregnant animals to 6025 ± 403 ml/min (156.7 ± 7.9 ml/kg/min)near term. The major increase in output occurred after about 90 days. Insufficient data are available at 30 days gestation but at 60 days the cardiac output was significantly higher than in non-pregnant ewes. Amongst individual organ blood flows only mammary gland and uterine blood flow in the maternal circulation showed a statistically significant gestational trend. The main increase in uterine flow occurred after about 90 days and in mammary flow after about 120 days gestation. Uterine and umbilical flow in the control animals was within the range reported previously. In contrast, in ewes carrying post-mature adrenalectomised foetuses while uterine blood flow/(kg uterus and contents) was in the low normal range, umbilical blood flow/(kg foetus) was about half that found in normal foetuses or in adrenalectomised foetuses examined just before normal term. In hypophysectomised fetuses the umbilical flow/(kg weight of foetus) was low while in their mothers the uterine flow per unit weight was half that found in the other groups. In normal animals uterine blood flow before 120 days appeared to keep pace with the growth of the uterus and its contents but after 120 days both uterine and umbilical flows per unit weight were lower.

INTRODUCTION

Weber (1850), Bayliss and Starling (1894), Starling (1918) and more recently Guyton et al (1973) have provided analyses of the circulatory system which allows us to make certain predictions about the behaviour of the system in different pathological and physiological circumstances. There has been extensive investigation of the effects of exercise on cardiac output (a condition in which acute changes in metabolic demand may be expected to produce rapid changes in cardiac function) but there has been relatively little investigation of the effects of pregnancy on cardiac output and its distribution (pregnancy being a condition in which more gradual adaptation to metabolic demands may be anticipated). The

present investigation defines the extent of the changes in cardiac output during pregnancy in ewes with normal foetuses and describes the changes in blood flow to individual maternal tissues in these animals. We have also examined uterine and umbilical blood flows in ewes carrying normal, hypophysectomised or bilaterally adrenalectomised foetuses.

METHODS

37 pregnant and 9 non-pregnant Welsh sheep were used in the present study. The ewes were prepared for study in one of the following ways.

1) Implantation of thermistor and catheters for thermal dilution measurements of cardiac output. Under Halothane (I.C.I. Ltd.) anaesthesia a catheter was introduced non-occlusively through a small incision in the right jugular vein until its tip lay at or near the atrio-caval junction. The position of this catheter was confirmed at post-mortem. A second catheter with a small bead thermistor (U23US ITT Ltd.) mounted in the tip was introduced into the descending aorta through either the left carotid artery or the right femoral artery so that the catheter tip lay in the descending thoracic aorta. The injection of a small quantity (5-10 ml) of saline at room temperature into the right atrium produced a fall in blood temperature which was detected at the bead thermistor. A small analogue computer (Bower and Ead, 1976) was used to compute the cardiac output from the recorded temperature signals and a knowledge of the injected volume. The details of the method have been described (Barnes et al, 1980). Readings from individual animals taken at least 5 days after surgery and averaged over a period of 4-7 days provide single points in Figure 1.

2) Foetal hypophysectomy and adrenalectomy. Both of these techniques have been described in full elsewhere, Comline et al. (1970) and Barnes et al. (1977).

3) Catheterisation of ewes and foetuses. Ewes with normal foetuses and with operated foetuses were prepared for the injection of radioactively labelled microspheres. The techniques for implantation and maintenance of catheters have been described (Comline and Silver, 1970; 1972). In those ewes in which maternal cardiac outputs were to be measured 2 PTFE catheters (Southern Syringe Co. Ltd., 1.5 mm o.d., 1 mm i.d.) were introduced through branches of the right femoral artery centrally so that the tip of one, the injection catheter, lay within the left ventricle while the tip of the other lay in the abdominal aorta just above the bifurcation. Foetuses in which umbilical flows were measured were prepared with inferior vena caval catheters for injection and femoral arterial catheters for sampling. In all experiments at least 4 days were allowed to elapse between surgery and the first measurement of blood flow. The blood gas tensions, PCV and pH were measured as a routine and if these were outside the normal range (Barnes et al. 1977) flow measurements were not made. At the end of each experiment the ewe and foetus were anaesthetised with sodium pentobarbitone (May & Baker Ltd.) and the ewe was exsanguinated through a carotid arterial catheter. All visceral organs, the heart, the brain, the endocrine glands and the mammary gland were removed, cleaned and placed in weighed polypropylene pots (Dines Plastics Ltd.). The pots were reweighed and organ weights obtained by subtraction. The foetus was treated similarly to the ewe but because the arterial reference sample was obtained from the descending aorta

below the entry of the ductus anteriosus only blood flows to the viscera, the placenta and hindquarters could be estimated.

Blood flow by microspheres

Blood flow was determined by the reference organ technique (Makowski et al. 1968) using withdrawal rates of 25 ml/min in the ewe and 4.4 ml/min in the foetus. The volume (<15 ml) withdrawn from a fetus was replaced by a similar volume of dextran saline. Microspheres of 15μ diameter (Riker, 3Ms or N.E.N.) labelled with up to six different nuclides were used in each animal. At least 1 million spheres were contained in a tightly coiled spiral of P.V.C. Tubing. This was counted as a point source some 80 cm from a 2 inch NaI (Tl) crystal before and after flushing through with dextran solution to determine by difference the amount injected. Tissue samples were counted between a pair of 6 inch crystals in a whole body counter. The general technique (Dobson, 1979) has been improved in one respect. The effect of tissue mass on the gamma spectrum of each isotope was determined, and due allowance made for this in solving for the activities present. The error correction for the effect of tissue mass was not trivial and details of this method will be published elsewhere (Dobson, in preparation). All blood flows were calculated using IBM 370/165 facilities in the University of Cambridge, and Fortran IV programs. As with the thermal dilution studies the results from an individual animal averaged over a period from 1-3 days provide a single data point on each relevant Figure.

RESULTS

Normal ewes: cardiac output

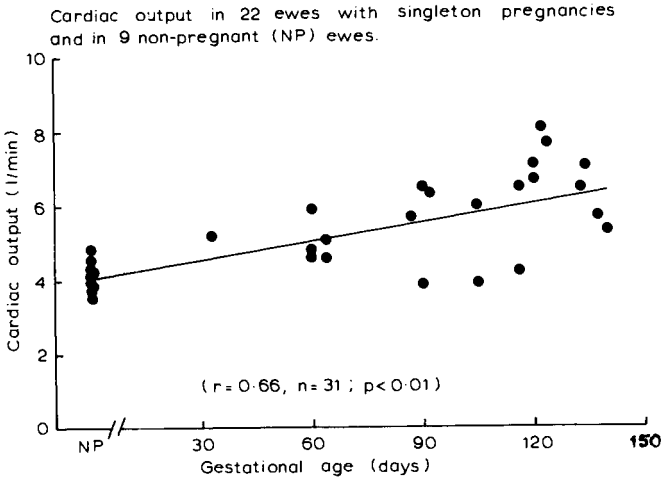

Figure 1. Cardiac output (litre/min) plotted as a function of duration of pregnancy. The regression line shows a highly statistically significant correlation between output and gestational age.

Preliminary analysis of the data showed no significant difference between cardiac output measurements obtained by thermal dilution and those obtained by microsphere injection. All cardiac output data have therefore been combined. Cardiac output in the non-pregnant animals was 4131 ± 135 ml/min (mean ± SEM, n = 9). The output rose significantly by 48% during pregnancy. The cardiac output rose progressively throughout gestation, but if the cardiac output be expressed in terms of body weight of the ewe it is only in the last third of gestation that the output per unit weight is significantly higher than in non-pregnant animals (Figure 2). Much of the early increase in output is therefore related to the increase in weight of the ewe during this part of pregnancy.

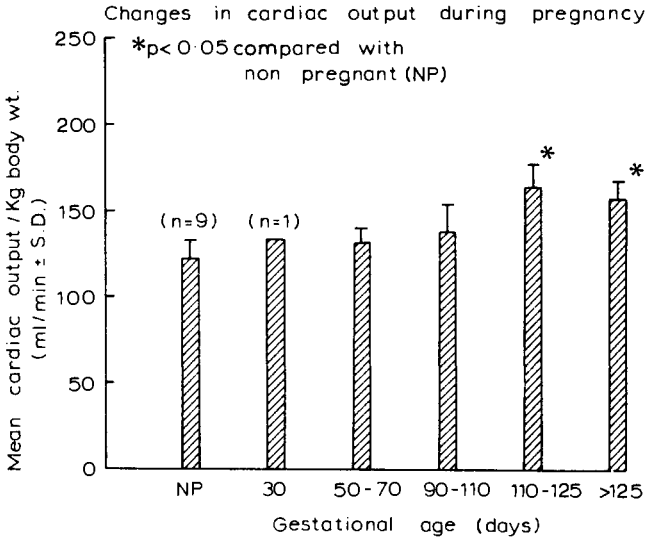

Figure 2. The cardiac output per kg body weight in six groups of ewes at different stages of pregnancy. The differences between the mean values in the two groups of foetuses older than 110 days and the value in the non-pregnant animals are significant ($p > 0.05$).

Normal Ewes: distribution of cardiac output

Blood flow to non-sexual tissues

In non-pregnant sheep the mean blood flow to some of the non-reproductive tissue was 305 ± 22 ml/min (kidneys), 925 ± 110 ml/min (portal tract), 142 ± 18 ml/min (heart) and 102 ± 12 ml/min (brain). The flows to these organs showed no significant gestational trends (Figure 3) although flow to kidney and gut in particular might have been expected to increase during pregnancy. The wide variation in portal tract blood flows may reflect the difficulties inherent in examining a system with such

a wide range of individual organ flows (Barnes, Comline and Dobson, in preparation. In the whole series of pregnant sheep the renal blood flow (635 ± 46 ml/min) was significantly higher than in the non-pregnant sheep (305 ± 22 ml/min) but while the mean portal flow appeared higher (1125 ± 116 ml/min as against 925 ± 110 ml/min) the wide range of the values in both series means that the difference is not statistically significant. Coronary and brain blood flows were very similar in pregnant and non-pregnant animals.

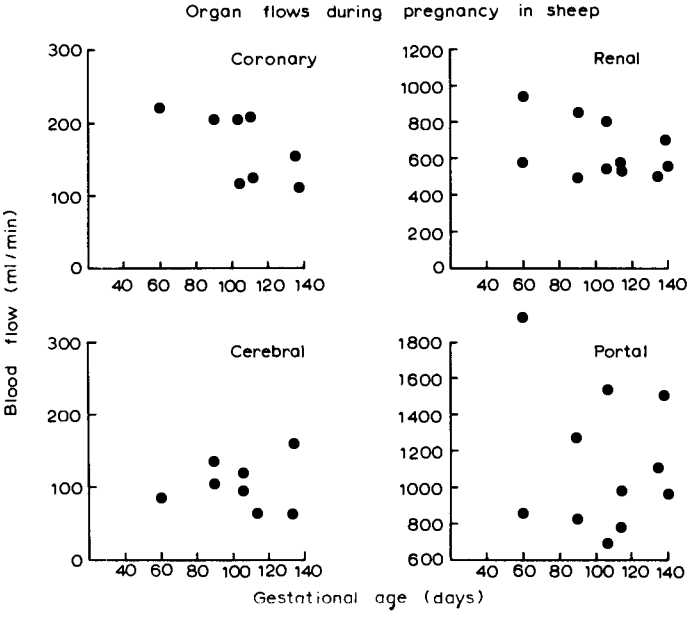

Figure 3. Organ blood flows during pregnancy in sheep.

Blood flow to sexual tissues

Mammary gland

Mammary gland blood flow increased very slowly from the non-pregnant flow rate (less than 15 ml/min) until about 120 days gestation and thereafter rose more rapidly, especially in the ten days before delivery (Figure 4). This confirms the findings of Burd et al. (1975). The flow per unit weight of tissue increased from about 10 ml/100 g tissue/min at 60 days to 30 ml/100 g tissue/min near term. The correlation between gestational age and mammary blood flow per unit weight of tissue was statistically significant ($r = .804$, $n = 11$).

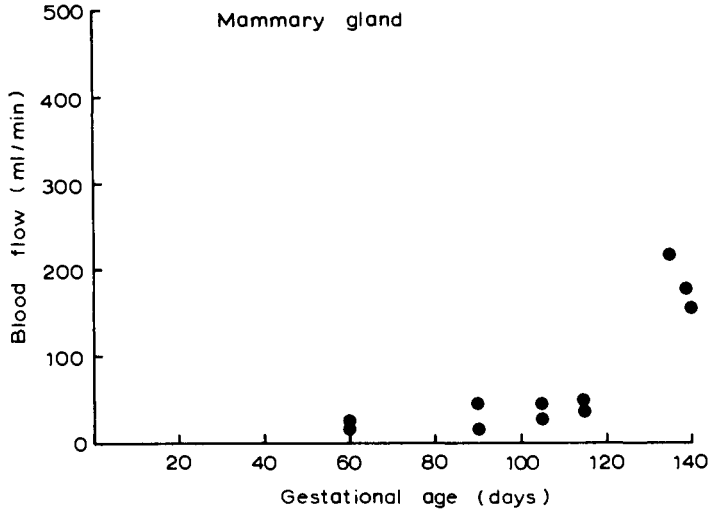

Figure 4. Mammary gland blood flow (ml/min) plotted against gestational age.

Uterine blood flow

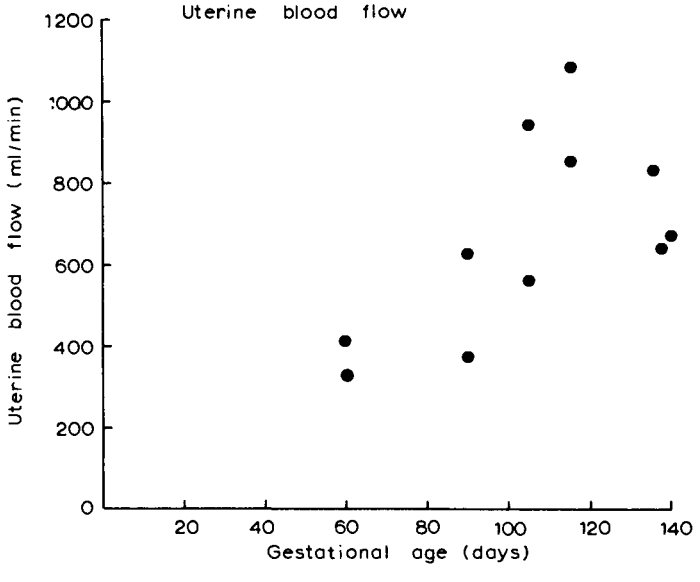

Figure 5. Uterine blood flow (ml/min) plotted against gestational age.

Uterine blood flow increased from less than 10 ml/min (60 ml/100 g tissue/min) in the non-pregnant animal to between 1 and 2 litres per min near term (Figure 5). Uterine blood flow does not increase linearly but instead (Barron, 1970; Rosenfeld et al. 1974) tends, at least until about 130 days gestation, to increase in parallel with the growth of the uterus and its contents. In the oresent study the mean uterine flow/kg uterus and contents was 300 ml/min at 100-130 days but in three ewes was only 200 ml/kg/min nearer to term.

Umbilical blood flow

Umbilical blood flow was measured by the microsphere technique in control foetuses between 100 days gestation and term and in bilaterally adrenalectomised or hypophysectomised foetuses either shortly before normal term or in the postmature period (Table 1). In normal foetuses between 100 and 120 days the mean flow was 231 $\pm$ 17 ml/kg foetus/min while in older foetuses the mean flow was 126 ml/kg/min. In postmature hypophysectomised foetuses and in adrenalectomised foetuses near term umbilical flow was similar to values found in the controls near term. In the postmature adrenalectomised foetuses umbilical flow per unit weight was about half that found in the other groups.

Uterine blood flow in ewes with operated foetuses

In two ewes with hypophysectomised foetuses the uterine blood flow per unit weight was less than half that found near term in either normal ewes or those with adrenalectomized foetuses. In ewes carrying adrenalectomized foetuses the uterine flow per unit weight was within the range found for normal ewes in late gestation.

Table 1

Uterine and umbilical blood flow in normal and operated groups of animals

Animals	Uterine blood flow ml/kg uterus and contents/min			Umbilical blood flow ml/kg foetus/min		
	Mean	SEM	n	Mean	SEM	n
Normal Foetuses						
90-120 days	321	29	5	231	17	4
120 days	209	20	6	126	-	2
Hypophysectomised						
156 days	112	-	2	135	15	4
Adrenalectomised						
130-140 days	338	87	3	164	20	3
156 days	219	76	3	76	4	5

DISCUSSION

Clapp (1978) investigated the relationship between cardiac output and the increase in uterine blood flow during pregnancy in acutely anaesthetised ewes lying on their sides. In these animals he found that 75% of the increased cardiac output could be accounted for by the increased perfusion of the uterine tissues. Rosenfeld et al. (1974) investigated the changes in blood flow to the reproductive tissues in conscious ewes during pregnancy using a radioactive microsphere technique but did not measure cardiac output at the same time. Subsequently (Rosenfeld et al, 1976) they did estimate uterine flow as a proportion of cardiac output in a number of animals but they did not give the gestational ages of these animals so that it is impossible to compare their results directly with the present study.

The results presented here indicate that there is an increase of about 3% in cardiac output above the values found in non-pregnant animals, and that this increase occurs throughout pregnancy. There are not sufficient data to be certain that the first sixty days of gestation show a gradual progressive rise in output but preliminary data using implanted electromagnetic flow probes (Barnes, unpublished) support this contention.

There is a suggestion in the present results that cardiac output may reach a plateau at about 110-130 days and thereafter may even decline slightly during the last part of pregnancy. Possibly the adaptive capacity of the maternal circulation is exceeded in this period. In this respect it is important to note that uterine blood flow per unit weight of uterus and its contents decreased in the last part of gestation in the present study. The suggestion that the uterine blood flow is more closely related to the growth of the uterus and its contents than to the growth of the placenta (Barron, 1970) is supported by this and many other studies but we now have evidence to suggest that the growth of the uterus and its contents may exceed the capacity of the uterine blood flow to adapt. The observations of Liggins and Kennedy (1968), Drost and Holm (1968) and Barnes, et al. (1977) that the ewe may support prolonged pregnancy and growth in hypophysectomised and adrenalectomised foetuses suggested that the uterus and its circulation had an almost infinite adaptive capacity. The present observations on normal foetuses and on operated foetuses cast doubt on this assumption.

The blood flows reported in the control foetuses and ewes in the present study were within the range of values found in the literature (for references see Silver, 1976). The very low flow in the umbilical circulation in the adrenalectomised foetuses deserves comment. In order to test the possibility that the low flow was an artefact caused by shunting the small (15μ) microspheres, sequential flow determinations, within 10 minutes, were made with 15, 50 and 100μ microspheres in three normal and three adrenalectomised foetuses. The blood flows measured by the three sizes of sphere were within 5% in each case.

We conclude that the differences between the uterine and umbilical flows in these groups are genuine and the investigation of these phenomena should provide useful infomation about the normal control of uterine flow. In particular it is very interesting that foetal hypophysectomy can effect maternal uterine flow.

The observation (Clapp, 1978) that uterine flow can account for 75% of the increase in cardiac output may depend upon the precise conditions of the experiment. In the present study the contribution of raised uterine blood flow to the cardiac output increment was nearer to 50%. The difference between the two studies may well be attributed to the combined effects of anaesthesia and 72 hours starvation in the experiments of Clapp.

An apparent 20% difference between the mean blood flows to the portal tract in the pregnant and non-pregnant state was not statistically significant but the wide variation in blood flow to different parts of the gut and in total portal blood flow at different stages of a feeding-fasting cycle in the ruminant (Barnes et al, in preparation) suggests the possibility that a real increase in the vascular supply to the gastro-intestinal tract during gestation may be hidden by much larger feeding related changes in flow. We are now conducting a study of gut blood flow in pregnant and non-pregnant ewes with careful control of dietary and feeding schedules. If there is a significant difference in gastro-inestinal blood flow between the two groups then this, together with the raised renal and mammary blood flows, may account for much of the increment in cardiac output which cannot be accounted for by the raised uterine perfusion.

We are grateful to the Welcome Trust for generous support of this study.

REFERENCES

Barnes, R.J., Comline, R.S. and Silver, M. (1977). The effects of unilateral adrenalectomy or hypophysectomy of the foetal lamb in utero. J. Physiol. 274, 429-447.

Barnes, R.J., Bower, E.A. and Rink, T.J. (1980). Haemodynamic responses to stimulation of the cardiac autonomic nerves in the anaesthetised cat with closed chest. J. Physiol. 299, 55-73.

Barron, D.H. (1970). The environment in which the fetus lives: lessons learned since Barcoft. Chapter VI in Prenatal Life. Wayne State. University Press. Detroit.

Bayliss, W.M. and Starling, E.H. (1894). Observations on venous pressures and their relationship to capillary pressures. J. Physiol. 16, 159-202.

Bower, E.A. and Ead, H.W. (1976). An extrapolating analogue computer for measurement of cardiac output by thermodilution. J. Physiol. 263, 108-110P.

Burd, L.I., Lemons, J.A., Makowski, E.L., Battaglia, F.C., and Meschia, G. (1975). Relationship of mammary blood flow to parturition in the ewe. Amer. J. Physiol. 229, 797-800.

Clapp, J.F. III (1978). Cardiac output and uterine blood flow in the pregnant ewe. Am. J. Obstet. Gynecol. 130, 419-423.

Comline, R.S. and Silver, M. (1970). Daily changes in foetal and maternal blood of conscious pregnant ewes with catheters in umbilical and uterine vessels. J. Physiol. 209, 587-586.

Comline, R.S., Silver, M. and Silver, I.A. (1970). Effect of foetal hypophysectomy on catecholamine levels in the lamb adrenal during prolonged gestation. Nature, London, 225, 739-740.

Comline, R.S. and Silver, M. (1972). The composition of foetal and maternal blood during parturition in the ewe. J. Physiol. 222. 233-356.

Dobson, A. (1979). The choice of models relating tritiated water absorption to subepithelial blood flow in rumen of sheep. J. Physiol. 297, 111-121.

Drost, M. and Holm, L.W. (1968). Prolonged gestation in ewes after foetal adrenalectomy. J. Endocrinol. 40, 293-296.

Guyton, A.C., Jones, C.E. and Coleman, T.G. (1973). Cardiac output and its regulation. W.B. Saunders Co. Philadelphia, London, Toronto.

Higgins, G.C. and Kennedy, P.C. (1968). Effects of electrocoagulation of the foetal lamb hypophysis on growth and development. J. Endocrinol. 40, 371-381.

Makowski, E.L., Meschia, G., Droegemueller, W. and Battaglia, F.C. (1968). Measurements of umbilical arterial blood flow to the sheep placenta and fetus in utero. Circulation Res. 23, 623-631.

Rosenfeld, C.R., Morriss, F.H.Jr., Makowski, E.L., Meschia, G. and Battaglia, F.C. (1974). Circulatory changes in the reproductive tissues of ewes during pregnancy. Gynecol. Invest. 5, 252-268.

Rosenfeld, C.R., Barton, M.D. and Meschia, G. (1976). Effect of epinephrine on distribution of blood flow in the pregnant ewe. Am. J. Obstet. Gynecol. 124, 156-163.

Silver, M. (1976). Fetal energy metabolism. In: Foetal Physiology and Medicine eds. Beard, R.W. and Nathanielsz, P.W. W.B. Saunders, London.

Starling, E.H. (1918). The Linacre Lecture on the Law of the Heart. Longmans, Green and Co. London.

Weber, E.H. (1850). Ueber die Anwendung der Wellenlehre auf die lehre vom kreislauf des blutes und insbesondere auf die pulslehre. Ber. Verh. sächs. Akad. Wiss. 164-204.

Adv. Physiol. Sci. Vol. 8. Cardiovascular Physiology. Heart, Peripheral Circulation and Methodology
A. G. B. Kovách, E. Monos, G. Rubányi (eds)

CARDIOVASCULAR RESPONSES OF THE FETAL PIG TO AUTONOMIC STIMULATION

A. A. Macdonald* and B. Colenbrander
with the technical assistance of U. Biermann
Institut für Tierzucht und Tierverhalten, 3057 Neustadt 1, FRG

INTRODUCTION

The functional status of the cardiovascular system of the pig fetus is unknown. However, the presuckling behaviour of the piglet suggests that it is born with a fairly mature ability to maintain cardiovascular homeostasis; each piglet in the litter has to contend with energetic competition from its siblings for the position at the udder giving best access to the supply of milk (Fraser, Thompson, Ferguson and Darroch, 1979). It is therefore surprising that when the newborn piglet is anaesthetised, and components of its cardiovascular system are examined, that there is physiological evidence of functional immaturity (see literature reviewed by Gootman, Buckley and Gootman, 1978). Anaesthesia and surgical stress are known to have a comprimising effect on the autonomic nervous system (Korner, 1971; Kirchheim, 1976) and thereby may have influenced the results of these acute studies. We therefore chose to investigate the cardiovascular physiology of the unanaesthetised piglet, before birth, and to measure its response to the autonomic nervous system agonists acetylcholine, isoprenaline and methoxamine.

MATERIALS AND METHODS

Chronic preparation

We anaesthetised seven German Landrace sows with Azaperone and Methomidate (Janssen Pharmaceutica), and through a lateral abdominal laparotomy exposed a portion of the uterus in which lay one fetus. We made an incision through the uterine and placental tissues and inserted polyvinyl catheters ID 0.5 mm OD 1.0 mm into the fetal carotid artery and jugular vein such that the tips lay in the brachiocephalic artery and superior vena cava respectively. A polyvinyl catheter ID 1.0 mm OD 2.0 mm was placed in the amniotic cavity and the wound

* Present address: Department of Veterinary Anatomy, State University Utrecht, Yalelaan 1, 3508 TD Utrecht, The Netherlands.

sutured closed (fig. 1). In three sows a second fetus was likewise catherised. Antibiotics were given to the sow intravenously (1,000,000 U of penicillin G and 500 mg of Kanamycin) and to the fetus intraamniotically (500,000 U of penicillin G and 250 mg of Kanamycin) on the day of surgery and every 1-2 days thereafter.

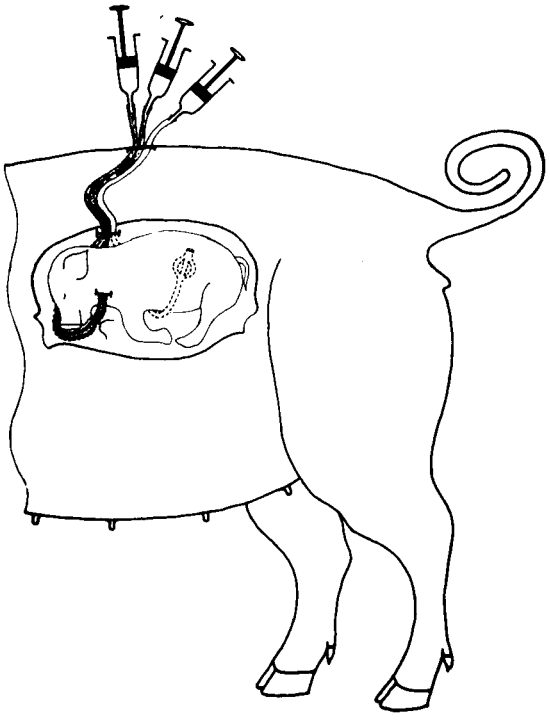

Fig. 1 A schematic diagram of the pig fetus in utero with polyvinyl catheters placed chronically in the carotid artery, jugular vein and amniotic cavity.

Observations and analyses

We studied the fetuses at least 3 days after surgery when they were aged between 103 and 107 days of gestation, and body weight was estimated to be about 1 kg. Fetal arterial blood and intraamniotic pressures were measured with Statham P23 Db pressure transducers and the arterial pressures reported with amniotic pressures as zero. Heart rate was obtained electronically from the blood pressure signal. All records of pressure and heart rate were made on a Beckman chart recorder. At the beginning of each study we drew a 0.6 ml sample of fetal arterial blood and measured pH and blood gases using an Instrument Laboratories IL 431 blood gas analyzer with the appropriate electrodes. Hematocrit was measured following microcapillary tube centrifugation. We measured the fetal blood pressure and heart rate responses following intravenous injection of the parasympathetic agonist acetylcholine (10 μg) and the β and α sympathetic agonists isoprenaline (0.2 μg) and methoxamine (0.5 mg) respectively. These observations were compared with the responses to injections of equivalent volumes (< 0.5 ml) of saline as controls.

Results were summarized as means ± SEM. Statistical tests were done by analysis of covariance and unpaired t test, except for sets of paired observations which were evaluated by paired t test (Zar, 1974).

RESULTS

Blood gases

Fetal arterial pH was 7.38 ± 0.03, Po_2 was 22 ± 1, Pco_2 was 43 ± 1 and haematocrit was 28 ± 1.

Blood pressure and heart rate

The control arterial mean blood pressures averaged 58 ± 2.6 mmHg. The fetal heart rate before each experiment averaged 166 ± 4 beats/min.

Response to saline

There were no measurable changes in fetal arterial blood pressure or heart rate in response to injections of less than 0.5 ml saline.

Response to acetylcholine

The peak fetal blood pressure and heart rate responses to intravenous injections of acetylcholine are illustrated in figure 2. Mean arterial blood pressure decreased ($P < 0.05$) by an average of

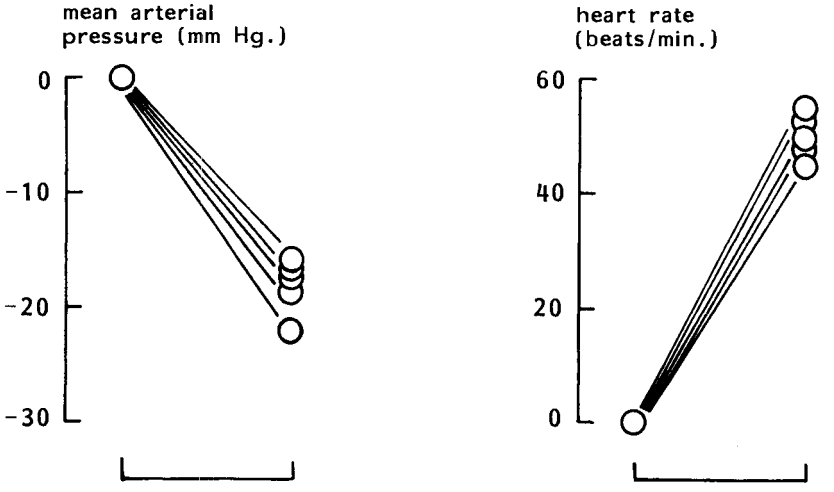

Fig. 2 The peak changes in mean arterial blood pressure and heart rate of pig fetuses in utero to an intravenous injection of 10 µg of Acetylcholine, the parasympathetic agonist.

16 ± 1 mmHg which represented a fall of 25 ± 2% from control blood pressures. This resulted in a reflex tachycardia which averaged 50 ± 2 beats/min., an increase of 31 ± 1% over control heart rate values ($P < 0.05$).

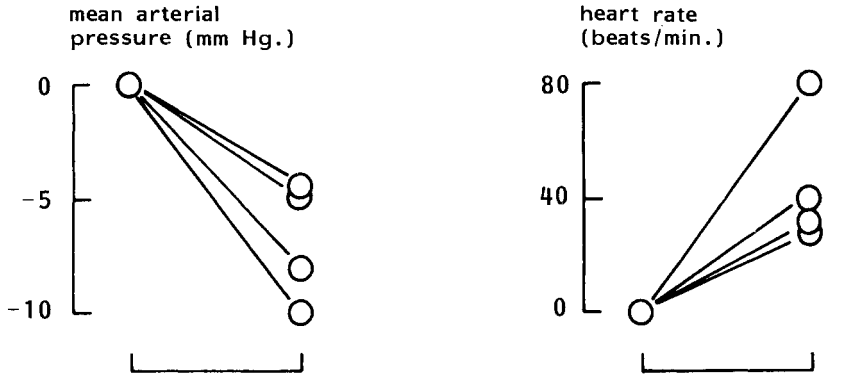

Fig. 3 The peak changes in mean arterial blood pressure and heart rate of pig fetuses in utero to an intravenous injection of 0.2 µg Isoprenaline, the β sympathetic agonist.

Response to isoprenaline

Fetal heart rate increased in response to isoprenaline as indicated in figure 3. The rise in heart rate ($P < 0.05$) averaged 46 ± 13 beats/min., an increase over control values of 25 ± 6% . Fetal blood pressure decreased by 7 ± 1 mmHg, a decrease from control values of 11 ± 1% ($P < 0.05$).

Response to methoxamine

There was a consistent increase in fetal blood pressure in response to methoxamine as may be seen in figure 4. The rise in mean arterial blood pressure averaged 9 ± 2 mmHg or 18 ± 3% over control values ($P < 0.05$). There was no consistent pattern of change in heart rate in response to methoxamine.

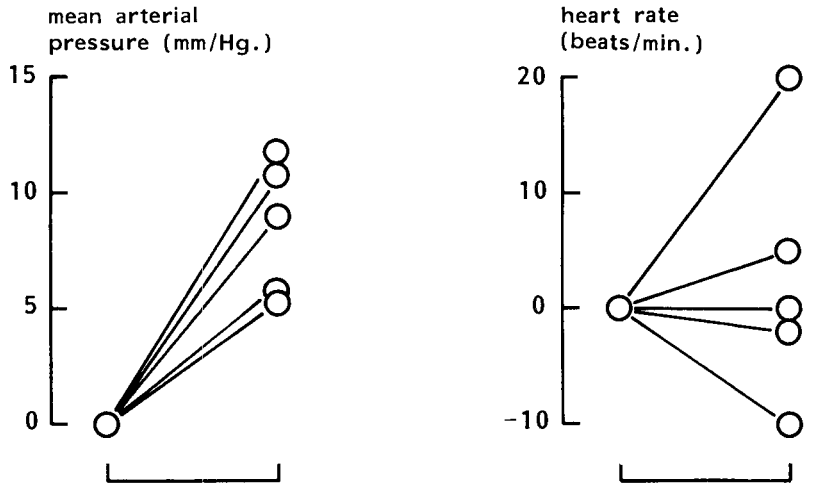

Fig. 4 The peak changes in mean arterial blood pressure and heart rate of pig fetuses in utero to an intravenous injection of 0.5 mg Methoxamine, the α sympathetic agonist.

DISCUSSION

The mean arterial blood pressure measured at the start of each of the present series of fetal studies were lower than those found in the neonatal piglet by LeBlanc and Mount (1968), Gruskin, Edelmann and Yuan (1970) and Buckley, Gootman, Gootman, Reddy, Weaver and Crane (1976), but higher than those in fetuses at 85 days gestation (Macdonald, Rudolph and Heymann, unpublished observations). Thus the pattern if increasing blood pressure with advancing age described in the neonatal pig by Gruskin et al (1970) and Buckley et al (1976) would seem to be the continuation of a trend begun in utero.

The average of the control fetal heart rates was lower than those reported for anaesthetised neonates by Buckley et al (1976) but within the range of values from uncatheterised pig fetuses measured using an ultrasonic Doppler method (Fraser, Nagarathnan and Callicott, 1971). It was concievable that the faster heart rate after birth resulted from the depressive action of anaesthetic on endogenous vagal tone (Korner, 1971; Kirchheim, 1976). However, von Engelhardt (1966) in his review of heart rates from unanaesthetised neonatal piglets also quotes faster heart rates than seen in the present study. It is conceivable that the differences in heart rate between the preterm fetus and neonate may be due to the larger blood volume of the fetus resulting from the placental circulation.

In earlier studies on the anaesthetised newborn piglet Adams, Hirvonen, Lind and Peltonen (1958) observed a decrease in arterial pressure in response to an intravenous injection of acetylcholine. Our observations on the unanaesthetised fetal pig support and extend these observations, demonstrating by the vasodilatatory response that peripheral cholinergic receptors are present before birth. It is interesting to note, however, that although acetylcholine produced a comparable hypotension in the lamb fetus, there was a bradycardic heart rate response in that species; not until one to two weeks after birth was tachycardia observed in the lamb (Nuwayhid, Brinkman, Su, Bevan and Assau, 1975). The pig fetus, however responded with a reflex increase in heart rate when arterial pressure decreased, as seen in the present study, or following hypotension induced by haemorrhage (Biermann, Forsling, Ellendorff and Macdonald, 1979).

Intravenous injection of the β sympathetic agonist isoprenaline stimulated the heart of the fetal piglet directly. The tachycardia produced was similar in magnitude to the reflex response following acetylcholine administration. Adams et al (1958) stated that tachycardia seldom resulted from the administration of adrenaline to the anaesthetised newborn piglet although the more recent studies of Gootman et al (1978) demonstrated the converse. When the latter authors used the specific β sympathetic agonist isoproterenol they observed an increase in heart rate which was comparable to that seen in the present study. Competence of the heart to respond to β sympathetic stimulation is thus present in the preterm pig fetus.

The fetal hypotension seen in response to isoprenaline was similar to that observed in the piglet immediately after birth (Gootman et al, 1978), and indicated the presence of β receptors in the peripheral circulation of the pig fetus.

That α adrenergic receptors are also present in the pig fetus was demonstrated by the hypertensive reaction to methoxamine. Earlier studies by Adams et al (1958), LeBlanc and Mount (1968) and Gootman et al (1978) clearly showed that both norepinephrin and epinephrin had vasopressor effects on the vasculature of the newborn piglet. That both substances are present in the adrenal of the newborn pig has been demonstrated by Stanton and Woo (1978). Although catecholamine concentrations appear not to have been measured in the tissues of fetal pigs, it is known that the enzymes responsible for their inactivation are present before term (Stanton, Corneto, Mersmann, Brown and Mueller, 1975).

ACKNOWLEDGEMENTS

We wish to acknowledge with gratitude that this work was supported by the Deutsche Forschungsgemeinschaft and by a NATO Science Fellowship to B.C. granted by the Netherlands Organisation for the Advancement of Pure Research (Z.W.O.).

REFERENCES

Adams, H., Hirvonen, L., Lind, J. and Peltonen, T. (1958). Physiologic studies on the cardiovascular status of newborn pigs. Etudes Néo-Natales 7, 53-61.

Biermann, U., Forsling, M.L., Ellendorff, F. and Macdonald, A.A. (1979). The cardiovascular responses of the chronically catheterised pig fetus to infused lysine vasopressin and to haemorrhage. J. Physiol. Lond. 296, 28-29P.

Buckley, N.M., Gootman, P.M., Gootman, N., Reddy, G.D., Weaver, L.C. and Crane, L.A. (1976). Age-dependent cardiovascular effects of afferent stimulation in neonatal pigs. Biol. Neonate 30, 268-279.

Engelhardt, W. von (1966). Swine cardiovascular physiology - a review. In: "Swine in Biomedical Research" (eds. L.K. Bustad, R.O. McClellan and M.P. Burns) Battelle-Northwest: Richland.

Fraser, A.F., Nagaratnam, V. and Callicott, R.B. (1971). The comprehensive use of Doppler ultra-sound in farm animal reproduction. Vet. Rec. 88, 202-205.

Fraser, D., Thompson, B.K., Ferguson, D.K. and Darroch, R.L. (1979). The "teat order" of suckling pigs. 3. Relation to competition within litters. J. Agric. Sci. 92, 257-261.

Gootman, P.M., Buckley, N.M. and Gootman, N. (1978). Postnatal maturation of the central neural cardiovascular regulatory system. In: "Fetal and Newborn Cardiovascular Physiology, Vol. 1. Developmental Aspects" (eds. L.D. Longo and D.D. Reneau) p. 94-152. Garland STPM Press: New York.

Gruskin, A.B., Edelmann, C.M. and Yuan, S. (1970). Maturational changes in renal blood flow in piglets. Pediat. Res. 4, 7-13.

Kirchheim, H.R. (1976). Systemic arterial baroreceptor reflexes. Physiol. Rev. 56, 100-176.

Korner, P. (1971). Integrative neural cardiovascular control. Physiol. Rev. 51, 312-367.

LeBlanc, J. and Mount, L.E. (1968). Effects of noradrenaline and adrenaline on oxygen consumption rate and arterial blood pressure in the newborn pig. Nature 217, 77-78.

Nuwayhid, B., Brinkman, C. R., III, Su, C., Bevan, J.A., and Assau, N.S. (1975). Systemic and pulmonary hemodynamic responses to adrenergic and cholinergic agonists during fetal development. Biol. Neonate 26, 301.

Stanton, H.C., Corneto, R.A., Mersmann, H.J., Brown, L.J. and Mueller, R.L. (1975). Ontogenesis of monoamine oxidase and catechol-o-methyl transferase in various tissues of domestic swine. Arch. Int. Pharmacodyn. 213, 128-144.

Stanton, H.C. and Woo, S.K. (1978). Development of adrenal medullary function in swine. Am. J. Physiol. 234, E137-E145.

Zar, J.H. (1974). Biostatistical analysis. Prentice Hall: Eaglewood Cliffs.

Adv. Physiol. Sci. Vol. 8. Cardiovascular Physiology. Heart, Peripheral Circulation and Methodology
A. G. B. Kovách, E. Monos, G. Rubányi (eds)

THE ROLES OF PARASYMPATHETIC AND ß-ADRENERGIC ACTIVITY IN BEAT TO BEAT FETAL HEART RATE VARIABILITY (FHRV)

J. T. Parer, R. K. Laros, D. C. Heilbron and J. R. Kreuger

Department of Obstetrics, Gynecology, and Reproductive Sciences, and Cardiovascular Research Institute, University of California, San Francisco, San Francisco, California 94143, USA

Fetal heart rate variability (FHRV) is generally accepted as a useful index of fetal wellbeing. It is our opinion, however, that clinical FHR interpretation will remain stagnant until more is learned about the basic mechanisms and regulation of fetal heart rate patterns and FHR variability.

There is a widely held and frequently stated belief--largely undocumented-- that FHRV is the result of interactions of the activity of two inputs to the heart, that from the parasympathetic and that from the sympathetic system. We have tested this theory in the postsurgical, acutely hypoxic monkey fetus.

Definitions and methods

FHRV is measured using a non-averaging cardiotachometer, in our studies a Hewlett Packard Clinical FHR monitor, which displays a heart rate equivalent for each interval between beats, generally at a specific paper speed of 3 cm/min and results in patterns which become recognizable to the clinician. Heart rate scaling is 30 bpm/cm, and is used throughout this discussion. Heart period discrimination is 1 msec.

Two classes of variability are recognized: firstly, short-term variability, or a difference in interval between adjacent or several beats which appear as jitter. Secondly, long-term variability, or irregular, crude sinewave-like oscillations with a frequency of about 3 to 6 per minute.

In the clinical setting, variability is subjectively defined as normal, decreased, or absent.

The presence of variability has been assumed, and is empirically confirmed, to denote absence of asphyxia. The absence of FHRV, however, may be due to asphyxia or a large number of nonasphyxic causes, e.g. drugs or neurologic anomalies.

A number of authors have attempted to quantitate each type of FHRV. At least 8 different indices have been used to date by our count. We have previously compared several of these indices (1) and have shown that when used to quantitate either simulated pure short term or long term FHRV, the indices of the Dutch workers, de Haan, van Bemmel, et al. (2), are the most sensitive and specific, exhibiting the least interdependence.

De Haan et al.'s indices are derived with computer assistance by plotting consecutive time intervals against each other. Two functions are derived to quantitate each type of variability. The first, the argument (θ), is the angle formed by the line from each plotted point to the

origin. The magnitude of this angle is sensitive to sporadic changes in successive heart beat intervals, and is thus used as an index of short term or beat-to-beat variability.

The modulus is another derived function. This is the length of the line from the plotted point to the origin. Its magnitude is sensitive to persistently increasing or decreasing heart interval periods, so it is used as an index of long term variability.

To quantitate each type of variability, frequency histograms of the values of argument or modulus are prepared, and the interquartile range calculated. For example, if values of the argument are clustered around the 45° point, this signifies very little STV. On the other hand, a moderately well-distributed histogram of the frequency of the modulus values would signify a moderate degree of LTV.

We have previously studied and reported the influence of acute hypoxia on FHRV in Macaca muletta monkeys 1 to 3 days after surgery, maintained in restraint chairs (3). They were prepared at 136 days of gestation with fetal electrodes, and fetal and maternal intravascular and amniotic catheters. Gases, either room air or a mixture with decreased O_2 content with added CO_2, passed at 17 L/min through a plexiglass hood over the animals' heads, and blood and FHR sampling, or drug injection, were an average of approximately 20 minutes after induction of hypoxia. Fenoprofen, an inhibitor of prostaglandin synthesis, was infused overnight to suppress uterine activity.

Results

Acute hypoxia in the previously normoxaemic fetus resulted in bradycardia. The heart rate declined 28 bpm from 198 bpm, and there was an increase in both STV and LTV. Fetal arterial PO_2 declined from approximately 25 to 18 mm Hg, maternal arterial PO_2 from 100 to 46 mm Hg, and a mild fetal metabolic acidosis developed, base excess decreasing from -3 to -6 mEq/L.

As mentioned, our aim in this study was to test the hypothesis that FHRV in the hypoxic monkey fetus was due to an interaction of the vagal and sympathetic nervous systems' actions on the heart, because each operates with a different time constant. According to this theory, blockade of either of these branches should totally abolish FHRV.

The effects of a totally blocking dose of the vagolytic drug atropine (200 μg/kg) was to produce a smoothness of the FHR tracing and a tachycardia after treatment. FHR increased from 158 to 188 bpm. The mathematical indices for ST and LTV decreased to 30 and 19% of control values respectively.

When totally blocking doses (1 mg/kg) of propranolol, a β-adrenergic blocker, are administered to the fetus, there is a bradycardia and there visually appears to be a decline in the long term fluctuation, but little influence on the beat-to-beat jitter. FHR decreased from 185 to 152 bpm, and the index of STV did not change. The LTV index declined to 51% of control, though in the 4 animals studied this did not reach statistical significance.

Discussion

These observations do not support the theory that FHRV is a result of an interaction between the vagal and sympathetic nervous systems. Rather they support the concept that STV is primarily vagally mediated without sympathetic input. LTV, on the other hand, is primarily vagally

mediated, but with a modest β-adrenergic input.

An unsolved question persistently arises: What is the origin of FHRV? We believe it is the result of a large number of inputs, primarily from the cerebral cortex and brain stem impinging on the cardiac integratory centers. Thus, anencephalics (with complete absence of cortex), and severely and centrally asphyxiated or narcotized fetuses do not have FHRV.

Recent work suggests that there may be important species differences in FHRV and its etiology. Earlier this month, Adrian Walker and his Melbourne coworkers reported findings consistent with the interactive theory in normoxic sheep (4). They did, however, use a FHRV index which is different from ours, and, we believe, is measuring different variability factors. Furthermore, our own preliminary analyses in hypoxic fetal sheep tend to confirm Walker's findings.

These two important questions, i.e. 1) the origin of FHRV, and 2) the validity of species differences, remain unresolved.

REFERENCES

1) Laros, R.K., Wong, W.S., Heilbron, D.C., Parer, J.T., Snider, S.M., Naylor, H., and Butler, J.: A comparison of methods for quantitating fetal heart rate variability. Am. J. Obstet. & Gynecol. 128:381-392, 1977.

2) de Haan, J., van Bemmel, J.H., Versteeg, B., Veth, A.F.L., Stolte, L.A.M., Janssens, J., and Eskes, T.K.A.B.: Quantitative evaluation of fetal heart rate patterns. Europ. J. Obstet. Gynec. 3:95-102, 1971.

3) Parer, J.T., Laros, R.K., Heilbron, D.C., Krueger, T.R., Rubsamen,R.M. and Wong, W.S.: The effect of acute hypoxia and hypercarbia on fetal heart rate variability in awake monkeys. Abstracts of Scientific Papers, 26th Annual Meeting of Soc. Gynecol. Invest., San Diego, p. 93, 1979.

4) Walker, A.M., Cannata, J., Wilkinson, M., Yardley, R.,Bowes, G., Ritchie, B.C., and Maloney, J.E.: Nervous contributions to heart rate variability in fetal lambs. Abstracts of Scientific Papers, 7th International Workshop on Fetal Breathing, Oxford, England, p.2, 1980.

Adv. Physiol. Sci. Vol. 8. Cardiovascular Physiology. Heart, Peripheral Circulation and Methodology
A. G. B. Kovách, E. Monos, G. Rubányi (eds)

CONCLUDING REMARKS ON CARDIOVASCULAR FOETAL PHYSIOLOGY

Robert S. Comline
Physiological Laboratory, Downing Street, CB2 3EG, Cambridge, UK

There was a lively discussion on many of the papers. After Cassin's presentation, Will asked about the normal regulation of pulmonary blood flow. Cassin thought that the position was probably a balance between the effects of vasodilators and vasoconstrictors. Bland mentioned the relative absence of effects if active substances were given by aerosols to neonates and suggested that the absorption might occur after the sensitive structures. The paper by Mott was followed by a long discussion on the effect of nephrectomy on foetal blood pressure. Faber pointed out that in his experience the systemic arterial pressure was not changed even after three weeks. Bland cited the results of G.D. Thorburn while Lumbers suggested that the capricious effects on arterial pressure and cardiac hypertophy indicated that there might be a role for the foetal kidney in the maintenance of fluid volume. Faber however, could not agree that the foetal kidney is important in this respect since so much of the urine passed into the amniotic sac and is re-circulated through foetal drinking.

After Will's paper Mott queried the role of the angiotensin system in the rabbit and Lumbers pointed out that captopril when given to ewe augments the effects of hypoxia, in that it causes a fall in foetal pO_2 and a rise in pCO_2 probably related to a fall in maternal arterial pressure. Will could not agree, although he had noted death in foetal rabbits and that those close to the cervix were usually the first to be affected. Fore asked after the paper by Barnes, Comline and Silver, whether the umbilical blood flow after foetal adrenalectomy or hypophysectomy reflected changes in cardiac output; Mott asked whether in these preparations the foetal O_2 consumption was reduced. The preliminary results could not offer good definitive answers to the questions. Parer suggested that the response to atropine in the foetal pig obtained by Macdonald and Colenbrander might have been exacerbated by hypoxia. There was a discussion on the time of onset of vagal tone in the foetal pig towards the end of gestation.

The papers by Nemeth, Papp and Resch were taken together for the discussion. There was speculation in the relative maturity of the foetal heart of the human and rabbit; it was pointed out that slow Na^+ flux appears before the fast Na^+. The paper by Faber et al was extensively discussed. Mott suggested that in view of the absence of effective pressure in the IVC the caval flow was more relevant than atrial pressures to the function of the foramen ovale. There was a brisk discussion with Bland on the role of the right heart and the normal pO_2 in the pulmonary vessels of the foetus. The possibility was raised that in experiments on the foetus an unwitting selection of the experimental population could influence the conclusions. After the paper by Parer et al, Walker pointed out the difference between the development of the innervation of the foetal heart between the lamb and the human. Bland's presentation on lung lymph flow was followed by a brisk discussion that continued after the end of the formal session.

Adv. Physiol. Sci. Vol. 8. Cardiovascular Physiology. Heart, Peripheral Circulation and Methodology
A. G. B. Kovách, E. Monos, G. Rubányi (eds)

METHODOLOGY OF THE SIMULTANEOUS, NONDESTRUCTIVE DETERMINATION OF METABOLISM, BLOOD FLOW AND BLOOD VOLUME WITHIN SUPERFICIAL MICROAREAS OF THE BRAIN CORTEX BY MICROFLUOROREFLECTOMETRY

András Eke and Arisztid G. B. Kovách

Experimental Research Department, Semmelweis Medical University, 1082 Budapest, Üllői út 78/a, Hungary

The fine adjustment of the blood supply to the neuronal metabolic demand is one of the crucial factors assuring the functional integrity of the brain. This complex adjustment by the effect of metabolites on the microcirculatory units takes place in microareas throughout the brain, where the neuronal tissue comes in contact to its supplying microvessels. Simultaneous, nondestructive measurements of metabolism and blood supply in these microareas, mostly in rest-to-activity or activity-to-rest transitions when the typical features of the control mechanisms are the most apparent, is desired and is on the way to become an important area of studies. The demand for an equally good time and spatial resolution in the applied methodologies is obvious. It seems, though, that the presently available methods can provide one or none of these features. The following combination of two in situ photometric techniques providing means to measure NADH-level - as a metabolic parameter - and blood supply in superficial microareas of the brain cortex at a rate of max. 4 measurements per minute, could be a useful alternative.

MEASUREMENT OF NADH LEVEL AS A METABOLIC PARAMETER

The tissue NADH-level as a metabolic parameter can be monitored by the fluorometric method of Chance et al. [1]. According to its principle, the NADH molecules within the tissue compartments can be excited at 366 nm by the light of a mercury arc lamp and their secondary fluorescence detected at 450 nm For the details of the measuring system see Fig. 1! With a suitable correction for the disturbing effect of blood on the fluorescent reading, it is a measure of the NADH-level in the illuminated area /mrNADH/. Until now, we have applied the correction technique of Harbig et al. [2], which computes mrNADH as follows

$$mrNADH = F - k\,I \qquad /1/$$

where F and I are fluorescence and reflectance intensities and k - the correction factor - is defined as the ratio of F- and I-enhancment during bolus perfusion of the monitored

area by an intracarotid injection of a dextran-saline solution. The tissue NADH-level itself is not a specific metabolic parameter. Therefore, well designed tests - like brief anoxia, activation of the monitored area etc. - should be arranged throughout the experiment in order to properly interpret a given response in the mrNADH.

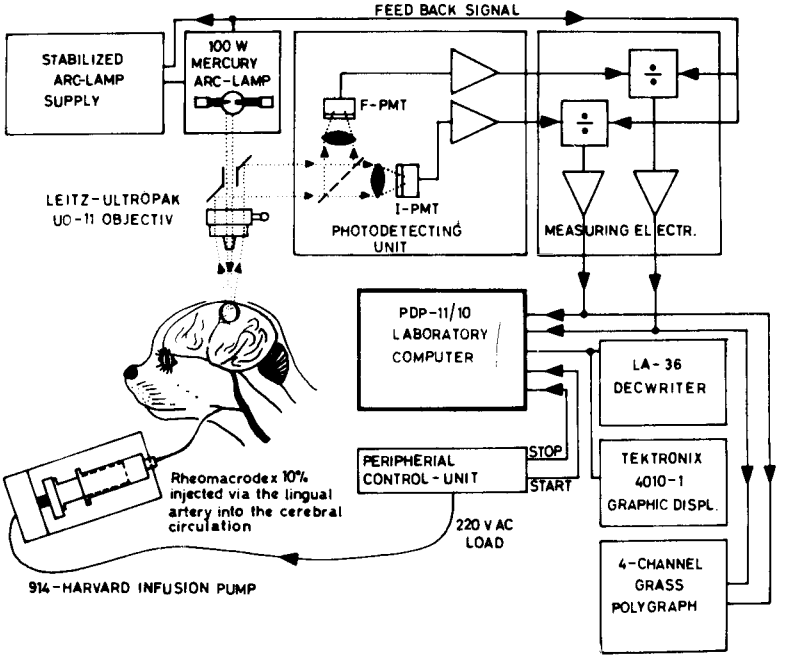

Fig. 1. Schematic diagram of the microfluororeflectometric system and experimental arrangement. The light of a 100 W DC mercury arc lamp is filtered at 366 nm and focused onto the surface of the brain through a glass window implanted into the skull of an anesthetized cat. The light diffusely scattered from the tissue /I, reflectance/ and that emitted by the NADH molecules /F, fluorescence/ is detected through the circumferential lens and directed to the measuring phototubes. The amplified outputs are linked to the A/D ports of a PDP 11/10 laboratory computer. A control unit initiates the fully automative measurements of the NADH-level, blood flow and blood volume by activating the infusion pump for 0.6 sec - thus performing bolus perfusion of the brain by isotonic Rheomacrodex 10% solution - and providing control signal to the computer for data acquisition from the F and I channels. The maximal rate at which the system can output a set of data is 4/minute.

MEASUREMENT OF BLOOD FLOW AND BLOOD VOLUME

The blood-dilution method of Eke et al. [3] using the same optics and the reflectance photometric channel measures the absolute values of microregional blood flow /mrCBF/ and blood volume /mrCBV/ by analyzing the optical density /OD/ of the tissue at 366 nm during bolus perfusion. The OD of the tissue is calculated from the ratio of diffusely scattered light intensity for a given instant to that of the blood-free cerebro-cortical tissue. A calibration function, which linearly correlates the OD and the blood content of blood samples, makes it possible to use the circulating red blood cells as "endogenous" indicator for determing mrCBV from the measured OD in vivo. To measure mrCBF, bolus perfusion of the monitored area is performed by injecting an isotonic dextran-saline solution /Rheomacrodex 10%/ as nondiffusible indicator into the cerebral circulation. The subsequent hemodilution is monitored as an OD change /Figs. 2 and 3/. This temporary change in the OD during the microregional transit of the bolus is interpreted as indicator dilution and provides the data for computing the microregional mean transit time /mrMTT, t/ of the bolus /Fig. 2/. It was shown, that the mrCBV monitored by the baseline of these functions is an accurate measure of distribution of the traversing bolus. This made it possible to apply the principle of Meier and Zierler [5] to calculate the mrCBF as the ratio of mrCBV and mrMTT. The reader is referred here for further details to ref. [3]. Here, we are restricted to give the nomenclature for the equations and the equations themself.

Nomenclature:

I_o	Reflectance intensity without blood /determined at the end of the experiment by measuring reflectance intensity following washing out of blood from the brain/.
I_b	Reflectance intensity with blood anywhere between dilutions.
I_{bi}	Linearly extrapolated reflectance baseline intensity with blood during indicator transit.
I_e	I_{bi} extrapolated to time when the peak reflectance intensity is detected during indicator transit.
I_i	Reflectance intensity with blood during indicator transit.
t_o	Time at which the indicator is injected into the cerebral circulation.
t_a	Appearance time of the indicator in the monitored area.
t_d	Disappearance time of the indicator.
$\overline{OD}$	Normalized optical density.
V_{wb}	Concentration of blood with its hematocrit measured before diluting it for photometric measurements in in vitro model studies.
Hct_a	Large vessel arterial hematocrit.
Hct	Mean microregional hematocrit.

d	Depth of light penetration in the brain cortex.
C_i	Indicator concentration in the monitored area.
h_i	Fraction of the bolus traversing the monitored area at a given moment.
H(t)	Cummulative function, step response.

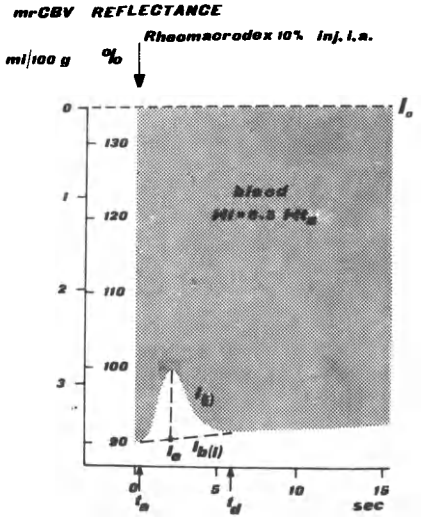

Fig. 2 Schematic representation of the bolus perfusion induced hemodilution in the monitored area. The microreflectometric parameters involved in the computation of mrCBF anf mrCBV are indicated.

Calculations:

$$OD = \log(I_o/I) \qquad /2/$$

$$\widehat{OD} = OD/(Htc_a \times d) \qquad /3/$$

The in vitro obtained calibration function:

$$\widehat{OD} = m \times V_{wb} + b \qquad /4/$$

where m and b are constants.

$$mrCBV = (\widehat{OD} - b) / m \qquad \text{ml blood/100 g tissue} \qquad /5/$$

where $\widehat{OD}$ similarly to Eq. 3 is

$$\widehat{OD} = (\log I_o/I)/(Htc \times d) \qquad /6/$$

Based on data reported by Chance [1] :

$d \approx 800$ micra

Based on data provided by Sklar [4] :

$Htc \approx Htc_a \times 0.5$

$$C_i = \Delta mrCBV = \Delta\widehat{OD}_i/m = (\log I_i - \log I_{bi})/(0.5 \times m \times Htc_a \times d) \qquad /7/$$

$$h_i = C_i / \int_{ta}^{td} C(t)\,dt \qquad /8/$$

$$H(t) = \sum_{n=0}^{\infty} h_T (t - nT) \qquad /9/$$

$$\bar{t} = \int_{ta}^{td} 1 - H(t)\,dt \qquad /10/$$

$$mrCBF = mrCBV/t = \frac{\frac{\log I_o/I_e}{Hct \times d} - b}{m \times t} \times 60 \quad ml/100g\ min \qquad /11/$$

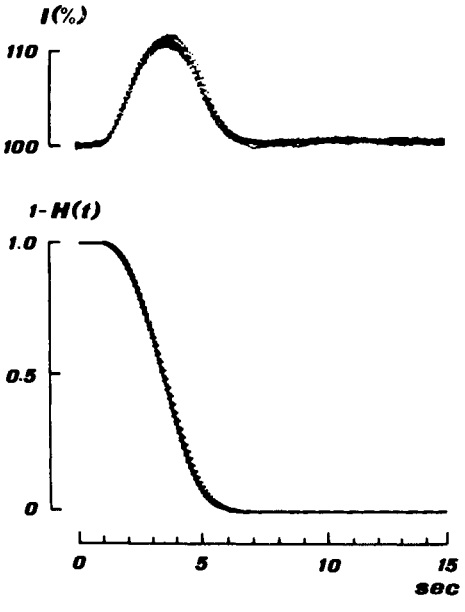

Fig. 3 Microreflectometric recordings of bolus perfusion induced cerebrocortical hemodilutions. Note, that 10 curves are superimposed with identical t_o! These curves were recorded to test the reproducibility of the method during serial measurements of mrCBF in a steady state. mrMTT was calculated from the 1 - H/t/ function as the area under the curve in the range between the appearance and disappearance of the indicator. Photographic copy of original data stored on megnetic diskette and displayed point by point on the Tektronix graphic terminal. The reproducibility of these mrCBF measurements is within 1%.

EXPERIMENTAL EXAMPLES

Epileptic seizures have been selected to demonstrate the usefulness of the presented method in correlating mrNADH, mrCBF and mrCBV when these are rapidly and vastly changing.

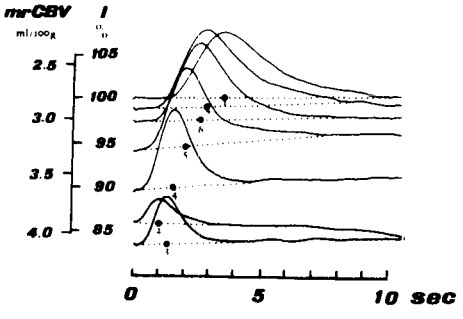

Fig. 4 A typical set of microreflectometric recordings during epileptic seizure. One should note the marked reduction of the baseline indicating a great vasodilation and the extreme shift of mrMTT towards t_o because of the manyfold increase in the velocity of blood flow.

APP.T.	MTT	MRBV	MRBV%	MRBF%	MRBF	CF	-K-
1.5	2.32	2.54	100	100	65.66	0	3.27
.3	.59	3.56	145	545.34	358.09	-7.3	2.05
.4	.71	3.75	154	477.09	313.27	-13	1.67
.4	.99	3.25	131	299.38	196.58	-8	1.91
.6	1.64	2.91	116	162.12	106.45	-9	2.01
.9	1.76	2.71	107	140.47	92.24	-6.8	2.08
1	2.28	2.61	103	104.65	68.72	-6.8	2.25
1.2	1.84	2.49	97	123.34	80.99	-5.7	2.63
1.5	2.24	2.5	98	101.82	66.86	-.8	2.74
1.2	2.14	2.49	97	106.14	69.69	-2.8	2.71

Fig. 5 Computer print out for the response shown on Fig. 4. Measurements were made in every 30 second. Appearance time /APP.T./ and the mrMTT /MTT/ are given in seconds, mrCBF /MRBF/ in ml/100g min, mrCBV/MRBV/ in ml/100g and the mrNADH /CF/ in % of a control level.

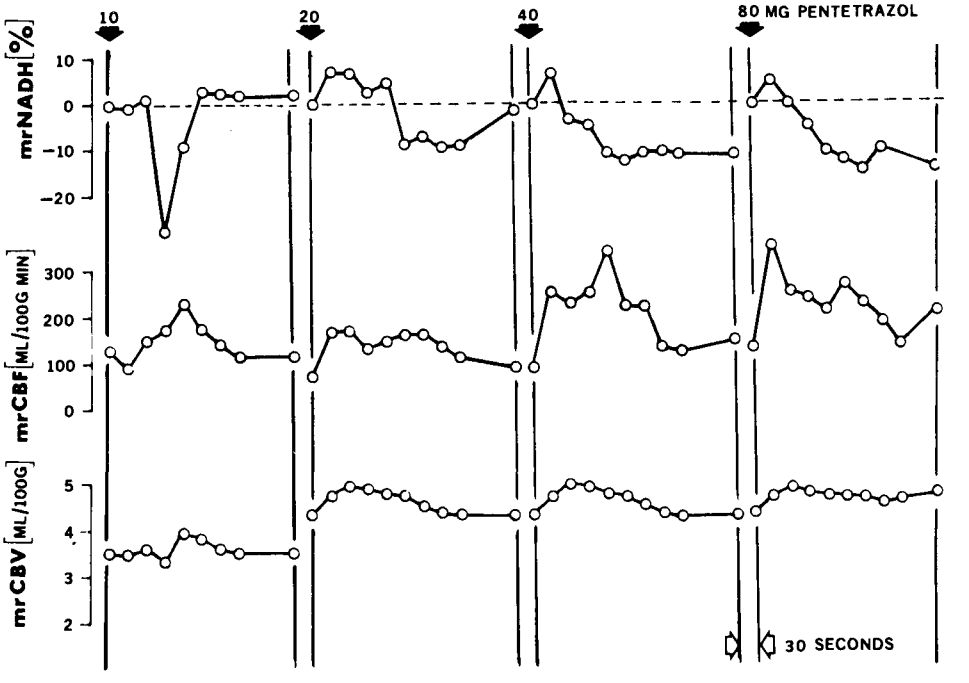

Fig. 6 Serial measurements of mrNADH, mrCBF and mrCBV following repetitive intra-arterial administration of Pentetrazol. Note the capability of the method to describe faithfully the changing pattern of metabolic and hemodynamic responses.

Seizures were triggered by injecting Pentetrazol /a Metrazol equivalent/ into the cerebral circulation . Right after the injection a series of automatic measurements of mrNADH, mrCBF and mrCBV was started at a rate of 2/minute. Fig. 4 shows a typical set of microreflectometric recordings during an epileptic seizure. On Fig. 5 the computer print out with the evaluated data for the same response can be seen. The whole cycle of a single measurement / injection - data acquisition - computation - data storage - print out / took 30 seconds. As it can be seen on Fig. 6, such a measuring frequency is sufficient to describe the fastest changes in blood flow and metabolism.

CONCLUSIONS

From our results the following advantages of the method can be enumerated:

1./ Provides measures in a tiny superficial volume in the brain cortex.
2./ High time and spatial resolution results from its use.
3./It measures nondestructively in an intact tissue volume with fully preserved structure and function.
4./ The method is fully computer controlled: Determinations of tissue NADH-level, blood flow and blood volume and other microcirculatory parameters are quick, accurate and highly reproducible.

We are aware of the crutial importance of the appropiate correction for the hemodynamic artifact on the NADH-fluorescence in vivo. Although our results obtained by the correction of Harbig et al. [2] are selfconsistent, our method easily permits the application of other techniques of correction provided it would be more reliable than the presently used one.

REFERENCES

1. Chance, B.,P.Cohen,F.Jöbsis, and B.Schoener. Intracellular oxydation-reduction states in vivo. Science 137:499-508,1962.
2. Harbig, K.,B.Chance,A.G.B.Kovách, and M.Reivich. In vivo measurement of pyridine nucleotide fluorescence from the cat brain cortex. J. Appl. Physiol. 41:480-488,1976.
3. Eke, A.,Gy.Hutiray, and A.G.B.Kovách. Induced hemodilution detected by reflectometry for measuring microregional blood flow and blood volume in cat brain cortex. Am. J. Physiol. 236/5/:H759-H768,1979.
4. Sklar, F.H.,E.F.Burke Jr., and T.W.Langfitt. Cerebral blood volume:values obtained with ^{51}Cr-labeled red blood cells and RISA. J. Appl. Physiol. 24:79-82,1968.
5. Meier, P., and K.L.Zierler. On the theory of the indicator dilution method for measurement of blood flow and volume. J. Appl. Physiol. 6:731-744,1954.

Adv. Physiol. Sci. Vol. 8. Cardiovascular Physiology. Heart, Peripheral Circulation and Methodology
A. G. B. Kovách, E. Monos, G. Rubányi (eds)

APPLICATIONS OF OPTICAL TECHNIQUES TO BRAIN PHYSIOLOGY

Myron Rosenthal and Joseph C. LaManna
University of Miami School of Medicine, Departments of Neurology and Physiology/Biophysics, Miami, Florida 33101, USA

Biological systems are not at equilibrium but at a steady state which requires metabolic energy for its maintenance. For many tissues, this energy requirement is so great that its nonsatisfaction can affect specific functional activities and lethal consequences may ensue. In fact, the energy requirements of certain tissues such as heart and brain can be satisfied only by continuous supply of energy derived from the mitochondrial oxidative reactions. This requirement leads to the conclusion that a full understanding of tissue physiology and pathophysiology must reflect three interrelated processes; functional "work"; circulatory provisioning; and metabolic conservation of free energy.

In this review, we consider how such an understanding is being approached in mammalian brain by optical techniques that directly monitor metabolic activity. These procedures take advantage of signals provided by the components of the mitochondrial respiratory chain as they go about the reactions of energy conservation. As an apologia, we submit that much new work is reported here that is only now being prepared for full publication. Thus reference is made, in several instances, to preliminary communications. However, our aim here is to exhibit the advantages that optical techniques provide to investigate functional activities and to show, by example, that this approach offers significant aid in many tissues. This work also illustrates that optical studies, together with investigations using techniques such as 2-deoxyglucose autoradiography for measuring glucose utilization, O_2-micropolarography for measuring tissue oxygen tension, hydrogen electrodes and other blood flow probes, and the potential for significant contributions by positron emission tomography and NMR probes give hope that we will someday bridge the gaps between physiology and biochemistry of brain and other tissues.

Since brain is our demonstration model, some applicable facts should be reviewed. One is that central nervous tissues are highly dependent upon metabolism and their viability is threatened by very short periods of anoxia or ischemia. Another is that when the coupling between energy supply and transport is broken, transmembrane ion gradients are not maintained, transmembrane voltage differences are lost and nervous functioning is sacrificed. Third is that there is little about energy conservation that is unique to brain except its disproportionate use. Brain, at only 3% total body weight, consumes approximately 20% of the total body oxygen and receives nearly 15% of the total cardiac output (Schmidt,

1964). Finally, it must be emphasized that brain's anatomy and physiology present special difficulties to an understanding of its energy metabolism. For one, electrical functioning is impaired, and critical relationships between cells and circulation are altered when brain tissues are examined as simpler systems such as homogenates, slices or isolated organelles. Another difficulty is that brain harbors specific regulations of its circulation which are lost with relatively minor manipulations. Another complication is the presence of a "blood-brain-barrier" which limits access of many experimentally useful molecules. In addition, nervous tissues are continuously active with a high metabolic rate so that basal conditions cannot properly be defined.

The advantage of optical probes of metabolism is that they allow continous and simultaneous measurements of "physiological" function in the presence of normal circulation. The principle of these methods is simple (c.f. Fig 1). When glucose or other substrates are broked down to CO_2 through glycolysis, the tricarboxylic acid cycle or other specific pathways, hydrogen ions and electrons are passed through the mitochondrial respiratory chain from one reactant to the next up the ascending redox potentials to molecular oxygen. This passage of reducing equivalents is coupled to the formation of high energy phosphate bonds from the free energy liberated in oxidation-reduction reactions at three sites along the chain. Thus, the respiratory chain is the "final common pathway" for the conservation of energy from substrates in the form of ATP (ATP or its precursors are considered to be involved in most or all of the energy requiring functions of cells). The respiratory chain consists of a series of coenzymes (NAD and Fp) and cytochromes. Each of these exists in either an oxidized or reduced form depending upon whether it is donating or accepting reducing equivalents (see e.g. Jöbsis, 1964). Changes in these oxidation/reduction states provide the basis for optical probing of metabolism because of a fortuitous circumstance. Each reactant absorbs light, or fluoresces, at specific wavelengths and the absorption or fluorescence is dependent upon whether the molecules are in an oxidized or reduced state. It was by light absorption that the components of the respiratory chain were identified (see e.g. Keilin, 1966), and such absorption differences provide the basis for spectrophotometric measurements of concentrations and redox shift kinetics as pioneered by Chance (1951a,b).

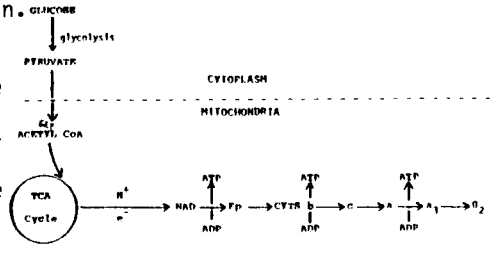

Figure 1. Simplified schematic of cellular energy conservation included here to provide some indication of the relationships among the cytoplasmic and mitochondrial reactions, the respiratory chain and oxidative phosphorylation of ADP.

By such spectrophotometry, Chance and Williams (1956) defined five mitochondrial "states" and found that redox ratios depend upon the supply of ADP, substrate or oxygen. For example, ADP (or more recently, the phosphate potential) controls the rate of electron transport and oxidative phosphorylation. Upon addition of ADP to mitochondria, whose respiration is ADP limited in state 4 ("rest"), all components but cytochrome c oxidase (cytochrome a,a_3) became more oxidized. The latter remained

nearly fully oxidized in either the state 4 or state 3 ("active") condition consistent with the concept of a "critical pO_2" for full oxygen utilization (see e.g. Jöbsis, 1972). Redox ratios changed to full reduction in anoxia (state 5) and shifted to full oxidation under substrate limitation (state 2). These states have served valuably as reference to the situation found *in vivo*. The applicability of state-5 to the functioning brain was shown when, as expected, decreased inspired oxygen produced increased ratios of reduced NAD (Chance et al., 1962) and cytochrome a,a_3 (Rosenthal, LaManna et al., 1976). Mitochondrial redox shifts were also assessed during and following increased brain activity which presumably parallels a state 4-3 transition of isolated mitochondria. With evoked potentials (Rosenthal and Jöbsis, 1971), seizures (Jöbsis et al., 1971) and spreading cortical depression (Rosenthal and Somjen, 1973), NAD became transiently more oxidized, exactly as expected.

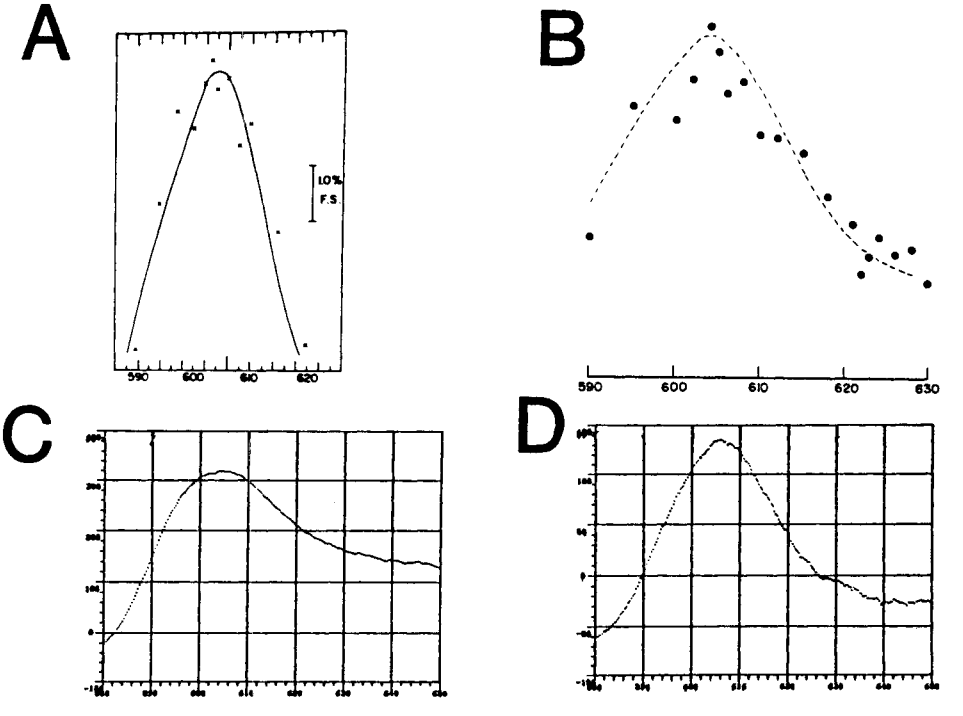

Figure 2. Difference spectra of cytochrome a,a_3 from brain tissues *in vivo*. Trace A represents the difference spectrum between 5% O_2 and 95% O_2/5% CO_2 inspiration recorded from rat neocortex. Trace B shows a reaction spectrum of the amplitude of optical signal responses to dorsal root stimulation. Traces C and D represent difference spectra recorded from rat neocortex at "rest" and when the animal was breathing 100% N_2. Trace C represents the spectrum in the presence of hemoglob in while B was recorded after full blood replacement with an oxygen-carrying fluoronated hydrocarbon solution (hematocrit less than 1%).

However, cytochrome $\underline{a},\underline{a}_3$ also became more oxidized, indicating that on a tissue level it is not fully oxidized as it is under "resting" conditions in isolated mitochondria. This apparent discrepancy led us first to examine the validity of reflectance spectrophotometry in brain and then to consider the steady-state condition of cytochrome oxidase.

REFLECTANCE SPECTROPHOTOMETRY OF CYTOCHROME OXIDASE

Many experiments were performed to demonstrate that the signals recorded by reflection spectrophotometry in brain are indicative of cytochrome oxidase redox changes. This was especially important since hemoglobin absorbs light strongly in the visible region of the spectrum and its absorption differs with oxygen saturation. To identify the optical signals, absorption spectra from intact brains were found comparable to spectra from mitochondria in the presence and absence of hemoglobin (Jobsis et al., 1977). Also, reaction spectra recorded during hypoxia-hyperoxia transitions and during stimulus-evoked increases in metabolic intensity were compared to mitochondrial spectra (Figure 2A-B). Most recently, our new procedure of rapid scanning spectrophotometry, modified from the instrument of Mandel et al (1977) found very comparable reflection spectra from rat neocortex previous to and following the substitution of an oxygen-carrying fluoronated hydrocarbon solution (Fluosol) for hemoglobin (Figure C-D and LaManna, Pikarsky et al., in press). To verify reference wavelength compensation for changes in hemoglobin volume, additional comparisons were made. Cytochrome $\underline{a},\underline{a}_3$ reduction was found equal in terminal anoxia and complete ischemia although the former was accompanied by hemoglobin volume increases and the latter by large decreases (Rosenthal, Martel et al., 1976). Conversely, hyperoxia produced by 100% O_2 or by inspiration of 95% O_2 with 5% CO_2 each produced increased ratios of oxidized cytochrome oxidase. However, inspiration of the former gas mixture was accompanied by decreased blood volume (Fig 3A) presumably due to vasoconstriction, while inspiration of the latter was accompanied by increased blood volume (Fig 3B) likely associated with CO_2 vasodilatation. Also, the extent of cytochrome $\underline{a},\underline{a}_3$ oxidation with hyperoxia was related to the increase in tissue oxygen tension (PtO_2) and not to hemoglobin volume (LaManna et al., 1979). To examine the adequacy of reference compensation for shifts in Hb/HbO_2, changes at a wavelength of maximal difference in absorption of these (577 nm), with reference to an isobestic wavelength (585 nm), were found considerably smaller than those recorded for cytochrome $\underline{a},\underline{a}_3$. This is in spite of greater absorption by hemoglobin in this spectral region and the greater difference between Hb/HbO_2 when compared to that between re-

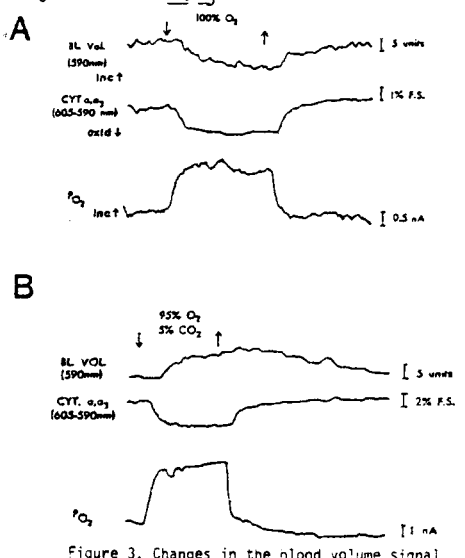

Figure 3. Changes in the blood volume signal, cytochrome $\underline{a},\underline{a}_3$ redox state and tissue oxygen tension recorded in rat neocortex during changes in inspired gases (reprinted courtesy of N. Kreisman and T. Sick).

duced and oxidized cytochrome $\underline{a},a_3$. Also, the kinetics of cytochrome oxidase redox changes and Hb/HbO_2 shifts were different and changed independently of each other during and after repetitive ischemic episodes (Rosenthal, Martel et al., 1976). In addition, at hyperbaric oxygen pressures at which no further Hb/HbO_2 shift occurred, continued oxidation of cytochrome oxidase was recorded (Hempel et al., 1977; Hempel, 1979). Other confirmations of technique are provided by triple wavelength compensation experiments (Jöbsis et al., 1977) and the fact that cytochrome oxidase absorption in the infrared region, which is essentially beyond the range of hemoglobin absorption, demonstrates very similar directions and kinetics as reactions recorded in the visible region (Jöbsis, 1977).

THE STEADY STATE CONDITION

The redox state of the mitochondrial reactants in brain has received much examination. Early studies showed that decreased oxygen availability produced reduction of all respiratory chain members (see above). Decreased energy turnover, produced with CNS depressant drugs, had similar effects (Chance et al., 1962; LaManna, Sylvia et al., 1976; LaManna, Younts et al., 1977). However, increased oxygen tension resulted in increased oxidation of cytochrome $\underline{a},a_3$ (Rosenthal, LaManna et al., 1976) as did the diminution of blood glucose levels (Bryan et al., in press) and increased energy demand of evoked potentials, seizures and spreading depression. Sylvia and Rosenthal (1978) calculated that cytochrome oxidase is approximately 30% reduced under "resting" conditions in rat cerebrum but higher ratios of reduced cytochrome $\underline{a},a_3$ were found in cat spinal cord, which we speculated might be related to the lower resting oxygen consumption of spinal tissues (Rosenthal et al., 1979). In contrast, recently implanted cortical and subcutaneous tumors exhibited highly oxidized cytochrome $\underline{a},a_3$ (Sylvia et al., 1979). The cytochrome oxidase redox state was shown to be unaffected by chronological aging but was changed by lung pathology (Sylvia and Rosenthal, 1978). This ratio was also unaffected by virtually complete absence of cerebral norepinephrine (LaManna, Harik et al., in press).

Conclusions from these experiments include: 1) brain tissue average cytochrome oxidase redox state varies with both oxygen availability and energy demand; 2) if cytochrome oxidase is presented with more oxygen, it will become more oxidized; 3) there must be some control or regulation at the cytochrome oxidase level *in vivo* preventing the fully oxidized state of isolated mitochondria. This control or regulation sets its limits specifically in different CNS areas; 4) there is no level of oxygen which can be defined, in the classical sense, as the "critical pO_2" in brain tissue. Whether cytochrome oxidase redox differences in tissue and mitochondria are due to isolation procedures, or more likely to tissue conditions (such as O_2 heterogeneity) remains to be established.

A major outcome of the "steady-state" experiments, however, is that a limitation must be applied to any conclusions based upon static measurement of biochemical parameters *in vivo*. Such measurements do not address whether energy demand is equal under all conditions. For example, the redox ratio of cytochrome oxidase did not vary with aging, with no-

repinephrine depletion, and recently we showed that its full recovery after ischemia did not indicate EEG or evoked potential recovery in rat cerebral cortex (Rosenthal et al., 1980; Duckrow et al., 1980). Such results are difficult to reconcile with reports of changes in brain metabolism or function in each of these conditions. What is measured optically, or with any biochemical or autoradiographic assay, under static conditions, is a balance between energy supply and demand that is subject to the turnover rates of oxygen, substrates and high energy intermediates. These complications demonstrate the necessity of considering the regulations of metabolism and tissue functional activity, and presumed influences upon each of these, in the dynamic or "active" state when energy demand is increased.

THE "ACTIVE" STATE

In brain and spinal cord, evoked potential activity produced transient oxidations of NAD and cytochrome a,a$_3$ (Fig.4 and Rosenthal and Jobsis, 1971; Rosenthal, LaManna et al., 1979). These oxidations were correlated in time and linearly related in amplitude to the negative shifts of extracellular voltage and to the increased activity of extracellular potassium which accompanies such stimulation (Lothman et al., 1975; Rosenthal, LaManna et al., 1979). Pentobarbital attenuated the amplitude and slowed the recovery rate of all parameters (LaManna, Cordingley et al., 1977). Since this drug is not thought to alter functining in white matter, this indicates that the labile optical signals originate from central gray matter. These data confirm in vivo that the major fraction of oxidative energy spent after stimulation is expended in restoring disturbed ion balance (Somjen et al., 1976). Ouabain slowed the rate of oxidation after stimulation demonstrating that the transition from "resting" to "active" states in vivo, as in vitro, is dependent upon the supply of ADP and that oxygen turnover in brain is regulated by energy demand (Rosenthal and LaManna, 1975).

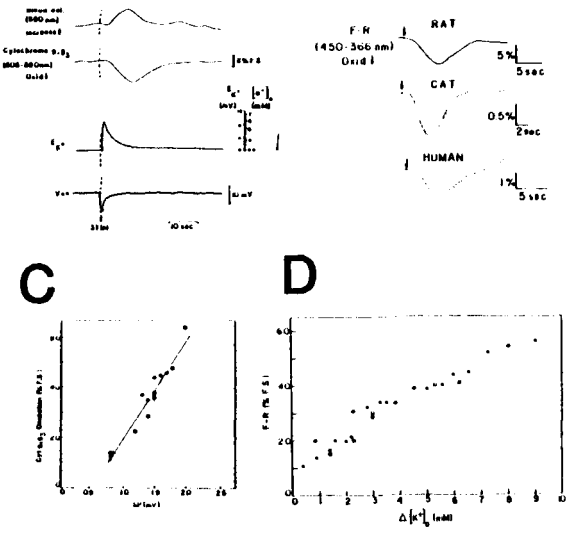

Figure 4. Stimulus-induced responses in cortex and spinal cord. A = raw traces recorded in cat spinal cord with a one sec train of pulses applied to the dorsal root at the dashed line. B= averaged fluorescence changes (NAD oxidations) in rat, cat and human neocortex with one second trains of pulses applied at the arrows. C and D show relationships among optical and electrical changes after cord (C) and cortical (D) stimulation in cat

Responses to increased energy demand can be used to test metabolic

capabilities and influences under many conditions. For example, small decreases in PaO_2 result in decreased SP shift amplitudes and smaller mitochondrial oxidations due, likely, to decreased excitability. However, when PaO_2 was decreased to 40-50 torr in rats, stimulation still produced SP shifts but oxidations of NAD and cytochrome $\underline{a},a_3$ were replaced by transient reductions at higher stimulus intensities. Further decreases in PaO_2 lowered the stimulus intensity required to produce transient reductions. We conclude that ADP availability results in increased substrate "pressure" on the respiratory chain and a buildup of reducing equivalents occurs when energy demand is increased. Another example of the value of such a metabolic testing system occurred in studies of aging. As already described, "resting" redox ratios were unchanged in brains of aged rats and even evoked potential responses were not altered. However, transient reductions of cytochrome $\underline{a},a_3$, rather than oxidations as expected, were recorded in aged brains under the very intense metabolic demand associated with spreading depression. It appears that oxygen utilization capability may be adequate for "resting" but not for intensely active conditions in the aged CNS (Sylvia and Rosenthal, 1979).

The effects of cerebral norepinephrine depletion provide another example of the benefit of considering metabolic capabilities in the "active" state. As in aging, NE depletion had little effect on "resting" redox ratios in rat neocortex. However, in norepinephrine-depleted cerebral hemispheres, rates of oxidation and re-reduction of respiratory chain members were slowed following stimulation (Harik et al., 1979) which confirms directly that NE has a role in modulating oxidative processes in the cerebral cortex. Most recently, we ruled out the possibilities that the NE influence resides within the respiratory chain itself (LaManna,Harik et al., in press) or that these effects result from influences on the clearance of extracellular potassium (Sick et al., in press). Rather, these data are consistent with the possibility that the NE influence is mediated through an effect on cerebral circulation, an area currently under exploration.

An additional example of the value of the in vivo approach derives from studies of metabolic capability after ischemia. Previously, we showed that baseline redox states and metabolite levels are recovered before EEG activity is restored in rats after restoration of flow following carotid and vertebral arterial ligation (Rosenthal et al., 1980). An indicator that appears better to signal metabolic recovery is the evoked potential induced metabolic response sequence. Duckrow et al (1980) showed that stimulus induced increases in blood volume and mitochondrial oxidations were changed and then recovered at characteristic times after ischemia in a manner predicting recovery of tissue capability. Thse data confirm that the important parameter to consider in terms of metabolism is turnover and that biochemical parameters such as ATP/ADP ratios can give the false appearance of recovery under conditions where energy demand is changed.

These studies lead to the following conclusions. 1) under physiological conditions, when oxygen and circulation are capable of response, there is continuous adjustment of energy supply to meet energy demand. The system is flexible. It can handle greater demands for energy if required. Increased brain activity is associated with increased ion transport activity which results in increased ADP availability. This results

in increased oxygen consumption and microflow increases so that energy supply meets energy demand; 2) the linear relationships among K^+o load, O_2 consumption and mitochondrial metabolic intensity strongly support the concept that a very large portion of metabolic energy is spent after brain activation in the reestablishment of transmembrane ion gradients; 3) the oxidative changes that occur with stimulation demonstrate that, on a tissue level, the production of ATP from ADP is not proceeding at maximum rate. This emphasizes the efficiency of energy conservation of brain. However, certain conditions such as aging, ischemia and norepineprhine depletion pose a threat to the ability of the brain to increase energy conservation in proportion to increased energy demand; 4) brain cannot maintain ion homeostasis when small decreases in oxygen occur. There appears to be little capability for adjustment. Ongoing metabolism appears already to be at a critical level. More oxygen will allow increaed metabolism. Less O will quickly result in metabolic deficit. These data confirm that there is a continuum of dependency of oxidative metabolic functioning in brain on oxygen. Hypoxia must be defined in terms of a functional system. Metabolic sufficiency must be defined for each level of metaboic demand.

SUMMARY

We have demonstrated how optical techniques can be used in combination with other probes of functional activity to approach an understanding of the physiology of working tissues. Two factors should be most obvious. One is that no single technique allows the full developmenet of such an understanding. Metabolism must be considered in terms of, and coordinated with, the specific activities for which energy is expended. The second is that optical techniques provide the unique advantage that they allow, kinetically, such relationships to be investigated in tissues whose on-going activities remain undisturbed. This approach should provide new understandings of functional activities in not only brain but in many other tissues of the body.

ACKNOWLEDGEMENTS

It is our priviledge to acknowledge the many contributions of collaborators R.B.Duckrow, S.I.Harik, N.R.Kreisman, A.I.Light, S.J.Peretsman, S.M.Pikarsky and T.J.Sick whose preliminary work is quoted within. This research has been supported in part by PHS grants NS 14319 and NS 14325 and RCDA award NS 00399 (to JCL).

REFERENCES

Bryan, R, R.Duckrow, J.LaManna, M.Rosenthal and A. Sylvia, Changes in the redox state of cytochrome a,a_3 in rat cerebral cortex during hypoglycemia, Neurosci. Absts., in press

Chance,B, Rapid and sensitive spectrophotometry: I and II, Rev.Sci.Inst., 22, 619-627(a) and 634-638(b),1951

Chance,B, P. Cohen, F. Jöbsis and B. Schoener, Intracellular oxidation-reduction states in vivo, Science, 137, 499-508, 1962
Chance, B. and G. Williams,The respiratory chain and oxidative phosphorylation, Adv. Enzymol.,17, 65-134, 1956
Duckrow, R, J. LaManna and M. Rosenthal, Reversible alterations of oxidative metabolism in rat cerebral cortex after transient ischemia, Fed. Proc., 39,534,1980
Harik, S, J. LaManna, A. Light and M. Rosenthal, Cerebral norepinephrine: Influence on cortical oxidative metabolism in situ, Science 206,69-71, 1979
Hempel, F, Oxygen tensions measured in cat cerebral cortex under hyperbaric conditions, J. Appl. Physiol., 46, 53-60, 1979
Hempel, F, F. Jöbsis, J. LaManna, M. Rosenthal and H. Saltzman, Redox levels of cytochrome a,a in cat cerebral cortex during hyperbaric oxygenation, J. Appl. Physiol., 43, 873-879, 1977
Jöbsis, F, Basic Processes in cell ular respiration, In: Handbook of Physiology, Am. Physiol. Soc., 63-124, 1964
Jöbsis, F, Non-invasive, infrared monitoring of cerebral and myocardial oxygen sufficiency and circulatory parameters, Science, 198, 1264-1267, 1977
Jöbsis, F, J. Keizer, J. LaManna and M. Rosenthal, Reflectance spectrophotometry of the intact cerebral cortex. I. Dual wavelength technique, J. Appl. Physiol., 43, 858-872, 1977
Jöbsis, F, M. O'Connor, A. Vitale and H. Vreman, Intracellular redox changes in functioning cerebral cortex. I. Metabolic effects of epileptiform activity, J. Neurophysiol., 34, 735-749, 1971
Keilin, D., The History of Cell Respiration and Cytochrome, Cambridge Univ. Press, 416 pp., 1966
LaManna, J., G. Cordingley and M. Rosenthal, Phenobarbital actions in vivo: Effects on extracellular potassium activity and oxidative metabolism in cat cerebral cortex, J. Pharmacol. Exptl. Therap., 200, 560-569, 1977
LaManna, J, S. Harik, A. Light and M. Rosenthal, Norepinephrine depletion alters cerebral oxidative metabolism in the "active" state, Brain Research, in press
LaManna, J, S. Pikarsky, T. Sick and M. Rosenthal, Blood substitution: II. Effects on cytochrome oxidase spectrophotometry in vivo, The Physiologist, in press
LaManna, J, M. Rosenthal, T. Sick and N. Kreisman, Stroke 10, 7-8, 1979
LaManna, J, A. Sylvia, D. Martel and M. Rosenthal, Fluorometric monitoring of the effects of adrenergic agents on oxidative metabolism in intact cerebral cortex, Neuropharmacology, 15, 17-24, 1976
LaManna, J, B. Younts and M. Rosenthal, The cerebral oxidative response to acute ethanol administration in rats and cats, Neuropharmacology 16, 283-288, 1977
Lothman, E, J.LaManna, G.Cordingley, M.Rosenthal and G.Somjen, Responses of electrical potential, potassium levels, and oxidative metabolic activity of the cerebral neocortex of cats, Brain Research 88, 15-36, 1975
Mandel, L, T. Riddle and J. LaManna, A rapid scanning spectrophotometer and fluorometer for in vivo monitoring of steady-state and kinetic optical properties of respiratory enzymes, In: Oxygen and Physiological Function, F.Jobsis ed, Prof. Inf. Lib, Dallas, 79-89, 1977

Rosenthal, M. and F. Jöbsis, Intracellular redox changes in the functioning cerebral cortex. II. Effects of direct cortical stimulation, J. Neurophsyiol., 34, 750-762, 1971
Rosenthal, M. and J. LaManna, Effect of ouabain and phenobarbital on the kinetics of cortical metabolic transients associated with evoked potentials, J. Neurochem., 24, 111-116, 1975
Rosenthal, M, J. LaManna, F. Jöbsis, J. Levasseur, H. Kontos and J. Patterson,jr., Effects of respiratory gases on cytochrome a in intact cerebral cortex; Is there a critical PO ? Brain Research 108, 143-154, 1976
Rosenthal, M, J. LaManna, S. Yamada, B. Younts and G. Somjen, Oxidative metabolism, extracellular potassium and sustained potential shifts in cat spinal cord in situ, Brain Research, 162, 113-127, 1979
Rosenthal, M, D. Martel, J. LaManna and F. Jöbsis, Oxidative energy metabolism in situ during and following short periods of transient cortical ischemia in cats Exptl. Neurol. 50, 477-494, 1976
Rosenthal, M, S. Peretsman, J. LaManna, O. Alonso, R. Busto and K. Kogure, Recovery patterns of mitochondrial respiratory state and EEG in intact cerebral cortex after ischemia, Stroke 11, 129, 1980
Rosenthal, M. and G. Somjen, Spreading depression, sustained potential shifts and metabolic activity of cerebral cortex of cats, J. Neurophysiol., 36, 739-749, 1973
Schmidt, C, The measurement of oxygen in tissues, In: Oxygen in the Animal Organism, F.Dickens and E.Neil, eds., vol 31, Pergamon Press, London, 433-446, 1964
Sick, T,S. Harik,J. LaManna and M. Rosenthal, Effect of norepineprhine depletion on potassium transport in cerebral cortex, Trans.Am.Neurol.Assoc. in press
Somjen, G, M. Rosenthal, G. Cordingley, J. LaManna and E. Lothman, Potassium, neuroglia and oxidative metabolism in central gray matter, Fed. Proc., 32, 1266-1271, 1976
Sylvia, A. and M. Rosenthal, The effect of age and lung pathology on cytochrome a,a redox levels in rat cerebral cortex, Brain Research, 146, 109-122, 1978
Sylvia, A. and M. Rosenthal, Effects of age on brain oxidative oxidative metabolism in vivo, Brain Research, 165, 235-248, 1979
Sylvia, A, G. Somjen, D. Bigner and M. Rosenthal, Redox properties of cytochrome a,a and vascular reactivity of astrocytomas and neuroblastomas in vivo, J. Neurochem., 32, 1371-1377, 1979

Adv. Physiol. Sci. Vol. 8. Cardiovascular Physiology. Heart, Peripheral Circulation and Methodology
A. G. B. Kovách, E. Monos, G. Rubányi (eds)

ABSOLUTE REFLECTION PHOTOMETRY AT ORGAN SURFACES

D. W. Lübbers and J. Hoffmann
Max-Planck-Institut für Systemphysiologie, Rheinlanddamm 201, 4600 Dortmund 1, FRG

Methods of absorption photometry are sensitive enough to measure in vivo natural pigments such as hemoglobin, myoglobin and cytochromes which participate in oxygen supply. Since the influence of light on the chemical reaction in which these substances are involved can generally be made small, transmission and reflection photometry measurements are useful tools for studying the oxygen transport mechanisms in vivo. Photometric measurements as applied to biology have a long history. Without going into detail I might recall only the first studies of McMunn (1886) on respiratory pigments. These were followed by the work of Keilin (1925) and Warburg (1926) in the 1920's. To apply these methods to experiments in situ Kramer (1934), Matthes (1934) and Millikan (1942) developed the two wavelength technique, in which one wavelength is used to measure the change in oxygen saturation or the redox state, the other one to compensate for non specific changes caused by the tissue. In the 1950's the two wavelength method was very much improved by Chance (1954).
The photometric techniques as applied in biology have been very much improved during the last two decades, but the methods of evaluation especially for reflection spectra have not followed in the same proportion. For evaluation mostly the two wavelength method or similar methods are used which assume the validity of the Bouguer-Lambert-Beer law (BLB-law); but to our knowledge there was up to now no method available by which the validity of the BLB-law could be continuously tested. In the following we would like to present a method by which a quantitative analysis of reflection spectra in situ can be performed. In order to explain the basic problems of the quantitative analysis of reflection spectra we take as an example the reflection spectrum of the skin. In skin the spectrum is mainly determined by a single substance, the hemoglobin present in the capillaries and the deeper vascular plexus. Since the hemoglobin has different extinction spectra dependent on its state of oxygenation we deal with a two component system. The idea of our modus procedendi was to bring the hemoglobin within the skin to a state the spectrum of which is known - for example in a state of full oxygenation - and compare this spectrum with the spectrum of a cuvette which contains a solution of also fully oxygenated hemoglobin. By analysing the difference between both spectra it should be possible to find the laws by which differences can be explained and to work out a proper evaluation technique.
Fully oxygenated hemoglobin in the capillary blood of the skin was

obtained by heating up the skin and respiring pure oxygen. Fig. 1 shows the HbO_2 spectrum of the skin (upper trace) and the extinction spectrum of the corresponding HbO_2-solution. The spectra were registered by the rapid-spectroscope (Kieler Howaldtswerke, Kiel) which was developed together with Koehler and Niesel (9).The scanning time for a single spectrum is 1/100 of a second. The difference between both spectra is obvious. In the skin spectrum the peaks of the HbO_2-solution are flattened similar to that which was observed in a turbid solution (2). To quantify these changes the extinction of both spectra is compared wavelength by wavelength. When the extinctions of the reflection spectra are taken as ordinate and the extinctions of the cuvette spectra at the same wavelength as abscissa one obtains the function the graph of which is shown in Fig. 2. By this function the spectrum of oxyhemoglobin within the skin is transformed to the spectrum of oxyhemoglobin solution or vice versa. One observes a monotonously increasing curve which has several branches in its upper part. In the following we will show that this curve, this transformation, can be explained

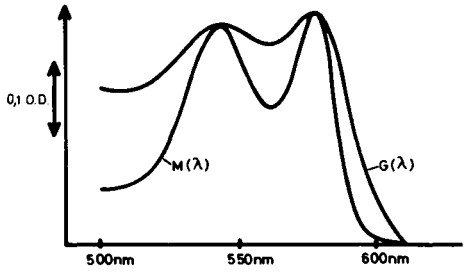

Fig. 1: Cuvette spectrum, M(λ), and skin spectrum of HbO_2 G(λ) (11)

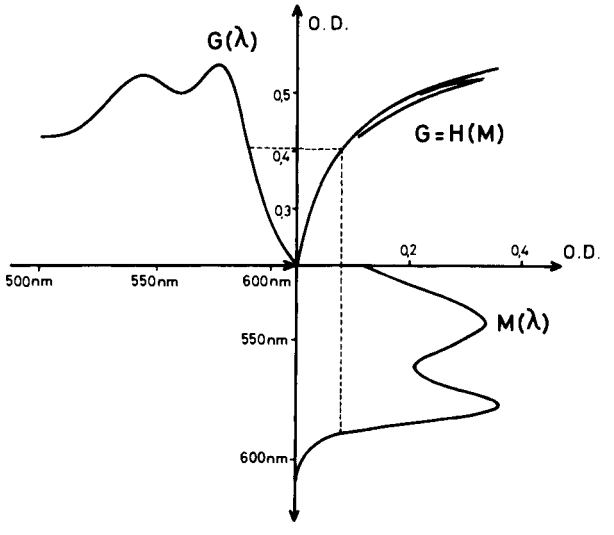

Fig. 2: Construction of the transformation G = H(M) (11)

1. by the effect of inhomogeneous distribution of light pathes,
2. by the effect of light scattering.

1. Influence of inhomogeneous light paths

When hemoglobin is homogeneously distributed in a cuvette - as shown in

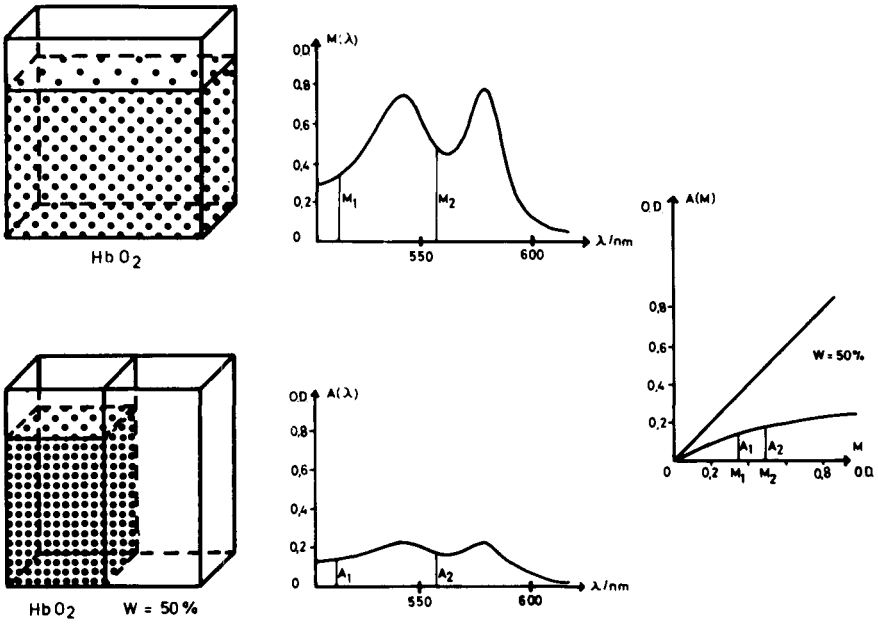

Fig. 3: Influence of an inhomogeneous light path on the spectrum (11)

the upper part of Fig. 3 - the spectrum is described by the Bouguer-Lambert-Beer law.

$$I = I_o \cdot \exp(-E(\lambda)) \tag{1}$$

$$\ln \frac{I_o}{I} = E(\lambda) = c \cdot \varepsilon(\lambda) \cdot x = c \cdot \phi(\lambda) = a(\lambda) \cdot x \tag{2}$$

I, light intensity (zero, incident light); $E(\lambda)$, extinction; c, molar concentration of the dye stuff; $\varepsilon(\lambda)$, molar absorbance; x, length of the light path; $a(\lambda) = c \cdot \varepsilon(\lambda)$; $\phi(\lambda) = \varepsilon(\lambda) \cdot x$.
In a multicomponent system the total extinction is the sum of the single extinctions.

$$a(\lambda) = a_1(\lambda) + a_2(\lambda) + \ldots + a_i(\lambda) \tag{3}$$

$$M(\lambda) = \sum_i c_i \cdot \phi_i(\lambda) \tag{4}$$

If the spectra of the single components of a mixture are known the sum spectrum of the mixture can be analysed by applying the least square method of Gauss taking into account a special weight function (10).
In the lower part of Fig. 3 the hemoglobin is unevenly distributed. To make it simple, hemoglobin is only in one half of the cuvette whereas the other one is free of hemoglobin. In this case the BLB-law has to be applied separately to each homogeneous compartment.

$$I = I_o(\Psi_1 \cdot \exp(-E(\lambda)) + \Psi_2) \tag{5}$$

ψ, fractional size of the compartment
or more general

$$A(\lambda) = \ln \frac{I_o}{I} = \sum_j c_j \cdot \exp(-\sum_i a_i(\lambda) \cdot x_j) \qquad (6)$$

In this case the sum spectrum is not a linear combination of the extinctions, but a sum of exponential functions. Therefore, by comparing $A(\lambda)$ and $M(\lambda)$ wavelength by wavelength one obtains a curve, a transformation the slope of which depends on the distribution of the light paths.

$$A(\lambda) = H(M(\lambda)) = H\ (\sum_i c_i \cdot \phi_i(\lambda)) \qquad (7)$$

The equation shows that the transformation caused by the inhomogeneous distribution is a one to one transformation, i.e., for a given transformation the deviation from the linearity depends only on the magnitude of extinction.
In tissue experiments the transformation can be approximated by

$$H(y) = \frac{a \cdot y + b}{c \cdot y + 1} \qquad (8)$$

This approximation is applied to determine the factors a, b, c and the fractional concentrations c_i using a non-linear least square method. Fig. 4 shows an example of the application of this evaluation method. The hemoglobin spectrum was measured by a microscope photometer (UMSP, Zeiss, Oberkochen) and obtained from a blood filled vessel in a tissue slice which was quickly frozen, cut at -80°C and kept at -100°C for the measurements (kryophotometric measurement, Grunewald and Lübbers, 1975). The experiments were carried out by V. Schwarzmann. In panel A the measured spectrum (trace with noise) and a recalculated spectrum is shown. For this recalculation the ordinary multicomponent analysis is used. A' displays the deviation between both curves (ca. 20 times enlarged). In B the transformation (eq. 8) is introduced and the coefficients a, b, c and the degree of oxygenation is calculated by iteration. B' shows that the deviation is reduced to statistical deviations, whereas in A' the deviation remains large and wavelength dependent. The final transformation (B'') clearly shows the one to one relationship between $A(\lambda)$ and $M(\lambda)$. The excellent fit emphazises the fact that for this application the evaluation method was more appropriate. The ordinary multicomponent analysis using only the BLB-law resulted in a HbO_2 saturation of 75%, the value obtained by considering inhomogeneities with this method amounts to 83%.
We can conclude also that the curved form of the measured transformation (Fig. 2) can be explained by the inhomogeneous distribution of the blood in the skin, but the different branches of the transformation need further explanation.

2. The effect of light scattering

To describe the effect of light scattering rather sophisticated methods have been worked out (see for example 6). However, the more sophisticated the method the more parameters are needed to describe the scattering effect. Since the types of information which we can obtain by photometric measurements in situ are restricted, we tried together with F. Hannebauer at first the simplest approach which was developed by Kubelka and Munk (1931). They assumed that in a medium light is absorbed and scattered in such a way that light is evenly distributed in all directions in space; they showed that this is equivalent to the case in

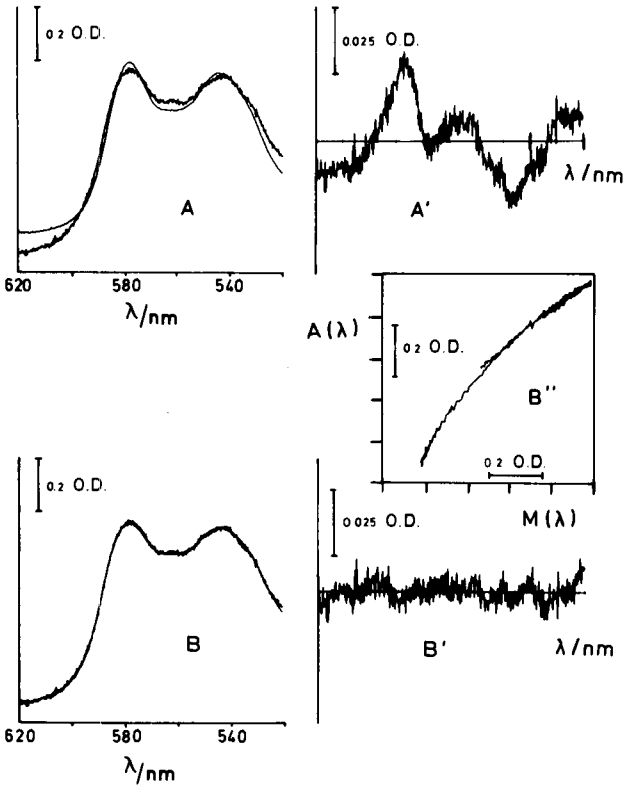

Fig. 4: Evaluation of HbO_2 saturation in a blood vessel in a frozen tissue slice

which light is distributed in only two directions: in the direction of the incident light and in the opposite direction, the direction of the reflected light. If the fraction of light which is absorbed or scattered is proportional to the actual light intensity we obtain

$$dI = -a(\lambda) \cdot I \cdot dx - s(\lambda) \cdot (I-J) \cdot dx \quad (9)$$

$$-dJ = -a(\lambda) \cdot J \cdot dx - s(\lambda) \cdot (J-I) \cdot dx \quad (10)$$

J, intensity of scattered light; $s(\lambda)$, scattering coefficient ("light exchange" between the direction of I and J).The solution of these two differential equations is

$$I(x) = c_1(1-\beta) \cdot \exp(k \cdot x) + c_2(1+\beta) \cdot \exp(-k \cdot x) \quad (11)$$

$$J(x) = c_1 \cdot (1+\beta) \cdot \exp(k \cdot x) + c_2 \cdot (1-\beta) \cdot \exp(-k \cdot x) \quad (12)$$

with

$$k = (a(\lambda) \cdot (a(\lambda) + 2s(\lambda))^{1/2} \; ; \; \beta = (a(\lambda)/(a(\lambda)+s(\lambda))^{1/2} \quad (13)$$

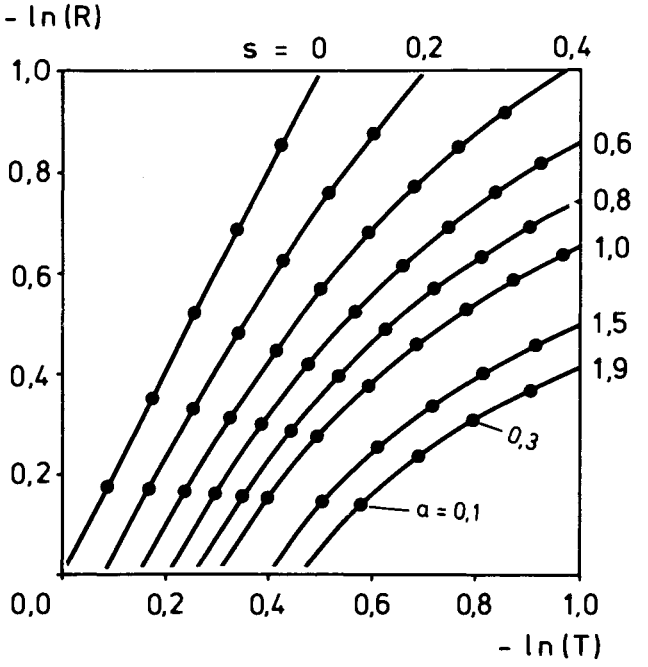

Fig. 5: Reflectance vs. transmittance according to the two-flux theory (8)

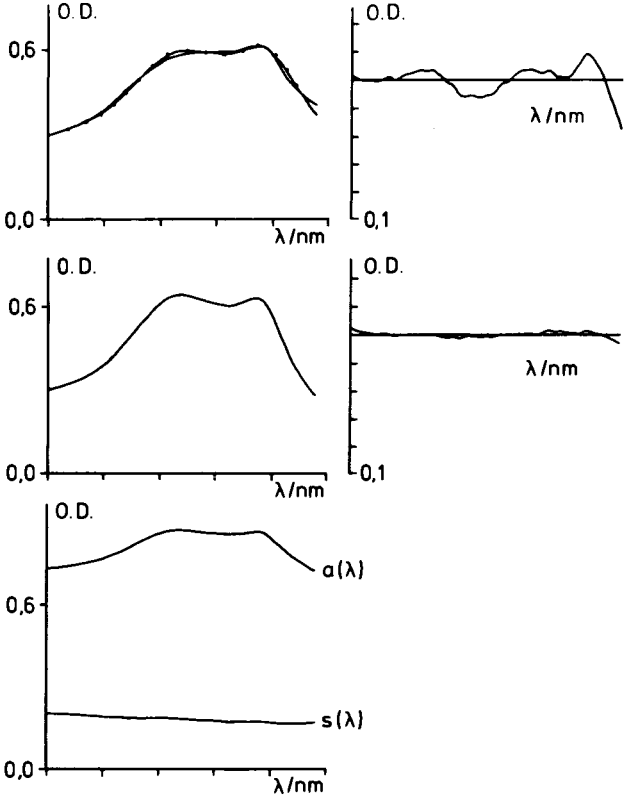

Fig. 6: Evaluation of a skin spectrum (pig)

c_1, c_2 are constants given by the measuring conditions. The equations show that one needs the transmission and reflection spectra of the same sample to calculate the true absorbance and scattering coefficients.
a) In model experiments which were performed together with U. Heinrich we tested the two flux theory using mitochondria, tissue homogenates and capsules of different diameters as different scattering particles as well as cuvettes of different thicknesses. The scattering particles were suspended in a hemoglobin solution. For reflection measurements the backside of the cuvette was covered with a white cardboard so that the light path is doubled. We measured the spectra of the same sample in transmission, $T(\lambda)$ and reflection, $R(\lambda)$

$$T(\lambda) = \frac{I}{I_o} \tag{14}$$

$$R(\lambda) = \frac{J}{I_o} \tag{15}$$

Fig. 5 shows in which way the scattering changes the extinction of the transmitted and the reflected light. Without scattering (s=0) one obtains a straight line with a slope of 2, since, as mentioned the reflected light passes the cuvette twice. With increasing s the curve moves to the right and becomes steeper. From this figure it can be deduced that for constant scattering one obtains a one to one transformation. When s is wavelength dependent then several curves are involved and consequently the transformation looses its one to one relation and obtains several branches. The conclusion is that the branching of the transformation measured in skin (Fig. 2) can be caused by wavelength dependent scattering. For our model experiments the Kubelka-Munk theory gave sufficiently good results (4). b) For the quantitative determination of $a(\lambda)$ and $s(\lambda)$ we need the reflection and the absorbtion spectra, however, in most of the experiments in situ only the reflection spectra can be measured since the thickness of the organs is so large that the transmitted light is unmeasurably small. Since the two flux theory describes the effect of scattering well enough with finite thickness of cuvette, we can assume that the theory holds also for samples of infinite thicknesses. For this case we find

$$R_\infty(\lambda) = \frac{1 - \beta}{1 + \beta} \tag{16}$$

or

$$\frac{a(\lambda)}{s(\lambda)} = \frac{1 - R_\infty^2}{2R_\infty} = \frac{1}{2}\left(\frac{1}{R_\infty} - R_\infty\right) \tag{17}$$

To solve the equation for $a(\lambda)$ und $s(\lambda)$ we would need a second independent measurement. As discussed above this is not possible directly but we can obtain additional information by the following procedure:
1) which components are present is determined from other information and their separate, cuvette spectra ("book spectra") are obtained;
2) a thin tissue piece or a homogenate is analysed as described before. Thereby the true absorption spectrum and scattering spectrum of this sample are calculated.
This additional information can be used to evaluate the reflection spectrum $R(\lambda)$. In a first step $R(\lambda)$ is analysed by multicomponent

analysis described above taking into account inhomogeneous distribution and constant light scattering ($s(\lambda)$ = constant), in other words, assuming a one to one transformation. The reflection spectra R (λ) and the calculated absorption spectra yield the scattering spectra $s(\lambda)$. These spectra should resemble the experimentally determined scattering spectra. An important criterion of the scattering spectra is that it should be a monotonously decreasing function. This can be achieved by several iterations. Fig. 6 shows the analysis of a reflection spectrum of pig skin measured by H.R. Figulla. In the upper left panel the measured spectra and the recalculated spectra (marked with dots) using a one to one transformation is shown and in the upper right panel the deviation between both curves (5 times enlargement). There are still wavelength dependent disturbances. In the middle left panel the scattering corrections by iterations as described have been carried out. In the middle right panel one sees that it was possible to reduce the error to statistical deviations. In the lowest panel the true absorption spectra and scattering spectra resulting from this analysis are shown.

Summary

These experiments have shown that for a quantitative evaluation of a reflection spectrum one has to take into account
1. the inhomogeneous distribution of light paths and
2. the effect of scattering.

The problem of inhomogeneous distribution was solved by applying the methods developed by Wodick and Lübbers (10, 11, 15 - 19). The scattering is described according to the two flux theory of Kubelka and Munk (8). To obtain - after correction for the inhomogeneities - the true absorption spectra, one has to determine the scattering coefficients. This is possible only by two independent observations. With thin tissue layers this can be achieved by measuring the transmission and reflection spectra of the same sample. With thicker layers only the reflection spectra can be registered. We were able to show that the necessary additional information can be obtained from knowing the "book spectra" which compose the reflection spectra and from the (general) form of the scattering spectra. This information allows the calculation of the true absorption spectra by an iteration process using the form of scattering spectra as criterion. This method works for skin spectra; it has to be tested with other organs. Further work is in progress to compare the complete analysis with the more simple evaluation methods which use two ore more wavelengths.

References

1. Chance, B.(1954): Spectrophotometry of intracellular respiratory pigments'. Science 120, 767-775.
2. Duysens, L.N.M. (1956): The flattening of the absorption spectrum of suspensions as compared to that of solutions. Biochim. biophys. Acta 19, 1-11.
3. Grunewald, W.A. and Lübbers, D.W. (1974): Die Bestimmung der intracapillären HbO_2-Sättigung mit einer kryo-mikrofotometrischen Methode angewandt am Myokard des Kaninchens. Pflügers Arch. 353, 255-273.
4. Heinrich, U., Hoffmann, J. and Lübbers, D.W. (1980): Quantitative analysis of reflection spectra by simulation experiments on tissue. Satellite Symposium "Oxygen Transport to Tissue", Budapest, July 8-12.

5. Keilin, D. (1925): On cytochrome, a respiratory pigment, common to animals, yeast and higher plants. Proc. R. Soc. Lond. B98, 312.
6. Kortüm, G. (1969): Reflexionsspektroskopie. Grundlagen, Methodik, Anwendungen. Berlin, Heidelberg, New York, Springer.
7. Kramer, K. (1934): Fortlaufende Registrierung der Sauerstoffsättigung im Blute an uneröffneten Blutgefäßen. Klin. Wschr. 13, 379-380.
8. Kubelka, K. and Munk, F. (1931): Ein Beitrag zur Optik der Farbanstriche. Z. Tech. Phys. 11a, 593-603.
9. Lübbers, D.W. and Niesel W. (1959): Der Kurzzeit-Spektralanalysator. Ein schnellarbeitendes Spektral-Photometer zur laufenden Messung von Absorptions- bzw. Extinktionsspektren. Pflügers Arch. ges. Physiol. 268, 286-295.
10. Lübbers, D.W. and Wodick, R. (1969): The examination of multicomponent systems in biological materials by means of a rapid scanning photometer. Appl. Optics 8, 1055-1062.
11. Lübbers, D.W. and Wodick, R. (1975): Absolute reflection photometry applied to the measurement of capillary oxyhaemoglobin saturation of the skin in man. In: Oxygen Measurements in Biology and Medicine, J.P. Payne, D.W. Hill (eds.). pp. 85-109. London and Boston, Butterworths.
12. Matthes, K. (1934): Über den Einfluß der Atmung auf die Sauerstoffsättigung des Arterienblutes. Naunyn-Schmiedebergs Arch. exp. Path. Pharmak. 176, 683-696.
13. Millikan, G.A. (1942): The oximeter, an instrument for measuring continuously the oxygen saturation of arterial blood in man. Rev. scient. Instrum. 13, 434-442.
14. McMunn, C.A. (1886): Researches on myohaematin and histohaematins. Phil. Trans. R. Soc. 177, 267.
15. Wodick, R. and Lübbers, D.W. (1973): Methoden zur Bestimmung des Lichtweges bei der Photometrie trüber Lösungen oder Gewebe mit durchfallendem oder reflektiertem Licht. Pflügers Arch. 342, 29-40.
16. Wodick, R. and Lübbers, D.W. (1973): Quantitative Analyse von Reflexionsspektren und anderen Spektren mit inhomogenen Lichtwegen an Mehrkomponentensystemen mit Hilfe der Queranalyse. I. Das Verfahren der Queranalyse bei Mehrkomponentensystemen mit unbekannten, inhomogenen Lichtwegen. Hoppe-Seyler's Z. Physiol. Chem. 354, 903-915.
17. Wodick, R. and Lübbers, D.W. (1973): Quantitative Analyse von Reflexionsspektren und anderen Spektren mit inhomogenen Lichtwegen an Mehrkomponentensystemen mit Hilfe der Queranalyse. II. Die Bestimmung wellenlängenabhängigen Störungen und darin enthaltenen unbekannten Komponenten an Mehrkomponentensystemen mit Hilfe der Queranalyse. Hoppe-Seyler's Z. Physiol. Chem. 354, 916-922.
18. Wodick, R. and Lübbers, D.W. (1973): Ein neues Verfahren zur Bestimmung des Oxygenierungsgrades von Hämoglobinspektren bei inhomogenen Lichtwegen, erläutert an der Analyse von Spektren der menschlichen Haut. Pflügers Arch. 342, 41-60.
19. Wodick, R. and Lübbers, D.W. (1974): Quantitative evaluation of reflexion spectra of living tissues. Hoppe-Seyler's Z. Physiol. Chem. 355, 583-594.

Adv. Physiol. Sci. Vol. 8. Cardiovascular Physiology. Heart, Peripheral Circulation and Methodology
A. G. B. Kovách, E. Monos, G. Rubányi (eds)

NMR AS A NONINVASIVE MONITORING TECHNIQUE IN PHYSIOLOGY AND MEDICINE

O. Jardetzky, D. Wemmer and N. Wade-Jardetzky
Stanford Magnetic Resonance Laboratory, Stanford University, Stanford, California 94305, USA

Nuclear Magnetic Resonance (NMR) is a spectroscopic method widely used in Chemistry and Biochemistry for the identification of compounds and the study of molecular structure and dynamics (Pople, Schneider and Bernstein, 1959, Jardetzky and Roberts,1981).

The method is based on the fact that atomic nuclei in bulk matter absorb radiofrequency radiation when placed in a magnetic field. The absorption signal can be picked up by a tuned coil surrounding the sample and displayed after manyfold amplification on any suitable recording device. The frequency at which absorption is observed depends on the strength of the imposed magnetic field and to a first approximation on the nature of the nucleus--e.g. in a field of 100 KGauss protons will absorb at 420 MHz ^{13}C at 105 MHz and ^{31}P at 170 MHz. The intensity of the generally bell-shaped resonance absorption line is directly proportional to the number of nuclei in the sample. Beer's Law is strictly obeyed, which accounts for the usefulness of the method for analytical purposes. The width and in many instances the splitting of lines are determined by interactions between nuclei and carry a wealth of structural and dynamic information.

NMR absorption was first detected by F. Bloch at Stanford and E.M. Purcell at Harvard in 1945. Interest in chemical applications was sparked by the discovery made in 1949-1950 by several investigators that a chemical compound can be identified by a pattern of lines in the spectrum of a single isotope, each line representing a different chemical group. Methyls can be distinguished from methylenes in either the hydrogen or the carbon spectrum, and methyls in different molecules from each other. Such "chemical shifts" of resonance lines are very much smaller (of the order of 10-10,000 Hz) than the difference in the absorption frequencies of different isotopes and very homogenous magnetic fields (1 part in 10^9) are required to resolve them. The shifts are extraordinarily sensitive to both molecular structure and molecular environment.

Research at the Stanford Magnetic Resonance Laboratory was supported by grants from the National Institutes of Health (RR00711) and from the National Science Foundation (GP23633 and PCM 78-07930).

Observations of NMR signals from living matter did not lag far behind the discovery of the phenomenon. Among the legends in the field are F. Bloch's examination of the water line on his finger and E.M. Purcell's and N. Ramsey's attempt to erase human memory by resonance absorption on the hypothesis that memory was stored in the orientation of nuclear spins (personal communications). It is not surprising that the first recorded physiological observations made by NMR were on blood or its cellular components. Odeblad et al (1956) attempted to measure the exchange rate of deuterium across the red blood cell membrane by ^{1}H NMR of the water line. Jardetzky and Wertz (1956) examined the state of sodium in blood by ^{23}Na NMR. This experiment, reproduced in Fig. 1 showed that there was no significant binding of sodium in plasma, since the shape and width of the line was identical to that found in physiological saline, but that a significant number of sodium binding components was released on hemolysis, as manifested in pronounced broadening of the line. A large number of different cellular constituents can produce such line broadening by forming weak sodium complexes (Jardetzky and Wertz, 1956, 1960).

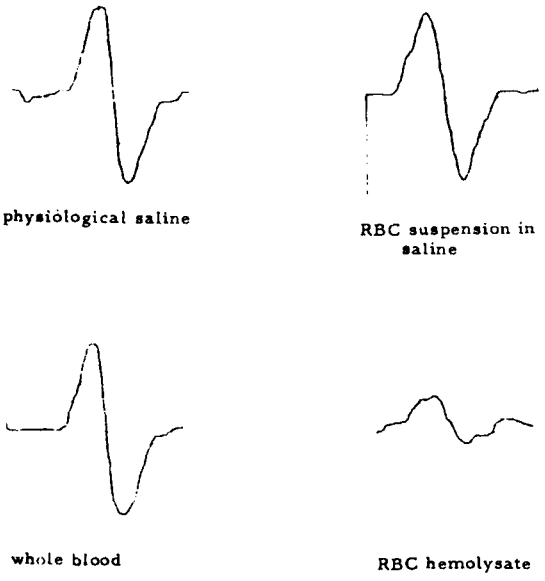

Figure 1
^{23}Na resonance in blood and red blood cell suspensions

Using the well known pH dependence of the chemical shift of the phosphate ^{31}P NMR line, Moon and Richards (1973) proposed a method for estimating intracellular pH in red blood cells. The pH dependence of the ^{31}P chemical shift is shown in Fig. 2 (Roberts, et al, 1980) which also illustrates that separate resonance lines will be seen for the same compound in different cellular compartments, if the compartments differ in pH or composition.

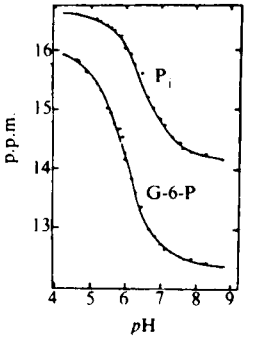

Figure 2

Graph of chemical shift (in p.p.m.) by ^{31}P NMR vs. pH for P_i (inorganic phosphate) and G-6-P (glucose-6-phosphate)

Physiological applications of NMR have received a very significant impetus in 1974 from the demonstration by G.K. Radda and his coworkers at Oxford that the combined ^{31}P spectra of ATP, creatine phosphate, sugar and nucleotide phosphates and inorganic phosphate can be simultaneously observed in intact cells and tissues. (Hoult et al, 1974) Such spectra have now been recorded on bacteria, yeast, erythrocytes, skeletal and cardiac muscle, liver, kidney and brain (Gadian et al, 1979, Hollis, 1979) and references therein).

Anoxia and death are accompanied by a progressive disappearance of the creatine phosphate and ATP spectra, a dramatic rise in the concentration of inorganic phosphate and a fall of pH, as illustrated in Fig. 3 (Grove et al, 1980). The possibility of measuring the rates of appearance or disappearance of metabolites with a time resolution of about 1 - 2 min. (given the best of present technology) is also apparent in the figure. NMR spectra recorded in vivo reveal only soluble cell constituents of small molecular weight, present in concentrations of 10^{-3}M or higher. Spectra of macromolecules, membrane phospholipids, and bound metabolites are too broad to be observed under these conditions, although they can be studied on purified systems in vitro. Furthermore, the concentrations of individual molecular species of different proteins, nucleic acids and lipids tend to be below the limits of sensitivity of the method which lie at about 10^{-4} - 10^{-3}M.

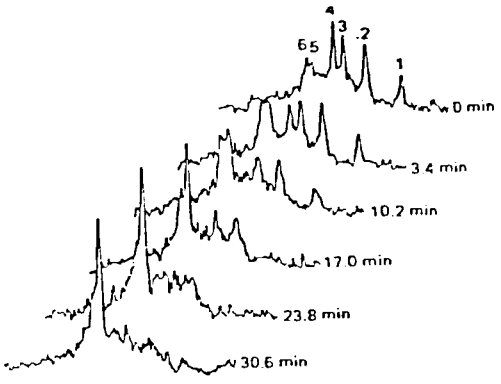

Figure 3

^{31}P NMR Spectra of in vivo rat heart recorded as a function of time during respiratory arrest. (Grove et al,1980)

Simultaneous observation of several cell constituents, such as is possible for the phosphorylated metabolites, is of great importance to the successful use of NMR in physiological investigation or medical diagnosis. Fairly extensive in vivo NMR work has been done over the past two decades on single lines particularly those of water and inorganic ions. Among the more successful applications using the water resonance has been the measurement of blood flow (Halbach et al, 1979). Otherwise the results have generally been disappointing, for understandable reasons. The spectrum observed for species rapidly exchanging between different environments is an average of the spectra in individual environments (e.g. bound and free). Average spectra contain relatively little information. (Jardetzky and Roberts, 1981). The claims put forth by Damadian (1971) and others that differences in the characteristics of the water line between normal and malignant tissues could be used for a diagnosis of malignancy, have been shown to be ill founded, since the differences are correlated with the water content, rather than the cytological type of tissue. Similarly in vivo NMR studies of Na^+, K^+ and Cl^- have not led to any striking findings that were not previously obtained by other techniques (Shporer and Civan, 1977). In contrast, when several cell constituents, whose concentrations are sensitive to physiological states, can be observed simultaneously, interpretation can be based on comparisons of concentrations and rates and a much more detailed assessment of the physiological state becomes possible. For example, the use of creatine phosphate (P_C) to inorganic phosphate (P_i) ratio as an index of the cellular energy supply has recently been proposed by Chance (1980). Under conditions of normal oxygenation the Pi concentration is low and the ratio is high. In anoxia the P_C level falls, the P_i level rises and the ratio is low.

Thus far in vivo NMR studies have dealt largely with cell suspensions or perfused organs and only one report of a ^{31}P spectrum obtained on a live animal, the head of a mouse, has appeared in the literature (Chance, et al, 1978). Relatively broad lines, attributable to the γ, α and β phosphate of ATP, P_c and P_i could be identified. Decapitation resulted in a disappearance of organic phosphate peaks, increase in P_i concentration and a fall in pH, as estimated from the P_i chemical shift. By careful correlation of NMR and chemical measurements it was shown that 60% of the signal originated from the brain and the remainder from blood and surrounding tissues.

The interpretation of NMR spectra of intact organisms obviously presents greater difficulties than for simple compounds of even homogeneous tissues and organs. The observed spectrum is a superposition of the spectra of all tissues within the coil. Since the chemical shift is sensitive not only to chemical structure, but also to the molecular environment, the lines of the same compound in different compartments may not be exactly superimposed. This may be manifested as either a broadening or splitting of lines, depending on the differential shift, as seen in Fig. 2. Identification of lines which in simple spectra such as those in Fig. 3 can be made from the relatively large differences in chemical shifts and standardization of intensity measurements on overlapping lines may thus become a formidable problem.

Whether the method is sensitive to reversible metabolic and mild physiological perturbations in the face of these difficulties has so far remained an open question. Two types of experiments carried out over the past year in our laboratory in collaboration with the groups of Dr. M. Weiner and Dr. E.D. Robin from the Departments of Medicine and Physiology, Stanford University School of Medicine, have clearly shown that reversible perturbations of the metabolic state are observable by ^{31}P NMR in the intact animal.

In the first type of experiment, radiofrequency coils were chronically implanted around the kidneys of Sprague-Dawley male rats (120-200 gm). A small glass capillary containing 0.05 m phosphoric acid, pH 8.5 was attached inside the coil to serve as an internal standard for chemical shift measurements. The wires were carried under the skin and brought out behind the neck so as to be inaccessible to the animal. After the wound was closed and the animal recovered, the coils remained in place for as long as 4 - 6 weeks without signs of infection or rejection. For in vivo ^{31}P NMR measurements the animal (awake or anesthetized to reduce movement) was placed in an electrically shielded probe box 2" x 3" x 5" and the leads soldered to the transmitter and preamplifier connections. The spectra were obtained at ambient temperature, without proton irradiation, on a Varian XL-100 Spectrometer with a Nicolet 1180 data system and an external D_2O lock at a ^{31}P frequency of 40.5 MHz.

The results are shown in Fig. 4. Tracing A represents the control, with the marker peak at 0 ppm, the sugar phosphate P_s, inorganic phosphate (P_i), phosphocreatin (P_c)and ATP peaks at 13,14,16,22,27, 35 ppm respectively. This spectrum is similar to that previously reported for the perfused kidney. (Sehr et al, 1977). Anesthesia per se does not perceptibly alter the appearance of the spectrum although small changes in the concentration of phosphorylated metabolites would not be detected.

To determine whether NMR spectroscopy has the sensitivity to detect changes in phosphate metabolism, more subtle than those associated with complete anoxia (so far the only condition studied), fructose (40 mol/g body weight) was administered intraperitoneally. Fructose is known to diminish ATP and Pi concentration while increasing ADP and hexophosphate concentrations (Morris et al, 1978). Figure 4B shows a marked reduction of the β-phosphate peak of ATP and a rise in the intensity of the P_S resonance 30 min. following fructose administration. Subsequent administration of adenosine (2 mol/g) reversed this trend within 20 min. (Figure 4C) (Sanchez, 1974).

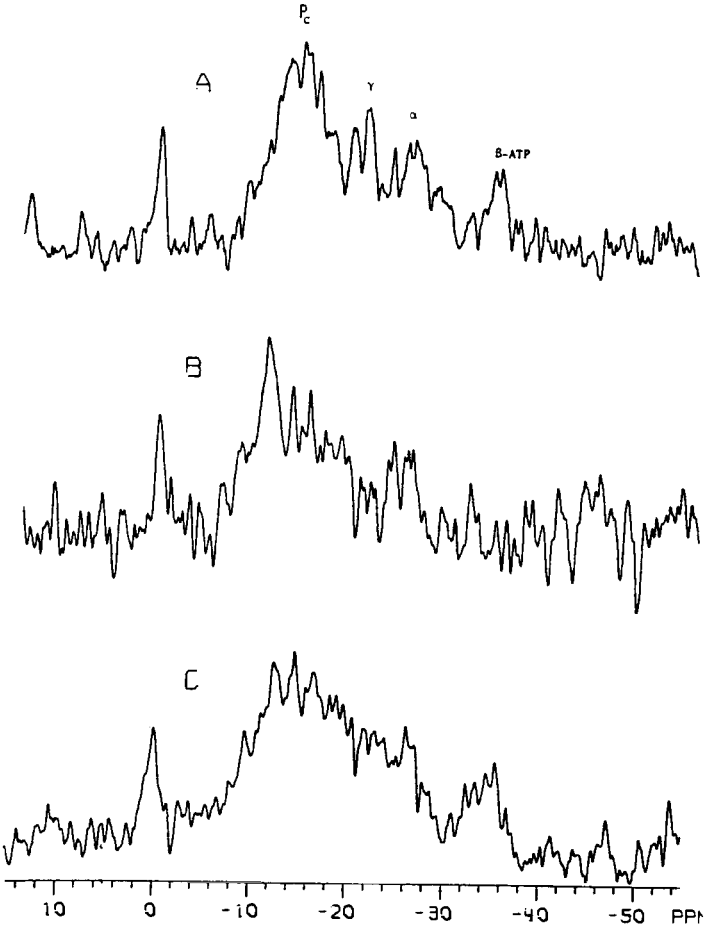

Figure 4

^{31}P NMR spectra of an in situ rat kidney A-control, B-after administration of fructose, C-after subsequent administration of adenosine.

The second type of experiment involving no surgical intervention was performed on intact healthy ($\sim$ 10-25 g) freshwater turtles (Pseudemys scripta elegans) capable of sustaining a prolonged dive. For the NMR experiment the turtle's head was held by a single silk suture looped through the chin muscle and tied to a teflon chuck inserted into a 12 mm NMR cell at a level adjusted to reproducibly position the center the head at the center of the coil. The NMR cell also contained a sealed (1 mm x 15 mm) capillary

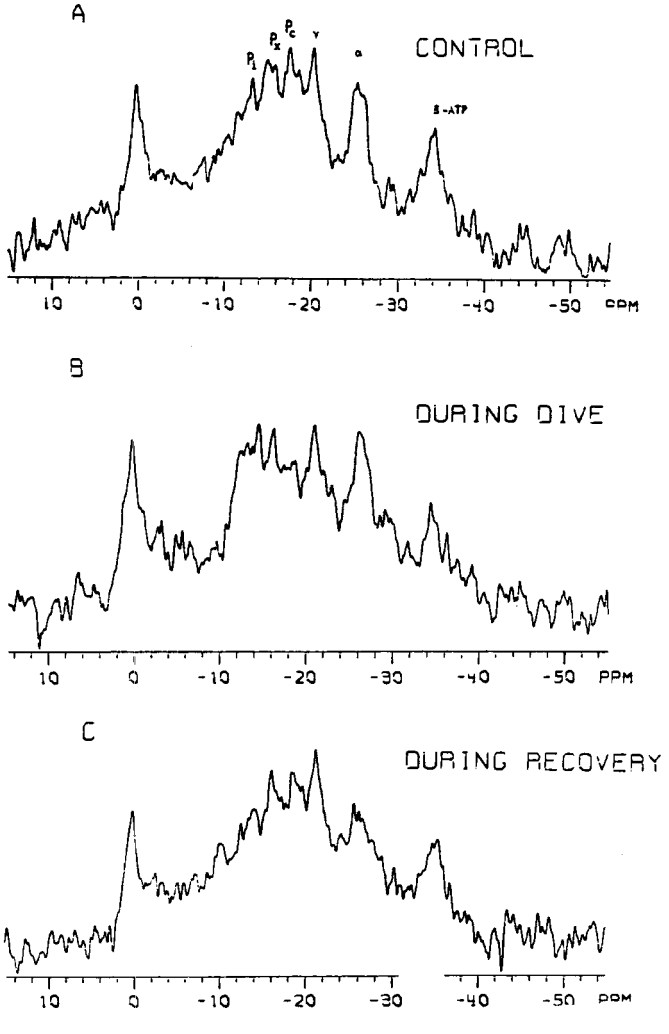

Figure 5
^{31}P NMR spectra of the head of a freshwater turtle

of 0.05 M methylene diphosphonic acid in tris buffer at pH 8.7 cemented inside the tube at the level of the turtle's head. A constant flow of air (50-150 ml/min) was maintained around the turtle's head during the control and recovery periods. The experimental dive was accomplished by filling the NMR cell with tap water until the turtle's head was completely submerged. Every effort was made to ensure that the turtle was in a normal stable physiological state during spectral accumulation.

A typical ^{31}P NMR spectrum of the turtle head in a controlled air environment, showing the expected resonances from inorganic phosphate (P_i), phosphocreatine (P_c) and adenosine triphosphate (ATP), is seen in Fig. 5A. Individual peaks have been identified on the basis of relative chemical shifts and published analyses of phosphate compounds present in the turtle head. Tentative identification of peaks whose resonances appear in the expected region of shifts for sugar phosphates, nicotine adenine dinucleotide and phosphodiesters may also be made, although according to rigorous NMR criteria, no assignments have been made at the present time. The unidentified resonance (Px at 15.5 ppm) has a shift similar to unidentified peaks previously reported in spectra from both frog and toad (Gadian et al, 1979).

The most obvious difference observed during the dive (Fig. 5B) is the ~84% decrease in the intensity of the β-ATP peak. Decreases in the peak areas of P_c and P_x and increases in the peak areas of P_i and ADP are also apparent in these spectra. These changes are partially reversed after a 4 hour recovery (Fig. 5C) but complete recovery requires approximately 15-16 hours.

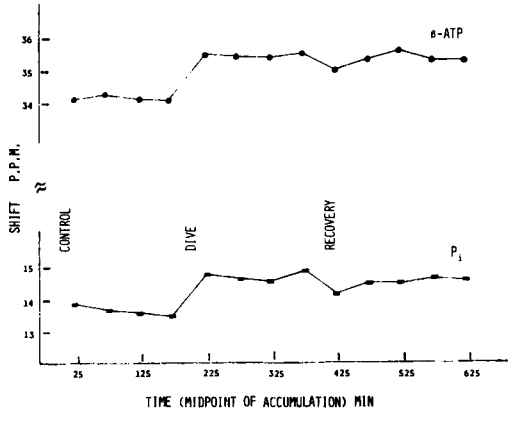

Figure 6
Graph of chemical shifts of inorganic phosphate (P_i ■) and β-ATP(●) vs. time during a period of 12 hours

Fig. 6 shows the time course of the chemical shift changes for the P_i, and -ATP resonances during the 3 phases of the experiment. At the onset of the dive there is a definite shift of P_i and -ATP resonances toward higher field indicating a decrease in pH. During recovery the P_i shift toward higher field continues for a period nearly equal to the time of the dive and then gradually returns to the control value as the pH rises. The maximal observed difference in pH is approximately 1 pH unit from about pH 7.7 to about pH 6.6 taking uncorrected values from the calibration curve (Fig. 2). In contrast to the difference, the absolute value of the initial and final pH are uncertain, since the calibration curves were obtained on a medium of different composition.

These experiments show clearly that the reversible physiological changes occurring during the dive are reflected in the ^{31}P spectra of the turtle head in some detail. Some of these changes, as those cited, are interpretable. There are however others that require further investigation. There are multiple peaks in the region of the P_i, P_c and P_s resonances. Since one is simultaneously observing brain, cerebrospinal fluid, blood, muscle and bone, the possibility remains that some of the peaks reflect the same constituents in different tissues. The possibility that they reflect other, as yet unidentified phosphorylated metabolites in the amphibian brain is also open. To attach quantitative significance to the estimates of pH and ATP, P_c and P_i concentrations requires far more extensive calibrations than have been reported thus far. Experiments in which a turtle did not recover from the dive indicate that the rise of the sharp P_i peak beyond a certain level precedes death and signals irreversibility. The exact P_i level at which survival is endangered remains to be established. Extensive correlation of the spectroscopic findings with biochemical, anatomical and physiological measurements will be required to answer the more detailed questions. Nevertheless, the experiments unequivocally demonstrate that reversible physiological changes can be monitored by high resolution NMR in the intact animal.

References

Chance, B. (Personal Communication)

Chance, B., Nakase, Y., Bend, M., Leigh, J.S. and McDonald, G. (1978) Proc. Nat. Acad. Sci. 75, 4925. "Detection of ^{31}P Nuclear Magnetic Resonance Signals in Brain by In Vivo and Freeze-trapped Assays".

Damadian, R. (1971) Science 171, 1151 "Tumor Detection by Nuclear Magnetic Resonance"

Gadian, D.G., Radda, G.K., Richards, R.E. and Seeley, P.J. in "Biological Applications of Magnetic Resonance", R.G. Shulman Ed., Academic Press, N.Y. 1971, 463-529.

Grove, J.H., Ackerman, J.J.H., Radda, G.K. and Bore, P.J. (1980) Proc. Nat. Acad. Sci. 77, 299, "Analysis of Rat Heart In Vivo by Phosphorus Nuclear Magnetic Resonance".

Halbach,R.E., Battocleti, J.H., Sances, A.,Jr., Bowman, R.L., Kudravcev, V. (1979) Rev. Sci. Instrum. 50 428-434,"Cylindrical Crossed-Coil NMR Limb Blood Flowmeter".

Hollis, D.P. (1979) Bull. Mag. Res. 1, 27, "Nuclear Magnetic Resonance Studies of Cancer and Heart Disease".

Hoult, D.I., Busby,S.J.W., Gadian, D.G., Radda, G.K., Richards, R.E. and Seeley, P.J. (1974) Nature 252, 285-287, "Observation of Tissue Metabolites Using ^{31}P Nuclear Magnetic Resonance".

Jardetzky, O., Ph.D. Thesis, Univ. of Minnesota (1956) "A Study of Interactions of Aqueous Sodium Ion by Nuclear Spin Resonance".

Jardetzky, O. and Roberts, G.C.K. "NMR in Molecular Biology", Academic Press, New York, 1981 (in press).

Jardetzky, O. and Wertz, J.E. (1956) Am. J. Physiol. 187, 608,"Declaration of Sodium Complexes by Nuclear Spin Resonance".

Jardetzky, O. and Wertz, J.E. (1960) J. Am. Chem. Soc. 82, 318, "The Complexing of Sodium Ion with Some Common Metabolites".

Moon, R.B. and Richards, J.H. (1973) J. Biol. Chem. 248, 7276-7278, "Determination of Intracellular pH by ^{31}P Magnetic Resonance".

Morris, R. Curtiss, Jr., Nigon, Kathleen, Reed, Elizabeth R. (1978) J. Clin. Inves. 61, 209-220, "Evidence that the Severity of Depletion of Inorganic Phosphate Determines the Severity of the Disturbance of Adenine Nucleotide Metabolism in the Liver and Renal Cortex of the Fructose-Loaded Rat"

Odebald, E., Bhar, N. and Lindstrom, G. (1956) Arch. Biochem. Biophys. 63, 221, "Proton Magnetic Resonance of Human Red Blood Cells in Heavy-Water Exchange Experiments".

Pople, J.A., Schneider, W.G. and Bernstein, H.J., "High Resolution Nuclear Magnetic Resonance" McGraw-Hill Book Co., New York (1959).

Roberts, J.K.M., Ray, P.M., Wade-Jardetzky, N.G. and Jardetzky, O. (1980) Nature 283, 870, "Estimation of Cytoplasmic and Vacuolar pH in Higher Plant Cells by ^{31}P NMR".

Sanchez, V. Chagoya de, Brunner, A., Sanchez, M.E., Lopez, C., Pina, E., (1974) Arch. Biochem. Biophys. 160, 145-150, "Utilization of Adenosine as a Tool in Studies on the Regulation of Liver Glycogen Biosynthesis".

Sehr, P.A., Radda, G.K., Bore, B.J. and Sells, R.A. (1977) Biochem. Biophys. Res. Commun. 77, 195, "A Model Kidney Transplant Studied by Phosphorus Nuclear Magnetic Resonance".

Shporer, M. and Civan, M.M. (1977) Curr. Top Membr. Transp. 9, 1-69 "Structuring of Water and Immobilization of Ions within the Intracellular Fluids: The Contribution of NMR Spectroscopy".

Adv. Physiol. Sci. Vol. 8. Cardiovascular Physiology. Heart, Peripheral Circulation and Methodology
A. G. B. Kovách, E. Monos, G. Rubányi (eds)

THE PROBLEMS OF THE CORRECTION AND EVALUATION OF IN VIVO NADH FLUORESCENCE MEASUREMENTS

E. Dóra, T. Nagy-Dóra, L. Gyulai and A. G. B. Kovách
Experimental Research Department and 2nd Department of Physiology, Semmelweis Medical University, H-1082, Hungary

The interpretation of in vivo NADH fluorescence measurements is quite difficult when optical properties of tissues /water content, blood content,refraction index,penetration depth of the incident light, etc./ change.
In case of blood perfused organs the increase in blood content result in NADH fluorescence decrease,though the tissue NADH concentration did not change /Dóra and Kovách 1978,Kovách et al. 1977/ and vice versa when the blood content is decreased.Because of the possibility to have such an artifact the people who work with fluorometry in vivo look for such a tissue field where big vessels are lacking.However this way the problem can not be solved.In the brain cortex one have to face up with a very dense capillary network /Fig. 1/.To eliminate this type of virtual NADH concentration change in NADH fluorescence reading one have to apply an appropriate correction method.In our laboratory the correction method of Harbig et al. /1976/ is used,since a linear relationship was obtained between the hemodilution induced tissue reflectance and fluorescence changes and the hemodilution does not make the brain hypoxic.The great drawback of this correction procedure is that the correction factor has to be determined frequently and the fast changes can not be measured exactly.
In neural tissues the ion and water movements are regular concomitants of altered electrical activity /Lipton 1973,Hodgkin and Keynes 1957/. This can cause a serious artifact again,since the increase in cellular volume might act as if NADH concentration were decreased when the NADH fluorescence is measured by in vivo fluorometry.These virtual NADH fluorescence changes can be eliminated only if the cellular volume changes were measured simultaneously.

In the present report our results concerning the factors /background NADH fluorescence,illumination angle,type of ultropak/ which influence the value of correction factor,determined by artificial haemodilution,are summarized.A part of these results has been published earlierly /Kovách et al. 1977,Dóra and Kovách 1978/.
In the second part of this presentation some problems of the correction of NADH fluorescence measured in isolated ganglia and hearts of Helix Pomatia will be mentioned.

METHODS

One part of the experiments was performed on rat's and cat's

brain.The animals were anaesthetized,immobilized and artificially respirated.The tissue NADH fluorescence and UV reflectance were measured with a light pipe fluorometer /Zeuthen et al. 1979/ and with a microfluorometer /Kovách et al. 1977/.The correction factor determined by artificial haemodilution was around 1 in rat brain and it varied between 1 and 6 in cat brain.The arterial blood gases were controlled and maintained in physiological range.
The effect of the background NADH fluorescence,illumination angle and type of ultropak on the value of correction factor was analysed in cat brain.The backgound NADH fluorescence was altered by a stepwise bleeding from the control level to 80,60 and 40 mm Hg mean arterial blood pressure.
To see the effect of illumination angle and the type of ultropak the brain cortex was excited with angles of 90^{o} and 45^{o} using Wetzlar ultropaks of 3.2,6.5 and 11.

The oesophageal ganglia and hearts were carefully dissected from the animals and placed in a special chamber containing oxygenated Meng solution.The temperature of the bathing solution was maintained at 23 ^{o}C.The stimulating electrodes were placed on the surface of the ganglia and hearts so that the illuminated spot lied from equal distances from the electrodes.In these experiments a micro fluororeflectometer was used.The illumination angle was 60^{o}.When the ganglia was stimulated the efferent neural electrical activity was also recorded from the intestinal nerve.In these experiments the effect of various stimulation strength on tissue NADH fluorescence and UV reflectance was studied. For correction the reflectance changes were subtracted from the fluorescence changes with a ratio of 1.

RESULTS

The importance of appropriate correction of NADH fluorescence changes measured in vivo in blood perfused brain is clearly demonstrated by Fig. 2.In this Fig. the effect of nitrogen gas breathing is shown on cortical pO_2,UV reflectance,corrected NADH fluorescence,NADH fluorescence and on mean arterial blood pressure in rats.In these experiments a correction factor of 1 was used.The anoxia induced corrected NADH fluorescence response is very similiar to the response that was obtained on isolated liver /Scholz et al. 1969/.The uncorrected NADH fluorescence trace shows at the same time a reoxidation of NADH during nitrogen breathing which is certainly an artifact caused by the continuous increase of cortical blood content /see reflectance/.

Importance of background NADH fluorescence

The correction factor determined by artificial haemodilution is defined as the ratio of haemodilution induced fluorescence and reflectance responses /Harbig et al. 1976/.Therefore it is reasonable to presume that the background NADH fluorescence should have a considerable effect on the value of the correction factor.To test this hypothesis we increased the background NADH fluorescence of the cat brain cortex by arterial bleeding.As Fig. 3 shows arterial hypotension resulted in a marked increase in background NADH fluorescence.In agreement with the above postulated hypothesis the value of the correction factor increased significantly during arterial hypotension however,a linear relationship was not found between the changes of background NADH fluorescence and correction factor /Figs. 3 and 4/.This indicates that there are other factors,probably the changes in microcirculation,which also have an effect on the value of the correction factor during bleeding.

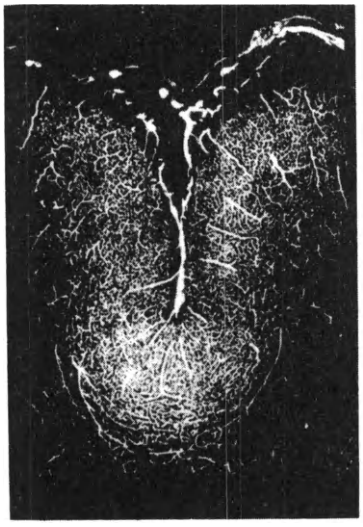

Fig. 1.A microscopic picture from the cat brain cortex.The brain was perfused with colloid carbon at normal arterial pressure and later fixed in 10 % formaldehyde solution. Ater embedding 100 µ thick slices were made from the brain with a Zeiss microton.

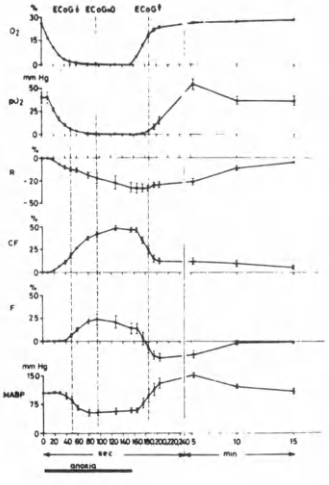

Fig. 2.Effect of nitrogen anoxia on cortical oxygen tension /pO_2/, UV reflectance /R/,corrected NADH fluorescence /CF/,NADH fluorescence /F/ and mean arterial blood pressure /MABP/ in 8 rats. The duration of anoxia is marked below the time scale by a vertical bar.

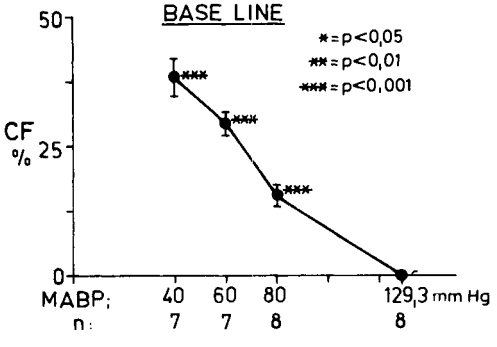

Fig. 3.Changes in the background NADH fluorescence of the cat brain cortex. Asterisks show the degree of significant changes as compared to control. For abbreviations see Fig. 2.

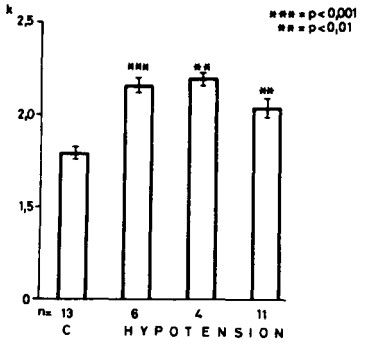

Fig. 4.Changes in the value of correction factor /k/ during arterial hypotension in cat brain cortex.Abbreviations: C=control period,n=number of experiments.

Importance of the type of ultropak and illumination angle

In Fig. 5 one can see that the correction factor can very from 1 to 6 when different ultropak is applied at an illumination angle of 90^{o}.On the basis of this result it seems that the mirror reflectance is a very important factor in the determination of correction.If the mirror reflectance is decreased by an illumination of 45^{o} the values of the correction factor decreased significantly,though ultropak 6.5 gave higher correction factors than ultropak 11.

Fig. 6 shows the effect of nitrogen anoxia on cerebrocortical corrected NADH fluorescence,NADH fluorescence and reflectance at different illumination angles using ultropak 6.5.This Fig. is a good demonstration of the appropriateness of this correction procedure,since the corrected NADH fluorescence changes during anoxia were identical at the different illumination angles.

At high focal length ultropaks /3.2/ the reflectance changes to any intervention are smaller and the correction factor is much larger than at short focal length ultropaks /11/.If in such a case the correction factor is not determined the interpretation of the results can be misleading.

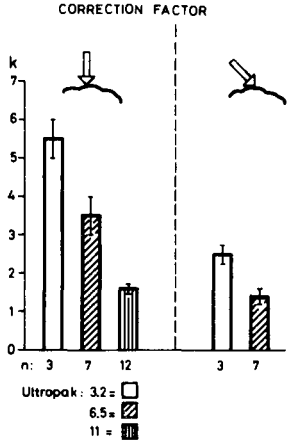

Fig. 5.Effect of the type of ultropak and illumination angle on the value of the correction factor /k/ determined by injecting o.1-o.3 cc oxygen saturated saline into the lingual artery. n shows the number of experiments used for calculation.

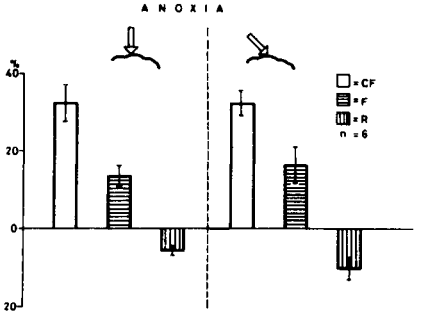

Fig. 6.Effect of nitrogen gas breathing on the cat's brain corrected NADH fluorescence /CF/,NADH fluorescence /F/ and reflectance /R/ at different illumination angles using ultropak 6.5.n shows the number of experiments used for calculation.

Measurements on Helix Pomatia hearts and ganglia

According to the work of Lipton /1973/ the light scattering is a good indicator of changes in cellular volume.When the cellular volume is increased the intensity of the scattered light is decreased.

To see the influence of stimulation strength on cellular volume and

NADH fluorescence changes the hearts were paced at different frequencies and stimulation voltages /Figs. 7 and 8/.When the heart was stimulated with 10 cycl.,10 V, 2 msec the reflectance slightly decreased and the uncorrected and corrected NADH fluorescence increased /Fig. 7/.The contractions of the heart are indicated by small spikes on both recordings.When the frequency of the stimulation was increased to 60 cycl. the corrected NADH fluorescence responses became more pronounced though the reflectance responses did not alter very much.Since in this case the reflectance and NADH fluorescence responses were opposite in direction the increase in corrected fluorescence certainly came from the increase of the number of NADH molecules.
In Fig. 8 the stimulation voltage was increased to 15 V.The stronger stimulation resulted in more marked reflectance and corrected NADH fluorescence changes and interestingly enough the responses at 40 cycl. has been changed fundamentally.At this time the reflectance increased during stimulation and the corrected NADH response became biphasic,namely after the initial corrected NADH fluorescence increase a longlasting decrease occured in corrected NADH fluorescence.The response in the uncorrected NADH fluorescence however was very similiar to the responses obtained before.In this case the interpretation of the corrected NADH fluorescence response is not so simple,since the reflectance and the uncorrected NADH fluorescence changed in the same direction. It is also a question whether the spike-like changes in the corrected trace shows a real NAD reduction,or it is caused by the movement of the heart.However,since the heart was fixed by metal pins and the reflectance and uncorrected NADH fluorescence spikes were opposite in direction it is supposed that these rapid changes are real and they are showing the alterations of the NAD/NADH redox state during heart beats.The increased NADH fluorescence during heart muscle contraction can not be the sign of tissue hypoxia,it probably originates from the increased glycolysis and concomitant cytoplasmic NAD reduction.

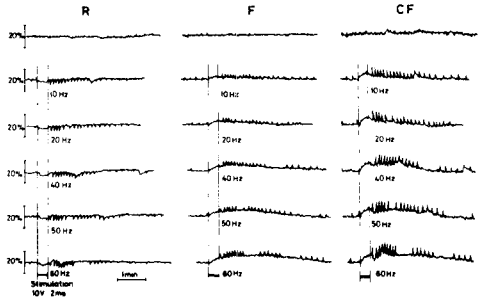

Fig. 7.Effect of direct electrical stimulation of Helix Pomatia isolated heart on reflectance /R/,NADH fluorescence /F/ and corrected NADH fluorescence /CF/ in a typical experiment.The duration of stimulation is shown by two vertical lines and by a horizontal bar.

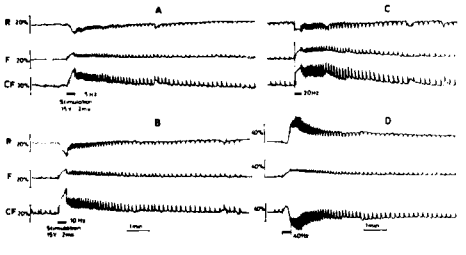

Fig. 8. Effect of direct electrical stimulation on R,F and CF in the same experiment as it was shown in Fig. 7.Note that the stimulation voltage was increased to 15 V.

In Figs. 9 and 10 the effect of the direct electrical stimulation of the Helix Pomatia ganglia on reflectance,NADH fluorescence and corrected NADH fluorescence and on the spontaneous activity of intestinal nerve is demonstrated in such an experiment where the stimulation resulted in an increase in the activity of intestinal nerve.In 4 from the 12 experiments the electrical stimulation of the ganglia resulted in an inhibition in the activity of the intestinal nerve.These results are in a good agreement with the work of Rózsa et al. /1973/ who found a mixed population of inhibitory and excitatory neurons in the oesophageal ganglia of Helix Pomatia.
In the demonstrated experiment the 4 V,1 msec,40 cycl. electrical stimulation led to a marked increase in reflectance and NADH fluorescence. The interpretation of the corrected NADH fluorescence response is difficult since R and F changed in the same direction /Fig. 7/.When the stimulation voltage was elevated to 15 and 20 V opposite changes appeared in reflectance and uncorrected NADH fluorescence.The reflectance response became triphasic while the uncorrected NADH fluorescence increased monotoneously.The increase in corrected NADH fluorescence correlates nicely with the alterations of the activity of intestinal nerve.Increasing the stimulation voltage to 25 and 30 V the uncorrected NADH fluorescence response turned to the opposite direction and the reflectance response became more pronounced.If a 1:1 correction were made the corrected NADH fluorescence woud indicate NAD reduction but again it is difficult to decide whether this correction was proper.

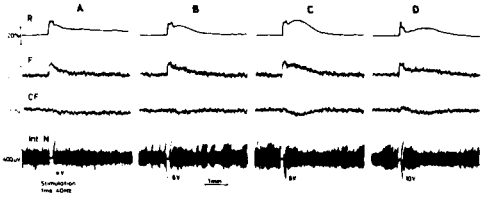

Fig. 9. Effect of direct electrical stimulation on the reflectance /R/, NADH fluorescence /F/ and corrected NADH fluorescence in isolated oesophageal ganglia of Helix Pomatia in a typical experiment.The electrical activity of the intestinal nerve was recorded bipolarly by silver wire electrodes.During stimulation the spontaneous electrical activity of the intestinal nerve was not recorded.

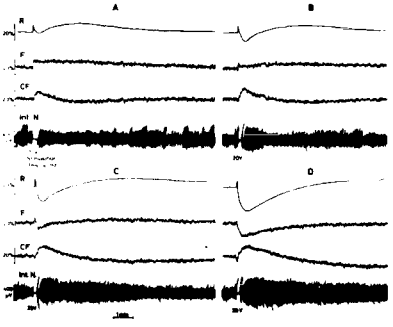

Fig. 10.Effect of direct electrical stimulation on R,F, CF in isolated oesophageal ganglia of Helix Pomatia and on the spontaneous electrical activity of intestinal nerve in the same experiment as in Fig. 9.

DISCUSSIONS AND CONCLUSIONS

First Chance et al. /1962/ demonstrated that the blood content variations can cause virtual NADH concentration changes when the NADH fluorescence is measured in vivo in intact blood perfused organs. The red blood cells absorb and scatter the exaltation light and quench the emitted NADH fluorescence light.When the blood vessels are dilated and the tissue blood content is increased the NADH fluorescence can decrease without any real changes in tissue NADH concentration.This artifact can be eliminated by a correction method based on artificial haemodilution /Jöbsis et al. 1971,Harbig et al. 1976,Kovách et al. 1977/,although Jöbsis et al. /1971/ questioned the usefulness of this correction procedure because of the large variability of this correction factor.
Our results /Kovách et al. 1977,Dóra and Kovách 1978,Zeuthen et al. 1979/ show,however,that this type of correction gives good results and if the correction were not applied improbable results were obtained /Fig. 2/.

According to our experience the correction factor can vary in a broad range depending on the type of objective used,on the illumination angle,on the intensity of background NADH fluorescence and on the arrangement of microcirculation,etc.Though the value of the correction factor can vary it does not effect the results when the correction is made with the appropriate factor /Fig. 4/.
If such an objective were used which has a great focal length /ultropak 3.2/ the reflectance changes to any intervention /anoxia,electrical stimulation,epilepsy,etc./ are small but they can not be neglected since,the value of the correction factor is high /Fig. 3/.

In isolated organs the cellular volume changes generally are not recorded and not considered in the evaluation of the NADH fluorescence recordings /Chance and Jöbsis 1959,Rodriguez-Estrada 1975/.It is surprising since the NADH concentration and the intensity of the NADH fluorescence light can be decreased if the cellular volume were increased,though the NAD/NADH ratio did not change.Ji et al. /1979/ tried resolve this problem and with complicated calculations corrected the NADH fluorescence responses that were evoked by electrical stimulation of the isolated heart papillary muscle.Surprisingly enough he was unable to show consistent NADH fluorescence changes during forced contraction in contrast to Chapman who obtained always NADH oxidation in the same condition but did not correct for cellular volume changes /1972/.
According to our experience obtained on isolated hearts of Helix Pomatia the increased mechanical work was accompanied to NAD reduction. This NAD reduction can not be the result of relative tissue hypoxia since the hearts were bathed in oxygen saturated Meng solution.In those cases where the reflectance and the uncorrected NADH fluorescence changed in the same direction the NADH fluorescence alterations were not evaluated because of the incertainity of correction.In our experiments the reflected light was measured at 366 nm and probably additional measurements at 589 nm would help to elaborate a more sophisticated method for the correction of NADH fluorescence changes in Helix Pomatia hearts.

In isolated ganglia electrical stimulation resulted in NAD reduction mostly but in some cases NADH oxidation appeared during and after

stimulation.The appearance of NAD reduction or NADH oxidation was not dependent on the stimulation strength.In some cases the small stimulating parameters resulted in NAD reduction and this response was changed to NADH oxidation when high stimulating parameters were applied and vice versa in other cases.This certainly excludes the role of tissue hypoxia in the NAD reductive response.It is suggested that the direction of tissue NADH fluorescence responses during increased activity is fundamentally influenced by the initial NAD/NADH redox state and by the intactness and capability of the glycolytic system at least in the demonstrated experiments.

REFERENCES

Chance, B.,Jöbsis, F.F. /1959/.Changes in fluorescence in a frog sartorius muscle following a twitch.Nature 184:195-196.

Chapman, J.B. /1972/.Fluorometric studies of oxidative metabolism in isolated papillary muscle of the rabbit.J. gen. Physiol.59:135-154.

Dóra, E.,Kovách, A.G.B. /1978/.Origin of cerebrocortical NADH fluorescence measured by in vivo surface fluorometry and the correction of the mirror reflectance.Acta physiol. Acad. Sci. hung.52:156-157.

Harbig, K.,Chance, B.,Kovách, A.G.B.,Reivich, M. /1976/.In vivo measurement of pyridine nucleotide fluorescence from the brain cortex. J. appl. Physiol.41:480-489.

Hodgkin, A.L.,Keynes, R.D. /1957/.Movements of labelled calcium in squid giant axon.J. Physiol./London/.138:253-281.

Ji, S.,Chance, B.,Nishiki, T.,Smith, T.,Rich, T. /1979/.Microlight guides:a new method for measuring tissue fluorescence and reflectance. Amer. J. Physiol.263: C144-C156.

Jöbsis, F.F.,O'Connor, M.J.,Vitale, A.,Vreman, H. /1971/.Intracellular redox changes in functioning cerebral cortex.I.Metabolic effects of epileptiform activity.J. Neurophysiol.34:735-749.

Kovách, A.G.B.,Dóra, E.,Eke, A.,Gyulai, L. /1977/.Effects of microcirculation on microfluorometric measurements.In:Oxygen and Physiological Function,Ed.:Jöbsis, F.F.,Professional Information Library,Dallas, Texas,111-132.

Lipton, P. /1973/.Effects of membrane depolarization on light scattering by cerebral cortical slices.J. Physiol./London/.231:365-383.

Rodriguez-Estrada, C. /1975/.Reduced nicotinamide dinucleotide and depolarization in neurons.Amer. J. Physiol.288:996-1001.

Rózsa-S, K.T.,Kiss, I.,Szőke, V./1973/.On the role of bioactive substances in the rhytm regulation of heart muscle cells of Gastropoda and Insecta.In:Neurobiology of Invertebrates.Mechanism of Rhytm Regulation.Ed.:Salánki, J.,Akadémiai Kiadó,Budapest,67-181.

Scholz, R.,Thurman, R.G.,Williamson, J.R.,Chance,B.,Bücher,T. /1969/. Flavine and pyridine nucleotide oxidation-reduction changes in perfused rat liver.J. biol. Chem.244:2317-2324.

Zeuthen, T.,Dóra, E.,Silver, I.A.,Chance, B.,Kovách, A.G.B. /1979/. Mechanism of cerebrocortical vasodilatation during anoxia.Acta physiol. Acad. Sci. hung.54:305-318.

INDEX

The page numbers refer to the first page of the article in which the index term appears.